Hormones during *Drosophila* metamorphosis

by
Stephen Paul Bainbridge

Doctor of Philosophy

University of Edinburgh
1984

CONTENTS

PAGE

List of Figures

List of Tables

Acknowledgements

Abstract

CHAPTER ONE: INTRODUCTION 1

1.1 Metamorphosis 1

1.2 The Approach 2

1.3 Metamorphosis timed 3

1.4 The Cuticles 6

1.5 The Hormones 9

1.6 Direct radioimmune assay (RIA) - A preliminary investigation of ecdysteroid titre 13

1.7 Analytical methods 14

1.8 Objectives 17

CHAPTER TWO; MATERIALS AND DEVELOPMENT OF METHODS 18

2.1 Rearing Conditions 18

2.2 Observation and timing of the sequence of changes during metamorphosis 18

2.3 Duration of stages estimated by frequency 19

2.4 Microscopy and Photography 20

2.4.1 Dissecting microscopy 20

2.4.2 Nomarski phase interference microscopy 20

2.5 Collection of staged material for radioimmune assay (RIA) and chromatography: 21

2.5.1 Small-scale collections of stages LIII-A3, sexes separated, for (RIA) 21

2.5.2	Large-scale collections of stages P1, P7 and P10-13	23
2.6	Extraction of ecdysteroids for direct RIA	24
2.7	Characterisation of the Horn I2 antiserum	25
2.8	Monitoring of the assay system	26
2.9	Correction for variable scintillation quenching (Q)	27
2.10	Protocol for direct RIA of ecdysteroids	28
2.11	Thin-layer chromatography (TLC):	30
2.11.1	TLC: loading density vs. R_F	30
2.11.2	TLC: Development-time vs. R_F	30
2.11.3	TLC: Elution-contaminants	30
2.12	Test Beers-Lambert Law	32
2.13	Trial fraction-collection after HPLC	33
2.14	HPLC sample-preparation	33
2.15	Preparative and analytical HPLC	38
2.16	HPLC eluate volume-reduction:	40
2.16.1	Determination of optimal solvent composition for loading HPLC eluate fractions into C_{18} cartridges	41
2.16.2	Protocol for sample volume-reduction using C_{18} cartridges	42
2.16.3	Volume-correction to realise nominal sample volume (1 ml)	42
2.16.4	Monitoring recovery efficiency of ecdysteroids through C_{18} cartridges used for fraction volume-reduction	43
2.17	Preparation of a mouse anti-20-OH-ecdysone polyclonal antiserum (MAS):	44
2.17.1	Carboxymethyloxime-derivatisation of 20-OH-ecdysone	44
2.17.2	Conjugation of 20-OH-ecdysone-CMO to BSA	45

2.17.3 Raising anti-20-OH-ecdysone mouse antiserum 46
2.18 Characterisation of MAS 46
2.19 Monitoring of the radioimmune assay (MAS) 48
2.20 Protocol for HPLC-coupled RIA using MAS 49
2.21 Predicting HPLC retention times 50
2.22 Treatment of data from HPLC-RIA: 50
2.22.1 HPLC relative retention times (RRTs) as peak-area segment boundaries 51
2.22.2 Screening HPLC-fractional concentrations as components of ecdysteroid titres 52
2.23 Sample preparation for GLC-MF analysis of ecdysteroids: 53
2.23.1 Extraction/purification 54
2.23.2 Derivatisation (Full silylation) 55
2.23.3 Sample-TMS-ethers: work-up for GLC 55
2.23.4 GLC-MF of silylated ecdysteroids 55
2.23.5 Quantification 56
2.24 Identification of juvenile hormone (JH) in D. melanogaster: 56
2.24.1 Sample-collection 56
2.24.2 GC-MF 58
CHAPTER THREE:
DESCRIPTION AND TIMING OF THE STAGES OF METAMORPHOSIS 60
3.1 Definition of the stages 60
3.2 Differentiation of cuticles during metamorphosis 65
3.3 Timing the stages of metamorphosis at 25°C: 66
3.3.1 Estimation of durations of stages L1-A2 by frequency 66
3.3.2 Variability of timed cultures with respect to stages 69
3.4 Metamorphosis at temperatures other than 25°C: 71

3.4.1 Frequency-estimates of stage durations at 18°C + 29°C 72

3.4.2 Direct timing of P1-4 at 18°C + 29°C 73

3.5 Collecting staged material: 74

3.5.1 Cold-shock 74

3.5.2 Collection-methods for staged material 79

3.6 Stages in other Drosophila species 80

3.7 Note on previous uses of staging criteria 81

CHAPTER FOUR: DIRECT RADIOIMMUNE ASSAY (RIA) FOR ECDYSTEROIDS: WHOLE-BODY TITRE PROFILES 83

4.1 Standard response curves 83

4.2 Correlation of developmental status with stage, net age 84

4.3 Ecdysteroid titre profiles: 84

4.3.1 The data 84

4.3.2 Treatment and analysis of the data 86

4.3.3 An ecdysteroid(s) titre profile 88

CHAPTER FIVE: ANALYTICAL AND PREPARATIVE HIGH PERFORMANCE LIQUID CHROMATOGRAPHY (HPLC); HPLC-COUPLED RIA 91

5.1 Sample preparation 93

5.2 HPLC-separations of ecdysteroids 93

5.3 Quantitative HPLC-UV spectrophotometry 94

5.4 Preparative HPLC: collection of eluate fractions for RIA 94

5.5 Eluate volume-reduction: monitoring recovery-efficiency 96

5.6 Treatment of the HPLC-RIA data: 98

5.6.1 Background correction 98

5.6.2 Analysis of HPLC-RIA data 100

CHAPTER SIX: ANALYSIS OF HORMONES BY CHROMATOGRAPHY-COUPLED MASS FRAGMENTOGRAPHY (MF) 108

6.1 GLC-MF of ecdysteroids 108

6.2 GC-MF of juvenile hormone(s) (JH) 110

CHAPTER SEVEN: DISCUSSION OF CHAPTER FOUR TO SIX 114

7.1 Ecdysteroid titre-profiles 114

7.2 Makisterone A 117

7.3 Ecdysteroid identifications and titres 119

7.3.1 20, 26 di-hydroxyl-ecdysone 119

7.3.2 Comparisons of stages P7/P10-13 and HPLC-RIA/GLC-MF 120

7.3.3 Stage P1 121

7.3.4 Stage P7 123

7.3.5 Stages P10-13 124

7.3.6 General 125

7.4 Ecdysteroids: Sources and Biosynthesis 125

7.5 Ecdysteroid Metabolism 127

7.6 Ecdysteroid functions 128

7.6.1 Production and modification of cuticle 128

7.6.2 The testes 130

7.6.3 The ovaries/vitellogenesis 132

7.7 Ecdysteroids and JH: The cuticle cycle 137

7.8 The modified "classical scheme" 146

APPENDICES

A1: GLOSSARY 151

A2: TIMECOURSE OF METAMORPHOSIS 165

A3: ANALYSIS OF THE PUPAL CUTICLE POLYPEPTIDES 174

A3.1 Introduction 174

A3.2 Materials and methods 175

A3.3 Results 176

A3.4 Discussion 177

A4 ECDYSTEROID RECOVERY EFFICIENCIES 181

A4.1 Materials and methods 182

A4.2 Experiments 184

A4.3 TLC: general conclusions 193

A5 HPLC: THEORETICAL AND TECHNICAL INFORMATION 196

A5.1 Aspects of liquid chromatography theory 196

A5.2 HPLC-system operation (Waters/LKB) 198

A5.2.1 Apparatus 198

A5.2.2 HPLC Program 199

A5.2.3 Technical details 203

A6: CAN DROSOPHILA IMAGINAL DISCS SERVE IN AN ECDYSTEROID BIOASSAY 206

A7: TWO su(f) MUTANTS

A7.1 Introduction

A7.2 Results

A7.3 Discussion

A8: STAGING THE METAMORPHOSIS OF Drosophila melanogaster

By S. Paul Bainbridge and Mary Bownes (1981)

J. Embryol. exp. Morph. 66, 57-80.

BIBLIOGRAPHY

LIST OF FIGURES

		Section
1.1	Schematic insect cuticle: changes during moulting/ metamorphosis	1.4
1.2	Tyrosine metabolism at pupariation in calliphora erythrocephala	1.4
1.3	Pupariation + puparium formation in Sarcophaga bullata	1.4
1.4	Ecdysteroid structures and cholesterol	1.5
1.5	Juvenile Hormones (JH)	1.5
1.6	Composite profile of reported ecdysteroid titres	1.5
1.7	Classical scheme for the control of moulting (Holometabola)	1.5
2.1	Removal of the puparium	2.4.1
2.2	Optimisation of the RIA extraction procedure for ecdysteroids	2.6
2.3	Scatchard plot (c.f. Scatchard, 1949) for 0.44% antiserum Horn I2 (16 wk) with ^{3}H-ecdysone (S.A. = 63.5 Ci/mmol).	2.7
2.4	Typical standard response curves of antiserum Horn I2 (16 wk) for ecdysone (α) and 20-OH-ecdysone (β) competing with ^{3}H-ecdysone (63.5 Ci/mmol) in 0.44% solution	2.7
2.5	Monitoring RIA solutions: Horn I2 (16 wk) antiserum with ^{3}H-ecdysone (NEN)	2.8
2.6	Quench Calibration Curve	2.9
2.7	TLC: R_f vs. $\log_{10}$ chromatogram development time	2.11.2
2.8	TLC Elution Contaminants	2.11.3
2.9	TLC Elution Contaminants: λ max scans	2.11.3
2.10	Direct proportionality of HPLC - UV spectrophitometry peak areas and ecdysteroid concentration	2.12
2.11	Pipetting error for variable-volume pipette (Gilson	

	pipetman P 200)	2.12
2.12	U.V.-absorption λ_{max} determinations of ecdysteroid HPLC eluate fractions	2.13
2.13	Derivatisation of 20-OH-ecdysone as an immunogen	2.17.1
2.14	Immunisation schedule for production of MAS	2.17.3
2.15	MAS 12 dilution vs. binding of ^{3}H-ecdysone	2.18
2.16	Scatchard plots for MAS 7 and MAS 12 with ^{3}H-ecdysone	2.18
2.17	Standard response curves of MAS	2.18
2.18	MAS 12 with ^{3}H-ecdysone: % binding cpm vs. MAS/label volumes	2.19
2.19	Optimum working dilutions for degraded MAS aliquots	2.19
2.20	Protein/Serum in competition with ^{3}H-ecdysone for binding to MAS	2.19
2.21	Quench callibration curve	2.20
2.22	Retention time ratios	2.21
2.23	HPLC Ecdysteroid peak traces	2.22.1
2.24	RRT vs. Cummulative percentage total O.D-peak area	2.22.1
2.25	O.D. peak segment area (cm^2) vs. % total peak area, (simulation)	2.22.2
2.26	Calibration of GLC-MF ecdysteroid peak areas	2.23.5
2.27	JH derivatization	2.24.2
3.1	Stages L1 (Post-feeding) to P2 (Brown puparium)	3.1
3.2	Stages P3 (Bubble) to P4 (Buoyant)	3.1
3.3	Stages P4 (Moving bubble) to P5	3.1
3.4	Stages P5 (Malphigian tubules migrating) to P7 ("yellow body")	3.1
3.5	Stages P8 (Yellow-eyed) to P11 (Thoracic bristles)	3.1
3.6	Stages P11 to P15 (Meconium)	3.1
3.7	Female of Stage P1 (puparium formation)	3.1
3.8-10	Stage P5 ii (White Malphigian tubules)	3.1

3.11	Stage P8 (Yellow-eyed)	3.1
3.12	Stage P9 (Amber)	3.1
3.13-15	Stage P12 i (Wing-tips grey)	3.1
3.16	Early stage P13 (Wings black)	3.1
3.17-18	Late stage P13 (Wings black)	3.1
3.19-20	Stage P14 (Mature bristles)	3.1
3.21	Stage P15 i (Meconium)	3.1
3.22	The appearance of the translucent testes (g) of larva/prepupa	3.1
3.23	The gas bubble (b) in an animal from Stage P4 i (Buoyant)	3.1
3.24	Gas bubble movements within the puparium, and head eversion, unequal time-lapse series	3.1
3.25	Diagrammatic interpretation of the morphogenetic events of stage P4 ii	3.1
3.26	State of the thoracic imaginal discs towards the end of pupal morphogenesis	3.1
3.27	Displayed visceral dissection of the pupa	3.1
3.28	Relationship between the Malphigian tubules (Mt) and the "yellow-body"	3.1
3.29	Mature relationship between the green Malphigian tubules (Mt) and the "yellow body"	3.1
3.30	Folding of the imaginal wing before eclosion	3.1
3.31	Comparison of the sexes after the darkening of the male specific sex comb	3.1
3.32	Thoracic appendages of early pupa	3.2
3.33	Tarsal morphogenesis in young pupa	3.2
3.34	Wing blade tip (unfolded) from pupa	3.2
3.35	Wing from young pharate adult (P8) folded inside pupal	

	cuticle	3.2
3.36	Progressive melanisation disto-proximally from middle of stage P8 wing	3.2
3.37	Thoracic Appendages, partly differentiated cuticle, P8	3.2
3.38	Stage variability within cultures timed from puparium-formation	3.3.2
3.39	Increasing asynchrony with time after pupariation	3.3.2
3.40	Testing predicted stage transition-times	3.3.2
3.41	Relative durations of stages at three temperatures	3.4.1
3.42	Dependance of stage durations (h) on temperature	3.4.1
3.43	Stage P4-Stage P5 50% transition-graphs	3.4.2
3.44	Susceptibility of P-stages to cold-shock	3.5.1
4.1	Composite standard curves of Horn I2 (16 wk) response to ecdysone (α) and 20-OH-ecdysone (β)	4.1
4.2	Stage-titre correlation	4.2
4.3	Mean ecdysteroid titres	4.3.1
4.4	Pooled male and female ecdysteroid(s) titre-measurements (untransformed)	4.3.1
4.5	RIA Variance (S^2) vs. assay sample-number (n)	4.3.2
4.6	Dependence of variance upon the mean and its source in the form of the standard response curve	4.3.2
4.7	Natural logarithm transformation of data for peaks and troughs apparent in Fig. 4.4	4.3.2
4.8-4.11	Log_e-transformed data as profiles of ecdysteroid titre during metamorphosis	4.3.2
(4.8	Female stages compared)	4.3.2
(4.9	Male stages compared)	4.3.2
(4.10	Female/male comparison within each stage)	4.3.2

(4.11	Pooled female and male data: stages compared)	4.3.2
4.12	An understanding of the direct RIA data	4.3.3
5.1	P1 (no mak. A)	5.1
5.2	Stages P1, P7, P10-13 (+ mak. A)	5.1
5.3	Chromatograms from HPLC-UV spectrophotometry	5.2
5.4	Multiple use of C_{18} cartridges: recovery efficiency	5.5
5.5	Ecdysteroid background correction curves	5.6.1
5.6	Independence of titre and variance, and of variance and sample-number	5.6.1
5.7 (a-g)	Histograms showing ecdysteroid concentrations in HPLC eluate fractions	5.6.1
5.8	Composites of eluate fraction sets I and II	5.6.1
5.9	Log-log plot of fractional concentration vs. percentage total titre	5.6.2
5.10	Superimposition of log-log plots	5.6.2
6.1	Mass fragmentography of ecdysteroids	6.1
6.2	GLC-Mass chromatograms of ecdysteroid-TMS ethers	6.1
7.1	Sarcophaga bullata: reported direct RIA ecdysteroid titres	7.1
7.2	Schematic pathway for ecdysone synthesis in larvae	7.4
7.3	Metabolic conversion of ecdysone	7.5
7.4	The Tenebrio Cuticle Cycle	7.7
7.5	Determinations of ecdysteroids and JH in Drosophila	7.7
7.6 (a)	Ecdysteroid and JH titres during the fifth (last) larval instar of the tobacco hornworm, M sexta	7.7
7.6 (b)	Ecdysteroid concentrations in developmental stages of the queen (o) and worker (o) of the honey bee	7.7
7.6 (c)	Simultaneous variations of JH, and 20-hydroxyecdysone during the last larval instar and the pupal instar of pieris	7.7

7.7	Ecdysteroid and JH titres in Manduca	7.8
7.8	JH and Drosophila cell lines secreting cuticle	7.8
A3.1	Pupal cuticle from stage P5 ii dorsal view	A3.1
A3.2	Pupal cuticle fragments - dissection scheme	A3.2
A3.3	Pupal cuticle, polypeptides separated by SDS - polyacrylamide gel electrophoresis	A3.3
A3.4	Molecular weight conversion curve	A3.3
A3.5	Comparison of polypeptide components of pupal cuticle	A3.3
A4.1	Recovery of ^{3}H-ecdysone from TLC by ethanol elution	A4.2
A4.2	Distribution of counts (^{3}H-ecdysone (α)) recovered from TLC	A4.2
A4.3	Recovery from TLC zones by successive 300 ul ethanol elutions	A4.2
A4.4	Independence of recovery by 0.9ml elution volume and load	A4.2
A4.5	Effect of silica-gel plate-area on proportional recovery of ^{3}H-ecdysone in serial elutions	A4.2
A4.6	Effect of loading density	A4.2
A4.7	Effect of loading density on recovery of ecdysteroids through the HPLC preparation protocol	A4.2
A4.8	Analysis of sources of HPLC-UV spec. peaks in the protocol adopted for Drosophila sample preparation (λ = 254nm)	A4.2

LIST OF TABLES

		Section
1.1	Reported durations of metamorphosis at three temperatures (h)	1.3
2.I	TLC Elution-Contaminants	2.11.3
2.II	Recovery of ecdysteroids through C_{18} cartridges:-	2.16.1
2.III	50% inhibition of ^{3}H-ecdysone binding to MAS	2.18
3.I	Sampling procedure	3.3.1
3.II	Frequencies of Stages L1-A2, expressed as percentage of Total P (i.e. P1-P15)	3.3.1
3.III	Stage frequencies cf. extremes of timed observations	3.3.1
3.IV	Stage transition times calculated from both frequencies and ages of stages L1-A2 at 25°C	3.3.1
3.V	Durations of period P1-P15 inclusive at 3 temperatures	3.4.2
3.VI	The genus Drosophila: A comparison of species based on the stages of D. melanogaster metamorphosis, L1-A3	3.6
3.VII	Staging criteria adopted by other authors for D. melanogaster	3.7
5.I	Samples analysed by HPLC-RIA	5.1
5.II	Ecdysteroid quantification by HPLC-UV spectrophotometry (λ - 254nm)	5.3
5.III	Makisterone A as internal standard in stage P1 extract	5.6.2
5.IVa)	HPLC/RIA measurements (P1/7/10-13)	5.6.2
b)	Contribution, Fraction sets I and II (%)	5.6.2
5.V	Endogenous ecdysteroid titres determined by HPLC-RIA in selected stages	5.6.2
6.I	GLC-MF analysis of ecdysteroids in stages P1, P7 and	

	P10-13	6.1
7.I	Summary of findings, P1, P7 and P10-13	7.3
7.II	Comparison of HPLC-RIA with GLC-MF	7.3.2
7.III	Proportional representation of ecdysteroids at three stages of metamorphosis	7.3.2
A2.I	Time elapsed between mid-points of stages	A2
A4.I	Recovery from (A + B) (% total loaded)	A4.2
A4.II	Steroid recovery through TLC determined by HPLC-UV spectrophotometry.	A4.2
A4.III	Summary: Ecdysteroid recovery estimates	A4.3
A6.I	Ecdysteroid bioassay trial	A6

Acknowledgements

I have been lucky enough to have the cooperation of many people during the preparation of this report. Professor J. D. O'Connor kindly provided the Horn I2 antiserum, and standard ecdysteroids including makisterone A were supplied by Drs. David Morgan and Ian D. Wilson. Dr. Huw Rees, Professor Heinz Rembold and Dr. Chris Redfern have all given me the benefit of their expertise in collaborative experiments and Dr. David Finnegan advised me during the course of the work. I should like to thank Jo Rennie and Graham Brown for their help with the photography, Margaret Daniels for technical assistance, and Marilyn Ritchie for typing the manuscript.

It has been my great privilege to do this work as a member of "The Bownes Group", often droning away in the background of its constant activity to the consternation of my supervisor and thus confounding her patient workers who, it might be noted in passing,

> ..."always avoid turning their backs on (their) queen. No sooner has she approached a group than they will invariably arrange themselves so as to face her...and walk backwards before her (as) a token of respect";
>
> (Maeterlinck, 1901).

But I exaggerate. We are not quite so formal; but such respect would be entirely appropriate here. Dr. Bownes has been a constant help and source of friendly encouragement to me, and I am also pleased to acknowledge her guidance in writing the report, although its faults are not hers.

My wife was an invaluable assistant in preparing the manuscript. I wish to thank my parents, and parents-in-law for their financial assistance. The project was supported by the Science and Engineering Research Council.

Abstract

Metamorphosis in the fruit-fly Drosophila melanogaster was characterised with respect to visible changes, and the relationship between stages of postembryonic development and time was established at three temperatures. The staging system so devised for the collection of animals at equivalent points in their development was employed to determine a profile of whole-body ecdysteroid titres throughout metamorphosis in each sex using a radioimmune assay. Males and females were found to be very similar in this respect, showing elevated titres shortly before the onset of deposition of pupal and adult cuticles (stages P1 and P7 respectively) and at melanisation of the latter in the pharate adult (stage P11). An anti-ecdysteroid antiserum was prepared and used in conjunction with high performance liquid chromatography to measure the free ecdysteroid titres and to identify the ecdysteroids present at these stages. At each stage ecdysone was found to be the more common compared to 20-OH-ecdysone, suggesting active secretion of the prohormone for imminent conversion to the active "moulting" hormone. The measured ecdysteroid titres at stages P1 and P10-13 were about 1.4 and 0.6 times that of stage P7, respectively. A parallel analysis by gas-liquid chromatography/mass fragmentography suggested the presence of 20,26-dihydroxyecdysone at stage P7. Gas chromatography/mass fragmentography was used to identify C16 juvenile hormone (JH-III) during metamorphosis; and this was found to be present both before and after head evagination (equivalent to pupal ecdysis in the Lepidoptera). The involvement of these hormones in the coordinate control of dipteran metamorphosis is discussed with particular reference to the cuticle cycle in comparison with what is known of the Lepidoptera.

CHAPTER 1

INTRODUCTION

1.1 Metamorphosis

The imaginal discs of *Drosophila* have been widely used in the study of animal development because they exhibit a wide difference between the time of cell determination and that of the expression of the determined state which results in the formation of the adult cuticle. The embryo is the site of the formation of the discs; the larval instars are the sites of cellular proliferation and the source of the discs for experimentation; and the adult bears the results of such experiments in the form of cuticle markers, either on its surface or on metamorphosed implants in the abdomen; so these phases of development are well-known. But the events of metamorphosis have generally received less attention, possibly because of the technical difficulties involved. In the cyclorrhaphous Diptera, including *Drosophila*, the last larval cuticle is tanned and retained throughout metamorphosis as a hard case inside which the developing imaginal hypoderm is at first extremely delicate. In addition, much of the larval structure disintegrates as the various organ systems are histolysed and reconstituted. Nevertheless, metamorphosis has attracted attention because during this period the realisation of the determined state is achieved in differentiation. This study represents an attempt to apply biochemical techniques towards the elucidation of one aspect of this process, namely the involvement of hormones, especially

steroids, in the control of insect metamorphosis.

1.2 The Approach

Methods for staging a continuous developmental process have been established for several systems: e.g. for the embryos of *Locusta* (Maltete, 1962), *Drosophila* (Bownes, 1975) and *Schistocerca* (Bentley *et al.* 1979); for *Tenebrio* larvae (Stellwaag-Kittler, 1954); and for the metamorphosis of *Xenopus* (Nieukoop and Faber, 1967), the lepidopteran insects *Manduca* and *Hyalophora* (Jungreis, 1979 Appendices), and of the hymenopteran *Apis* (Rembold *et al.*, 1980).

No such method has been described for *Drosophila* metamorphosis however; and in addition, most biochemical studies of postembryonic development in this genus take no account of differences between the sexes. Asynchrony in a developing population can be a serious problem but, at least with *Drosophila*, it is possible to collect symphasic animals, i.e. animals which *look* the same without necessarily being of the same age and developing at the same rate, (synchronic). This might be expected to reduce the error likely to result from asynchrony since changes in appearance must reflect the underlying biochemical status of an animal; and, quite apart from asynchrony, it is more convenient to collect material by appearance rather than over time when analysing a long period of development, (here about 4 days). Chapter 3 therefore presents a practical system for the staging of living "prepupae", "pupae" and "pharate adults" (Section 3.1 and

Appendix A1) based on twenty-four criteria including morphology, colour and behaviour. The durations of the stages of metamorphosis are estimated there, and in Chapter 4 a rough estimate is made of the ecdysteroid titres in separate crude preparations of males and females, based on this staging system and using a radioimmune assay (RIA). Subsequent chapters (4, 5 and 6) are concerned with the identification and measurement of hormones, especially ecdysteroids at three staged high-points in the RIA-profiles of ecdysteroids during metamorphosis.

1.3 Metamorphosis timed

Although staging has not been developed systematically for metamorphosis, several authors have noted some useful staging-criteria in the course of timing various aspects of metamorphosis, (see A2, and 3.7). Thus Mitchell and Mitchell (1964) employed positive buoyancy for mass-selection of living prepupae "synchronised" at about 5h after pupariation. Wehman (1969) gave a system for staging wing discs on ultrastructural features, but this is destructive. From fixed and sectioned animals timed from pupariation Robertson (1936) determined the sequence of changes which constitutes metamorphosis, and living prepupae were observed in order to establish the course of events leading to "pupation". Bodenstein (1950) reviewed these and other data and compiled a typical time-course for the various discs and organ systems from pupariation to eclosion in D. melanogaster at 25°C.

Much work has been carried out using timed batches of animals

to establish the rate of progression through metamorphosis, the effects upon this rate of temperature-changes, and the effect of a diurnal rhythm upon eclosion, (reviewed by Ashburner and Thompson, 1978). Bliss (1926) found that females eclose before males and reported a diurnal fluctuation in eclosion; (75% of flies emerged 1-9h after they seemed to have completed development). He also identified four "markers" which might be used to estimate the time reached by an individual in its metamorphosis, these being: pupariation; pupation (i.e. head eversion); the first appearance of eye colour; and the (coincident) appearances of head bristles and red-eye colour. But only the first of these was found to be reliable (synchronous) and his study was therefore restricted to the prepupal period defined by two sharp temporal markers. Using these, he observed the effect of exposure to a range of temperatures upon the duration of the prepupal period.

Ludwig and Cable (1933) used alternation between different temperatures to identify a developmental threshold during the period from pupariation to eclosion. This period was regarded as a single homogeneous stage - they gave "percentage development per day". Extremes of temperature retarded development and caused higher mortality in the "pupae", these effects being most pronounced early in metamorphosis. Later animals became less susceptible, not only to this treatment, but also to X-ray exposure (Mavor, 1927). So the "pupal" period was not to be seen as homogeneous - morphogenesis of the adult organs had already occurred and they now had only to undergo tissue-differentiation.

Powsner (1935) presented data in agreement with those of Ludwig and Cable (1933) in a study designed to test the applicability of the Van't Hoff and Arrhenius equations to development. (The idea of an underlying master chemical reaction was, not surprisingly it now seems, found to be inappropriate to metamorphosis). The effect of a diurnal rhythm upon eclosion was found to be inconsistent, sometimes resembling that described by Bliss (1926) but not reproducibly so. Eclosion times were established for a range of temperatures.

Kalmus (1940) reported a diurnal eclosion rhythm of 24h under natural lighting conditions at all temperatures. The rhythm was inherent and temperature-sensitive in the dark, but in cultures maintained in continuous darkness no such rhythm developed, although a light-pulse of 4h could reinstate the normal (24h) rhythm. Bakker and Nelissen (1963) observed that the time of pupariation in the day/light cycle was related to the time of eclosion, and also that the time of oviposition itself appeared to have some effect. Since no mention was made of staging criteria during metamorphosis it is not clear whether the whole period was adjusted to bring eclosion to the appropriate time in the cycle or, alternatively, whether animals pupariating late in the light-phase were blocked as pharate adults until they could eclose in the "morning"; The data of Harker (1965) show that various staged sub-periods of metamorphosis are similarly affected by photoperiod, but Pittendrigh and Skopik (1970) were unable to repeat these findings.

David and Clavel (1966, 1967) estimated the physiological optimum temperature for metamorphosis in <u>D. melanogaster</u> to be 19°-

-25°C (c. 21°C; although the pupariation-eclosion period was shortest at 29.5°C, at which temperature mortality was relatively high).

Reported timings of pupariation-head eversion and pupariation - eclosion at four temperatures are given at Table 1.I and their ratios to $t_{25°C}$ are calculated for comparison, (see also Section 3.4). In quantitative biochemical work over time the sexes must be considered separately and cultures must be maintained in the dark permanently if it is required that any possible coupling of metamorphic events to a photo-rhythm be avoided.

1.4 The Cuticles

The production and modification of cuticles is a major function of, and a major burden on, metabolism during metamorphosis, so it will now be described briefly.

The third instar larval cuticle is functionally analogous to the cocoon of lepidopterans in that it supports the developing organism, and its tanning and separation from the epidermis (larval/pupal apolysis) constitute the formation of the hard, brown puparium unique to the higher Diptera (cyclorrhapha). At pupariation the larval epidermis begins puparium formation and soon begins to secrete the transparent pupal cuticle which is featureless but quite tough - tough enough to offer protection. The larval cuticle, in being retained, then affords both a means of anchorage to the substrate and a scaffolding against which the movements

TABLE 1.I Reported durations of metamorphosis at three temperatures (h)

		18°C	25°C	29°C
(A) pupariation - head evertion (Bliss, 1926)	F	22.3	11.3	9.4
	M	22.8	11.8	9.8
(B) pupariation - eclosion (i) (Powsner, 1935)	F	195.3	94.3	76.2
	M	204.2	97.5	80.9
(ii) (Ludwig and Cable, 1933)	M	211.2	102	78

RATIOS:		$t_{18°}/t_{25°}$	$t_{29°}/t_{25°}$
(A)	F	1.97	0.83
	M	1.93	0.83
	(FM)	(1.95)	(0.83)
(B) (i)	F	2.07	0.81
	M	2.09	0.83
(ii)	M	2.07	0.76
	(FM)	(2.08)	(0.80)
A + B (n = 5)	(FM)	2.03	0.81

F = Female, M = Male, FM = sexes mixed.

involved in pupal morphogenesis, including gas displacement, might be effected (Section 3.1).

In some cyclorrhaphous systems diapause occurs at this stage, i.e. before pupal/adult apolysis is detectable histologically (Fraenkel and Bhaskaran, 1973) - in this respect the higher dipterans resemble the Lepidoptera.

Another apolysis then becomes detectable histologically, and the adult cuticle is secreted in its turn beneath the pupal. Note that in Sarcophaga bullata there is an exuvial phase after the pupal/adult apolysis (when the epidermis is bare of cuticle; see Fraenkel and Bhaskaran, 1973) before adult cuticle is deposited. This would provide an opportunity for bristle morphogenesis to occur, which, involving as it does a remoulding of the surface of the animal, must necessarily be free of close attachment to the pupal cuticle. However, such an exuvial phase has not been explicitly reported for Drosophila.

So a pharate adult Drosophila bears three cuticles, each of them having been constructed as shown in Fig. 1.1.

At each apolysis much of the hard exocuticle and the epicuticle is wasted, but components of the endocuticle are resorbed before apolysis, (a feature which may be especially significant in a closed nutritional system). The puparium, then, is only part of the true larval cuticle (exo- and epi-cuticles). The remains of the endocuticle persist in Drosophila as a thin membrane over the pupa

Figure 1.1

Schematic insect cuticle: changes during moulting/ moulting/metamorphosis (after Rees, (1977), Neville, (1978), and Weis-Fogh (1970)).

Chitin = linear polysaccharide of β (1,4)- linked N-acetyl-D-glucosamine; (degraded to N-acetyl-D-glucosamine by moulting-fluid).

Sclerotization (tanning) = hardening due to cross linkage of proteins by N-acetyldopamine (orthoquinone derived from tyrosine) at -NH and -SH groups; forming a network with chitin.

Melanin = polymer of indole- 5, 6- quinone; fills in the cross-linked chitin-sclerotin matrix; darkens and hardens the cuticle.

Procuticle also contains extracellular enzymes, water, lipids, sterols, diols, alcohols, fatty acids, esters, aliphatic aldehydes, phospholipids, branched hydrocarbons and shellac, ± uric acid and sugars.

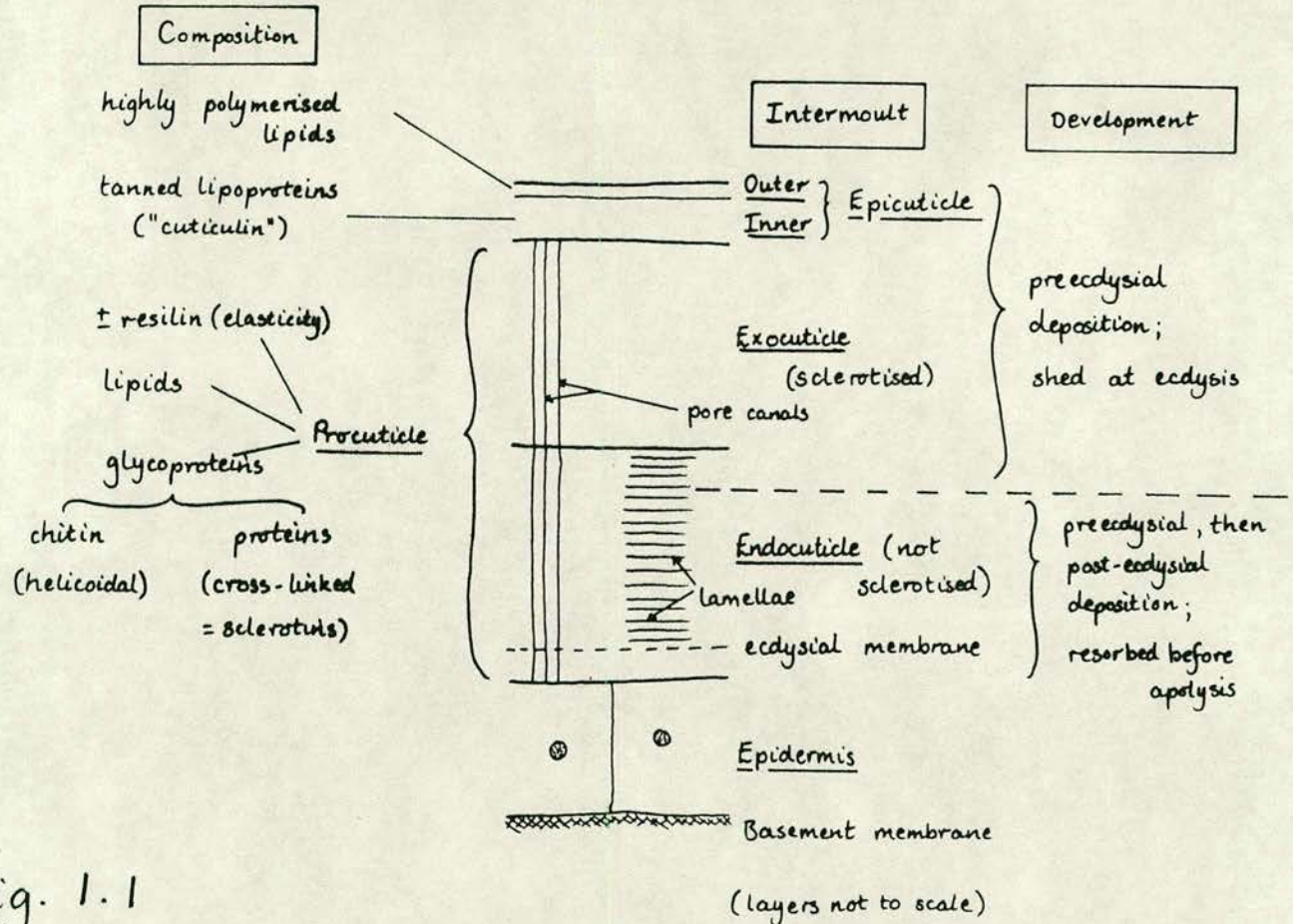
Composition
highly polymerised lipids
tanned lipoproteins ("cuticulin")
± resilin (elasticity)
lipids
glycoproteins
Procuticle
chitin (helicoidal)
proteins (cross-linked = sclerotins)
Intermoult
Development
Outer
Inner
Epicuticle
Exocuticle (sclerotised)
pore canals
Endocuticle (not sclerotised)
lamellae
ecdysial membrane
Epidermis
Basement membrane
preecdysial deposition; shed at ecdysis
preecdysial, then post-ecdysial deposition; resorbed before apolysis
(layers not to scale)

Fig. 1.1

(Poodry and Schneiderman, 1970). This has been mistaken for an "intra-puparial fourth larval instar cuticle", eg. by Robertson (1936), but it lacks both chitin and moulting fluid (Mitchel et al., 1971). Between moults the composition of a cuticle changes. Deposition of structural protein and chitin continues (see Appendix 3), and sclerotization and melanization alter the cuticle's structural properties. The production of sclerotin involves N-acetyldopamine derived from tyrosine (Fig. 1.2), the conversion of which is mediated in some respects by ecdysteroids; and pupariation/puparium formation in particular is mediated not only by ecdysone from the ring gland and its effector (PTTH=ecdysiotropin) but also by at least two other factors from the brain, and pupariation is a complicated transformation involving at least four distinct coordinated changes. (Fig 1.3, Sarcophaga. Note that in this study the criterion held to be diagnostic of pupariation is irreversible cessation of locomotion when the prepupa is wetted - see 3.1; A2).

In contrast to puparium formation, sclerotisation of adult cuticle in newly-eclosed Drosophila, which is mediated by N-acety-dopamine (and therefore by DOPA-decarboxylase), does not appear to be controlled by ecdysteroids (Kraminsky et al., 1980). A proteinaceous neurohormone, "bursicon", is thought to be responsible for controlling tanning of the adult exocuticle and post-moult deposition of endocuticle in Calliphora, (see Doane 1973; Wyatt, 1972).

Figure 1.2

Tyrosine metabolism at pupariation in Calliphora erythrocephala

(after Rees, 1977 and Neville, 1978).

*ecdysteroid(s) implicated.

Fig. 1.2

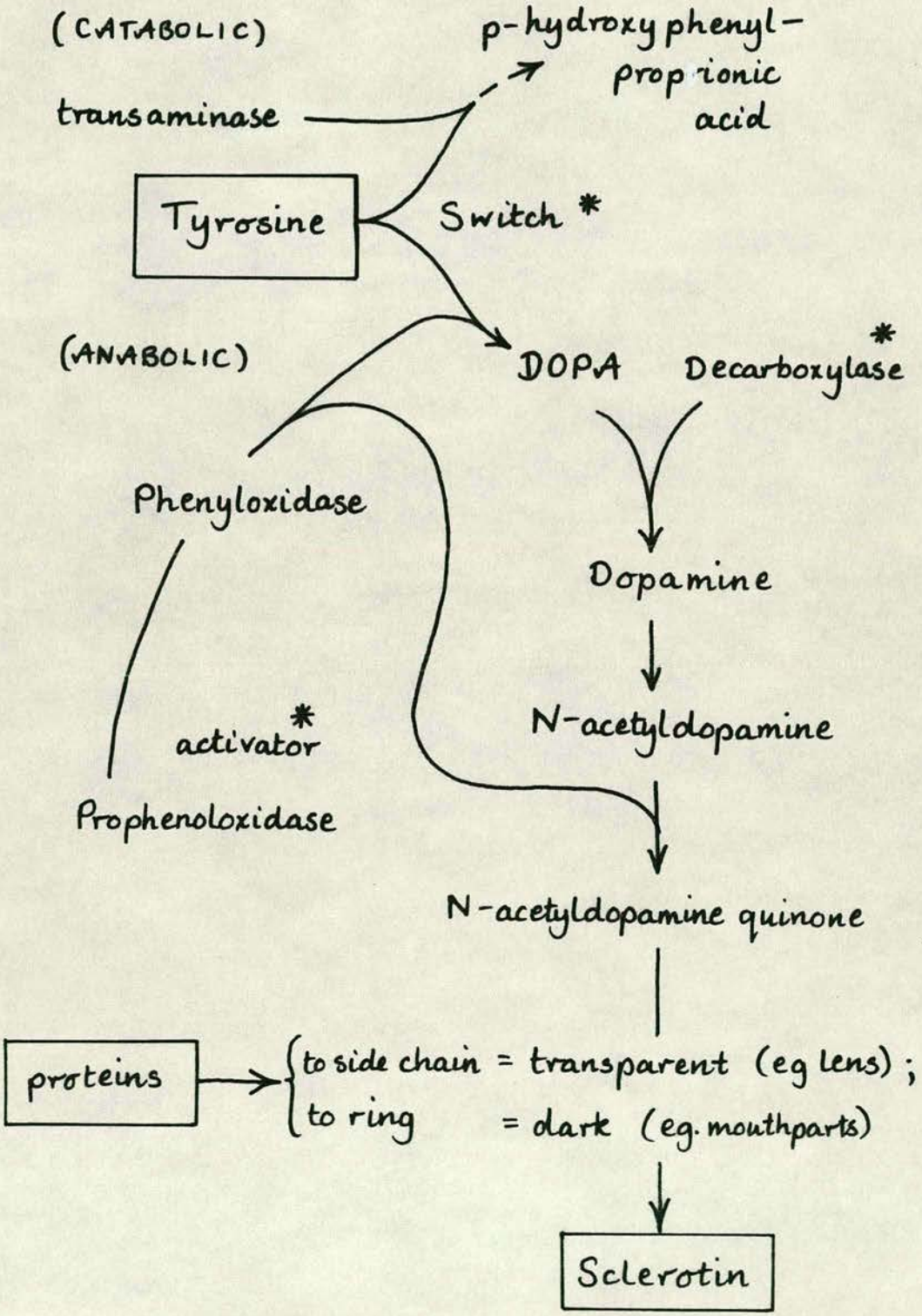
(CATABOLIC)
p-hydroxy phenyl-propionic acid
transaminase
Tyrosine
Switch *
(ANABOLIC)
DOPA
Decarboxylase *
Phenyloxidase
Dopamine
N-acetyldopamine
activator *
Prophenoloxidase
N-acetyldopamine quinone
proteins
to side chain = transparent (eg lens);
to ring = dark (eg. mouthparts)
Sclerotin

Figure 1.3

Pupariation and puparium formation in Sarcophaga bullata

(Modified after Sivasubramanian *et al.* (1974)). CNS, central nervous system; PTTH; prothoracicotropic hormone; ARF, anterior segments retraction factor; PTF, puparium tanning factor; (1) longitudinal contraction to barrel-shape; (2) cuticular shrinkage to smoothen the larval cuticle; (3) retraction of the anterior segments; (4) *Drosophila*: the animal no longer crawls away from water (see Chapter 3); (5) tanning of the larval cuticle. Note that the order of these events in *Drosophila* is: 3, 1, 2, 4, 5 (see Appendix 2).

Fig. 1.3

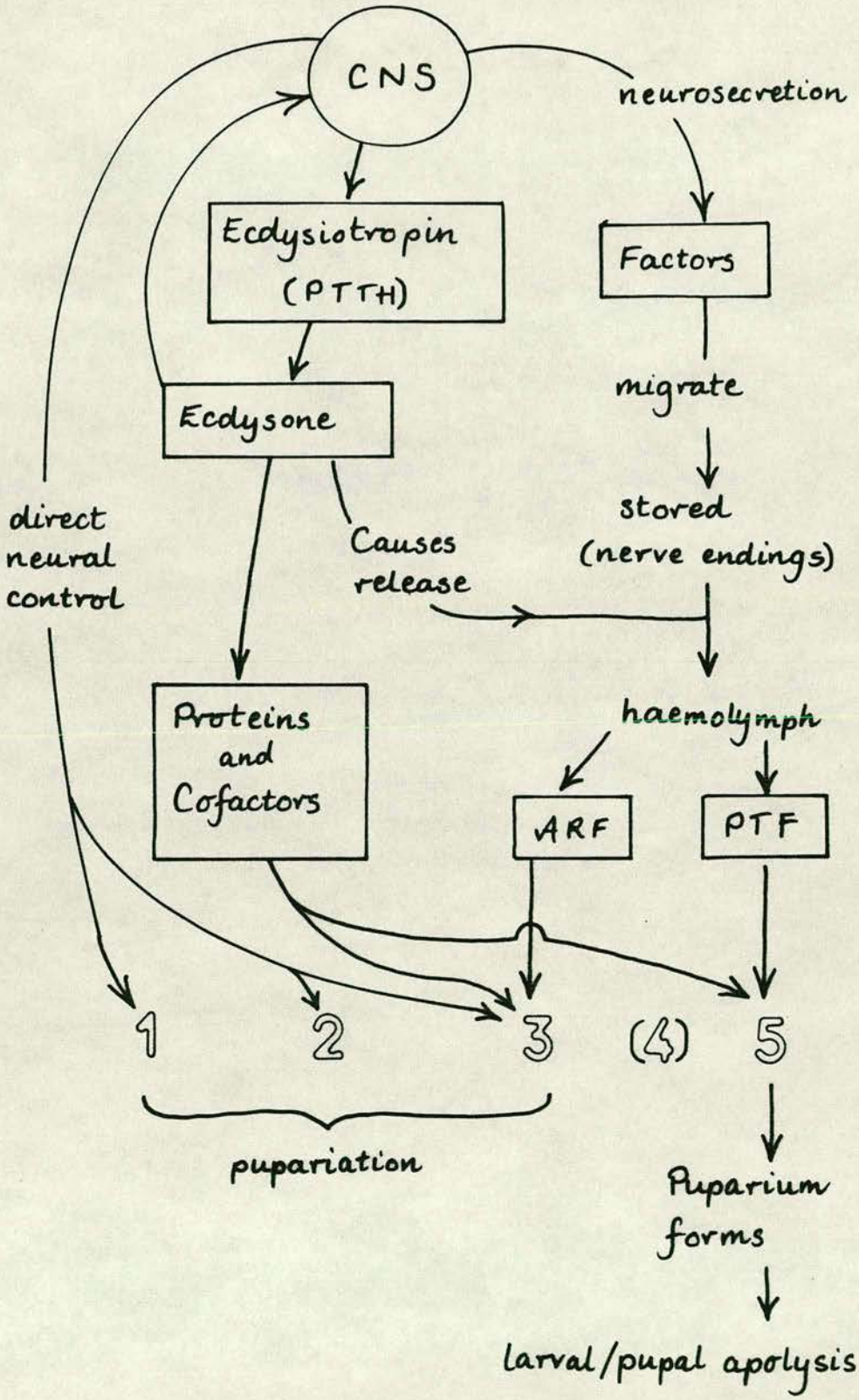
CNS
neurosecretion
Ecdysiotropin
(PTTH)
Factors
Ecdysone
migrate
stored
(nerve endings)
direct
neural
control
Causes
release
Proteins
and
Cofactors
haemolymph
ARF
PTF
1
2
3
(4)
5
pupariation
Puparium
forms
larval/pupal apolysis

1.5 The Hormones

Insect moulting and metamorphosis are under the joint control of ecdysterone and juvenile hormone (Riddiford, 1980). Ecdysterone is a member of the family of related steroid molecules called ecdysteroids, three of which are shown in Fig. 1.4 with their trivial names and the abbreviations employed in this report. They are metabolites of cholesterol which is consequently an obligate component of the diets of carnivorous insects and is derived from plant sterols by phytophagous insects (Rees 1977). "α-ecdysone" (= ecdysone) was the first to be isolated from Bombyx by Butenandt and Karlson (1953), while "β-ecdysone" ("ecdysterone", = 20-OH-ecdysone) was more active in the Calliphora bioassay (premature induction of pupariation). Measurements of ecdysteroid titres have been made by many workers interested in the hormonal regulation of developmental programs and patterns of cellular differentiation. Such measurements were made in vivo initially, using one insect or another as a bioassay system which, ostensibly, gave estimates of the whole-body content of biologically active ecdysteroids (bioassay units; Karlson and Shaaya, 1964) at various times during postembryonic development; e.g. in the dipterans Calliphora (Shaaya and Sekeris, 1965) and Sarcophaga (Ohtaki and Takahashi, 1972) and in the lepidopteran Bombyx (Shaaya and Karlson, 1965; Hanaoka and Ohnishi, 1974). However, with the development of a radioimmune assay (RIA) for ecdysteroids it has become possible to estimate very small quantities of extractable ecdysteroids in absolute units (pg) without the risk of metabolic interference which is implicit in bioassay systems employing whole organisms.

Figure 1.4

Ecdysteroid structures and cholesterol

(after Roberts and Caserio, 1964)

a) Ecdysteroids

Ecdysone ("Alpha-ecdysone") Pentahydroxycholest-7-en-6-one α = $C_{27}H_{44}O_6$ (=464)

20-Hydroxy-ecdysone (Crustecdysone", "ecdysterone". "β-ecdysone") Hexahydroxycholest-7-en-6-one β = $C_{27}H_{44}O_7$ (= 480)

24-Methyl-20-Hydroxy-ecdysone ("Makisterone A") μ = $C_{28}H_{44}O_7$ (= 494)

These compounds will be symbolised in subsequent figures as α, β, and μ respectively.

b) 3-epi-configuration (e.g. 3-epi-ecdysone; cf. Chapter 7).

c) Cholesterol, $C_{27}H_{46}O$ (= 386).

Fig. 1.4 Ecdysteroids

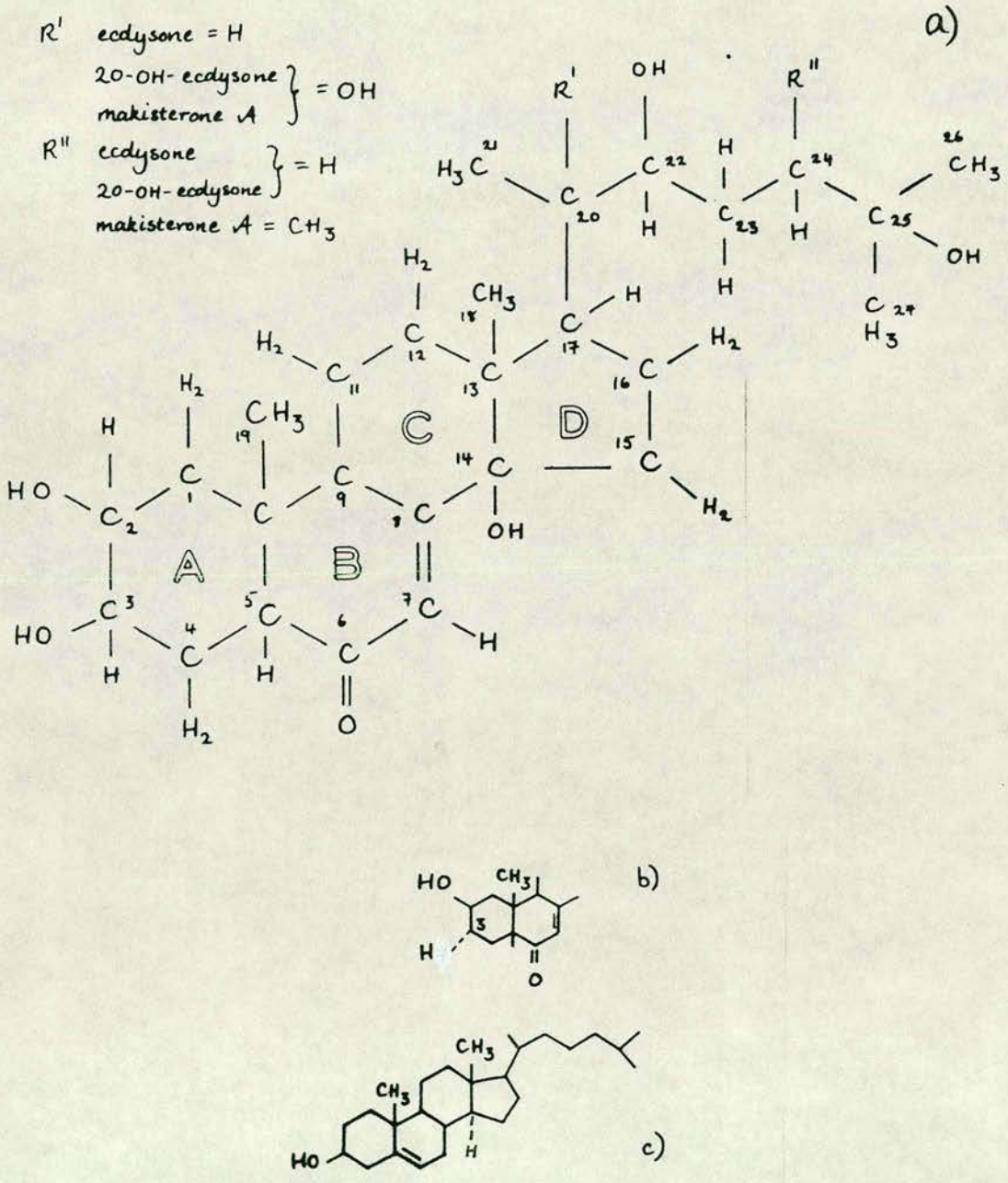

In chapter 4 RIA has been used to ask if there are any peaks of hormone obviously associated, firstly, with sex-specific gene functions, (e.g. spermiogenesis or primary induction of vitellogenesis in the female fat body), and secondly, with stage-specific functions, (e.g. cuticle development).

Juvenile hormones (JHs) are often considered to be absent from Drosophila during metamorphosis (e.g. Srdic et al., 1979) but it is quite likely that they are involved here if Drosophila resembles other systems. In Manduca, high juvenile hormone titres at the time of the pupariation ecdysteroid peak are thought to prevent precocious differentiation of adult structures (see Riddiford, 1980). In many hemimetabolous insects egg development appears to be controlled by juvenile hormone alone (Hanoaka and Hagedorn, 1980). Isolated adult Drosophila abdomens show reduced yolk synthesis which is restored by juvenile hormone application (Jowett and Postlethwait, 1980). Pre-vitellogenic adult ovaries will mature in metamorphosing female Drosophila abdomens (Bodenstein, 1947) as a result of ovarian yolk protein synthesis (Srdic et al., 1979), and, since such ovarian synthesis may require the presence of juvenile hormone (Jowett and Postlethwait, 1980), its presence is quite likely, at least sometimes, after pupariation. For these reasons a preliminary analysis of the juvenile hormone(s) present in Drosophila during metamorphosis has been performed in collaboration with Dr. H. Rembold (Martinsried, W. Germany), (Section 6.2). The family of JHs so far identified in insects is presented in Figure 1.5.

Figure 1.5

Juvenile Hormones (JH)

(After Rembold et al. 1980; Gilbert and Goodman, 1981; Richards, 1981b).

Aliphatic sesquiterpene hydrocarbons:

(n x (C_5H_8, 2-methyl-1, 3-butadiene)).

JH-0 $C_{19}H_{32}O_3$

JH-I $C_{18}H_{30}O_3$

JH-II $C_{17}H_{28}O_3$

JH-III $C_{16}H_{26}O_3$

cis- 10, 11-epoxy-3, 7, 11 - trimethyl-
trans, trans- 2, 6 - tridecadienoic
acid methyl ester.

or

methyl (2E, E)-(10R) - 10, 11- epoxy-
3, 7, 11-trimethyl-2, 6 - dodecadienoate

Fig. 1.5 Juvenile Hormones

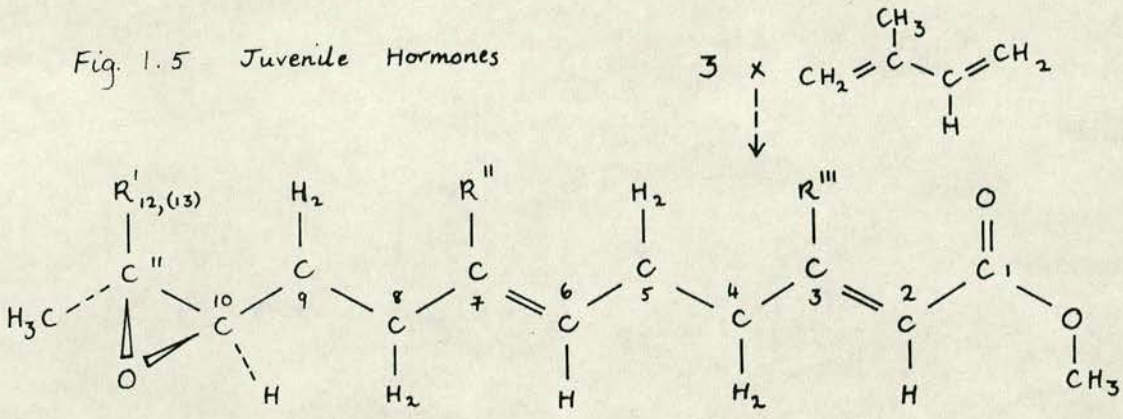

JH-0 $R' = R'' = R''' = C_2H_5$

JH-I $R' = R'' = C_2H_5$ $R''' = CH_3$

JH-II $R' = C_2H_5$ $R'' = R''' = CH_3$

JH-III $R' = R'' = R''' = CH_3$

To return to ecdysteroids; radioimmune assay (RIA), when used alone, is unable to distinguish between cross-reacting ecdysteroids, including 20-OH-ecdysone; nor can it necessarily recognise free hormone as opposed to its bound and conjugated states. Nevertheless, RIA has been employed for titre determinations in several metamorphosing insects including Drosophila (Review by Richards, 1981), Sarcophaga (Briers and de Loof, 1980, Wentworth, et al., 1981), the lepidopteran Galleria (Maroy and Tarnoy, 1978) and the coleopteran Tenebrio (Delbecque et al., 1978). The studies of Drosophila which extend beyond larval life are not in full agreement where they overlap (See Fig. 1.6). One extensive study, however, that of Kraminsky et al. (1980) based on timed animals of mixed sex reveals a profile in agreement with the general picture which has emerged from bioassay and RIA determination of ecdysteroid titres in other dipterans and in insects of other orders (e.g. Bombyx: Hanoaka and Ohnishi, (1974); Calliphora; Shaaya and Karlson, (1964) and Shaaya and Sekeris (1965)):- There is a sharp peak at pupariation or its equivalent (Richard's peak 9) followed by an extended elevation in titre in the pupa/pharate adult (Richard's peak 11).

This pattern fits well with the classical understanding of the respective roles of "ecdysone" (i.e. unspecified ecdysteroid(s)) and JH in controlling insect metamorphosis (see Fig. 1.7) since each peak closely precedes or is roughly coincident with the production of a new cuticle, (pupal at pupariation; adult at pupa/pharate adult). But, in looking for evidence of control of functions other

Figure 1.6

Composite profile of reported ecdysteroid titres (radioimmune assay, D. melanogaster; updated from Richards (1981), Figs. 1 and 2a).

Data normalised on peak 9 (pupariation). Ordinate: relative ecdysteroid titre expressed in terms of equivalence to 20-OH-ecdysone in the RIA (approx. ng 20-OH-ecdysone equivalents per mg fresh weight). Abscissae: stadium (based effectively on staging criteria) and time after oviposition, in days, normalised to 25°C. (E, embryo; L, larval instars; PP, prepupa; P, pupa; A, adult. No one study reports titre elevations at all eleven points:

Richards' peak numbers 1-11:

Reference	1	2	3	4	5	6	7	8	9	10	11
Borst, et al. (1974)									+		(+)
de Reggi, et al. (1975)								+	+		
Garen, et al. (1977)		+			+				+		
Berreur, et al. (1979)							+		+		+
*Kraminsky, et al. (1980)	+		+		+				+		+
Maroy, et al. (1980)				+		+			+		
Klose, et al. (1980)									+	+	+
**Handler (1982)									+	+	+

*This study re-presents the data of Hodgetts et al. (1977) and extends the titre- profile back to embryonic development.

**Arrows show apparent fluctuations in peak 11, (confidence limits not stated). (See also Figs. 4.4 and 4.12).

Fig. 1.6

Ecdysteroid (s) titre - profile

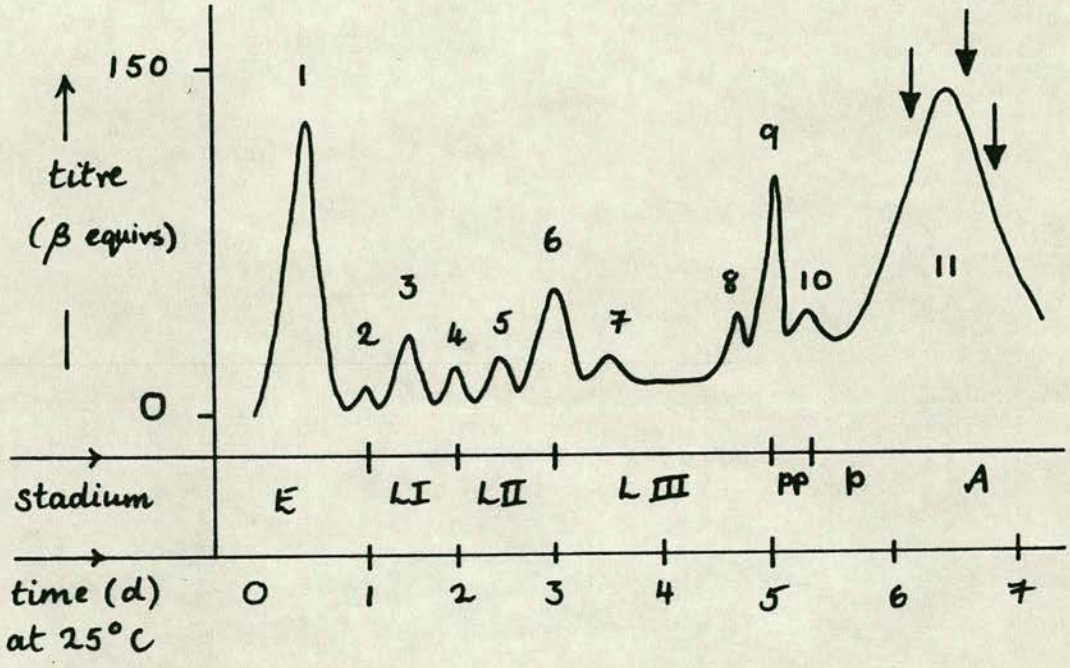

Figure 1.7

Classical Scheme for the control of moulting in the Holometabola

(modified from Rembold *et al.* 1980)

Moulting to another larval stadium (L), the pupa (P) or the adult (A) is governed by coordinated control of the exposure of tissues (including imaginal discs) to "moulting hormone" (MH = ecdysteroid, ecdysone) ± "juvenile hormone" (JH). AH, Allatotropic Hormone; PTTH, Prothoracicotropic Hormone (Ecdysiotropin); CC, Corpus cardiacum; CA, Corpus allatum; PTG, Prothoracic gland. (Note that, in *Drosophila* and other cyclorrhapha, cells with the functions of CC (ventral) CA (dorsal) and PTG (lateral) are associated in the Ring gland (RG) (Bodenstein, 1950; Redfern, 1984) which encircles the dorsal aorta). On this basis JH titres would be expected to decline at metamorphosis to prevent continued juvenilisation, but "JH" is thought to have other functions in controlling development apart from determining the nature of a moult (especially reproductive development), and it may increase in titre during or after metamorphosis (see text).

Fig. 1.7

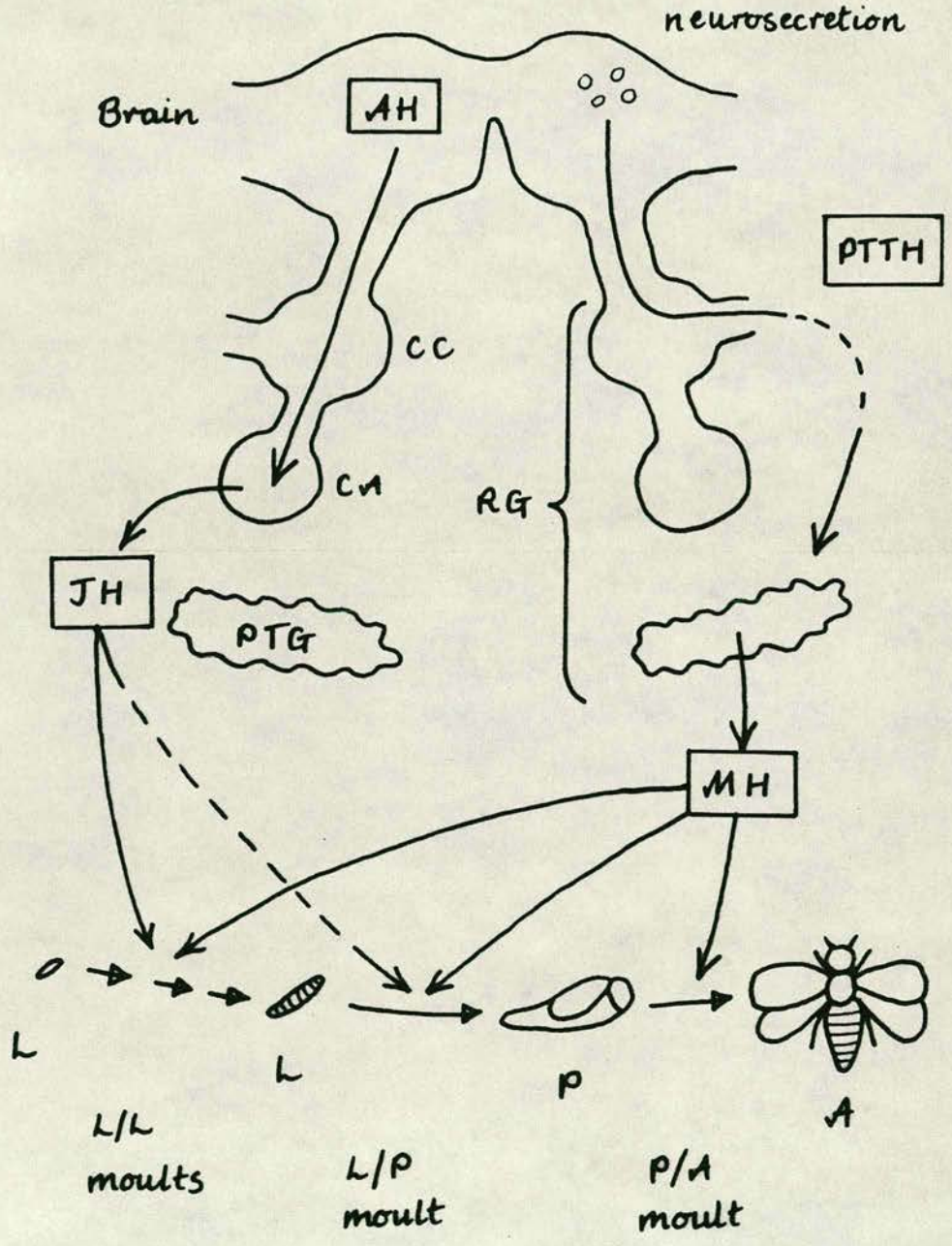
neurosecretion
Brain
AH
PTTH
CC
CA
RG
JH
PTG
MH
L
L
P
A
L/L
moults
L/P
moult
P/A
moult

than these, the existing profiles are beset by two problems: they take no account of increasing asynchrony in a timed population and, (with the exception of Handler, 1982) they are based on samples of mixed sex. An additional problem, that of tissue-specificity, is not eliminated in this study; but males and females of all stages during metamorphosis have been examined here by ecdysteroid RIA, firstly to look for differences between the sexes. Bombyx mori, for instance, has been shown by means of a Sarcophaga bioassay (cf. Appendix 6) to exhibit one titre-peak two days after pupal ecdysis (equivalent to P5+) in the male but two peaks in the female (Hanoaka and Ohnishi, 1974), the second peak being followed by rapid growth of the ovary. (Milner et al. (1982) also report a second peak in Spodoptera, associated with the ovaries; but note that in Drosophila the most significant increase in size of the ovary occurs after eclosion as a result of vitellogenesis.) The second reason for performing these assays was to identify high points in the titre profiles held in common between the sexes - crude whole-body, mixed-sex extracts from such stages would be worthy of more sophisticated chromatographic analysis. The profile of ecdysteroid titre will be compared with that found in mixed-sex, whole-body extracts of Sarcophaga bullata (Wentworth et al., 1981) which shows three major elevations in titre during metamorphosis, in contrast to the two generally recognised in Drosophila (Richard's peaks 9 and 11), (see Chapter 7).

1.6 Direct radioimmune assay (RIA): A preliminary investigation of ecdysteroid titre

RIA is based on the principle of competitive binding *in vitro* to polyclonal antibodies produced by stimulation of a mammalian immune system *in vivo*. A mouse anti-ecdysterone antiserum (MAS) was prepared for part of this study (Sections 2.18 and 5.6); but another antiserum (Horn I2 rabbit anti-ecdysone) was used for the initial determinations of male and female titre-profiles. An uncoupled ecdysteroid is too small to provoke an immune response and is made antigenic by coupling as a hapten to a protein capable of challenging the immune system, (e.g. ecdysone-22-hemisuccinate - thyroglobulin, Horn I2; 20-OH-ecdysone-carboxymethoxime - bovine serum albumin, MAS). Antiserum is raised against this antigen and is sometimes found to be enriched for binding sites specific to the hapten. Although some antisera are extensively characterised against the available pure analogues of their "preferred", original antigens, few show anything approaching absolute specificity; and this, coupled with their variable affinities for the range of analogues of biological significance, suggests that misleading measurements could be obtained unless samples be first characterised chemically (e.g. by TLC or, preferably, HPLC) and then their components investigated quantitatively by RIA.

In using an anti-ecdysteroid antiserum to measure hormone titres, tissue samples are weighed and their ecdysteroids extracted and allowed to compete with a labelled analogue for binding sites on

the mixed population of antibodies present in the antiserum. During this incubation period ^{3}H-ecdysone binds to the available sites to a greater or lesser extent according to the amounts and natures of the native species also present. The "antigen"-antibody complexes are then precipitated and resuspended in a scintillant for liquid scintillation counting (LSC). The extent to which counts are bound reflects the presence of native ecdysteroids according to a standard response curve prepared from known quantities of a pure analogue (e.g. ecdysone); so counts-per-minute bound are translatable into "equivalents" (pg) of a given ecdysteroid per weight of tissue. This method was applied to the stages of Drosophila metamorphosis in each sex, and points in their development when ecdysteroid(s) are relatively abundant were identified.

1.7 Analytical methods

Having identified which stages might most usefully be characterised with respect to ecdysteroids, samples were collected in quantities large enough to subject them to High Performance Liquid Chromatography (HPLC). Ecdysteroids absorbs UV-light maximally at 240-245nm (characteristic of the unsaturated ketone 7-en-6-one; see Fig. 1.4) (Morgan and Wilson, 1980); so insect extracts prepared using a protocol which includes delipidation and group-separation (Lafont et al., 1980) may be resolvable in terms of their ecdysteroid components using HPLC-UV absorption spectrophotometry alone (254nm); but this is rarely used (cf. Hori, 1969 for crude crustacean extracts; and Holman and Meola, 1978 for

purified Heliothis zea pupal extracts) because many other compounds also absorb strongly at 254nm. In this study, therefore, HPLC was used primarily as a preparative step (effecting group-separation) before measurements were made by RIA (5.4-5.5). However, HPLC-UV quantification is reported in Chapter 5 for comparison, (5.3; Table 5.1).

For more accurate quantification an anti-ecdysteroid antiserum was prepared (2.18) and used in the RIA performed on HPLC-eluate fractions as reported in Chapter 5 (5.6). HPLC-RIA has been adopted by several groups, in preference to TLC-RIA because HPLC offers improved recovery and resolution, and the method has yielded information both about the ecdysteroids secreted *in vitro* by cultured organs and also about the quantities of ecdysteroid(s) present in tissues and whole animals (see Lafont *et al.* 1981 for review). Handler (1982) supplemented direct RIA of Drosophila ecdysteroids with HPLC-RIA to measure the ratio ecdysone:20-OH-ecdysone at three points during metamorphosis. His results will be compared with those of Chapter 5 in the discussion (Chapter 7).

HPLC as used in this study is a type of liquid-solid affinity chromatography based on the distribution of solutes between the liquid mobile phase and sites on the solid stationary phase for which the solutes have different affinities. (This affinity chromatography is one species of absorption chromatography - the stationary phase has rigidly-fixed absorption sites; e.g. TLC, cf. liquid-liquid partition chromatography). Normal-phase LC involves a non-polar mobile phase traversing a polar material (e.g.

chloroform/alcohol across silanol groups), whereas Reverse-phase LC, as adopted here for HPLC and short-column LC, utilises a polar mobile phase with a non-polar (hydrocarbon) stationary phase coating the solid support (water/methanol across octadecylsilane, C_{18}).

An analysis of ecdysteroids in selected stages, performed in parallel with that by HPLC-RIA using Gas-Liquid Chromatography-coupled-Mass Fragmentography (GLC-MF), is reported in Chapter 6. This method has the advantage over HPLC-RIA of chemical specificity: Using GLC-MF, ecdysteroids are quantified but, more importantly, they are recognised on the basis of the mass- to-charge ratios of molecular fragments produced by electron bombardment and also on the basis of the steroid retention-times on GLC. The fragments so produced include those characteristic of ecdysone-type and 20-OH-ecdysone-type molecules, which allows a more positive identification of ecdysteroids to be made than is possible with HPLC alone. (Note that in HPLC-RIA the selection of a standard response curve for quantification depends upon an identification made on one criterion only by HPLC, namely retention time). GLC-MF is destructive because the hormones once extracted must first be derivatised to make them volatile and then, eventually, cleaved to yield charged fragments. Mass fragmentography (or Selected Ion Monitoring, SIM) is based upon a knowledge of the mass-spectra of a group of compounds, judiciously chosen ions being monitored as their parent molecules elute from a chromatography column. GLC-MF and GC-MF have been used to determine ecdysteroids in several insects, including Pieris, Tenebrio and Locusta (see review by Lafont et al. 1980), and in this study GLC-MF has confirmed the identities

of ecdysone and 20-OH-ecdysone suggested by HPLC and has provided independent estimates of titre in selected stages for comparison with the HPLC- RIA data. In addition, GC-MF has been used to identify a juvenile hormone found in Drosophila during metamorphosis (6.2).

1.8 Objectives

This report is concerned, then, with establishing a method of staging the metamorphosis of D. melanogaster and using it to refine the measurement of ecdysteroid titres in males and females examined separately, particularly in the pharate adult when asynchrony in populations timed from pupariation is likely to constitute an obstacle to accurate quantification of hormones. Stages which show an elevation in titre in both sexes will then be examined in more detail with regard to the chemical characterisation of the ecdysteroids which contribute to such titre-elevations; and the presence of juvenile hormone during metamorphosis will be reported in this species. These two classes of insect hormones will then be discussed in relation to some of the principle activities of the metamorphosing insect, particularly cuticle production.

Chapter Two

Materials and Development of Methods

2.1 Rearing Conditions

Drosophila melanogaster of Ore-R stock were maintained on yeasted Lewis's medium at 18°, 25° or 29°C in permanent darkness in Gallenkamp incubators (± 1°C) or were exposed to a 12:12h light-cycle at 25°C, as stated. The colour of the "yellow body" was found to be consistent when checked on Instant Drosophila Food (Carolina Biological Supply Co.).

2.2 Observation and timing of the sequence of changes during metamorphosis

White prepupae were picked from the sides of culture bottles at random times throughout the day/night cycle, sexed, and placed in sealed petri-dishes lined with moist filter paper (pupation plates). Collections continued for about 20 minutes, after which some individuals had become pale brown and were discarded (= too late). Any larvae still able to crawl were also discarded (= too early). The plates were stored in the dark and withdrawn for observation at various times throughout metamorphosis. Time zero was therefore pupariation +maximum 20 minutes. Observations were made at 30 minute intervals and the data were pooled. The flies remained fairly similar in appearance during prepupation, becoming less so as pupation proceeded. Two hundred and fifty six observations were

made of 44 plates, each of which contained about 25 flies. In a separate experiment, viability under these conditions was found to be 97% (100% = 975).

The typical sequence of visible changes was determined together with a range of times at which each event had been seen to occur in each sex. The animals were examined against a white background using a Wild dissecting microscope with lateral illumination close to the stage, interposing the tip of a pair of watchmaker's forceps between the lamp and the puparium to cast a shadow over features which are obscured by surface reflection but which show up with light scattered inside the animal (particularly the Malpighian tubules and the meconium). The animals were observed wet.

2.3 Durations of stages estimated by frequency in an artificial population approximating to a continuous age distribution:

Mature flies (5 females, 5 males) were placed in each of 4 fresh culture bottles and kept in constant darkness to encourage continuous egg-laying. On days 11-14 mixed populations of prepupae and pupae could be seen on the sides of the bottles. Adult flies were etherised, sexed, staged and counted. Prepupae and pupae were then removed, washed, staged and counted. Staging was performed on a random sample from the population of each bottle and lasted no more than one hour because development may continue during this time. Living animals were scored since freezing and fixation altered their colouration and other staging characters; and frequencies were based on populations of mixed sex because sexing

of the pupa and early pharate adult is not reliable, (the only criterion being the larger mean size of the females compared to males, which is a population effect).

2.4 Microscopy and photography employed for chapter 3

2.4.1 Dissecting Microscopy

Animals were collected, washed and staged as above, (b). The characteristics employed here as staging criteria may be observed through the puparium, but this was removed before photographs were taken (Fig. 2.1). Dissections and photography were performed using animals submerged in 1% agar in a tissue culture dish. A Wild dissecting microscope was used (X50 objective) with a Photoautomat MPS 55 and camera attachment, (Film: Ilford PanF).
Illumination was from above using Volpi Intralux Fibre Optics 150H against a dark field.

2.4.2 Nomarski phase interference microscopy

Specimen preparation for stages P5-P6

1. Puparium moistened with 70% ethanol/water;
2. Animals returned to water;
3. Puparium removed in insect Ringers solution;
4. Pupal cuticles split dorsally;
5. Vortexed vigorously (eviscerated);
6. Rinsed (3 x in water);
7. Mounted with 1% BSA (Sigma);

Figure 2.1

Removal of the puparium

This was done without puncturing the pupal cuticle or adult hypodermis/cuticle after completion of the larval-pupal apolysis (12h+; stage P5). Dissections were performed using watchmaker's forceps in 1% agar to prevent the animals from floating.

Directions: (1) grip the base of the posterior spiracles; (2) pull away the anterior spiracles and operculum; (3) insert the tip of the forceps over the wing hinge and gently pull off a ring of cuticle; repeat until the pupa/adult rests in a cup of cuticle; (4) grip the abdomen gently and ease it free of the posterior spiracles.

Fig. 2.1

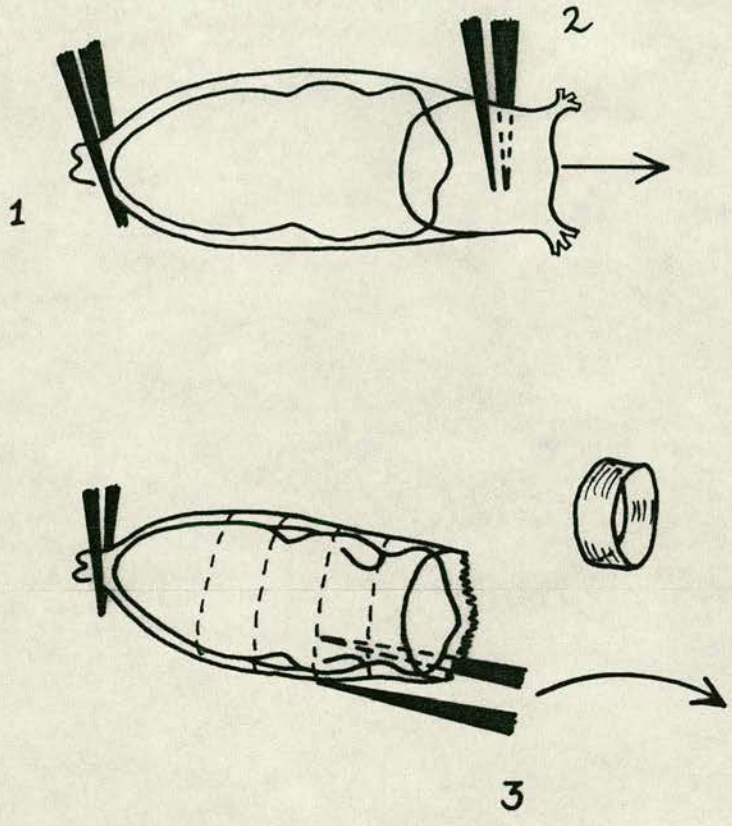

8. Dried;
9. Fixed (3:1 Acetic Acid/Ethanol);
10. Dehydrated (50, 70, 90, 100% Ethanol);
11. Cleared (Xylol, Xylene);
12. Mounted (Euparal).

Specimen preparation for stages P7 and P8 only

1. Puparium cut between anterior spiracles longitudinally with microknife;
2. Returned to water;
3. Puparium removed in insect Ringers solution;
4. Pupal and adult cuticles split dorsally;
5. Thorax dissected out;
6. Cuticles vortexed vigorously (eviscerated);
7. Hydrolysed (5 M HCl, 1 hour, hotplate);
8. Vortexed vigorously in water x 3;

   then as above, steps 7-12.

Microscopy:- Photographs were taken with a Zeiss Photomicroscope III equipped with Nomarski interference optics and using Ilford Pan F film.

2.5 Collection of staged material for radioimmune assay (RIA) and chromatography

(See Section 3.1 for definition of stages)

2.5.1 Small-scale collections of stages LIII-A3, sexes separated, (for direct RIA).

LIII Collected by sugar floatation - culture bottle walls were

scraped clean of animals; bottles were filled with saturated sucrose solution; the largest larvae were selected, but they were neither staged nor timed.

LI Wandering on bottle wall. The uncrowded culture-bottles selected had larvae either only close to the food ("early") or only close to the stopper ("late").

L2 Picked from bottles along with P1 (everted anterior spiracles, anterior segments retracted). When placed on wet filter paper they began to crawl - this included some apparent P1s (retraction of segments not irreversible when wetted).

PI Animals stuck to the glass were dislodged with a stiff brush from bottles containing wandering larvae. They were collected for 20 minutes, ("early" frozen within about 10 minutes of retraction of segments becoming irreversible); sexed on wet black filter paper; rinsed briefly in 70% ethanol (water rinse X 2) to remove glue and adhering food and the colour of the cuticle was checked on a white background (brown = P2).

LIII - PI Frozen immediately in liquid nitrogen.

P2-A1 Symphasic batches were collected from cultures set up as P1 plus maximum 20 minutes (= time 0) on damp filter paper in sealed petri-dishes (sexes separated), stored in the dark at 18°C, 25°C or 29°C as appropriate, (e.g. 18°C for P4 (ii)). Animals were examined wet in strong cold light directed from the side, frozen in liquid nitrogen (e.g. about 24 hours, P4(ii)) and accumulated at -60°C. (See Section 3.5.2).

A1-A3 Culture bottles were cleared of exarate adults, the food pellets were mascerated in about 5cm water (room temperature) and removed; bottles were rinsed (X2, water at room temperature) and tiss

paper was pressed into the bottles and dampened; flies were removed and lightly etherised at 1 hour intervals (A1+A2). Stage A3 was collected at 24 hour intervals, (i.e. "d1" = 0.5d ± 0.5d after eclosion). Flies were frozen (liquid nitrogen) and stored at -60°C.

LN1-A3 Stored for up to 12 months; briefly defrosted, dried (tissue paper), weighed (Mettler balance) and quickly refrozen before extraction of steroids.

2.5.2 Large-scale collections of stages P1, P7 and P10-13, mixed sex (for HPLC-RIA and GLC-MF)

P1:* White prepupae (stationary*, stuck to glass, anterior spiracles everted, colour as larvae) were picked from walls of culture bottles maintained at 18°C or 25°C in the dark or on 12:12h photocycle and plunged immediately into liquid nitrogen. Batches were then spread over a bed of dry ice and resorted for colour by eye. Any animals slightly brown in comparison to the norm were discarded. Stored at -60°C.
*NB. The criterion "irreversibly stop crawling (no locomotion when challenged with water)" was not applied here, (i.e. "P1" may be contaminated with L2).

P7 and P10-13 Food pellets in bottle-cultures (18° or 25°C, reared in the dark) were removed by maceration in c. 5cm depth of water (room temperature). The bottles were rinsed and animals stuck to the walls were scraped into a fine seive and washed in running water (room temperature) for 1 minute. Living batches were sorted (dissection microscope) for: yellow body +, eye colour - (=P7) and

red eyes +, tarsal bristles and claws dark - (=P10- 13). Animals were frozen in liquid nitrogen and stored at -60°C.

Animals were weighed fresh or briefly defrosted, dried with tissue paper, quickly weighed and counted on a bed of dry ice before being homogenized.

2.6 Extraction of ecdysteroids for direct RIA

Extractions were performed initially by pestle-homogenisation in cold 70% methanol, but the RIA titres were found to escalate when successive extractions were performed on the same tissue. With approximately 40mg tissue extracted twice in 3 x 100µl methanol (70%), 3000% more ecdysteroid(s) by weight (ecdysone equivalents per mg fresh weight) was sometimes obtained in a second extract compared with the first. Various homogenisation techniques were considered, as were the effects of time and/or volume on extraction efficiency. Cummulative titres from successive extractions performed on female white prepupae (stage P1) are shown in Figure 2.2. Pestle-homogenisation was compared with blending and sonication, and less tissue was used (c. 10mg). The resulting standardised extraction procedure (performed at 4°C; all plastics and glassware siliconised using "Repelcote" and autoclaved,) is as follows:-

1. Freeze-thaw 2-5 whole animals three times in microcap tubes;
2. To each tube add 600µl cold 70% methanol (Rathburns HPLC), plus phenylthiourea (Sigma) x 10^{-3}M and one perforated ceramic insulation bead;
3. Blending: vortex extraction tubes holding the tubes

Figure 2.2

Optimisation of the RIA extraction procedure for ecdysteroids

RIA was performed on successive extracts obtained from samples of five stage-P1 females (approx. 10mg fresh weight). Pestle-homogenisation (o), blending by vortexing with a pellet (x) and sonication (+) are compared. Abscissae: extracts were taken over a period of 1 h at intervals of 10 min or less, each in 300µl cold 70% methanol (+PTU, 10^{-3}M) per 10 min. Thus by the 10th minute, 300µl MeOH had been used. Ordinate: cumulative titres are expressed in pg ecdysone equivalents per mg fresh weight. $\bar{x}$, mean final cumulative titres. It seems that 600µl (20 min) is adequate for achieving the maximum extractable yield of cross-reactive ecdysteroids and that blending, although less efficient than pestle-homogenisation, gives a narrower spread of the results. It was decided, therefore, to use 700µl (including wash) of extraction medium; to extract from 2-5 animals over a period of 1 h (excess); and to combine blending and sonication in one protocol which may be completed in a single tube without transfers.

Fig 2.2

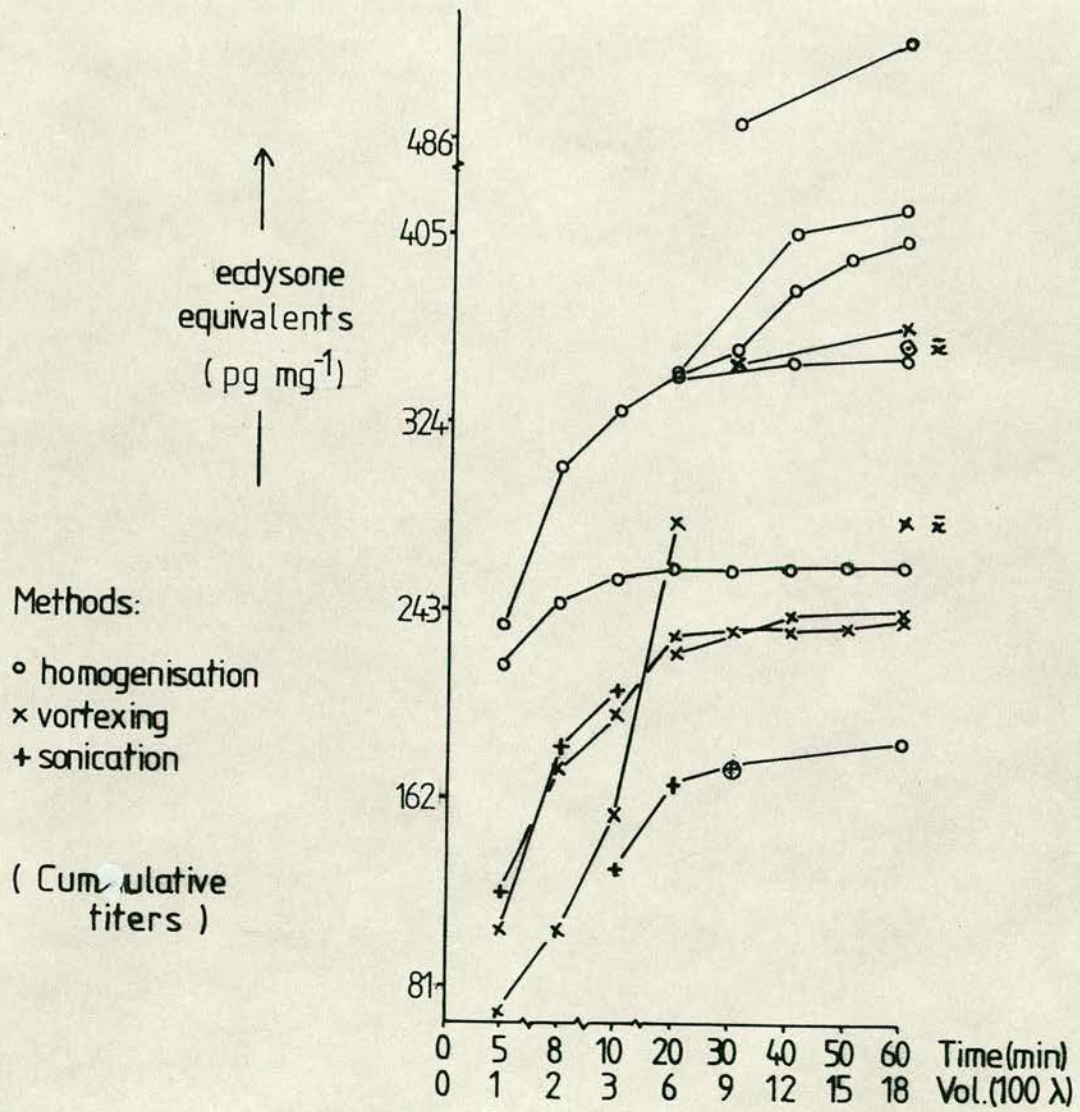
ecdysone
equivalents
(pg mg-1)
Methods:
° homogenisation
× vortexing
+ sonication
(Cumulative
titers)
486
405
324
243
162
81
0 5 8 10 20 30 40 50 60 Time(min)
0 1 2 3 6 9 12 15 18 Vol.(100 λ)

horizontally until the beads rattle, 20 sec;

4. Sonicate (Dawes Soniprobe converter) 10 sec;
5. Blend again, 20 sec.;
6. Remove beads with forceps, spin tubes at 12,000g in the cold for 3 minutes, transfer supernatants to assay tubes;
7. Wash pellets in 100µl methanol, spin 3 minutes, pool wash-supernatants with extracts and store at -60°C until assay.
8. Dry down under nitrogen (Organomation N-Evap 106) at about 35°C (c. 45 min).

Twenty samples took about 1 hour using this protocol (steps 1-8). After the preliminary assays had been done extracts were prepared from the numbers of animals appropriate to give values for % binding which lay on the linear part of the standard response curve.

2.7 Characterisation of the HornI2 antiserum

This antiserum, which was generated in response to a thyroglobulin-coupled ecdysone-22-hemisuccinate antigen (Horn *et al.*, 1976) was the generous gift of Dr. J. D. O'Connor, (serum code Horn I2 16 wk) and was used diluted to 0.44%.

A Scatchard analysis (Fig. 2.3) was performed using constant volume of antiserum with varying volumes of tritiated ecdysone (NEN) and a control series of incubations employing anti-*Drosophila* yolk protein antiserum (Bownes) to give values for non-specific binding of labelled ecdysone to Horn I2. Corrected bound controls were converted through disintegrations-per-second to mM labelled

Figure 2.3

Scatchard plot (cf. Scatchard, 1949) for 0.44% antiserum Horn 12 (16 wk) with ^{3}H-ecdysone (S.A. = 63.5 Ci/mmol).

Ordinate: ratio of bound (B) to free (F) antigen. Abscissa: bound antigen (B), nmol/l x 10^{-2}. Slope y/x = association constant, K_a = 1.2 x 10^{9} l/mol. Intercept on x (= binding sites) = 1.2 x 10^{9} nmol/l.

Figure 2.4

Typical standard response curves of antiserum Horn 12 (16 wk) for ecdysone (α) and 20-OH-ecdysone (β) competing with ^{3}H-ecdysone (63.5 Ci mmol^{-1}) in 0.44% solution

Counts (c.p.m.) are corrected to 10% efficiency of counting. "100% Bound" represents counts in the absence of unlabelled competitor. Standard amounts of pure ecdysone and 20-OH-ecdysone (pg) are plotted semi- logarithmically v. % Bound. This gives a linear portion of the curve in which unknowns are to be read. At 50% bound the 20-OH- ecdysone titre is 9.2 times higher than that of ecdysone.

Fig 2.3

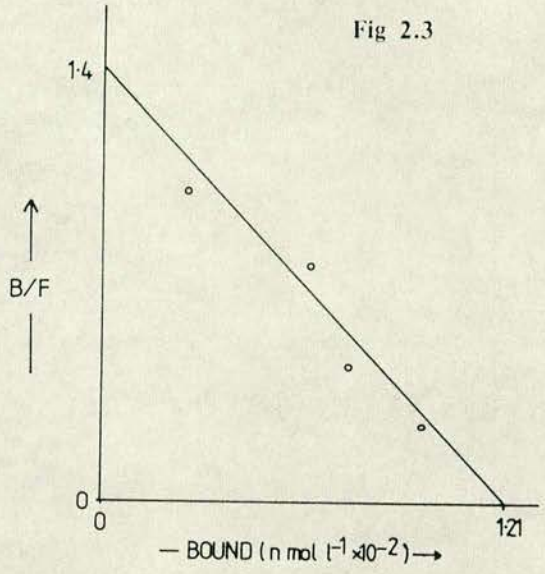
1·4
B/F
0
0
1·21
— BOUND (n mol l⁻¹ x10⁻²) →

Fig 2.4

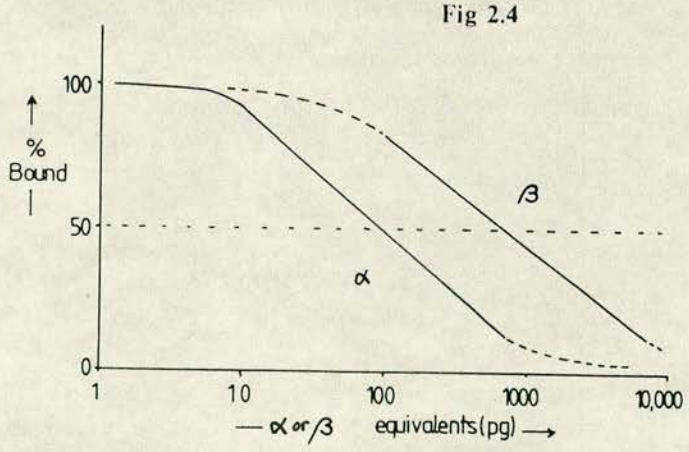
100
%
Bound
50
0
β
α
1
10
100
1000
10,000
— α or β equivalents (pg) →

ecdysone. Bound/Free vs. Bound has slope $y/x = K_a$, the Association Constant of the binding reaction (1 $mole^{-1}$):

$$\text{Ecdysone}^* + \text{Antibodies} \underset{K_d}{\overset{K_a}{\rightleftharpoons}} \text{Antibody-ecdysone complexes}$$

$$K_a = \frac{[\text{complexes}]}{[\text{antibodies}]\,[\text{ecdysone}]}$$

(units = 1/mol)

The Association constant K_a of this antiserum with ^3H-ecdysone is 1.2×10^9 1 mol^{-1}. An earlier bleed (14 wk) showed only a 1.5 x difference in the ecdysone/20-OH-ecdysone affinities (Redfern, 1981).

The standard response curves for ecdysone and 20-OH-ecdysone (Fig. 2.4), show that the affinity of ecdysone over 20-OH-ecdysone for the antiserum is between 9- and 10-fold greater at 50% binding. Results are expressed in terms of ecdysone equivalence (pg ecdysone equivalents mg^{-1}) fresh weight, but this is not to say that ecdysone is necessarily the ecdysteroid under scrutiny - clearly in the case of 20-OH-ecdysone it is not.

2.8 Monitoring of the assay system

During routine use of this antiserum for RIA it was found that the binding of counts dropped occasionally. This might be due either to degradation of the antiserum or to loss of specific

Figure 2.5

Monitoring RIA solutions:

Horn I2 16 wk antiserum with ^{3}H-ecdysone (NEN)

Assay-tubes were prepared at 4°C and 29°C containing varying ratios of antiserum to ^{3}H-ecdysone (by volume). Bound counts (as % available counts, 100µl = 100% = 8909 cpm) were plotted as ordinate against the volume- ratio antiserum: ^{3}H-ecdysone (abscissa). a) increasing antiserum compound; b) increasing ^{3}H-ecdysone component. A negative slope would indicate reduced specific activity of the ^{3}H-ecdysone (i.e. with storage at 4°C). The positive slope indicates a reduction in the avidity of the antibodies for ecdysone (e.g. with storage as aliquots in borate buffer at 4°C).

Fig. 2.5

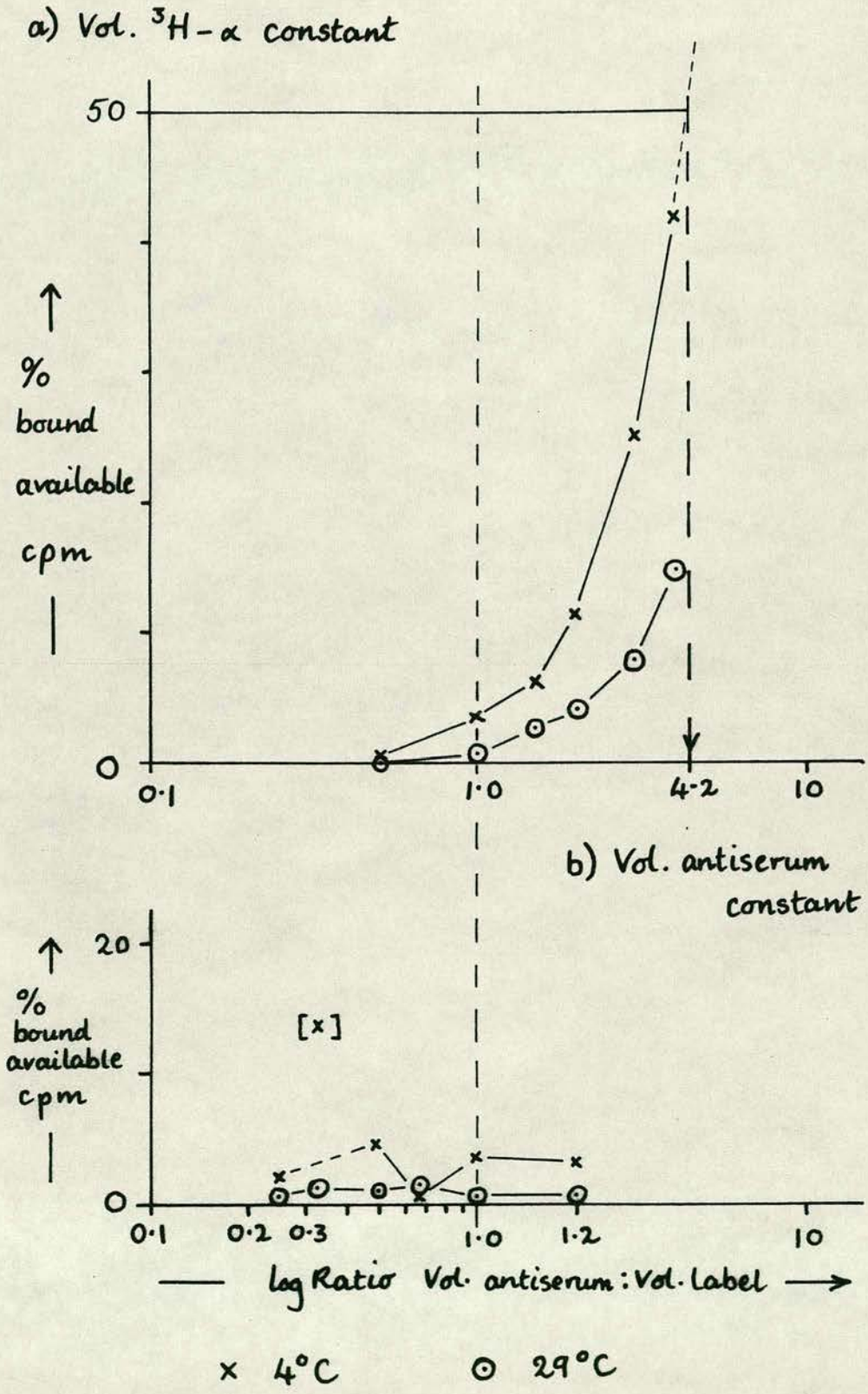
a) Vol. ^3H-α constant
50
0
% bound available cpm
0·1
1·0
4·2
10
b) Vol. antiserum constant
20
0
% bound available cpm
[x]
0·1
0·2
0·3
1·0
1·2
10
log Ratio Vol. antiserum : Vol. label
× 4°C
⊙ 29°C

activity of the tritiated ecdysone used as labelled competitor. Fig. 2.5 shows how the second explanation was rejected, all solutions employed in the assay having been prepared afresh.

2.9 Correction for variable scintillation quenching (Q)

Scintillation counting depends upon the property of the scintillant whereby the energy of radioactive decay is transduced into light energy by excitation of the scintillant. Quenching, Q of the photon emission may occur to differing extents in the various assay tubes, and was compensated for by Digital Count-rate Normalisation (DCN) using a quench calibration curve (ie. efficiency determination) prepared as follows.

A series of identical ^{3}H-standards was spiked with varying volumes of acetone as a quencher. The samples were counted, using an Intertechnique SL-3000 Liquid Scintillation Counter (LSC) coupled to a Texas Silent 743 KSP data terminal, in the presence of an external ^{137}Cs gamma-ray source, once using a wide energy window (E1) and then again using an overlapping but narrower window (E2). The ratio cpm_{E1}/cpm_{E2} is the external standard ratio, ESR. The samples were then counted a third time in the lower 3H-energy range (beta-emission) to give Q-uncorrected counts per minute (dpm) and plotted against ESR as shown in Fig. 2.6. This curve was used to bring all unknowns to a common LSC efficiency, (eg. 10%), and until a new curve was determined none of the following conditions were allowed to vary: scintillant, volume, vial-size, vial material, specific activity of ^{3}H-ecdysone, and instrument settings.

Figure 2.6

Quench Calibration Curve (Absolute counting efficiency)

Example used until April, 1981.

Ordinate: counting efficiency = cpm/dpm (see text)

Abscissa: External Standard Ratio, ESR (see text)

(Compare Fig. 2.21, relative counting efficiency).

Fig 2.6

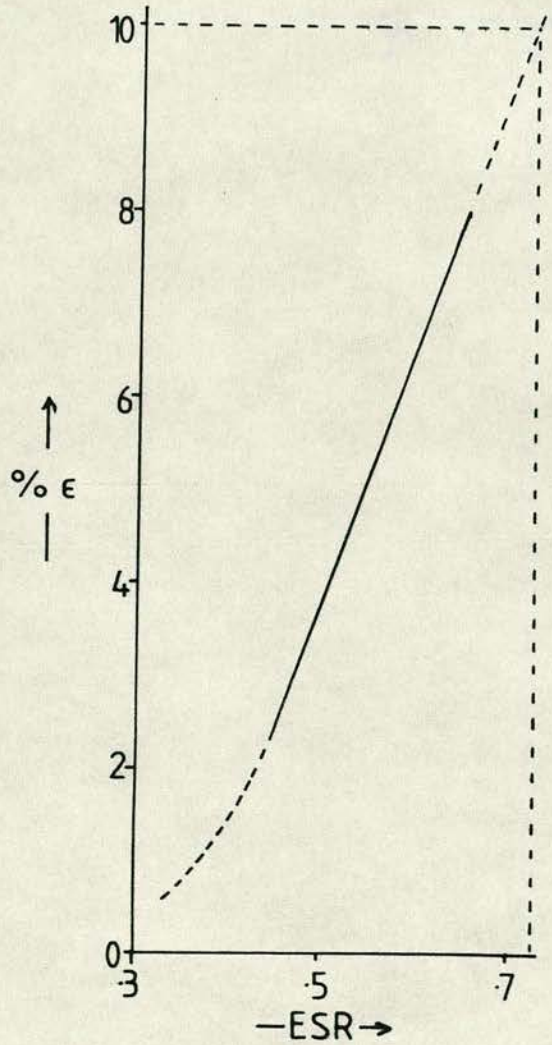

2.10 Protocol for direct RIA of ecdysteroids based on O'Connor, 1980 (personal communication).

Animals were weighed with a Mettler balance and ecdysteroids were extracted according to Section 2.6. The extracts were reduced to dryness under nitrogen (Organomation Ass. N-Evap 106) at about 35°C and taken up in 100µl tetraborate buffer (pH8.4) containing approximately 5000 cpm 23,24-^{3}H-ecdysone, 63.5 Ci/mmol (NEN). The mixture was vortexed and an equal volume (100µl) of antiserum, made up to 0.44% in tetraborate buffer (+1% B.S.A.), was added. Under these conditions about 2000 c.p.m. were bound in the absence of competing unlabelled antigen. After further mixing the resulting solutions were incubated at 4°C overnight. An equal volume of saturated Ammonium sulphate solution (in borate buffer) was added to separate bound from unbound antigen, and the precipitate was washed once with 50% saturated Ammonium sulphate solution. 20 min. micro-centrifugations were performed at 4°C. Bound ^{3}H-ecdysone was then dispersed in 125µl distilled water. Water-miscible scintillant (toluene/Triton x-100,/PPO,/POPOP) was added (1ml per tube) and the tubes were allowed to stand for one hour in the dark before scintillation counting began, (Intertechnique SL 3000, Program 21). Counting efficiency was between 6% and 9% and was corrected to 10% for all assay tubes. Standard curves were prepared for each run of the assay, based on duplicate values (c.p.m.) for 100% binding of label in the absence of a competitor;

Solutions: a) Extraction medium:

10^{-3}M Phenylthiourea (Sigma)

(= Phenylthiocarbamide) in 70% aqueous methanol. Stored at room temperature.

b) RIA Borate Buffer

6.184g Boric Acid (0.1m),

9.536g Borax (= Sodium tetraborate) (0.1M),

4.383g NaCl (0.075M).

These were dissolved in 1 litre distilled water aseptically and brought to pH 8.4. Stored at 4°C.

c) Horn I2 anti-ecdysone antiserum 16 week bleed.

A generous gift from Dr. J. D. O'Connor (Los Angeles). Received lyophilized. Taken up in distilled water and stored at 4°C in small aliquots to avoid repeated freeze- thawing. Diluted to 0.44% with 1% BSA in tetraborate buffer aseptically. (See Horn et al. (1976) for details of antiserum preparation).

d) Standard solutions of ecdysone and 20-OH-ecdysone

10^{-7} - 10^{-10} stock solutions in Analar Ethanol. Stored at -60°C.

e) Scintillant (Aqueous-miscible)

PPO/POPOP in Triton X/Toluene 1:2.

100ml Triton X-100,

(200ml Toluene),

1.2g PPO,

0.012g POPOP,

300ml.

Stored in brown bottle.

All glassware and plastics were siliconised using "Repelcote" and autoclaved.

2.11.1 Thin-layer chromatography (TLC): Loading density vs. R_F

A silica-gel TLC plastic plate (Eastman Chromagram Sheet 13181 400 cm^2 with UV-fluorescent indicator No. 16060) was washed three times in AR Methanol (BDH); loaded with 2, 4, 6, 8, 10, 12, 14 or 16 drops 20-OH-ecdysone at 10^{-5}M from a 25µl capillary tube; developed for 60 minutes with 3:1 Methanol/Chloroform (Rathburns); and visualised under UV-illumination (Ultra-Violet Products Inc.). The markers showed similar R_F values (0.776 ± 0.022; $p = 0.05$) over an 8-fold loading-density range, suggesting that R_F-markers are a reliable guide to the position of unknowns despite the variation in loading-density.

2.11.2 TLC : Development-time vs. R_F

As 2.11.1, using constant load, and development time being multiples of 15 minutes. See Fig. 2.7. (Increasing the development time makes progressively less difference to the separation of an ecdysteroid from the origin).

2.11.3 TLC : Elution-contaminants

Two silica-gel TLC plates were washed in AR ethanol, dried and

Figure 2.7

TLC: R_F vs. $\log_{10}$ chromatogram development time (min)

for 20-OH-ecdysone (β) on a silica-gel plate developed with 3:1 methanol/chloroform.

Figure 2.8

TLC elution contaminants

Unloaded TLC plates developed in methanolic and ethanolic solvent systems, A and B, respectively. Ecdysone and 20-OH-ecdysone R_F-markers would run in zones 2.

Fig. 2.7

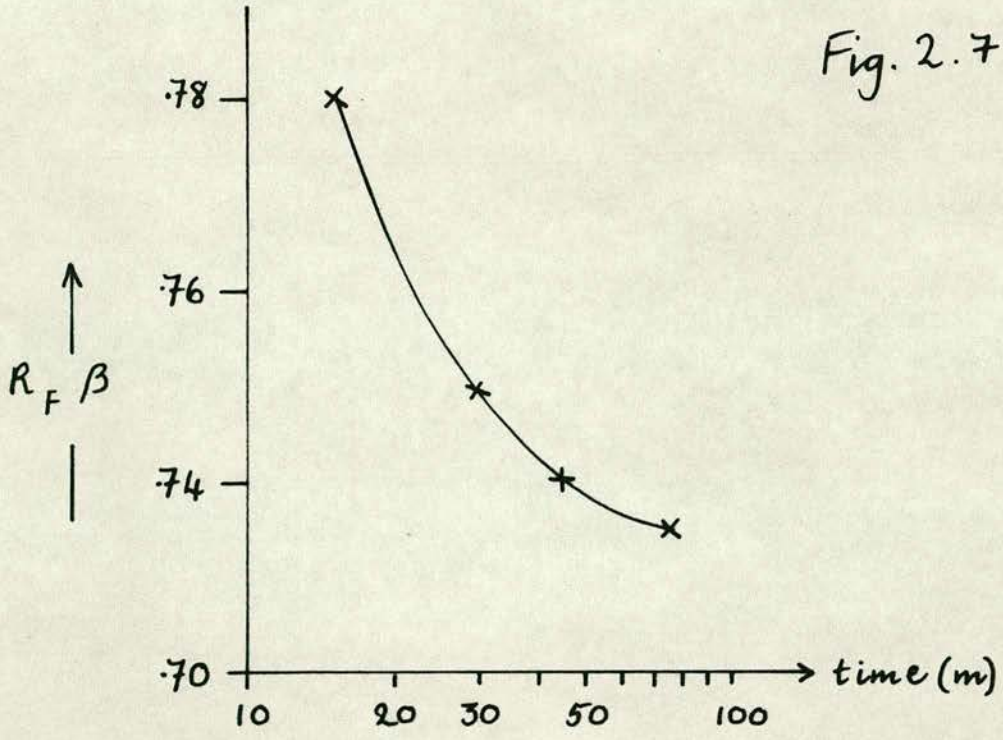
·78
·76
·74
·70
R_F β
10
20
30
50
100
time (m)

Fig 2·8

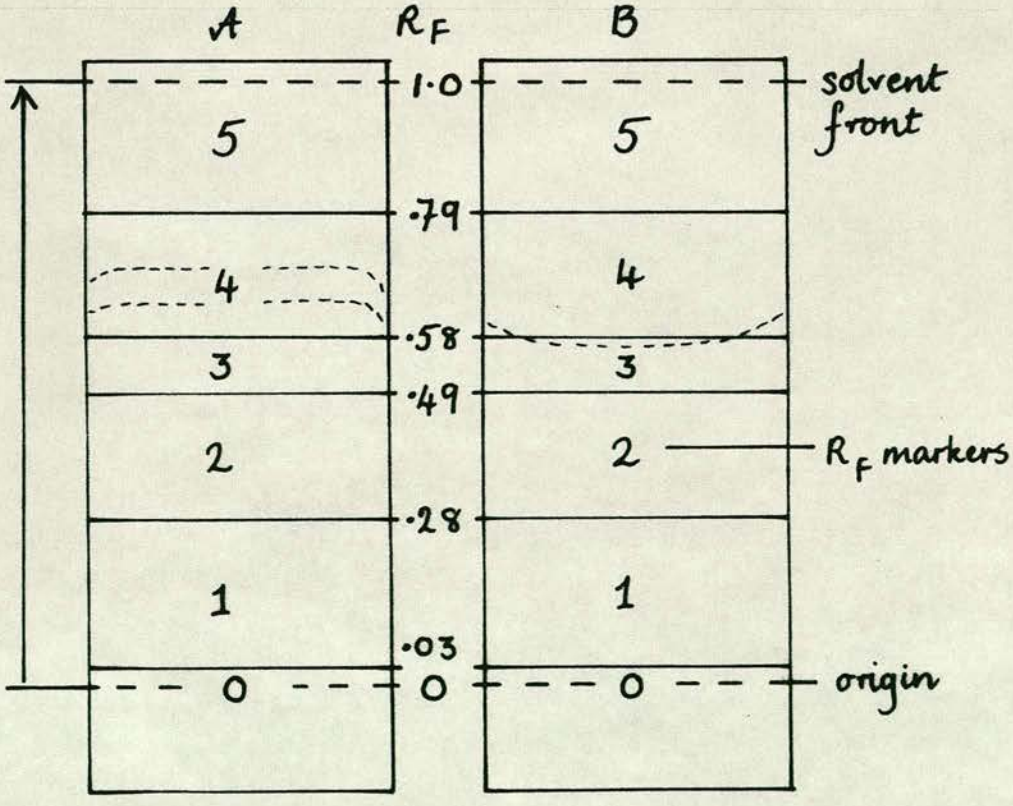
A
R_F
B
1·0
solvent front
5
5
·79
4
4
·58
3
3
·49
2
2
R_F markers
·28
1
1
·03
0
0
0
origin

Figure 2.9

TLC Elution Contaminants: λ_{max} scans

λ_{max} scans of ethanolic eluates from TLC zones A 0-5 and B 0-5 (see Fig. 2.8) blanked against AR ethanol (1 cm quartz cuvette). OD: optical density (units); λ wavelength (nm). λ_{max} was identified by reducing the scan speed and increasing the chart speed until readings were consistent. (Scans above 300nm not shown).

Fig. 2.9 A0-5

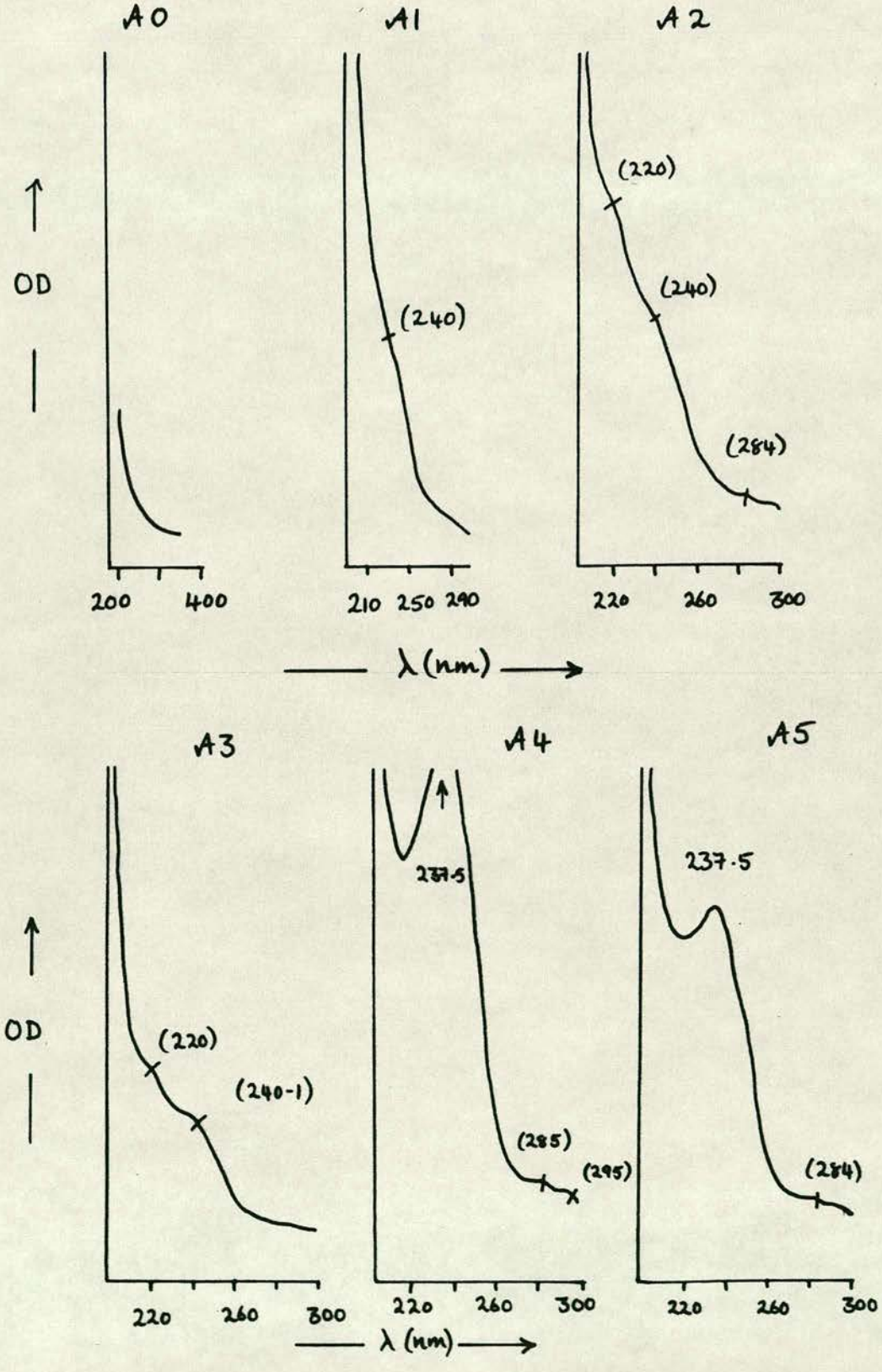
A0
A1
A2
OD
(240)
(220)
(240)
(284)
200
400
210
250
290
220
260
300
λ (nm)
A3
A4
A5
OD
(220)
(240-1)
237·5
(285)
(295)
237·5
(284)
220
260
300
220
260
300
220
260
300
λ (nm)

Fig. 2.9 B0-5

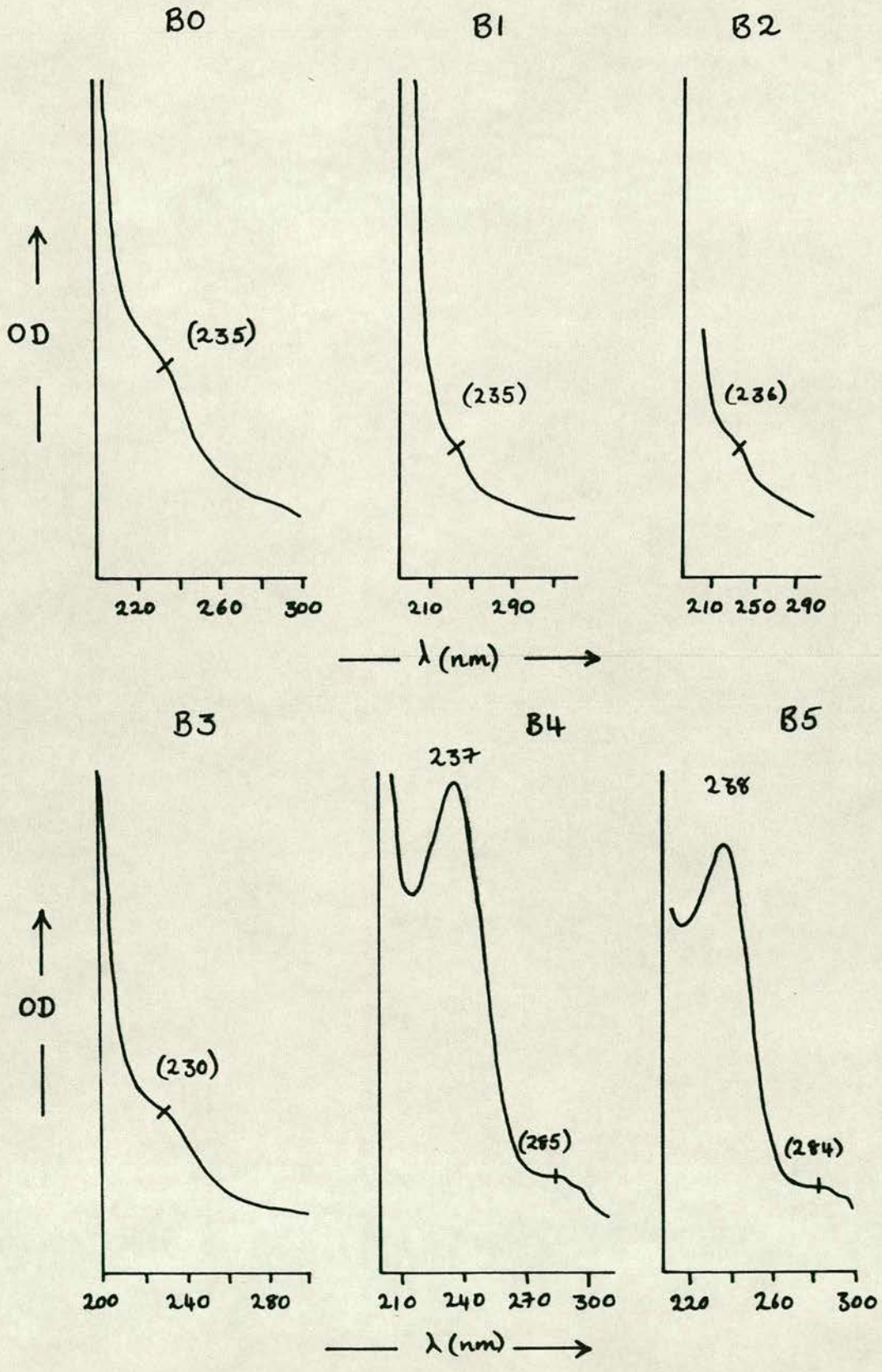
B0
B1
B2
OD
(235)
(235)
(236)
220 260 300
210 290
210 250 290
λ (nm)
B3
B4
B5
237
238
OD
(230)
(285)
(284)
200 240 280
210 240 270 300
220 260 300
λ (nm)

"developed" in 3:1 Methanol/chloroform (A) or 3:17 95% Ethanol/Chloroform (B) for about 15 minutes to compare the effects of the two alcoholic solvent-systems on elution of contaminants. Bands from the origin to the solvent front (Fig. 2.8) were eluted in 1ml AR Ethanol and the eluates compared for UV-absorbing compounds by performing UV-absorption max. scans (200-350nm) using a Perkin Elmer 320 spectrophotometer. Dilutions were not constant; (qualitative analysis).

Figure 2.9 shows the spectrophotometer scans in the ecdysteroids-region ($\lambda_{max.}$ 243), and Table 2.1 shows ethanol-elutable contaminants by their $\lambda_{max.}$ for each R_F-zone.

The only distinct peaks in these scans occur in zones 4 and 5 (i.e. distant from ecdysteroids) and their $\lambda_{max.}$ (237-8nm) is lower than that characteristic of an ecdysteroid-type nucleus (243nm); so the major elutable contaminants from TLC do not occur in the ecdysteroids zone.

To keep contamination to a minimum, ethanol (B) has been adopted as the TLC solvent-system because its use resulted in fewer compound-types being eluted compared to the use of methanol (A); (but whatever the $\lambda_{max.}$ of a compound, it may be measurable at 254nm with the HPLC UV-detector (fixed wavelength) and, should it co-elute with ecdysone or 20-OH-ecdysone, it may lead to false-positive identifications or inaccurate quantification by UV spectrophotometry at that stage; see A4.2,f).

TABLE 2.I TLC elution contaminants

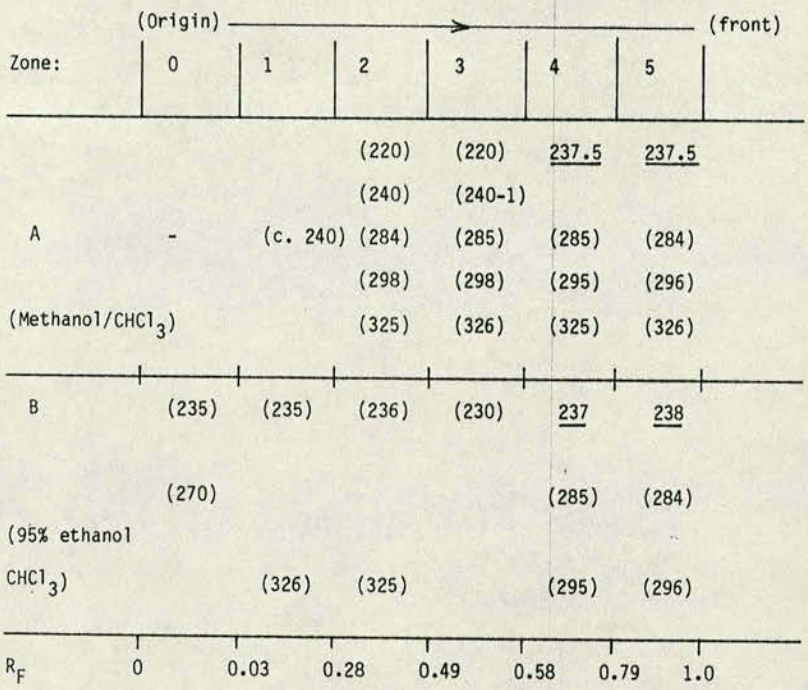

Compare A v. B: Fewer contaminants eluted with ethanol than with methanol.

(Values for λ_{max} in parentheses were not distinct peaks).

Ecdysteroids correspond to zone 2.

2.12 Test Beers-Lambert Law for ecdysteroids at maximum sensitivity of HPLC UV-detector; and
Test pipetting error for variable-volume pipette.

The HPLC system used for this study performs quantification of concentrations by computing a response factor relating UV-absorption peak area to the defined concentration of one dilution of a reference solution, and then applying this factor automatically to all unknowns (with recalibration ad lib). So compounds of interest must obey Beer's Law (see Glossary), throughout the range of application of the detector.

Six dilutions were made of a 10^{-5}M solution containing two ecdysteroids using a variable-volume pipette (Gilson Pipetman). These dilutions were subjected to HPLC-UV spectrophotometry and their peak areas were determined as shown in Fig. 2.10. Peak area was directly proportional to concentration, confirming that it is acceptable for these compounds, under these conditions, to be quantified by the application of a single response factor for each steroid (i.e. the relation is linear within this range near the limit of sensitivity of the fixed-wavelength detector).

These data offer an opportunity for assessing the accuracy of the 200µl variable-volume pipette which was used to prepare dilutions. Fig. 2.11 shows that the use of such a pipette involves an error of greater than 5% at volumes less than 12.5% maximum volume capacity. This was also considered when using the 1ml and 20µl-models.

Figure 2.10

Direct proportionality of HPLC-UV spectrophotometry peak areas and ecdysteroid concentration

a) Representative HPLC chromatogram showing ecdysone (α) and 20-OH- ecdysone (β) UV- absorption peak areas quantified by comparison with a concentration standard solution (10^{-5}M). Instrument: Waters tri-module HPLC system; column: C_{18} Rad-Pak; Injection: 3 x 50µl; mobile phase: 50% aqueous methanol 1ml/min; isocratic 20 min. alternating with a methanol flush and equilibration. UV-absorbance at 254nm; integration by calibration averaging.

b) Linear relation between ecdysteroid concentration and UV absorption peak area over the 10^{-5}-10^{-6}M range (= lower limit for accurate quantification by detector/integrator). Concentration as percentage stock 10^{-5}M standard mixture of ecdysone (α) and 20-OH-ecdysone (β).

Fig. 2.10

a)

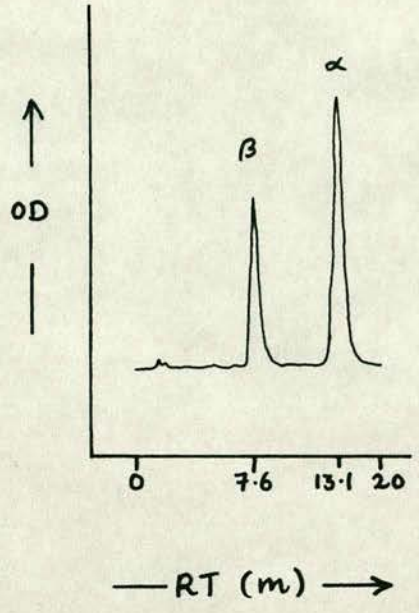
α
β
OD
0
7·6
13·1
20
RT (m)

b)

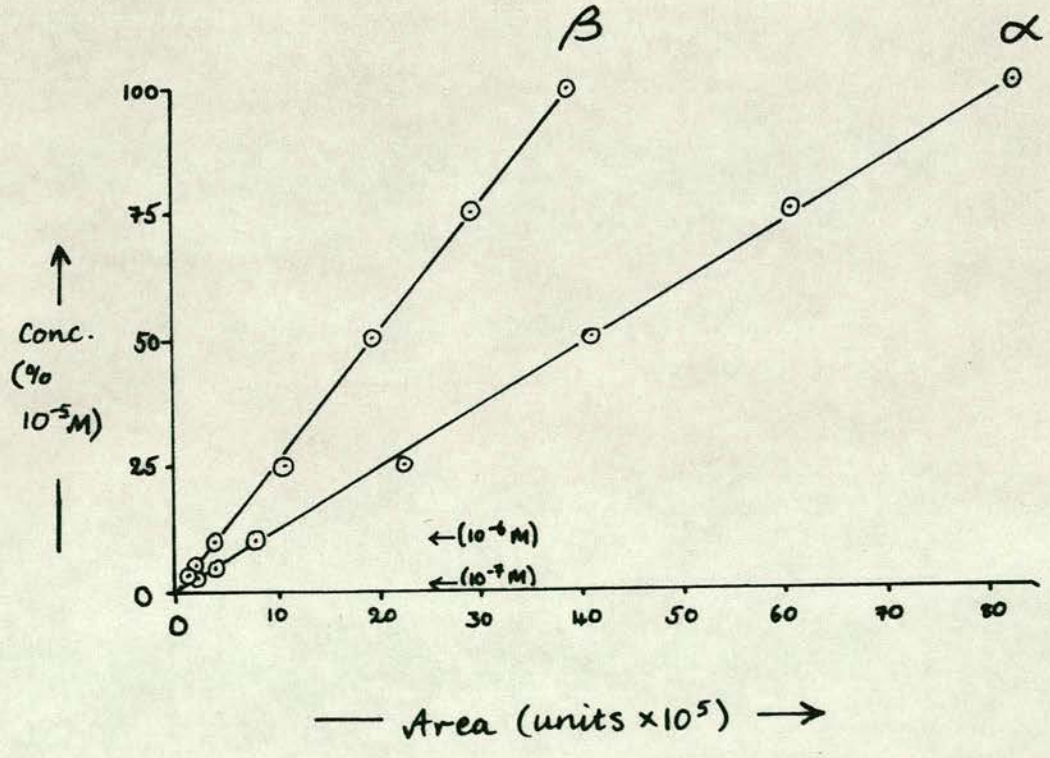
β
α
100
75
50
25
0
Conc. (% 10⁻⁵M)
←(10⁻⁶M)
←(10⁻⁷M)
0
10
20
30
40
50
60
70
80
Area (units ×10⁵)

Figure 2.11

Pipetting error for a variable-volume pipette (Gilson pipetman P200) over the range 6-200µl (abscissa). Ordinate = positive or negative percentage error as determined by quantitative HPLC-UV spectrophotometry using 10^{-5}-10^{-6}M ecdysone/20-OH-ecdysone in aqueous methanol. Errors are based on means for the two ecdysteroids (three injections of each dilution). Volumes less than 25µl (= 12.5% nominal volume) are subject to an error of more than 5%.

Fig. 2.11

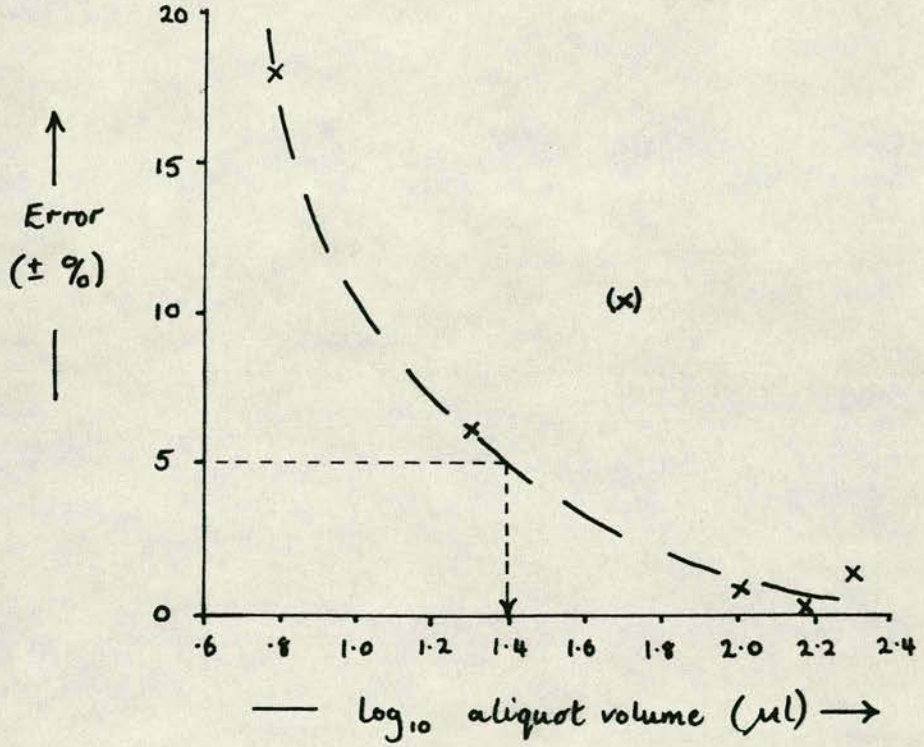
20
15
10
5
0
Error
(± %)
(x)
·6
·8
1·0
1·2
1·4
1·6
1·8
2·0
2·2
2·4
log10 aliquot volume (µl) →

2.13 Trial fraction - collection after HPLC.

The use of the fraction collector (LKB 2211 Super Rac) was tested by subjecting standard 10^{-5}M ecdysone/20-OH-ecdysone (Simes; $\lambda_{max.}$ 243) to reverse-phase HPLC (conditions as Section 2.12) and collecting 30-sec. fractions of the eluate which were scanned from 300-200nm U.V., (see Fig. 2.12). HPLC peak retention times corresponded to timed fractions, allowing for a 35 sec. delay from UV-detector to fraction-collector dropper.

2.14 HPLC sample preparation

The following protocol was adopted for the extraction and purification of ecdysteroids from stages P1, P7 and P10-13 (See 3.1). Appendix A4 shows that the use of an internal standard was essential for quantification; and makisterone A (a gift from Dr. Wilson) was adopted for this purpose, being added to all stages before homogenisation. (This makisterone A showed no contamination with ecdysone or 20-OH-ecdysone when examined by HPLC-UV spectrophotometry). One preparation of stage P1 was made without exogenous makisterone A.

Solvents HPLC-grade water prepared by double-distillation and passage through a "Morganic" cartridge (Millipore, with filter HA 0.45µm).
Methanol, HPLC-grade (Rathburns)
Hexane (BDH)
Chloroform, HPLC-grade (Rathburns)

Figure 2.12

UV-absorption λ_{max} determinations of ecdysteroid HPLC eluate fractions

a) Example HPLC chromatogram showing separation of ecdysone (α) and 20-OH-ecdysone (β) 10^{-5}M. Conditions as Fig. 2.10; 30 sec. eluate fractions were collected using an LKB "SuperRac" from a 100µl injection x 15. Fractions were reduced to dryness, taken up in 0.5ml aqueous methanol and scanned in a quartz cuvette for UV-absorption λ_{max} using a Perkin Elmer 320 spectrophotometer blanked automatically vs. aqueous methanol.

b) λ_{max} UV-absorption scans of ecdysteroid fractions (30 sec). 243nm λ_{max} is characteristic of an ecdysteroid nucleus. Adjacent fractions beyond the HPLC peaks (< 4 min; > 8 min) showed no UV- absorption maxima between 200 and 300nm.

Fig. 2.12

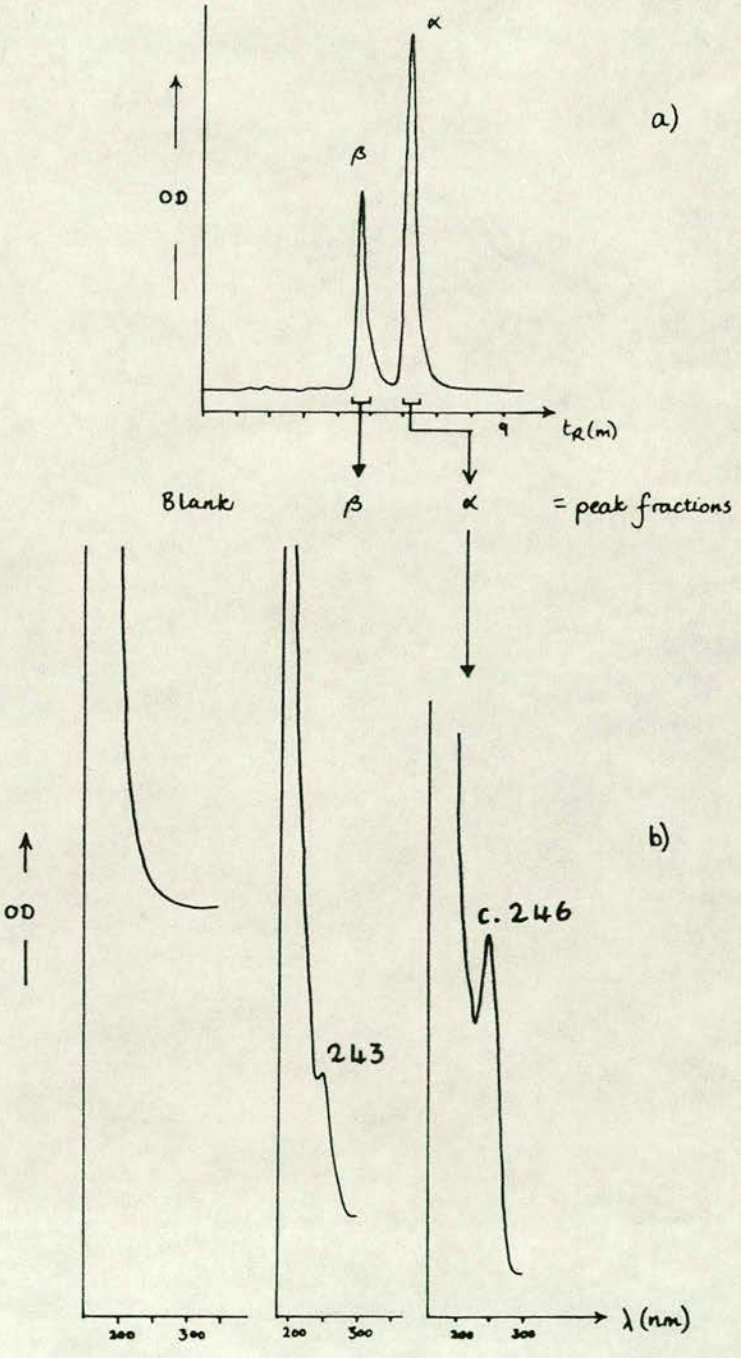

Ethanol, AR (BDH)

"Repelcote" (BDH) was used to siliconise all glassware.

All solvents were filtered (Millipore FH 0.5µm and HAWP 0.45µm)

Apparatus 20ml glass mortar with teflon pestle;

"Dry-ice bucket (-80°C);

Sonicator (Dawes);

30ml and 15ml centrifuge tubes (Corex);

Freeze-drying apparatus;

Rotary evaporator;

Short L.C.-columns, low pressure, C_{18} ("Sep-PAK" cartridges, Waters Ass.);

2mm-diameter glass beads;

Silica-gel plastic TLC plates, 400cm^2, with UV-fluorescent indicator (Eastman Chromagram 13181);

25µl glass capillary tubes;

Sheet-film 20in^2 (Ilford FP4

UV-lightbox, 254nm 365nm (Ultra-Violet Products Inc.);

Nitrogen sample-evaporator ("N-Evap" 106, Organomation Ass.).

Sample filtration apparatus (Waters; Filters Millipore FH/HA 0.45µm);

Centrifuge (Refrigerated Superspeed Sorval RC5B, Du Pont);

Protocol:

Extraction: 1) Incubate samples -20°C, 1h, in 7:3 methanol/water; Add 100µl makisterone A, 10^{-4}M (equivalent to 1ml 10^{-5}M = final sample volume cf. 10^{-5}M HPLC concentration standard);

2) Homogenise in sufficient changes of solvent (c.15) to bring off clear liquor with no debris remaining in mortar. Pool homogenates;

3) Sonicate c. 20 secs.;

4) Spin 10 minutes at 4°C (10K rpm). Remove supernatant, disaggregate pellet in 7:3 Methanol/water, spin, pool supernatant; repeat wash.

5) Reduce supernatant to small volume of water (rotary evaporation);

Purification 6) Partition twice vs. Hexane. Back-extract with water, pool aqueous phases;

7) Partition twice vs. Chloroform. Back-extract with water, pool aqueous phases.

8) Freeze-dry aqueous extracts overnight to reduce

volume.

9) Take up in a few mls. of water and load with rinses onto prepared C_{18}-cartridge (preparation = 3ml methanol, 5ml water). Wash cartridge with few mls. water. Repeat three times using transmitted water and new C_{18}-cartridges;

10) Elute steroids from C_{18}-cartridges in 4ml methanol (pooled per sample) and reduce to dryness (rotary evaporation);

11) Take up in 5 x 1ml ethanol using glass beads (vortex);

12) Spin off ground glass and insoluble material at 4°C 10 minutes (10K rpm). Repeat x 3 and pool supernatants. Volume reduced for TLC application;

13) Double-develop new TLC plates in 3:17 95% Ethanol/ Chloroform (70 min x 2). Load samples with rinses using capillaries in stream of cold air. Add R_F standard ecdysteroids.

14) Double-develop chromatograms in equilibrated TLC-tank lined with absorbent paper (70 min x 2) using 3:17 95% Ethanol/Chloroform.

15) Dry and mount chromatograms with double-sided sticky tape. Photograph under UV-illumination (254 and 365nm) using yellow and red filters;

16) Scrape chromatograms in ecdysteroid-region and up to, but excluding, other prominent fluorescence-masking or UV-fluorescent bands; (Some bands are dark, masking the fluorescence of the indicator in the plate coating while others fluoresce at characteristic wavelengths in response to UV-illumination.)

17) Elute ecdysteroids from silica-gel: Add 2ml ethanol, vortex, stand 1 hour (-80°C), vortex, spin 10 minutes (10K rpm), remove supernatant; repeat twice, pooling supernatants. (The P1 sample without exogenous makisterone A was eluted in 6 x 1ml ethanol.) Reduce to dryness (rotary-evaporation);

18) Take up in 1ml methanol using glass beads. Repeat twice and pool eluates;

19) Spin at 4°C 30 minutes (10K rpm) to remove ground glass and silica-gel. Reduce supernatants to dryness under nitrogen (room-temperature);

20) Take up ecdysteroids in 1ml 1:1 methanol/water and

freeze-thaw/vortex twice to facilitate dissolution. Sonicate 10 seconds.

21) Spin at 4°C, 30 minutes (10K rpm), to remove insoluble material. Remove supernatant and repeat twice using 500µl 1:1 methanol/water.

22) Filter samples and collect filtrates and washes in 4ml HPLC sample vials.

23) Reduce samples to dryness under nitrogen (room temperature) and bring to 1ml final volume in 1:1 methanol/water. Cap tubes with self-sealing PTFE HPLC septa (Waters Ass.), vortex, and store at -80°C.

2.15 Preparative and Analytical HPLC

Apparatus: Waters Tri-module HPLC system linked to programable fraction-collector (LKB "SuperRac") - See Appendix A6 for technical details.

Column: C_{18}, internal diameter 8mm, length 10cm (Waters Radial-PAK Cartridges)

Mobile Phase: Methanol/Water 1:1; premixed and degassed/filtered; stored covered on line to reduce selective evaporation.

Flow rate: 1ml min^{-1}

Temperature: Ambient.

Detector: 254nm

Operating pressure: approx. 500 psi (upper limit: 2000 psi).

Samples: (1ml) divided between limited-volume inserts (max. 120µl) for injection.

Injection volume: 100ul nominally.

Residual samples accumulated in single vial with washes. Final sample diluted progressively until UV-absorption undetectable. Sample vials caps kept loose to facilitate pressure redistribution during injection.

Chromatography: 20 or 30 min isocratic runs, alternating with methanol flushes of the column and re-equilibration to 1:1 aqueous methanol. (Purges of injector system not possible in conjunction with programmed fraction-collection; so injection volume subject to progressive decrease during automatic operation).

Quantification: Calibration of UV-absorption peak areas by reference to standard concentration mixture of ecdysone/makisterone A/20-OH-ecdysone 10^{-5} M, the makisterone-A concentration (designated 100) being the original concentration of the internal standard. Frequent recalibration (after three samples) to allow for variation in injection volume. Retention time recognition window = $5\%t_r$.

Eluate fractions-collection: 30 sec.-fractions collected exhaustively in 20ml siliconized test-tubes with programmed delay-time (detector to collector dropper) of 35 secs. Tubes covered with "parafilm" and stored at -80°C. Note that the standard ecdysteroids retention-times were monitored during collection, and when they changed significantly the remaining sample was collected in a fresh set of fraction-tubes.

2.16 HPLC Eluate volume-reduction

C_{18} L.C. cartridges ("Sep-PAK", Waters Ass.) were used to concentrate the 30 sec. HPLC-eluate fractions to a common small volume (1ml) prior to further analysis by RIA. The optimal concentrations for loading of fractions onto C_{18} cartridges was first determined (2.16.1) after which the fraction volumes were reduced (2.16.2) and a correction applied to bring the samples to 1ml methanol (2.16.3); and finally the efficiency of recovery of ecdysteroids through these C_{18} cartridges was determined retrospectively by testing the recovery through them of a further small volume of standard ecdysteroid solution (2.16.4). Note that the ability of new C_{18}-cartridges to retain ecdysteroids is reduced from 100% (cf. A4.2) by the repeated passage through them of large volumes of liquid, but that this reduction in efficiency has been monitored (2.16.4 and 5.5).

2.16.1 Determination of optimal solvent composition for loading HPLC eluate fractions onto C_{18} cartridges

Solutions of ecdysone/20-OH-ecdysone at 10^{-6}M were prepared in aqueous methanol (50%, 25% and 10%) and in water; and these were loaded onto prepared C_{18} cartridges (Sep-PAK, Waters Ass.) and eluted in aliquots of methanol. The loading volume was 1ml. Measurements were made of the ecdysteroid concentrations in transmitted loading-solvent, in aqueous washes (3ml) and in methanol eluates (3 x 1ml) by HPLC - UV spectrophotmetry (as at Section 2.15) with reference to the original 10^{-6}M 50% methanol steroids solution; (30µl injections x 2 per sample). A 50% methanol blank showed no absorption peaks at 254nm.

Table 2.II shows the recoveries measured in this way as percentages of recoverable ecdysteroid for each composition of the loading-solvent (recoverable ecdysteroid approached 100% of that loaded in these tests because the volumes passed through the cartridges were relatively small (about 7ml)).

For maximal recovery in a single methanol elution Table 2.II shows that the loading solvent should be about 1:3 methanol/water, (i.e. the HPLC-eluate fractions (1:1) should be doubled in volume with water).

2.16.2 Protocol for sample volume-reduction using C_{18} cartridges ("Sep-PAK", Waters Ass.).

C_{18} cartridge prepared (3ml methanol, 5ml water) and fitted onto a 20ml syringe (siliconized); HPLC-eluate fraction mixed with an equal volume of filtered water; ecdysteroids loaded slowly onto the cartridge in 1:3 methanol/water; mixing-beaker, loading-syringe and cartridge washed with 10ml water; 20ml air passed through the cartridge; cartridge transferred to 1ml syringe and struck across the hand to expel water-droplets; ecdysteroids eluted slowly in 1ml methanol into microcap tube (blow-out). Stored at -20°C. (therefore nominal sample volume = 1ml); cartridge flushed (3ml methanol, 5ml water; blow-out); cartridges used up to ten times. (Each use of a cartridge involved passage through it of about 50ml liquid and about 25ml air).

2.16.3 Volume-correction to realise nominal sample volume (1ml)

Samples were eluted from C_{18} cartridges in 1ml methanol, but some would remain in the packing after blow-out. The actual elution volume was determined volumetrically:-

A 1ml aliquot of methanol was blown through each of twelve used C_{18} cartridges, (number of uses ranged from 1-10). The dummy Eluates were collected in microcap tubes and their volumes measured using a new variable-volume pipette (Gilson pipetman P1000 with Gilson 1ml tip) mounted vertically in a clamp. (The pipette was set to slightly too high a volume; the sample taken up and the reading decreased until all the air had been expelled = sample volume (µl)).

Result: Eluate volume = 842.6 $\pm$ 36.7µl, (n = 12, p =

TABLE 2.II

Recovery of ecdysteroids through C_{18} cartridges:-

Monitoring proportional recovery (% recoverable steroid) by methanol elution as loading composition varies

	Loading composition (Methanol:water)							
	1 : 1		1 : 3		1 : 9		0 : 10	
ecdysteroid:	β	α	β	α	β	α	β	α
Transmitted at loading:	13.1	2.6	0	0	0	0	0	0
Eluted by aqueous wash:	11.9	6.2	0	0	0	3.8	0	0
Eluted in 1stml methanol:	75	90.2	100	100	100	96.2	93.7	97.7
2ndml	0	0.8	0	0	0	0	6.3	2.3
3rdml	0	0.2	0	0	0	0	0	0

α = ecdysone; β = 20-OH-ecdysone

0.05; Gilson accuracy specification (new) = 0.6% maximum volume). 1000 - 842.6 = 157.4µl, representing a -15.7% elution volume error from C_{18} cartridges.

Therefore the samples were brought to a final volume of 1ml in "methanol" by the addition of 157.4µl methanol. (Gravimetric determination of eluate volume was inaccurate at -3.7% error, because the methanol used for elution carried with it some residual water, so the specific gravity of the "methanol" was too high).

2.16.4 Monitoring recovery efficiency of ecdysteroids through C_{18} cartridges used for fraction volume-reduction

Used "Sep-PAKs" (Waters Ass.) were flushed with 3ml methanol after n uses and wrapped in foil until tested using 10^{-6} M ecdysone/20-OH-ecdysone (small volume, to avoid having the test constitute another use of the cartridge, n + 1).

Protocol: Prepare stored C_{18} cartridge (3ml Methanol, 5ml water); prepare ecdysteroids stock solution 10^{-6}M 1:1 methanol/water (blow-out); load 4ml 10^{-5}M ecdysteroid mixture in 1:3 methanol/water (= 2ml 1:1 methanol/water); wash cartridge (2ml water, blow-out); elute ecdysteroids in methanol, "1ml" (= 843µl); add 157µl methanol + 1ml water = 2ml 1:1 methanol/water; quantify recovered ecdysteroids with reference to 10^{-6}M 1:1 methanol/water stock solution by HPLC-UV spectrophotometry, (Injections 100µl x 3).

2.17 Preparation of a mouse anti-20-OH-ecdysone polyclonal antiserum (MAS)

This antiserum was prepared in collaboration with Dr. C. Redfern (Molecular Biology) and Dr. J. Ansell (Zoology), both of this University.

20-OH-ecdysone was rendered immunogenic by first converting the 6-keto group into the carboxymethyloxine (CMO) derivative and then coupling it to bovine serum albumen (BSA) through the resulting carboxylic function (Fig. 2.13b). The method was based on Borst and O'Connor (1974) and Porcheron et al. (1976) (reviewed by Hirn and Delaage, 1980).

2.17.1 Carboxymethyloxime-derivatisation of 20-OH-ecdysone

Five preparations of 20-OH-ecdysone-CMO were made. 10mg 20-OH-ecdysone (Sigma) were taken up in 1.5ml ARISTAR pyridine and 50mg carboxymethyloxamine (CMA) (K and K Laboratories) were added. The mixture was incubated at room temperature for 8 days to allow formation of 20-OH-ecdysone-CMO. Pyridine was eliminated by repeated washes with benzene and evaporation to dryness. The derivatised steroid and excess reaction-components were collected in the aqueous phase of an ethyl acetate 30% aqueous Methanol partition (10:1 v/v), reduced to dryness by rotary evaporation and taken up in a small volume of methanol for application to a silica-gel TLC plate (Eastman Chromagram 13181). The chromatogram was developed for 1 hour in Methanol/Chloroform 2:3 (1st dimension) which gave a

Figure 2.13

Derivatisation of 20-OH-ecdysone as an immunogen

a) λ_{max} scan of 20-OH-ecdysone- carboxymethyloxime recovered from a TLC plate by ethanol elution. λ_{max} = 253. (cf. 20-OH- ecdysone λ max. = 243; carboxymethoxamine was not recorded under these conditions).

b) Derivatisation of the ecdysteroid nucleus at position 6.

Fig. 2.13

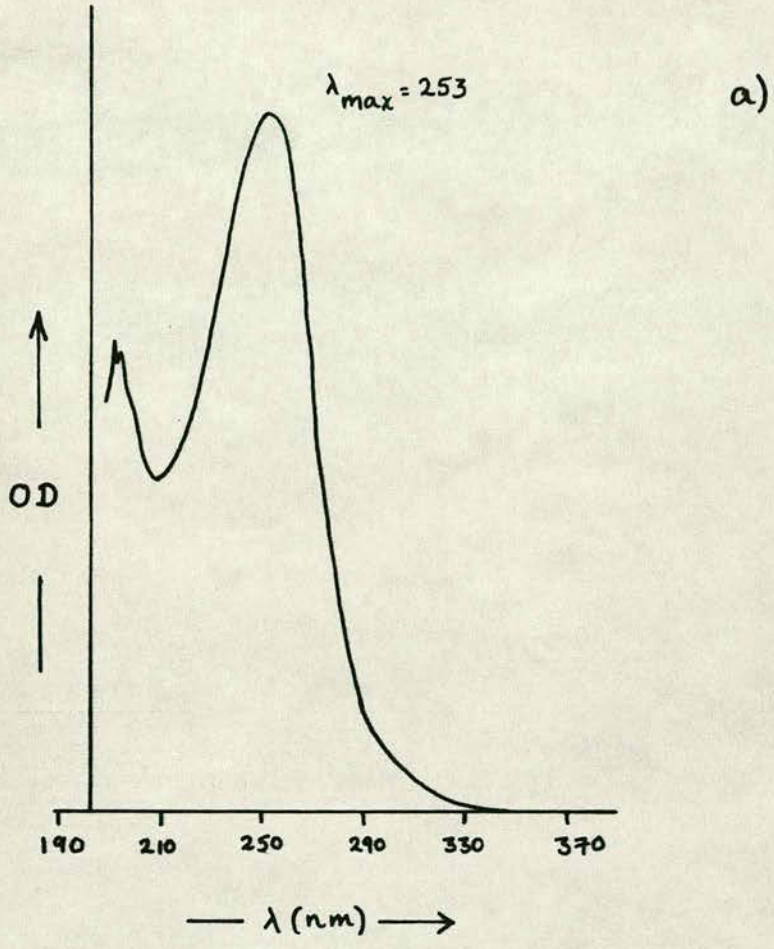
a)
$\lambda_{max} = 253$
OD
190
210
250
290
330
370
λ (nm)

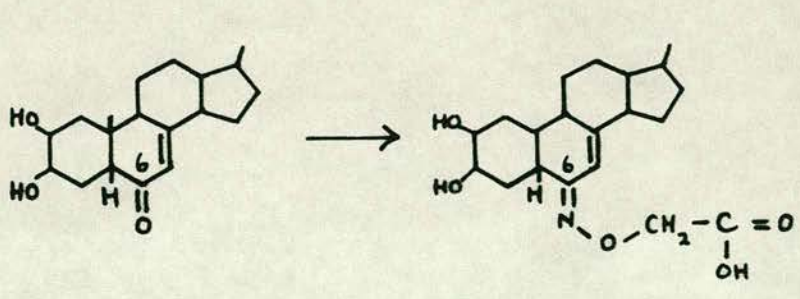
b)
HO
HO
6
H
O
HO
HO
6
H
N
O
CH_2
C
O
OH

relative R_F (20-OH-ecdysone = 1.0) of 0.36. The position of this derivative was unchanged in a second dimension (95% Ethanol/Chloroform 3:17, 1 hour) but excess 20-OH-ecdysone was removed from the vicinity of the derivative. 20-OH-ecdysone-CMO was eluted from the silica-gel by elution in 3 x 1ml Ethanol/water (7:3). The $\lambda_{max.}$ of the derivative was 253nm, (Fig. 2.13a; and see Borst and O'Connor 1974 (252nm) who give a molar extinction coefficient of 18,900). One such preparation was found to give 15.75mg 20-OH-ecdysone-CMO from 10mg steroid and 50mg CMA.

2.17.2 Conjugation of 20-OH-ecdysone-CMO to BSA

20-OH-ecdysone-CMO was reduced to dryness and taken up in 100µl freshly distilled dioxane. the medium was alkalinised by the addition of 126µmol tri-n-butylamine (Merck), and the carboxylic function was activated by adding 9.5µmol (excess) isobutyl chloroformate (Sigma), vortexing the mixture and incubating it at 0°C for 30 minutes. 6mg BSA (Sigma) was then added in water/dioxane 3:2, the mixture was vortexed and the conjugation performed at 4°C over 4 hours. The resulting 20-OH-ecdysone-CMO-BSA was dialysed against phosphate-buffered saline (0.1M pH 7.4) for 48 hours at 4°C and lyophilised. Molar ratios 20-OH-ecdysone: BSA ranged from 3.3:1 - 30:1 in these preparations (Redfern, personal Communication; cf. Borst and O'Connor (1974) 3.3:1, Porcheron et al. (1976) 20:1) but this is thought to make little predictable difference to the results of immunizations using this conjugate (Hirn and Delaage, 1980).

A similar procedure was adopted to produce 20-OH-ecdysone-CMO-ovalbumen; (for use see Fig. 2.15).

2.17.3 Raising anti-20-OH-ecdysone mouse antiserum (MAS)

Five mice of strain CBA/Ca were each immunised with 200µg 20-OH-ecdysone-CMO-BSA by intraperitoneal injection using 0.5ml 1% Tween 80 / 0.45% NaCl w/v. / 25% Freund's complete adjuvant as medium, (See Fig. 2.14). The final booster-injection was made using 250µg conjugate per mouse and the mice were sacrificed after about 11 weeks. The blood was stored for 12 hours at 4°C to allow clot retraction and the supernatant was collected and stored as 50µl aliquots at -20°C. Two bleeds designated MAS 7 and MAS 12 were both used for the experiments reported in Chapter 5.

2.18 Characterisation of MAS

^{3}H-ecdysone (NEN) of specific activity 70 or 80 Ci/mMol was used to determine the optimum dilution of the mouse antisera (bleeds 7 and 12 days after final booster-injection) and in the preparation of Scatchard and standard response curves. Redfern found MAS/7 to have an optimum dilution in BSA/borate buffer of 0.18% (1:550, personal communication). Fig. 2.15 shows the equivalent dilution for MAS 12 (i.e. the ability to bind 50% of 4000 cpm ^{3}H-ecdysone) to be 0.21% (author's finding).

Fig. 2.16 shows Scatchard plots (Scatchard, 1949) for the MAS bleeds. The binding constant for ecdysone is 1.4×10^{9} l/mole,

Figure 2.14

Immunisation Schedule for production of MAS:

Mice of strain CBA/Ca were challenged with 20-OH-ecdysone as hapten coupled to a carrier albumen over a period of 9 weeks, and the response was monitored by bleeding from the eye until a satisfactory titre was achieved. The first booster injection (5 weeks) was made using ovalbumen rather than BSA as the carrier, in the hope of eliciting a more specific response to the hapten, but this approach was unsuccessful. The mice were exsanguinated 5 d after the anti-ecdysteroid response was shown to have reached a high level. The two major bleeds were designated MAS 7 and MAS 12.

Fig. 2.14

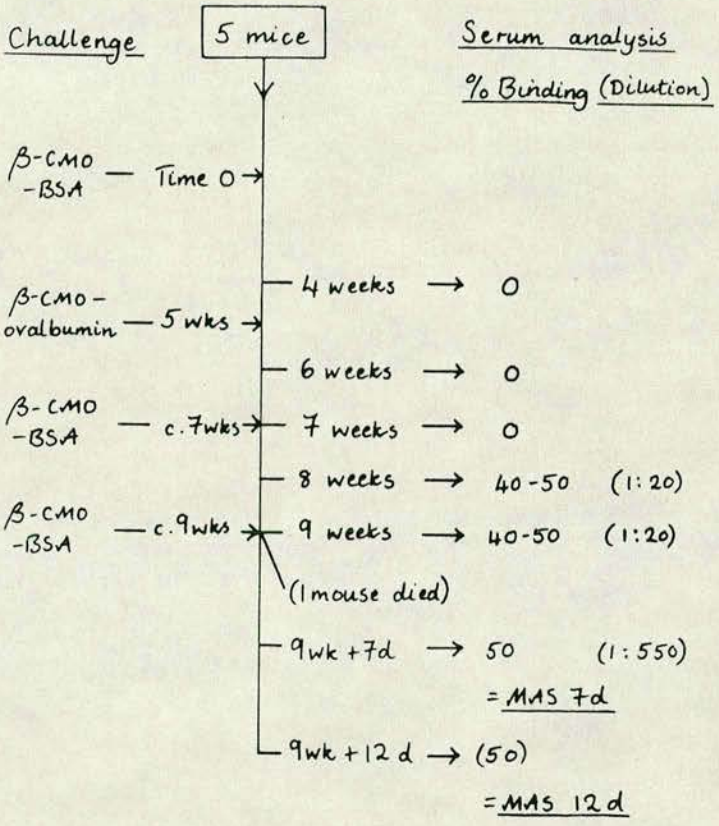
Challenge
5 mice
Serum analysis
% Binding (Dilution)
β-CMO -BSA — Time 0 →
β-CMO - ovalbumin — 5 wks →
β-CMO -BSA — c. 7wks →
β-CMO -BSA — c. 9wks →
4 weeks → 0
6 weeks → 0
7 weeks → 0
8 weeks → 40-50 (1:20)
9 weeks → 40-50 (1:20)
(1 mouse died)
9wk + 7d → 50 (1:550)
= MAS 7d
9wk + 12 d → (50)
= MAS 12 d

and during the five days which elapsed between MAS 7 and MAS 12 the number of ecdysone binding sites increased from 1.08 nMol litre ^{1} (MAS 7) to 1.85 nMol litre^{-1} (MAS 12).

Standard response curves for MAS 7 and MAS 12 are shown at Fig. 2.17 with unlabelled ecdysone, 20-OH-ecdysone and makisterone A competing with ^{3}H-ecdysone for binding to the two bleeds. Table 2.III shows values for each ecdysteroid equivalent to 50% inhibition of binding of ^{3}H-ecdysone. More makisterone A (24-methyl-20-OH- ecdysone) is required to compete equally with ^{3}H-ecdysone in the 12- day bleed compared with MAS 7, suggesting that this side-chain modification with respect to the original hapten (20-OH-ecdysone) becomes more significant to the specificity of the antiserum during the intervening five days. On the other hand, the C-20 reduction has little effect, i.e. the ecdysone and 20-OH-ecdysone curves are in the same relation to one another for the two bleeds. At 50% inhibition both antisera show a greater avidity for the immunogen (20-OH-ecdysone), but the linear portions of the ecdysone and 20-OH- ecdysone standard curves were not parallel and they converge at less than "100% bound", i.e. their respective affinities for the antisera are similar at low concentrations of competitor (about 300pg/200µl 0.1% MAS). This is not the case with makisterone A.

2.19 Monitoring of the radioimmune assay (MAS)

The MAS 7 and 12-day bleeds were stored as 50µl aliquots at -20°C. Aliquots were withdrawn for characterisation and use of the

Figure 2.15

MAS 12 dilution vs. binding of ^{3}H-ecdysone

The abscissa shows dilution of the antiserum prepared over the range 0.001-10% with RIA borate buffer (Section 2.10). 100µl aliquots of these dilutions were incubated overnight at 4°C with c. 4000 cpm ^{3}H-ecdysone (80 Ci/mMol) in 100µl 1.0% BSA/Borate buffer; the antibody- ecdysone complexes were separated from excess label by ammonium sulphate precipitation; and the bound label was counted in 1.2ml Aquasol (NEN) to determine the percentage binding of available counts (ordinate; 100% = 4024 cpm). The semi-log plot also shows data for another antiserum (rabbit) kindly donated by Dr. T. Briers (Louvain); raised against 20-OH-ecdysone. (Briers, personal communication) for comparison of titres. Both sets of data were corrected for non- specific binding of 3H-ecdysone to immunoglobulins using a rabbit anti- Drosophila yolk polypeptide antiserum made in Dr. Bownes' laboratory. The mid-point of the linear part of the dilution series curve for MAS 12 represents about 50% binding of the available cpm under these conditions. 0.21% MAS 12 (1:476 dilution) and Briers antiserum at 3.8% (1:26.3) bound half the available counts, and this dilution of MAS 12 was used in the RIA (cf. MAS 7: 0.18%). (This degree of binding of available counts in the absence of competing unlabelled ecdysteroid is designated "100% bound" in the RIA standard response curves).

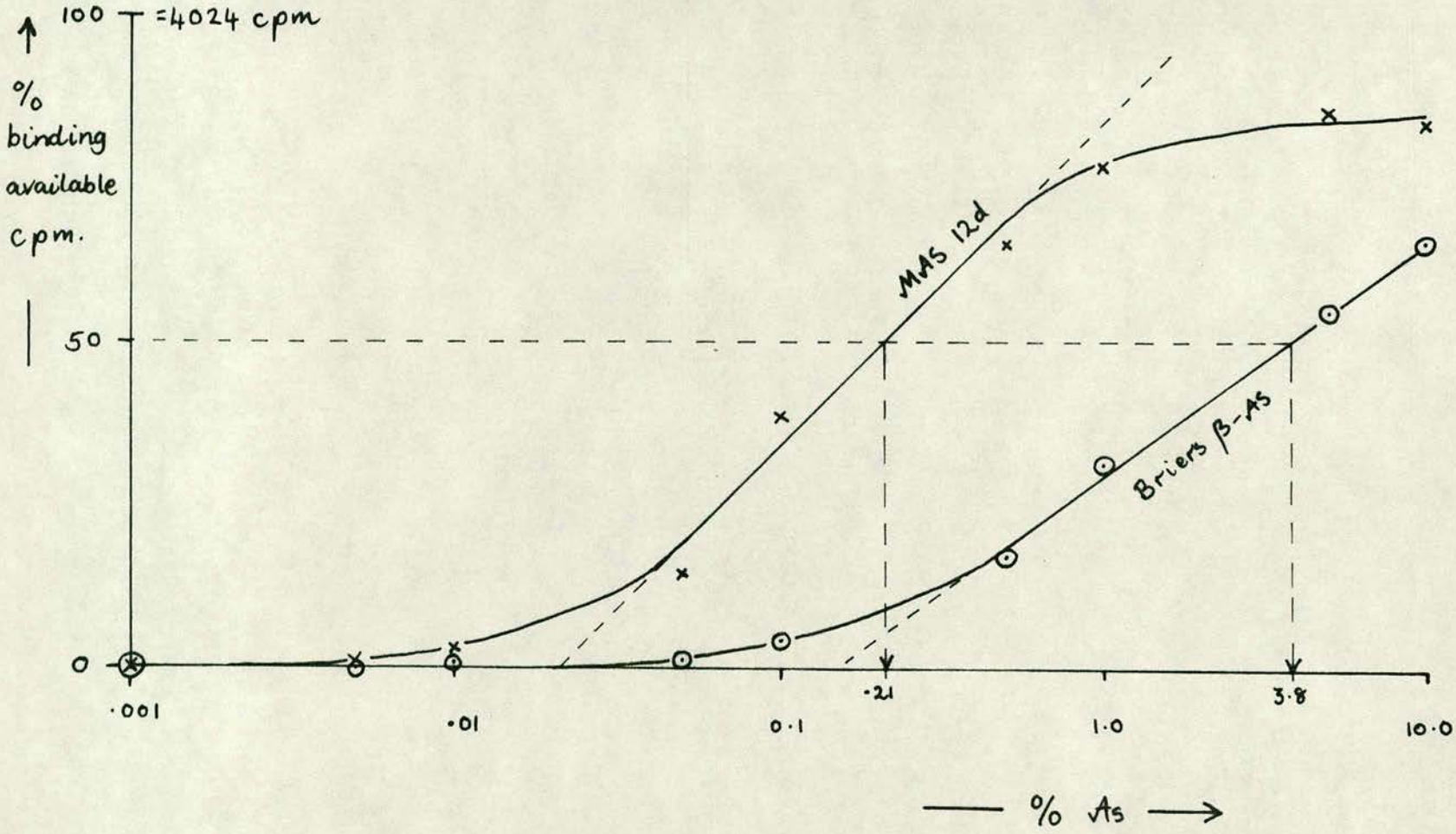
100
=4024 cpm
% binding available cpm.
50
0
MAS 12d
Briers B-AS
·001
·01
0·1
·21
1·0
3·8
10·0
% As

Fig. 2.15

Figure 2.16

Scatchard plots for MAS 7 and MAS 12 with ^{3}H-ecdysone

Aliquots of labelled ecdysone (NEN, 70 Ci/mMol) were incubated with 100µl antiserum (0.18% MAS 7; 0.15% MAS 12 with 1.0% BSA) in RIA borate buffer overnight at 4°C, precipitated with ammonium sulphate and counted in Aquasol. Abscissa: bound counts as disintegrations per minute; ordinate: ratio of bound counts to free. The intercept on x shows the number of binding sites in a 200µl incubation volume, equivalent to 1.08 nmol/l (MAS 7) or 1.85 nmol/l (MAS 12). The slope gives the binding constant, K_a = 1.4 x 10^9 l/mole.Binding of ^{3}H-ecdysone was adjusted to take account of any non-specific binding under these conditions to anti-yolk polypeptide antiserum.

Fig. 2.16

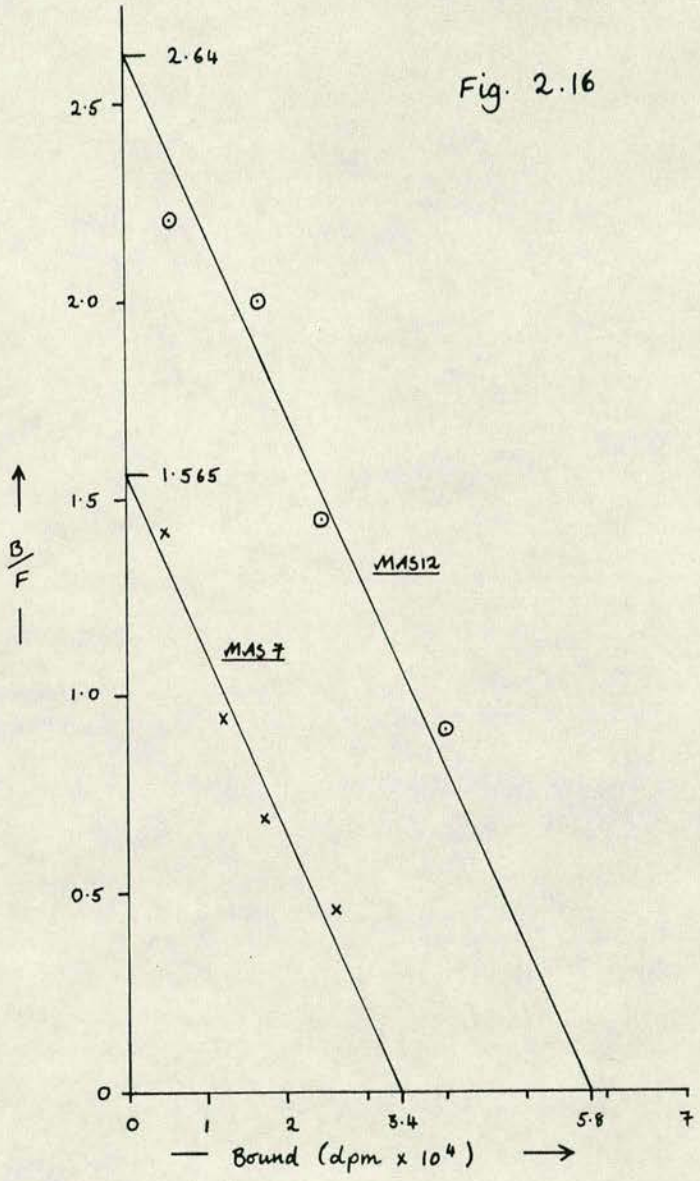

Figure 2.17

Standard response curves of MAS 7 and 12 day bleeds to ecdysone (α), 20-OH-ecdysone (β) and makisterone A (μ) as unlabelled competitors for binding sites with ^{3}H-ecdysone (NEN, 80 Ci/mMol). Curves are based on 5 runs of this incubation. Aliquots of standard-concentration unlabelled ecdysteroid were reduced to dryness and taken up in 100μl 3H-ecdysone (c. 4000 cpm) in borate buffer. 100μl antiserum at working dilution of c. 0.2% (see Fig. 2.15) was added in 1% BSA/borate buffer and, after incubation overnight at 4°C, the bound counts were precipitated with ammonium sulphate and counted in Aquasol/water (12:1). Abscissa: amount of unlabelled ecdysteroid ($\log_{10}$ pg) competing with 4000 cpm ^{3}H-ecdysone for binding to MAS. Ordinate: percentage binding of ^{3}H- ecdysone to MAS. "100% bound" represents binding of about half the available counts in the absence of unlabelled competitor (cf. Fig. 2.15). Values for 50% inhibition of binding of ^{3}H-ecdysone obtained with the three standard ecdysteroids are compared on the abscissa. Subtracted Control: non-specific binding to anti-yolk polypeptide antiserum.

Fig. 2.17

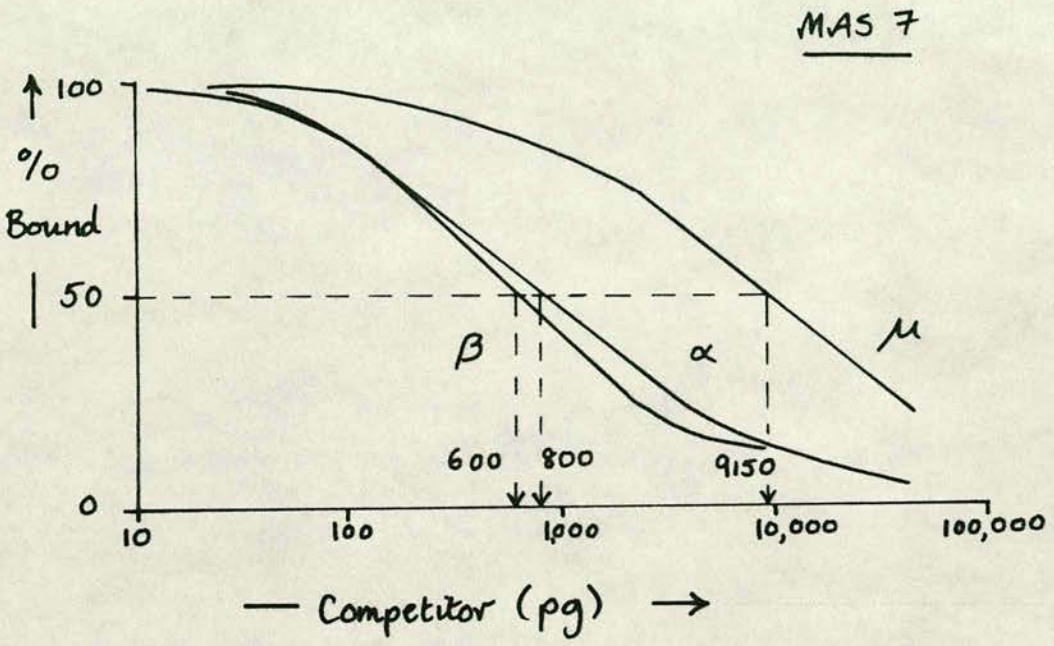
MAS 7
100
% Bound
50
0
β
α
μ
600
800
9150
10
100
1000
10,000
100,000
— Competitor (pg) →

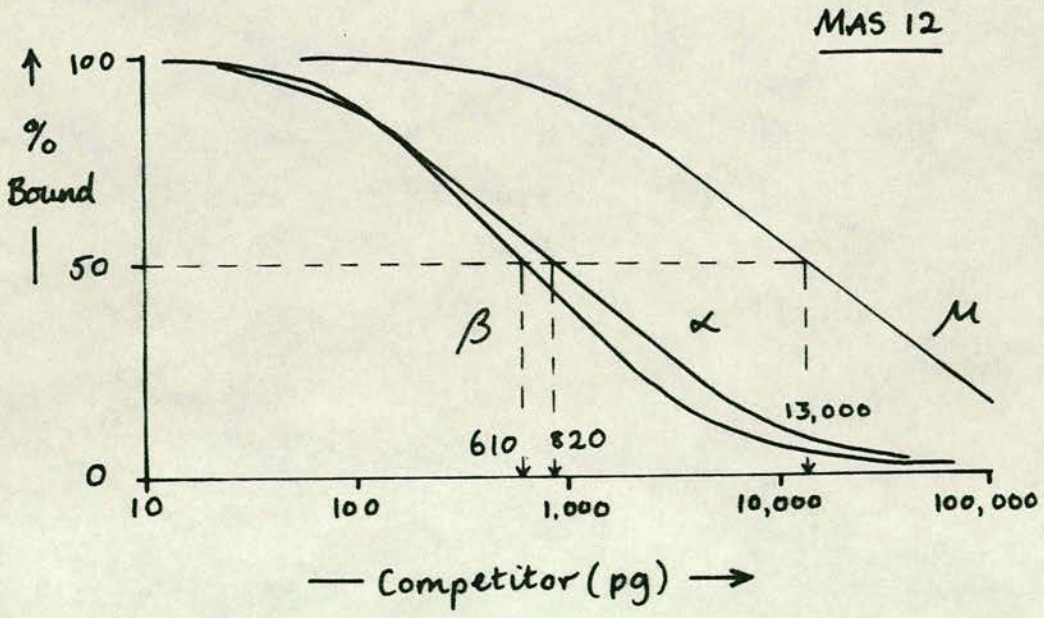
MAS 12
100
% Bound
50
0
β
α
μ
610
820
13,000
10
100
1,000
10,000
100,000
— Competitor (pg) →

TABLE 2.III

50% inhibition of 3H-ecdysone binding to MAS 7 and MAS 12 by ecdysone (α), 20-OH-ecdysone (β) and makisterone A (μ) from Fig. 2.17; expressed as picogram ratios

Comparisons:

A) between ecdysteroids

Denominator		Numerator		
		β	α	μ
MAS 7	β(600)	1	1.33	15.25
	α(800)	0.75	1	11.44
	μ(9,150)	0.07	0.09	1
MAS 12	β(610)	1	1.34	21.31
	α(820)	0.74	1	15.85
	μ(13,000)	0.05	0.06	1

B) between antiserum bleeds

Denominator (MAS 12)	Numerator (MAS 7)		
	β(600)	α(800)	μ(9150)
β(610)	0.98	1.31	15.00
α(820)	0.73	0.98	11.16
μ(13,000)	0.05	0.06	0.70

antisera in the RIA; but some were found to give unexpectedly low binding of ^{3}H-ecdysone counts. As in Section 2.18, by setting up incubations of antiserum and label in varying ratios it is possible to tell which component is being overloaded in the assay and hence which is no longer of optimum quality. Fig. 2.18 shows the results of such an experiment with an aliquot of MAS 12 and ^{3}H-ecdysone of 80 Ci/mMol. There is no evidence of loss of specific activity of the label but rather of degradation of the antiserum, (i.e. the slope of the plot percentage binding of available counts vs. ratio of volumes antiserum : ^{3}H-ecdysone is positive). Dilution-series made from suspect aliquots of both bleeds were found to give binding of half the available counts under assay conditions at much less favourable dilutions than had been determined for other aliquots (See Fig. 2.19).

Although the use here of BSA to increase the assay protein concentration is apparently questionable (since BSA was the carrier-component of the immunogen) it is unlikely that its use could provide an explanation for such a failure in the RIA system since failure was observed between ostensibly-identical aliquots of MAS - other aliquots gave satisfactory standard response curves at relatively high dilutions; and also, if BSA were to have a significant affinity for MAS, then it would constitute a third (unrecognised) competitor for binding sites when coincubated with labelled and unlabelled ecdysteroid, yet inhibition of ^{3}H-ecdysone binding by extreme quantities of ecdysone or 20-OH-ecdysone was observed to range from 0-100%, even in the presence of 5% BSA (cf. 1% used in the assay).

Figure 2.18

MAS 12 with ^{3}H-ecdysone: % binding cpm vs. MAS/label volumes

Antiserum volume (at 0.2% in 1% BSA/borate buffer) or labelled ecdysone (^{3}H-ecdysone, 4230 cpm) was kept constant while the other component was varied in two series of incubations. Binding under these conditions at volume ratio = 1.0 was expected to be 50% of available counts (i.e. c. 2000 cpm); and binding increased proportionally with additional antiserum, not with additional label.

Figure 2.19

Optimum working dilutions for degraded MAS aliquots

Compare Fig. 2.15 and previous dilutions determined for MAS 7 (0.18%, now greater than 11%) and MAS 12 (0.21%, now about 1%).

Figs. 2.18 and 2.19

Fig. 2.18

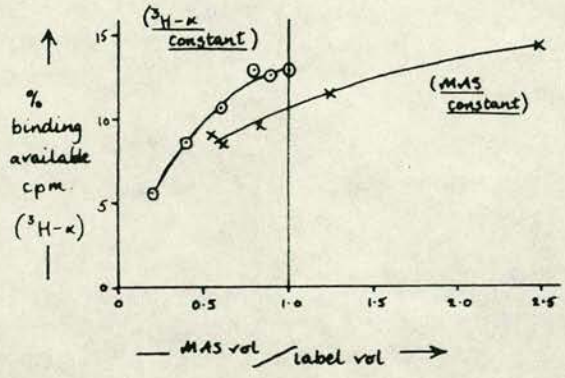

Fig. 2.19

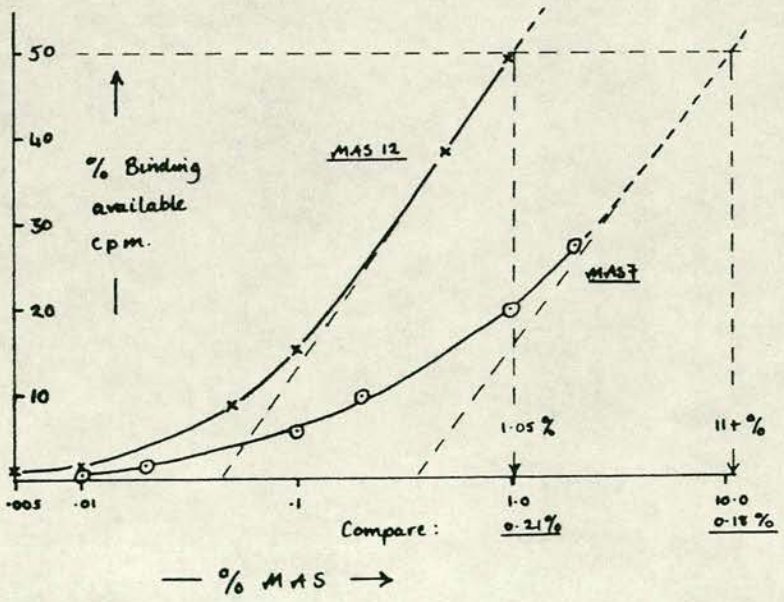

Nevertheless the competition for binding afforded by BSA was compared with ovalbumin and with two rabbit sera and borate buffer alone (See Fig. 2.20). Possibly, the antibodies stimulated by BSA as a component of 20-OH-ecdysone-CMO-BSA (or by excess BSA in the immunogen) constituted a separate population from those produced against the conjugate or specifically against the ecdysteroid; (this also applies to ovalbumin which was used as an alternative carrier in the immunisation schedule; (See Fig. 2.14); but concentrations of BSA much greater than that used here (>10%) do appear to out-compete ecdysone for binding sites (Fig. 2.20a), so the antisera may just have lower K_a values for the carrier as compared with the hapten.

2.20 Protocol for HPLC-coupled RIA using MAS

Aliquots of the reduced HPLC eluate fractions (20 or 30µl) were subjected to RIA as described in Section 2.10 with the following modifications: 100µl 3H-ecdysone (80 Ci/mMol) contained about 4000 counts in Aquasol (cpm over 10 minutes, with repeat counting); the second ammonium sulphate preparation was found to make little difference to the results here and was omitted; centrifugations in the cold lasted 15 minutes; liquid scintillant was 1.2ml cold Aquasol (NEN), and a correction for variable quenching in this medium was applied according to Fig. 2.21; plastic microcap tubes (new batch) were not siliconized as this destabilised the protein pellets.

Figure 2.20

Protein/Serum in competition with ^{3}H-ecysone for binding to MAS

100µl aliquots of MAS 7 (11%) and MAS 12 (1.05%) in RIA borate buffer were incubated with 4000 cpm ^{3}H-ecdysone in 100µl buffer containing between 0.044% and 12% albumen (w/v) or serum (v/v) or in buffer alone. Bound counts were determined by LSC in Aquasol (NEN). Controls for each sample were set up omitting MAS, and in all cases gave less than 15% binding of available counts, (background corrections applied). Competitors were: a) bovine serum albumen (Sigma), b) ovalbumen (Sigma grade IV), c) whole rabbit serum raised vs. immunoglobulins (Dr. Ford), d) rabbit anti-*Drosophila* yolk polypeptide antiserum (Dr. Bownes). Abscissa: log % competitor in borate buffer; ordinates: bound counts as percentage of available cpm ^{3}H-ecdysone (80 Ci/mMol). 1% competitor (e.g. BSA was the concentration of BSA adopted in the RIA.

Fig 2.20

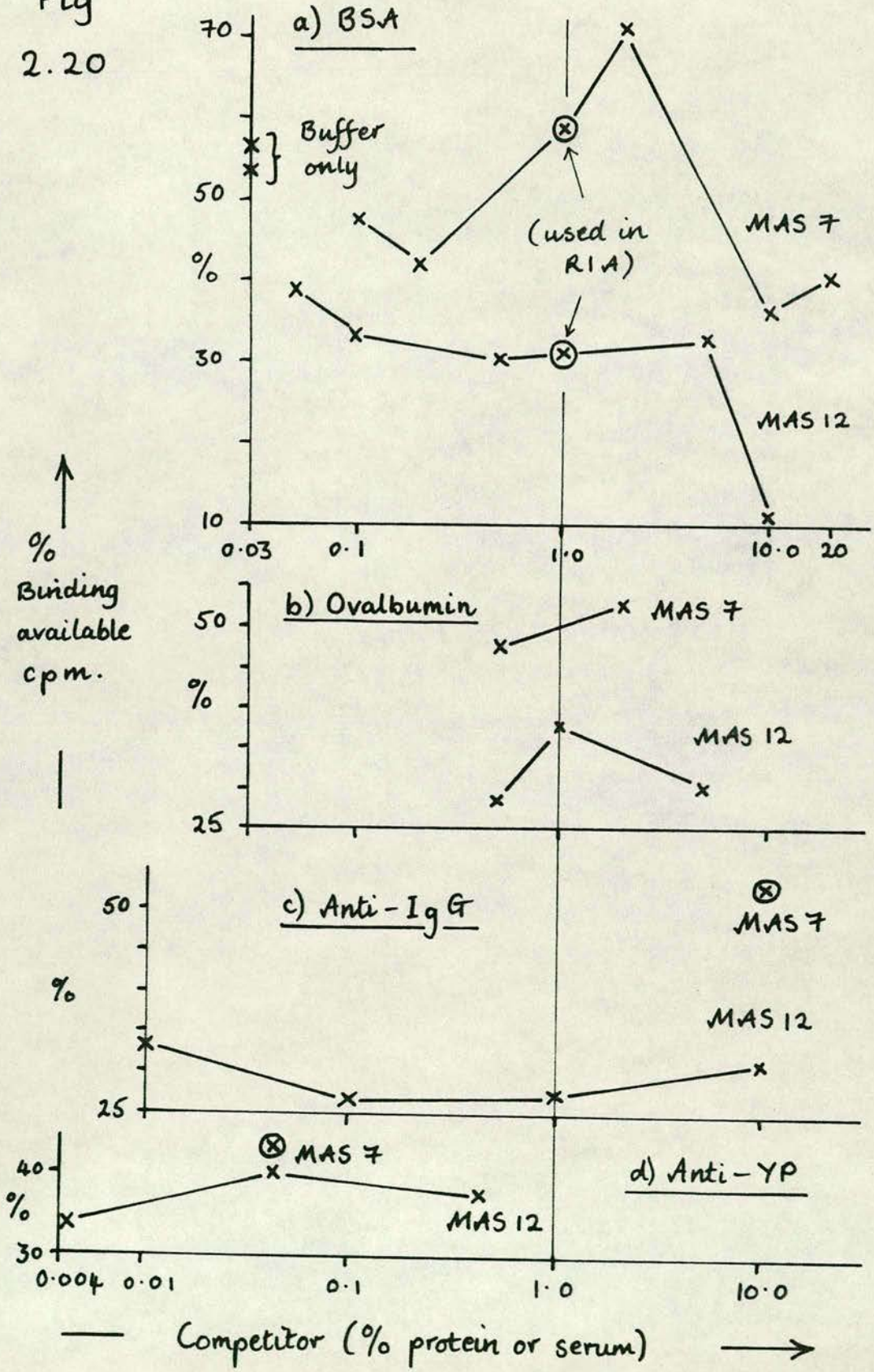
a) BSA
70
50
30
10
%
Buffer only
(used in RIA)
MAS 7
MAS 12
0·03
0·1
1·0
10·0
20
% Binding available cpm.
b) Ovalbumin
50
25
%
MAS 7
MAS 12
c) Anti-IgG
50
25
%
MAS 7
MAS 12
d) Anti-YP
40
30
%
MAS 7
MAS 12
0·004
0·01
0·1
1·0
10·0
Competitor (% protein or serum)

Figure 2.21

Quench callibration curve for 1.2ml Aquasol (NEN) + 100µl water with ^{3}H-ecdysone (< 4000 cpm):

Relative efficiency of counting is given as a percentage of the counts (cpm) recorded in the absence of acetone (= quencher) and is assumed to show a linear relation with external standard ratio (ESR) up to ESR = 0.8 (cf. Fig. 2.6). Samples when counted showed ESR values in the region 0.65 - 0.75 and were brought to a common relative efficiency of counting (100%) by application of the correction factors shown on the right-hand ordinate (cpm x F = 100%).

Fig. 2.21

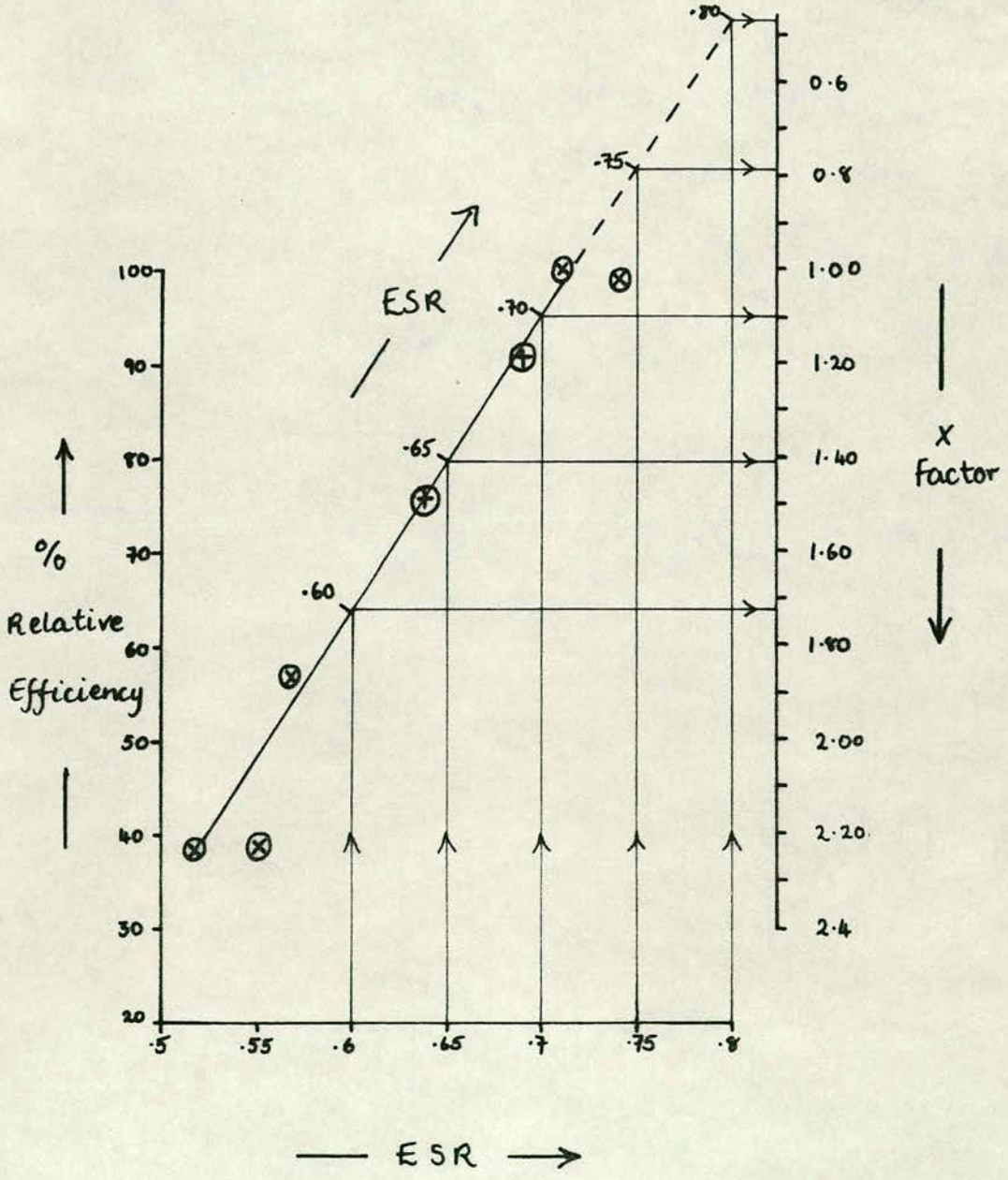
ESR
% Relative Efficiency
X Factor
100
90
80
70
60
50
40
30
20
·5
·55
·6
·65
·7
·75
·8
·80
·75
·70
·65
·60
0·6
0·8
1·00
1·20
1·40
1·60
1·80
2·00
2·20
2·4
ESR

2.21 Predicting HPLC retention times

The retention times of any of ecdysone, 20-OH-ecdysone and makisterone-A may be predicted on the basis of one another's retention times (RT) at a given composition of the whole phase. Since this composition, and other chromatographic characters, may vary slightly from run to run, and the relation between ecdysteroid retention times with them, relative retention times (RRT) were plotted for pairs of ecdysteroids against RT of the divisor - see Fig. 2.22. On this basis the RT, and hence the eluate fraction, of makisterone A could be predicted in a determination of endogenous levels (stage P1) without exposing the column to standard makisterone-A and risking contamination of the sample. In addition, chromatographic performance may be monitored by observing anomolous relations between standard RT's.

2.22 Treatment of data from HPLC-RIA

Chromatograms for ecdysteroids obtained by HPLC showed peaks which were not restricted in their spread to a single 30 sec. eluate fraction. Effective peak spreading also increases with multiple collections from a single sample. In addition, makisterone A and ecdysone were not completely baseline-resolved by HPLC under the conditions which obtained here. It was necessary, therefore, to measure the extent to which ecdysteroid concentration might be underestimated on the basis of fractional concentrations by excluding the peak tails (Section 2.22.1). Before summing the component fractions which constitute the middle segments of a given

Figure 2.22

Retention time ratios of ecdysone (α), Makisterone-A (μ) and 20-OH-ecdysone (β) vs. retention time (RT) of the denominator

Mobile phase: approx. 1:1 Methanol/water 1ml/min; stationary phase: C_{18}. Ordinate: relative retention time, unknown/known; abscissa: known RT of denominator (min). Based on 134 chromatograms, (scattergraph data not shown). The abscissa also corresponds to proportional increase in the methanol component of the mobile phase. Ratios are given for α/β, μ/β, α/μ, and their reciprosals.

Example:- When the peak RT of Makisterone- A is 10 min what would be the RT of Ecdysone?From curve (?RTα/RTμ) the Ratio at 10 min = 1.2 = RRT; i.e. RTα/RTμ = 1.2 = RTα/10. Therefore RTα = 1.2 X 10 = 12 min = Ecdysone peak RT (Check:- Predict RT of Makisterone A when Ecdysone elutes at 12 min: (?RTμ/RTα) at 12 min = 0.815 = RRT i.e. RTμ/12 = 0.815. Therefore RTμ = 0.815 x 12 = 9.78 (10 min) = Makisterone A peak RT)

Fig. 2.22

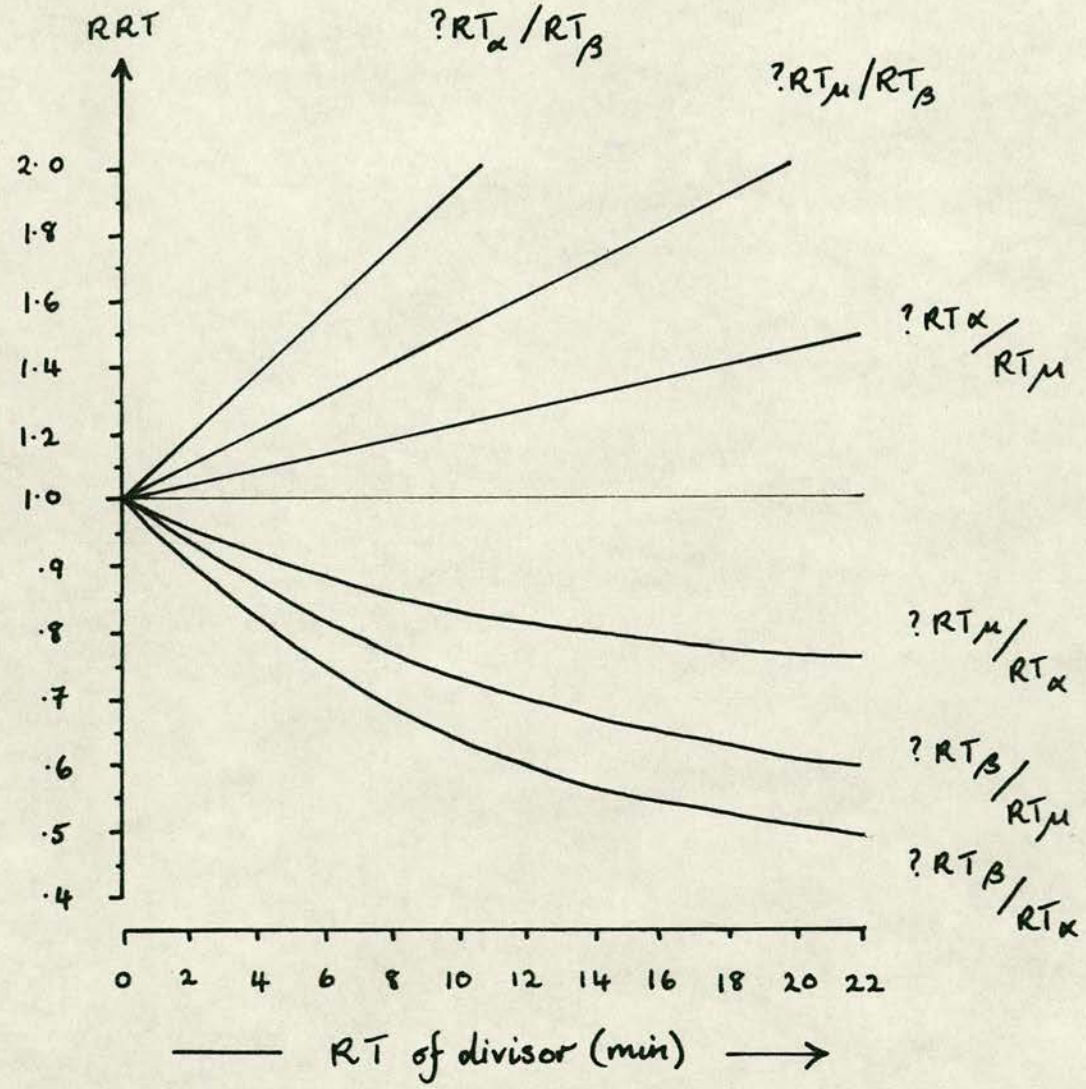
RRT
?RTα/RTβ
?RTμ/RTβ
?RTα/RTμ
?RTμ/RTα
?RTβ/RTμ
?RTβ/RTα
2·0
1·8
1·6
1·4
1·2
1·0
·9
·8
·7
·6
·5
·4
0 2 4 6 8 10 12 14 16 18 20 22
RT of divisor (min)

peak it was also necessary to check the accuracy of the concentrations determined for each fraction across the peak as members of a set (the real titre), especially since peak tails were the subjects of fewer replicate assays compared with the peak-fractions of highest concentration. A graphical method is given (2.22.2) for screening these concentration data.

2.22.1 HPLC relative retention times (RRTs) as peak-area segment boundaries

A group of typical peak traces for ecdysone, makisterone-A and 20-OH-ecdysone, of varying areas and retention times (Fig. 2.23), were divided into segments, the segment areas measured using an Olivetti P6040 programmable microcomputer coupled to a Ferranti Cetec digitiser (Fig. 2.23), and the data used to generate a representation of the relationship between segment area (in terms of total peak area) and relative retention time, RRT (peak RT = 1.0) (See Fig. 2.24). RTs of fraction/fraction boundaries relative to the RT at maximum peak height may thus be translated into residual peak areas.

Figure 2.23

HPLC Ecdysteroid peak traces

Three chromatograms A, B and C showing 20-OH-ecdysone (β), makisterone A (μ) and ecdysone (α) (10^{-5}M) obtained by HPLC-UV spectrophotometry using C_{18}/50% aqueous methanol (1ml min^{1}) at a chart speed of 2cm min^{1}), (absorbance units full scale deflection, AUFS = 0.01 or 0.02). Peak retention times vary from 7.17 - 13.48 min. Ordinate: optical density. Abscissa: retention time, RT. Relative retention times, RRTs are shown above the curves (peak retention time = 1.0). The RRT at the makisterone-A/ ecdysone trough is shown truncating all the peak tails at RRTs 0.92/1.14. 100% peak area was deemed to lie between RRT 0.84 - 1.24 in the analysis of peak-segment areas.

Figure D shows schematically how the traces were subdivided into segments, the areas of which, as proportions of the total peak area, were used to plot Fig. 2.24.

Fig. 2.23

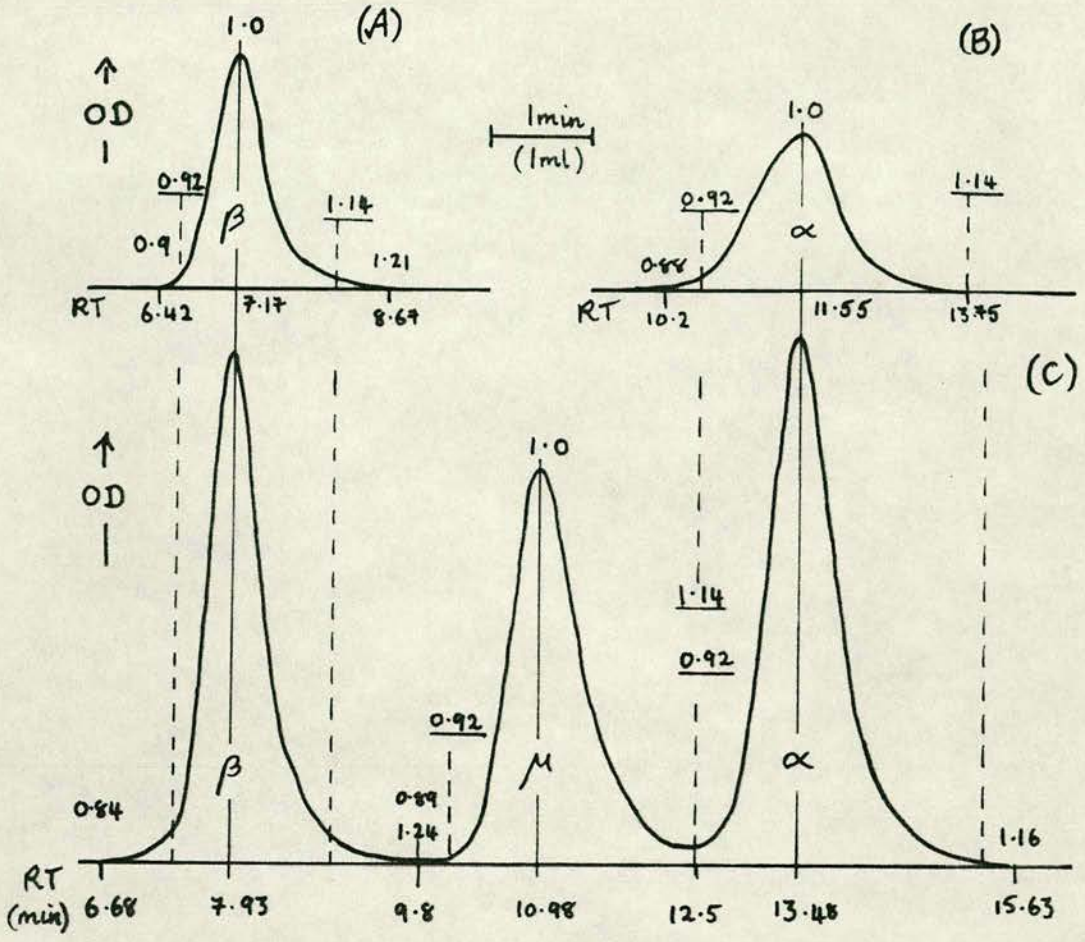
(A)
1·0
OD
0·92
0·9
β
1·14
1·21
RT
6·42
7·17
8·69
1min
(1ml)
(B)
1·0
0·92
0·88
α
1·14
RT
10·2
11·55
13·75
(C)
OD
1·0
0·92
0·84
β
0·89
1·24
μ
1·14
0·92
α
1·16
RT
(min)
6·68
7·93
9·8
10·98
12·5
13·48
15·63

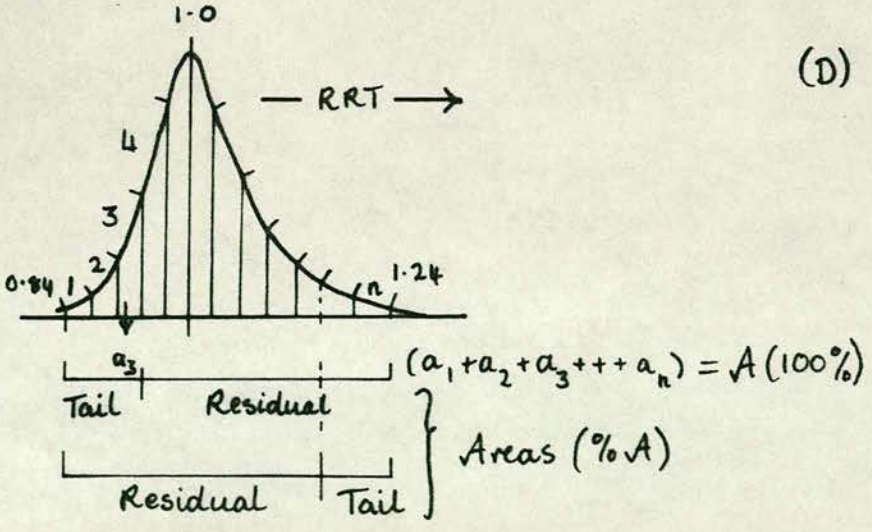
(D)
1·0
RRT
4
3
2
0·84
1
n
1·24
a_3
$(a_1+a_2+a_3+++a_n) = A\,(100\%)$
Tail
Residual
Residual
Tail
Areas (%A)

Figure 2.24

RRT vs. Cummulative percentage total O.D- peak area for a composite trace of ecdysteroid peaks (HPLC-UV spectrophotometry) based on Fig. 2.23. Abscissa: RRT (peak RT = 1.0). Ordinates (log_{10} scale): cummulative percentage area excluded when a peak flank is truncated at a given RRT; and residual area (as percentage total peak area) after truncation. Peaks are asymetrical about the maximum (43: 57% area). Errors represent $\pm$ 2 s.e.m. on x or y (n = 5) and increase towards the tails because of the log_{10} scale and also because of the inaccuracy of measurement of the progressively smaller segment-areas.

Fig. 2.24

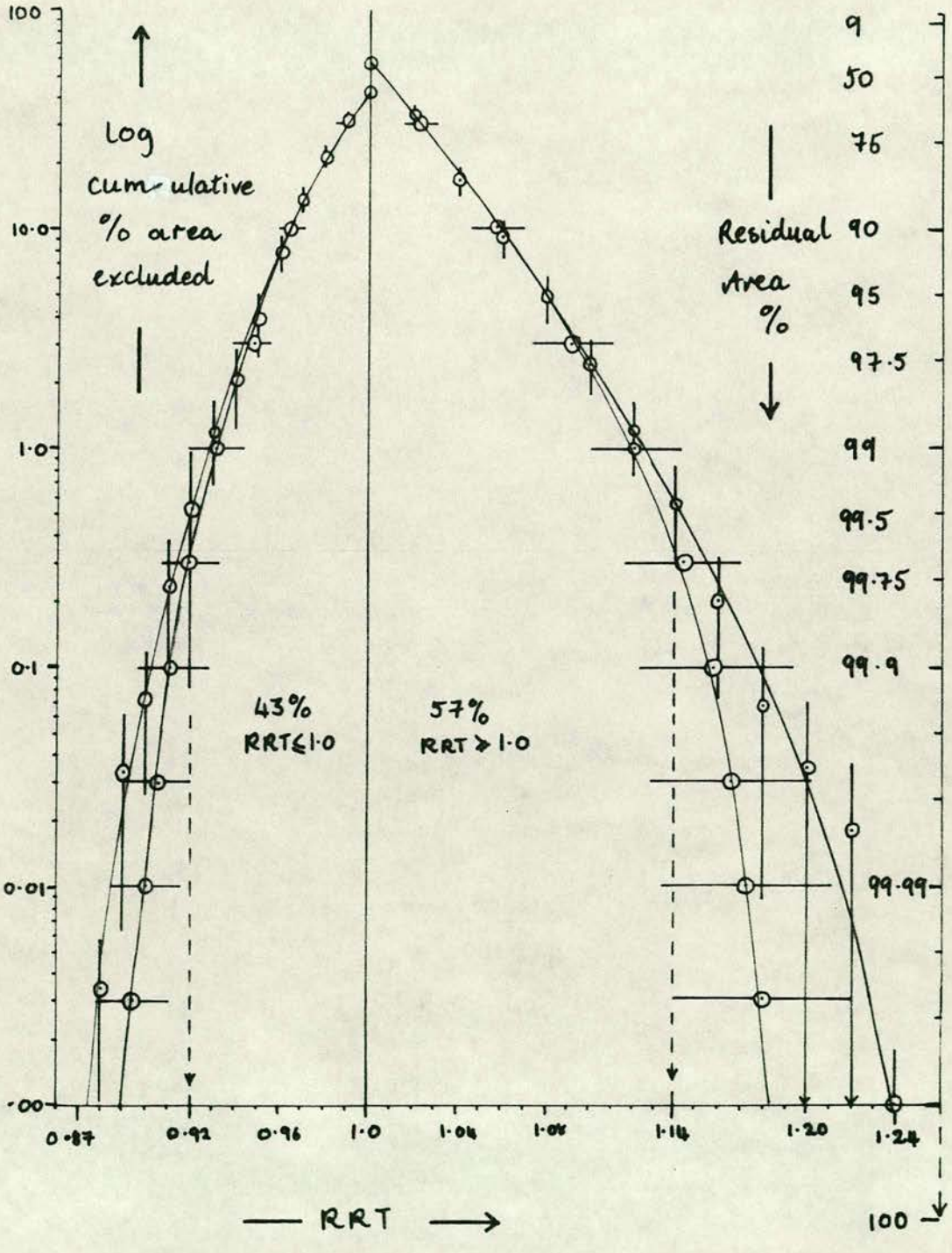
100
10·0
1·0
0·1
0·01
·00
Log cum-ulative % area excluded
43% RRT≤1·0
57% RRT≥1·0
Residual Area %
9
50
75
90
95
97·5
99
99·5
99·75
99·9
99·99
100
0·87
0·92
0·96
1·0
1·04
1·08
1·14
1·20
1·24
RRT

2.22.2 Screening HPLC-eluate fractional concentrations as components of ecdysteroid titres

Figure 2.25 shows that a log-log plot of peak segment areas vs. percentage total peak area lies parallel to the ratio 1:1. This means that only one segment area need be known to extrapolate the curve to the intercept with 100% and so to predict total peak area. Optical density is proportional to concentration (c.f. 2.12). By extension, since O.D.-peak area is therefore proportional to sample concentration for a given component, percentage area represented by a given segment (or eluate fraction) is proportioned to the total titre represented by the segments comprising the area of the peak. This will be equally true for single separations and for composite "peaks" produced by multiple pooled separations, providing that the chromatographic parameters do not change significantly during the accumulation of eluate fractions. Therefore, ideally, plots analogous to Fig. 2.25b using data from the RIA and peak areas equivalent to RT fractions (Fig. 2.24) would be parallel to 1:1, and those data which fail to lie on or near such a line should be suspected of shifting the 100%-value (i.e. the ecdysteroid titre) such that it becomes inconsistent with the rest of the data available on the component fractions.

This method is used (Section 5.7) to screen for spurious values of ecdysteroid-content in eluate fractions located at peak tails where the sample number may be too small to give a reliable mean value. There, it is also used, in effect, to reconstruct missing values when the concentrations of ecdysteroid in fractions at or

Figure 2.25

O.D. peak segment area (cm^2) vs. % total peak area, as a simulation of the relation: ecdysteroid concentration per peak segment area (ng ecdysteroid equivalents) vs. % total titre per sample (i.e. summation of fractional titres).

a) comparison of hypothetical peak of area $100cm^2$ with data for an ecdysone HPLC-UV spectrophotometry peak trace where total area is $29.23cm^2$ (RT of example = 13.48 min). Angles (theta) and gradients (m) are unequal.

b) log-log transformation (to base 10) of the same comparison. Angles (theta) are equal although gradients differ numerically (m= 1 cf. 3.4). The upper right quadrant excludes only 1% of the total peak area (negative logarithms).

Fig. 2.25

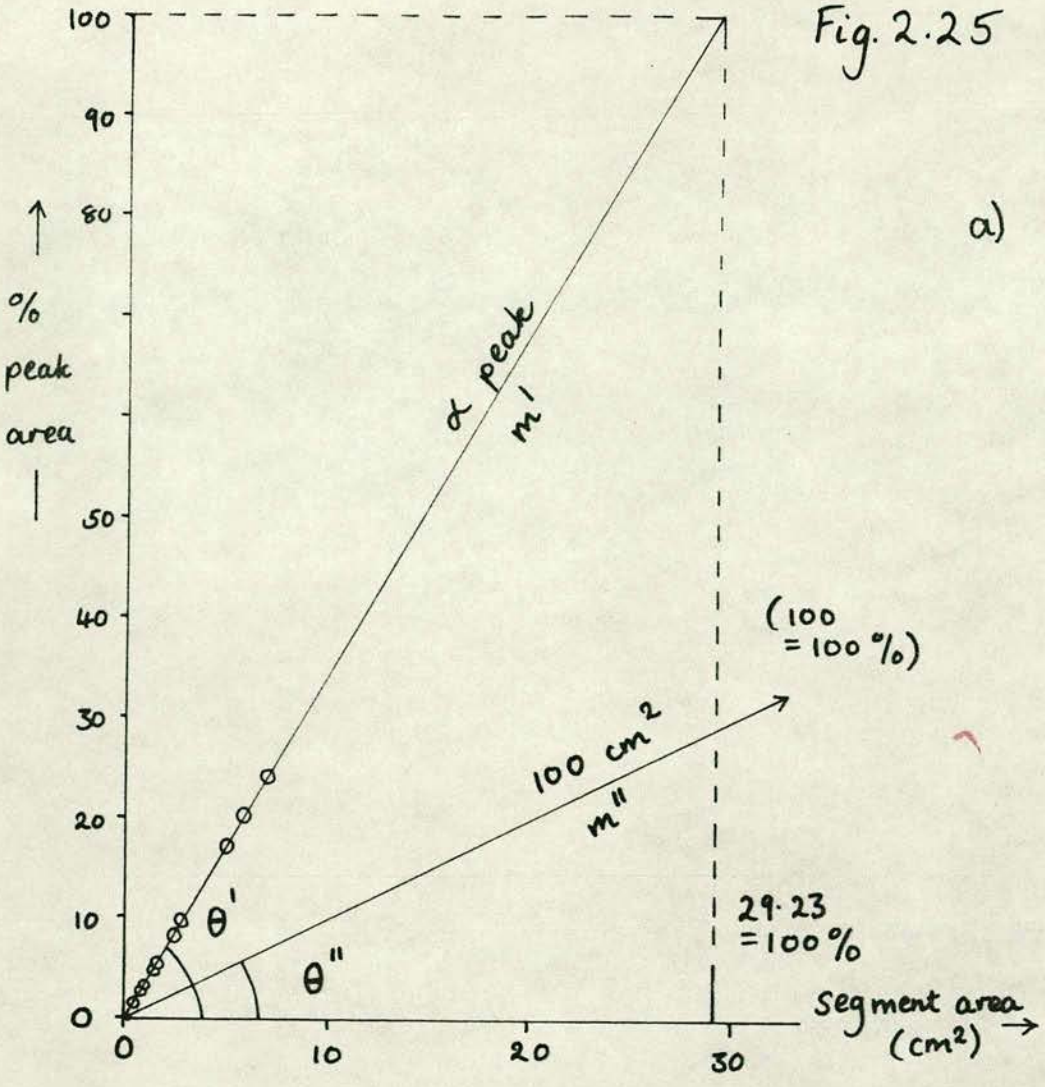
a)
100
90
80
50
40
30
20
10
0
% peak area
α peak
m'
(100 = 100 %)
100 cm²
m''
θ'
θ''
29·23 = 100 %
0
10
20
30
Segment area (cm²)

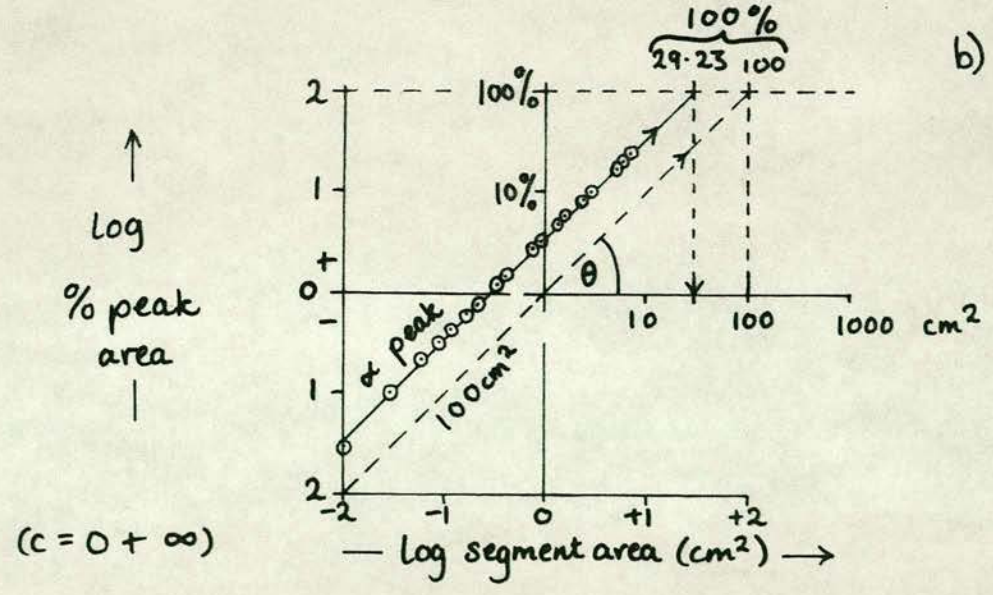
b)
100 %
29·23 100
2
1
0
1
2
100%
10%
θ
α peak
100cm²
10
100
1000 cm²
Log % peak area
(c = 0 + ∞)
-2
-1
0
+1
+2
— Log segment area (cm²) →

close to the peak retention time are anomalous (too low, due to experimental mishap). Then the unknown sample titre may be estimated in the absence of the highest value of the set of fractional concentrations. (In fact this was necessary only when there were two sets of fractions (I and II), the companion set being available to confirm that the fractions in question were components of a single peak). The use of log axes tends to remove spurious accuracy accumulated in treating the RIA data since it conforms to the logarithmic abscissa of the RIA standard response curves.

2.23 Sample-preparation for GLC-MF analysis of ecdysteroids

Samples of stages P1, P7 and P10-13 (as batches of 0.5g) were collected and prepared for derivatization. Initially this preparation was performed in Edinburgh, and the results of subsequent analyses by Dr. Rees (Liverpool) using gas-liquid chromatography and coupled mass fragmentography (GLC-MF) suggested the following (personal communication): methanolic extraction is preferable to the use of acetonitrite (less noisy signal produced); a silica-gel TLC step (preceded by hexane partition and treatment with a C_{18} cartridge), or its equivalent, is required to purify extracts (group separation, as with HPLC); and TLC-elution should be done with ethanol rather than methanol in which silica is more soluble, (silica masked the MF-signal generated by derivatised ecdysone). After TLC, eluates from the ecdysteroids zones of stages P7 and P10-13 showed UV-absorbance maxima at 215, 219, 273-4nm and shoulders on these peaks at 266 and 283nm, (no detectable maximum at 243nm).

After these samples had been thus roughly characterised in terms of their requirement for purification before GLC, further samples were frozen in liquid Nitrogen and sent to Liverpool packed in dry ice, for preparation as follows (personal communication).

2.23.1 Extraction/Purification

Samples weighing 500mg were homogenized using a Potter-Elvehjem homogenizer with 7:3 methanol/water; the extracts were centrifuged for 10min, at 12,000 rpm (microfuge); and the pellets were re-extracted by further homogenizations, once in the same solvent and twice in methanol. Supernatants were pooled, reduced to dryness (reduced pressure; with butanol at volume equal to water component, added to assist evaporation, and partitioned twice between 7:3 Methanol/water and hexane (25ml each; delipidation). The hexane was back-extracted, and the aqueous methanol phases were pooled and reduced to dryness. Extracts were taken up in methanol, evaporated onto Celite and loaded onto a silicic acid column (2g, packed in chloroform). The column was flushed with 20ml chloroform and the ecdysteroid(s) eluted in 20ml 3:7 methanol/chloroform. 10ml eluate were reduced to dryness and loaded onto a C_{18} cartridge (Waters, Sep-PAK) in 2ml 1:9 methanol/chloroform followed with an additional 4ml wash in the same solvent. The cartridge was flushed with 3:7 methanol/chloroform and the ecdysteroids were then eluted in 6:4 methanol/chloroform. Half of this eluate was transferred to a Reacti vial and derivatised. Overall, then, one quarter of the sample was silylated, equivalent to 0.125g staged material.

2.23.2 Derivatisation (full silylation)

Makisterone A (5ng) was added to each extract as an internal RT and concentration standard, and samples were reduced to dryness by vacuum dessication. N-Trimethylsilyl imidazole (TMSI; 60µl) was added as solvent and reactant, and samples were flushed with dry nitrogen before capping. They were then heated at 140°C for 17 h and allowed to cool.

2.23.3 Sample-TMS-ethers: work-up for GLC

Hexane/Ethyl acetate 7:3 (c. 0.5µl) was added to the silylation mixture and each sample was loaded, with washings (x3), onto a 2g silicic acid column made up in the same solvent. Ecdysteroid trimethylsilyl ethers were eluted in 20ml of this solvent, reduced to dryness by rotary evaporation at room temperature, and redissolved in 20µl hexane.

2.23.4 GLC-MF of silylated ecdysteroids

Method similar to Lafont et. al. 1980 (LKB 9000 GLC-MS apparatus; 28 eV; Ion source 310°C). Column: 5'x 0.125" OV - 1 (1%) on Gas Chrom Q (100-120 mesh); oven temperature 270°C, (Injector and Separator temperatures c. 285°C); gas 2 kg cm^{2}. Ions m/e = 567 (ecdysone-type molecule, major fragment), m/e = 561 (20-OH-ecdysone-type molecule) and, sometimes, m/e = 636 (also ecdysone- type molecule) were monitored. 5µl aliquots (of 20µl) were injected.

2.23.5 Quantification

GLC-MF of samples was preceded on each occasion by a run of ecdysteroid standards. Mass Chromatograms were obtained for each sample and the native ecdysteroids were identified on the basis of both their RRTs with respect to makisterone A and their main ions as characteristic of 20-hydroxylated or 20-deoxy ecdysteroid nuclei. Concentrations of native ecdysteroids were calculated on the basis of peak areas according to the plot shown at Fig. 2.26, correction having been made for the amount of sample which entered the GLC-MF apparatus; (but note that the internal standard was not added at the beginning of the extractions, and no estimate was made of recovery-efficiency through this procedure for the ecdysteroids being estimated). Rough measurements of concentration are presented in Section 6.1. (Table 6.I).

2.24 Identification of Juvenile Hormone (JH) in D. melanogaster

2.24.1 Sample-collection

Uncrowded bottle cultures were selected which contained both stages L1 and A2 together with empty puparia, and from them mixed stages P1-15 were collected by scraping the walls. The animals, of mixed sex, were cleaned in 70% ethanol followed by water at room temperature (brief rinses) and larvae (LIII-L2), exarate adults (A1-3) and damaged animals still undergoing metamorphosis were discarded. The remainder were checked for equivalent representation

Figure 2.26

Calibration of GLC-MF ecdysteroid peak areas on the basis of makisterone A (μ) as internal standard. Example log-log plot of unknown peak area/μ peak area x 100% vs. mass of ecdysone (α) or 20- OH-ecdysone (β) in grams. Peak areas were computed automatically during the analysis and converted to concentrations of ecdysteroid as ng/sample. A correction was made to return values to ng/500ng tissue according to the amount of sample proceding to GLC-MF after silylation etc.

Fig. 2.26

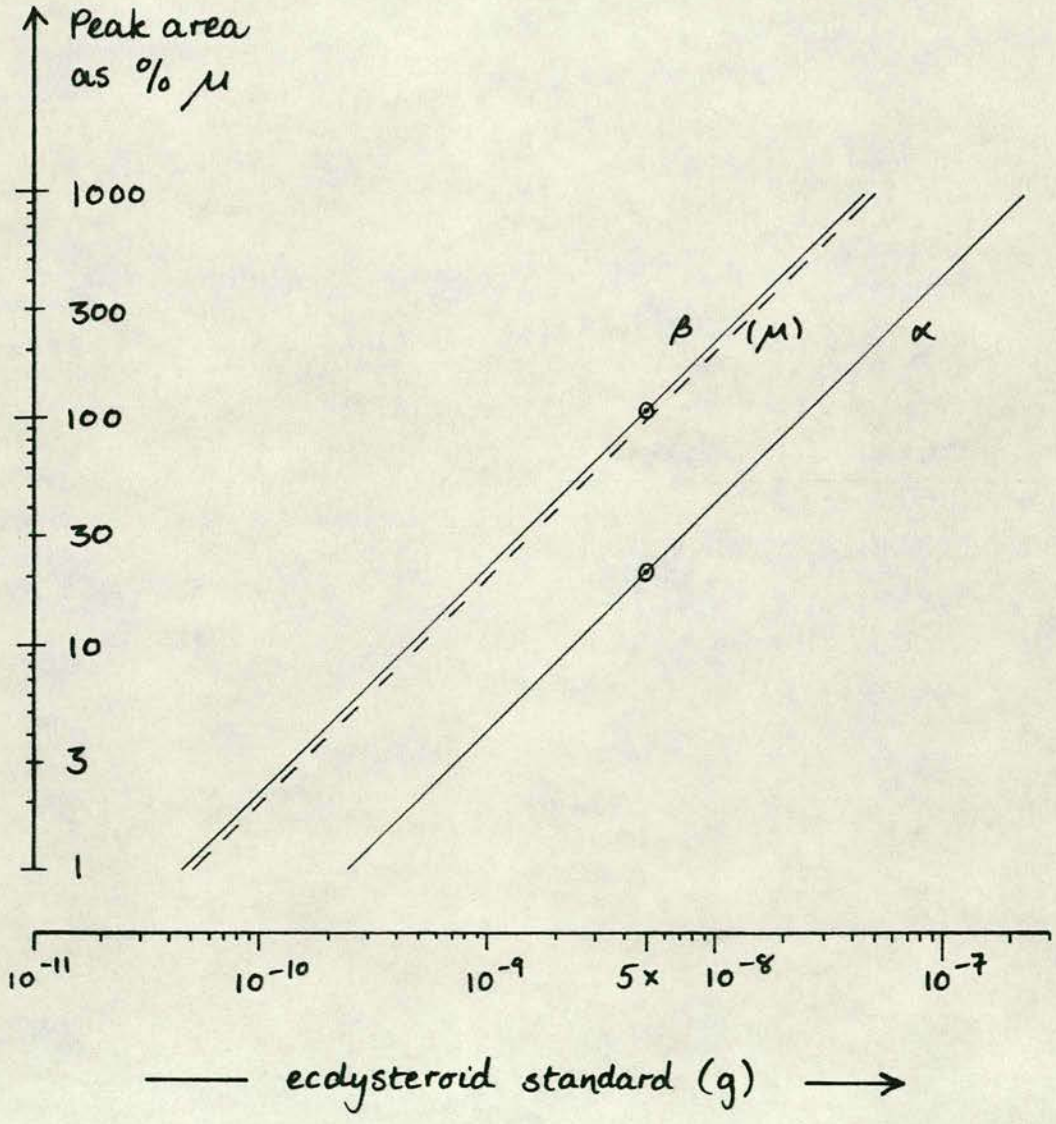
Peak area
as % μ
1000
300
100
30
10
3
1
β (μ)
α
10⁻¹¹
10⁻¹⁰
10⁻⁹
5x 10⁻⁸
10⁻⁷
ecdysteroid standard (g)

of the longer stages, very roughly, and then were frozen and accumulated at -60°C. The various batches of P1-15 were then defrosted, dried, mixed thoroughly and refrozen in liquid nitrogen before being submerged briefly in cold methanol to float off empty puparia. Again the animals were rinsed with water and dried. They were divided into 4 samples of 2g and homogenized (see below).

Further cultures were sorted for stages P1-4 (ii) (inclusive) which were accumulated individually at -60°C (stages represented to roughly the same extent) until there were sufficient to defrost, clean, dry and mix them and divide them like P1-15 into 4 samples of 2g each.

Each 2g sample was homogenized in 3 x 8ml HPLC-grade methanol (pooled). The extract was left to stand in the cold for 10 minutes and the crude supernatant was removed and retained. The remaining loose pellets were further extracted in 2 x 5ml methanol and then discarded, retaining the liquor. The total extract was divided between corex tubes and spun for 10 min. (5000 rpm). The supernatants were pooled, the centrifuge pellets were re-extracted in the same way, and the final extract was reduced to about 1ml (rotary evaporation). This material, including a freely-formed precipitate, was transferred in each case to an ampoule, evaporated to dryness under nitrogen and sealed in nitrogen for shipping to Munich.

2.24.2 GC-MF

Estimation of juvenile hormone content was performed by Professor Heinz Rembold (Martinsried, W. Germany) using glass capillary combined gas chromatography - selected ion monitoring mass spectrometry of derivatised juvenile hormones (Rembold et al., 1980). The procedure has been simplified (cf. Rembold, 1981) because of the high intensities and m/e values produced by this derivatisation (very similar to Bergot et al., 1981) and it need not involve HPLC. The derivatisation scheme is shown at Fig. 2.27. Briefly, the extracts were treated as follows by Professor Rembold:-

Break ampoules and take up extracts in methanol;
Add JH III-Et (Fig. 2.27) as internal standard;
Extract with ether - remove under Nitrogen;
Add Methanol/ether (1:1), cool on dry ice;
Centrifuge; wash precipitate; remove solvents under N_2;
Dissolve in ethyl acetate;
TLC (Silica-gel, 65:35 n-hexane/ethyl acetate);
Extract from silica-gel with ethyl acetate;
Sample (< 2mg) dissolved in nonafluorohexanol (NFH-OH)
Add NFH-OH/0.06% $HClO_4$; 30 min at room temp.;
Add ethyl acetate and remove NFH-OH under N_2 x 3;
TLC again;
Retrieve JH-derivative in ether or ethyl acetate;
(± TLC using CH_2Cl_2; sample > 1.5mg);e;
(+ TLC using CH_2Cl_2; sample > 1.5mg);
Add n-hexane;

Figure 2.27

JH derivatization (JHIII as example).

JHIII or analogue oxiran ring (1) is opened by the addition of alcohol (catalyst = perchloric acid) (2) and a C_{11} ether is produced (3) which shows a simple fragmentation pattern (///) yeilding fragments a-c. Esterification at C_{10} (4) can improve resolution in capillary-GC: The result is a 10-heptafluorobutyryloxy-11-nonafluorohexoxy-JH (JH- HFB-NFH). Internal standard = JH-analogous ethyl-10, 11-epoxyfarnesoate (JH-Et-NFH). Combining mass fragmentography with GC retention time allows JH 0-III to be identified and quantified in a single analysis:

		JHI-NFH	JHII-NFH	JHIII-NFH	JHIII-Et-NFH
GC t_R (min)		5.7	5.3	c. 4.4	(4.8)
m/e	a	319	319	305	(305)
	b	239	225	225	(239)
	c	207	193	193	(193)

Rel. Intensity

a	base peak
b	> 50%
c	> 40%

Reagents: n-1H, IH, 2H, 2H-perfluorohexanol (NFH-OH); heptafluorobutyrylimidazole (HFBI).

(From Rembold et al. 1980; Rembold, 1981; Rembold and Hagenguth, 1981).

Fig. 2.27

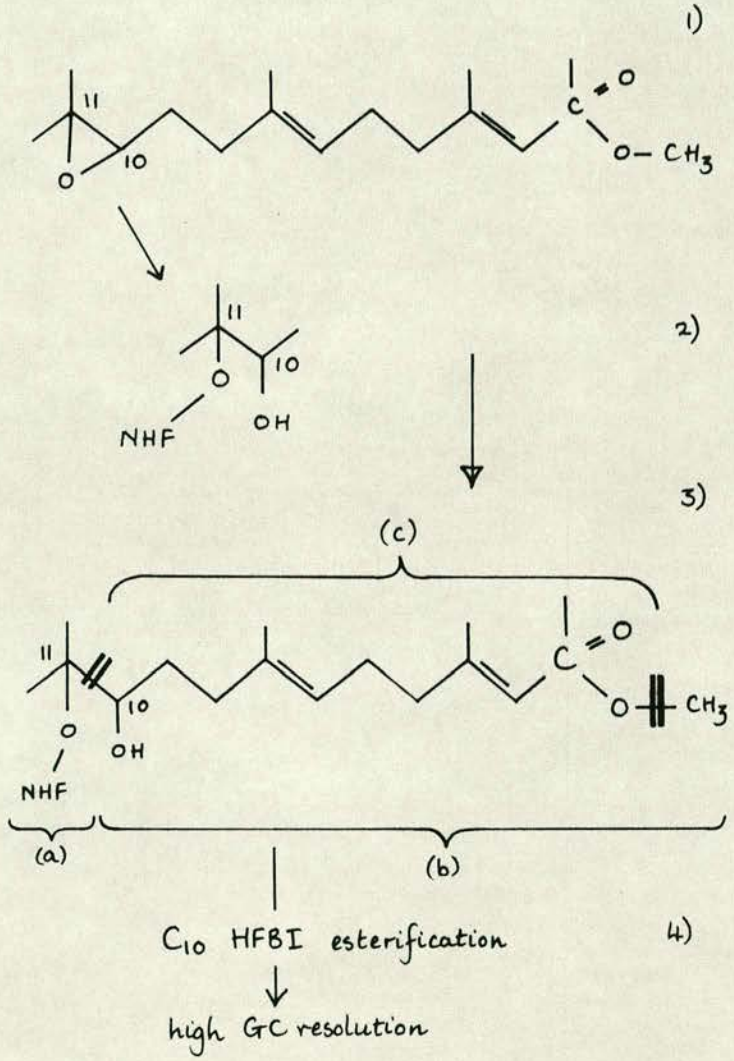
1)
11
10
O
C
O
O– CH3
2)
11
10
O
NHF
OH
3)
(c)
11
10
O
NHF
OH
C
O
O
CH3
(a)
(b)
C10 HFBI esterification
4)
high GC resolution

(± HPLC (samples = mg): n-hexane/12% ethyl ether 1.5ml/min over Lichrosorb Si 60, 5µm, UV absorption at 218nm);

GC-MF: 1440-Varian gas chromatograph with glass capillary column coated with SE 30 (250°C oven, 275°C injector, Helium 20cm/s) coupled with a Varian MAT mass spectrometer CH7A-DF (inlet 250°C, source 220°C, emission 2mA, 75eV, pressure 3×10^{-6} Torr).

(After Rembold et al., 1980).

Chapter Three

Description and timing of the stages of metamorphosis

3.1 Definition of the stages

Fifty-one changes were noted and their typical sequence determined by repeated observations at 25°C, (see Appendix A2). Only those changes which respect the sequence have been employed as criteria in devising this staging system,and in subsequent work animals which showed anomalous combinations of staging criteria were excluded from the analysis. Each stage is given a numerical and a verbal designation, and those features which are diagnostic of accession to the various stages are underlined.

The stages are illustrated systematically in Figs. 3.1-3.6 and a developmental series of photographs of whole animals is presented (Figs. 3.7-3.12) while photographic details of some staging criteria are given in Figs. 3.13-3.31. Events revealed by sectioning (taken from the literature) are given in Appendix A2.

Stage designation	Description (criteria underlined)	Figure
Third instar LARVA (LIII)	(Feeding or) still in food.	
LI (Post-feeding)	animal wandering on bottle wall; later, stops crawling (irreversibly).	3.1

L2 (Spiracles everted)	anterior spiracular papillae present (stationary); Puparation/puparium formation begins with withdrawal of anterior three segment; body shortens;	3.1
PREPUPAL period of LIII		
P1 (white)	animal fails to crawl when challenged with water; body short; stuck to glass; stops wriggling.	3.1, 7
P2 (Brown)	larval cuticle stiff and brown (completion of puparium formation); oval armature movements and heart-pumping stop.	3.1
P3 (Bubble)	abdominal gas bubble visible between lobes of fat-body; oval armature stationary; heart not pumping.	3.2, 22
(*Cryptocephalic, Pharate PUPA)	(*See Section 3.3.1 for explanation)	

P4 i (Buoyant)	animal floats on water; distinct opercular ridge; (puparium apolysed); trunk tracheae become obscured; abdominal contractions visible through puparium; everted imaginal discs visible.	3.2, 2
P4 ii (Moving bubble)	Pupa displaced forward inside puparium by gas pocket, and abdominal gas bubble disappears (c.P1+12 h at 25°C) (= "pupation"); gas moves to anterior; head everted; oval armature and tracheal connections expelled.	3.3, 24-26
(*Phanerocephalic, Pharate)	(*See Section 3.3.1 for explanation).	
PUPA:		
P5 i (Malphigian Tubules (Mts) migrating)	Bubble has moved to anterior and head has everted. Legs and wings visible. MTs visible at thorax/ abdomen junction. Best viewed in shadow of forceps.	3.4
P5 ii (White MTs)	MTs are invisible or may just be seen in shadow of forceps.	3.5-7

P6 (Green MTs) — Pair of MTs clearly visible in position on either side of dorsal mid-line, pale green elongated "initial segments". — 3.4

P7 ("Yellow body") — Dark green structure visible; moves from thorax/abdomen junction to lie between the MTs. (Later becomes very prominent). — 3.4

*Pharate ADULT: — (*See Section 3.3.1 for explanation)

P8 (Yellow-eyed) — Perimeter ofeye, then whole eye pale yellow, later bright yellow. — 3.5,11,27

P9 (Amber) — Eye pale brownish colour; colour deepens. — 3.5,12

P10 (Red-eye bald) — Eye perimeter pink, then whole eye bright red. No bristles visible. — 3.5

P11 i (Head Bristles) — Major head bristles have darkened to visibility through puparium. — 3.5

P11 ii (Thoracic Bristles) — Microchaetes, then macrocheates visible dorsally on thorax. — 3.6, 28,29

P12 i (Wing tips grey)	"Tips" of folded wings very pale grey.	3.6, 13-15
P12 ii (Wings grey)	Abdominal tergite bristles visible; Wings grey; Sex comb darkens.	3.6
P13 (Wings black)	(Sex comb visible). Wings very dark.	3.6, 16-18, 30,31
P14 (Mature bristles)	Tarsal bristles have darkened and claws are black. Flies may twitch their legs.	3.6,19, 20.
P15 i (Meconium)	Green patch visible dorsally at tip of abdomen; MTs and yellow body become obscured.	3.6, 21
P15 ii (Eclosion)	Ptilinum expands, opening operculum; Fly emerging. (c. P1+100 h at 25°C).	

Exarate ADULT:

A1 (Newly-enclosed)	Adult has emerged; Abdomen elongated plus pale; Wings still folded.	3.30
A2 (Wings extended)	Wings extended plus hardened; Abdomen adult in shape.	

Figures 3.1-3.6

Diagrammatic representations of the visible events observed during metamorphosis. Segments of individual figures are presented in reading order: a, b, c, d. Not all changes are employed as criteria for staging (numbers in parentheses correspond to the series of 51 visible changes listed at Appendix A2 and are included here to indicate the sequence of events). Figs. 3.1-5 are dorsal views, Fig. 3.6 ventral.

Figure 3.1

Stages L1 (Post-feeding) to P2 (Brown). The left side shows half of the uncontracted late third instar larva, drawn the same length as its other half a few hours later, which is shown on the right. Thus the boundary divides the drawing unequally, and the two halves are not to scale.

Figure 3.2

Stages P3 (Bubble) to P4 (Buoyant). The bubble which appears within the abdomen is shown, firstly small, and often to one side of the animal, and secondly large and visible dorsally. Contracting muscles are seen stretched across the surface of the bubble.

Fig. 3.1

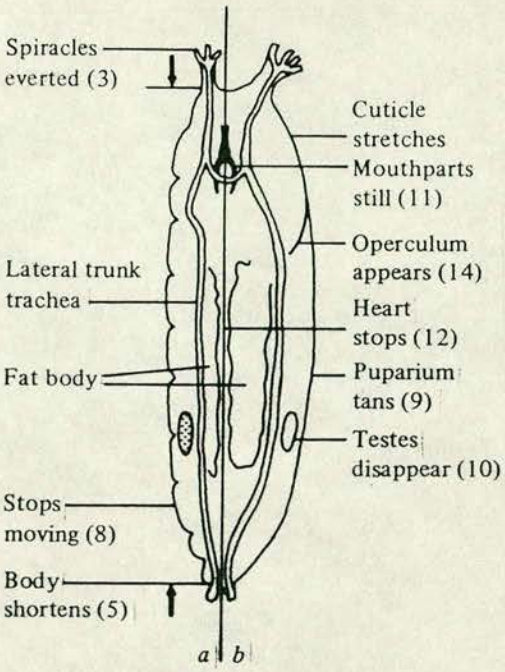
Spiracles everted (3)
Cuticle stretches
Mouthparts still (11)
Operculum appears (14)
Lateral trunk trachea
Heart stops (12)
Fat body
Puparium tans (9)
Testes disappear (10)
Stops moving (8)
Body shortens (5)
a
b

Fig. 3.2

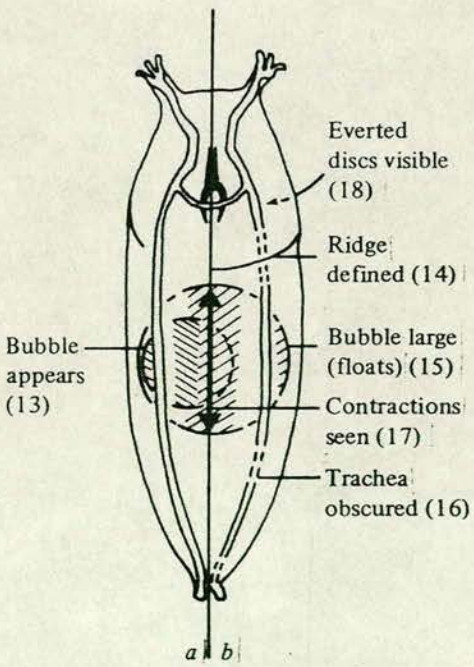
Everted discs visible (18)
Ridge defined (14)
Bubble appears (13)
Bubble large (floats) (15)
Contractions seen (17)
Trachea obscured (16)
a
b

Figure 3.3

Stages P4 (Moving Bubble) to P5.

The pupa is shown in two positions within the puparium, firstly at the anterior end during shedding of the posterior tracheal linings, and secondly in its final position after displacement of gas to the anterior end (see also Figs. 3.24-26) and head eversion have occurred. All tracheal connections with the outside of the puparium are broken. The arrow represents ventral extension of the appendages by hydrostatic pressure. The pupal spiracle marks the insertion of the lateral trunk trachea in the larva/pupa.

Figure 3.4

Stages P5 (Malphigian tubules migrating) to P7 ("Yellow body").

The white enlarged initial segments of the anterior Malphigian tubules (MTs) are first visible in the thorax but move through the constriction into the abdomen where they may at first be completely obscured. Later, they become faintly visible again and eventually turn green. The "yellow body" appears at the thorax-abdomen junction as a dark shadow and is most prominent after moving to lie between the MTs.

Fig. 3.3

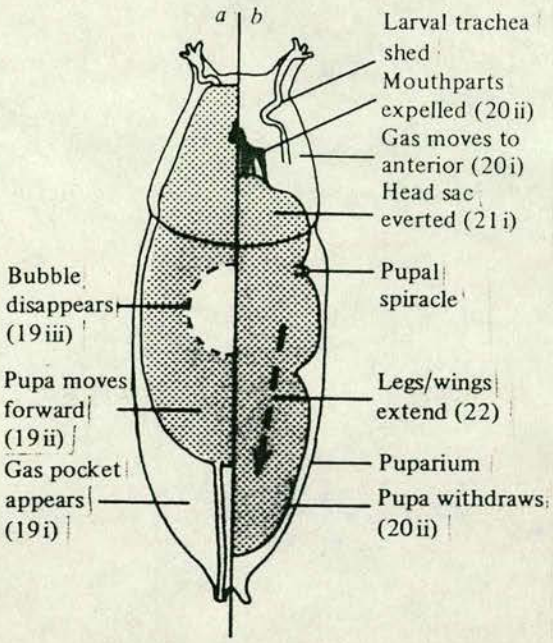
a
b
Larval trachea shed
Mouthparts expelled (20ii)
Gas moves to anterior (20i)
Head sac everted (21i)
Pupal spiracle
Bubble disappears (19iii)
Pupa moves forward (19ii)
Gas pocket appears (19i)
Legs/wings extend (22)
Puparium
Pupa withdraws (20ii)

Fig 3.4

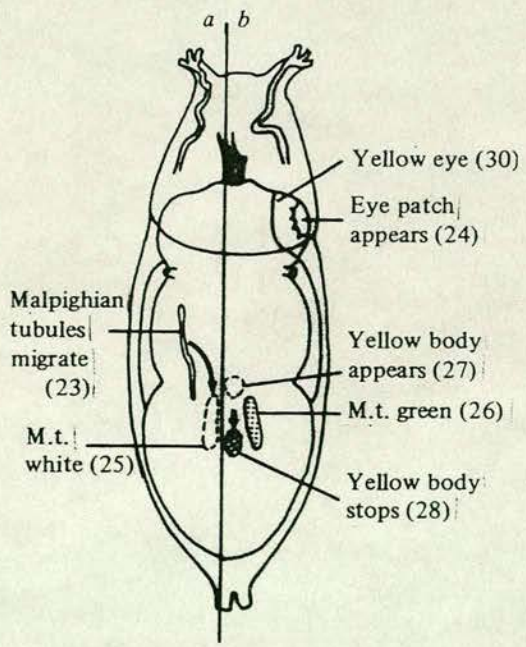
a
b
Yellow eye (30)
Eye patch appears (24)
Malpighian tubules migrate (23)
Yellow body appears (27)
M.t. green (26)
M.t. white (25)
Yellow body stops (28)

Figure 3.5

Stages P8 (Yellow-eyed) to P11 (Thoracic bristles)

Pigmentation of the eye begins with the yellowing of the perimeter. The rest of the eye colours (P8) and later darkens to amber (P9). The perimeter followed by the whole eye becomes pink at the beginning of P10 and this colour darkens to the mature bright red of adults (P10).

Figure 3.6

Stages P11 to P15 (Meconium)

The "distal" part of the folded wing blade becomes grey (P12(i)), then the whole blade darkens (P12(ii)). The wings then undergo further darkening to appear black when folded, usually beginning with the "distal" part again (P13). Tanning of the sex comb in P12(ii) allows one to separate the sexes from now on instead of sexing prepupae. Tarsal claws do not darken until P14 when the legs may also begin to twitch. The meconium appears dorsally as a green patch (P15(i)) which persists until eclosion (P15(ii)). Then, the ptilinum, an extensible sac between the eyes, is expanded by hydrostatic pressure from the contracting abdomen. The operculum breaks open anteriorly, the fly emerges and the ptilinum contracts while the abdomen shortens and widens (A1). The wings are unfurled (A2) and the banding of the abdomen becomes distinct (A3).

Fig. 3.5

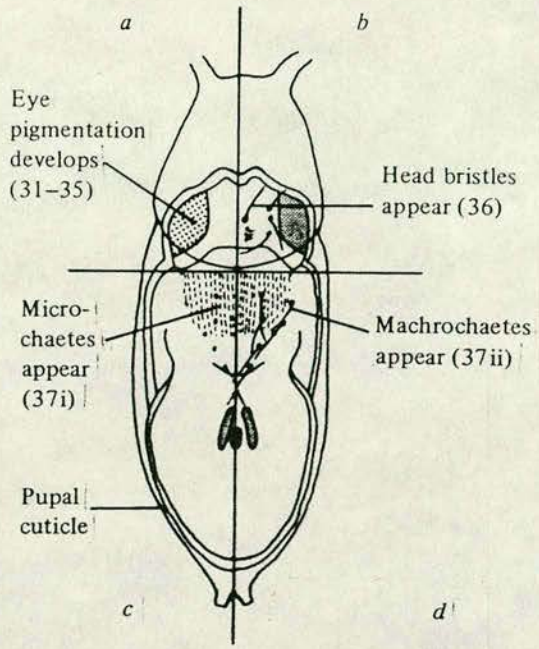
a
b
Eye pigmentation develops (31–35)
Head bristles appear (36)
Micro-chaetes appear (37i)
Machrochaetes appear (37ii)
Pupal cuticle
c
d

Fig. 3.6

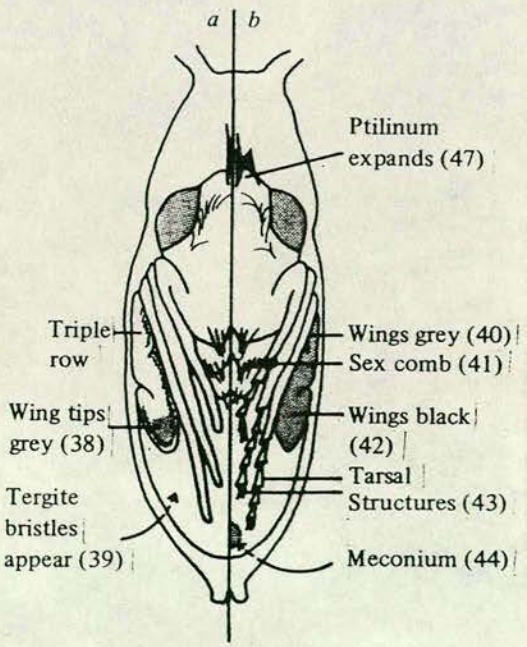
a
b
Ptilinum expands (47)
Triple row
Wings grey (40)
Sex comb (41)
Wing tips grey (38)
Wings black (42)
Tarsal Structures (43)
Tergite bristles appear (39)
Meconium (44)

Figure 3.7

Female of Stage P1 (white), dorsal view

Everted anterior spiracle (as); fat body (fb); lateral trunk trachea (t). Scale smaller than subsequent figures - contraction of the cuticle is incomplete.

Figures 3.8-10

Stage P5 ii (white Malphigian tubules), dorsal, lateral and ventral aspects respectively, after removal of the puparium. Pupal morphogenesis is complete. Fat body cells (fb) have entered the wing pouches by hydrostatic pressure and line the hypoderm except in the middle of the eye (e). Malphigian tubules must be viewed in shadow at this stage. The first signs of the "yellow body" (yb) are visible here but it will move posteriorly by stage P7. The pupal spiracles (ps) were severed from the anterior larval spiracles at head eversion (P4/5). Pupal cuticle (pc); gas pockets (g) adhering to pc.

Figure 3.11

Stage P8 (Yellow-eyed), lateral view

Yellow pigment defines the extent of the compound eye. Abdominal segment margins (s) would not be distinct through the puparium.

Figure 3.12

Stage P9 (Amber), lateral view. Eye colour has darkened. The wing is visibly folded within its sleeve of pupal cuticle (w).

Figs 3.7 – 3.12

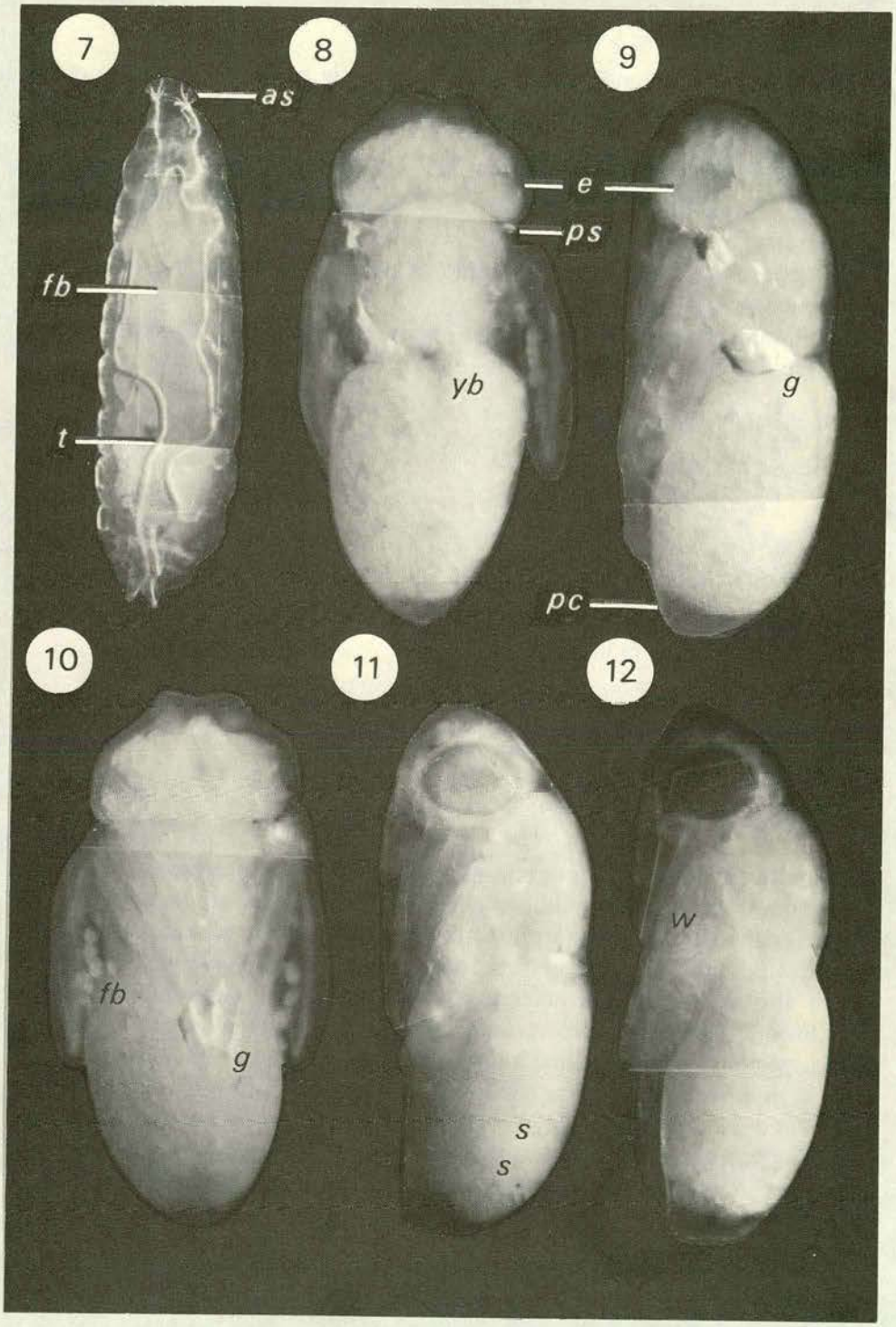

Figures 3.13-15

Stage P12 i (Wing-tips grey), dorsal lateral and ventral views respectively. Macrochaetes along the posterior margins of the abdominal tergites are beginning to darken (m). The wing hinge region (h) is untanned while the distal blade has darkened (db). Triple row (tr); dark proximal leg bristles (1); untanned tarsi (t).

Figure 3.16

Early stage P13 (Wings black), lateral view. The wing has darkened further. Macrochaetes of tergites 2 to 6 (m).

Figures 3.17 and 3.18

Late stage P13 (wings black), lateral and dorsal views respectively. The whole wing is deeply-tanned. After the pupal-adult apolysis, the degradation of the pupal cuticle (pc) continues. Here it is torn during removal of the puparium. At eclosion it is left inside the puparium. The Malphigian tubules and yellow body are no longer prominent. Tergite macrochaetes are very dark (m).

Figs 3.13 – 3.18

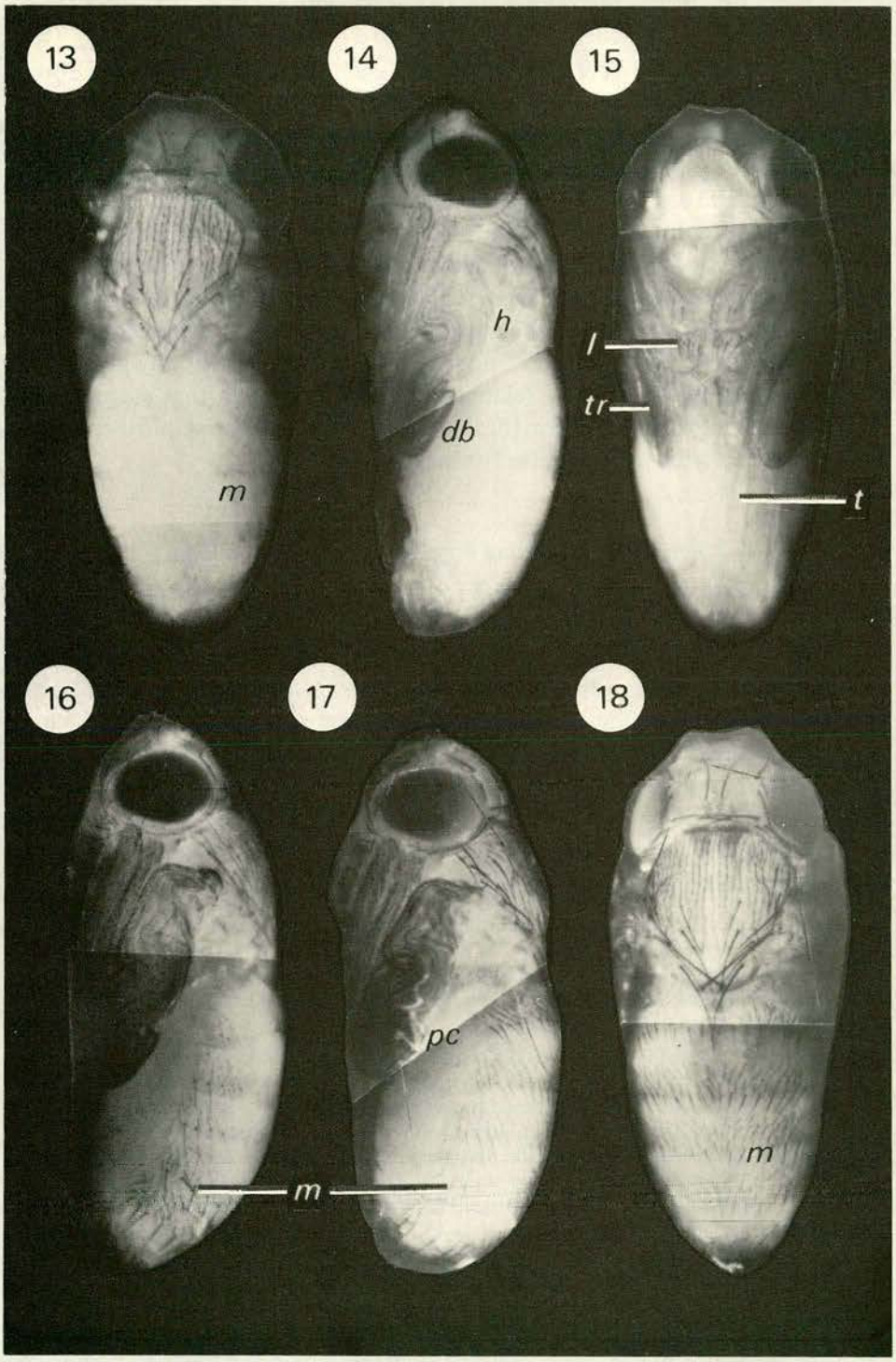

Figures 3.19 and 3.20

Stage P14 (Mature bristles), female and male ventral aspects respectively. Tarsal bristles (t), claws (c), sex comb (sc) and triple row (tr) are black. The genital disc derivatives are obscured by the posterior spiracular papillae until the puparium is removed.

Figure 3.21

Stage P15 i (meconium), dorsal view. The meconium (m) is a pale green patch. It will be expelled soon after eclosion (A1) or sometimes inside the puparium during eclosion (P15 ii). It is composed of fluid derived from the "yellow body" (Robertson, 1936).

Figure 3.22

The appearance of the translucent testes (g) of the larva/prepupa, seen here still visible in Stage 3 (Bubble) and distinct from the gas bubble (b). The ovaries are indistinguishable from fat body. Later view.

Figure 3.23

The gas bubble (b) in an animal from Stage P4 i (Buoyant), lying between and beneath the lobes of the fat body. The lateral trunk tracheae are still intact and, since head eversion has yet to occur, the pupa is cryptocephalic. Opercular ridge (or). Dorsal view.

Figures 3.24-3.26

Show pupal morphogenesis of the head and thorax in Stage P4 ii (Moving bubble).

Figure 3.24

Gas bubble movements within the puparium, and head eversion, unequal time-lapse series. Dorsal view. The first three photographs represent 1 min, and the whole process takes from 2-10 mins. Note the absence of a gas bubble. Posterior gas chamber (pgc); posterior tracheal lining (pt); gas pocket (p); larval oval armature (oa); anterior tracheal lining (at); anterior gas chamber (agc).

Figs 3.19 – 3.24

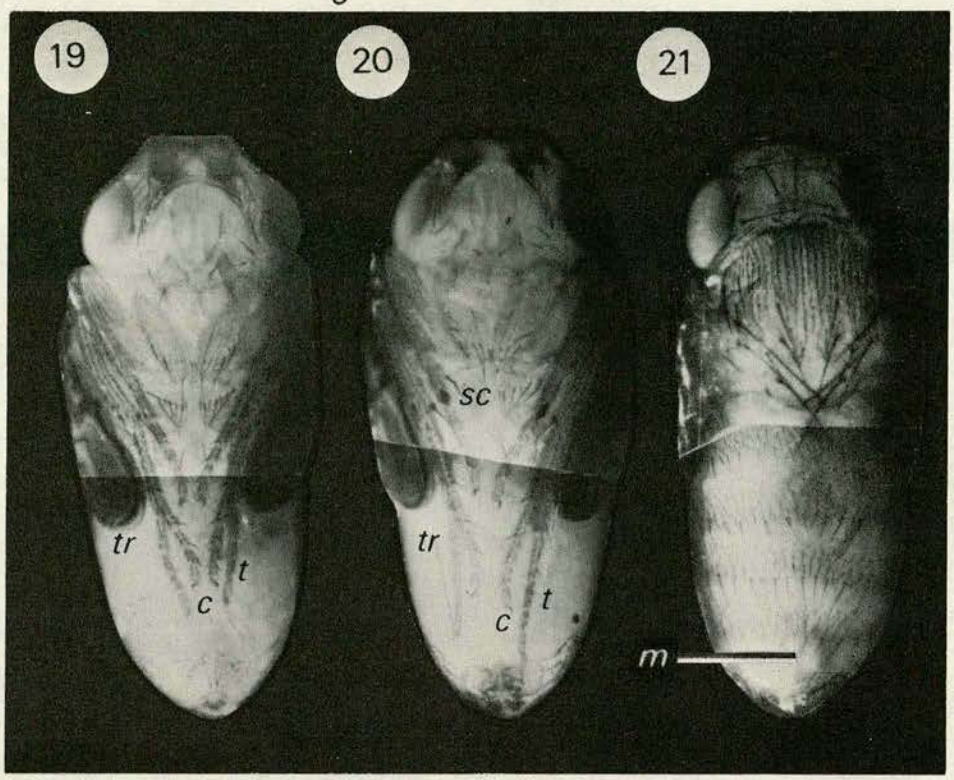

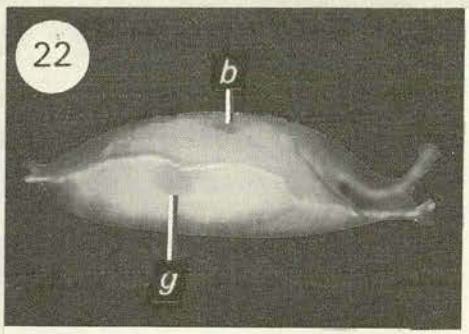

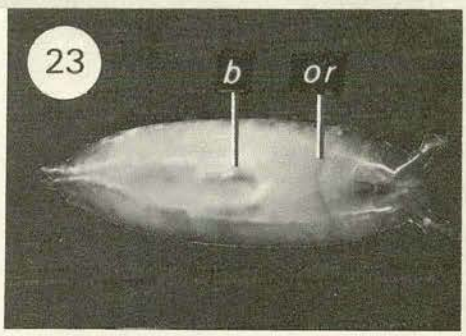

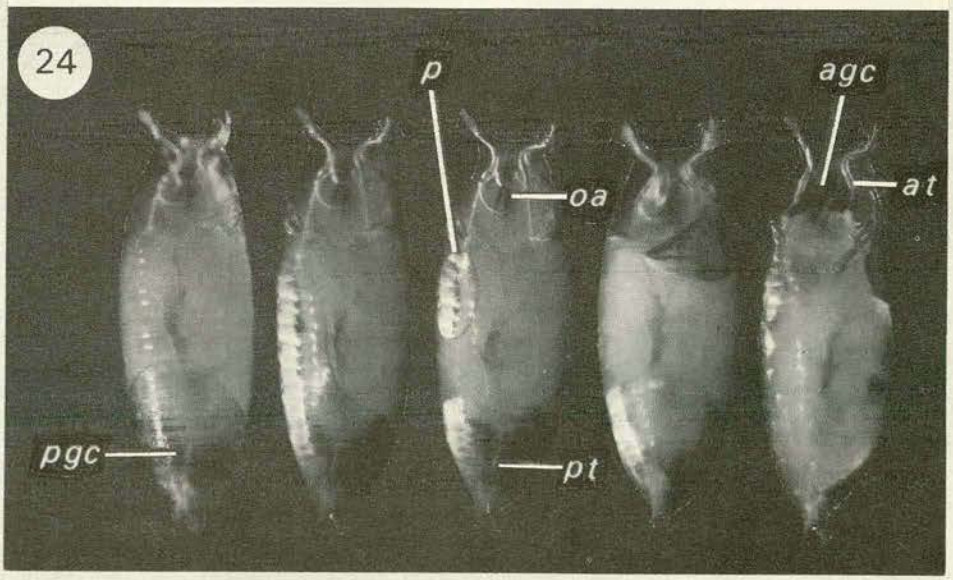

Figure 3.25

Drosophila "pupation": Diagrammatic interpretation of the morphogenetic events of stage P4 ii shown at Fig. 3.24. Numbered arrows represent the sequence of events: (1) The bubble within the animal disappears as (2) the posterior gas chamber develops inside the puparium and the animal moves accordingly toward the anterior spiracles. As a result, the posterior linings of the lateral trunk tracheae are stretched across the chamber and so are shed (Robertson, 1936; Whitten, 1957 a and b). Tracheal connections shown are schematic, and gas may also exit through more anterior abdominal ecdysial openings (Whitten 1957a). (3) The gas is shunted forward by slow wriggling using the larval abdominal muscles. Small pockets of gas pass between the pupal cuticle and the larval endocuticle or lining of the puparium (formerly called the "prepupal cuticle"; Robertson, 1936, Poodry and Schneiderman, 1970), thus effecting the dissociation of the larval and pupal cuticles. The pupal cuticle is already continuous and rather tough. (4) The increase in size of the anterior gas chamber is accompanied by the backward-displacement of the pupa (5) and the withdrawal of the anterior tracheal linings. These and subsequent changes are independent of all the spiracles (Robertson, 1936) and the pupa now has no tracheal connections with the puparium. Pupal spiracles mark the sites of connections to the larval anterior spiracular papillae, (see Fig. 3.8). (6) By sudden muscular contractions haemolymph and dissociated larval fat body is pumped into the folded head sac, which then everts into the anterior gas chamber. The larval oral armature is expelled and lies ventrally

inside the puparium. X-X marks the level of the antennal hypoderm within the puparium. The leg and wing discs, which are already evaginated, evert more slowly and extend along the abdomen during Stage P5 i to reach their pupal/adult positions (see Fig. 3.10).

Fig 3.25

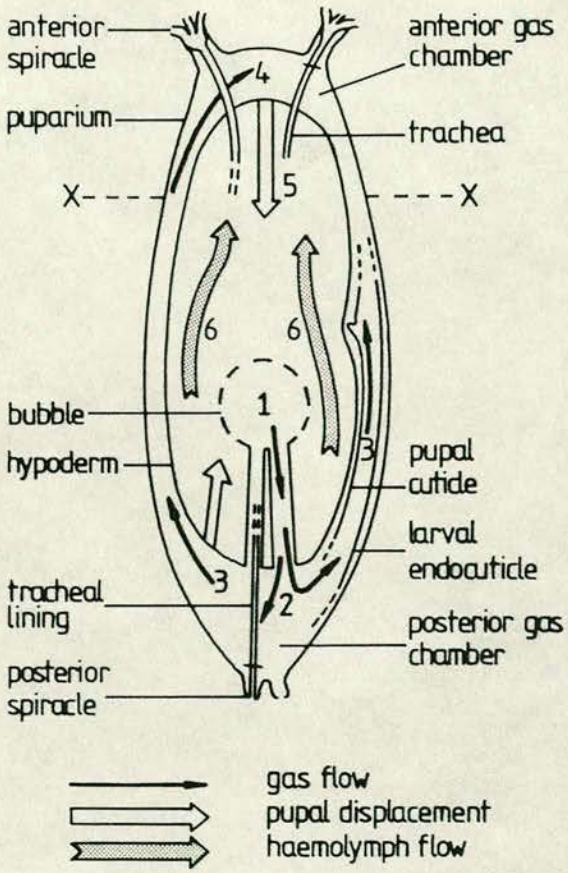
anterior spiracle
puparium
X
X
bubble
hypoderm
tracheal lining
posterior spiracle
anterior gas chamber
trachea
pupal cuticle
larval endocuticle
posterior gas chamber
1
2
3
3
4
5
6
6
gas flow
pupal displacement
haemolymph flow

Figures 3.26-3.28

Fig 3.26 State of the thoracic imaginal discs towards the end of pupal morphogenesis, stage P4 ii. The complex of fused discs with its continuous layer of pupal cuticle has been dissected out of the puparium. Evertion of legs (1) and wings (w) by hydrostatic pressure is incomplete. In the intact pupa, the anterior region is translucent while the abdominal hypoderm, of larval origin, is opaque.

Fig. 3.27 Displayed visceral dissection of the pupa shown at Fig. 3.11 to show the Malphigian tubules and "yellow body" in Stage P8 (yellow- eyed). Dissection performed in 1% agar. Enlarged initial segments (i) of the anterior pair of Malphigian tubules join the more slender posterior pair (p) which are invisible in the intact animal. The "yellow body" (yb) is the imaginal mid-intestine containing the larval mid- intestine, gastric caecae and proventriculus (Bodenstein, 1950).

Fig. 3.28 Relationship between the Malphigian tubules (Mt) and the "yellow body" (yb) in situ. Dorsal view, stage P11 ii (Thoracic bristles). These structures are by now distinctly green. Note also the orbital and ocellular bristles, and the dark (i.e. red) eyes. Reflections are due to gas trapped beneath the puparium.

Figures 3.29-3.31

Fig. 3.29 Mature relationship between the green Malphigian tubulues (Mt) and the "yellow body" (yb, almost black) in their most prominent condition in a Stage P11 (ii) animal before they begin to be obscured. Dorsal thoracic macrochaetes (dtm).

Fig. 3.30 Folding of the imaginal wing before eclosion. the puparium and pupal cuticle of the pharate adult shown at Fig. 3.16 (Stage P13 Wings black) have been removed, allowing the wing blade to unfurl prematurely. Compare Fig. 3.31.

Fig. 3.31 Comparison of the sexes after the darkening of the male-specific sex comb (sc) in Stage P12 ii. Ventro-lateral views, early Stage P13 (Wings black). The wings are blackening disto-proximally. Droplets of water line the puparium.

Figs 3.26 – 3.31

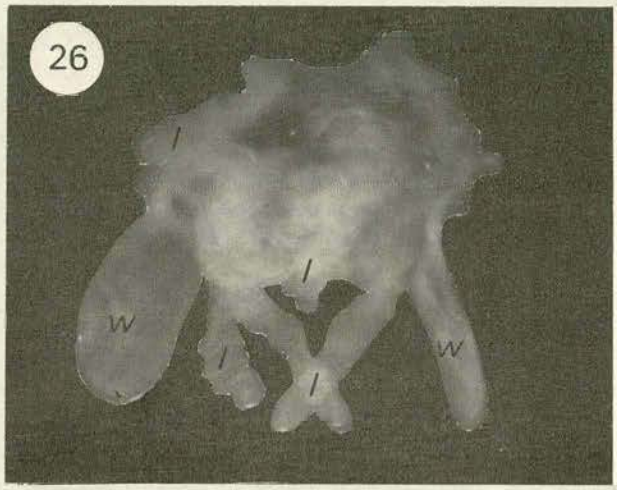

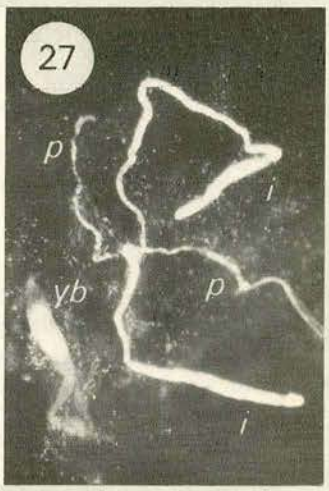

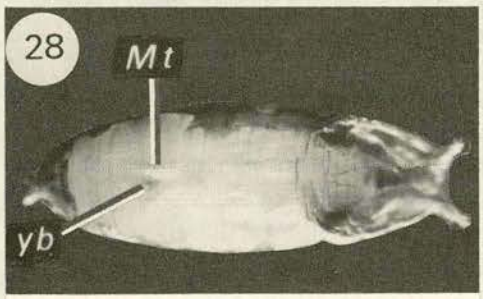

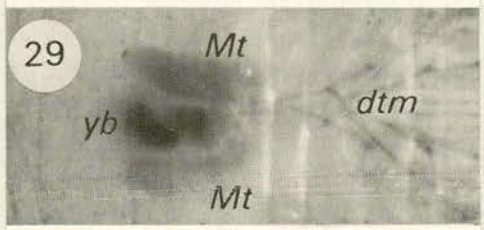

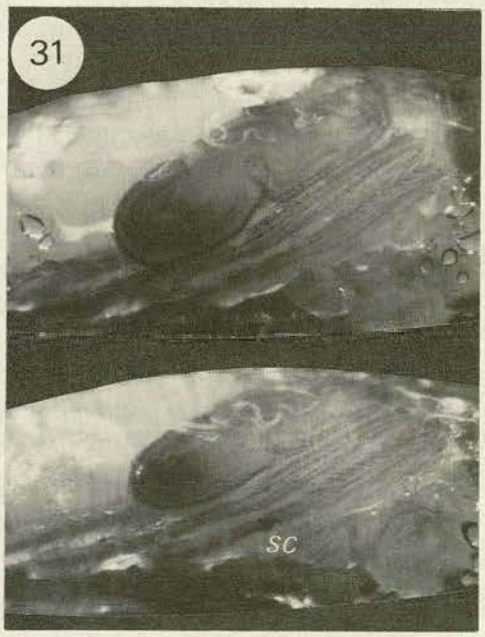

A3 (Tergites tanned) Abdominal tergites tanned

through grey to shiney brown

3.2 Differentation of cuticles during metamorphosis

The pupal cuticle is featureless and transparent throughout metamorphosis, though its texture changes after the pupal-adult apolysis. Its chemical composition appears to change during the period P4 ii - P15, (Appendix A3). The adult cuticle which develops underneath it bears markers, some of which make useful staging criteria. The abdominal bristles, however, were found not to darken reliably in stage P12 (i) and appeared asynchronously across the abdomen, eg. on the second tergite first, then along the flanks then dorsally. (This may be related to Trepte's observation (1980) that in Sarcophaga the chromosome puffing-pattern of bristle cells and the associated differentation of bristles are autonomous in various regions of the body).

The darkening of the tarsi is less variable, although it is not restricted to P13; but the darkening of leg cuticle does follow a sequence in which the tarsi come last, whereas the tarsal claws come first in order of morphogenesis on the young adult leg (distal to proximal; Figs. 3.32 - 3.37).

Darkening of the cuticle on both leg and wing seems to begin medially and proceeds proximo-distally (Figs. 3.35-3.37); which is exactly the reverse of the order of acquisition of competence to differentiate shown by leg imaginal discs taken from larvae and put

Figures 3.32-3.37

Adult cuticle differentiation (Nomarski phase interference micrographs)

Fig. 3.32 Thoracic appendages of early pupa (early P5-7). Legs ( ) and wings (w) fully evaginated. No adult cuticle or bristle morphology visible beneath pupal cuticle (pc). Magnification x 476.

Fig. 3.33 Tarsal morphogenesis in young pupa (P6-7). Claws (c) formed. pc; pupal cuticle. X 717.

Fig. 3.34 Wing blade tip (unfolded) from pupa (P7). Hairs (h) on posterior margin but no cuticle melanisation. Perforated pupal cuticle, pc. x 717.

Fig. 3.35 Wing from young pharate adult (P8) folded inside pupal cuticle (pc). d; distal blade; p, proximal blade. Hairs (h) absent proximally on margin; melanisation (m) of adult cuticle occurs first in mid-blade. x 249.

Fig. 3.36 Progressive melanisation disto- proximally from middle of stage P8 wing. Marginal hairs (h) present proximally x 249.

Fig. 3.37 Thoracic appendages, Partly- differentiated cuticle, P8. Wing blade (w) melanised but not tarsi (t), which bear bristles; femur (f) and tibia (ti) do not. pupal cuticle, p.c. x 311.

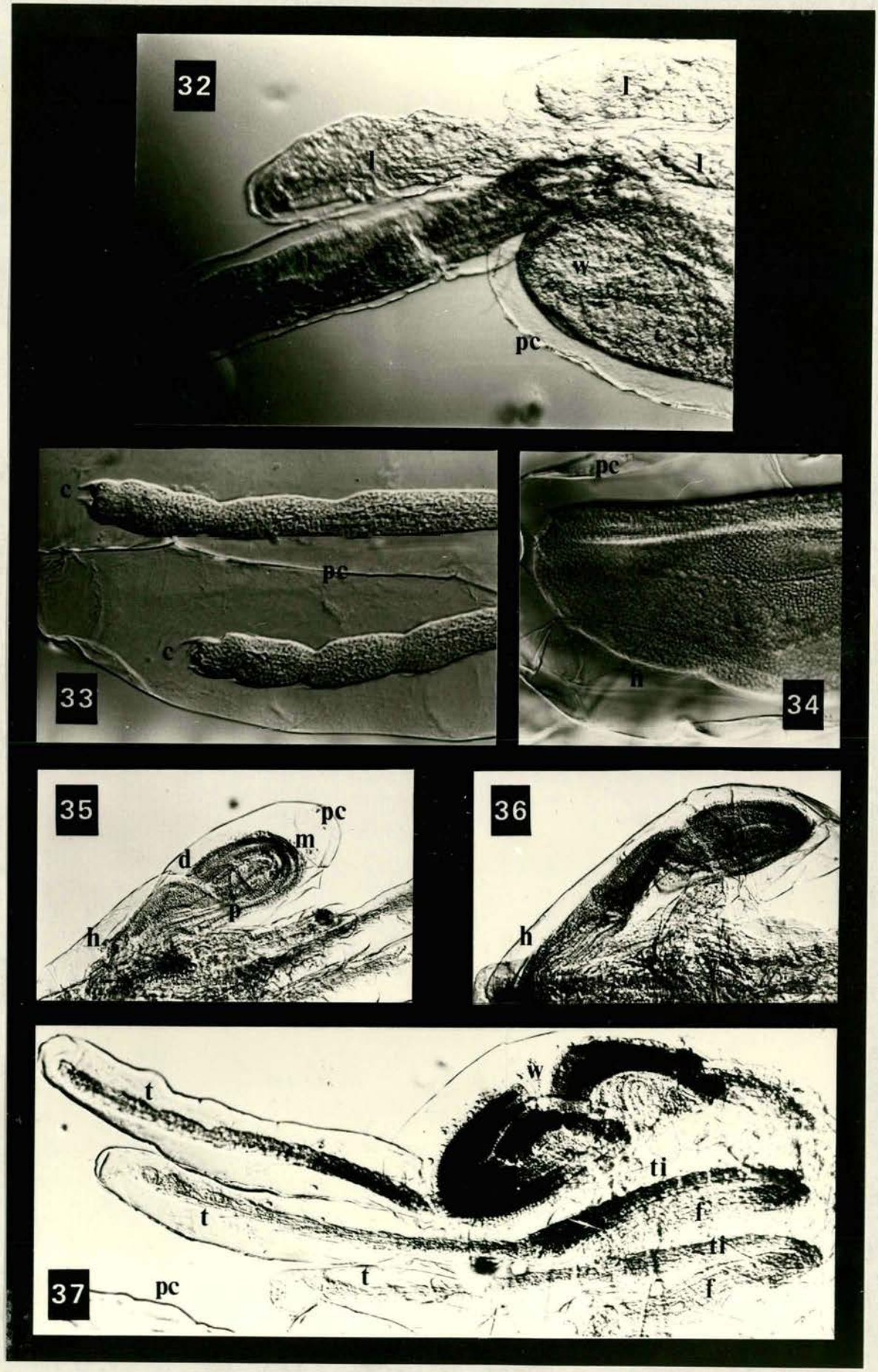
32
l
l
l
w
c
pc
c
pc
c
33
pc
n
34
35
pc
m
d
p
h
36
h
37
t
t
t
pc
w
ti
f
ti
f

through metamorphosis prematurely - i.e. disto-proximal to medial (Schubiger, 1974).

The wings are folded inside the pupal cuticle, so apparent darkening of the "tips" diagnostic of P12 (i) represents medial tanning or melanisation. Eventual darkening of the tarsal cuticle constitutes accession to P14.

3.3 Timing the stages of metamorphosis at 25°C

Two sources of data were employed to estimate typical stage transition times - direct timings of pupation-plate cultures to establish extreme timings at 25°C (See 2.2, cf. 3.1) and frequency-estimates (Section 2.3 and ff.).

3.3.1 Estimation of durations of stages L1-A2 by frequency

Adult females in new culture bottles will not lay continuously for a period equal to that of metamorphosis; so animals were scored from cultures of four ages, namely 11,12, 13, and 14 days. These cultures contained both first generation adults in stage A3 and postfeeding larvae (stage L1).

Since laying commenced on day 0 and eclosion on day 10, the composite population approximated to a continuous age distribution, and mean percentage frequencies were then obtained for each stage within it. Table 3.1 shows the sampling procedure and the proportions L:P:A involved.

TABLE 3.I Sampling Procedure

Days after oviposition begins:		11	12	13	14	Mean
L1-A3 (Total = 2286)		367	688	373	858	571.5
Sample size (= 100%)		159	140	196	119	
Classes within sample:						
L%		3.1	5.7	2.5	1.7	3.25%
P%		93.1	88.6	71.5	44.5	74.4%
	(Total*)	(148)	(124)	(140)	(53)	
A%	Female	3.2	2.9	18.4	30.3	13.7%
	Male	0.6	2.8	7.6	23.5	8.6%
	Total	3.8	5.7	26.0	53.8	22.3%

*These values become 100% in Table 3.II (q.v.).

Table 3.II shows the frequencies of each stage in the various cultures, and frequency-means. To make it possible to relate these frequencies to a known time-span at 25°C the scores for all stages (L1-A2) are expressed as percentages of the total P1-P15 taken from Table 3.I (*). The time taken from pupariation to eclosion was estimated from the observation of pupation plates. The mid-point of the range of eclosion times was about 100h, that for females being 98 (93-103h) and that for males 102 (98-106h) a difference of 4h which is in agreement with that reported by Powsner (1935), (3.7h at 25°C). So for a mixed-sex population the approximate duration of the period P1-P15 is 100 h. Assuming that the frequency of any given stage in a continuous sample is directly related to the time spent in that stage, then a stage frequency of 1% indicates a duration for that stage of 1 hour. This principle is applied in Table 3.III where cummulative mean percentages suggest a timecourse for metamorphosis which is compared with extremes of the direct (timed) observations. Where the two sets of data are contradictory, i.e. an estimated transition-time lies beyond the observed time-limits, priority is given to the latter. The resulting timecourse of metamorphosis is presented in Table 3.IV and is recalculated there for each sex. These values form the basis for estimates of stage durations in all subsequent experiments.

The estimated duration of L1 may be too low because during the period of scoring for frequency ($\leqslant$ 1h) all other stages could, given development proceeding normally, loose individuals to their

TABLE 3.II Frequencies of Stages L1-A2, expressed as precentages of Total P (i.e. P1-P15; See Table 3.I*)

Day after oviposition begins:	11	12	13	14	Mean%
Total P	148	124	140	53	
Stage:					
L1	2.0	5.6	3.6	3.8	3.8
L2	1.4	0.8	0	0	0.5
P1	0	0.8	2.1	3.8	1.7
P2	1.4	3.2	2.1	5.7	3.1
P3	0.7	2.4	0.7	0	1.0
P4 i	3.4	1.6	4.3	0	2.2
P4 ii	0	0	0.7	0	0.2
P5 i	0.7	0	0	3.8	1.1
P5 ii	8.8	7.3	12.1	9.4	9.4
P6	14.9	27.4	10.7	1.9	13.7
P7	23.6	16.1	2.1	5.7	11.9
P8	20.3	19.4	5.7	3.8	12.3
P9	17.6	12.9	14.3	11.3	14.0
P10	0.7	0.8	1.4	13.2	4.0
P11 i	0	0.8	0.7	3.8	1.3
P11 ii	0	0	0.7	1.9	0.7
P12 i	0	0.8	0.7	1.9	0.9
P12 ii	0.7	1.6	2.1	0	1.1
P13	2.7	0	2.8	7.6	3.3
P14	4.1	2.4	15.0	16.9	9.6
P15 i	0.7	1.6	20.7	9.4	8.1
P15 ii	0	0.8	0.7	0	0.4
A1	0	0	4.2	3.8	2.0
A2	0	0.8	8.6	45.3	13.7
					Total P = 100%

TABLE 3.III Stage frequencies cf. extremes of timed observations

Stage	% P1-15	+%'s	Observed end-stage transition times (L2/P1+h)		Data fail to correspond (X)
			Extremes	Typically	
(L.111)		- 4.3			
L1	3.8	- 0.5	-		
L2	0.5	0	-		
P1	1.7	+ 1.7	0.3-1.0	.3	X
P2	3.1	4.8	0.3-3.0	2.0	X
P3	1.0	5.8	6.5-7.0	6.75	X
P4 i	2.2	8.0	12-13.5	12	X
P4 ii	0.2	8.2*	12-13.5	12.2	X
P5 i	1.1	9.3	13-48	13.3	X
P5 ii	9.4	18.7	13-48		
P6	13.7	32.4	25-46		
P7	11.9	44.3	43-47		
P8	12.3	56.6	49-57		
P9	14.0	70.6	71-78	74.5	X
P10	4.0	74.6	71-77		
P11 i	1.3	75.9	72.5-77		
P11 ii	0.7	76.6	-		
P12 i	0.9	77.5	73-78		
P12 ii	1.1	78.6	75-86		
P13	3.3	81.9	-		
P14	9.6	91.5	87-103		
P15 i	8.1	99.6	93-c.105		
P15 ii	0.4	100.0	-		
A1	2.0	102.0	(P15/A1+0.5)	100.5	X
A2	13.7	115.7	-		

* anomalous value - see text.

TABLE 3.IV Stage transition times calculated from both frequencies and ages of stages L1-A2 at 25°C

Stage	P1-15 incl =	FM estimated stage duration (h) 100	Cumulative times stage ends (h) FM 100	F 98	M 102
Third instar larva (LIII)		-	-4.3	-4.2	-4.4
L1	(Post-feeding)	3.8	-0.5	-0.5	-0.5
L2	(Spiracles everted)	0.5	0	0	0
Prepupa					
P1	(white)	0.3	+.3	+0.3	+0.3
P2	(brown)	1.7	2.0	2.0	2.0
P3	(Bubble)	4.75	6.75	6.7	6.8
(Cryptocephalic pupa)					
P4 i	(Buoyant)	5.25	12	11.8	12.2
P4 ii	(Moving bubble)	0.2	12.2	12.0	12.4
P4		5.45			
Phanerocephalic) Pupa					
P5 i	(Mts.* migrating)	1.1	13.3	13.1	13.5
P5 ii	(White Mts.)	5.4	18.7	18.4	19.0
P5		6.5			
P6	(Green Mts.)	13.7	32.4	31.8	33.0
P7	("Yellow body")	11.9	44.3	43.5	45.1
Pharate Adult					
P8	(Yellow-eyed)	12.3	56.6	55.5	57.6
P9	(Amber)	17.9	74.5	73.0	75.9
P10	(Red eye bald)	0.1	74.6	73.1	76.0
P11 i	(Head bristles)	1.3	75.9	74.4	77.3
P11 ii	(Thoracic bristles)	0.7	76.6	75.1	78.0
P11		2.0			
P12 i	(Wing tips grey)	0.9	77.5	76.0	78.9
P12 ii	(Wings grey)	1.1	78.6	77.1	80.0
P12		2.0			
P13	(Wings black)	3.3	81.9	80.3	83.4
P14	(Mature bristles)	9.6	91.5	89.7	93.3
P15 i	(Meconium)	8.1	99.6	97.6	101.6
P15 ii	(Eclosion)	0.4	100.0	98.0	102.0
P15		8.5			
Exarate Adult					
A1	(Newly-eclosed)	0.5	100.5		102.5
A2	(Wings extended)	15.2	115.7		118.0

* = Malphigian tubules (Mts.) F = female M = male

successors and themselves be supplied with new members from the preceding stage; but since no food was collected there were no LIIIs to maintain the frequency of L1 constant. (But note that the population was washed briefly before scoring - see 3.5.1 - so development may have been arrested before the stages were recorded).

Table 3.IV shows metamorphosis divided into larval, prepupal, pupal (cryptocephalic and phanerocephalic) and adult (pharate and exarate) phases. These distinctions refer to the status of the various cuticles and derive from reported timings and definitions of the larval-pupal and pupal-adult apolyses.

The prepupa is merely a very distinctive phase of the last larval instar, not a discrete stadium, (it has no unique cuticle). Pupal cuticle has been distinguished in electron micrographs at about 3h after pupariation (Poodry and Schneiderman, 1970) i.e. c.P3. Fraenkel and Bhaskaran (1973) place the start of apolysis of the larval cuticle at 4-6h (P3), beginning anteriorly; (but note that the beginning of an apolysis may only be recognisable using the electron microscope (Delachambre et al., 1980); and presumably apolysis precedes any secretion of specifically pupal cuticle). The resulting pupa is cryptocephalic until eversion of the head sac at P4 (ii). This change is accomplished with much wriggling inside the puparium (Figs. 3.24 and 3.25) and involves the shedding of the larval tracheal linings (Whitten, 1957), so it resembles a more conventional ecdysis; and, by analogy with other ecdyses, pupation (P4 ii) is often referred to as "pupal ecdysis" or "the pupal moult".* Pupation does not really mark the beginning of the pupa,

however, unless we consider the sliding of the pupal cuticle beneath the overlying larval endocuticle lining the puparium to be the last step in the larval-pupal apolysis, which it is not. The mechanical dislocation of the alignment between the two cuticles is effected by the displacement of the pupa, bearing a pupal-specific product (Appendix A3) of a pupally-committed epidermis, within the puparium. Stage P4 will therefore be considered to be a pupa (cryptocephalic until P5).

(*Note: The term "moult" is applied loosely in the literature to both apolysis and ecdysis. However, large elevations or peaks in moulting hormone titre tend to precede apolysis rather than ecdysis).

Fraenkel and Bhaskaran (1973) place the pupal-adult apolysis at 34-50h (P6-7) starting posteriorly (cf. the larval-pupal apolysis, which commences with the disc-derivatives).

3.3.2 Variability of timed cultures with respect to stages

Observations of some pupation-plate cultures were analysed to show their composition by stages. Using the stage durations in Table 3.IV these data may be used to make a rough test of the accuracy of this timecourse: the largest stage classes in each culture should lie close to the following ratio:-

$$\frac{\text{Time after pupariation}}{\text{Cummulative duration of stages}} = 1.0$$

Figure 3.38 shows that the general pattern of relative stage durations is correct.

One advantage of employing a staging system is that it may correct for developmental asynchrony if individuals change at very different rates after zero-time.

There are many late stages distinguishable during Drosophila metamorphosis, which is fortunate if asynchrony does increase with time. Fig. 3.39 shows the relation between real and developmental time based on the stage-composition of cultures at various times after pupariation. The correlation is significant; but anyway staging is more convenient than timing as a means of collecting experimental material, and also young cultures (eg. 5h) are already sufficiently heterogeneous with respect to stage for staging to be preferable to simple timing.

The heterogeneity of these cultures may be in part an effect of a diurnal rhythmn since these cultures were set up from stock bottles maintained on a 12:12h photocycle so both oviposition and preparation had occurred under these conditions. (It seems likely, however, that the diurnal rhythm, if it has an effect, induces a block in the latter part of pupation: some flies eclosed before the meconium became visible, while others retained this character but did not eclose for some time; but cf. Harker 1965. However, any effects of the day/night cycle are decreased in the estimation of stage durations by frequency, as both oviposition and puparium

Figure 3.38

Stage variability within cultures timed from puparium-formation

Abscissa: Composition of pupation plate cultures at various times after pupariation (25°C, sexes mixed). Vertical bars show spread of component stages (Table 3.IV) in hours to midpoints of extreme stages projected from the ordinate. Horizontal bars indicate relative abundance of stages in a given culture (not projected from abscissa - inset shows 100%). Slope = 1:1 (h:h). Proximity of longest horizontal bars (i.e. major component stages) to 1:1 is a measure of the reliability of the estimates of stage durations represented on the ordinate (Based on 1309 observations, 19 cultures).

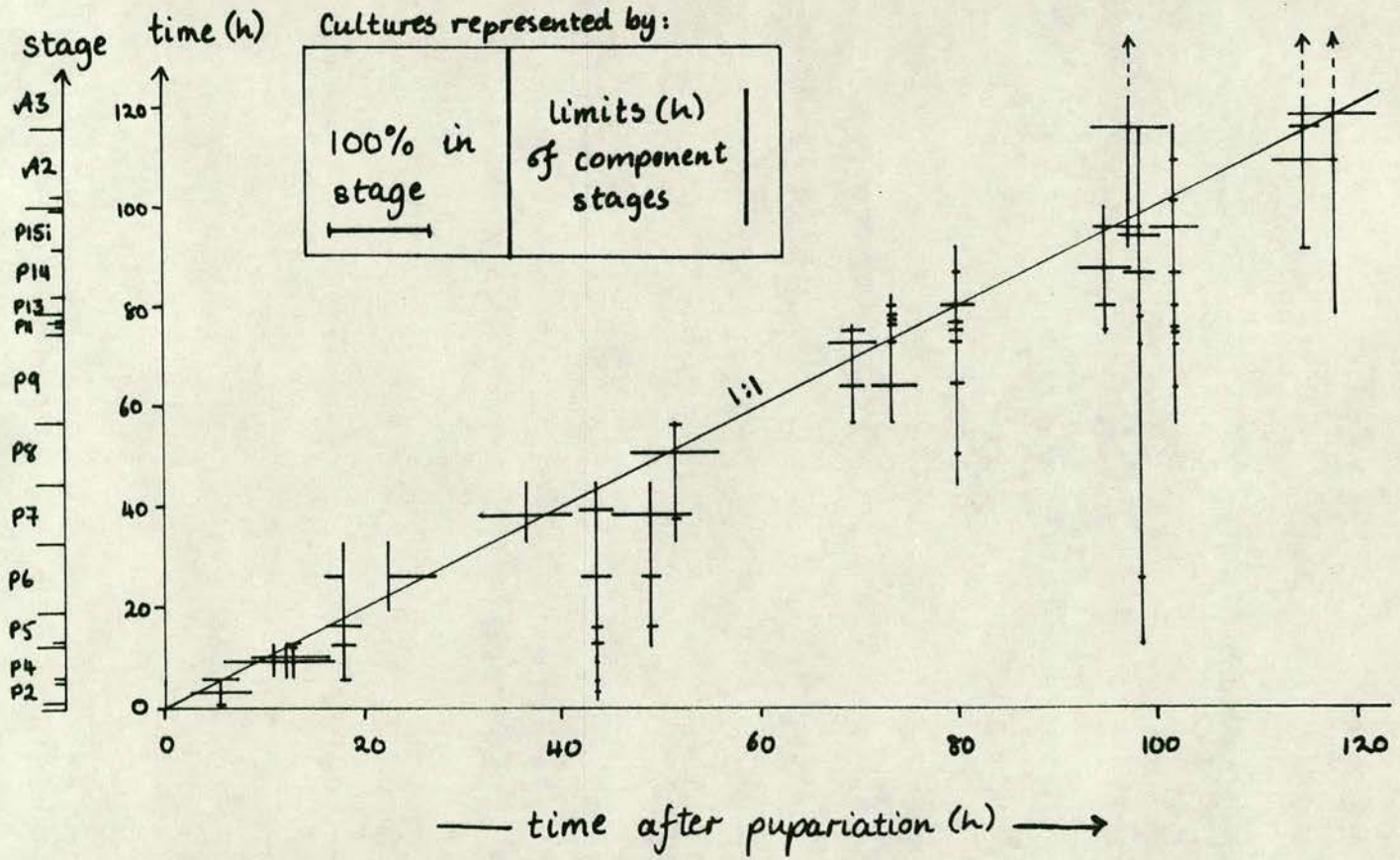
stage
time (h)
Cultures represented by:
100% in stage
limits (h) of component stages
A3
A2
P15i
P14
P13
P9
P8
P7
P6
P5
P4
P2
0
20
40
60
80
100
120
1:1
time after pupariation (h)

Fig. 3.38

Figure 3.39

Increasing asynchrony with time after pupariation

Estimated maximum period (h) represented by component stages in mixed-sex pupation-plate cultures at 25°C (ordinates) against time of observation (hours after pupariation). Data as Figure 3.38 but without open ended values where cultures included stage A3. Correlation coefficient, r is significant at the 1% level of confidence ($r = +0.69 > 0.61$, $p = 0.01$, $n-1 = 15$).

Fig. 3.39

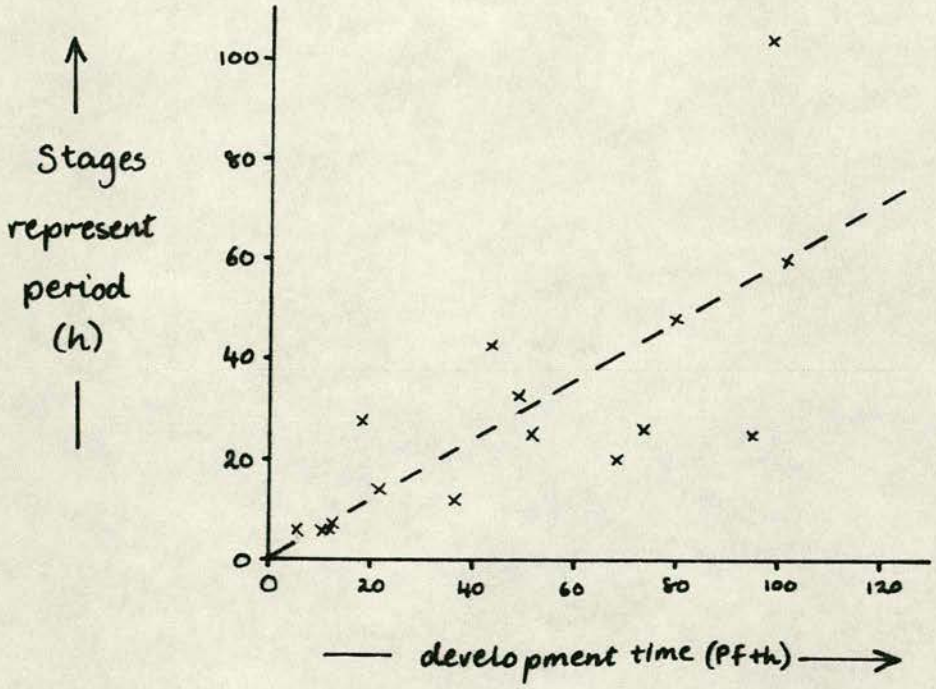
Stages represent period (h)
100
80
60
40
20
0
0
20
40
60
80
100
120
development time (PF+h)

formation took place in the dark.)

The difference between males and females is established early, to the extent that, if pupae are segregated on the basis of early or late accession to P5 (i.e. head evertion), then they are also segregated sexually with an accuracy of about 70%.

The stage durations in Table 3.IV predict the stage transition times of the median class of individuals in a developing population but they suggest nothing about the accuracy of the predictions or the size of the median class (i.e. the yield of the predicted stage). Figure 3.40 shows an analysis of the composition of single-sex cultures compared with their stage as predicted from the time elapsed since pupariation. The accuracy of the predictions is quite good until eclosion, but it is clear that timed batches of animals are usually highly heterogeneous with respect to appearance.

3.4 Metamorphosis at temperatures other than 25°C

In order to investigate the sexes separately it is necessary to sex prepupae and to collect the required stages at intervals after pupariation until P14 when the sex-combs become black: it is not possible to select stages from a mixed population. It is therefore desirable that other temperatures should be available for legitimate exploitation and that they be characterised with respect to stages, in order that all stages may be collected at convenient times of day. Presumably the criteria employed in staging must in general reflect the metabolic processes underlying metamorphosis, so it is

Figure 3.40

Testing predicted stage transition-times

Analysis of some pupation-plate cultures compared with predicted stage transition-times based on frequencies of stages in a continuous age-distribution at 25°C. Estimates of cumulative male and female stage durations are superimposed on a time axis (ordinate; hours after pupariation). Cultures were set to time-zero at pupariation and kept in the dark and analysed w.r.t. stage(s) as %. Based on 753 observations. Underlining indicates correspondence between predictions and observations (e.g. P8). Length of boxes represents proportion of culture in a given stage.

Fig. 3.40

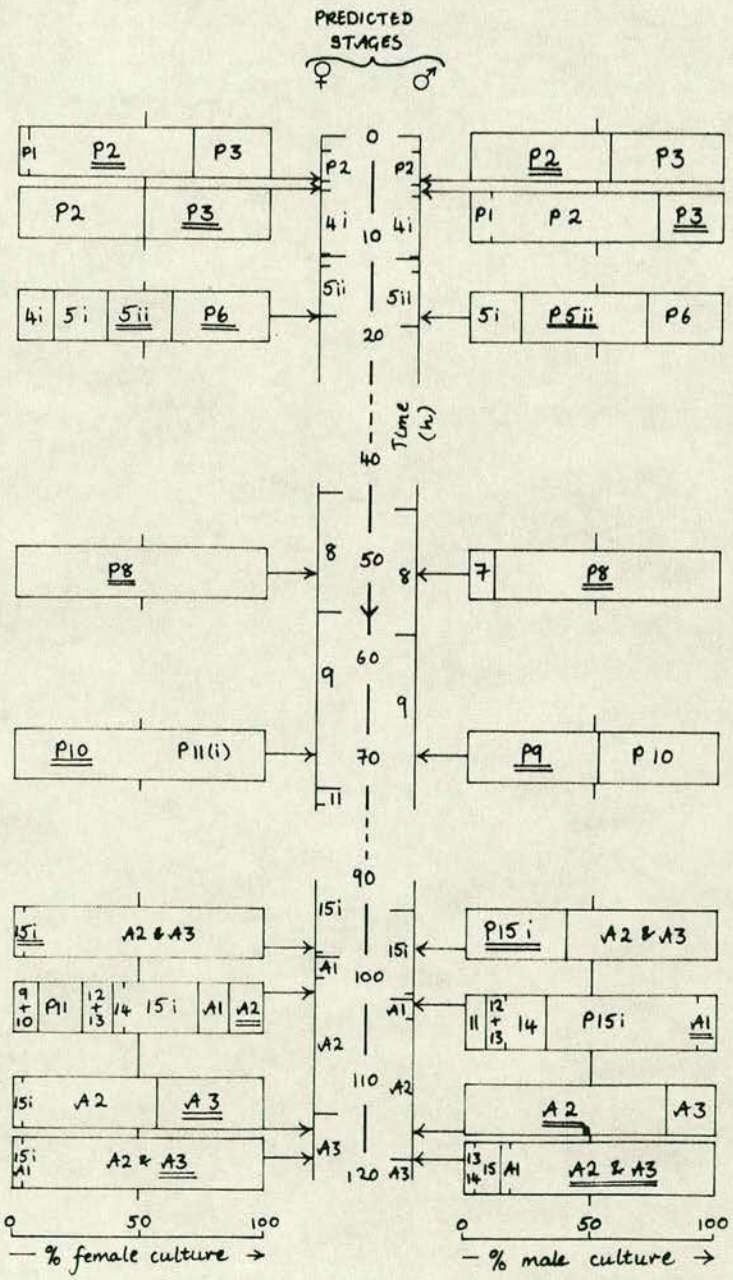
PREDICTED STAGES
♀
♂
P1
P2
P3
4i
5i
5ii
P6
0
10
20
40
Time (h)
8
50
60
9
P8
7
P10
P11(i)
P9
11
70
90
15i
A1
A2
A3
100
110
120
A2 & A3
P15i
9 + 10
12 + 13
14
15i
A1
A2
A3
0
50
100
% female culture
% male culture

unlikely that they will be uncoupled from metabolism when they occur at different temperatures; (cd. a correlation of an ecdysteroid titre peak with a given appearance of the animal; and see Section 4.2 for evidence of this at the biochemical level). However, the proportions of development time (P1-15) devoted to progression through given stages should vary with temperature in so far as the stage-specific metabolic processes vary in their temperature-dependence. Are the various stages differentially temperature-dependent ? The relative and absolute durations of stages P1-15 have been estimated at two other appropriate temperatures to establish whether they share a pattern with 25°C.

3.4.1 Frequency - estimates of stage durations at 18°C and 29°C

Artificial populations approximating to a continuous age distribution were constructed at 18°C and 29°C as they were at 25°C (cf. Sections 2.3; 3.3.1) and these were scored by stage-frequency. The data are presented as proportions of the development period P1-P15 in Figure 3.41 which shows no striking differences between the temperatures or trends with change in temperature. The same data are represented in Fig. 3.42 to ask: is there a critical duration for any period of metamorphosis which would show its independence of temperature Some anomalous values are produced by the inaccuracy of the frequency-estimate method (cf. 25°C); but when clusters of stages are considered the dependence of stage durations on temperature becomes clear.

So it is reasonable to use the corrected stage durations

Figure 3.41

Relative durations of stages at three temperatures

Percentage $t_{P(1\text{-}15)}$ as calculated from stage frequencies at 18°C and 29°C in artificial populations constructed to resemble continuous age distributions (mixed sex), against temperature: 18°C and 29°C compared to 25°C data from Table 3.IV. 18°C values from cultures of ages 22-29d. (972 scored); 29°C values from cultures of ages 7-9d. (1563 scored). Cultures were raised in bottles in the dark. The values for P1-P5i are likely to be as inaccurate at 18°C and 29°C as they were at 25°C.

Fig. 3.41

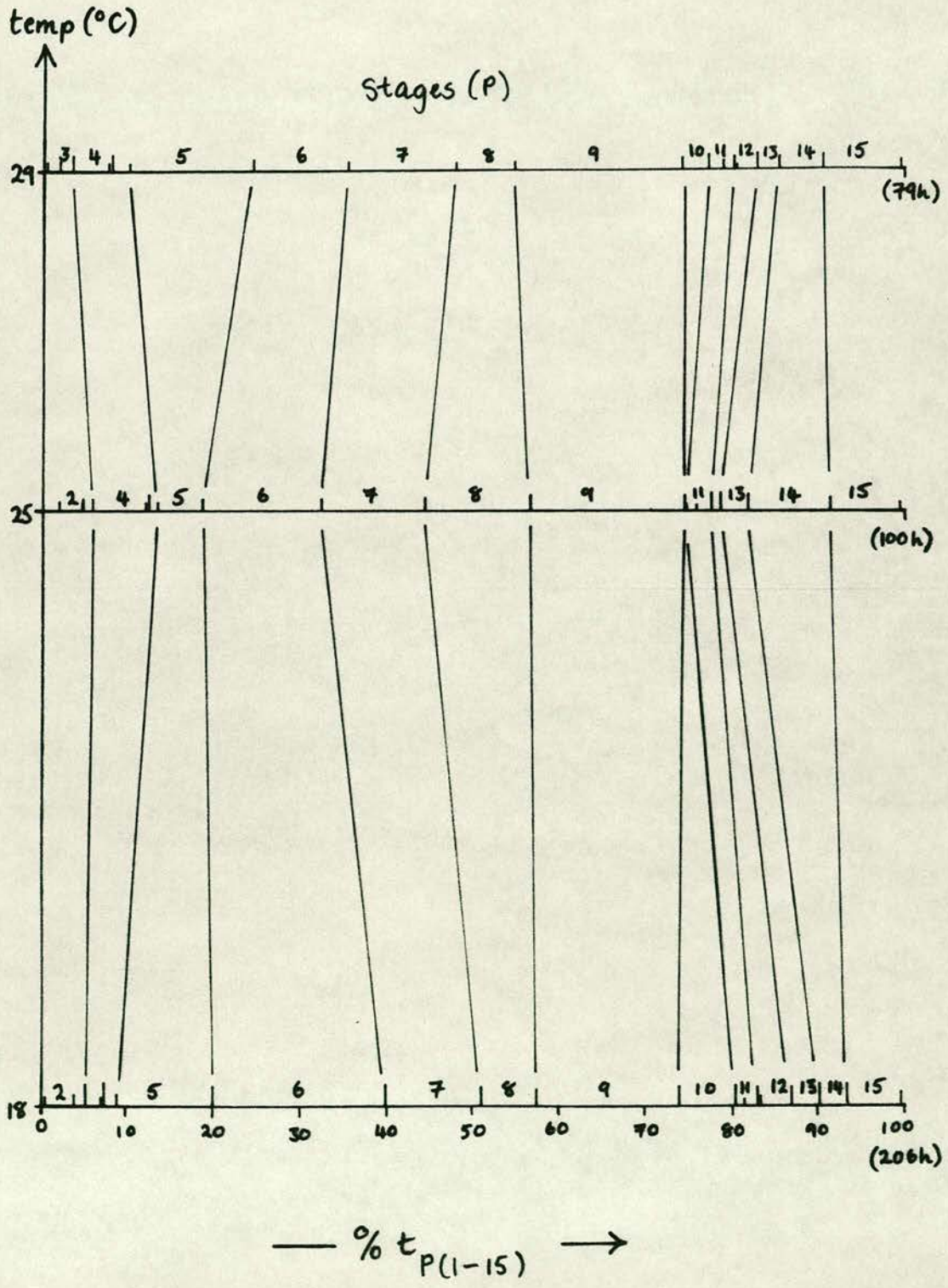
temp (°C)
Stages (P)
29
25
18
(79h)
(100h)
(206h)
0
10
20
30
40
50
60
70
80
90
100
— % $t_{P(1-15)}$ →

Figure 3.42

Dependence of stage durations (h)

on temperature

Data as Figure 3.41. Absolute durations of stages P1-15 and selected groups of stages are shown at 18°C, 25°C and 29°C, as calculated from stage frequencies in populations of approx. continuous age distribution and mixed sex. Some points are linked to show their deviation from the norm, that being: The higher the temperature, The shorter the stage. P1-3 Prepupa; P4 Cryptocephalic pupa; P5-7 Phanerocephalic pupa; P8-15 Pharate Adult; P10- 13 cuticle-darkening; P14+15 legs twitch. (Durations of period P1-15 = 100% taken from Table 1.I).

Fig. 3.42

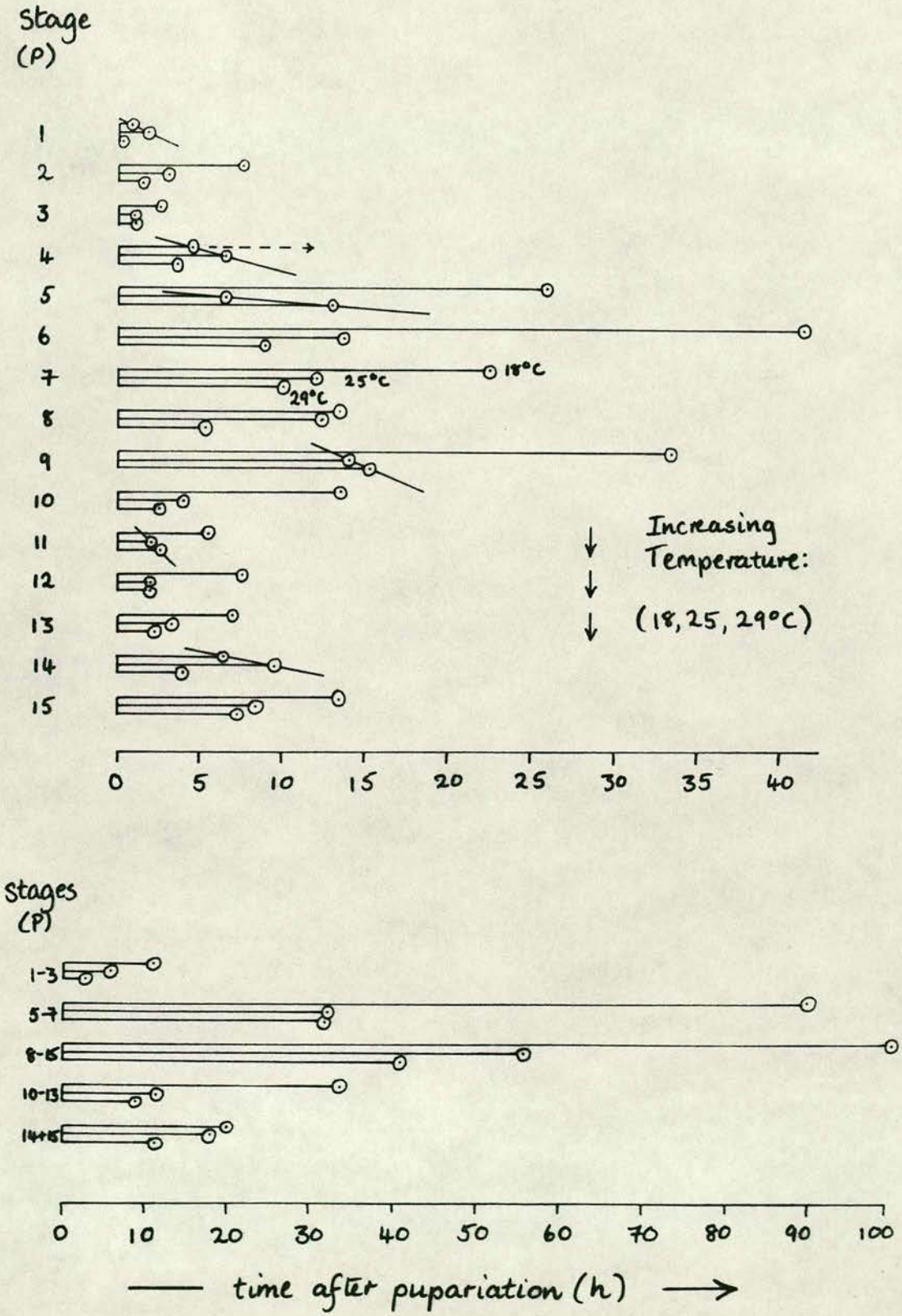
Stage
(P)
1
2
3
4
5
6
7
8
9
10
11
12
13
14
15
18°C
25°C
29°C
Increasing
Temperature:
(18, 25, 29°C)
0
5
10
15
20
25
30
35
40
Stages
(P)
1-3
5-7
8-15
10-13
14+15
0
10
20
30
40
50
60
70
80
90
100
time after pupariation (h)

determined at 25°C as proportions of development-time at 18°C and 29°C. It remained for the actual durations of metamorphosis at these temperatures to be determined.

The values employed in Fig. 3.42 are derived from published figures (Table 1.I), and such estimates are reported in the following section, although for convenience they were restricted to stages P1- 4 inclusive. (This is acceptable practice. The relation of duration to temperature is very similar for the periods P1-4 ("prepupal period", Bliss, 1926) and P1-15 ("pupal period" of Powsner 1935); and Harker (1965) has shown that the P4/5 and P15/A1 transition- times co-vary with another environmental factor, namely photoperiod; so the times of these events are closely related).

3.4.2 Direct timing of P1-4 at 18°C and 29°C

Animals were selected at pupariation and, the times of head evagination having been roughly identified previously, cultures were scored for the proportion having effected head-evertion by time t at each temperature. Figure 3.43 shows the data as they indicate typical stage transition times (i.e. 50%-time): at 18°C, c. 25h; at 29°C, c. 9.7h. In relation to the time determined at 25°C these are x 2.05, x 0.80 respectively, which correspond well with the data collected from the literature and shown in Table 1.I (x 1.95, x 0.83 respectively). So under our conditions, and using this Ore-R stock, the relation between durations of P1-4 at 18°, 25°C and 29°C are standard, and from Table 1.I it can be seen that the relation applies also to the period P1-15; so, taking the mean of all 5

Figures 3.43 (a) + (b)

Stage P4-Stage P5 50% transition graphs

To estimate time of accession to stage P5 at 18° and 29° by direct timing of cultures from pupariation. a) 18°C (sexes observed separately) b) 29°C (mixed-sex cultures only) % pre-stage P5 (i) (ordinate) vs. time after pupariation (h). Diagnostic feature = head evagination.

Fig. 3.43

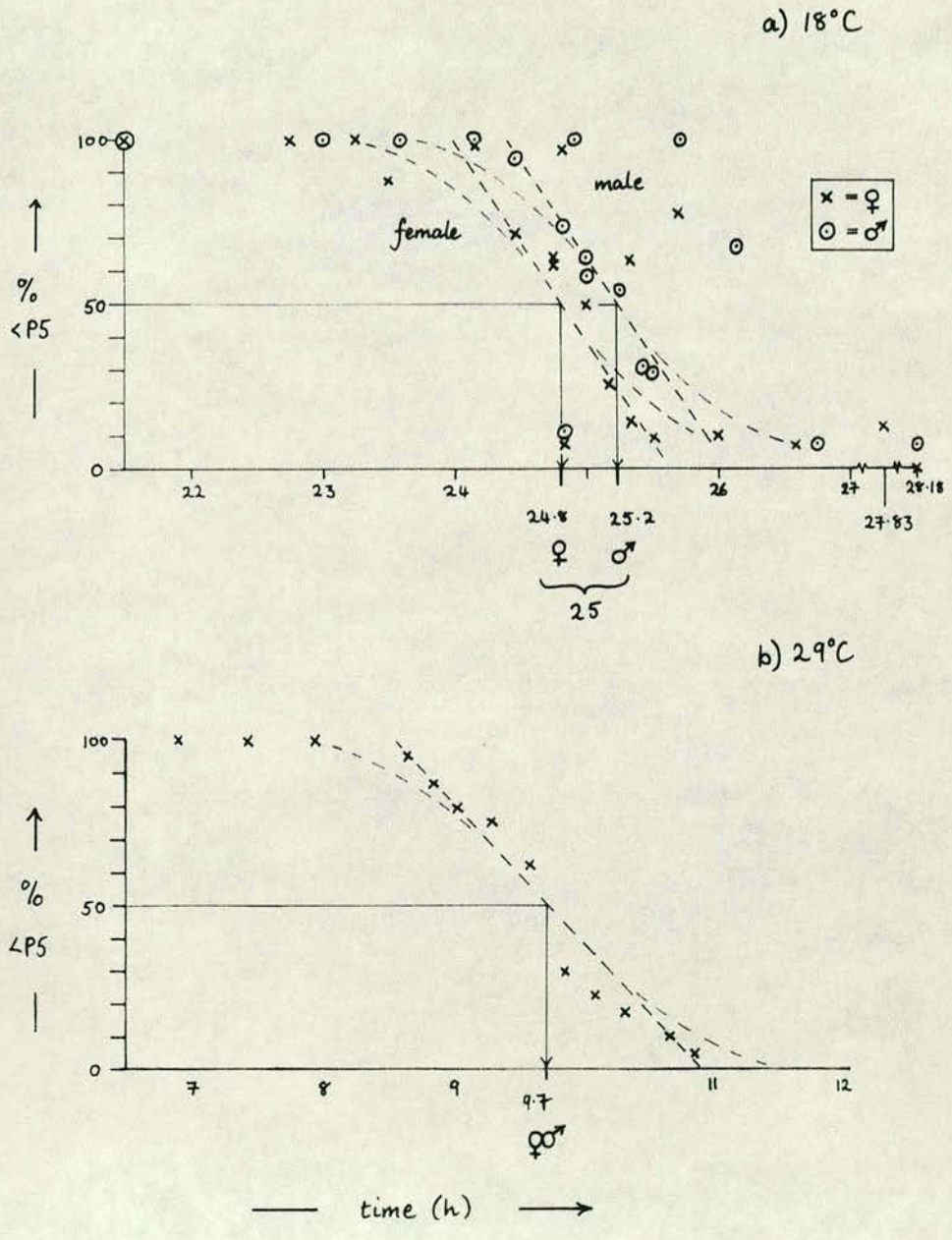
a) 18°C
100
50
0
% <P5
female
male
× = ♀
⊙ = ♂
22
23
24
24·8
25·2
26
27
28·18
27·83
♀
♂
25
b) 29°C
100
50
0
% <P5
7
8
9
9·7
11
12
♀♂
time (h)

reported ratios we have:

a) Duration P1-15 at 18°C = duration at 25°C x 2.03;

b) " " " 29°C = " " " x 0.81.

These factors are applied in Table 3.V to the observed duration of metamorphosis in males and females at 25°C; and they may equally well be applied in conjunction with Table 3.IV to estimate other approximate stage transition-times.

3.5 Collecting staged material

Drosophila undergoing metamorphosis may be obtained for analysis by scraping the walls of bottle-cultures but they need then to be washed in running water before staging; and, unless water of the appropriate temperature is used, washing may constitute a cold-shock. What are the effects of cold-shock ?

3.5.1 Cold-shock

Preliminary observations:- It was observed that:

1) Of animals cultured at 18°C and washed briefly in mains (cold) tap-water, some in stage P9 eclosed when transferred to 29°C but none in stage P10 did so; and

2) Animals cultured at 18°C and then shifted to 7°C for 12h

TABLE 3.V Durations of period P1-P15 inclusive at three temperatures

Temp (°C)	Factor	Estimated durations (h) Female	Male
		our conditions:	our conditions:
25	x1	98	102
	reported:	calculated:	calculated:
18	x2.03	199	207
29	0.81	79	83

(refrigerator) appeared as follows after a further 10d at 29°C:

Stage P9 (n = 21)	c. 24% =	had eclosed
	c. 48% = c. P13	dead, or
	c. 28% = c. P10	development arrested.
Stage P10 (n = 79)	0% =	had eclosed
	8% = c. P13	dead, or
	92% = P10	development arrested.

Controls (no wash or cold-shock):

Stages P9 and P10 (n > 20)	100% = eclosed.

These observations suggested that there may be a block in development induced by cold-shock, and the following experiments were performed to investigate this a little further:

Experiments A-C 18°C bottle-cultures were developed, their walls cleared of "pupae" by scraping, and the animals were washed for 1 minute in tap-water (= short cold-shock).

Experiment A: No further cold-shock

Groups of animals (mixed-sex) were selected in stages P3 and 4, P7, P9, P10, and P15 (i) and returned to 18°C in pupation plates for observation which continued for 10 days. See Fig. 3.44A.

Experiment B: Extended Cold-Shock

Groups of animals (mixed-sex) were selected as for experiment A in the stages P3 and 4, P7, P9, P10 and P15 (i). These were stored in pupation plates at 7°C for 36h and then shifted back to 18°C for observation (10 days). See Fig. 3.44B

Results Of the stages examined here, pharate adults in P9 are relatively unaffected by cold-shock, but the responses of the other stages are marked. Stages P3-4 and P10 are especially susceptible, and the longer cold-shock causes high lethality at these points in developments

Experiment C: Fertility after extended cold-shock

Some pharate adults eclosed during the 36h period at 7°C (Experiment B) but remained motionless thereafter. These flies were anaesthetised, separated into food-vials as mating-pairs, and shifted to 29°C for 10 days.

Figure 3.44

Susceptibility of P-stages to cold-shock

Animals were subjected to A) short cold- shock (1 min, tap-water) or B) extended cold- shock (tap-water wash followed by 3h at 7°C) and observed regularly over 10 days. Abscissa: stage immediately after tap-water wash, weighted by estimated stage-durations (cf. Table 3.IV). Stages: P3 and P4 = prepupa/cryptocephalic pupa; P7 = phanerocephalic pupa; P9-15i = pharate adult. Ordinate: percentage composition of cultures after 10 days (total = 100%) according to the following classes: a) stage A3 (dead or alive); b) retarded (or dead) within the puparium (i.e. pre-A1); c) dead (discoloured) within the puparium (i.e. pre-A1). There was no class (b) after extended cold-shock (B) - i.e. animals either eclosed within 10 days or were obviously dead inside the puparium. Histograms under the curves represent successful completion of metamorphosis as percentages of cultures.

Fig. 3.44

A)

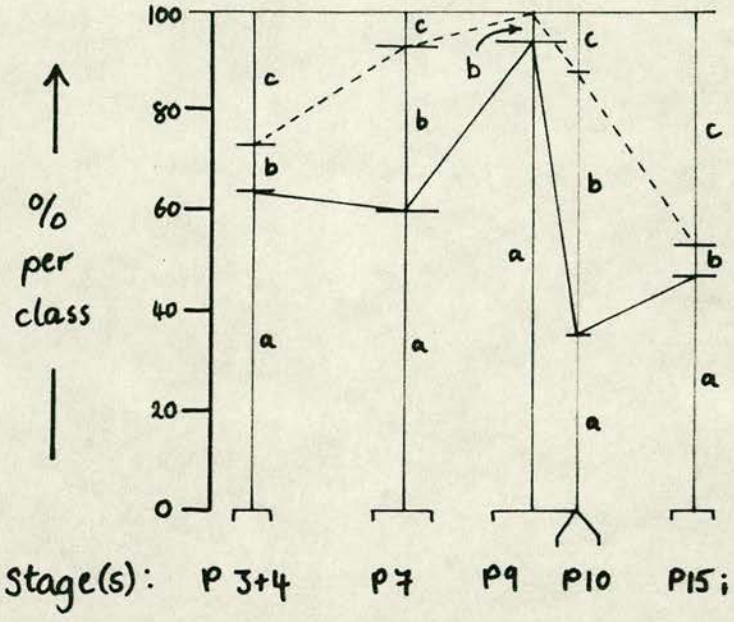
100
80
60
40
20
0
% per class
a
b
c
Stage(s): P 3+4 P 7 P 9 P 10 P 15 i

B)

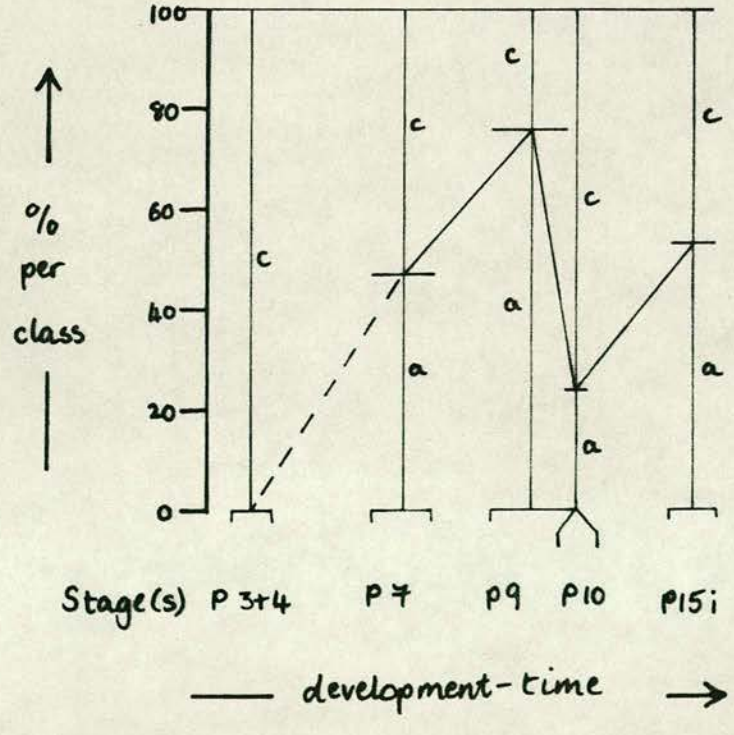
100
80
60
40
20
0
% per class
a
c
Stage(s) P 3+4 P 7 P 9 P 10 P 15 i
development-time

Results: About half of the vials developed larvae and "pupae" while half had none, (cf. control-vials (no cold-shock) which all developed larvae/"pupae"). The sexes were not examined separately; but clearly, fertility may be reduced by prolonged exposure of pharate adults to 7°C.

Experiment D: Extended cold-shock to larvae

(Could *Drosophila* stocks be maintained as larvae at 7°C?)

Larvae (LI-LIII) were collected by sugar-floatation from 18°C bottle-cultures and shifted in groups of 10 or more to c. 7°C in yeasted food-vials (foam bungs taped at the neck, the bungs covered with aluminium foil to hinder dessication). Vials were removed at intervals of 2 weeks and shifted to 25°C (in the dark) where they were observed for up to one month.

*Temperature ranged from 5.5-8.0°C over two months; mean temperature = 6.7°C.

Results: After 2 weeks at 7°C - viable (inbred to two generations).

After 4 weeks at 7°C - survival much reduced;
both sexes were fertile when
out-crossed to flies from 18°C
cultures (no cold-shock).

After 6 weeks at 7°C - Some development through P-

stages; no eclosion.

After 6+ weeks at 7°C - P-stages dead (± dessicated within the puparium).

Some larvae entered metamorphosis within two weeks of the shift to 7°C, and this accounts for all the animals which survived this cold-shock. All remaining larvae were dead (black) at the time of transfer to 25°C, which suggests that one response to cold-shock in D. melanogaster larvae may be a (premature) protective entry into metamorphosis analogous to diapause, i.e. that a depressed metabolic rate species can only be sustained in a post-pupariation condition (cf. Sarcophaga, in which diapause does occur between the larvae/pupal and pupal/adult apolyses, i.e. c. P4-6; Fraenkel and Bhaskaran, 1973; but note that it is controlled by photoperiod, not by temperature); and there is probably a critical period in the third larval instar before which the challenge of prolonged cold-shock cannot elicit premature accession to stage P1. Presumably those animals which did respond to cold stress by pupariating were already in the so called "facultative feeding" phase (Shaaya and Levenbook, 1982) of the last larval instar before which starvation is lethal to the larvae of both Calliphora and Drosophila ("obligate feeding" phase).

Cold-Shock: General conclusions

Metamorphosing Drosophila are especially susceptible to cold-

shock before P5 and at about P10. Brief exposure to cold tap-water is effective, (so animals collected from bottle-cultures should be washed before staging using water at the temperature of the culture, or at least at room temperature; and animals should be used fresh (homogenised) or frozen immediately. In addition, pupation-plates should be lined with absorbent paper to avoid incubating animals beneath a water meniscus.

Larvae can protect themselves from the lethal effect of cold shock by proceeding to stage P1, so the early period of maximum susceptibility to cold-shock is probably between P2 and P4.

Wild-type larval stocks may not be maintained at 7°C for more than two weeks.

3.5.2 Collection-methods for staged material (cf. Section 2.5).

As with the estimation of a timecourse for stages, so for other experiments staged material may be taken from two sources: (a) unsorted populations at unspecified time, and (b) batches timed from pupariation. The latter is essential for pupae/pharate adults of known sex (P4-P12) and is also useful and convenient for prepupae (0-c. 6h) which may be collected from cultures at the appropriate times to enrich for a selected stage. Both methods were adopted for experiments in the following chapters, (see Section 2.6).

With practice it is possible to distinguish and also to subdivide the colour-stages easily, e.g. P8 (yellow-eyed), P9

(amber). In distinguishing between colours ambiguity is avoided by sorting the animals into three groups and discarding the intermediate group.

The indiscriminate grouping together of symphasic animals may be refined to some extent by acknowledging that developmental time is continuous even though the staging system suggests stepwise development. Given a large enough timed culture, subdivision of stages may also be effected by treating the developmental status of the culture as a whole as an internal standard of developmental time; so "late" P8 would be those in P8 when most of the culture has proceeded to P9, and likewise, "early P9" a minority amongst P8s.

3.6 Stages in other Drosphila species

Other representative species of the genus Drosophila were checked for the presence of the staging criteria defined for D. melanogaster (see Table 3.V1), although the sequence of stages was not checked, (i.e. groups of metamorphosing animals of mixed ages were simply sorted according to stages L1 ... A3). There is no pattern to suggest a correspondence between similarity of appearance during metamorphosis and proximity to D. melanogaster in phylogenetic terms amongst the species examined, but in general the stages in closely-related species are similar; so it is likely that the staging system defined here for one species would be applicable to sibling species and beyond, and this could help greatly in making inter-species comparisons. However, it is to be

TABLE 3.VI

The genus Drosophila: A comparison of species based on the stages of D. melanogaster metamorphosis, L1-A3.

Taxonomy ⊕				Staging: Diagnostic criteria not observed:						Sexing: Sex comb	Tergites
Genus	Subgenus	Group	Spp.	L1	P5i	P5ii	P7	P11i	P13	P12ii	A3
Drosophila	Sophora	Melanogaster	melanogaster								
			simulans*	•							
			mauritiana	(•)							
			Teissieri		•		•		•		
		Obscura	pseudoobscura*	(•)			•				•
		Saltans	saltans	(•)		•				•	•
	Drosophila	Funebris	funebris	(•)						•	•
		Virilis	virilis								
		Repleta	hydei	(•)			(•)	(•)		•	•

⊕ From Bownes (1980). *expanded in the text.

• indicates staging or sexing criterion not observed.

expected that the proportional durations of any recognisable stages will vary between species. This is certainly the case in a comparison between genera: e.g. Wentworth et al. (1981) give "onset of sclerization: claws darkening" in Sarcophaga bullata at 91% of total time (P1-15 inclusive), which in D. melanogaster occurs in P13, i.e. before c. 82% of time P1-15 (cf. Table 3.IV); but this 9% difference is neither especially large nor a significant obstacle to the wider use of a common staging-system.

Examples:

D. simulans (sibling species) is very similar to D. melanogaster except for the site of metamorphosis (on the food) which makes it impossible to collect L1 (post-feeding) as wandering larvae. D.pseudo-obscura (obscura group) also shows this character to a lesser extent, but some individuals do move away from the food. However, the diagnostic feature of Stage P7 is lacking in this species since the "yellow body" is not observed until P8 and even at P9 has still to move into position between the Malphigian tubules. In both species the larval male gonads and the sex comb (s) (two in D.pseudo-obscura) are available as criteria for the sexing of individuals.

3.7 Note on previous uses of staging criteria

As mentioned in the introduction (Section 1.3) many authors have employed timings at a given temperature to define points in post-embryonic development. Sometimes these can be roughly related

to the staging system discussed here; e.g. Wolsky (1930) used four "stages" of D. melanogaster metamorphosis defined in terms of time after pupariation at 25°C when eclosion occurred at between 90 and 100h. Taking P15/A1 to be 95h = 100% P1-P15 inclusive, these stages appear to correspond to: I = P3-4i; II = P6; III = P8-9, and IV = P13-14, (Wolsky 1938, cf. this study, Table 3.IV). These interpretations are only approximations but may be reasonably accurate since they involve a comparison using the same species and temperature, and because stages I-IV are not continuous but allow a margin for error in interpretation.

However, some authors have adopted a limited version of this staging system, employing some of its diagnostic criteria to increase the resolution and/or convenience of their experiments. The criteria which have been used by these authors - Bliss (1926) has already been mentioned - are shown in Table 3.VII which suggests that the subtle features of pharate adult development have been relatively neglected on this basis.

TABLE 3.VII

Staging criteria adopted by other authors for D. melanogaster

Reference	Criteria (stage-stage transitions):							
	L2/P1	P3/4	P4/5	P7/8	P9/11	P10/11[x]	P11/12	P15/A1
Bliss, 1926	+		+	+	+			+
Harker, 1965	+		+	+		(+)	+	+
Pittendrigh and Skopik, 1970	+		+	+		+		+
Chomyn et al. 1979	+	+		(*	*	*	*)	
In common use:	+		+					+

[x]Bliss reports the almost coincident appearance of head bristles and red eye colour, i.e. P9/10 and P10/11 are not distinguished, (cf. Section 3.1).

****Animals were "selected for synchronous development of pigmentation (eye colour, wing colour)".

Chapter Four

Direct radioimmune assay for ecdysteroids: Whole-body titre profiles

Animals in all stages of metamorphosis, LIII-A3, were collected (Section 2.5.1) and subjected to methanolic extraction of ecdysteroids (2.6) and direct whole-body radioimmune assay (RIA) using antiserum Horn I2 (16 wk) (2.10). In this chapter the standard response curves used in RIA are presented (4.1) and the appropriateness of the staging system in this context is tested (4.2). Section 4.3 shows the RIA results and the variability of the data is discussed. A transformation is applied, and comparisons are made, within the limits of the data, between stages and between the sexes. Finally, three periods in the developmental timecourse are selected for further analysis.

4.1 Standard response curves

Curves showing the response of Horn I2 (16wk) to ecdysone and 20-OH-ecdysone are shown at Fig. 4.1. These are composites of the curves which were prepared with each run of the assay protocol to allow for variable conditions during the runs. There is a nine-fold difference between the affinities of the antiserum for ecdysone and 20-OH-ecdysone, and the linear portions of the curves extend to three orders of magnitude (pg).

Figure 4.1

Composite standard curves of Horn I2 (16 wk)

response to ecdysone (α) and 20-OH-ecdysone (β)

Ordinate:- binding of counts (cpm) as % maximum binding in the absence of an untritiated competitor (c. 2000 cpm). Abscissa:- $\log_{10}$ mass of unlabelled ecdysteroid (pg) competing with ^{3}H- ecdysone for binding to the antiserum: For the purposes of the assay this axis was read as "pg ecdysone-equivalents", i.e. binding competitors of unknown composition were expressed in terms of their equivalence to ecdysone with respect to this particular antiserum bleed. Error-bars on the ordinate represent 95% confidence-limits about the mean (ecdysone curve only). Values for 50% binding of ^{3}H-ecdysone are projected onto the abscissa and differ x 9.3, i.e. nine times more 20-OH-ecdysone than ecdysone is required to compete equally with ^{3}H-ecdysone.

Fig. 4.1

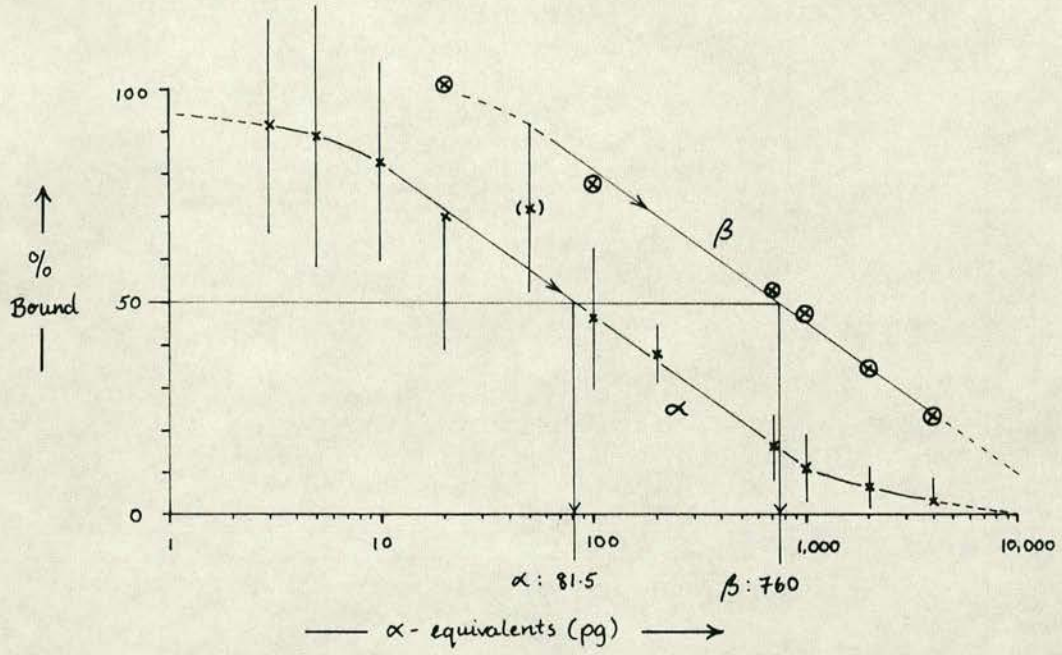
100
50
0
% Bound
(*)
β
α
1
10
100
1,000
10,000
α : 81·5
β : 760
α - equivalents (pg)

4.2 Correlation of developmental status with stage, not age

In preparing titre-profiles, samples for assay were drawn from plates incubated at both 18°C and 25°C, and animals were selected by stage regardless of whether or not they were typical of their group or age. Some individuals known to be atypical were assayed and their titres were compared with the norm in order to test the relation between stage and titre and to ask if these two parameters can show disjunction under varying conditions. Figure 4.2 shows the resulting titres. The trend which emerges from this test is consistent with the claim that animals which are either fast or slow with respect to their contemporaries show a titre characteristic of their stage rather than of chronology; and this appears to be the case irrespective of the temperature at which they were incubated, even though this 7°C temperature-difference doubles the time between pupariation and eclosion. In this connection it is also relevant that Handler (1982) obtained very similar results from Drosophila at 20°C and 25°C when using an RIA to measure ecdysteroid titres during metamorphosis (i.e. curves over % time P1- 15 almost superimposable). It can be assumed, therefore, that staged animals are admissible for assay and comparison, regardless of their origins.

4.3 Ecdysteroid titre profiles

4.3.1 The data

Fig. 4.3 shows the profiles of mean titre measurements in each

Figure 4.2

Stage-titre correlation:

Mean titres of ecdysteroid(s) (pg ecdysone equivalents per mg fresh wt; data untransformed) and 95% confidence intervals for selected stages. The norm compared with "slow" and "fast" animals at two temperatures.

a) At 18°C, "slow" males in P6 should have reached P14 but their tires are not representative of the later stage.

b) "Fast" females in P7 (25°C) should still be in P6 but their titres correspond to that of normal animals in P7.

c) P7 females at 18°C tend to show the same titres as those at 25°C shown at (b),

"The norm"/"normal" refers here to animals which in appearance respect the predictions of Table 3.IV; while "fast" and "slow" animals notably deviate from these predictions.

Fig 4.2

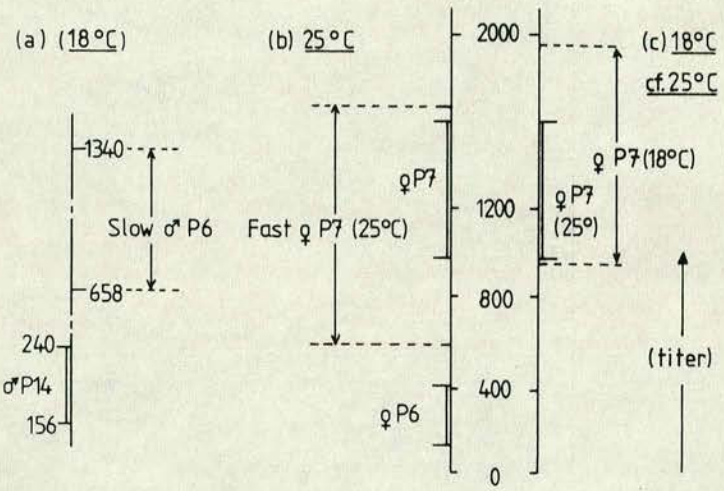
(a) (18°C)
1340
Slow ♂ P6
658
240
♂P14
156
(b) 25°C
Fast ♀ P7 (25°C)
♀P7
♀P6
2000
1200
800
400
0
(c) 18°C
cf. 25°C
♀ P7 (18°C)
♀P7
(25°)
(titer)

Figure 4.3

Mean ecdysteroid titres

RIA ecdysteroid titres of females (top) and males (bottom) from the stages of Drosophila metamorphosis. Mean titres are weighted along the abscissa by estimates of stage durations taken from Table 3.IV to produce comparable profiles. Ordinate: titres as pg ecdysone- equivalents x 10^3 per mg fresh wt whole animals. Abscissa: a) stages from third instar larvae (LIII) to mature adults (A3); sub-stages (i) and (ii) indicated by half ticks. "Early", "mid-" and "late" stages are arbitrary divisions into two or three equal periods; b) time (h) from P.F. (puparium formation). Both abscissae apply to both histograms. Adults are timed in days, thus: "d1" = (0.5 $\pm$ 0.5)d post eclosion.

Fig 4.3

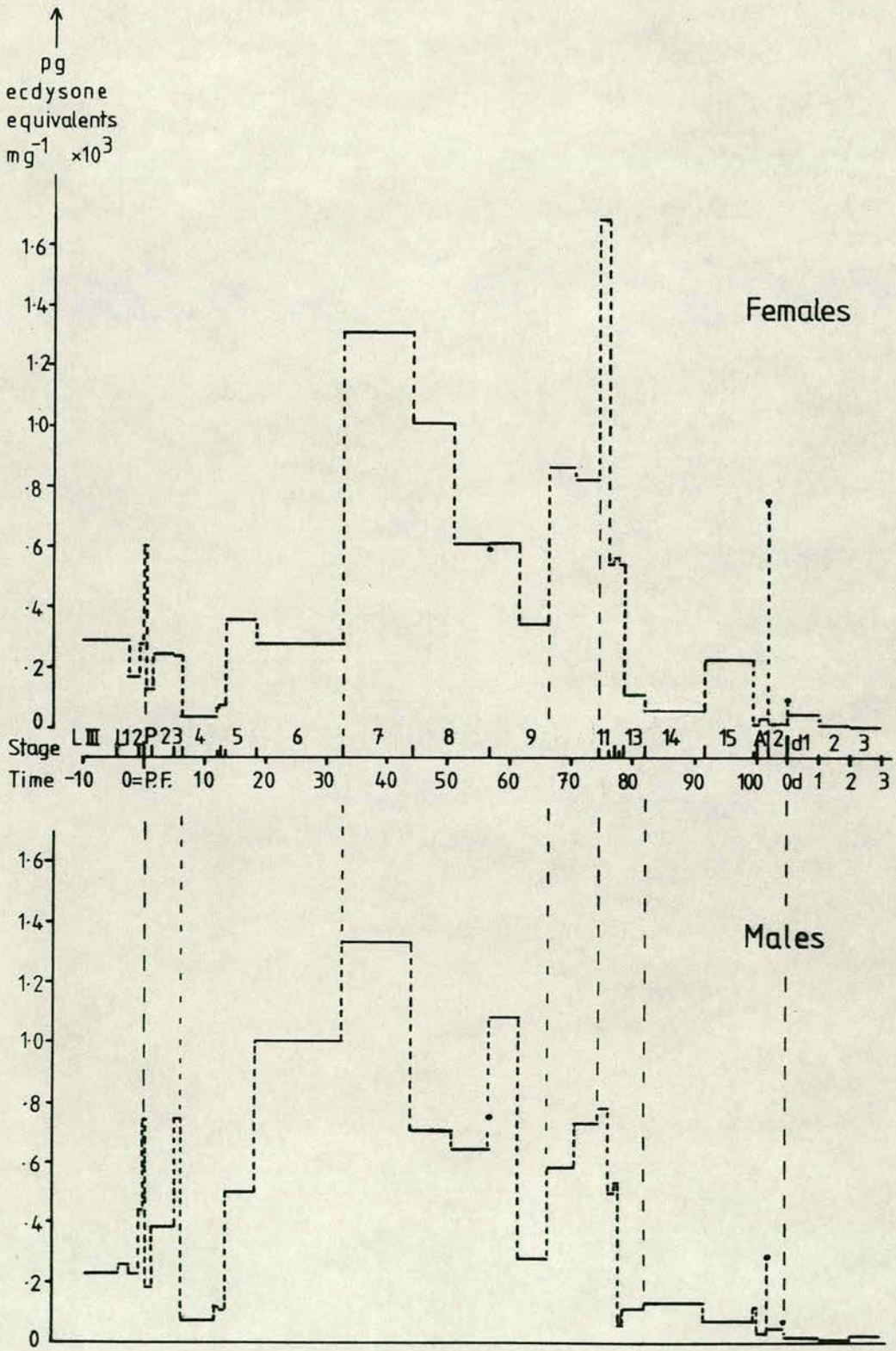
pg
ecdysone
equivalents
mg⁻¹ ×10³
1·6
1·4
1·2
1·0
·8
·6
·4
·2
0
Females
Stage L III I1 I2 P 2 3 4 5 6 7 8 9 11 13 14 15 A1 2 d1 2 3
Time −10 0=P.F. 10 20 30 40 50 60 70 80 90 100 0d 1 2 3
Males

sex in stages LIII-A3. The values are presented by stage, the stages being weighted by their estimated durations (Table 3.IV). These data suggest that both female and male profiles exhibit elevations of titre not only at P1 and P7 (cf. Hodgetts et al., 1977; these correspond to peaks 9 and 11 in Richards, 1981) but also at P2, P5 (ii), P10 and A1/A2. In addition, there appear to be sex-specific peaks at P3 (male), early P9 (male), P11 (i) (female) and P15 (i) (female).

Data for stages A1 and A1/A2 have been corrected for an estimated 9% loss in weight at eclosion due to loss of the puparium (estimate made by comparing weights before and after eclosion, at 10 minute intervals, eclosions occurring in the absence of food on dry filter-paper).

These apparent peaks are deceptive, however, because the variances are often very large, to the extent that when the sexes are compared in their limits of confidence (95%) only two stages show a significant difference (P6 and P12 (ii)). Fig. 4.4 shows the data for both sexes pooled where there is no apparent difference between their means ($\pm$ 2 s.e.m.) i.e. they may come from the same population of values. This profile suggests that there may be peaks common to both sexes at: P1; P3; P7; "early" P9; P11 (i); P14-15 (i) and A1/A2. However, the variability of the data makes such conclusions premature.

Figure 4.4

Pooled male and female ecdysteroid(s) titre-measurements (untransformed).

Whole-body titres of ecdysteroid(s) measured by RIA using the Horn I2 (16 wk) antiserum. Male and female data are pooled except where the 95% confidence limits of their means (± 2 s.e.m.) do not overlap. Data are presented for the stages of *Drosophila* metamorphosis, LIII - A3. Ordinate: equivalence to ecdysone in the RIA (pg ecdysone-equivalents per mg fresh weight); Abscissa: series of stages, L111, L1- 2; P1-15; A1-3; (note that this is not a *time* axis - the stages are equally weighted). Some stages are sub-divided into "early" (e), "mid-" (m) and "late" (l). A1 and A1/2 are shown uncorrected for weight-loss at eclosion (loss of puparium), but this makes little difference to the shape of the profile of means.

Apparent peaks in titre (cf. Figs. 1.6 and 4.12):-

P1 (= Richards' peak 9 (1981));

P3 (this is not the peak reported by Klose *et al.* (1980) at 12h after pupariation in *D. melanogaster* (25°C) (Richards' peak 10): P3 finishes before 7h (cf. Table 3.IV). Both Klose *et al.* (1980) and Handler (1982) report titre-elevations at times corresponding to late P4 (Handler's second peak, c. 10h) but neither present confidence limits when comparing points in their time courses);

P7 (= Richards' peak 11, the second peak in

Hodgetts et al. 1977; this corresponds to Handler's fourth peak (1982) which is the second of a group of three between 30h and 48h at 25°C - these three peaks, if they are not due to experimental error (reproducible at 22°C), are not resolved to baseline (lowest recorded titre) so they constitute minor fluctuations in the titre- elevation represented by Hodgett's second peak);

"Early" P9; P11 (i) (follow a drop to less than half the maximal titre (c. P7) in both Hodgetts' and Handler's reports);

(P14- 15 (i)) (Briers and de Loof (1980) report a small peak just before eclosion in Sarcophaga which is not found by Wentworth et al. (1981);

A1/2 (i.e. unfolding of the wings. This apparent brief elevation in titre was not confirmed by further assays of animals at A1, A1/2 and A2 (Redfern and Bainbridge, data not presented).

Fig. 4.4

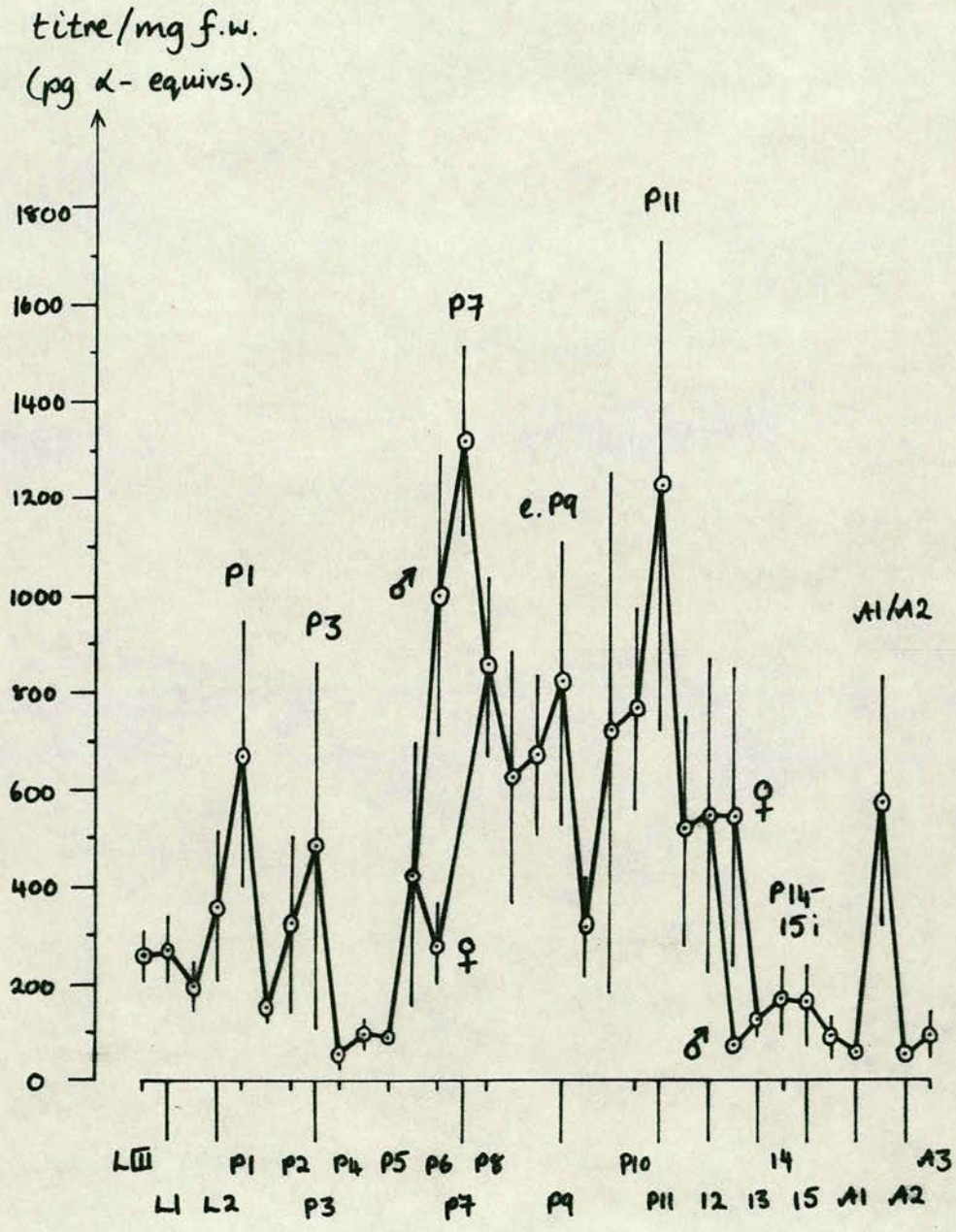
titre/mg f.w.
(pg α- equivs.)
1800
1600
1400
1200
1000
800
600
400
200
0
P1
P3
♂
P7
♀
e. P9
P11
♀
P14-15i
♂
A1/A2
LIII
P1
P2
P4
P5
P6
P8
P10
14
A3
L1
L2
P3
P7
P9
P11
12
13
15
A1
A2

4.3.2 Treatment and analysis of the data

Sample-numbers are often small (n = 5-18) but Fig. 4.5 shows that there is no tendency for the variance to decrease with increasing number of measurements of a given stage: Considering only the apparent peaks and troughs in Fig. 4.4 the correlation of variance with sample number is not significant at the 90% level of confidence. However, the variances of these points are dependent upon the mean, (see Fig. 4.6).

Although the measurements of titres were not each strictly derived from any particular portion of the standard response curve for ecdysone (Fig. 2.5) the linear part of the curve is large (10-1000 pg ecdysone-equivalents) and would accommodate a tendency for high-titre animals to be read from the distal portion of the curve and low-titre animals from the proximal portion. (To avoid this would require that the numbers of animals per assay be precisely tailored to the known titre, so placing all readings in the same part of the curve; i.e. many assays would be required to establish a good estimate of titre before a set of definitive measurements could be made - this was not attempted because of the number of stages, the limited value of direct RIA-measurements and the consequently limited objectives of this preliminary investigation). This being the case, the semi-logarithmic nature of the standard response curve suggests itself as a major factor contributing to any close relationship between variances and means. In fact, the relation variance to mean can be very precisely simulated for means based on 5 measurements by taking a set of dummy readings from the standard

Figure 4.5

RIA Variance (s_2) vs. assay sample-number (n)

Data for peaks and troughs in Fig. 4.4 are used to test for a correlation between (increasing) sample number (i.e. the number of measurements, not the number of animals analysed) and (decreasing) variance of the data. Ordinate: $\log_{10}$ variance x 10^5; Abscissa: number of assays per stage or substage. Correlation coefficient, r = + 0.15 (cf. 0.549, n-1 = 8, p = 0.1).

Fig. 4.5

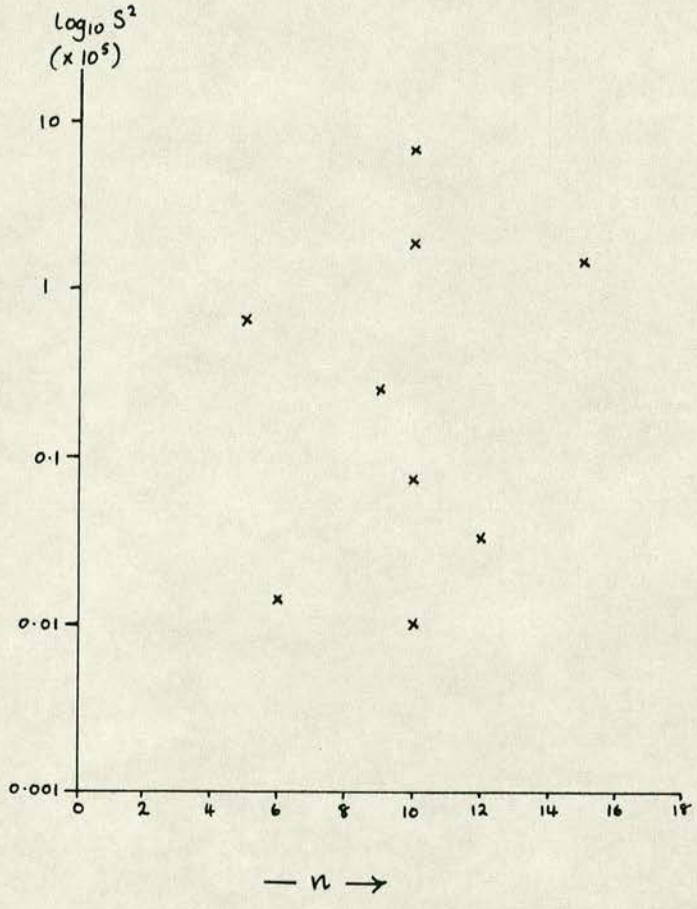

curve over a range of up to ± 10% maximum binding of counts. This simulation is presented in Fig. 4.6 together with the measured values for the apparent peaks and troughs shown by Fig. 4.4. Some degree of variability may also derive from inequalities in the efficiencies of extractions, and perhaps unusually high variances at particular points in the titre-profiles could be taken to indicate rapid change in titre within a stage; but to detect this it would be necessary first to equalize the variances in so far as they derive from the mean and hence, apparently, from the form of the standard response curve (semi-log).

To equalize the variances the data must be transformed, and Fig. 4.7 shows the natural logarithm transformation applied to the data used in Fig. 4.6. Logarithms of the ecdysteroid titres are the most appropriate functions to employ in that they best scramble the linear relation:

(A1, A2, P4 (i)) < P13 < lL1 < mP9 < A1/A2 < (e.P1, P11 (i), P7)

...which is true of both the variance and the mean. This scrambling is to be expected if, as seems to be the case, the variance derives in large part from the logarithmic abscissa of the standard curve in the first place. Natural logs are slightly more effective in scrambling this relation than $\log_{10}$ (r (non-log plot) = -0.192 cf. -0.302; neither significant at P = 0.1); and $\log_e$ has been used in preparing the following titre profiles.

The $\log_e$-transformed data have been used to calculate 95% confidence limits of the population means in each stage of metamorphosis, and the resulting titre profiles are presented in

Figure 4.6

Dependence of variance upon the mean and its source in the form of the standard response curve

a) Data for apparent peaks and troughs in the mixed-sex ecdysteroid titre-profile (Fig. 4.4) showing linear relation between mean titre ($\bar{x}$) and sample variance (S^2). Parallel to this curve is a set of simulations of variability in readings from the composite ecdysone standard curve (see Fig. 4.1). There were constructed as shown at (b): b) Schematic semi-log standard response curve showing simulation of readings, x along the abscissa (log pg ecdysone-equivalents) for values of p, percentage binding $\pm$ q percentage binding of ^{3}H-ecdysone cpm (ordinate; 100% = binding in the absence of unlabelled competitor). q ranged from 5 to 10% bound (5, 7 and 10% shown); p for the $\pm$ 5% simulation ranged from 10 to 55% bound, and for each value of p five readings on x were taken, at (p-q), (p- q/2), p, (p+q/2) and p+q). (Example: when p = 70% bound and q = $\pm$ 10%, values for x (Fig. 4.1) are 43, 31, 22.7, 16.5 and 12, mean = 25 (S^2 = 151.6); cf. when p = 25% (still q = $\pm$ 10%), x = 775, 560, 405, 296 and 213, mean = 449.8 (s^2 = 49908.7)).

Simulated variances were plotted vs. mean for increasing values of q until the simulation almost coincided with the RIA data at q = 10%. The relation does not hold for p $\pm$ q' when q' is a proportion of p itself, but only when q is a constant proportion of "100% bound" as p varies; i.e. the semi-log nature of the standard curve only serves to explain the observed variance-mean correlation if we assume that for a given incubation the extent of the variability in % binding (q) does not decrease with increasing % binding (p) - a reasonable assumption.

Fig 4.6

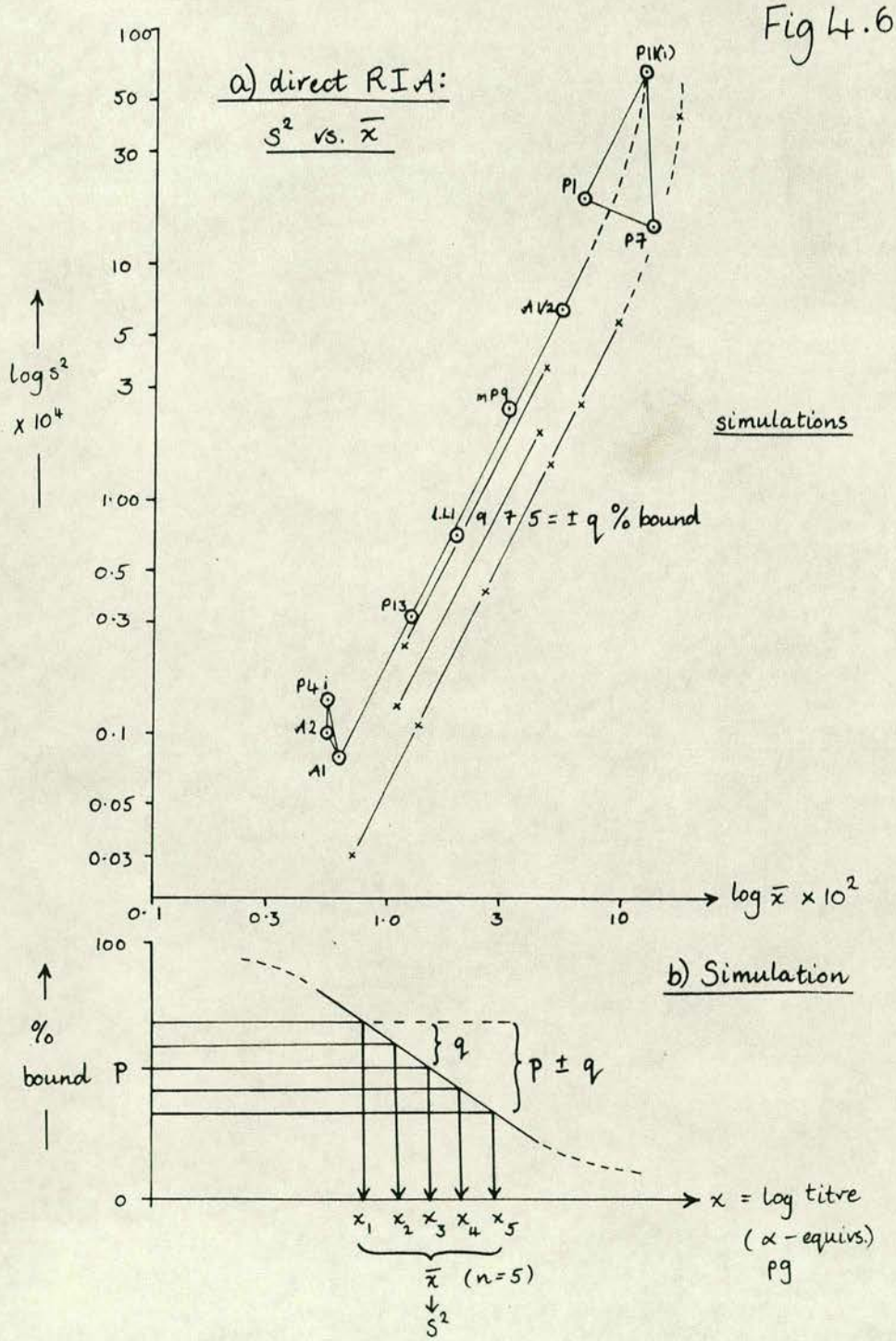
a) direct RIA:
s^2 vs. $\bar{x}$
100
50
30
10
5
3
1·00
0·5
0·3
0·1
0·05
0·03
log s^2 x 10^4
P1K(1)
P1
P7
A1/2
mPg
simulations
1.11
q 7 5 = ± q % bound
P13
P4 i
A2
A1
0·1
0·3
1·0
3
10
log $\bar{x}$ x 10^2
b) Simulation
100
% bound
P
q
P ± q
0
x_1 x_2 x_3 x_4 x_5
x = log titre
(∝ - equivs.)
pg
$\bar{x}$ (n=5)
s^2

Figure 4.7

Natural logarithm transformation of data

for peaks and troughs apparent in Fig. 4.4

Means of $\log_e$-transformed data (lnx) vs. variance (s^2) showing data-points connected in order of their untransformed relation and the scrambling of this relation (arrows) due to the transformation. Log_{10} has a similar effect. Functions of x which conserve the relation (linear or curved) are Reciprocal, Roots and Trigonometric functions.

Fig. 4.7

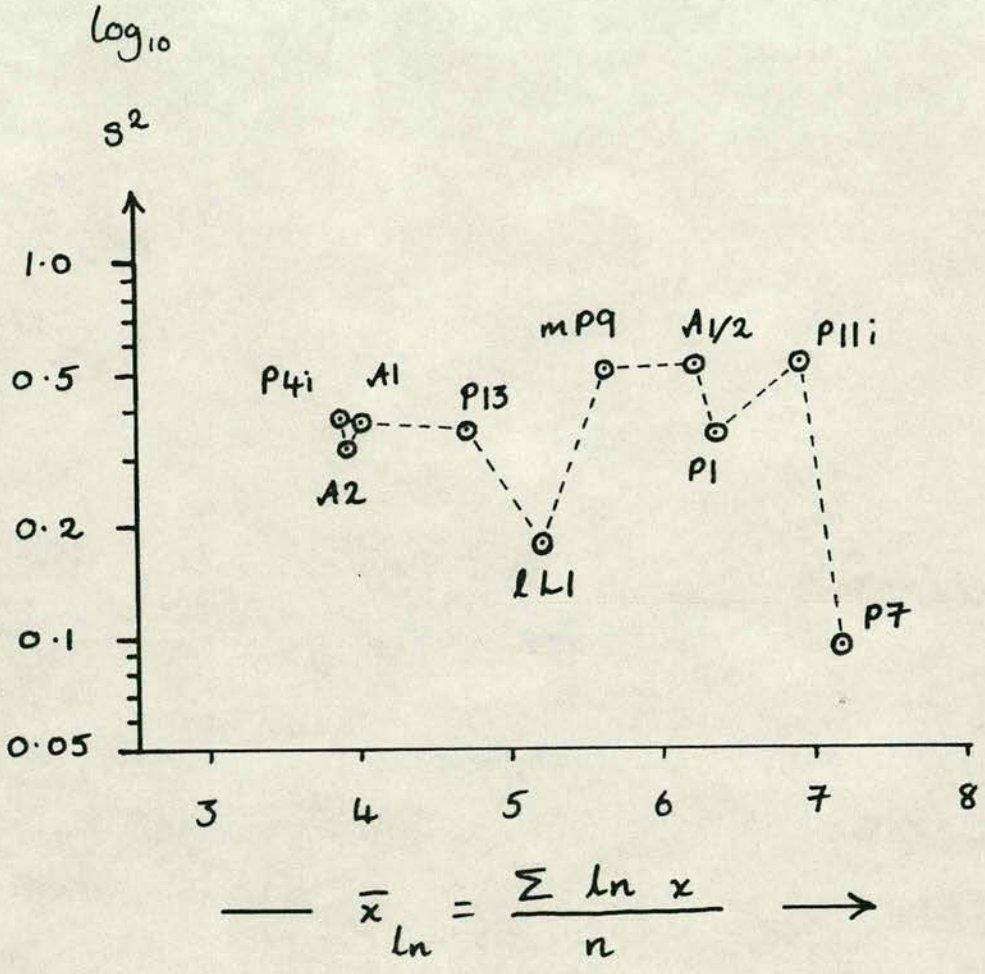
log10
s2
1·0
0·5
0·2
0·1
0·05
P4i
A1
A2
P13
mP9
A1/2
P1
P11i
lL1
P7
3
4
5
6
7
8
$\bar{x}_{ln} = \frac{\Sigma \ln x}{n}$

Figs. 4.8 - 4.11.

Few significant differences between the titres are revealed but there are sufficient to suggest a course of action in proceeding with a chromatographic analysis of ecdysteroids during metamorphosis. Only one difference is apparent between the sexes, however, at stage P12 (ii) (Fig. 4.10) when the male titre is lower than the female. The mean titres in males are consistently higher than the female mean titres throughout the first part of metamorphosis (late L1 - P7). In the female, early titres are exceeded during pharate adult development (late P1 and P5 (i) cf. P7--P8 and P12 (ii)); and the titre has dropped by the end of metamorphosis (P12 (ii) cf. A2). Likewise in the male, a relatively low titre after prepupation (P5 (i), cf. early P1) is exceeded in the pupa/pharate adult (P5 (i) cf. P6-P7 and P10) and the titre has dropped by stage A1 (cf. P10). The pooled data from both sexes emphasise the relatively high titres of the pharate adult as late as P11 (i) compared to P5 (i), a difference of 62.5h or about 60% of metamorphosis. Either the classical pupal/adult peak (Richards 1981 peak 11; expected and found here at stage P7) is of much greater duration than previous profiles have suggested (cf. Figs. 1.6, 4.4 and 4.12) or there is another peak during adult development (c. stage P11) which has only been resolved because of the use here of a staging system (Fig. 4.12 (c)).

4.3.3 An ecdysteroid(s) titre profile

The titre-elevation at "early" stage P1 is not significant

Figures 4.8-4.11

Log_e-transformed data as profiles of ecdysteroid titre during metamorphosis

Transformed RIA measurements presented as sample means with 95% confidence limits of population means, $\bar{y} \pm (t_{.95} \times S_{n-1})$

Fig. 4.8 Female stages compared

Fig. 4.9 Male stages compared

Fig. 4.10 Female/male comparison within each stage

Fig. 4.11 Pooled female and male data: stages compared.

Ordinate: log_e ecdysteroid measurement (pg ecdysone-equivalents per mg fresh weight). Abscissa: stages of metamorphosis. (Table 3.IV). Horizontal broken lines point out comparisons distant in the sequence of stages, (Figs. 4.8, 4.9 and 4.11). Stages P15 (ii), A1 and A1/2 include the weight of the puparium (feeding is assumed to commence in A2). The means shown in Fig. 4.11 are represented at Fig. 4.12 against time.

Fig. 4.8

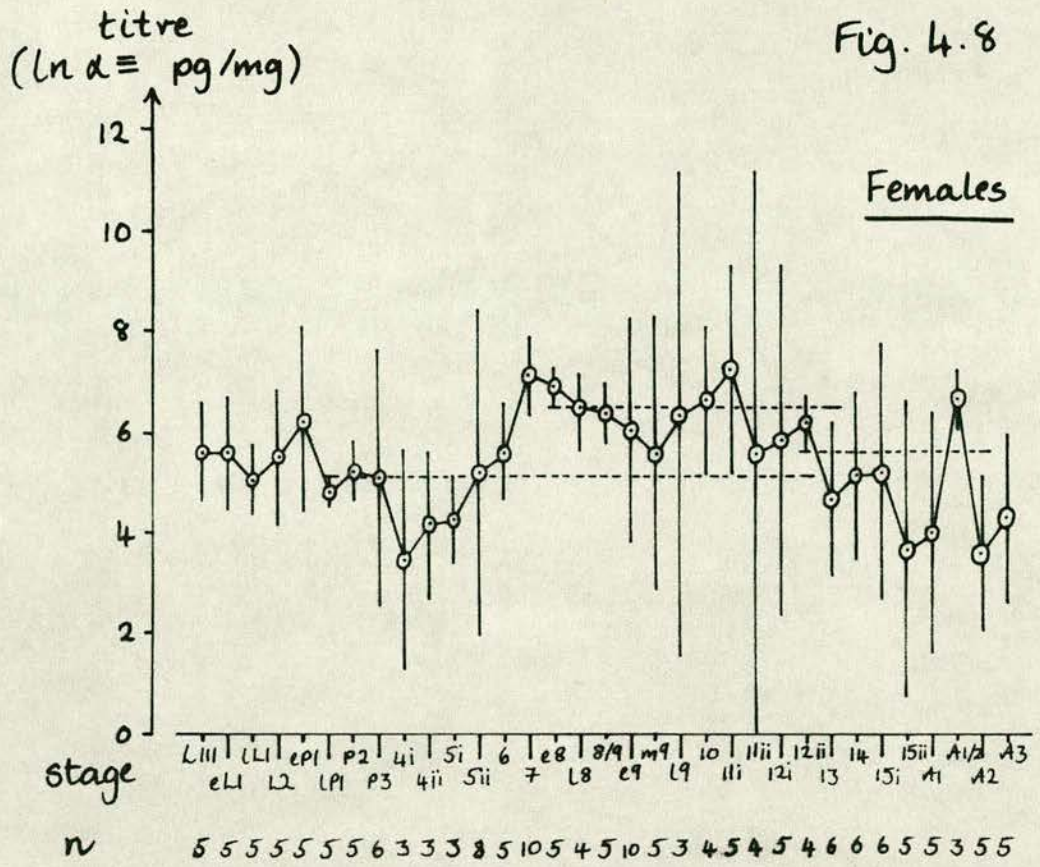
titre
(ln α ≡ pg/mg)
Females
12
10
8
6
4
2
0
stage
LIII eLI LI L2 ePI LPI P2 P3 4i 4ii 5i 5ii 6 7 e8 L8 8/9 e9 m9 L9 10 11i 11ii 12i 12ii 13 14 15i 15ii A1 A1/2 A2 A3
n
5 5 5 5 5 5 6 3 3 3 8 5 10 5 4 5 10 5 3 4 5 4 5 4 6 6 6 5 5 3 5 5

Fig. 4.9

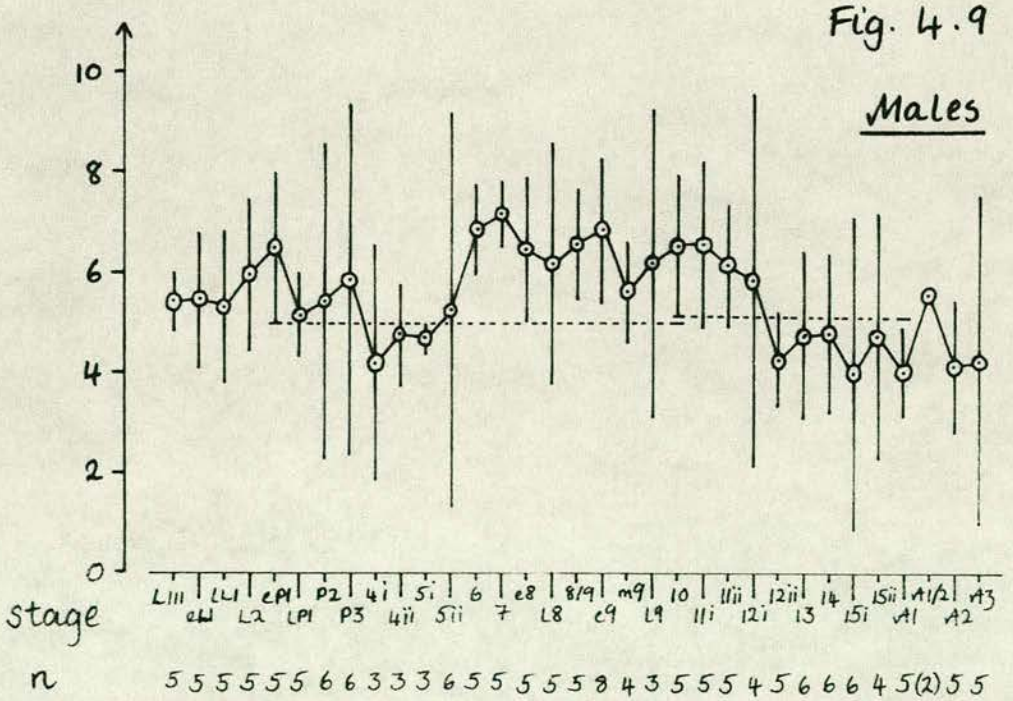
Males
10
8
6
4
2
0
stage
LIII eLI LI L2 ePI LPI P2 P3 4i 4ii 5i 5ii 6 7 e8 L8 8/9 e9 m9 L9 10 11i 11ii 12i 12ii 13 14 15i 15ii A1 A1/2 A2 A3
n
5 5 5 5 5 5 6 6 3 3 3 6 5 5 5 5 5 8 4 3 5 5 5 4 5 6 6 6 4 5 (2) 5 5

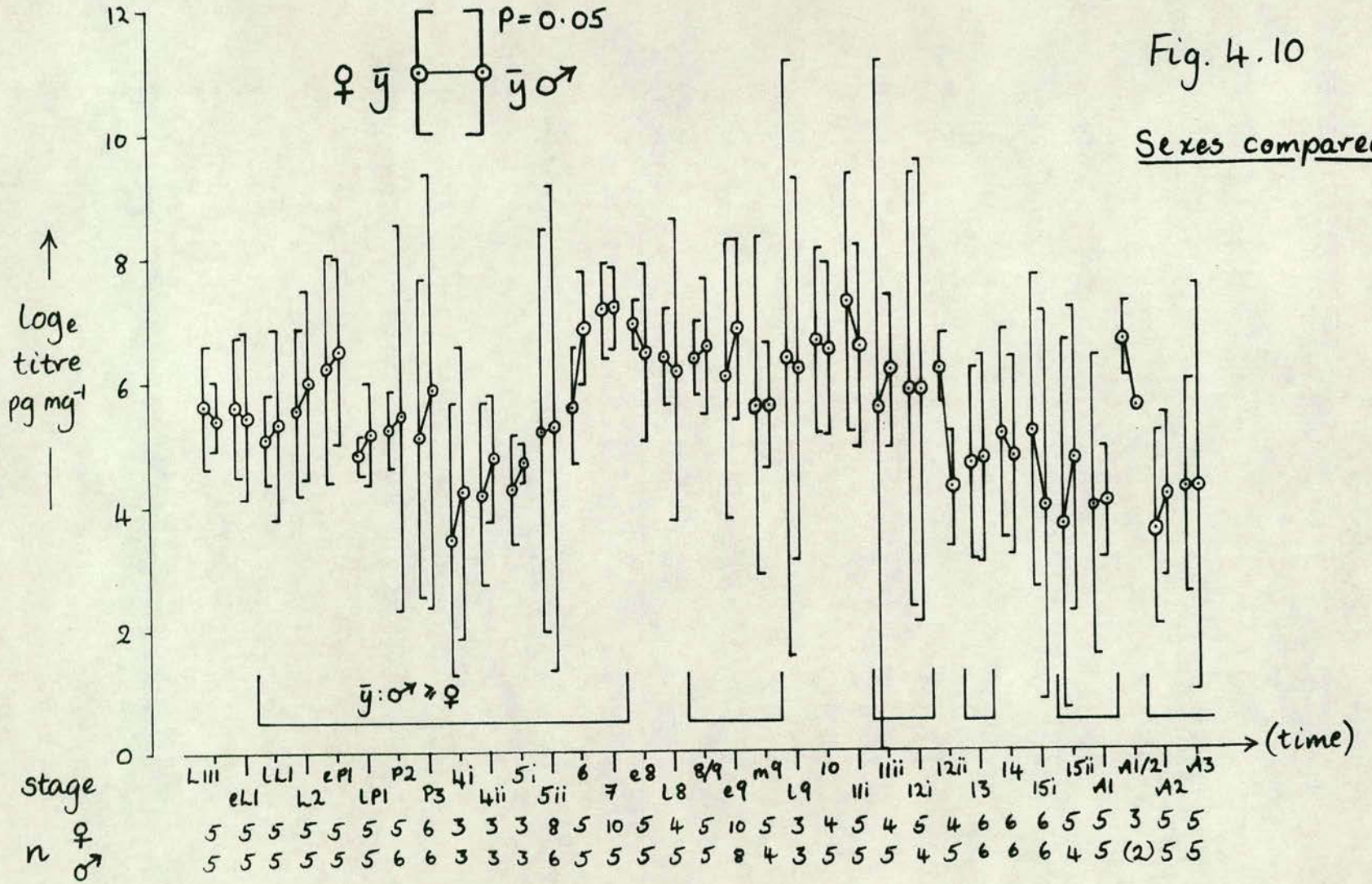
P=0·05
♀ ȳ
ȳ ♂
Fig. 4.10
Sexes compared
12
10
8
6
4
2
0
loge titre pg mg⁻¹
ȳ: ♂ ≠ ♀
(time)
stage
L III
eL1
LL1
L2
eP1
LP1
P2
P3
4i
4ii
5i
5ii
6
7
e8
L8
8/9
e9
m9
L9
10
11i
11ii
12i
12ii
13
14
15i
15ii
A1
A1/2
A2
A3
n ♀
5 5 5 5 5 5 5 6 3 3 3 8 5 10 5 4 5 10 5 3 4 5 4 5 4 6 6 6 5 5 3 5 5
n ♂
5 5 5 5 5 5 6 6 3 3 3 6 5 5 5 5 5 8 4 3 5 5 5 4 5 6 6 6 4 5 (2) 5 5

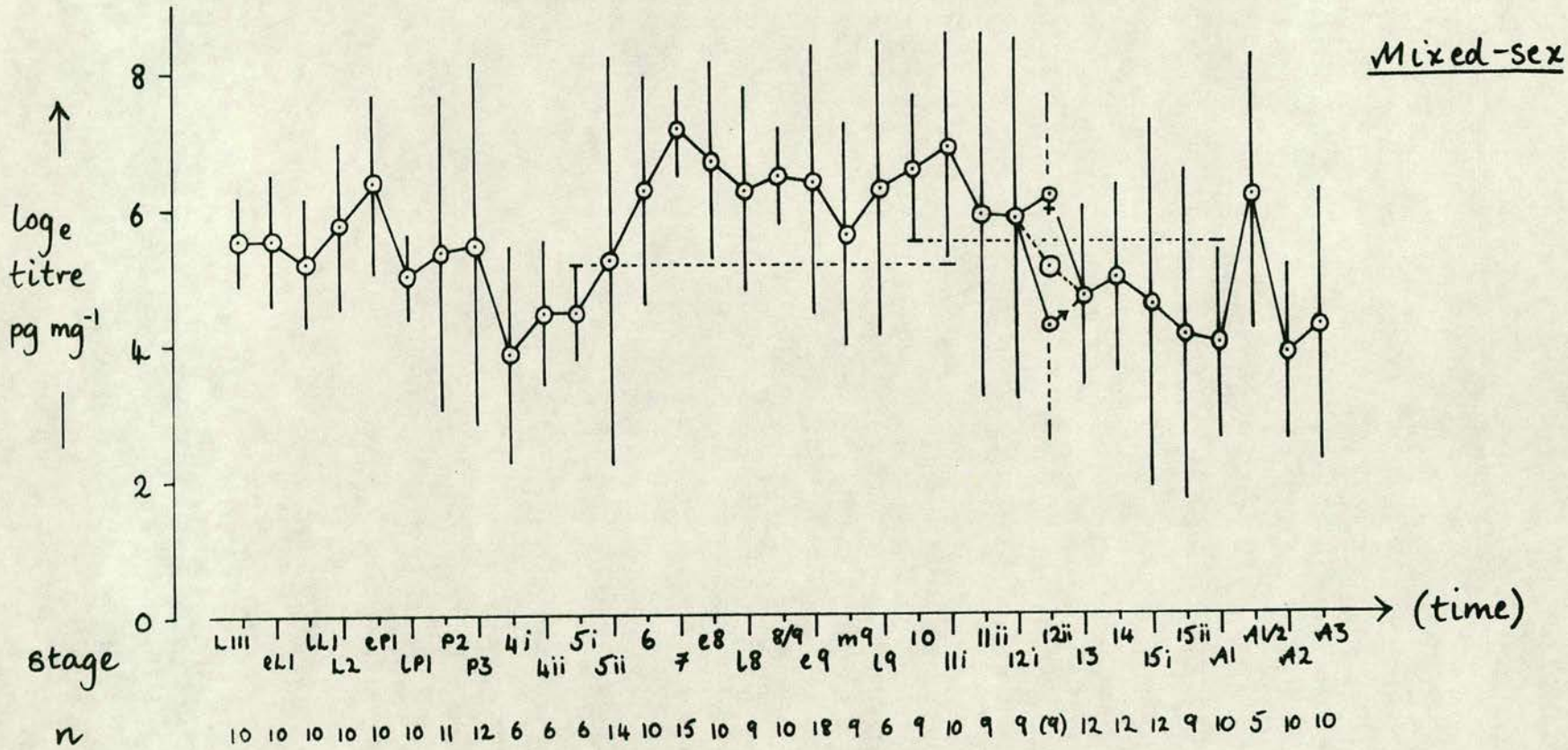
Mixed-sex
log e titre pg mg⁻¹
8
6
4
2
0
(time)
stage
L III eL1 LL1 L2 eP1 LP1 P2 P3 4i 4ii 5i 5ii 6 7 e8 L8 8/9 e9 m9 L9 10 11i 11ii 12i 12ii 13 14 15i 15ii A1 A1/2 A2 A3
n
10 10 10 10 10 10 11 12 6 6 6 14 10 15 10 9 10 18 9 6 9 10 9 9 (9) 12 12 12 9 10 5 10 10

Fig. 4.11

according to the transformed data, so strictly they cannot be said to demonstrate a pupariation peak (Richard's peak 9, (1981)); but it is suggested by the profiles of means alone in both sexes (Figs. 4.8, 4.9 and 4.12), and such a peak, just before, at, or soon after pupariation or its equivalent is widely reported, in Drosophila and in comparable species, (eg. Roberts et al. (1982), in Sarcophaga bullata; Steel et al. (1982), in Rhodnius; see reviews by Jungreis (1979) and Richards (1981, 1981b)). Such differences in reported titres may sometimes be explained as deriving from the variously different affinities of ecdysone, 20-OH-ecdysone etc. for the respective antisera if the ratios of one ecdysteroid to another change over developmental time. Alternatively the sample-numbers here may be simply too small; but for present purposes stage P1 will be considered to represent an elevation in ecdysteroid titre. Peak 11 of Richards (1981) is demonstrated by these data, at stage P7. After that, Fig. 4.12 (c) shows that the mean transformed titres show a trend to decrease linearly with estimated real time (m_1; the correlation of $\log_e$ titre with time is highly significant) as do the $\log_e$ titres of Hodgetts et al. (1977) (from their Fig. 2; for m (t = 38-96hrs, n = 5) $r = -0.735 > r\ (p = 0.1)$, $< r\ (p = 0.05)$). This decrease appears to be interupted, however, by a titre-elevation commencing at mid-P9, peaking at P11 (i) and declining until P12 (ii). The gradients m_2 and m_3 show lower correlation coefficients because of the limited number of sub-stages involved; but the fact that the gradients can be recognised suggests, first, that although the data are highly variable (Fig. 4.11) their sample-means may not deviate too seriously from an underlying relationship between titre

Figure 4.12

An understanding of the direct RIA data

Comparison of the pattern of transformed data (mixed-sex; from Fig. 4.11) with previous reports for Drosophila based on timed animals of mixed sex at 25°C. Ordinates: titre (units); Abscissa: developmental time (zero = pupariation, L2/P1).

a) Composite curve based on Hodgetts et al. (1977) and Klose et al. (1980) modified after Richards' 1981 review, which numbers the apparent peaks 9-11, (see Fig. 1.6). Ordinate: pg 20-OH-ecdysone-equivalents mg^{-1} fresh weight; Abscissa: time (h) after pupariation with stage-transitions mentioned by Hodgetts et al. (1977) whose metamorphosis data-points are marked (X). The measurements of Klose et al. (1980) (marked O; selected points only) are only loosely comparable with these (different antiserum; much higher maximum at P1; separate set of data for peak 11) but are included for the sake of Richards' peak 10 (their Fig. 3b) at 12-14h.

b) Ecdysteroid(s) titre-profile estimated from Handler (1982), adapted from similar curves at 20°C and 25°C. Data not presented, but the fifth peak in the profile of means, in particular, was probably not significant at 20°C, and neither the second nor the fifth putative peaks were confirmed in either sex assayed separately. Ordinate as (a).

c) Mean $\log_e$ titre-values from Fig. 4.11, stages weighted according to estimates of their durations (Table 3.IV; data points at mid- points of each (sub-)stage). For these mixed- sex data, 100% t_{P1-15} = 100h. Richards' peaks 9 and 11 are marked.
For gradients, m in the pharate adult (fitted by inspection) correlation coefficients are: for m_1 (P7-m.P9, P12ii-P15ii, n = 11) $r = -0.89 > r(p = 0.001)$; for m_2 (mP9-P11:; n = 4) $r = +0.74 < r(p = 0.1)$; for m_3 (P11i-P13; n = 5) $r = -0.76 > r(p = 0.1), < r(p = 0.05)$.

Fig. 4.12

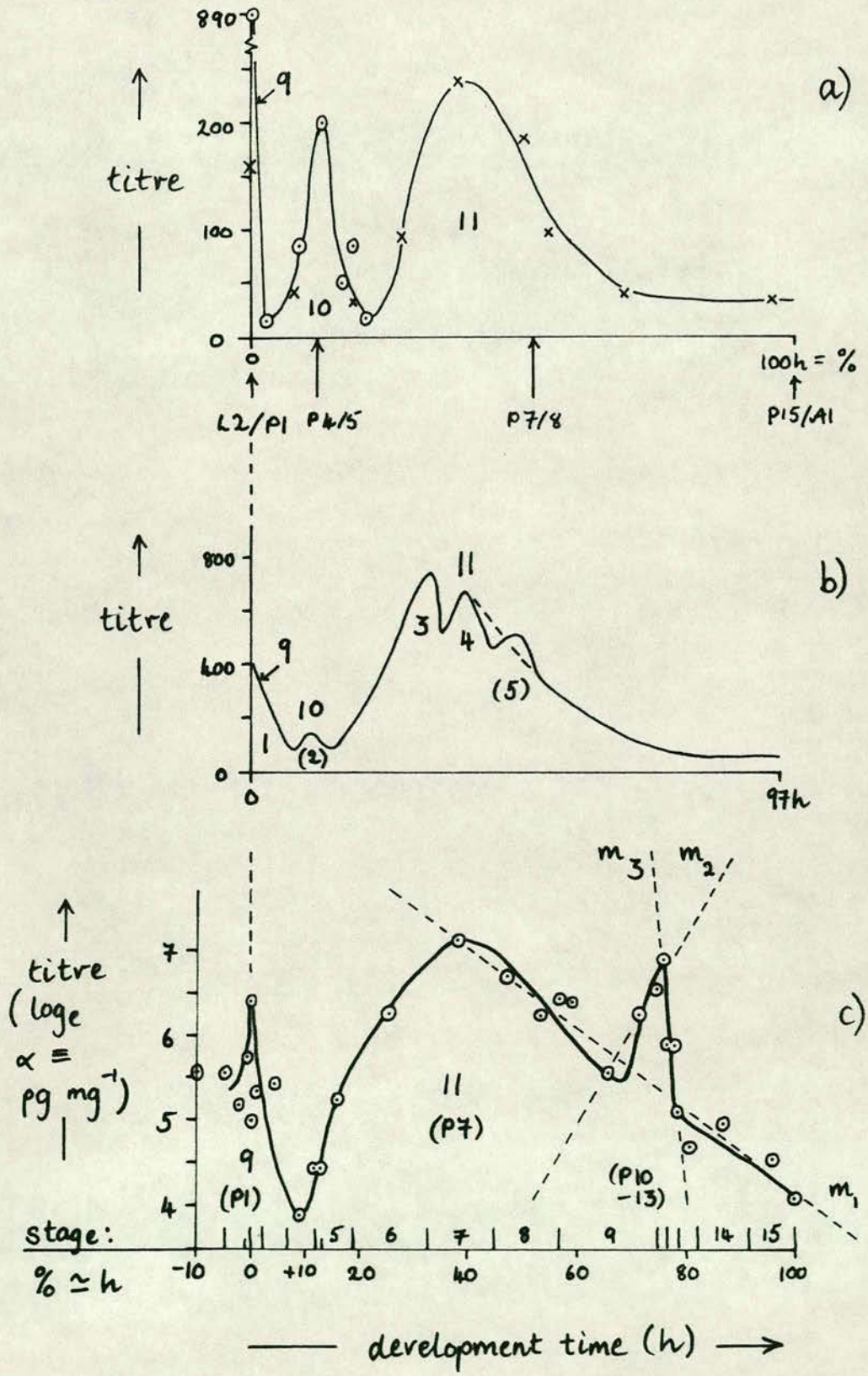
a)
titre
890
200
100
0
9
10
11
0
100h = %
L2/P1
P4/5
P7/8
P15/A1
b)
titre
800
400
0
9
10
1
(2)
3
11
4
(5)
97h
c)
titre (log$_e$ α = pg mg^{-1})
7
6
5
4
9 (P1)
11 (P7)
(P10 −13)
m_3
m_2
m_1
stage:
5
6
7
8
9
14
15
% ≃ h
-10
0
+10
20
40
60
80
100
development time (h)

and developmental age which is therefore recognisable at Fig. 4.12 (c). Secondly, the gradients argue against these pharate adult data being seen as representing a shoulder on the P7-peak because they are rather clearly defined changes in slope. It is therefore more likely that the use of stages P7-15 has exposed a hitherto hidden ecdysteroid(s) titre peak which is usually concealed by developmental asynchrony. Were the data presented in this chapter to represent an extension of, or shoulder on, the P7-peak the area under the graphs shown at Fig. 4.12 would be significantly greater, which should have influenced the previous reports based on timed animals. It is therefore more consistent with the published profiles of whole-body titre to interpret these new data in terms of a spike in the titre-profile confined to a small group of stages of short duration in the pharate adult (as shown at Fig. 4.12.(c)).

On the basis of these measurements it was decided that stages P1 (Richard's peak 9), P7 (Richard's peak 11) and P10-13 should be analysed further, these showing titre-elevations common to both sexes at stages which are relatively easy to collect in bulk; (P11 alone is not). P1 shortly precedes pupal cuticle production and, similarly, P7 precedes production of the adult cuticle, while P10-13 encompasses the darkening of this cuticle.

Chapter Five

Analytical - preparative high performance liquid chromatography (HPLC); HPLC - coupled RIA

Selected stages of *Drosophila* metamorphosis were subjected to small-scale preparative HPLC and it was found to be necessary to prefix this with a purification procedure which included thin-layer chromatography (TLC) which itself required to be preceded by a low pressure reverse-phase chromatography step (short C_{18} columns ("Sep-pak" cartridges, Waters Ass.) were used - see Shackleton and Whitney, 1980 and Appendix 4). These samples were such that untreated extracts were incompatible with the HPLC column and samples not first cleaned up on an affinity column were immobilised on the silica-gel TLC plates.

Recovery efficiencies for ecdysteroid concentration standards taken through this protocol were found to be highly variable (Appendix A4), necessitating the introduction into the extracts of an ecdysteroid as an internal concentration standard whose proportional recovery could be monitored at the HPLC level and followed qualitatively through the subsequent analysis by radioimmune assay (RIA). In selecting an ecdysteroid for this purpose from amongst those available (ecdysone, 20-OH-ecdysone; then ponasterone A, cyasterone, polypodine B, inokosterone, makisterone A and muristerone) it was necessary that the chosen compound be not a subject of the analysis, that it behave similarly to the compounds of interest with regard to recovery efficiency, and that it should

not co-elute with these compounds in reverse phase HPLC but yet have a similar retention time. Makisterone A (Fig. 1.4) was found to elute freely during HPLC (using aqueous methanol/C_{18}), between ecdysone and 20-OH-ecdysone, and it shares these compounds recovery characteristics through TLC (See A4.2 f). The other ecdysteroids listed above either fail to elute under the same conditions as ecdysone or they show peak retention times very similar to 20-OH-ecdysone (Wilson et al. 1982; and author's observations); so Makisterone A (24-methyl-20-OH-ecdysone) was used in the preparations described in this chapter (and also for the parallel analysis by gas-liquid chromatography; chapter 6).

Preliminary quantitation of ecdysteroids after HPLC was performed by HPLC-coupled UV-spectrophotometry; but this was found to give false positive identifications of, especially, 20-OH-ecdysone in control experiments (A4.2, d and f). Therefore HPLC elution fractions were collected and analysed further by RIA to confirm ecdysteroid identifications and to make accurate measurements of endogenous concentrations of ecdysone and 20-OH-ecdysone. Only one of the stages selected for analysis was examined in this way both with and without additional makisterone A, and this extract was found to contain a certain amount of the steroid endogenously. The data for the other stages, therefore, are not concerned with naturally-occurring makisterone A; but the quantity employed as an internal standard was large enough (10^{-5}M) to make possible reasonably accurate estimations of the other ecdysteroids, were there to be makisterone-A present in the extracts of a concentration similar to that of ecdysone/20-OH-ecdysone.

5.1 Sample preparation

Sample weights are shown at Table 5.I. Stage P1 was analysed by HPLC both with and without exogenous makisterone A as internal concentration standard. The sample without added steroid (P1-Mak.A) makes it possible to ask whether native makisterone A occurs at this stage in development; but it was not prepared in quite the same way as the corresponding sample with added steroid (P1+Mak.A), so it is not strictly comparable in terms of recovery-efficiency. (This sample was about five times heavier than the others; and it differed from them in TLC loading-density and elution area, and also in the duration of storage after HPLC). However, it is possible to make a rough estimate of the native concentration of makisterone A in this stage by calculating the efficiency of recovery of ecdysone and 20-OH-ecdysone with reference to these compounds in the sample spiked with makisterone A.

After addition of makisterone A, the samples were prepared as described at Section 2.14. Their purifications included the use of thin-layer silica-gel chromatography (TLC) which is illustrated at Figs. 5.1 and 5.2.

5.2 HPLC separations of ecdysteroids

After ethanol-elution, the samples are prepared for and subjected to reverse-phase HPLC as described at Section 2.15 to separate the component ecdysteroids on the basis of their

TABLE 5.I

Samples subjected to HPLC-RIA

Sample	Total mass (g)	Number of animals	Fresh Weight (mg/animal)
without internal standard:-			
P1	5.175	3018	1.175
with internal standard:-			
P1	1.0	655	1.53
P7	1.0	783	1.28
P10-13	1.0	758	1.32

Figure 5.1

P1 (without mak.A)

Silica-gel TLC, stage P1 methanolic extract (without exogenous makisterone A) observed under UV-illumination. R_F standards are: makisterone A (μ), 20-OH-ecdysone (β) and ecdysone (α). Loading zone 12cm x spot diameter. Plate scraped for ethanol-elution from R_F 0.29-0.78 (relative R_F (μ = 1.0) 0.53-1.41). (This plate represents 4/5 of the sample, the remainder having been run on a separate plate (see A4.2 f, sample 9)).

Fig. 5.1

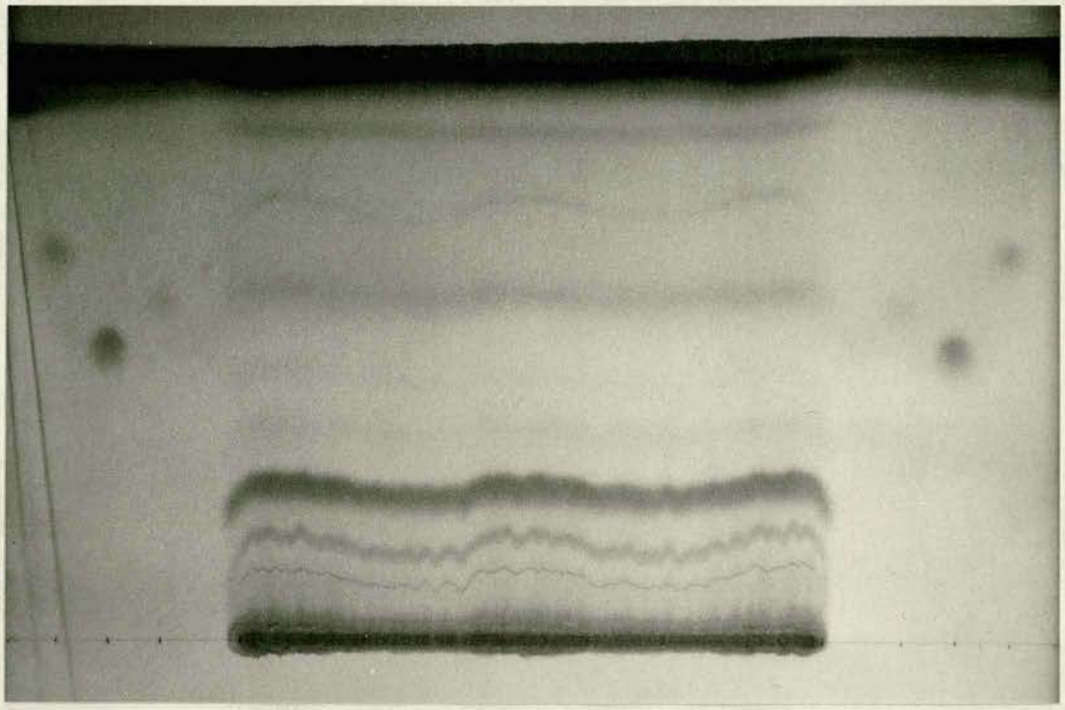

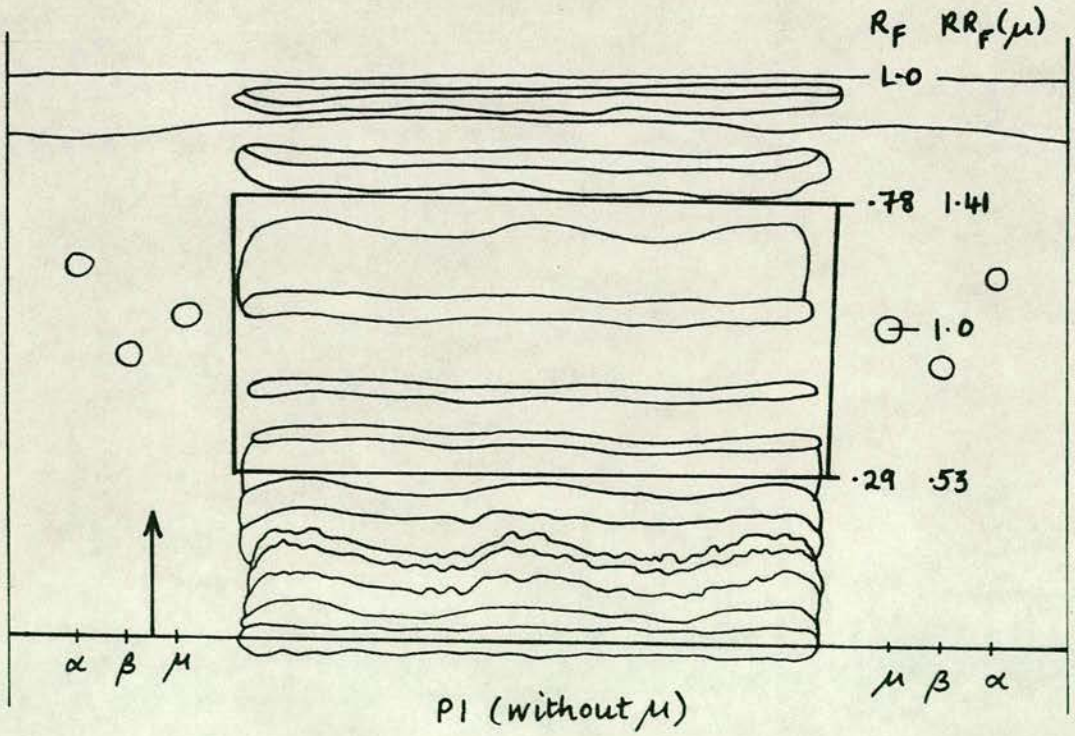

Figure 5.2

Stages P1, P7, P10-13 (+ mak.A)

Silica-gel TLC methanolic extracts (with makisterone A (μ) as internal concentration standard) observed under UV-illumination. R_F standards include ecdysone (α) and 20-OH- ecdysone (β). Ethanol elution from R_F 0.14- 0.63, RR_F (mak.A = 1.0) 0.4-1.81. Loading zone = 4cm x spot diameter.

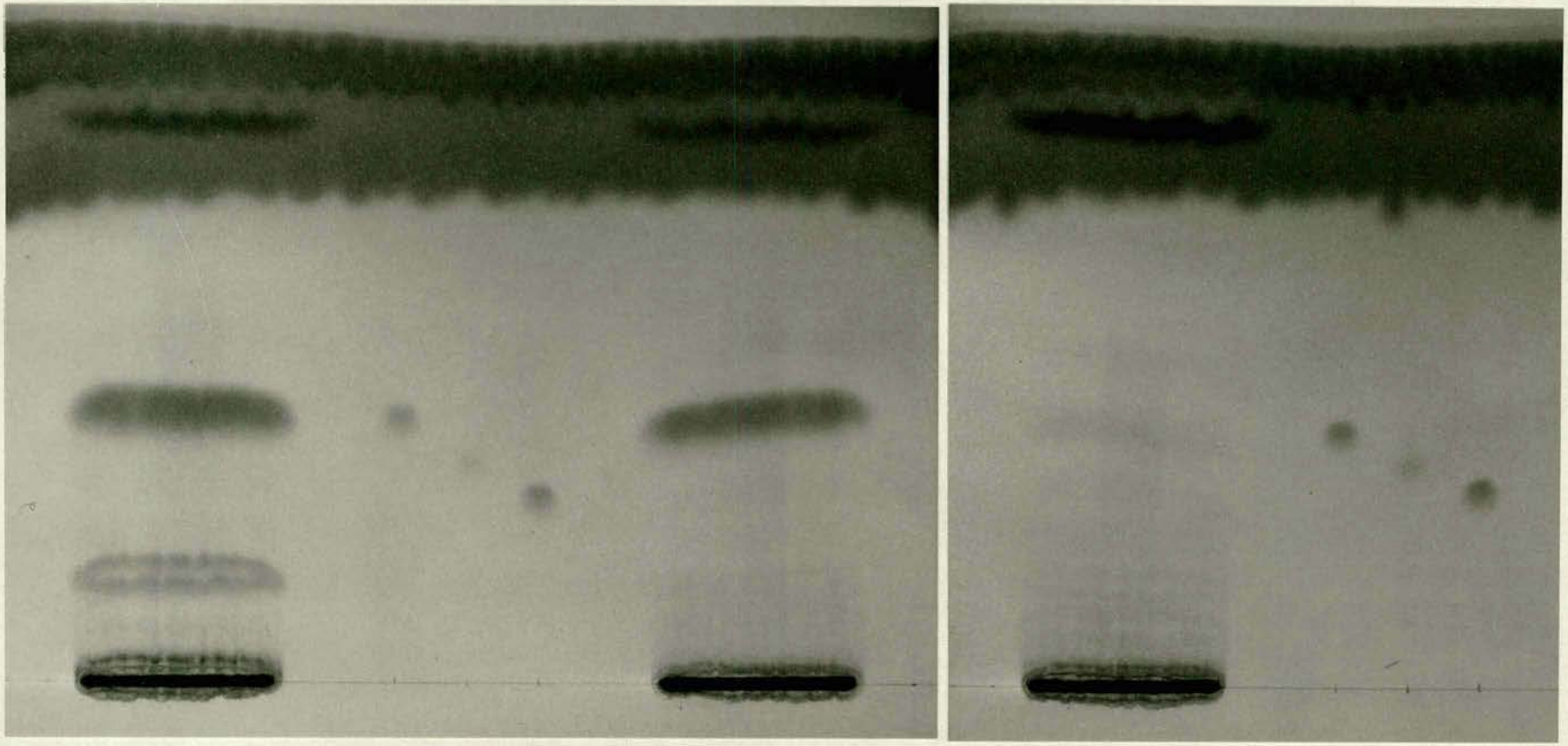

Fig 5.2

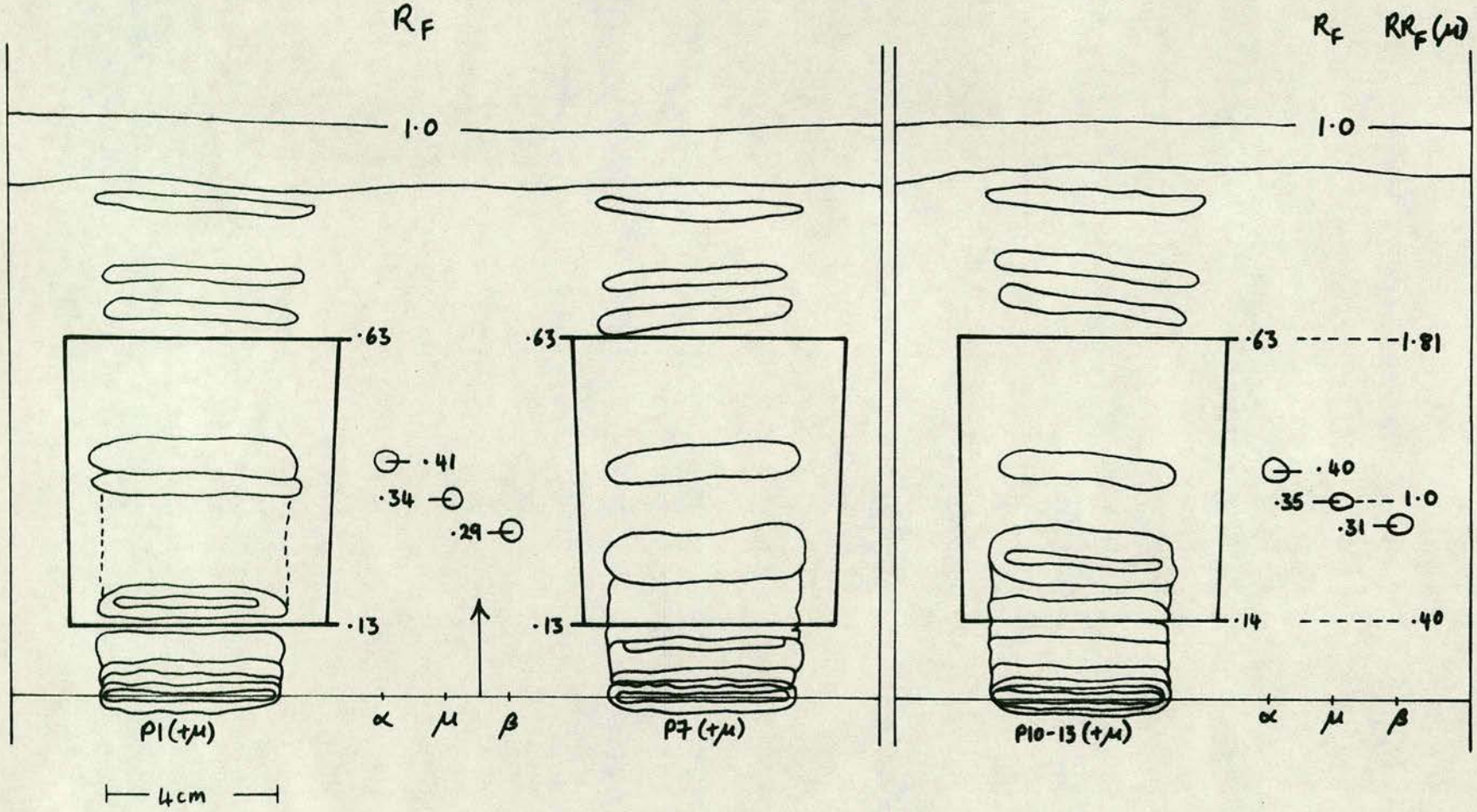
R_F
1·0
·63
·13
·41
·34
·29
α
μ
β
P1 (+μ)
P7 (+μ)
4cm
R_F
$RR_F(\mu)$
1·0
·63
1·81
·40
·35
1·0
·31
·14
·40
α
μ
β
P10-13 (+μ)

Fig. 5.2 (Key)

differential distribution between C_{18} (Octadecylsilane) and aqueous methanol. Ecdysteroids were provisionally identified by their similarity to a standard 10^{-6}M ecdysteroids solution with respect to UV-OD peak retention times $\pm$ 5%. Representative chromatograms are illustrated at Fig. 5.3.

5.3 Quantitative HPLC-UV spectrophotometry

Ecdysone and 20-OH-ecdysone concentrations in stages P1, P7 and P10-13 were measured with reference to makisterone A as an internal concentration standard by computation of UV-absorption peak areas during HPLC elution and comparison with peaks generated by external concentration standards including Makisterone A, (see Section 2.15). Table 5.II shows the results of this preliminary analysis (which was not applicable to 20-OH-ecdysone in stages P7 or P10-13 because of the complexity of the chromatograms in this region). Makisterone A recovery-efficiencies (approx. 10%) differ slightly with developmental stage. These limited data suggest that the three stages show similar concentrations of ecdysone (approx. 20 ng mg^{-1}).

5.4 Preparative HPLC: collection of eluate fractions for RIA

Samples of ecdysteroids separated by HPLC were collected as 30 second fractions of the HPLC eluate allowing for a delay between the detector cell and the delivery dropper of 35 seconds. The volume of each injection of a given sample concentration was kept relatively small in order to avoid overloading the column and so making the

Figure 5.3

Chromatograms from HPLC-UV spectrophotometry

HPLC reverse-phase chromatography (C_{18}/aqueous methanol), stages P1, P7 and P10-13 methanolic extracts: Blank = mobile phase; retention-time ecdysteroid standards were ecdysone (α) and 20-OH-ecdysone (β); TLC R_F standard markers served as retention-time controls. Stage P1 with and without makisterone A (μ) as internal standard, and P7 and P10-13 with internal standard. λ = 254nm. a) 50% aqueous methanol, (20 min.); b) ecdysone/20-OH-ecdysone retention-times (20 min, 100μl 10^{-6}M; Simes); c) 20-OH-ecdysone TLC R_F marker eluted in ethanol; d) ecdysone, as (c); e) and (f) stage P1 (-μ) before change in retention-times; g) and h) stage P1(-μ) after change in retention times; e and g) ecdysone/20-OH-ecdysone (α/β) retention- times standard solution (20 min. isocratic + 5 min. gradient 50-100% methanol; 45μl); f and h) P1 without exogenous makisterone A (as (e) = 4.5% sample vol.). j) stage P1 with makisterone A as internal standard (P1+μ); (Isocratic 20 min., 100μl = 10% sample; mean retention time of makisterone A for intercalated standards = 11.08 min.); k) stage P7 with makisterone A as internal standard (P7 + μ) (Isocratic 20 min. 100μl = 10% sample; mean retention-time of makisterone A for intercalated standards = 9.41 min. before shift in retention times) l) stage P7, as (k) after shift in retention- times (new mak. A retention-time from intercalated standards = 11.21 min.). m) stages P10-13 with makisterone A as internal standard (P10-13 + μ), (Isocratic 30 min, 100μl = 10% sample volume; mean retention-time of intercalated standard makisterone A = 10.94 min.).

Fig. 5.3 (a - d)

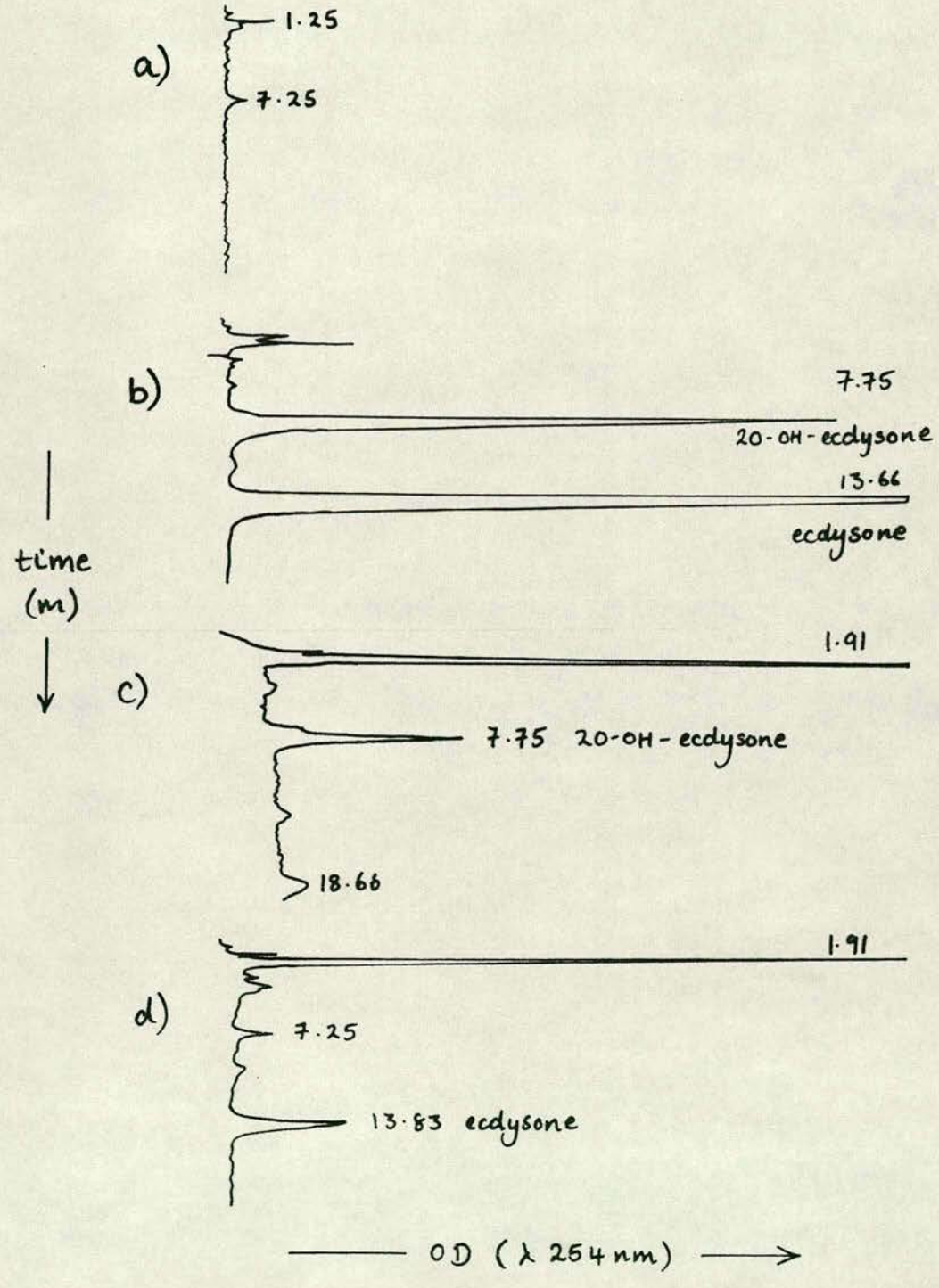
a)
1·25
7·25
b)
7.75
20-OH-ecdysone
13·66
ecdysone
time
(m)
c)
1·91
7·75 20-OH-ecdysone
18·66
d)
1·91
7·25
13·83 ecdysone
OD (λ 254 nm)

Fig. 5.3 (e-h)

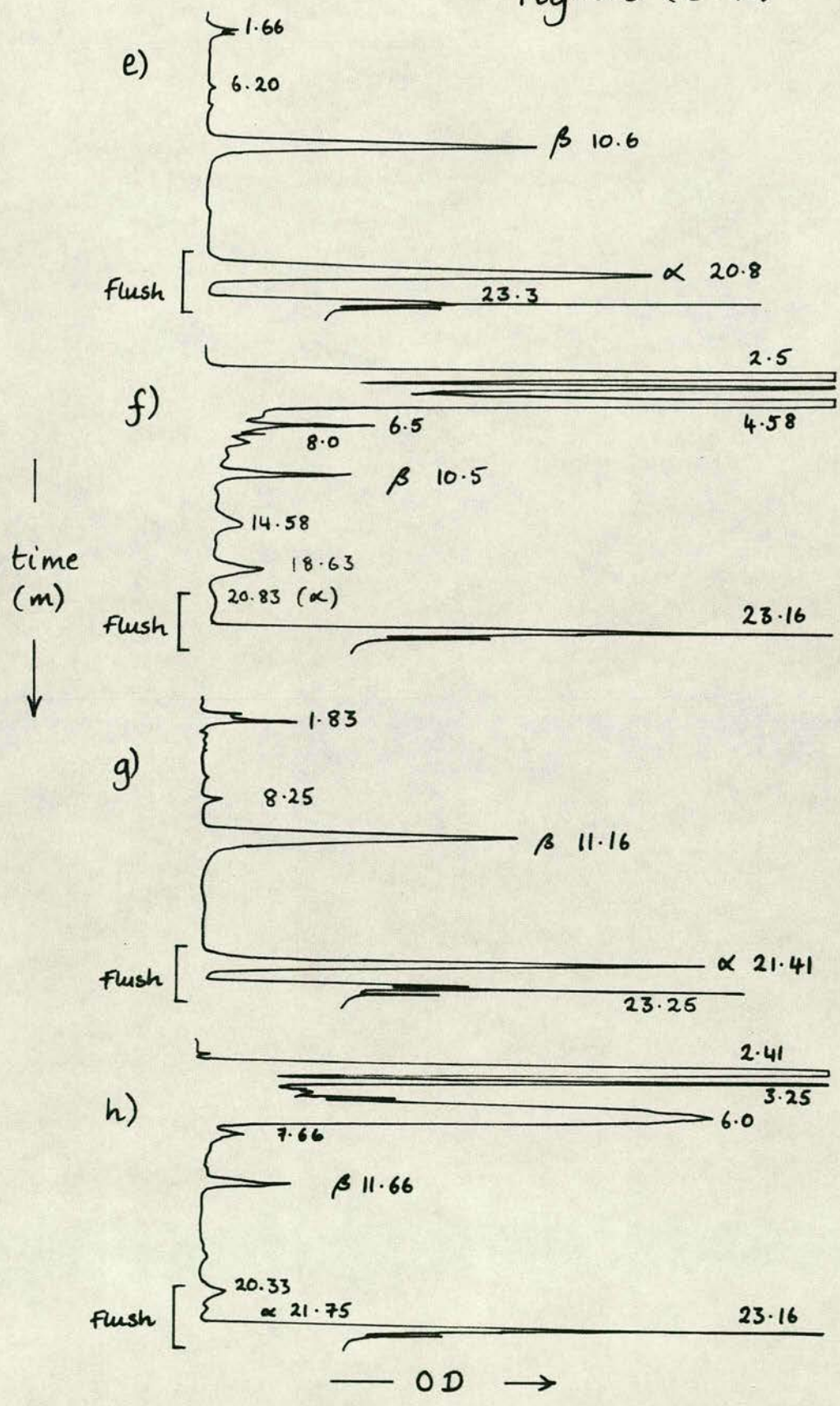
e)
1·66
6·20
β 10·6
α 20·8
Flush
23·3
f)
2·5
6·5
4·58
8·0
β 10·5
14·58
18·63
20·83 (α)
Flush
23·16
time
(m)
g)
1·83
8·25
β 11·16
α 21·41
Flush
23·25
h)
2·41
3·25
6·0
7·66
β 11·66
20.33
α 21·75
Flush
23·16
OD

Fig. 5.3 (j–m)

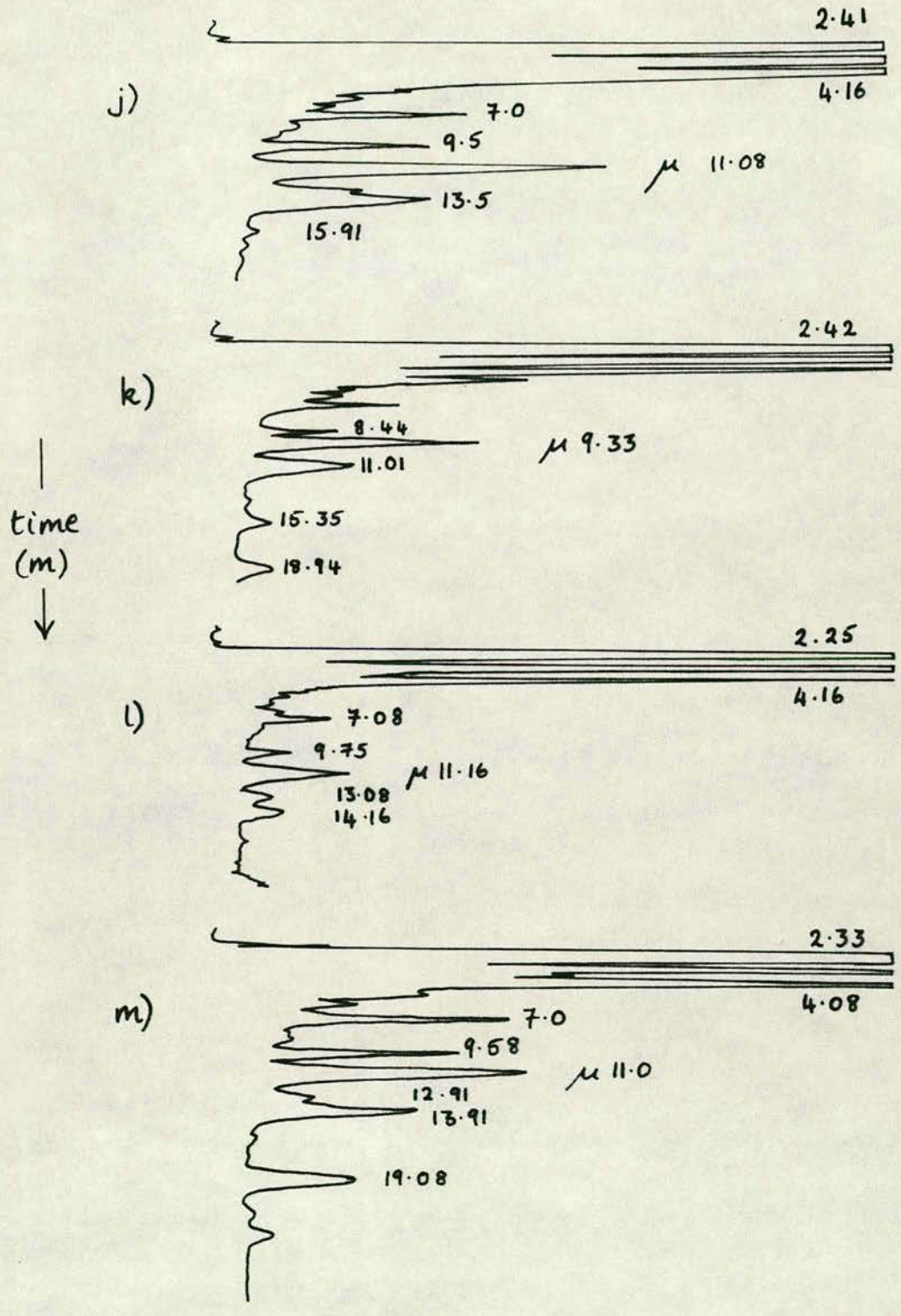
j)
2·41
4·16
7·0
9·5
μ 11·08
13·5
15·91
k)
2·42
8·44
μ 9·33
11·01
15·35
18·94
time
(m)
l)
2·25
4·16
7·08
9·75
μ 11·16
13·08
14·16
m)
2·33
4·08
7·0
9·58
μ 11·0
12·91
13·91
19·08
— O D →

TABLE 5.11

Ecdysteroid quantification by HPLC-UV spectrophotometry (λ= 254 nm)

Stage (lg)	P1		P7		P10-13	
Steroid	β	(μ) α	(μ)	α	(μ)	α
No. runs, n =	1	(10) 10	(6)	6	(21)	21
Concentration ($x10^{-6}$M)	0.30	(7.1) 4.6	(6.8)	4.3	(5.3)	2.8
Recovery (% μ)		(10.14)	(9.67)		(7.54)	
Therefore 100% = ($x10^{-6}$M)	3.0	(45.4)	(44.5)		(37.7)	
Steroid/extract (10^{-6}g/ml) = Steroid/tissue (μg/g)	1.42	21.05	20.63		17.49	
Proportion (%) steroid:fresh weight	0.00014	0.0021	0.0021		0.00175	
Animals/extract	655	655	783		758	
Mass/animal (mg)	1.527	1.527	1.277		1.319	
Steroid/animal (ng)	2.17	32.17	26.35		23.07	
Steroid/fresh weight ($ng\ mg^{-1}$)	1.42 =P1β	21.05 =P1 α	20.63 =P7 α		17.49 =P10-13 α	

β = 20-OH-ecdysone
μ = 24-methyl-20-OH-ecdysone (makisterone A)
α = ecdysone

chromatography erratic (see Appendix A5); so fractions were collected by multiple injection and exhaustive dilution of the 1ml extracts. A disadvantage of this strategy, however, is that the chromatographic conditions may change during the course of collection from a single sample, despite any precautions which might be taken, for instance, against aeration or selective evaporation of the mobile phase. On two occasions during the collection of fractions from these samples (P1 without Mak.A; P7+Mak.A.) a change was noticed in the retention-times of standard ecdysteroids intercalated between aliquots of the sample; so it became necessary to collect two sets of fractions (I and II) which were analysed separately by RIA and their results combined.

Because of this unreliability of the retention times, and also to facilitate quantification by UV-spectrophotometry, it was necessary to monitor the chromatography during each series of injections by intercalating injections of a mixture of ecdysteroids (standards for both concentration and retention-time) between sample injections. The standards were sent to waste while the sample eluates were collected repeatedly. It was not possible under these circumstances to program a purge of the injector system after each injection of ecdysteroid standards (which would reduce the risk of standards being carried over into the sample fractions during a subsequent run). Therefore a control preparation was made: 1ml of 50% methanol (= blank) was collected, in the same way as were samples P1/P7/P10-13, by multiple injection (100µl) of the blank alternating with injections of the standard solution of ecdysteroids used in conjunction with the Drosophila samples. The blank chromatograms

showed no UV-absorption peaks at 254nm; but the fractions so collected were subjected to further analysis by ecdysteroid RIA and treated as an HPLC-RIA background.

(Finally, a 1ml aliquot of the standard ecdysteroids mixture was fractionated by HPLC (multiple injection) and collected to be assayed by RIA. This allows the efficiencies of recovery of ecdysone, makisterone A and 20-OH-ecdysone through HPLC-RIA to be roughly compared).

The retention times of ecdysteroid standards intercalated between injections of samples and controls were surveyed to predict which eluate fractions required extensive analysis by RIA.

5.5 Eluate volume-reduction: monitoring recovery-efficiency (See 2.16).

HPLC eluates overall constituted a large volume of aqueous methanol which required to be reduced to a series of small volumes of alcohol for systematic RIA. In order to avoid either prohibitive evaporation under nitrogen or exposure of vacuum pumps to methanol and the glassware transfers involved in freeze-drying, the fractions were reduced in volume by concentration of their component ecdysteroids on C_{18} cartridges ("Sep-paks". Waters Ass.) (See Section 2.16.2) and subsequent elution in methanol which was brought to 1ml (the original internal standard equivalent volume) (See Section 2.16.3).

There were too many eluate fractions to use one C_{18} cartridge per fraction, so they were re-used several times (in accordance with Shackleton and Whitney, 1980) and their efficiency in retaining ecdysone and 20-OH-ecdysone (extremes of polarity amongst the ecdysteroid standards) was measured after they had passed large volumes of 1:3 methanol/water by the passage through them of a further small volume of ecdysone/20-OH-ecdysone solution (10^{-6}M) (See Section 2.16.4). Fig. 5.4 shows percentage recovery through C_{18} cartridges over a range of 1-10 x used for volume reduction, based on measurements by HPLC-UV spectrophotometry. There is a significant difference between the recoveries of ecdysone and 20-OH-ecdysone - 83.6% and 64.8% mean values respectively, but the data do not suggest a progressive degeneration of the cartridges with up to ten uses under the working conditions of Section 2.16; so the different extents to which they were used may be disregarded and these mean recoveries of ecdysone and 20-OH-ecdysone may be taken to be representative of C_{18} cartridges which have passed more than 50ml aqueous methanol.

The recovery of makisterone A (not measured) may be expected to be in the same relation to ecdysone/20-OH-ecdysone as the respective retention-times observed during HPLC since both depend upon the differential distribution of ecdysteroids between octadecylsilane and aqueous methanol. Calculation on this basis gives a value for recovery of makisterone A during fraction volume-reduction of 74.9% (data not presented; cf. mean recovery for ecdysone/20-OH-ecdysone = 74.2%).

Figure 5.4

Multiple use of C_{18} cartridges:

recovery efficiency

Mean values for recovery-efficiency of ecdysone (α) and 20-OH-ecdysone (β) on the ordinate vs. increasing number of previous uses of the cartridge (Sep-PAK, Waters Ass.) on the abscissa. Points represent means of 3-5 measurements of recovered concentration as % original concentration of a small volume of standard solution. There are no significant differences between recoveries of α and β at any one degree of x ($p = 0.05$); but the data treated as a whole do show such a difference and the mean values for the two steroids are shown (y_α, y_β). The apparent trend towards decreasing efficiency with number of uses for the recovery of ecdysone is not significant (correlation coefficient $r = -0.524 < r$ ($p = 0.05$, $n-1=9$) (cf. 20-OH-ecdysone: $r = + 0.164 < r$ ($p = 0.1$); and for Ratio α/β vs. previous uses $r = -0.600 < r$ ($p = -0.05$) (data not shown)). Nor does the variability of recovery vary significantly with x; (for variance on y, , S^2 vs. previous uses $r_\alpha = +0.278 < r$ ($p = 0.1$) and $r_\beta = +0.601 < r$ ($p = 0.05$), (data not shown)).

Fig. 5.4

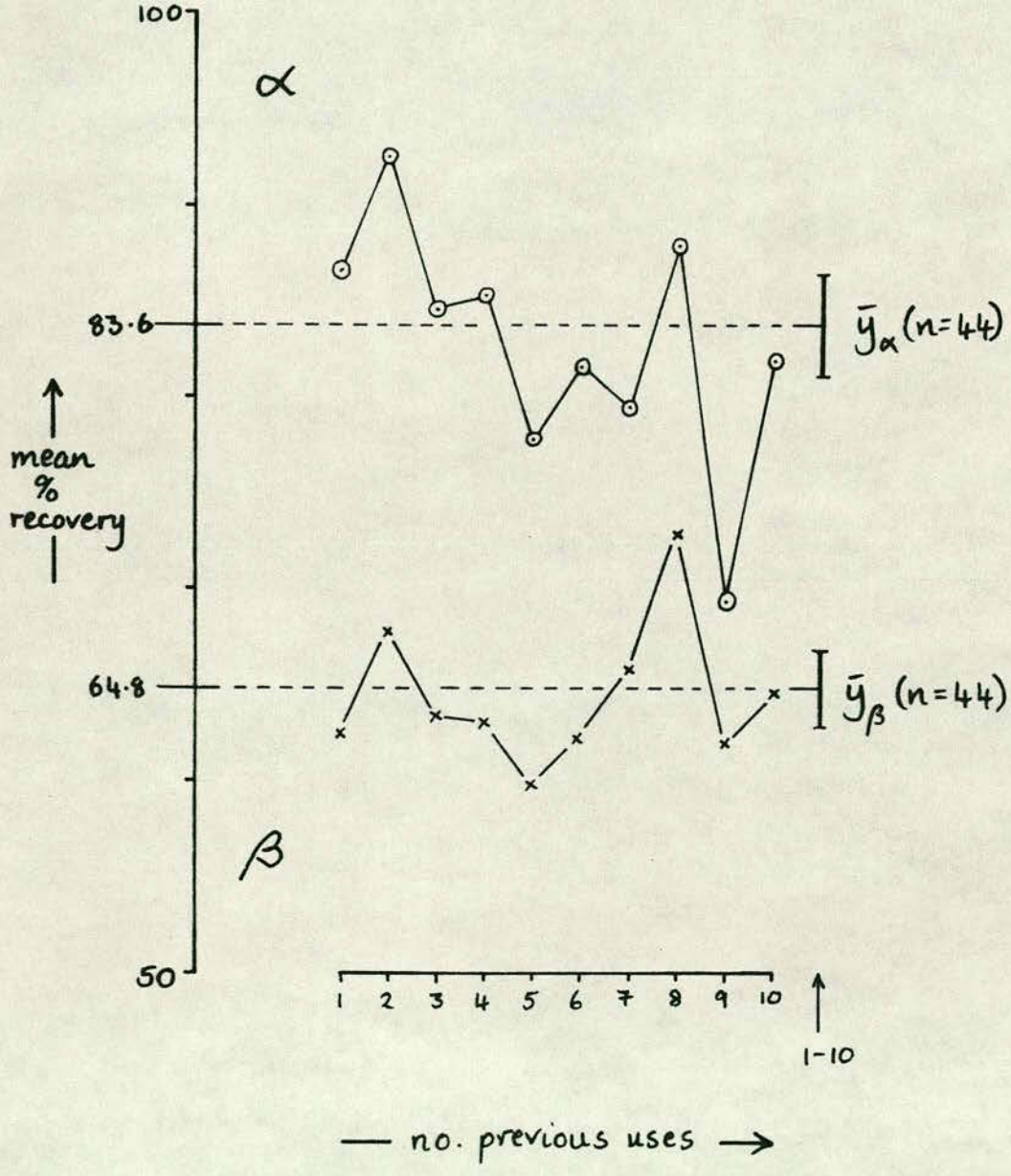
100
α
83·6
$\bar{y}_\alpha$ (n=44)
mean % recovery
64·8
$\bar{y}_\beta$ (n=44)
β
50
1 2 3 4 5 6 7 8 9 10
1-10
no. previous uses

5.6 HPLC-coupled RIA

A mouse antiserum (MAS) was raised against 20-OH-ecdysone-carbomethyloxime-bovine serum albumen as explained in Section 2.17 and used in a radioimmune assay of the ecdysteroid concentrations in HPLC eluate fractions (Section 2.20, using both 7d and 12d bleeds of MAS). In this Section a background correlation is applied to these RIA data (5.6.1) and the corrected data are analysed to determine ecdysteroid titres in the three stages selected for detailed investigation by HPLC-RIA (5.6.2). In this way the following titres were derived from the samples shown at Table 5.I:-

Stage P1:	20-OH-ecdysone	0.61	ng mg^{-1}
	makisterone A (endogenous)	0.62	" "
	ecdysone	3.24	" "
	Total	4.47	
Stage P7	20-OH-ecdysone	1.56	" "
	ecdysone	4.60	" "
	Total	6.16	" "
Stages P10-13:	20-OH-ecdysone	0.57	" "
	ecdysone	2.22	" "
	Total	2.79	" "

The following, then, is an account of how these measurements were obtained; and they are compared with those from HPLC-UV spectrophotometry at the end of the chapter (Table 5.V).

5.6.1 Background correction

Fractional concentration values were calculated per ml (the

original HPLC sample volume) for stages P1, P7 and P10-13 and corrected for background levels of ecdysone, 20-OH-ecdysone and makisterone A (the internal standard) due to WISP carry-over, etc. with reference to an HPLC run which was performed using only the mobile phase with standard ecdysteroids intercalated between the blanks (cf. Section 5.4). Retention times did not remain constant between samples; so this control run was analysed by RIA in terms of relative retention time (RRT) using a standard response curve for ecdysone, makisterone A or 20-OH-ecdysone, as appropriate (see Fig. 2.17). In this way the background could be deducted from all the samples, the midpoint of each 30 sec. fraction being expressed as RRT with respect to the nearest peak retention time (= 1.0). Background correction curves as applied to samples P1, P7 and P10-13 are shown at Fig. 5.5.

After these background values had been deducted from replicate assays of fractions from samples P1 and P10-13, means and standard deviations were calculated and the data were examined. Fig. 5.6 shows that, whilst the variance is high, its size is dependent neither upon the number of replicate assays performed nor upon the measured concentration of ecdysteroid (cf. 4.3.2). This is because the chromatograms gave a good indication of which fractions contained the ecdysteroids under analysis.

The background-corrected values for ecdysteroid content in stages P1, P7, and P10-13 are presented against HPLC retention time in Figs. 5.7 a-g, expressed in terms of equivalence to 20-OH-ecdysone, makisterone A and ecdysone. The sample of stage P1

Figure 5.5

Ecdysteroid background correction curves

Control HPLC injections (1:1 methanol/water) with intercalated injections of ecdysone (α)/makisterone-A (μ)/20-OH-ecdysone (β) (sent to waste) were assayed using MAS and the values for % binding for each eluate fraction were translated into α, μ or β (ng/ml) using the appropriate standard curve and plotted against relative retention time (RRT) with RT of α, μ or β as denominator. The profiles of steroid concentration have been smoothed out with time (RRT) to allow appropriate background levels to be read from the graphs for the midpoint of any sample eluate-fraction expressed as RRT with respect to the nearest peak retention time, (α, μ or β). Background levels are expressed here as a) 20-OH-ecdysone, b) Makisterone-A and c) ecdysone. Bars show the limits of application of each graph as they were subtracted from sample values. Broken lines indicate the absence of makisterone-A from the standard solution and the samples of stage P1 lacking an internal standard.

Fig. 5.5

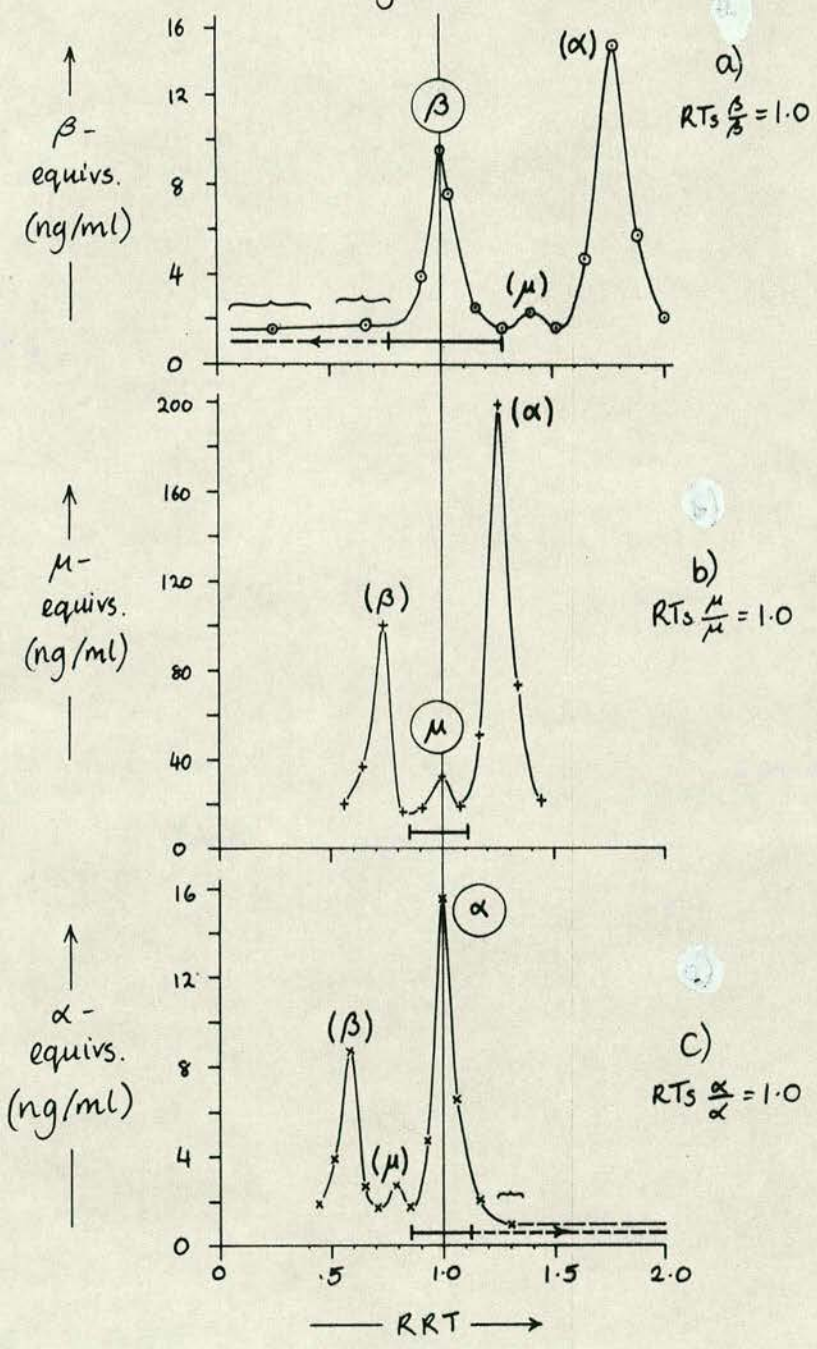
β - equivs. (ng/ml)
16
12
8
4
0
β
(α)
(μ)
a)
RTs β/β = 1·0
μ - equivs. (ng/ml)
200
160
120
80
40
0
(α)
(β)
μ
b)
RTs μ/μ = 1·0
α - equivs. (ng/ml)
16
12
8
4
0
α
(β)
(μ)
c)
RTs α/α = 1·0
0
·5
1·0
1·5
2·0
RRT

Figure 5.6

Independence of titre and variance,

and of variance and sample-number

HPLC-RIA data for stages P1 and P10-13 (taken as representative of the whole), ecdysone and 20-OH-ecdysone (similar standard response curves and titres*). a) mean titre/fraction vs. number replicate assays/fraction (n); b) variance, S^2 vs. n ($r = -0.001 < r\ (p = 0.1)$); c) variance, S^2 vs. mean titre ($r = +0.066 < r\ (p = 0.1)$*). The variance is not dependent upon the mean so a logarithmic transformation of the data is inappropriate; and it is unlikely to be reduced by a further limited number of replicate assays - it shows no dependence on n.

*(Note that if widely-differing standard response curves are included together (i.e. ecdysone/20-OH-ecdysone and makisterone A) then S^2 does show a strong apparent dependence upon the mean (e.g. Stage P1, $r = +0.828 > r\ (p = 0.001)$); but this is an artifact).

Fig. 5.6

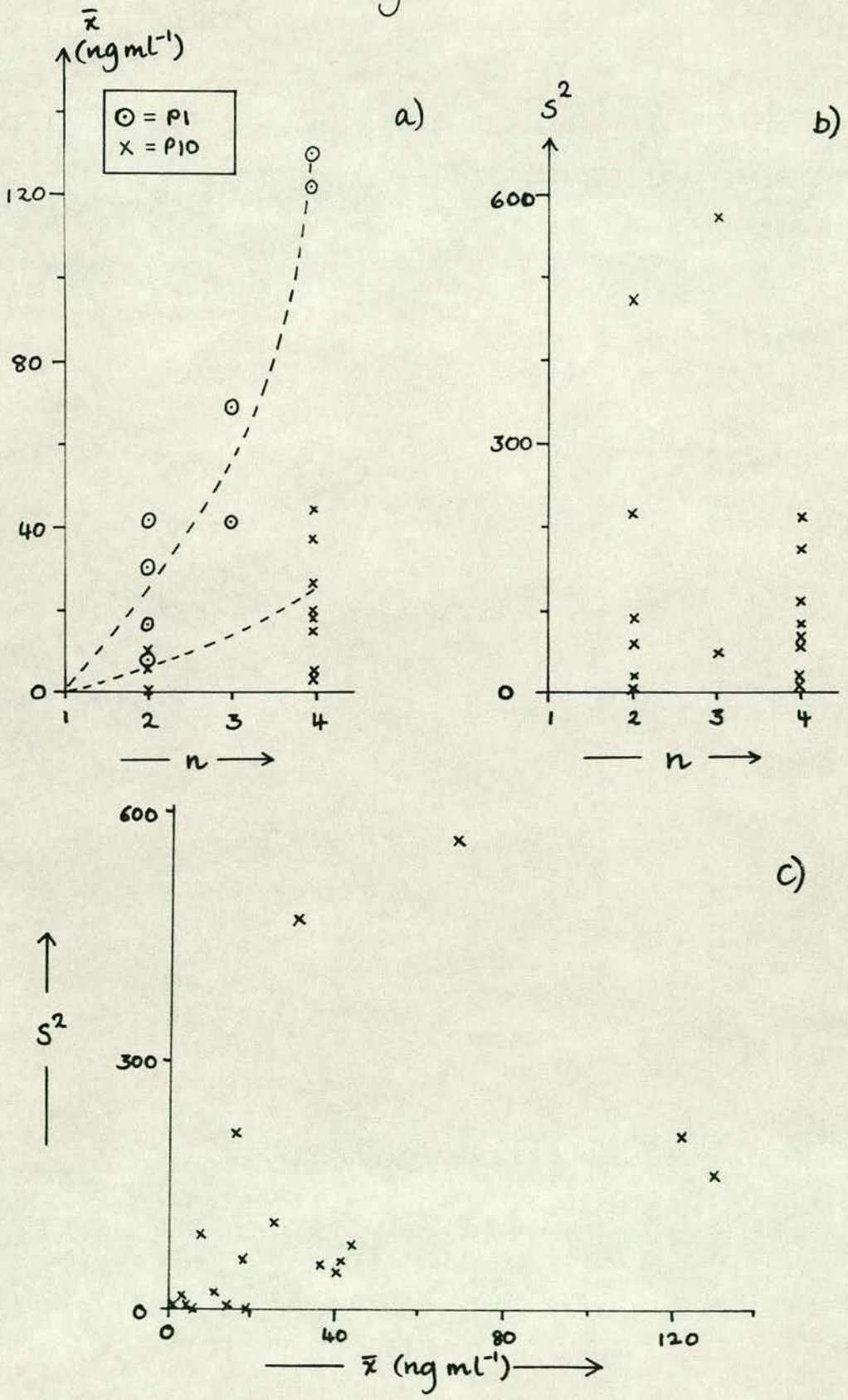
$\bar{x}$ (ng ml^{-1})
⊙ = P1
× = P10
a)
120
80
40
0
1
2
3
4
n
s^2
b)
600
300
0
1
2
3
4
n
c)
600
300
0
s^2
0
40
80
120
$\bar{x}$ (ng ml^{-1})

Figure 5.7 a-g

Histograms showing ecdysteroid concentrations in HPLC eluate fractions as measured by MAS-RIA (background-corrected). Abscissae: retention time as 30 sec. fraction number, also showing selected retention times RT (min) and relative RT's (RRT) and number of replicate assays (n). TLC cut-off points relate relative R_F of TLC ecdysteroid zones (scraped) to RT with reference to makisterone-A (=1.0). Ordinates: equivalence of eluate fractions to 20-OH- ecdysone (β), makisterone-A (μ) and ecdysone (α) in the RIA as concentration in ecdysteroid equivalents (ng ml^{-1}). STD indicates retention times of intercalated standard ecdysteroids. Construction lines indicate apparent peak retention times of endogenous ecdysteroids or (c-f) the internal standard, assuming fractions adjacent to the standard RT's to be of the same chemical nature. Mean concentration-values only are presented, and the variability was high. a, b) Fraction sets I and II, stage P1 without exogenous makisterone-A, respectively. (These values were corrected for loss to experiment f, Appendix A4); c) stage P1 with makisterone-A as internal concentration standard; d,e) fraction sets I and II, stage P7 with internal standard; f) stages P10-13 with internal standard; g) 10^{-5}M ecdysteroid standard mixture, HPLC-RIA control (fractions = 1 min).

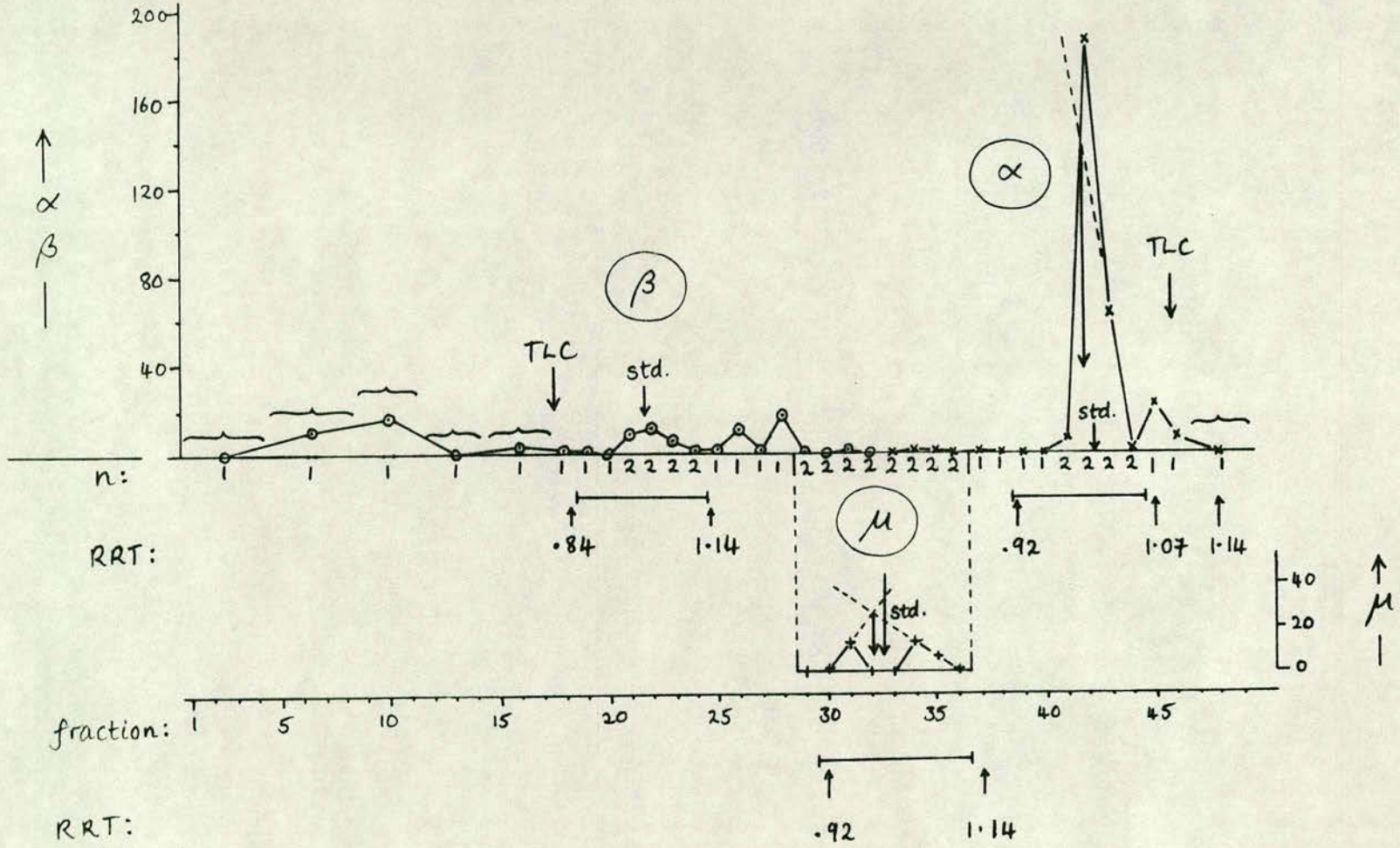

Fig. 5.7 (a)

Stage P1-μ, Set I

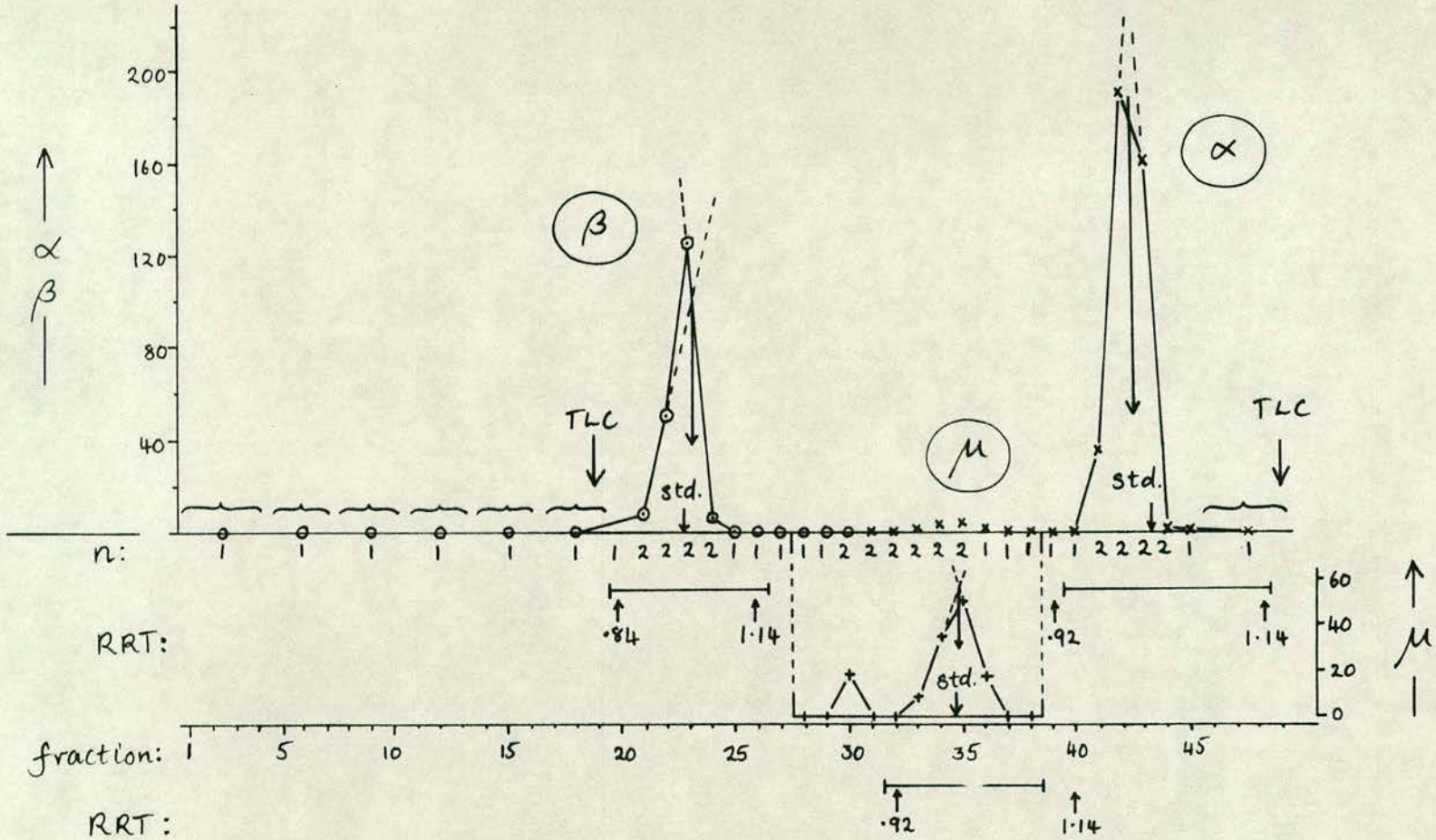

Fig. 5.7 (b)

Stage PI-μ, Set II

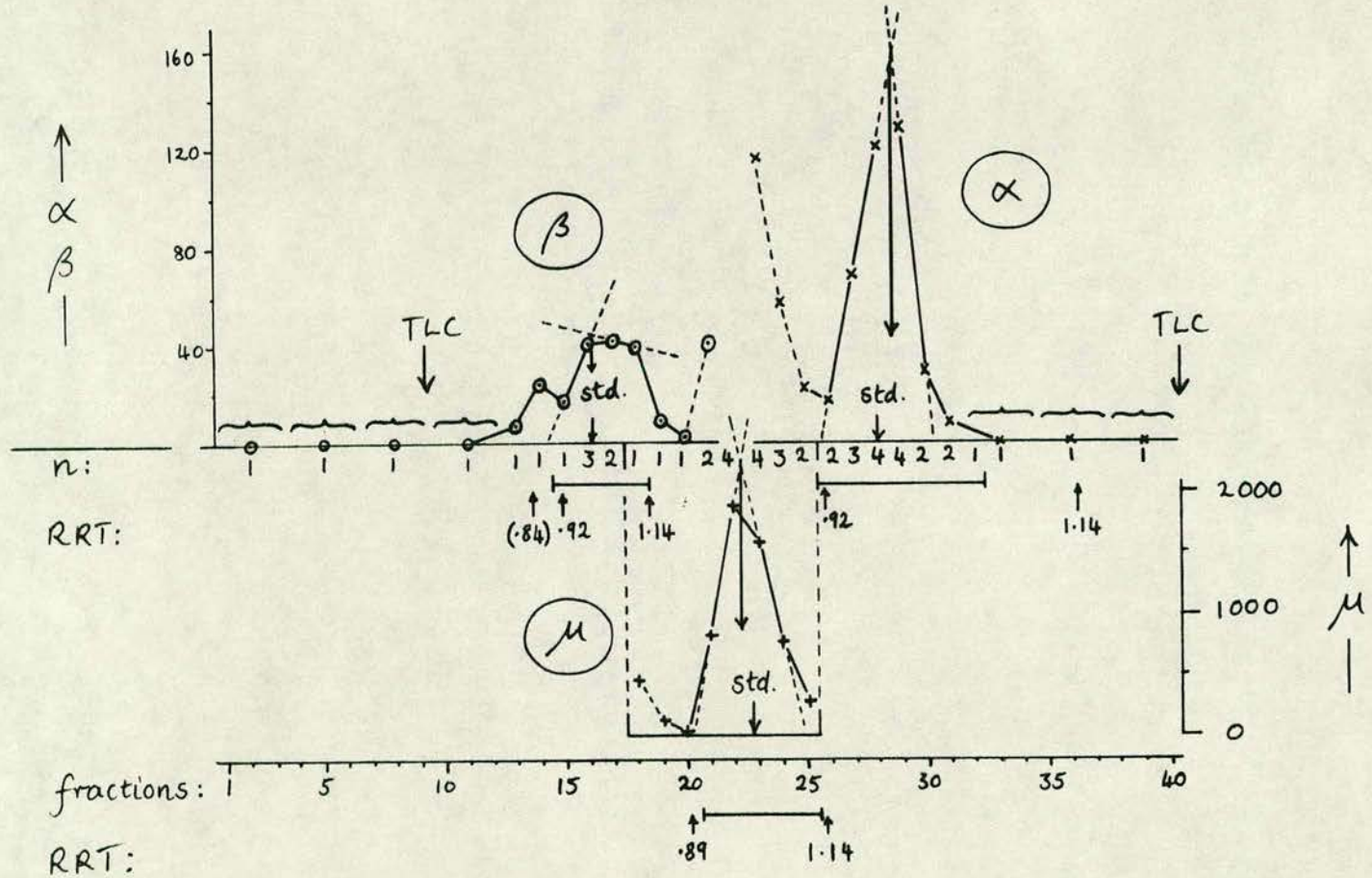

Fig. 5.7 (c)

Stage PI + μ

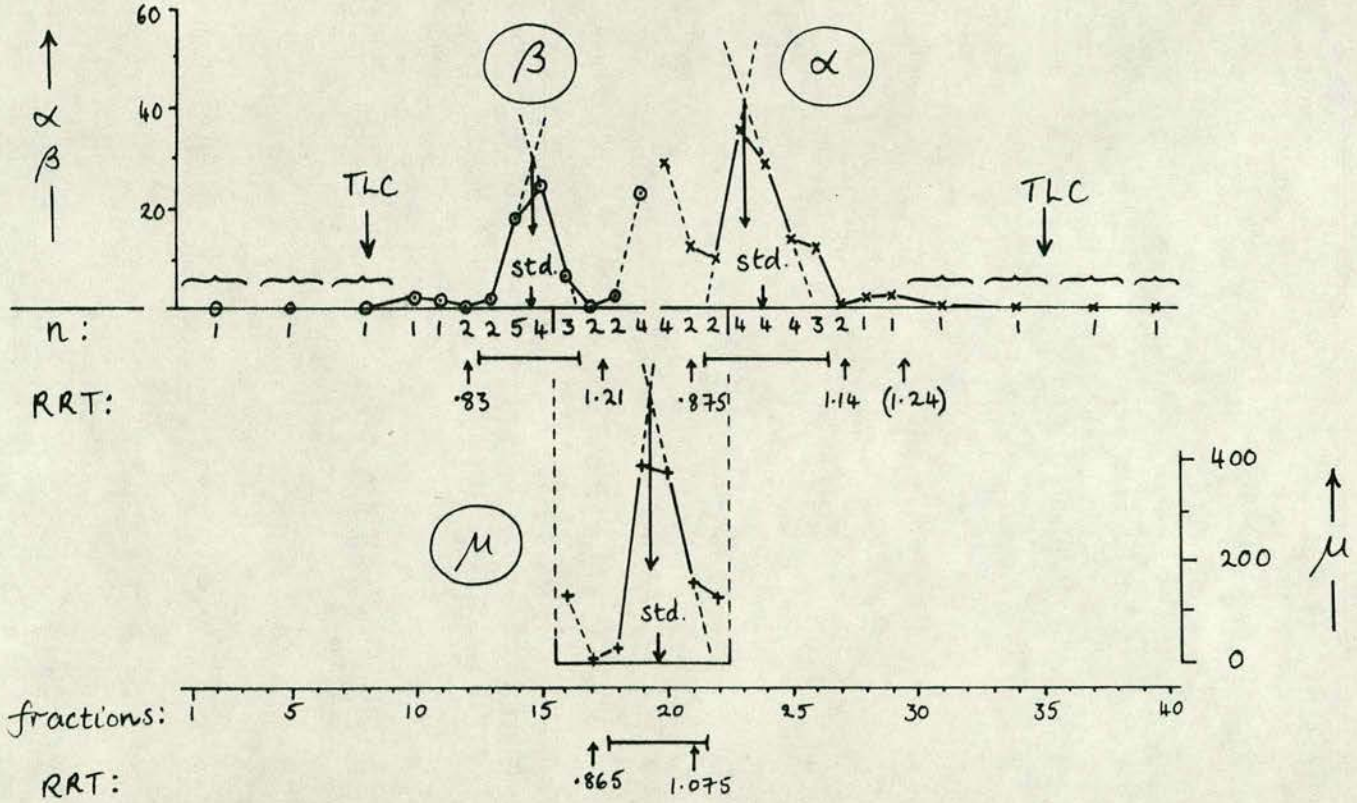

Fig. 5.7 (d)

Stage P7 + μ, Set I

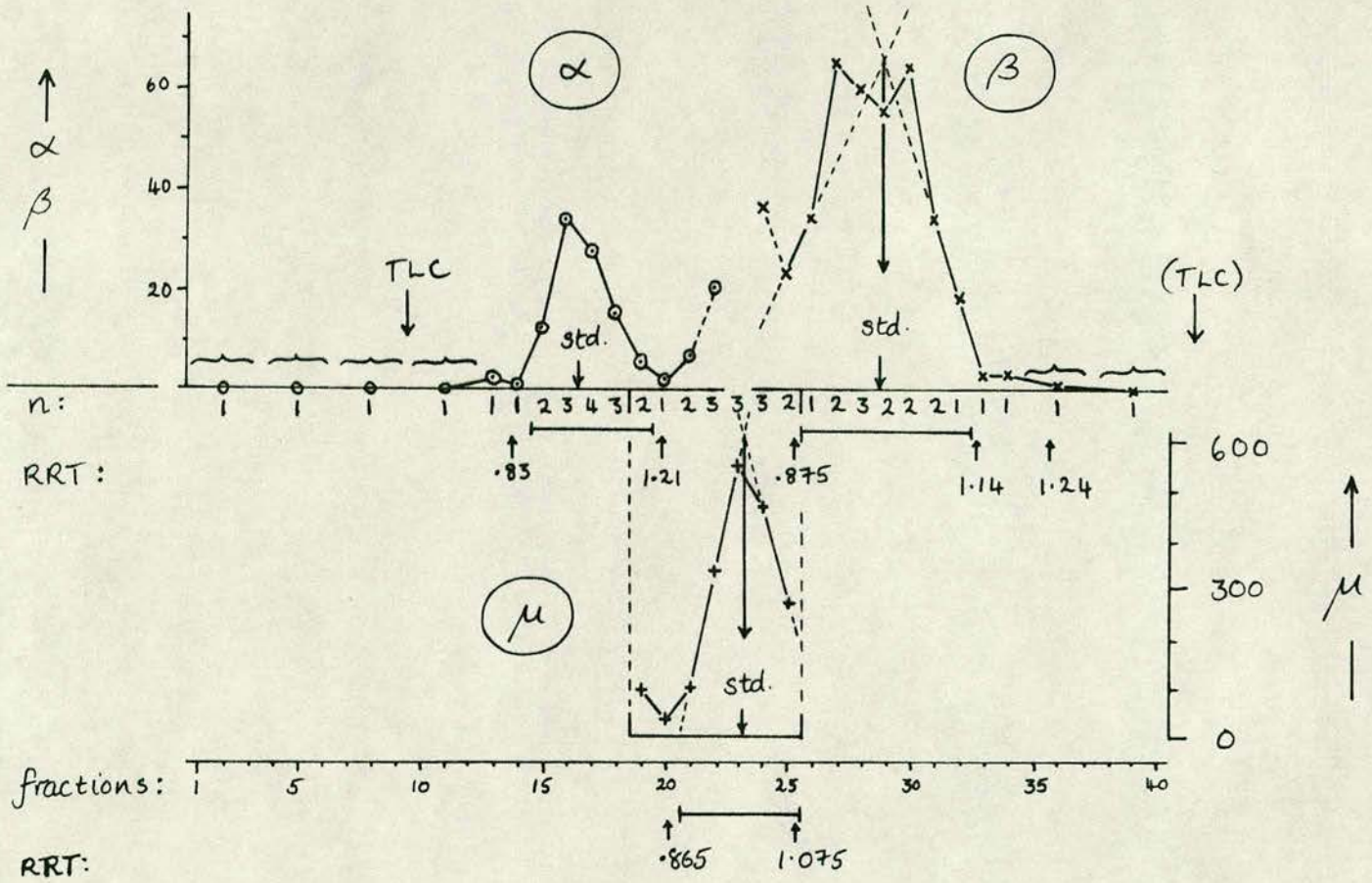

Fig. 5.7 (e)

Stage P7 + μ , Set II

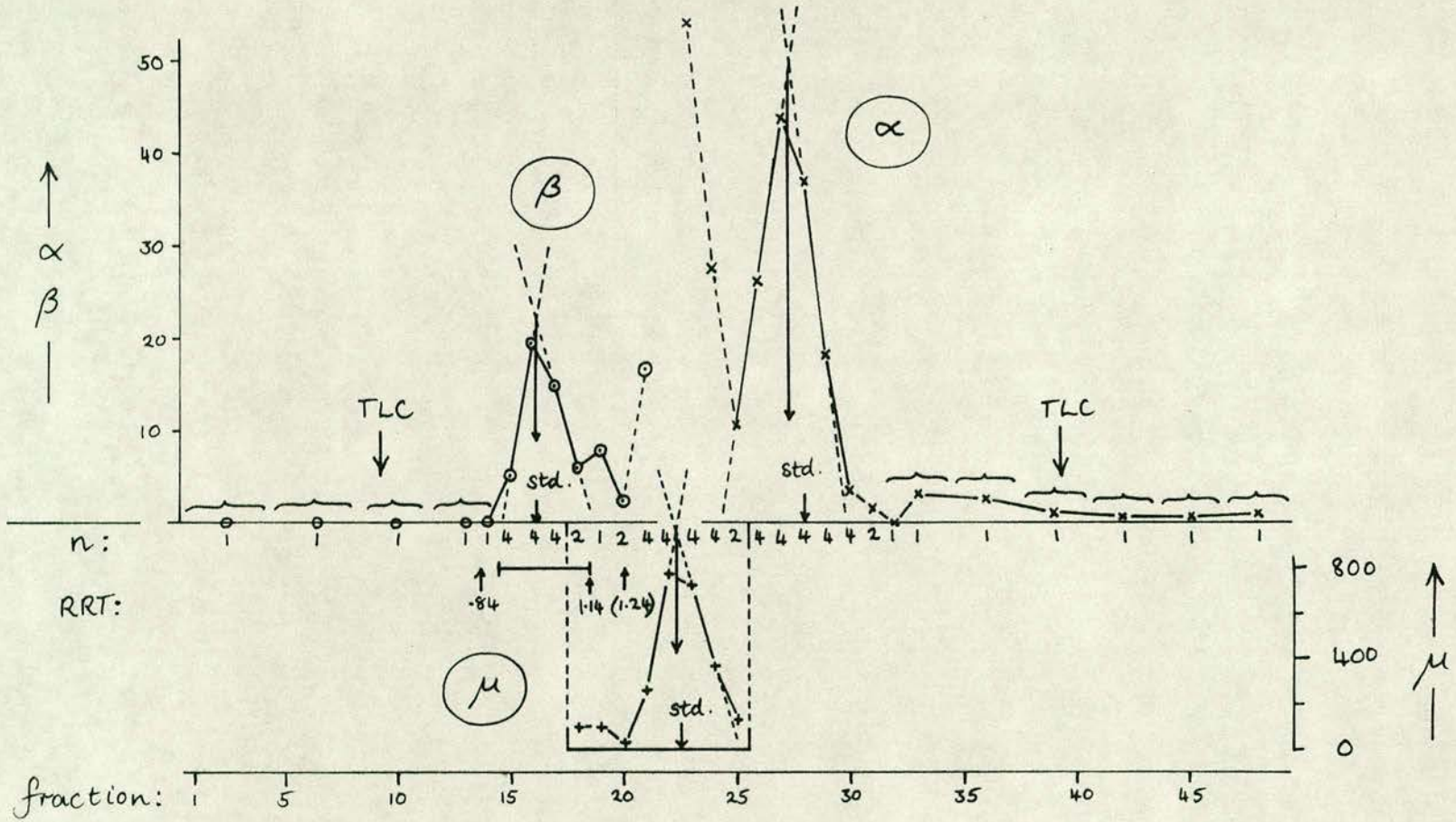

Fig. 5.7 (f)

Stages P(10-13)

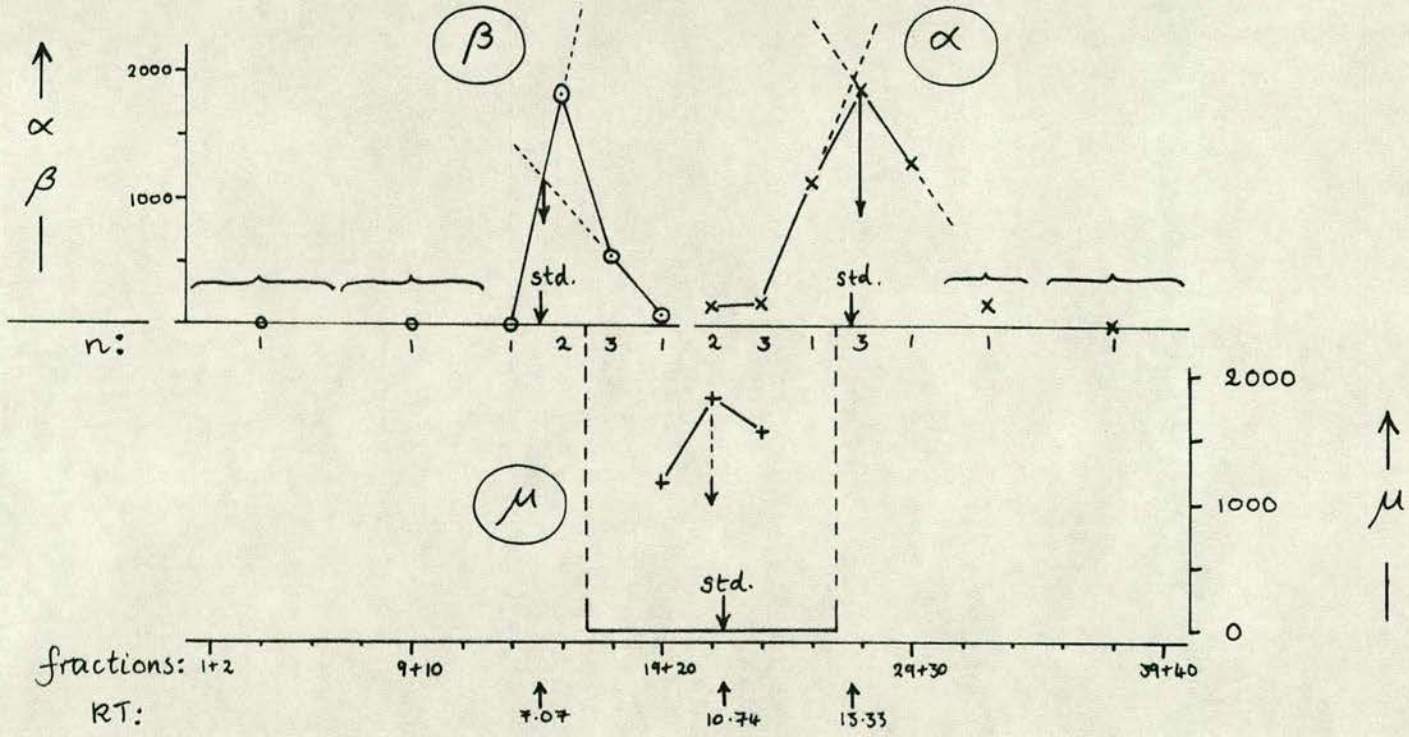

Fig. 5.7 (g)

Standards

without exogenous makisterone-A is chromatographically anomalous in that the two sets of pooled fractions, I and II show dissimilar RIA profiles and, in the second run, ecdysone has accumulated early with respect to 20-OH-ecdysone (cf. Fig. 2.22). This suggests that a further change in chromatographic conditions occurred during run II; but the shape of the profile (RIA-response vs. RT) for this sample, and also for stage P7, can be visualised by superimposing runs I and II in terms of relative RT as shown at Fig. 5.8. (This shows that over the RRT range 0.92-1.14 (cf. Section 2.22, Fig. 2.23) the superimposition curves are of regular form despite the contradictions between runs I and II).

5.6.2 Analysis of HPLC-RIA data (See 2.22)

HPLC-RIA produced sets of data for ecdysone, makisterone A and 20-OH-ecdysone for each set of fractions. The results are variable values of concentration centered about a series of means. Each mean is an estimate of concentration equivalent to only part of the total titre (peak area) for a given steroid in a given set of eluate fractions. Each part of the total titre may be visualised as a segment of O.D. peak area bounded by retention times (RRTs relative to the RT at the peak maximum; Fig. 2.23). When peaks are analysed in these terms they are found to share a common form. Tube sets were changed (I and II) when a change in standard RTs was noticed during HPLC, so although effective peak spreading may be expected to increase with multiple injection and fraction collection from a single sample, the net effect of this on distribution between eluate fractions has been minimised. Therefore the component fractions of

Figure 5.8

Composites of eluate fraction sets I and II, for samples P1 (no internal standard) and P7 (with internal standard) obtained by superimposition of smoothed histograms (cf. Fig. 5.7 a + b, d + e); fractions expressed as relative retention times (RRT) with respect to 20-OH-ecdysone (β), makisterone-A (μ) or ecdysone (α) = 1.0. Ordinates: concentration in ecdysteroid equivalents per fraction (ng ml^{-1}) in terms of the MAS-RIA.

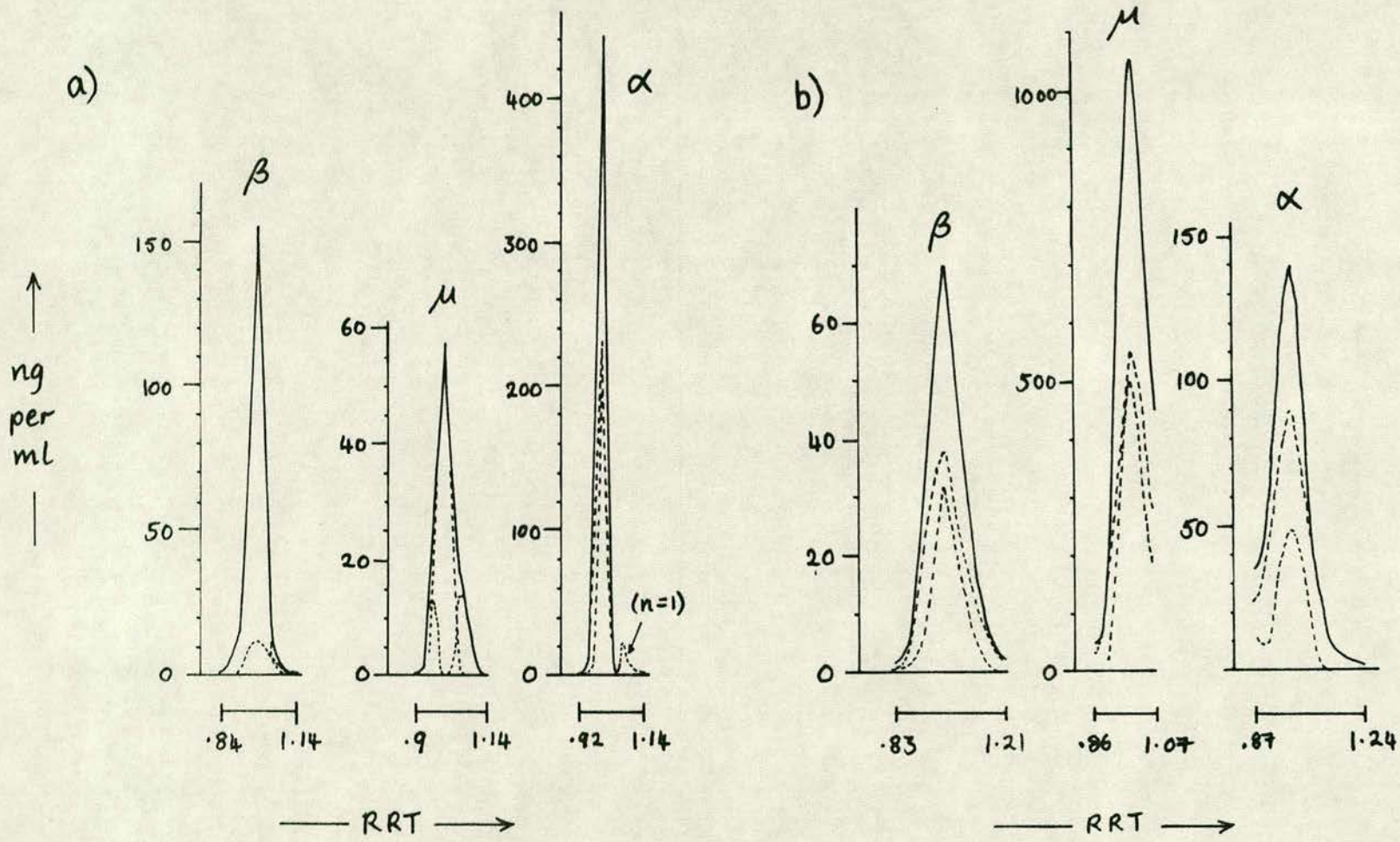
a)
b)
β
μ
α
ng per ml
150
100
50
0
60
40
20
400
300
200
100
1000
500
(n=1)
·84
1·14
·9
·92
·83
1·21
·86
1·07
·87
1·24
RRT

Fig. 5.8

an ecdysteroid titre may be analysed in terms of peak area with reference to an idealised relation between RRT and peak area for ecdysteroids separated under the same conditions, (Figs. 2.23-2.24).

HPLC eluate fraction times were translated into values of peak area on this basis (peak segments as proportions of total peak area) and compared with their measured ecdysteroid concentrations which may now be stated as proportions of the total concentration of the ecdysteroid in question distributed across several fractions. Consider, for example, the internal standard in sample P1, data for which are presented in Table 5.III: It is not clear from this which of the four calculations of 100% titre/tube set, which differ by up to 37%, is the more accurate.

In order to determine which fractions were to be excluded as unrepresentative they were all screened for conformity with the distribution of optical density in the idealised HPLC-peak according to Section 2.22.2. This treatment of the RIA data is presented at Fig. 5.9, and it can be seen that, for the internal standard in stage P1 (graph C), the most appropriate value for 100% titre is that obtained by calculation number 3 (Table 5.III), i.e. by excluding $n < 3$ which corresponds to the fractions expected to contain peak tails (especially the leading edge in this case, fraction No. 21). Some groups of data conform well to this relationship and each fraction could serve to predict 100% titre (e.g. stage P1 ecdysone graph C). Others conform less well, (e.g. stage P7, set II). The data for fractions at peak tails (and low

TABLE 5.111

Makisterone A as internal standard in Stage P1 extract (peak RT=11.08m)

Fraction No. (x30 sec)	19	20	21	22	23	24	25	26
RRT		.857	.903	.948	.993 (1.0)	1.038	1.083	1.128
Excluded tail area (%)		<.001	.098	4.2	34.5 43/57	19.5	4.58	0.9
Fraction Area (% total peak)		.098	4.102	30.3	46	14.92	3.68	
Fraction concentration (ng ml^{-1})		35.5	834.12	1880.33	1585.66	770.78	279.83	
(S_{n-1})		(-)	(100.17)	(600.08)	(438.22)	(108.35)	(174.42)	
n		1	2	4	4	3	2	

100% Computations (ml^{-1})

1 No. 20-25: 99.1 % = 5386.22 ng
100% = 5435.14 ng

2 No. 21-25: 99.002% = 5350.72 ng
100% = 5404.66 ng

3 No. 22-24: 91.22 % = 4236.77 ng
100% = 4644.56 ng

4 No. 23: 46% = 1585.66 ng
100% = 3447.09 ng

(cf. Fig 5.9(c))

Figure 5.9 (a-h)

Log-log plot of fractional concentration vs. percentage total titre for HPLC-RIA data by analogy with the plot of peak segment area vs. percentage total peak area (cf. Fig. 2.25). Fraction retention times were used to estimate fraction as % total peak area and compared with their ecdysteroid concentrations expressed as ng/ml 20-OH-ecdysone (β), makisterone-A (μ) or ecdysone (α). Each plot lies parallel to a hypothetical set of data which sum to 100ng = 100% titre, the variation in gradient being represented by a shift relative to this 1:1 relation. Numbered fractions lie on or are linked to the plots which generate readings from the abscissa of 100% titre (ng ml^{-1} original HPLC sample = ng/tube set). These are compared with the arithmetical predictions derived from the set of fractions which conform to the plots. Excluded data points and non-parallel relations between data points (unpermitted rotations) are indicated by broken lines. Values less than 1.0 on both axes are excluded. a, b) stage P1 without exogenous makisterone-A as internal standard, fraction tube sets I and II respectively; c) P1 + internal standard; d, e) P1 + internal standard, set I and II; f) P10-13 + internal standard; g, h) control ecdysteroid standards 10^{-5}M, 20-OH-ecdysone and makisterone-A/ecdysone respectively.

Fig. 5.9 (a and b)

a) Stage P1–4, Set I

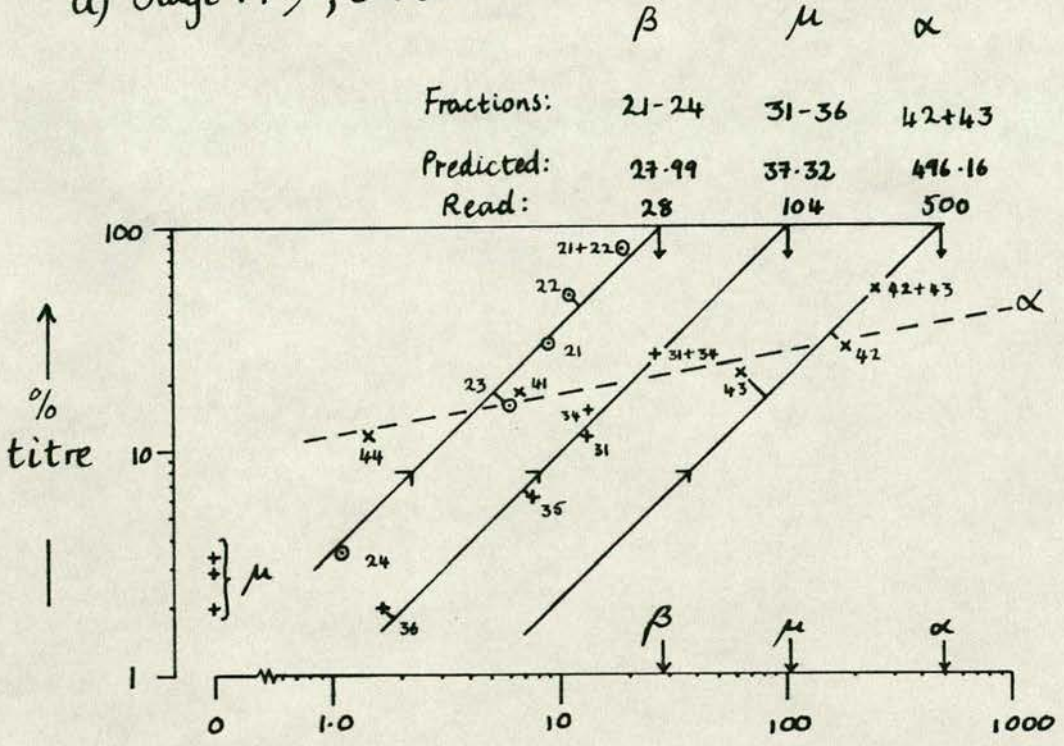

b) Set II

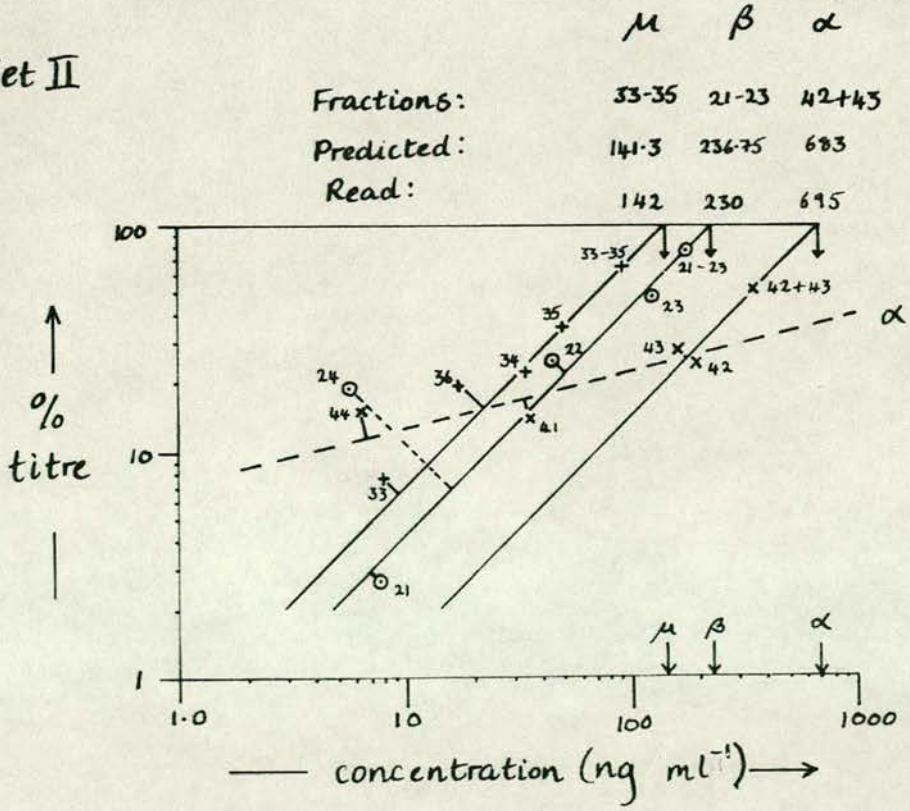

Fig. 5.9 (c and d)

c) PI + μ

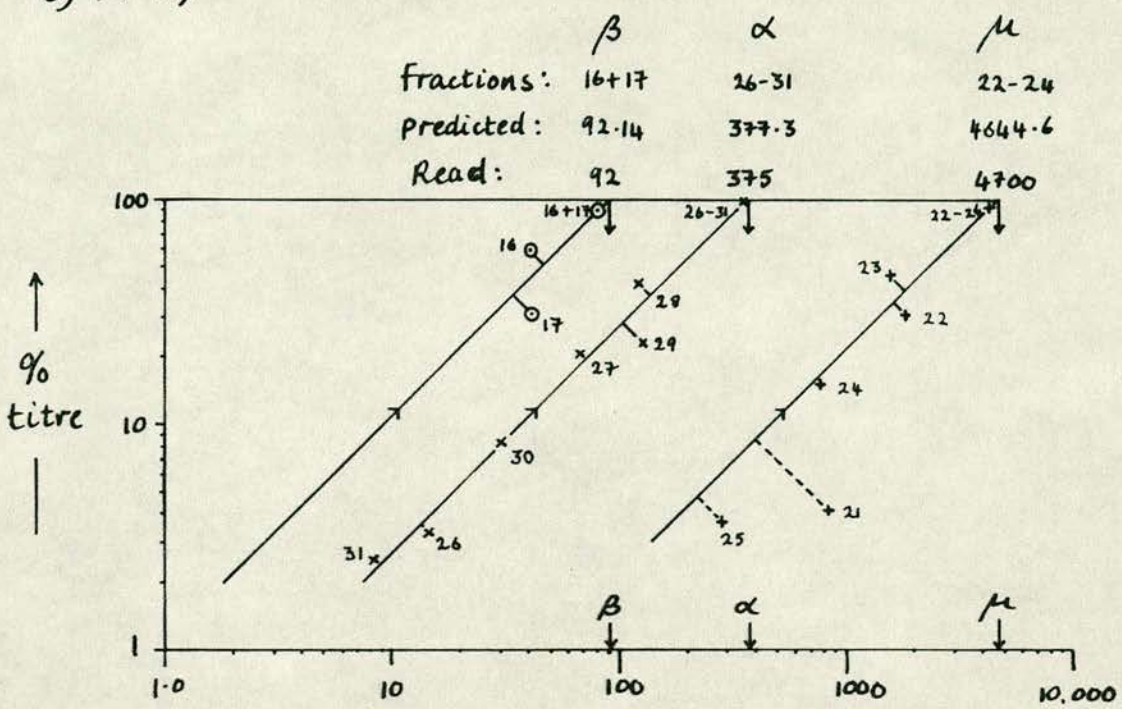

d) P7+μ, Set I

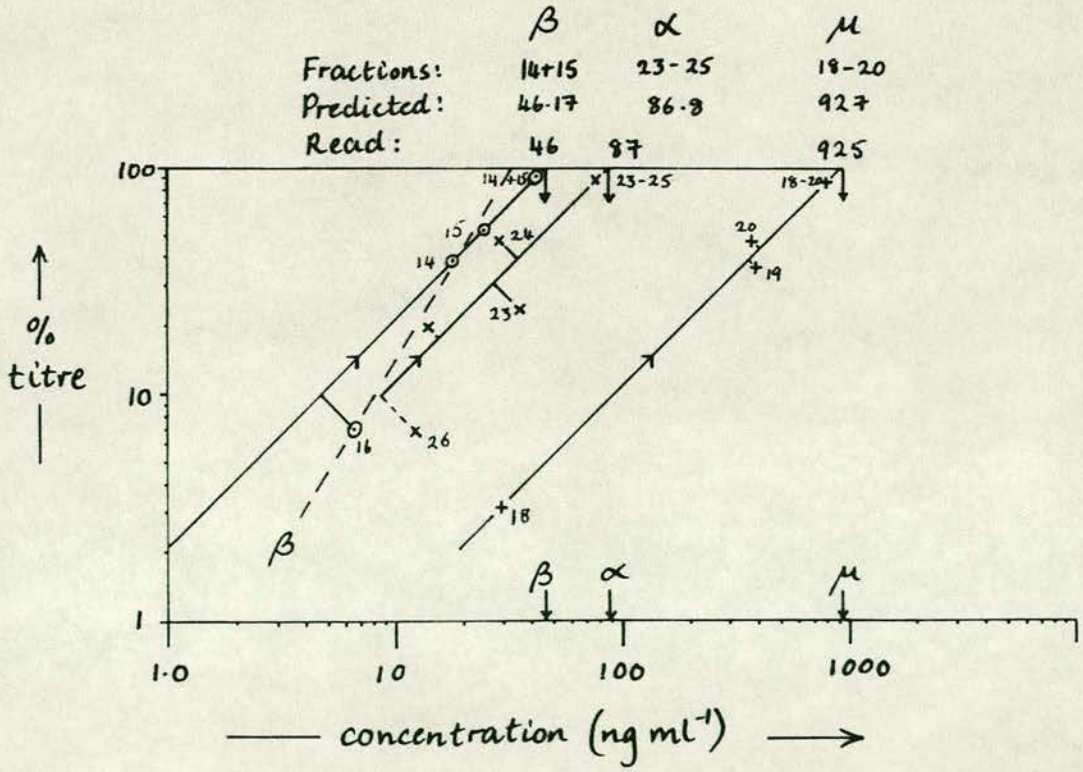

Fig. 5.9 (e and f)

e) P7+μ, Set II

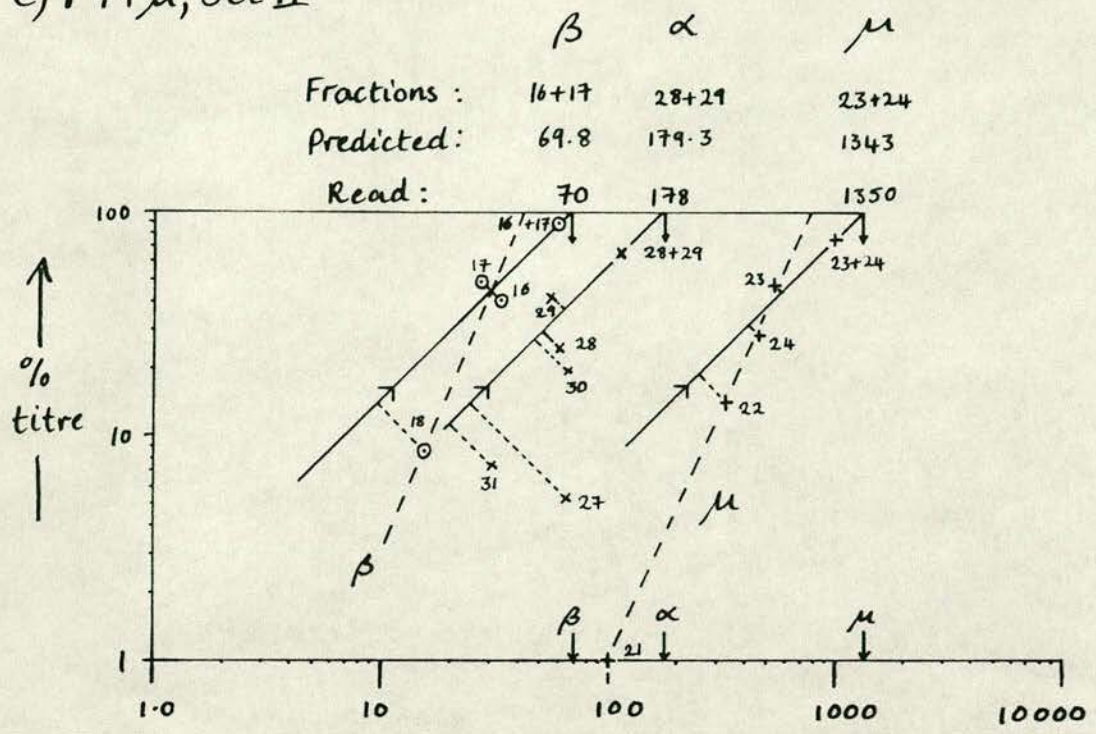

f) P(10-13)+μ

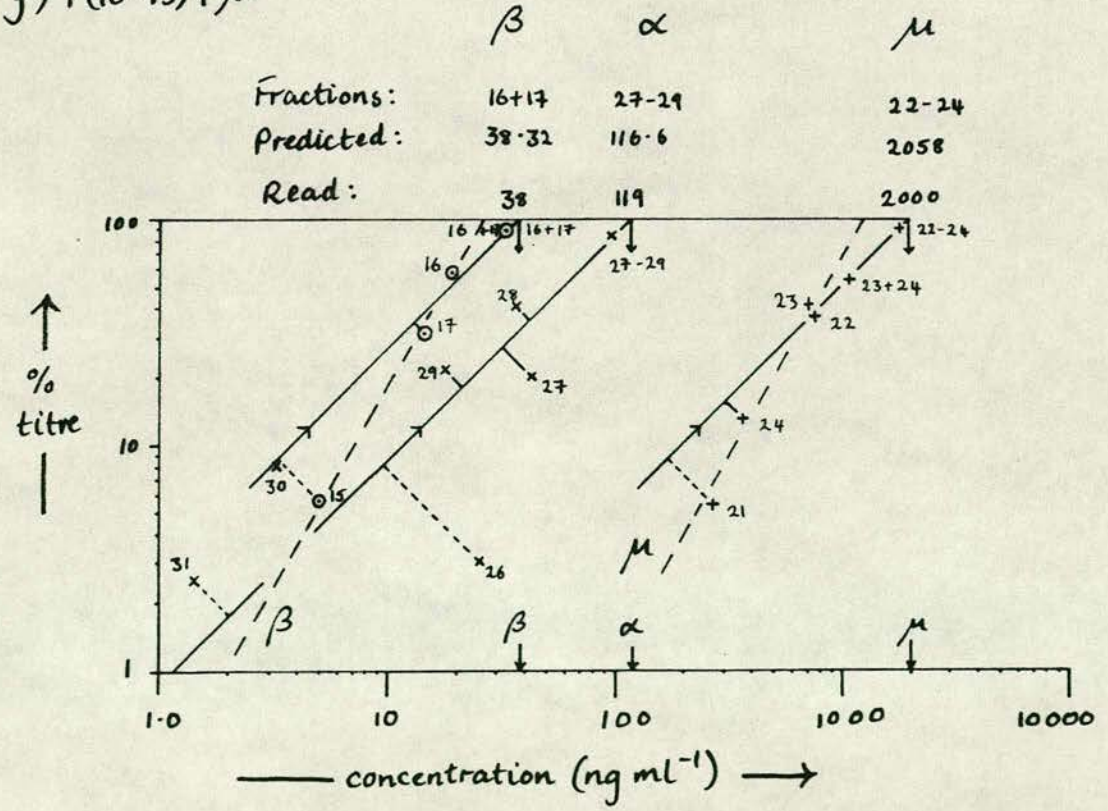

Fig. 5.9 (g and h)

g) Standard β

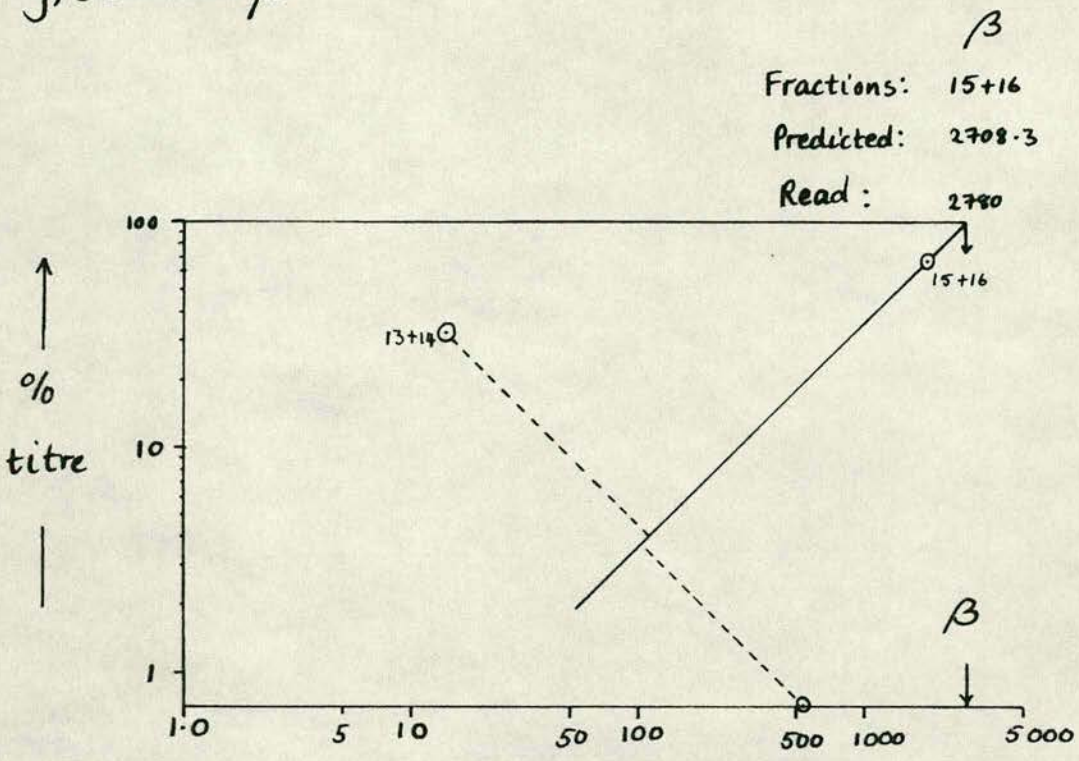

h) Standard μ and α

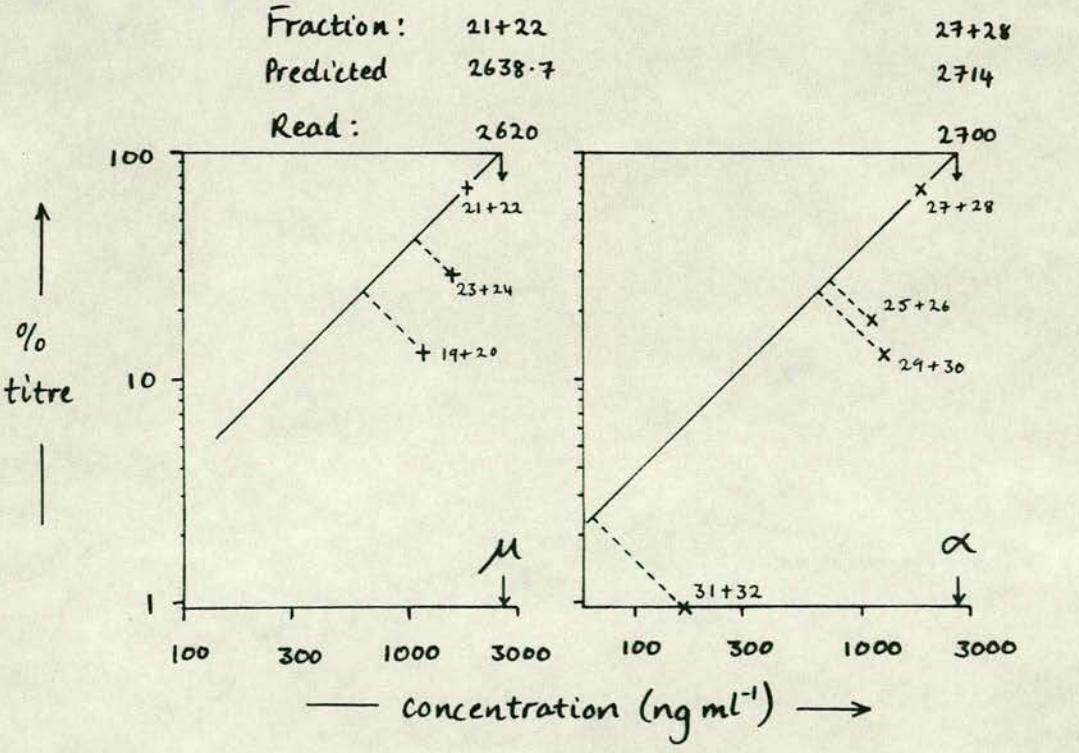

sample number) tend to rotate the plots shown in Fig. 5.9; but since the apparent rotation can be in either direction (Fig. 5.10) this does not seem to suggest that the use of an idealised OD-peak (Fig. 2.24) significantly misrepresents the peak-spreading produced by collecting these fractions through multiple injection. In the case of an apparent anti-clockwise rotation (stages P7, P10-13; Fig. 5.9 d-f) small sample sizes (and/or other factors) have resulted in values for fractional concentration which are spuriously high and which themselves suggest overly-high values for 100% titre (but which paradoxically, when taken in conjunction with fractions closer to peak retention time, suggest a graph which intercepts 100% titre at a spuriously-low value. The requirement for parallelism with 1:1 is thus especially useful in recognising this effect). Conversely, a clockwise rotation results from under- estimation of the concentration of fractions at peak tails (e.g. stage P1 without exogenous makisterone-A; ecdysone, Fig. 5.9 a and b).

In the case of native makisterone-A in stage P1 (Fig. 5.8 a) the highest peak values are missing and the estimate is based on the adjacent fractions. The companion set (graph b) suggests that there is indeed a single peak at the makisterone-A retention time, rather than two other compounds. Fractions set II for stage P7 (Fig. 5.9 e) again shows, apparently, two unresolved peaks (cf. Fig. 5.7 e) which set I suggests is a single peak at ecdysone RT; but here it is the fractions flanking the peak RT (27 and 30) which have been rejected as being inconsistent with the data for set I.

This graphical screening method depends upon several peak

Figure 5.10

Superimposition of log-log plots

a) Schematic example of log-log plot as used at Fig. 5.9. The use of this plot tends to exclude fractional measurements from peak tails - rotations are not permitted and the peak titres (2) generally define the position of the 1:1 or parallel gradient which defines total titre (T2). But could the other values (1 and 3) not generate equally acceptable values for the titre represented by 100% peak area (T1 or T3)? If the peak maxima can be shown to cluster together and define a line at, or parallel to, 1:1 around which the peak tails tend to spread evenly, then this line can be taken to represent a compromise between deviations (d) which increase towards the tails of O.D. peaks. b) Superimposition of the data in Figs. 5.9 a-f: the abscissa is normalised to 100mg = total titre represented by any of the peaks. The data-points are scattered above and below the 1:1 gradient. The deviations from this line above (d-) and below it (d+) were measured. Ratios for d+/d- with respect to the following are: numbers of points, n = 1.09; sums of the deviations, Σd = 1.08; means of the deviations, d = 0.99; standard deviation of the deviations, s = 0.776. So the peak maxima titres (e.g. number 2 in (a)) are more reliable than the peak tails in estimating total titres for a particular ecdysteroid.

Fig. 5.10

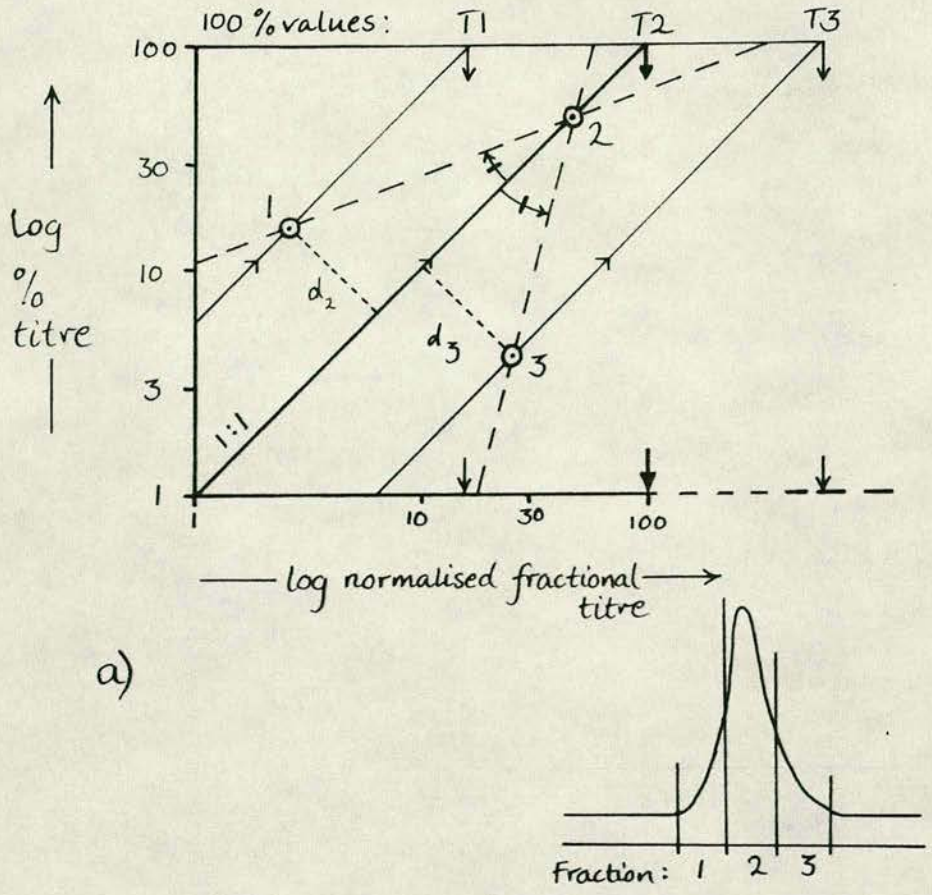
100 % values:
T1
T2
T3
100
30
10
3
1
Log % titre
1
2
3
d_2
d_3
1:1
1
10
30
100
log normalised fractional titre
a)
Fraction: 1 2 3

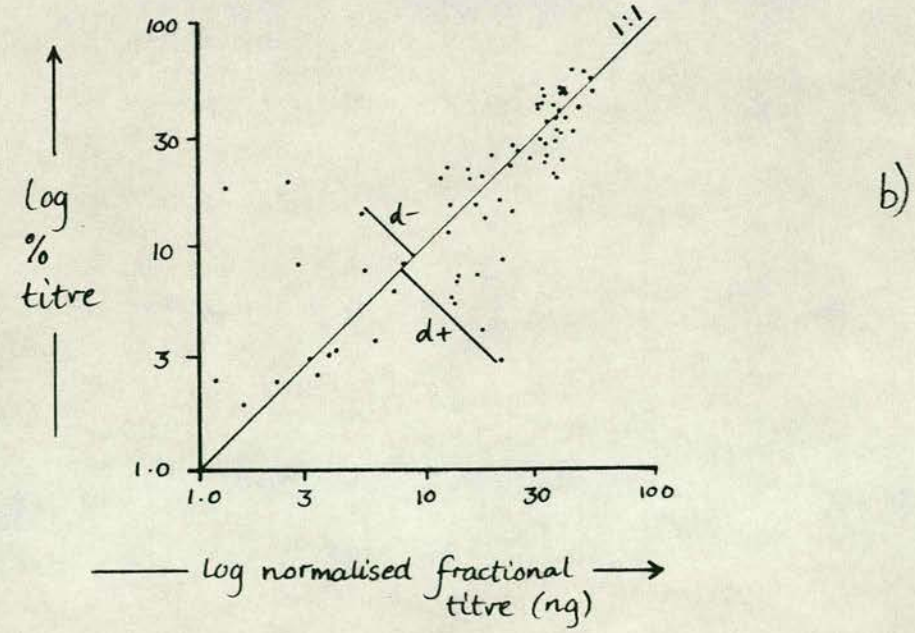
100
30
10
3
1.0
Log % titre
1:1
d-
d+
1.0
3
10
30
100
log normalised fractional titre (ng)
b)

segments being represented by eluate fractions, and is therefore inapplicable to the broader fractions (1 min.) of the standard-ecdysteroids control (Fig. 5.9 g and h).

Makisterone-A and ecdysone were not resolved to baseline by HPLC, so to some extent the response of the RIA to fractions from the trough between these compounds was ambiguous. Ecdysone concentrations for such fractions which were not rejected on the basis of the foregoing screening-procedure were adjusted for the contribution attributable to makisterone-A, bearing in mind the difference in sensitivity of the assay for the two ecdysteroids (x13.65, average for 7 and 12-day bleeds). However, this revealed an error of less than 0.8% ($p = 0.05$).

HPLC-RIA measurements of recovered titre per fraction set are summarised at Table 5.IV (a and b). It is not clear why, when on one occasion a single sample (P1 without internal standard) was collected as two sets of fractions (I and II), the distribution of 20-OH-ecdysone between the two sets should have differed from that of the other ecdysteroids measured (Table 5.IV b). However, when the two P1 samples (with and without internal standard) are compared overall they show very similar values for the ratio 20-OH-ecdysone: ecdysone (0.22, 0.24, with and without internal standard, respectively); so there is no justification for compensating for any apparent loss of 20-OH-ecdysone in the first fractions set. (Note that this also accounts for the change in sequence of 20-OH-ecdysone and makisterone in Fig. 5.9, a cf. b).

TABLE 5.IV(a)

HPLC/RIA measurements (P1/7/10-13)

Sample	Set(s)	Fraction(s)	% area	Sum of RIA means, (ng) → β	μ	α	100% = titre (ng/sample) β	μ	α	Check (100% from log-log graph) β	μ	α
P1(-I.S.)	I	21-24	96.24	26.936			27.99			28		
		31+(34-6)	34.4%		36.16			105.12			104	
		42+43	50.5			250.56			496.16			500
	II	21-23	74.95	177.45			236.75			230		
		33-35	64.58		91.28			141.34			142	
		42+43	51.5			351.9			683.3			695
	I+II						264.74	246.46	1179.5	258	246	1195
P1(+I.S.)		16+17	89.3	82.285			92.14			92		
		22-24	91.22		4236.8			4644.6*			4700	
		26-31	98.875			373.04			377.28			375
P7	I	14+15	91.52	42.25			46.17			46		
		18-20	85.72		795.45			927.96			925	
		23-25	89.92			78.02			86.76			87
	II	16+17	88.48	61.78			69.82			70		
		23+24	74.7		1003.3			1343.1			1350	
		28+29	64.8			116.19			179.3			178
	I&II						116.0	2271.1	266.1	116	2275	265
P10-13		16+17	89.3	34.22			38.32			38		
		22-24	90.72		1866.9			2057.9			2000	
		27+28	84.95			99.04			116.59			119
(stds)		15+16	67.7	1833.5			2708.3			2780		
		21+22	69.2		1826			2638.7			2620	
		27+28	68.3			1854.			2714.45			2700

* = 4562·4 when corrected for native μ (see text for calculation)

TABLE 5.IV (b)

Contribution, HPLC Fraction Sets I and II (%)

Sample	Set	β	μ	α
P1 (no internal standard)	I	10.6*	42.7	42.1
	II	89.4	57.3	57.9
	I+II	100%	100%	100%
P7 (+ internal standard)	I	39.8	40.9	32.6
	II	60.2	59.1	67.4
	I+II	100%	100%	100%

* See text.

Ecdysteroids:

β = 20-OH-ecdysone

μ = makisterone A

α = ecdysone

The data on the 1ml aliquot of standard ecdysteroids 10^{-5}_{M} taken through HPLC-RIA (Section 5.4) suggest that, at this stage of the analysis (including eluate volume-reduction using C_{18} cartridges) the three standards were recovered to roughly similar efficiencies, (20-OH-ecdysone 11.1%, makisterone-A 7.6%, ecdysone 6.9%, i.e. approx. 8.5%); but these data are of poor quality (Fig. 5.9 g and h) and this sample did not constitute a control for the extraction-purification steps, so no recovery estimates applicable to samples of P1, P7 and P10-13 are implied (cf. internal standard).

Stage P1 having been analysed with and without exogenous makisterone-A (i.e. ± I.S.), it is both possible to calculate the native concentration of this ecdysteroid and necessary to correct for its contribution to the apparent recovery of the internal standard, as follows (using the symbols α μ β as usual):-

Calculation

At an unknown Absolute Recovery Efficiency, compare P1 ± I.S. :-

92.14 ng/g β was recovered from 1 g P1 + I.S.

P1-I.S. sample weight = 5.175 g.

Therefore expected recovery of β from P1-I.S. = (92.14 x 5.175=) 476.84 ng

but observed " " " = 264.74 ng

so relative β Recovery = 55.52%

Similarly

377.28 ng/g α was recovered from 1 g P1+I.S.

Expected recovery of α from P1-I.S. = (377.28 x 5.175=) 1952.50 ng

but Observed " " " = 1179.50 ng

So Relative α Recovery = 60.41%

Let Relative μ Recovery be taken as (β+α/2=) 58.00%

Observed Recovery of μ from P1-I.S. = 246.46 ng/5.175 g

Expected Relative Recovery from P1+I.S. = 100%

Therefore Expected Observed Recovery of NATIVE μ from P1+I.S.

= 246.46 x 100/58

= (425.19 ng / 5.175 g=) 82.16 ng/g

- this is the native contribution to:

Total Observed μ in P1+I.S. = 4644.6 ng

Recovered I.S. = (4644.6- 82.16 =) 4562.4 ng (SEE TABLE 5.IV a)

Original I.S. (= Absolute Recovery Efficiency = 100%) = 34,580 ng

So for P1+I.S., Absolute Recovery Efficiency = 13.194%

The P1-I.S. sample represents 3018 animals.

Native μ in stage P1 = (82.16 x 100/13.194 =) 622.7 pg mg^{-1}

or about 363 pg/animal.

The HPLC-analysis of stage P1 without exogenous makisterone-A was performed before the column was exposed to this ecdysteroid. (The above calculation of native makisterone-A in stage P1, based on another sample containing this compound as an internal concentration standard, does not assume (a) that recoveries of the three ecdysteroids were in the same relation to one another in the two samples, or (b) that the percentage recovery of makisterone-A, being of a polarity intermediate between those of ecdysone and 20-OH-ecdysone, lay midway between the values for recovery of these two compounds, though this is approximately true on the basis of C_{18} retention times - See Section 5.5).

The titres of makisterone-A in stages P7 and P10-13 have not been measured, but the use of an internal standard concentration of 10^{-5}M makes it unlikely that native makisterone-A in these samples, if present, would seriously effect the accuracy of quantification - in stage P1 it has no significant effect (13.4% cf. 13.2% absolute recovery efficiency estimates). The recoveries of the internal standard in stages P7 and P10-13 were, on the basis of HPLC-RIA data (Table 5.IV), 6.56% and 5.95% respectively. These values have been used in calculating the equivalent values for ecdysone and 20-OH-ecdysone which are adopted for the construction of Table 5.V: the three ecdysteroids have been brought into the relations which they showed in respect of (i) their proportional recoveries through C_{18} cartridges and (ii) their HPLC retention times using C_{18}/aqueous methanol (cf. Section 5.5). (It was intended that these relations should be provided by the aliquot of standards-solution subjected to HPLC-RIA, but the results for this quantification were unreliable - see above).

Having treated the data in this way it is possible to present Table 5.V (q.v.) summarising the results of an HPLC-RIA analysis of ecdysone and 20-OH-ecdysone titres at those points during postembryionic development when direct RIA suggested there were elevated titres, probably of one or both of these steroids. The three periods show similar "total ecdysteroid" concentrations (within the limits of polarity analysed here). Ecdysone titres determined by HPLC-UV spectrophotometry (taken from Table 5.II) are consistently higher than those from HPLC-RIA but the two sets of

TABLE 5.V

Endogenous ecdysteroid titres determined by HPLC-RIA in selected stages

Stage	P1				P7			P10-13		
Ecdysteroid	β	μ	α	Total	β	α	Total	β	α	Total
Recovered Concentration (ng/sample)	92.14		377.28		116.00	266.10		38.32	116.59	
Recovery (%)	15.018	13.194	11.636		7.45	5.781		6.767	5.253	
100% concentration (ng/extract,g,ml)	613.53		3242.35		1557.05	4603.01		566.28	2219.49	
No. animals	655				783			758		
animal weight (mg)	1.527				1.277			1.319		
concentration per animal (ng)	0.94	0.36	4.95		1.99	5.88		0.75	2.93	
concentration per fresh weight (ng/mg) (% x 10^4)	0.61	0.62	3.24	4.47	1.56	4.60	10.76	0.57	2.22	2.79
COMPARE quantitation by HPLC-UV spec. (ng/mg)	(1.42)		21.05	22.47	?	20.63	(20.63)	?	17.49	(17.49)
HPLC-UV / HPLC-RIA	(2.3)		6.5	5.03	?	4.5	(1.92)	?	7.9	(6.27)

(β = 20-OH-ecdysone)
(μ = 24-methyl-20-OH-ecdysone (makisterone A))
(α = ecdysone)

results are in similar proportion from stage to stage. However, the relatively high titre of stage P7, shown by HPLC-RIA (cf. stage P1) and expected from the direct RIA results of this and other studies, was not revealed by HPLC-UV spectrophotometry, which in any case was incapable of resolving 20-OH-ecdysone effectively.

Chapter Six

Analysis of hormones by chromatography-coupled mass fragmentography (MF)

In the preceding chapter an analysis of ecdysteroids on the basis of chromatographic/immunological criteria was presented. A complementary analysis, based not on RIA activity but on mass spectrometric behaviour, was performed in collaboration with Dr. Huw Rees (Liverpool) using gas-liquid chromatography (GLC) and coupled mass fragmentography (MF = selected ion monitoring mass spectrometry, SIM-MS). This method was applied to the trimethylsilyl (TMS-) ethers of native ecdysteroids extracted from stages P1, P7 and P10-13, (Section 2.23), and the analysis, which was performed by Dr. Rees' laboratory using material collected in Edinburgh, forms the subject of the first part of this Chapter (6.1). In addition, a preliminary investigation of the juvenile hormone(s) of metamorphosing Drosophila was undertaken using mass fragmentography, again in collaboration, in this case with Professor Heinz Rembold (Munich). His laboratory subjected samples collected and extracted in Edinburgh (Section 2.24) to derivatisation and analysis by gas chromatography-coupled mass fragmentography (GC-MF). These experiments are reported briefly in Section 6.2 below.

6.1 GLC-MF of ecdysteroids

In this analysis, complementary to that by HPLC-RIA, GLC was employed to separate derivatized native ecdysteroids and mass

fragmentography was used to identify and quantify them, using an on-line mass spectrometer ion collector as the GLC detector (Morgan and Wilson, 1980; Lafont et al. 1980). Samples were prepared according to Section 2.23 where the full silylation of the hydroxyl functions to produce TMS-ethers is described. Figure 6.1 shows the silylation products and the major molecular ions derived from them by electron impact fragmentation. Ions of m/e 561 and 567 were chosen for continuous monitoring during GLC, these being characteristic of C20-hydroxy and C20-deoxy ecdysteroid nuclei respectively (e.g. 20-OH-ecdysone, vs. makisterone A and ecdysone).

Some of the resulting mass chromatograms for samples of stages P1, P7 and P10-13 are shown at Fig. 6.2. Native ecdysone, 20-OH-ecdysone and, possibly, 20-26-dihydroxyecdysone were identified on the dual basis of their retention times on GLC relative to makisterone A (internal standard) and their abundance as characteristic ions m/e = 567 or 561. No other ecdysteroids were identified on this basis from these stages (nor were any others found in stage P4 (i) - Redfern, personal communication). Quantification was based on peak areas in relation to makisterone A as internal concentration standard (see Section 2.23.5); and the resulting estimates of ecdysteroid concentration are presented at Table 6.1. Note that in this analysis no sample was analogous to the stage P1 sample without exogenous makisterone A which was subjected to HPLC-RIA (Chapter 5), so this steroid, if present endogenously at pupariation as the companion data suggest, was masked here by the internal standard.

Figure 6.1

Mass fragmentography of ecdysteroids

(Morgan and Wilson, 1980; Lafont et al. 1980)

A) Derviatization of ecdysteroids using trimethylsilylimidazole (TMSI) to modify the hydroxyl functions and render the compounds volatile.

B) Fully-silylated (hexa-TMS) derivative of 20-hydroxylated ecdysteroids (20-OH-ecdysone, R = H; Makisterone-A, R = CH_3) showing the cleavage site in a molecule under beta- bombardment (C20/22) to produce the most abundant molecular ion of mass-to-change ratio, m/e = 561 (proposed structure). This represents loss of the side chain and a silanol group at C14. (Incompletely silylated derivatives also give this ion, by loss of the sile chain and of water from the free hydroxyl group at C14).

C) Fully-silylated (penta-TMS) derivative of ecdysone, a 20-deoxyecdysteroid. Fragmentation is complex but yields major fragments at m/e 567 and 636 characteristic of this type of nucleus. In addition there is a major ion at m/e 171 derived from the side chain but not ecdysteroid-specific. Incompletely silylated derivatives show a characteristic nuclear fragment at m/e 564.

Fig. 6.1

A)

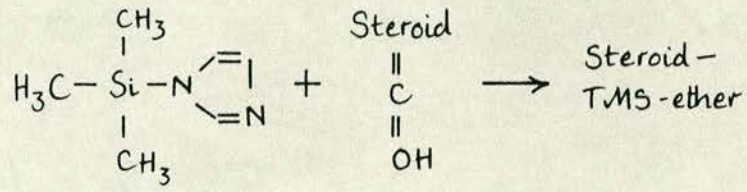
CH3
H3C – Si – N
CH3
=N
Steroid
C
OH
Steroid –
TMS-ether

B)

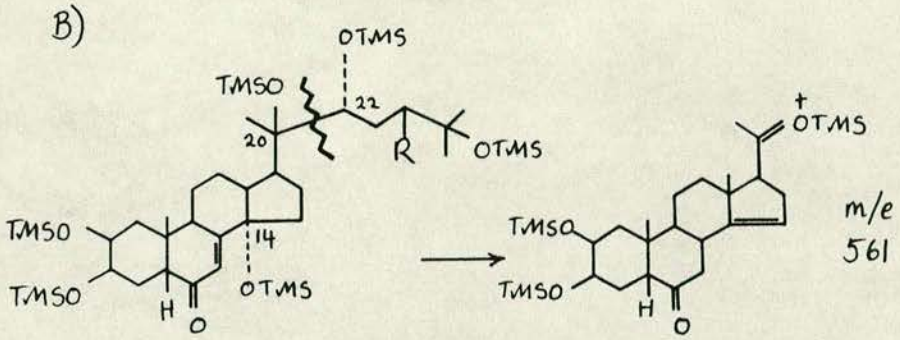
OTMS
TMSO
22
20
R
OTMS
TMSO
14
TMSO
OTMS
H
O
+
OTMS
TMSO
TMSO
H
O
m/e
561

C)

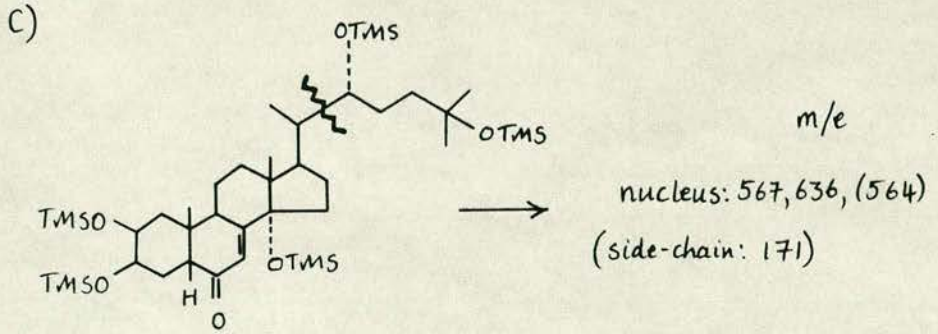
OTMS
OTMS
TMSO
TMSO
OTMS
H
O
m/e
nucleus: 567, 636, (564)
(side-chain: 171)

Figure 6.2 (a-d)

Example GLC-Mass chromatograms of Ecdysteroid- TMS ethers from stages of Drosophila metamorphosis. Fragments monitored = m/e 561 and 567 (±636) from ecdysone (α), 20-OH- ecdysone (β) and makisterone A (μ). Values in parentheses are relative retention times RRT_{μ} = 1.0, internal standard). Ordinates: (detector response) ion intensity relative to most abundant ion. Abscissa: analysis time in minutes. Profiles were summed to show the total signal. a) Example standard ecdysteroid mixture (α, 5ng; β, 5ng; μ, 1.25ng). (These chromatograms were produced in the same session as (c) below); b) Stage P1; c) Stage P7; d) stages P10-13. The m/e 561 peak in stage P7 at RRT_{μ} = 1.31 may be due to 20-26 dihydroxyecdysone (cf. standard, shows RRT_{μ} 1.25). The internal standard in stage P10-13 here shows an aberrant peak shape. The entire peak area (including the "shoulder") has been adopted in calculating concentrations of other ecdysteroids; but this would lead to underestimation of their concentrations should either the peak maximum or its shoulder be due to an impurity rather than to makisterone A. (Note: noisy signals have been smoothed out in the redrawing).

Fig. 6.2 (a)

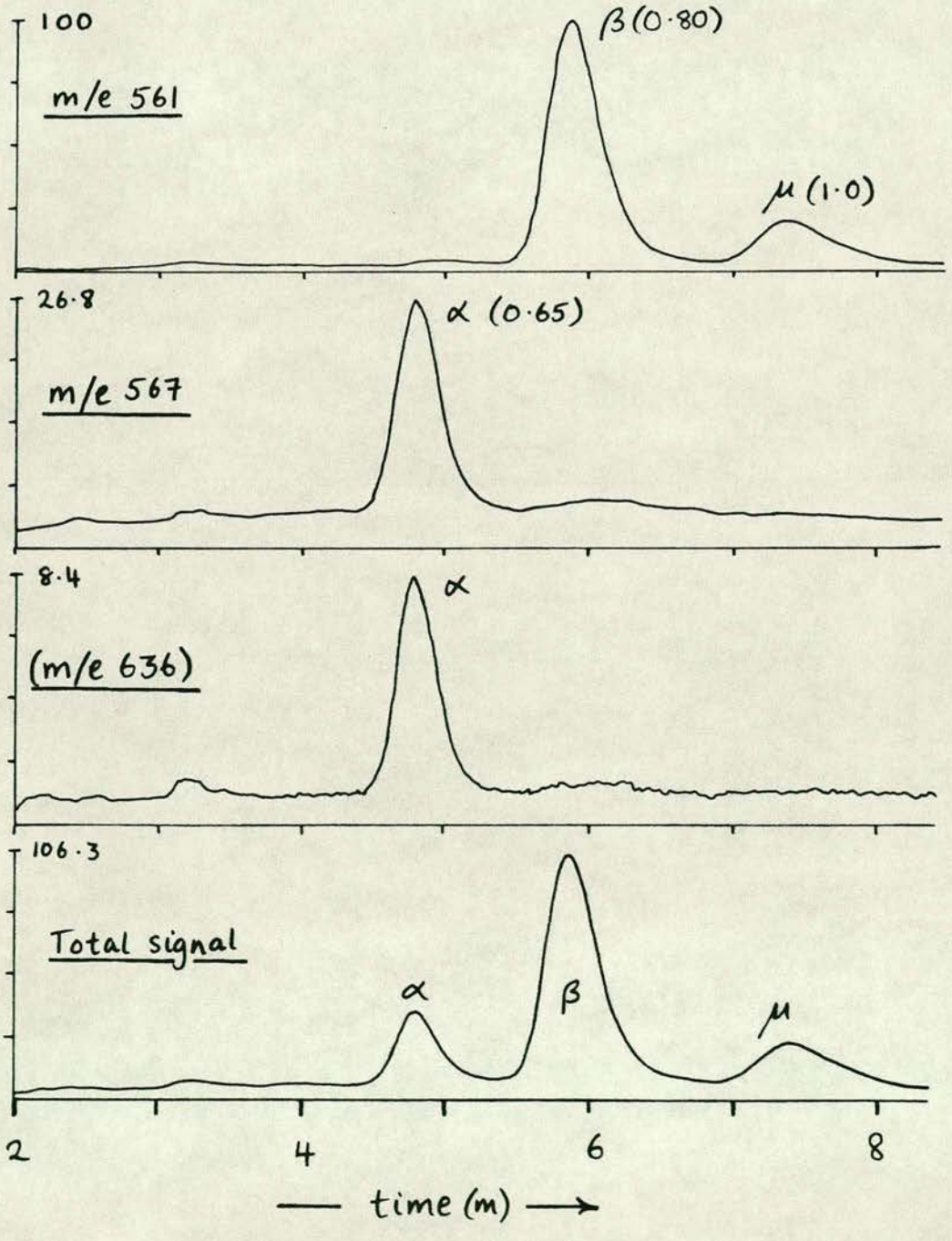
Standards
100
m/e 561
β (0·80)
μ (1·0)
26·8
m/e 567
α (0·65)
8·4
(m/e 636)
α
106·3
Total signal
α
β
μ
2
4
6
8
time (m)

Fig. 6.2 (b)

Stage P1

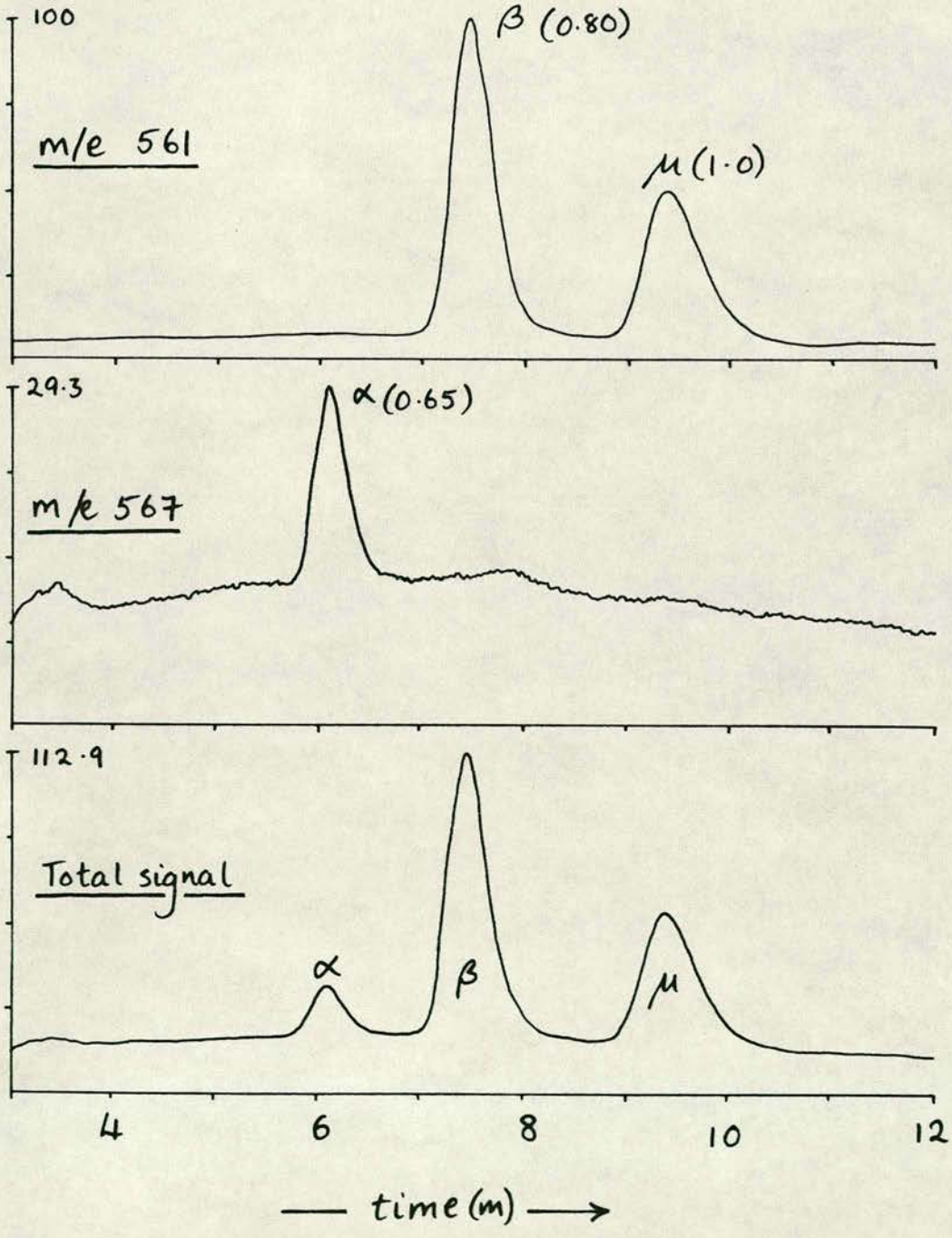

Fig. 6.2 (c)

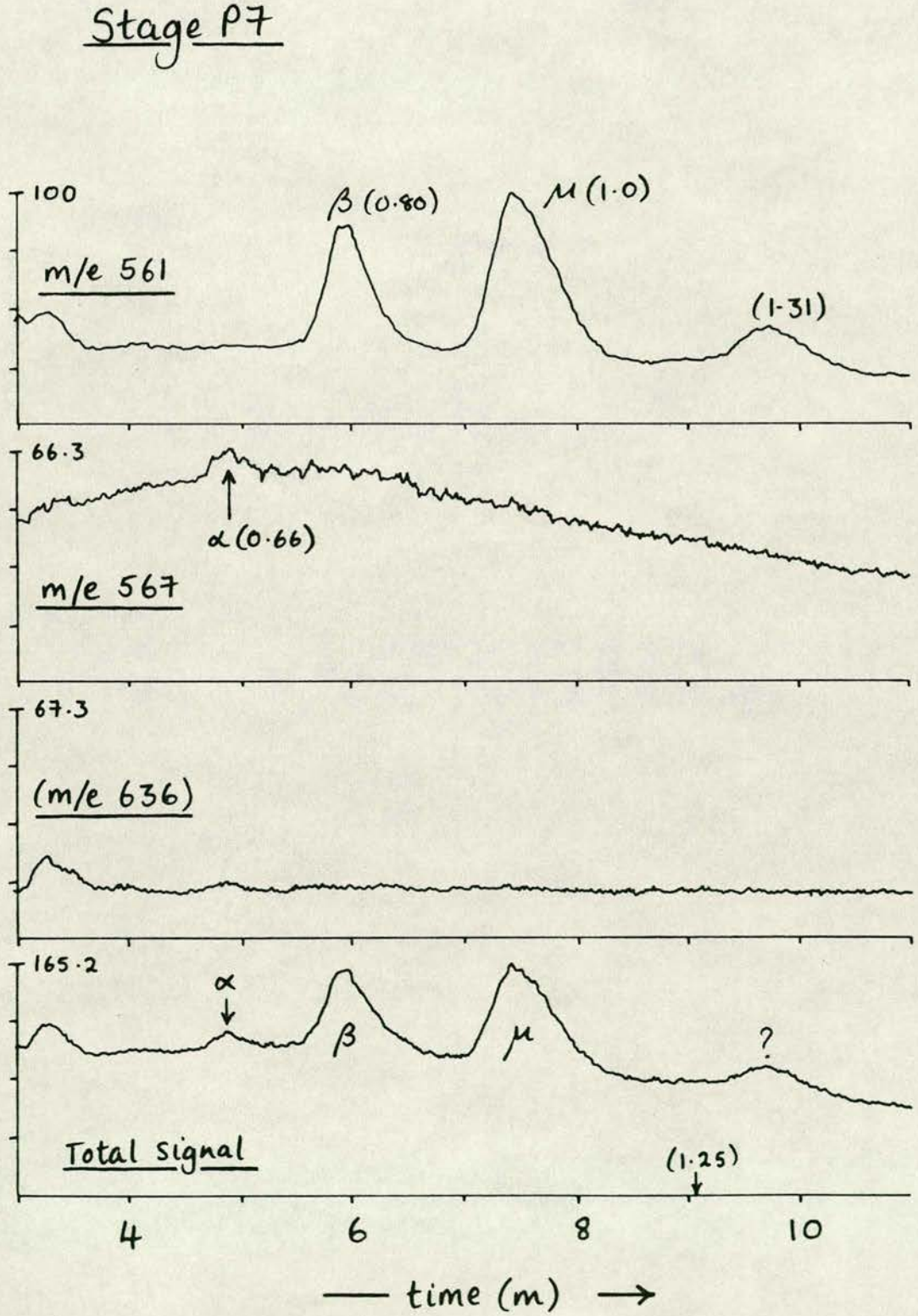
Stage P7
100
m/e 561
β (0·80)
μ (1·0)
(1·31)
66·3
α (0·66)
m/e 567
67·3
(m/e 636)
165·2
α
β
μ
?
Total signal
(1·25)
4
6
8
10
time (m)

Fig. 6.2 (d)

Stages P (10-13)

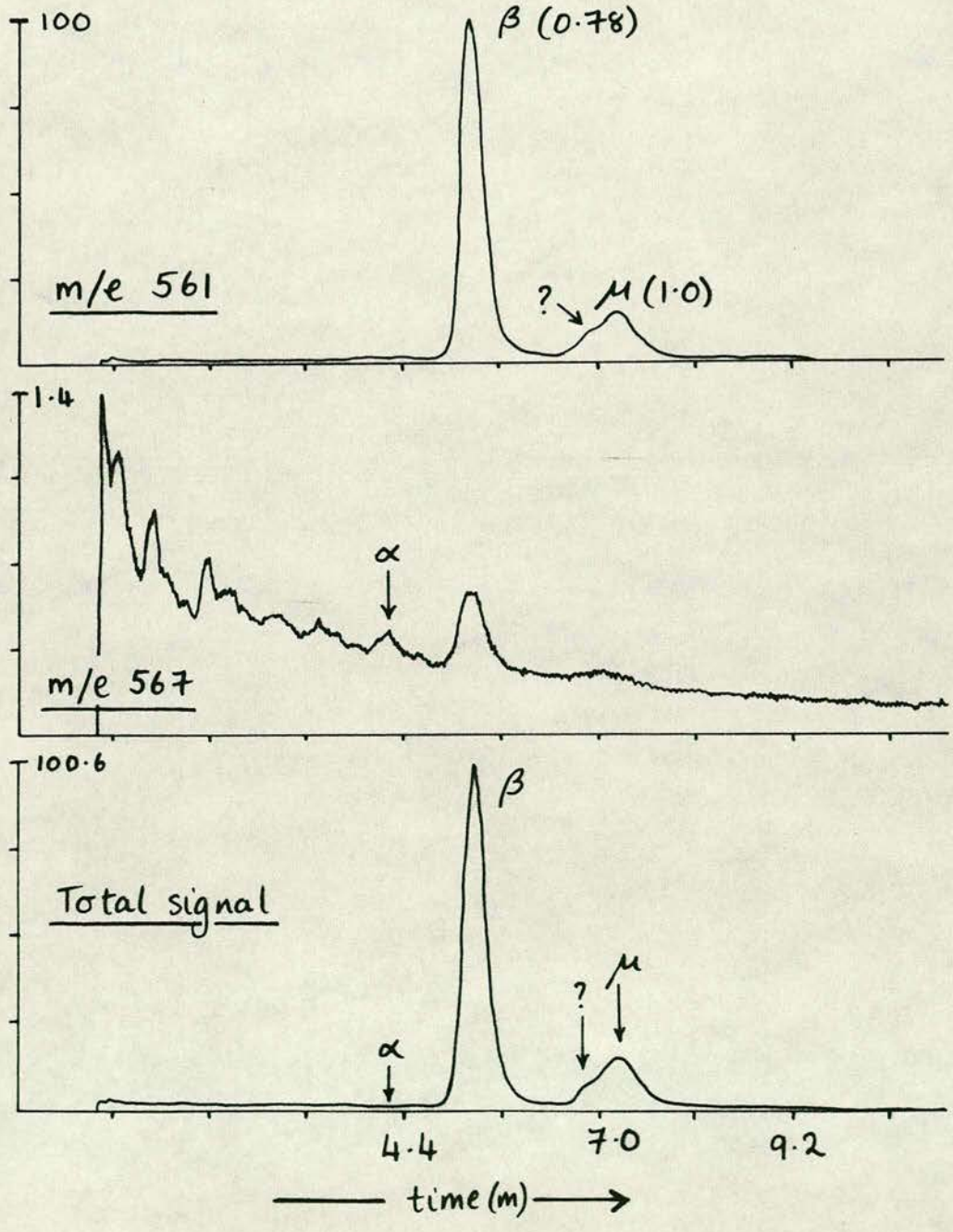

Table 6.1

GLC-MF analysis of ecdysteroids in stages P1, P7 and P10-13

Internal standard = makisterone A.

Estimated concentrations given as pg/mg fresh weight.

Steroid:	β	α	20,26-diOH-β	Total
Stage				
P1 (n=6, p = 0.05)	62 ± 51	70± 46	0	132
P7 (n=2)	18	12	6	36
n=1	+	+	?	
P10-13 (n=2)	212	5	0	217
n=2	+	+	-	

+ indicates compound identified but not quantified.

Note: Some runs of this analysis were rejected because they appeared to be based on degraded samples - the mass chromatograms were noisy and gave uncharacteristically low 20-OH-ecdysone titres in stages P10-13.

Ecdysteroids: β = 20-OH-ecdysone

α = ecdysone

20,26-diOH-β = 20,26-dihydroxyecdysone.

Because makisterone A was not introduced into the samples at the beginning of the extraction procedure, and also because it may be present endogenously in varying amounts according to stage, this analysis was not quantitative, (and note the different order of magnitude of these measurements compared to those of Table 5.V: pg cf. ng); but on the evidence of Table 6.I it seem that, contrary to expectations based on direct and HPLC-coupled RIA, the ecdysteroids titre at stage P7 is lower than that of either stage P1 or P10-13. Also, while the ratios of 20-OH-ecdysone to ecdysone appear to be similar in the earlier stages (P1 = 1.0, P7 = 1.5, approximately), in P10-13 the ratio seems to increase in favour of the 20-hydroxylated hormone (approx. 42.5 x ecdysone concentration) at a period in staged development which has not been scrutinised before. The results from this and the other sources of ecdysteroid-titre measurements will be compared in Chapter 7.

6.2 GC-MF of juvenile hormone(s) (JH)

It has been found that in the tobacco hornworm Manduca there are elevations in ecdysteroid titre during metamorphosis equivalent to those which occur in dipterans (Riddiford, 1980), e.g. in Drosophila at stages P1 and P7. In addition there is a small peak at the onset of wandering behaviour which is thought to "reprogramme" the epidermis for pupal cuticle production - a peak which, for the first time in the life cycle, does not coincide with a high JH titre (Riddiford, 1980) and which Richards (1981) suspects may be represented by the data of de Reggi et al. (1975) at a similar time in Drosophila larval life (peak 8, Fig. 1.6).

Thereafter, in Manduca the JH titre is found to rise to a peak coincident with the P1-equivalent ecdysteroid peak - this is thought to prevent precocious differentiation of the adult cuticle when ecdysteroids induce cuticle synthesis (Riddiford, 1980). So, given that JH has not been investigated as yet in Drosophila at the chemical level (cf. bioassays and RIAs), two questions arise in relation to the pattern of change in ecdysteroid titre: Which JH(s), if any, are present in Drosophila, particularly during metamorphosis, and secondly, does this species resemble Manduca with respect to coordination of the profiles of JH and ecdysteroid titres ? A preliminary attempt was made to answer these questions in collaboration with Professor Heinz Rembold (Martinsried).

Any samples ranging through the period of metamorphosis would serve to represent one or more analogues of JH should it be present at all during this period, although if titres were low and/or restricted in time JH might be undetectable - it is difficult to distinguish from other lipids in chromatographic procedures. The problem of sensitivity has been reduced considerably by the preparation of derivatives which yield intense fragments with high m/e values in mass fragmentography (see Section 2.24.2) (Rembold et al. 1980). Therefore homogeneous samples of mixed sex representing P1-P15 inclusive were prepared, extracted, derivatized and subjected to glass capillary gas chromatography-coupled mass fragmentography (GLC-MF). The only JH found in these samples was JH-III (C_{16}JH).

The second question - is there detectable JH at the time of the

pupariation ecdysteroid peak, and does it represent a JH peak? - was addressed by making a rough comparison between the average JH titres of stages P1-4 inclusive and P1-15 inclusive. If JH is more abundant at pupariation than (before or) after it this tactic should produce samples enriched for JH. However, preliminary results (per fresh weight) are as follows:

Stages P1-4 inclusive: 1.5pmol JH-III g^{-1};

Stages P1-15 inclusive: 5.0pmol JH-III g^{-1}.

In D. hydei "almost no JH-III seems to be present at (stage P1) and a first peak builds up around P3-4" (Rembold, 1983; personal communication, but cf. chapter 7).

It must be emphasised that this only constitutes a pilot-experiment, but there is no particular reason to doubt the identification of JH III during metamorphosis. The P1-4 and P1-15 extracts used in this analysis presented some difficulty when they were taken up into solution from the ampoules in which they were transported, and they were stored for some time before being analysed. Both of these factors might be expected to contribute if to anything then to underestimation of JH (e.g. by degradation, irrecoverability).

If we take the quantifications at face value, they suggest either that Drosophila does not have a pupariation JH-peak in common with Manduca or that the titre reaches a level at some later period to raise the mean titre P1-15 above that (detectable) level found over P1-4. P1-4 represents c. 12% of the P1-15 duration

(Table 3.IV). Arithmetically P4-15 then has a mean titre of about 5.5pmol g^{1}, 3.7 times higher than that of the earlier period. These measurements await confirmation and they indicate a need to look at the pharate adult in more detail. (cf. chapter 7 for data from Rembold and Bownes, personal communication).

Chapter Seven

Discussion of Chapters Four to Six

In this chapter the results of the preceeding experimental chapters are discussed, firstly to establish the particular findings of this report, taking into account contradictory strands of evidence, and secondly, in relation to other published findings concerning the roles of insect hormones during metamorphosis in an attempt to identify a working model for the control of some aspects of postembryonic development in Drosophila.

7.1 Ecdysteroid titre-profiles

The profiles of ecdysteroid titres of another cyclorrhaphous dipteran - Sarcophaga bullata - are shown at Fig. 7.1 for comparison with those of Drosophila (cf. Fig. 4.12). Briers and DeLoof (1981) give a profile very similar to that of Hodgetts et al. (1977; Figs. 1.6 and 4.12), showing the two major peaks of Richards (1981), i.e. numbers 9 and 11. There is no peak at or close to 75% of the period P1-P15 inclusive, which would be analogous to the putative peak at Drosophila stage P11 suggested by the data of chapter 4. Has any other study revealed such a peak ?

The data of Wentworth et al. (1981) are also shown at Fig. 7.1. Here it seems at first sight as though Sarcophaga does show a pharate adult ecdysteroid(s) titre peak, in this species at about 37% of "pharate adult" duration (cf. Drosophila stage P11 putative

Figure 7.1

Sarcophaga bullata: reported direct

RIA ecdysteroid titres

a) Briers and de Loof (1981) (30°C) Fig. 1; b) Wentworth et al. (1981) (25°C) Fig. 3

Abbreviations: L, larva; PP, prepupa; pu, pupa; Ph.A, Pharate adult; A, exarate adult (their diagnosis of stadia). Times in hours are converted to percentages of the period between puparium formation and eclosion. In (a) the pupal/pharate adult transition at 41% P(1-15) is said to mark "the transformation of the pupa into a pharate adult" (i.e. not the development of the pupal (and adult) form at head evagination; no source given but apparently not equivalent to P4/5). In Drosophila the pupal- adult apolysis occurs at about 38°C P(1-15) (Table 3.IV, mid-P7). Peaks 8, 9 and 11 are numbered according to Richards (1981). (No. 8 occurred "before the red spiracle stage"). 75% P(1-15) is marked (=P11i in Drosophila). In (b) the early pupal/pharate adult transition time (= apolysis) is probably misleading (24.5% P(1- 15)) since it is taken from another (diapausing) species (Tricholioproctia impatiens). The later time of 52% P(1-15) for secretion of the ecdysial membrane must be more realistic (cf. (a)) since this event represents one step in apolysis (in Tenebrio; Delachambre et al., 1980).

Fig. 7.1

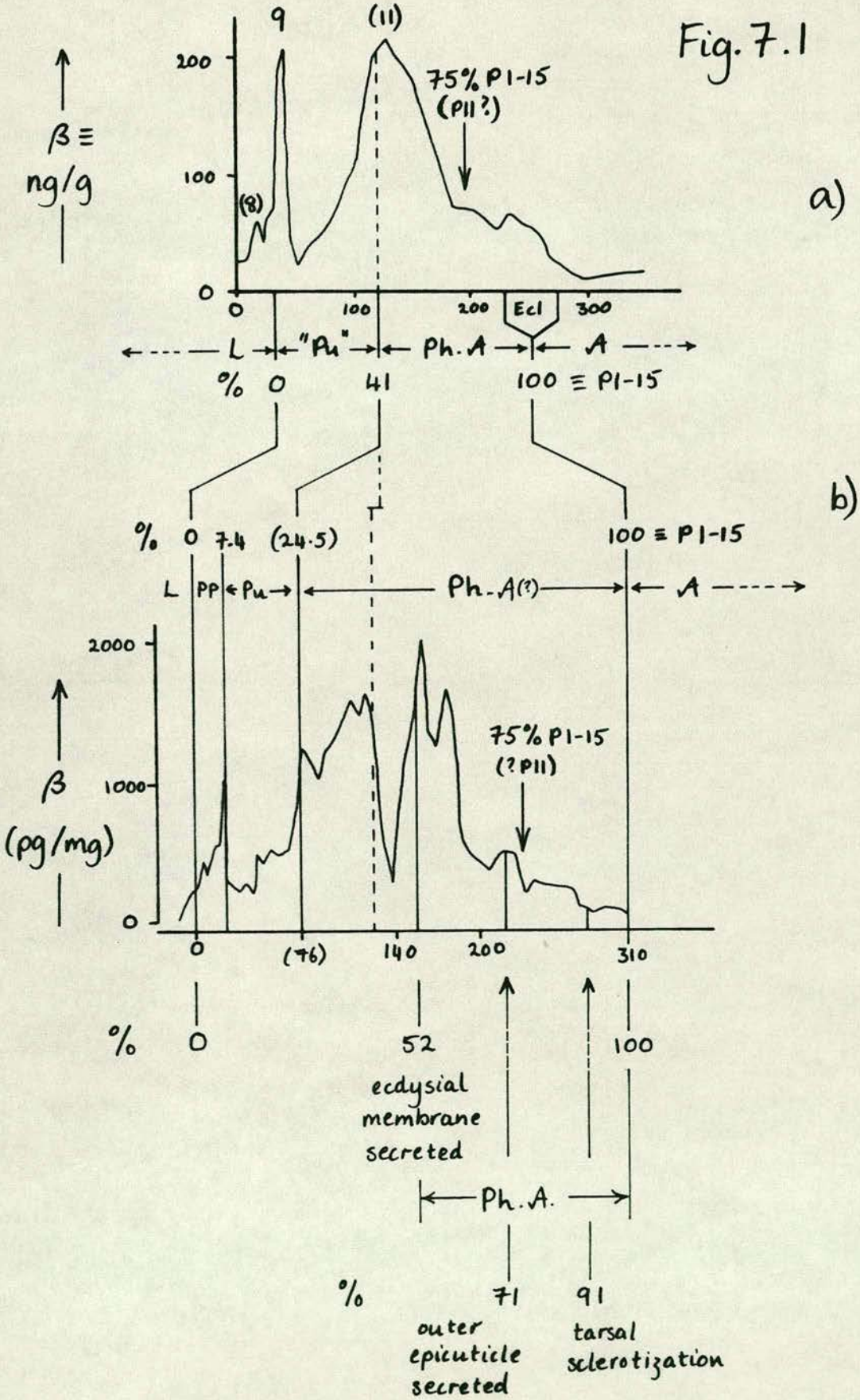
a)
β ≡ ng/g
200
100
0
9
(11)
(8)
75% P1-15 (P11?)
0
100
200
Ecl
300
L
"Pu"
Ph.A
A
% 0
41
100 ≡ P1-15
b)
% 0 7.4 (24.5)
100 ≡ P1-15
L PP Pu
Ph.A(?)
A
β (pg/mg)
2000
1000
0
75% P1-15 (?P11)
0
(76)
140
200
310
% 0
52
100
ecdysial membrane secreted
Ph.A.
% 71
91
outer epicuticle secreted
tarsal sclerotization

peak at approximately 62% of the period mid-P7-P15); i.e. there seem to be equivalents to the P1, P7 and later Drosophila peaks. But Wentworth et al. seem to have mis-placed the pupal/adult apolysis (see Fig. 7.1); and in fact their two major titre elevations flank the pupal/adult apolysis as does Hodgett's broad main peak (Richards' peak 11) in Drosophila. What is more, there is some evidence for peak 11 being resolved into more than one peak on at least one assay-system (Handler, 1982; see Fig. 4.12).

So it may be, then, that there is a drop in titre in Sarcophaga at or close to the pupal/adult apolysis, but there is no clear evidence of a peak close to the equivalent of stage P11, although Wentworth et al. (1981) do show some slight evidence of this - see Fig. 7.1(b), 75% of the period P1-15 inclusive; (and the two genera are reasonably similar with respect to stage at this period: "tarsal sclerotization" at 91% P1-15 in Sarcophaga (Wentworth et al. 1981) occurs at about 80% in D. melanogaster).

The ecdysteroid peak at stage P7 and the putative peak at P11 (Fig. 4.12) may well have different roles on physiological evidence. Wolsky (1938) presents a U-shaped curve for oxygen consumption during Drosophila metamorphosis. When these data are translated from times into stages on the basis of both time after pupariation at 25°C and reported morphology it appears that oxygen consumption declines from a maximum at P3(-4) until P6 and then increases from P8 to a maximum at P11(-14), the minimum by rough extrapolation being at late stage P7; i.e. oxygen consumption (and therefore metabolic rate?) declines as the P7 ecdysteroid titre peak climbs,

and then increases with the titre-increase towards stage P11.

Wolsky (1938) gives a fairly constant ratio of fresh to dry weights of Drosophila over this period (=c. 2.2 at c. P3-4, P6, P8 and P11-14). There is no detailed weight profile of Drosophila metamorphosis; (this could be obtained by growing up staged material in uncrowded cultures, measuring groups of staged animals, and plotting ratio (mean mass):(mean length) against stage;) but Joesten et. al. (1982) show that, in Manduca and Danaus, fresh weight is roughly constant between pupal ecdysis (=P4/5) and rejection of the meconium (=P15/A1). Manduca gains weight as a feeding larva (i.e. until =L1) and loses it again by the time of the pupal ecdysis (= P4/5), (Joesten et al. 1982). Glossina loses weight between pupariation and head eversion (=P1-P4/5), and furthermore this weight loss is accounted for by water, the volume of which is made up by the increasing size of the bubble involved in separation of the larval and pupal cuticles, (Langley and Ely, 1978; cf. Chapter 3); i.e. this prepupal weight-loss is not directly related to metabolic rate.

In general, then, it seems unlikely that absolute body-mass changes significantly in Drosophila between the P7 and P11 ecdysteroid titre peaks suggested by direct RIA; so if the data were re-expressed as "steroid mass per animal" (cf. per mg) the same pattern would emerge - any consideration of critical absolute steroid mass (e.g. per target organ), irrespective of actual body-size, would also be legitimate from this presentation of the data (mass per mg).

In comparing the direct-RIA data with those from HPLC-RIA and GLC-MF it is necessary to combine the set of titres obtained for the component stages of the band P10-13 which were not assayed separately by chromatographic procedures. The measured mean ecdysteroid titres of the sub-stages P10, P11i and ii, P12i and ii, and P13 shows a group mean of 580.1 pg ecdysone equivalents per mg (in terms of the Horn I2 anti-serum) but this figure becomes 440.6 pg when the component stages are weighted in accordance with estimates of their respective durations (Table 3.IV; i.e. according to the contributions they would make to a "P10-13" sample). So, when looking to the direct-RIA data for guidance as to peak ecdysteroid titres, we find:-

P1: 653.2 pg ecdysone equivalents;

P7: 1318.1 pg ecdysone equivalents;

P10-13: 440.6 pg ecdysone equivalents

... with respect to Horn I2 (16wk). These values match the data from HPLC-RIA in so far as P7 > P1 > P10-13 (cf. Table 7.I).

7.2 Makisterone A

Chapter 5 presents evidence for the presence of this C_{28} ecdysteroid in Drosophila stage P1. Most insect steroids are C_{27} compounds but makisterone A (24-methyl-20-OH-ecdysone) is found not only in plants and the Crustacea but also in Oncopeltus eggs at 4 days after oviposition (Kaplanis et al. 1980) where is is derived (without dealkylation) from the C_{28} compound campesterol - this is regarded as a dietary adaptation (substrate = sunflower seeds) by

evolution of the steroid biosynthetic pathways (Kaplanis et al. 1980). The compound has also been identified in fifth instar nymphs of the true bugs Nezara vivula, Podisus maculiventris and Dysdercus cingulatus (Aldrich et al. 1982) which show a peak in haemolymph titre of makisterone A (and little or no ecdysone or 20-OH-ecdysone) 5-8 days before "pupal ecdysis" (i.e. before P4/5 equivalent; cf. P1 titre-peak in Drosophila prepupae). In these species and in Oncopeltus Aldrich et al. (1982) find that makisterone A has ten times the activity of 20-OH-ecdysone in cuticulogenesis and they conclude that the C_{28} compound is active as a moulting hormone in the bugs (Hemiptera).

There is no direct evidence for a moulting-hormonal function for makisterone A in the Diptera, but it has been identified in Drosophila in another study (Redfern 1984) shortly before stage P1 (cf. Chapter 5). Redfern finds that ring glands taken from D. melanogaster raised on corn/yeast medium secrete 20-deoxy-makisterone A in vitro and that this compound is converted in vitro in the presence of fat body into makisterone A as identified by GLC-MF. The ring glands in these experiments were taken from larvae with partially or fully bloated salivary glands, i.e. "late wandering larvae" (Redfern 1984) representing stages L1 and/or L2. Their secretion of makisterone A appears to represent an adaptation to the presence of C_{28} or C_{29} phytosterols in the medium since ring glands from larvae raised axenically on a medium containing cholesterol as the only sterol do not secrete makisterone A. In the present study makisterone A has been found after growth on the same corn- yeast medium, shortly after L1-L2 (i.e. in stage P1).

In conjunction with Redfern's data (1984) this report, although lacking a molecular characterisation by mass fragmentography, strongly suggests the presence *in vivo* of makisterone A in *Drosophila* during the earliest period of metamorphosis.

7.3 Ecdysteroid identifications and titres

Table 7.1 summarises the quantitative findings of this report by the three techniques: direct RIA, HPLC-RIA and GLC-MF at stages P1, P7 and P10-13.

7.3.1 20,26-dihydroxyecdysone

This compound (Table 7.1, 26-OH-β) has been reported in *Manduca* (Kaplanis *et al.*, 1979) at the approximate equivalent of stage P7 when the most abundant ecdysteroid revealed by GLC-MF was 20-OH-ecdysone (cf. Table 7.I by GLC-MF); but Gilbert and Goodman (1981) did not confirm this, finding instead the *Manduca* ecdysteroid titre at P7-equivalent to be due largely to ecdysone (cf. Table 7.I, P7 by HPLC-RIA). There is some doubt, then, about the status of this report of a di-hydroxy-ecdysteroid present during *Drosophila* metamorphosis, and the identification must be confirmed independently.

Table 7.I

Summary of findings, P1, P7 and P10-13

	Ecdysteroids (pg/mg)			JH
	(direct RIA* α equivs.)	HPLC-RIA* (Quantification)	GLC-MF (Identification)	GC-MF
P1				
α		3242 (72%)	70 (46%)	
β		614 (14%)	62 (40%)	
26-OH-β			0 (0%)	
24-CH_3-β		623 (14%)		
Total	653	4479 (100%)	132 (86%)	
P7				
α		4603 (62%)	12 (33%)	
β		1557 (21%)	18 (50%)	
26-OH-β			6 (17%)	
Total	1318	6160 (83%)	36 (100%)	
P10-13				
α		2219 (80%)	5 (2%)	
β		566 (20%)	212 (98%)	
26-OH-β			0 (0%)	
Total	441	2785 (100%)	217 (100%)	
P1-4				
JHIII				+
P1-15				
JHIII				++

*Note: the two sets of data derive from different antisera (Horn I2 vs. MAS)

Ecdysteroids: α = ecdysone
β = 20-OH-ecdysone
26-OH-β = 20,26-dihydroxyecdysone
24-CH_3-β = 24-methyl-20-OH-ecdysone (makisterone A).

7.3.2 Comparisons of stages P7/P10-13 and HPLC-RIA/GLC-MF

Although the direct-RIA data do not demonstrate a distinction between the P7 and P10-13 ecdysteroid titres conclusively - i.e. P10-13 may represent an extension of the same titre-elevation - we may ask if the compositions of the two elevations differ with respect to ecdysone and 20-OH-ecdysone; i.e. are the ratios of ecdysone to 20-OH-ecdysone of the same order of magnitude at these two periods of metamorphosis ?

When this question is asked of the HPLC-RIA data the answer is no (Ratio at P7=3; at P10-13=4) although the ratios of ecdysone to 20-OH-ecdysone are dissimilar by GLC-MF (P7=0.7; P10-13=0.02) which tends to confirm the suggestion by direct-RIA mean titres of a distinct ecdysteroid peak at cuticle-melanisation in the pharate adult and raises the question of why there should be an increase in the rate of ecdysone hydroxylation at this time. However, the GLC-MF data are not strictly comparable with those from HPLC-RIA since they did not share a common, controlled recovery-efficiency. Table 7.II shows the ratios of absolute recoveries by the two techniques where they quantify the same ecdysteroid, and from this it is clear that, while recovery by GLC-MF is always the smaller, it is variably so.

But it is legitimate to compare the techniques by the proportions of total identified steroid represented by any given molecular type, (see percentages shown at Table 7.I). These should be admissable for comparison on an equal basis. Such a comparison

Table 7.II

Comparison of data from HPLC-RIA and GLC-MF

Ratios of titres (pg/mg) of common ecdysteroids
(HPLC-RIA:GLC-MF)

Stage	Ecdysone	20-OH-ecdysone	Both compounds
P1	46	10	29
P7	384	86.5	171
P10-13	444	3	13
(Mean all stages)	(291)	(33)	(71)

Table 7.III

Proportional representation (% total) of ecdysteroids at three stages of metamorphosis (from Table 7.I)

Stages:	P1		P7		P10-13	
Technique:	HPLC -RIA	GLC -MF	HPLC -RIA	GLC -MF	HPLC -RIA	GLC -MF
Steroid						
α	72	46	62	33	80	2
β	14	40	21	50	20	98
26-OH-β	?	0	?	17	?	0
24-CH_3-β	14	?	?	?	?	?
Ratio (α/β)	5.1	1.15	3	0.7	4	0.02
Factor (HPLC-RIA= GLC-MF x F)	F = 4.4		F = 4.3		F = 200	

Ecdysteroids:
α = ecdysone
β = 20-OH-ecdysone
26-OH-β = 20, 26-dihydroxecdysone
24-CH_3-β = 24-methyl-20-OH-ecdysone (i.e. makisterone A)

is made at Table 7.III; (but note that, when one of the techniques failed to identify a compound represented in the results of the other one, then it was assumed to have been present in both, in the same proportion - see Table 7.I,%).

Treating HPLC-RIA and GLC-MF as thus comparable, the ratios of proportional titres ecdysone:20-OH-ecdysone are not consistently of the same order of magnitude by the two techniques (Table 7.III, α/β), the discrepancy being greatest (x200) between the P10-13 samples. On the basis of HPLC-RIA alone, the ratios of ecdysone to 20-OH-ecdysone at stages P7 and P10-13 are similar (3 and 4 respectively; Table 7.III).

7.3.3 Stage P1

In stage P1 ecdysone is found to be present in greater abundance than 20-OH-ecdysone by both techniques (ratio = 5.1 or 1.15). In contrast to this Dean et al. (1980) found the 20-hydroxylated compound to be predominant in Calpodius at this stage (ratio = 0.15). Why should the prohormone be more abundant in Drosophila? The difference could well result from slight differences in staging of the larvae/prepupae, even were the comparison to be restricted to a single species (cf. Borst et al. 1974; Handler (1982) reports 20-OH-ecdysone as 18X more abundant than ecdysone at pupariation) - perhaps hydroxylation of the prohormone is more gradual in Calpodius. "P1" in Drosophila appears to be a period of rapid increase in size of the prohormone pool, presumably for subsequent very rapid conversion to the C_{20}-hydroxylated derivative. Perhaps,

also, makisterone A may play a minor role in the balance between precursors of and active hormones - it is itself a C_{20}- hydroxylated ecdysteroid which may not be present in Calpodius. But in general, if ecdysone is indeed the biologically less active pro-hormone (Smith et al. 1980), then it seems that the target process modulated by 20-OH-ecdysone is not at its most active if it is already in operation at stage P1 - that must occur later, (cf. pupal cuticle secretion).

So ecdysone appears to be more abundant than 20-OH-ecdysone near peak ecdysteroid titre. The reverse is the case at minimal ecdysteroid titre during metamorphosis: Redfern (personal communication) finds the ratio of ecdysone to 20-OH-ecdysone to be 0.64 at stage P4(i) (cf. Fig. 4.11); i.e. hydroxylation lags behind ecdysone synthesis/secretion by the ring-gland, and catabolism of the hydroxylated derivative of ecdysone lags behind that of the ecdysteroid pool as a whole.

Redfern's finding appears to contradict the requirements of the larval salivary glands: Richards (1976) has shown that these glands only exhibit a normal polytene chromosome puffing sequence in vitro when exposed to a very low 20-OH-ecdysone concentration between 3 and 8 hours after pupariation (i.e. approx. stages P3-P4i). This report (Fig. 4.11) and Redfern's observation offer no support to a prediction of baseline titres of 20-OH-ecdysone at 3-8 hours; but it must be remembered that these whole-body titres do not represent the hormone titres in circulation in the haemolymph bathing the salivary glands. Milner (1977) and Hodgetts et al.

(1977) speculate that particular tissues may become "isolated" in some way from hormones carried in the haemolymph at certain stages of development (perhaps they lack the receptor-protein, for instance); and Richards is in agreement that the salivary glands may not "see" the ecdysteroids represented by whole-body titres (personal communication) but feels that this is more likely to result from tissue-specific sequestration of steroid conjugates rather than effective compartmentalization of other tissues with respect to the haemolymph. The question could be resolved by precise analysis of the circulating titre at stage P4i using GLC-MF.

7.3.4 Stage P7

HPLC and GLC-MF differ in their identifications of the more abundant ecdysteroid at this stage, ecdysone or 20-OH-ecdysone (ratios = 3 or 0.7; Table 7.III) but their respective contributions to whole-body titre by the two techniques are of similar magnitudes. Gilbert and Goodman (1981) find ecdysone to be more abundant than 20-OH-ecdysone in Manduca at the approximate equivalent of stage P7, as found here by HPLC-RIA. On the other hand, Kaplanis et al. (1979) report 20-OH-ecdysone to be the more abundant, again in Manduca at approximately stage P7 - clearly there is a rapid change at around this time and precise timing of the sample is critical. Handler (1982) finds a ratio of 1:1 at about P6/7 in Drosophila (30h post-pupariation at 25°C). At a slightly later stage (45h after pupariation at 25°C; approx. P8) Gietz et al. (1983) find ecdysone:20-OH-ecdysone = 0.41, indicating subsequent hydroxylation at the C_{20} position.

The direct-RIA results of chapter 5 suggested that stage P7 represented a relatively high ecdysteroid titre-elevation in comparison with both P1 and P10-13. This is borne out by HPLC-RIA (Table 7.I; P7 total = 1.38 x P1 total pg mg^{-1}), but, although the samples submitted to HPLC-RIA and GLC-MF represented subgroups of a single homogeneous batch of animals at each stage, the GLC-MF data contradict this pattern (P7 total = 0.27 x P1 total pg mg^{-1}).

7.3.5 Stages P10-13

Ideally these samples would have been drawn from stage P11 or P10-11, but large-scale collection of such a narrow band of stages distinguished on subtle staging criteria proved to be impractical. In fact the samples included stage P13, by which time Fig. 4.12 shows the ecdysteroid titre to be on the decline.

As with stage P7, so here HPLC-RIA reveals ecdysone to be more abundant than the C_{20}-hydroxylated analogue, a fact which in itself lends support to the contention that there is a discrete peak in the pharate adult (i.e. there would appear to be synthesis of the "prohormone" as the free ecdysteroid pool increases in size; any subsequent hydroxylation at C_{20}, by analogy with the P1-P4 transition described above, has not been examined here). But the GLC-MF data suggest a high relative abundance of 20-OH-ecdysone at P10-13 (and a high ecdysteroids titre relative to stage P1).

7.3.6 General

In general the two techniques HPLC-RIA and GLC-MF must be regarded primarily as a means of confirming molecular identifications and of recognising 20,26-dihydroxyecdysone, whereas in this context the relative precision of the experiments suggest HPLC-RIA as a means of making accurate quantifications of the subjects of the analysis, given their presence confirmed by the complementary technique.

So the quantitative findings of this report are those shown at Table 7.I, HPLC-RIA (q.v.)

At each of the putative titre-peaks examined, ecdysone is the principle component of the whole-body free ecdysteroids pool; and the titres are considerable at the three stages P1, P7 and P10-13; but as to whether or not these stages really represent peaks in the titre-profile, the troughs in the mean titre-profile (Fig. 4.11 and 4.12) should also be characterised; and in addition the titre in stage P7 should be examined in detail in animals cultured at low temperature (cf. 25°C) to ask: "can Drosophila show a low ecdysteroid titre at some point within the P7 elevation as Sarcophaga appears to do at 140h after pupariation (Fig. 7.1)?"

7.4 Ecdysteroids: Sources and Biosynthesis de novo

Figure 7.2 illustrates schematically the derivation of ecdysone from its most rudimentary insect substrate, cholesterol, which is

Figure 7.2

Schematic pathway for ecdysone synthesis in larvae (After Richards (1981b) Fig. 3)

Major modifications to the cholesterol skeleton ($C_{17}H_{45}OH$; almost fully saturated) are required before the series of hydroxylation reactions inside the prothoracic gland (PTG). Ecdysone is hydroxylated at C_{20} peripherally by the P450 ecdysone-20-monooxygenase of the mitochondria (Gilbert and Goodman, 1981).

Fig. 7.2

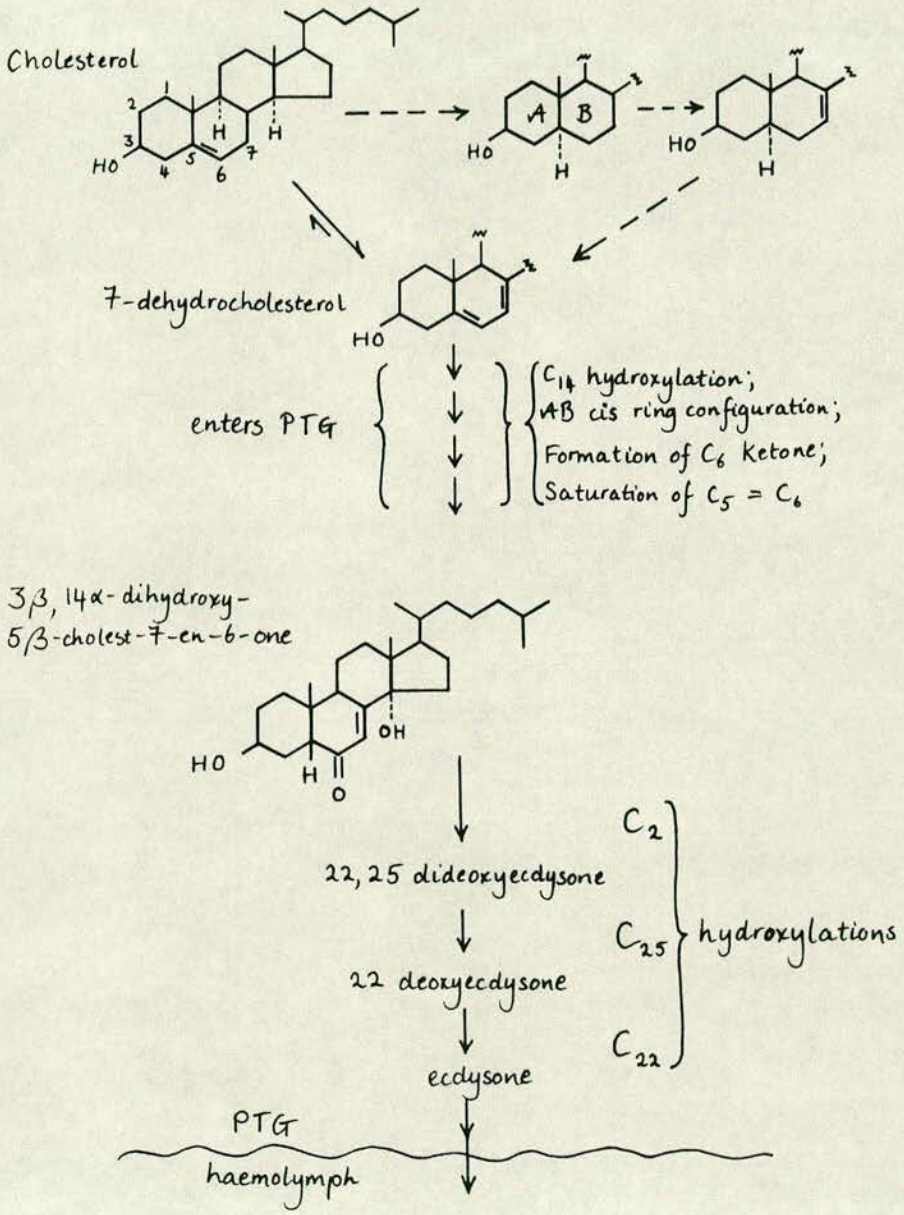
Cholesterol
HO
H
A
B
7-dehydrocholesterol
enters PTG
C14 hydroxylation;
AB cis ring configuration;
Formation of C6 ketone;
Saturation of C5 = C6
3β, 14α-dihydroxy-
5β-cholest-7-en-6-one
OH
O
22, 25 dideoxyecdysone
22 deoxyecdysone
ecdysone
C2
C25
C22
hydroxylations
PTG
haemolymph

oxidised to 7-dehydrocholesterol before entering the prothoracic gland cells of the larval ring-gland (Richards, 1981b) where it is modified and from where it is secreted to be hydroxylated at the C_{20} position peripherally, e.g. in the fat body (cf. Appendix 6) by a P450 20-monoxygenase system (in Manduca; Gilbert and Goodman, 1981).

This account is in accord with what is known of Drosophila at stage P1. The larval ring gland contains cells equivalent in function to the corpus allatum and the prothoracic glands of lower insects (Bodenstein 1950; King, 1970) as well as progenitors of the imaginal corpus cardiacum cells and the imaginal corpus allatum (Bodenstein 1950). This composite gland persists in the prepupa and moves posteriorly to the prothorax in the young pupa (c. P4i; Bodenstein 1950). Late third instar (LIII+) ring-glands secrete ecdysone in vitro (Redfern, 1983; Redfern and Bownes, 1984) and failure of certain mutants to pupariate tends to be cured by implantation of wild-type ring glands (Kiss et al., 1978). Despite the relative abundance of ecdysone at stage P1 found in this study it seems to be 20-OH-ecdysone which is the more active; e.g. administration of this compound tends to induce pupariation in the mutant ecd^1 at the restrictive temperature (Garen et al. 1977).

However, the ring gland is not the source of the ecdysone which gives an elevation in whole-body titre in Drosophila stages P6-7. Secretion from these glands, as tested in vitro, stops before stage P6 (Redfern and Bownes, 1984); and neither is it the cause of

any subsequent titre-elevation - the "prothoracic gland" cells degenerate after the "pupal moult" (Bodenstein, 1950). The ovaries are not significant sources of ecdysteroids or sites of ecdysone hydroxylation *in vitro*, neither at stage P9 nor in young exarate adults (Bownes *et al.* 1984; personal communication); but the oenocytes are candidates for the role of ecdysteroid source during metamorphosis (Ruhland and Romer, 1977); and Delbecque (1981) suspects differentiating structures in general of producing ecdysteroids during pupal development.

7.5 Ecdysteroid metabolism

Another possible "source" of active ecdysteroids (i.e. hormone) during metamorphosis is the reactivation of metabolites. Fig. 7.3 indicates the major modifications thought to occur in insects prior to ecdysteroid storage and/or excretion. Storage for subsequent reactivation is mainly by (reversible) conjugation; but note that this report is concerned essentially with aqueous methanol-extractable compounds - effectively "free" hormone. Non-polar compounds when extracted will have been left at the origin on TLC.

Elimination of molecules from the actual or potential hormone pool can be achieved by irreversible modification prior to excretion. The meconium of *Manduca* contains 3-epi-ecdysone and 3-epi-20-OH-ecdysone (Koolman, 1979; the meconium of *Drosophila* is expelled through the anus at eclosion).

The changing ratios of constituents of the ecdysteroid titre

Figure 7.3

Metabolic conversion of ecdysone

(After Koolman, (1982), Fig. 3)

Ecdysone is shown subject to catabolic modifications of the hormone (C_{20} hydroxylation is anabolic). Koolman (1982) also gives carboxylation of the side chain to produce highly polar "ecdysonoic acids" as a mechanism of inactivation prior to excretion, which is probably irreversible; and epimerisation at C_3 may be irreversible since it involves the loss of hydrogen peroxide.

Conjugate formation occurs prior to storage (e.g. in the Malpighian tubules). The highly polar conjugates of insect ecdysteroids include sulphate esters, glucosides, glucuronides, and phosphates (Koolman 1982), which may be reactivated later in development, especially in the embryo (Gilbert and Goodman 1981).

Calliphora ecdysone oxidase converts ecdysone and 20-OH-ecdysone to 3-dehydroecdysone (K_m=3.1x10^{-5}M) respectively plus H_2O_2 (i.e. effectively irreversible) (Gilbert and Goodman, 1981).

Manduca ecdysone reductase (3-epimerase) converts ecdysone irreversibly to 3-epiecdysone (K_m 1.7 x 10^{-7}M) and 20-OH-ecdysone to its 3- epi-derivative (K_m 4.7 x 10^{-7}M) via the 3-dehydro-ecdysteroid (Gilbert and Goodman 1981).

Fig. 7.3

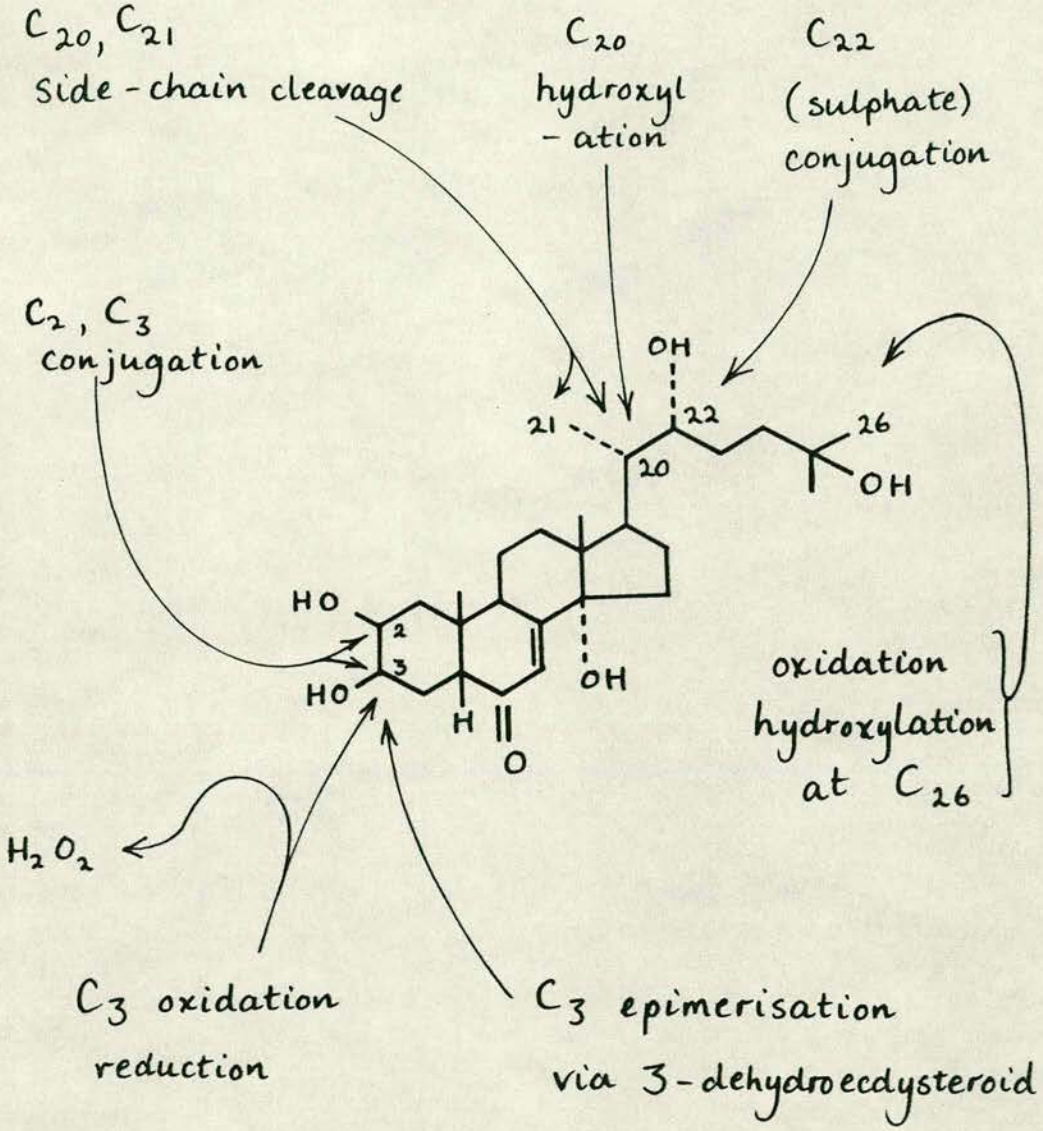
C_{20}, C_{21}
side-chain cleavage
C_{20}
hydroxyl-ation
C_{22}
(sulphate) conjugation
C_2, C_3
conjugation
OH
21
22
20
26
OH
HO
2
3
HO
H
O
OH
oxidation
hydroxylation
at C_{26}
H_2O_2
C_3 oxidation
reduction
C_3 epimerisation
via 3-dehydroecdysteroid

can be a valuable indicator of the timing of a target process, i.e. it is possible to look for evidence of hormone metabolism once the function of a titre-peak has been achieved. Kaplanis *et al.* (1979) found the active "moulting" hormone, 20-OH-ecdysone (with some 20,26-diOH-ecdysone) to be predominant at about equivalent-P7 in *Manduca* and later, at about equivalent-mid-P9, the ecdysteroid titre included epimerised molecules: ecdysone, 20-OH-ecdysone and 20,26-diOH-ecdysone and the 3-epi-analogues of each were all present as the general titre declined. This is highly significant in considering the putative distinction between the P7 and P10-13 titre peaks in *Drosophila* since mid-P9 represents a trough in the titre-profile obtained by direct-RIA (Fig. 4.12), and epimerisation is thought to be irreversible; i.e. if *Drosophila* resembles *Manduca*, the subsequent finding of an elevated titre at P10-13 consisting primarily of ecdysone must result from renewed ecdysone synthesis *de novo*.

7.6 Ecdysteroid functions

The consideration of control of cuticle secretion which follows will be returned to in discussing the interactions of ecdysteroids and juvenile hormone later in the chapter.

7.6.1. Production and modification of cuticle

The peaks in ecdysteroid titre at stages P1, P7 and c.P11 are found in both sexes (Figs. 4.8 and 4.9). The pupariation peak in *Drosophila* is required for sclerotization of the larval exocuticle

(Garen et al., 1977), for the normal sequence of salivary gland polytene chromosome puffing (Richards, 1976), and for eversion of the imaginal discs and subsequent secretion of the pupal cuticle (Milner, 1974; Fristrom, 1984). Kraminsky et al. (1980) report major peaks in ecdysteroid titre alternating throughout the life-cycle with peaks of the enzyme Dopa decarboxylase (DDC) involved in tanning of the most recently secreted cuticle - the two activities peak almost coincidentally at pupariation when pupal cuticle is very soon to become recognisable by electron microscopy (4-6h, c.P3; Poodry and Schneiderman, 1970) and, shortly after that, to tan. Delbecque et al. (1978) found a good correlation between moulting hormone peaks in Tenebrio and the beginnings of secretion of the pupal and adult cuticles. In this report a correspondence is shown between elevation in ecdysteroid titre at stages 6-7 and the onset of adult cuticle secretion: the pupal/adult apolysis (34h, Fraenkel and Bhaskaran 1973; approx. e.P7) is followed by imaginal differentiation of the thoracic appendages (approximately late P7; see chapter 3) and pigmentation of the femoral/tibial bristles is visible at about the time of first eye colouration (P7/P8; chapter 3); so presumably secretion of the thoracic adult cuticle must have begun by stage P8 (cf. Bodenstein 1950; P7/8 + 1h). In Bombyx a high ecdysteroid titre in the late pupa is thought to trigger adult development (Hanaoka and Ohnishi, 1974); and Ohtaki and Takahashi (1972) find that this pupal peak is absent from diapausing Sarcophaga in which, also, adult cuticle differentiation fails to occur. There is, then, both circumstantial and direct evidence for a causal relationship between ecdysteroids and cuticle production. The nature of the cuticle so produced

will be discussed in relation to juvenile hormone (section 7.7).

The flight-muscle primordia of Drosophila begin their morphogenesis in stage P6 (21h; Bodenstein, 1950); but they show no striations before mid-P8 (50h; Bodenstein, 1950) i.e. after the P7 ecdysteroid maximum; so, if synthesis of myofilaments is the differentiative equivalent in muscles of epidermal cuticle-secretion, then these thoracic muscles may be said to parallel the thoracic epidermis in their relation to the ecdysteroid titre profile.

The next DDC peak after the P7 ecdysteroid titre peak does not occur until P15/A1 (eclosion; Kraminsky, et al., 1980) by which time melanisation of adult bristles etc. has already occurred and has probably been preceded by a further elevation in ecdysteroid titre (late P9-P11; see Fig. 4.12). Tanning of the adult cuticle (as distinct from darkening) follows eclosion and the DDC peak; but the temporal relationship between increasing ecdysteroid titre and cuticle melanisation suggests a directive role for "moulting" hormone in cuticle maturation with no requirement for DDC.

7.6.2 The testes

While vitellogenesis and oocyte maturation begin at about the time of eclosion (King, 1970) the meiotic divisions in the testes take place at pupariation (Lindsley and Lifschytz, 1972), nearly-mature spermatozoa are present by stage P6 (24h; Bodenstein, 1950) and the testes at eclosion contain mostly mature spermatozoa

(Bodenstein, 1950); so the testes suggest themselves as a target tissue for, and/or a source of, ecdysteroids during metamorphosis, and limited evidence for this is shown at Fig. 4.10 (q.v.) where the mean male titre is seen consistently to exceed that of females from late stage L1 until stage P7 (and, excepting P8, until mid-P9) (pg mg^{-1}). Koolman et al. (1979) reported a high local concentration of ecdysteroids in the testes of adult Calliphora (and some evidence for their transfer at insemination). Because meiosis and subsequent germ-cell maturation occur so early in male Drosophila, if ecdysteroids should be sequestered in developing spermatozoa then sequestration might well be expected to begin during metamorphosis. The data of Bownes et al. (1984) concerning the first three days of exarate adult life do not reveal the testes to be a major reservoir of ecdysteroids relative to other tissues until day three, but they do show a relatively high titre for their weight (pg mg^{-1} testis), even on the second day. (They are not a significant source of secreted ecdysteroids in vitro: Bownes et al. 1984; eclosion + 3d). So, although data on testicular ecdysteroid titres are lacking during metamorphosis, it is conceivable that they sequester these compounds well before eclosion; and perhaps also their morphogenesis may be influenced by relatively high titres - elongation in stage P4i (11h; Bodenstein, 1950) and coiling in P6-7 (from 30h; Bodenstein, 1950) both occur during the period when the (mean) male ecdysteroid titre consistently exceeds that of the female (see above). On the other hand, pigmentation of the testes commences in mid-P9 when male and female titres are very similar and probably low relative to P7 and P11 (Figs. 4.10 and 4.11); so the matter is unresolved; but the

testes would be worthy of analysis with respect to ecdysteroids during metamorphosis.

7.6.3 The ovaries/vitellogenesis

King (1970) has described the timecourse of ovarian differentiation. Morphogenesis of ovarioles has begun by stage L1 (2h before pupariation at 25°C) when adjacent terminal filaments are already distinguishable. By P2/3 (pupariation+2h) the deposition of an acellular material, the tunica propria, around the ovarioles has started; germaria are visible by P6 (24h); and the first egg chambers bud off before mid-P7 (39h). Until this stage, then, there is a correspondence between ovarian and imaginal disc development in so far as morphogenesis begins in the larva (cf. disc folding and eversion) followed shortly after pupariation by secretion of lamellate material (cf. pupal cuticle) although disc differentiation, unlike that of the ovaries, is not accompanied by rapid growth; (the ovary doubles its volume once during stage P6 (24-30h) and once more by mid-P7 (30-36h)).

At about 39h (c. mid-P7) one pro-oocyte in the most basal cystocyte cluster of each ovariole switches to the nurse-cell differentiative pathway (King, 1970); but, although this coincides with maximal ecdysteroid titre (P7) the trigger for the switch is very likely to be ovary-autonomous since this event recurs repeatedly in the imaginal ovary. Subsequent development before eclosion is restricted to the pre-vitellogenic (yolk-depositional) stages of occyte maturation.

At eclosion each vitellarium contains 3-6 egg chambers in pre-yolk stages (i.e. pre-oocyte-stage 8; King 1970). Meiosis has still to occur - it is not completed even in stage 14 oocytes stored in the ovarioles of adults (King, 1970); but again, being a repetitive event in the mature ovary, this is unlikely to be coupled to gross hormone titres in Drosophila.

Do ecdysteroid titres control the production and/or deposition of yolk polypeptides - "vitellogenesis" - in Drosophila ? Until recently it was reasonable to think that they might since adult male Drosophila can, in common with several other insects (see Bownes et al. 1984), be induced to produce yolk polypeptides (YPs) in the fat body and to secrete them into the haemolymph by the administration of 20-OH-ecdysone (e.g. Bownes et al., 1983). But there is no unequivocal evidence for a significant difference in whole-body ecdysteroid titre between the sexes at stage P15+, when YP synthesis begins; (cf. Fig. 4.10, and Handler, 1982; although see Fig. 7.5(c) and (k) for evidence of a female-specific 20-OH-ecdysone peak (Bordes et al., 1983) 2h after eclosion).

The fat body is not the only source of YPs. Oocyte maturation can be ovary-autonomous with respect to YP synthesis and yolk deposition. Bodenstein (1947) and Bownes (1982) have shown that pupal ovaries (P5-6; 0.5-1d post-pupariation) undertake yolk deposition when transplanted into exarate adult abdomens; but Bownes (1982) also found that serial back-transplantation of adult ovaries into pupae of either sex resulted in the development of mature yolky

oocytes within the sub-imago; i.e. the ovarian follicle cells can themselves provide the YPs necessary for oocyte maturation.

So either expression of the YP genes is not regulated by ecdysteroids or the ecdysteroid trigger for induction of YP synthesis derives from the ovaries themselves. But both stage P9 ovaries and ovaries from exarate adults are known to secrete very little material which cross-reacts with the Horn I2 antiserum (Bownes, personal communication; and Bownes et al., 1984) and although by the third day after eclosion 30% of distributed ecdysteroids are traceable to the ovaries (Bownes et al., 1984) this tissue only accounts for less than 16% of whole-body titre on the first day (taking account of an unspecified amount in the haemolymph at this time; Bownes et al. 1984), i.e. at a time when YP synthesis is already established; so the trend towards concentration of ecdysteroid activity in the ovaries is perhaps more likely to represent sequestration in the eggs rather than indigenous control of YP gene expression.

When adult males are stimulated with 20-OH-ecdysone, transcription of the YP genes is induced in the fat body; and the transcription is also enhanced in females in body wall preparations (i.e. fat body + epidermis + oenocytes) but not in ovarian follicle cells (Bownes et. al., 1983). So induction of YP gene expression by "moulting" hormone represents a tissue-specific response (fat body) but it is not sex-specific; and this being the case, and there being no apparent difference between the sexes in native ecdysteroid titre, it has to be asked whether ecdysteroids really have any natural

function in directing expression of these genes. The male can be induced to synthesize YPs, but the dosage of 20-OH-ecdysone is very high (non-physiological) relative to mature female titres, so it would be unwise to infer a natural role for the hormone in female YP induction.

The fat body YP gene transcripts have been shown to be no more stable than the majority of Drosophila RNAs in adult females: when new transcripts were labelled with ^{3}H-ribonucleosides and YP-transcripts were selected and quantified by hybridisation to cloned YP-genes (Bownes et al., 1984b) the YP genes were found to be actively transcribed in both fat body and ovaries, and transcription corresponded well with the translatable YP-transcripts present in the female fat body. So Gavin and Williamson's findings (1976, 1978) that the YP RNAs may be relatively stable after induction, which depended upon the use of α-amanitin (which causes extreme cellular damamge in Drosophila - Bownes et al., 1984b), seems to be mistaken, and models for the regulation of YP-gene expression must account for the genes' continuing transcription in mature adult female fat body. Note that male fat bodies only show a transient response to 20-OH-ecdysone (Bownes et al., 1983), so either translation of YP-mRNAs stops fairly quickly in males or transcription is switched off again soon after induction. The stimulating hormone is very rapidly metabolised (80% in 10 mins) to high-polarity compounds in males (and, to a lesser extent, in females too) (Bownes et al., 1984c).

How, then, does 20-OH-ecdysone stimulate transcription of the

fat-body YP-genes, and how is their expression continuously regulated in normal females ? Their expression in normal flies as one aspect of the female phenotype points to an interaction of some kind with the series of sex-determining autosomal genes intersex, doublesex, transformer and transformer-2 (Bownes and Nöthiger, 1981). Mutations at these loci alter the expression of many genes such that genotypically-XX flies (normally female) can follow a male developmental pathway to become phenotypic pseudomales or intersexuals, and conversely, XY flies (normally male) can become intersexual. Pseudomale haemolymph lacks yolk polypeptides and intersexual haemolymph carries them but at a lower concentration than wild-type females, regardless of X-chromosome complement (Bownes and Nothiger, 1981; Bownes et al., 1983b).

Injection into female flies of cycloheximide, which inhibits protein synthesis, has been found to cause a reduction in transcription of the YP-genes; and males subjected to similar injections show a reduced ability to transcribe the YP-genes in response to 20-OH-ecdysone (Bownes et al., 1984c). There seems to be no feedback mechanism whereby transcription might be reduced in accordance with the amounts of YPs circulating in the haemolymph, (Bownes et al., 1983b) and in any case such a mechanism might be expected to increase transcription in the presence of cycloheximide rather than to suppress it; so, unless cycloheximide treatment leads to a protein transcription factor becoming a limiting factor in YP-gene transcription (Bownes et al., 1984c), these observations suggest that one or more other genes must be expressed in order to maintain transcription from the

YP-genes. Might these not be the "sex genes", dsx, tra and/or ix ?

One possible explanation of the modulation of circulating YP-titre is that a sex gene (cd. dsx; see Bownes et al., 1983b) acts on the fat body during metamorphosis, resulting in a difference between adult male and female fat bodies in terms of their ecdysteroid receptors such that they then exibit a differential response to similar hormone titres. Alternatively, dsx may regulate the YP-genes independently of hormones, perhaps throughout the reproductive period; and the observed YP-induction by 20-OH-ecdysone may be no more than an artifact of non-physiological dosage (Bownes, personal communication). The possibility of there being a difference in haemolymph ecdysteroid titres between the sexes which may be involved in YP-gene expression in the fat body cannot be ruled out merely because it has not been demonstrated consistently (and cf. Fig. 7.5); but Bownes et al. (1984c) consider it unlikely now that ecdysteroids could be shown to have a simple directive role in the sex-specific control of Drosophila yolk production.

7.7 Ecdysteroids and JH: The cuticle cycle

Tenebrio molitor, a coleopteran, is well characterised with regard to the temporal relation between cuticle ultrastructure and titres of the moulting hormones (Delachambre et al., 1980). This is shown schematically at Fig. 7.4. There it is apparent that the hormone titre peaks at the initiation of secretion of a new

Figure 7.4

The Tenebrio cuticle cycle

(based on Delachambre *et al.* (1980); cf. chapter 1, Fig 1.1).

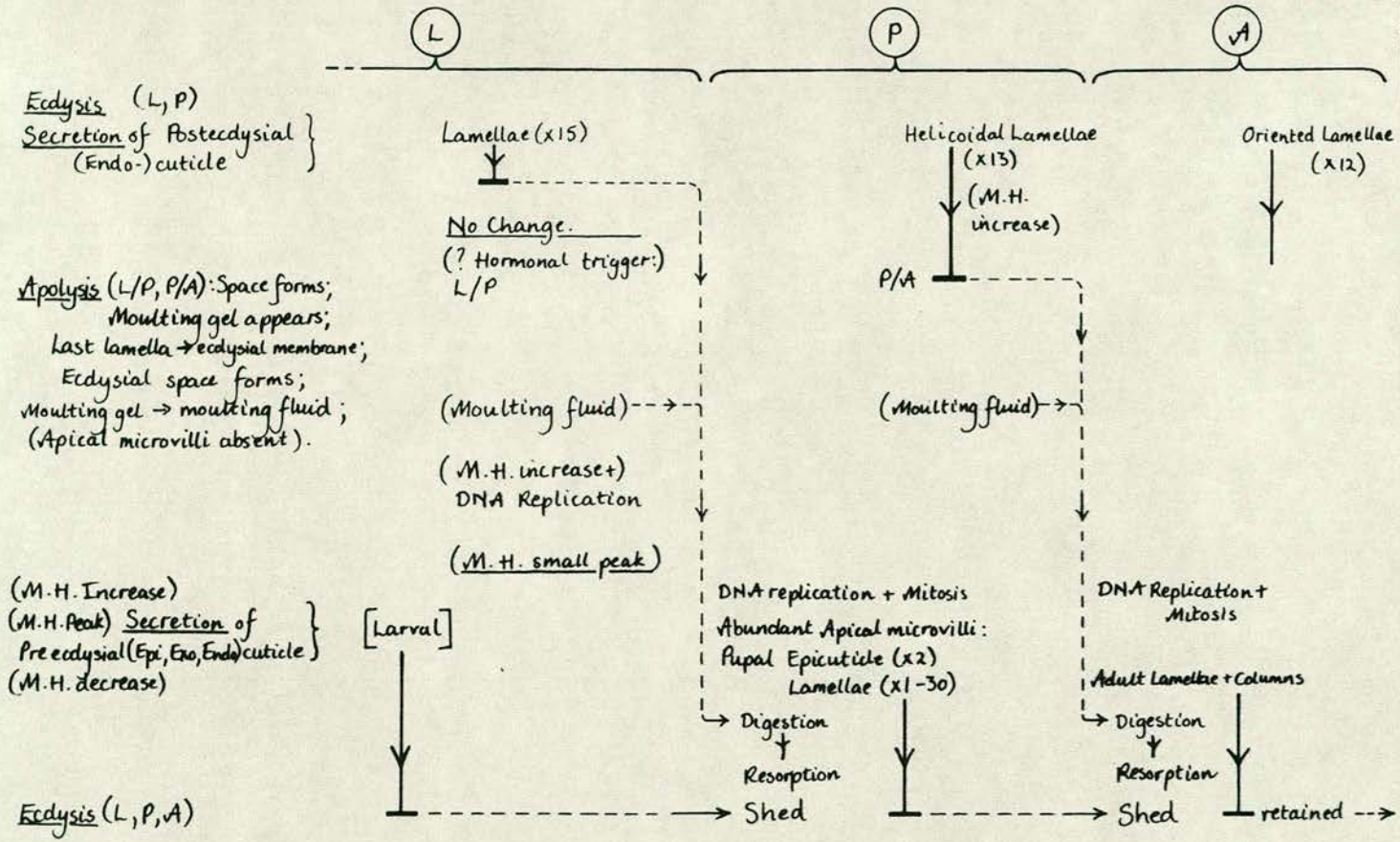
L
P
A
Ecdysis (L, P)
Secretion of Postecdysial (Endo-) cuticle
Lamellae (x15)
Helicoidal Lamellae (x13)
(M.H. increase)
Oriented Lamellae (x12)
No Change.
(? Hormonal trigger:)
L/P
P/A
Apolysis (L/P, P/A): Space forms;
Moulting gel appears;
Last lamella → ecdysial membrane;
Ecdysial space forms;
Moulting gel → moulting fluid;
(Apical microvilli absent).
(Moulting fluid)
(Moulting fluid)
(M.H. increase)
DNA Replication
(M.H. small peak)
(M.H. Increase)
(M.H. Peak) Secretion of Pre ecdysial (Epi, Exo, Endo) cuticle
(M.H. decrease)
[Larval]
DNA replication + Mitosis
Abundant Apical microvilli:
Pupal Epicuticle (x2)
Lamellae (x1-30)
DNA Replication + Mitosis
Adult Lamellae + Columns
Digestion
Resorption
Digestion
Resorption
Ecdysis (L, P, A)
Shed
Shed
retained

Fig. 7.4

cuticle rather than at apolysis, which is consistent with the secretion of pupal and adult cuticles in Drosophila if we allow either that the light-histological timings of the pre-requisite apolyses (Bodenstein, 1950) are likely to be late compared to those which might be expected from electron microscopy (see Delachambre et al. 1980) or that secretion follows soon after apolysis in Drosophila. Fristrom (1984) suggests, however, that 20-OH-ecdysone may itself cause apolysis in Drosophila.

Riddiford (1980) has described the interaction of ecdysteroids and juvenile hormone in determining which kind of cuticle is produced at metamorphosis in the lepidopteran Manduca. Each moult, larval, pupal and adult is preceded by a peak in ecdysteroid titre; and an additional peak during the last larval instar is thought to cause a change in commitment of the epidermis which next secretes not another larval cuticle but pupal cuticle. Such a peak during the third larval instar of Drosophila (LIII) has not been demonstrated (but see Fig. 1.6). Significantly, this "reprogramming" peak in Manduca occurs in the absence of JH, a situation not encountered by the epidermis before. It initiates wandering behaviour, i.e. the beginning of metamorphosis (cf. Drosophila stage L1), and 20-OH-ecdysone in the absence of JH is found to inactivate larval-specific genes irreversibly in Manduca (Riddiford 1982). Tenebrio, too, shows a "small but significant peak" in ecdysteroid titre during the last larval instar, associated with DNA replication (Fig. 7.4) which is thought perhaps to represent specific gene amplification in preparation for the secretion of a new set of (pupal) cuticle proteins (Delachambre et

al. 1980). Similarly, in Drosophila the abdominal epidermis must be reprogrammed since the abdominal histoblasts do not replace it until after the pupal cuticle has been secreted; (the thoracic pupal cuticle is the first product of the imaginal discs - see Appendix 3).

The next ecdysteroid titre peak induces "pupation" in Manduca and is accompanied by a peak in JH (Riddiford, 1980). In Tenebrio it marks the beginning of pre-ecdysial pupal cuticle secretion (cf. Fig. 7.4), and in Drosophila (stage P1) pupal cuticle is detectable shortly afterwards by E.M. (Poodry and Schneiderman, 1970). In Drosophila, as in Manduca, this is a period of detectable JH titre: chapter 6 presents evidence of the presence of JH III during the period P1-4; and Rembold and Bownes have recently repeated and extended these measurements in D. melanogaster. Their results for samples of 3g in duplicate are as follows (personal communication):-

Early LIII	0.56	pM JHIII/g fresh weight
	0.70	" "
P1-P3 (inclusive)	0.5(2)	" "
	0.3(9)	" "
P4-P8 "	0	" "
	0	" "
P9-P14 "	0.3(3)	" "
	0.43	" "

Drosophila hydei shows a similar pattern of distribution of JH over time during metamorphosis although the absolute titres are smaller cf. D. melanogaster, (Rembold and Emmerich, personal communication). In D. hydei the P(1-3) JH has been located at the end of this period (see section 6.2).

So Drosophila resembles Manduca (cf. Riddiford, 1980) in having minimal titres of both ecdysteroids and JH by stage P4i (cf. Fig. 4.12). Riddiford (1980) explains the presence of JH at the same time as ecdysteroids as being required for the prevention of precocious adult cuticle secretion by the imaginal discs/precursor cells of the eye, wing, genitalia and mouthparts in Manduca, and JH at this stage may also have a prothoracicotropic function to some extent (Riddiford, 1980), enhancing the production of ecdysone by the prothoracic glands (equivalent to ring gland cells). 20-OH-ecdysone is required at this time for the activation of most pupal-specific genes in Manduca (Riddiford, 1982).

Klose et al. (1980) reported an ecdysteroid peak at about

the time of the P4/5 transition in D. melanogaster (see Fig. 1.6; Peak 10 in Richards, 1981). This was not confirmed by the present study, nor is it exhibited by Manduca (Riddiford, 1980) or Tenebrio (Delachambre et al., 1980); and the vigorous movements of Drosophila at this time, analogous to pupal ecdysis, may be incompatible with elevated ecdysteroid activity - exogenous administration of 20-OH-ecdysone inhibits ecdysis in Tenebrio pupae (see Zdarek, 1981).

The next (stage P7) elevation in ecdysteroid titre, whose peak marks the onset of adult cuticle secretion in Tenebrio (Delachambre et al., 1980) and Drosophila (see 7.3.4 above) is accompanied in Drosophila and Manduca by basal levels of JH (see Rembold and Bownes, above; and Riddiford, 1980).

Since the onset of pupal cuticle secretion, the abdominal histoblasts have spread to form the new adult epidermis of the abdomen - this may be inhibited by JH-application at about stage P5 in Sarcophaga (Bhaskaran, 1972) - so once again ecdysteroid activity in the absence of JH may allow epidermal reprogramming to occur, but this time in the thorax, in preparation for adult cuticle secretion (Riddiford, 1980); and it has already been pointed out that the broad P7 ecdysteroid peak is represented by two peaks in Sarcophaga (Wentworth, et al., 1981; see Fig. 7.1) - perhaps there the first peak is responsible for reprogramming, the second for initiating secretion (cf. abdominal pupal cuticle, after peaks at LIII and P1 equivalent stages). Riddiford (1980) suggests that the small ecdysteroid peak observed

in Pieris after pupal ecdysis (Mauchamp et al., 1981) is responsible for reprogramming the epidermis for adult differentiation (see Fig. 7.6b). This time JH does not reappear during cuticle secretion (Drosophila stages P7-8).

The apparent P10-13 (P11) peak in ecdysteroid titre found in Drosophila has not been reported before, neither in this genus nor in Manduca or Tenebrio (cf. Riddiford, 1980; Delachambre et al., 1980). The results presented at section 6.2 suggest that an elevated JH titre is to be expected at least once during metamorphosis after stage P4 (i.e. JH titre P(1-15)> P(1-4), and the recent data of Rembold and Bownes (above) confirm the presence of JHIII during the period P(9-14); so there may well be roughly coincident peaks of ecdysteroid activity and JH at the onset of adult cuticle melanisation (P11i+) in D. melanogaster. Although this is suggestive of a role for JH in developing cuticular pigmentation, the limited comparative evidence is against such an explanation: JH is required, together with ecdysteroids, during the moult from the IVth to Vth larval instars in Manduca to prevent blackening of the next, normally unmelanised, larval cuticle (Riddiford, 1980). Alternatively, JH may enhance the production of ecdysteroids; but such a role in Drosophila at this stage (P9-14, cf. P1 above) would not be "prothoracicotropic" as such, since the cells of the ring gland with a prothoracic gland function have degenerated by this stage (Redfern, 1983).

There may be still further elevation(s) in JH titre during

metamorphosis after Drosophila stage P4 or its equivalent. In Pieris haemolymph, JH-I is reported at the end of pharate adult development when the 20-OH-ecdysone titre seems to be low (Mauchamp, et al., 1981; see Fig. 7.6b). The timing of this peak is perhaps suggestive of a reproductive target process; but it has been suggested that JH (I and) II have morphological functions during metamorphosis whereas JHIII is the gonadotropin (see El-Ibrashy, 1981). However, JHIII is the only homologue so far detected unambiguously (by GC-MF) in Drosophila (section 6.2), even in eggs, larvae and adults (Rembold and Bownes, personal communication); so it would seem that this dipteran ("advanced") insect employs the simplest JH-compound (Fig. 1.5) for all purposes in the life-cycle. Section 6.2 in conjunction with Rembold and Bownes' findings (above) gives some cause to expect more JH after stage P14 (i.e. JH titres: P(1-3)> P(9-14) but P(1-4)< P(1-15)). Fig. 7.5 shows a reworking of the data of Bordes et al. (1983) for Drosophila. There seems to be a spike in the JH-titre profile by HPLC-RIA when the ecdysteroid titre is decreasing (or, in the case of 20-OH-ecdysone in females, minimal). It is not clear how the animals were timed before eclosion in this report, nor is there mention of correction having been made for weight-loss at eclosion resulting from loss of the larval and pupal exuviae (and this would also require that subsequent weight gain be monitored during feeding); but neither of these technical problems would be expected to produce an artifactual peak in JH titre in each sex; so this may have contributed to the JH titre over P(1-15), although the effect would have been quite small. Since the spike is exhibited by both sexes it has no obvious gonadotropic role.

Figure 7.5 (a)-(s)

Determinations of ecdysteroids and JH in *Drosophila* (based on data from Bordes *et al.* (1983).

HPLC-RIA determinations of ecdysone (α), 20- OH-ecdysone (β) and juvenile hormones I (C_{18}) and III (C_{16}) in animals of approximate stages P14-A2.

a-c Female ecdysteroids (pmol per gram fresh weight)

d-f Male " " " " " "

g-l ratios for ecdysteroids:

g-h β:α

j-l Female:Male

m-p Female JHs (pmol per gram fresh weight)

q-s Male " " " " " "

m and q JHI

n and r JHIII

p and s JHs I and II.

(p) and (s) are superimposed on (c) and (f) respectively. Times on the abscissae are in hours before and after eclosion (estimated).

Fig 7.5 (a-f) : Ecdysteroids

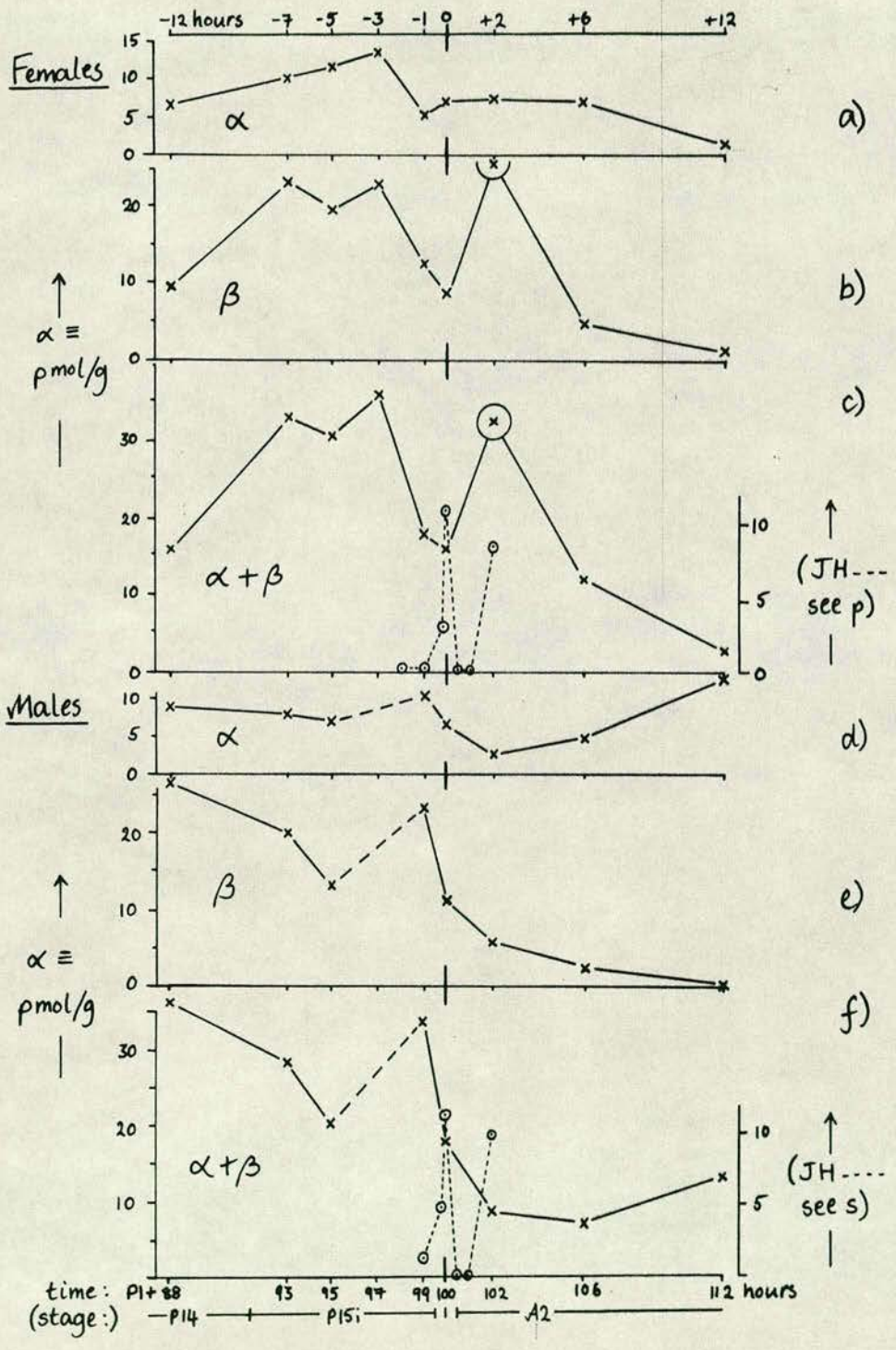

Fig. 7.5 (g-l) : Ratios

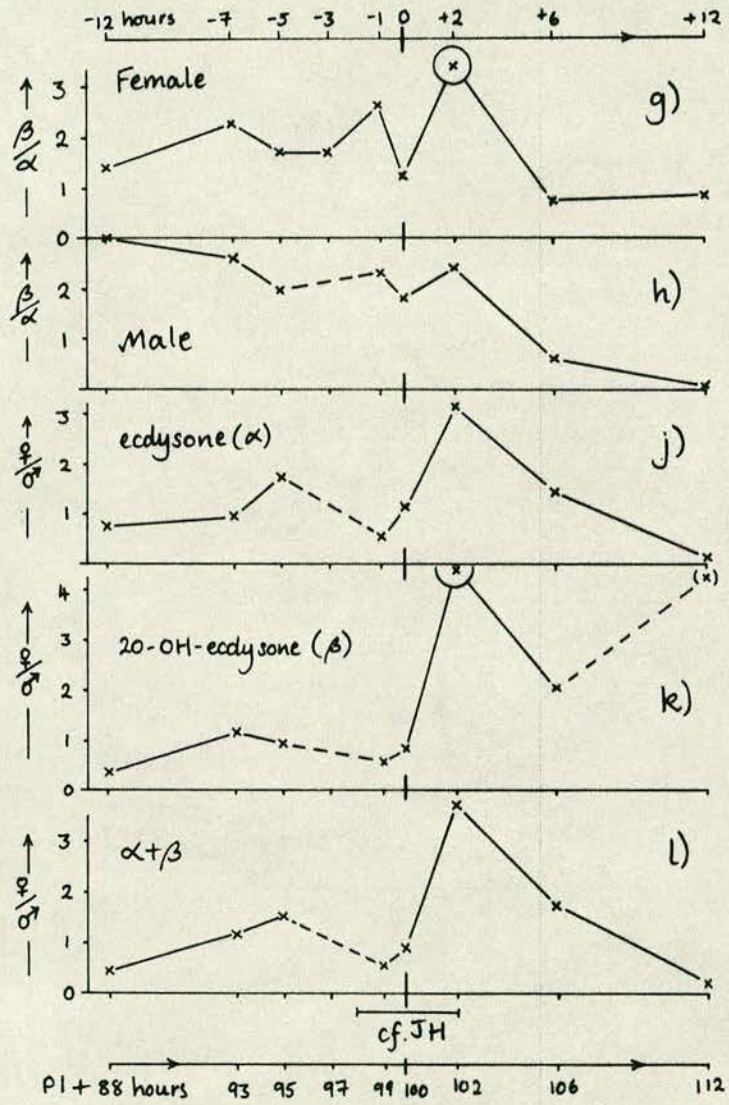

Fig. 7.5 (m-s) : JH

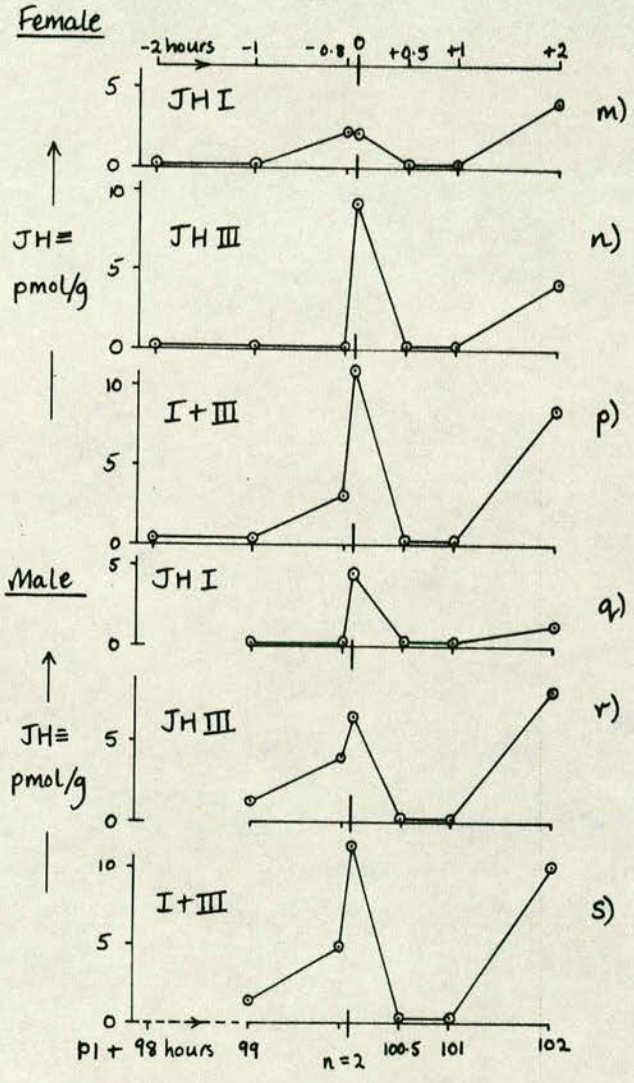
Female
-2 hours
-1
-0.8
0
+0.5
+1
+2
JH I
m)
JH III
n)
I+III
p)
JH≡ pmol/g
Male
JH I
q)
JH III
r)
I+III
s)
JH≡ pmol/g
PI + 98 hours
99
n=2
100.5
101
102

The apparent female-specific peak in 20-OH-ecdysone titre soon after eclosion has been referred to already in section 7.6.3. 20-OH-ecdysone has also been found to be the predominant ecdysteroid at eclosion itself by Handler (1982), who gives ratios of 20-OH-ecdysone:ecdysone of 13 and 9 in males and females respectively, declining to 7 and 2 respectively by the second day, but without any significant net difference between the sexes during the first day of exarate adult life or thereafter. The studies of both Handler (1982) and Bownes et. al. (1984a) would have failed to detect any female-specific ecdysteroid peak as precisely defined as that suggested by Fig. 7.5 at eclosion+2h; but note that Handler finds yolk polypeptide synthesis to begin before eclosion (see Handler, 1982; observation equivocal).

So what, then, is an appropriate model for the relations between these hormones and cuticle production during metamorphosis There are reports of systems which contradict the above Manduca pattern (Fig. 7.6), including data on Manduca itself for which insect the "reprogramming peak" model was developed by Riddiford: Fig. 7.6(a) does show the fifth instar ecdysteroid maximum held to cause a change in epidermal commitment, but the subsequent prepupal maximum (equiv.P1) is not accompanied by JH - instead this follows at pupal ecdysis (equiv.P4ii) (Sridhara, 1981; cf. Riddiford 1980 and Fig. 7.7). However, Drosophila appears to have coincident or closely associated JH and ecdysteroid maxima during stages P1-3 (see above). In Pieris, another lepidopteran, there are JH maxima before both pupal and adult ecdyses (equiv.P4 and approx.P14-15), in neither

Figure 7.6

Some reported ecdysteroid and JH titres

a) Manduca sexta: during the fifth (last) instar. W, PP and E represent the onset of the wandering stage, pharate pupal development, and ecdysis. From Sridhara, 1981 (Fig. 11).

b)Pieris brassicae: simulataneous variations of JHI and 20-OH-ecdysone during the last larval instar and the "pupal instar". From Mauchamp et al., 1981, (Figure 8).

c) Apis mellifera: Ecdysteroid concentrations in developmental stages of the queen (-) and worker (---) honey bee. L2-L5 = 2nd to 5th larval instars; LS = Spinning larva; PP = prepupa; Pw - Pvb = pupae with various eye and thorax colours; PA = pharate; A1 = 1-day-old adult.

d) A. mellifera: JH-III titres in development stages of the queen (-) and worker (---).

(c) and (d) from Rembold and Hagenguth, 1981 (Figs. 3 and 4).

Fig. 7.6

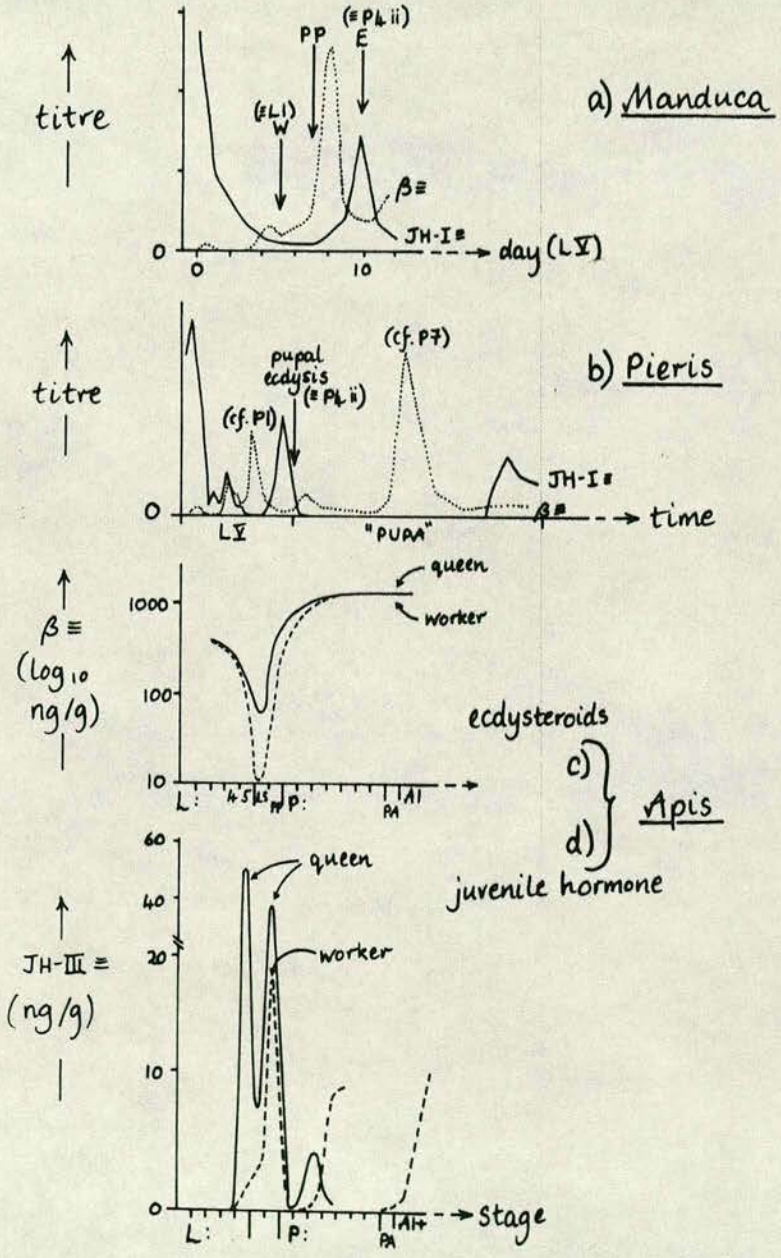
titre
(≡ Pharate ii)
PP
E
(EL1) W
β≡
JH-I≡
0
0
10
day (L V)
a) Manduca
titre
pupal ecdysis
(≡ Pharate ii)
(cf. P7)
(cf. P1)
JH-I≡
β≡
0
L V
"PUPA"
time
b) Pieris
β≡ (log10 ng/g)
1000
100
10
queen
worker
L:
4 5
P:
PA
A1
ecdysteroids
c)
d)
Apis
juvenile hormone
JH-III≡ (ng/g)
60
40
20
10
0
queen
worker
L:
P:
PA
A1+
Stage

case accompanied by ecdysteroids (Mauchamp, et al., 1981). Once again we know that Drosophila resembles Manduca in this respect at P1-3; but more significantly, Pieris appears to lack a "reprogramming peak" of ecdysteroids in the absence of JH before a moulting surge of ecdysteroids during the final larval instar. Instead the candidate peak in the ecdysteroids titre profile is coincident with a JH maximum; and the ecdysteroids-peak at pupariation, which in Manduca requires to be accompanied by JH to avoid premature adult differentiation of the newly-developing imaginal discs, is JH-free. It may be that Manduca and Galleria are atypical in having a distinct ecdysteroid peak to reprogram the larval epidermis. Riddiford (1980) credited Hodgetts et al. (1977) with finding such a peak, correlated with the onset of wandering behaviour, in Drosophila; but in fact these authors were unable to repeat the finding reported by De Reggi et al. (1975) of a small peak at about 8h before pupariation. It is possible that reprogramming is effected, in Pieris and in Drosophila, by the increasing ecdysteroid titre which leads in Drosophila to the maximum at stage P1 causally associated with disc morphogenesis and, as it begins to decline, with the subsequent onset of pupal cuticle production (Fristrom, 1984). This peak in Pieris is JH-free; (but there remains, therefore, the question of any need in this organism for inhibition of adult differentiation). The situation is reversed with respect to putative reprogramming of the epidermis for adult cuticle-production: Manduca lacks a distinct peak in ecdysteroid titre after pupal ecdysis, one which is evident in the Pieris profiles and which Riddiford (1980) suspects of performing this function, (Fig. 7.6b cf. Fig. 7.7). Finally,

Fig. 7.6 shows the hormone titre profiles of the honey bee Apis mellifera (Rembold and Hagenguth, 1981). Here the situation is complicated by the fact of caste polymorphism; but the ecdysteroid profiles at least are simple and atypical - there is no decrease in titre after the prepupal elevation (cf. P1+); and although as in Manduca (Fig. 7.7) both JH and ecdysteroid titres are maximal or increasing during the prepupal period, in Apis there is a return of JH before the pharate adult period, (cf. Manduca and Drosophila; Fig. 7.7). These data are very difficult to interpret on any modified "classical scheme" of endocrine control of metamorphosis (Rembold and Hagenguth, 1981) and they will not be referred to again, but they do serve here to suggest that the obvious advantages of a comparative approach to endocrinology may be accompanied by some risks.

7.8 The modified "classical" scheme

Figure 7.7 presents the hormone profiles of Manduca together with new information on Drosophila where the patterns appear to differ significantly. Riddiford's understanding (1980) of the interaction of ecdysteroids and JH in controlling the cuticle cycle is as follows:-

In Manduca high JH titres maintain the larvally-committed state of the epidermis and other tissues. They also maintain feeding behaviour and suppress the growth of the imaginal rudiments (discs and histoblasts); see Figure 7.7 (A). On reaching a criticial size ecdysteroids are released, leading to a larval/larval

Figure 7.7

Ecdysteroid and JH titres in Manduca

Titre-profiles for penultimate (IVth) larval instar to eclosion taken from reviews by Riddiford (1980, 1982) and Truman et al. (1984). Ecdysteroid titres refer to the haemolymph for the Vth instar larva, and whole-body extracts for other periods.

Truman et al. (1983) explain the declines in ecdysteroid titre after deposition of pupal and adult cuticle begins as facilitating both the completion of pupal and adult development respectively and also the release of Eclosion Hormone (a peptide) responsible respectively for pupal ecdysis behaviour (analogous to the events of stage P4(ii) in Drosophila) and adult ecdysis behaviour (=eclosion).

See text for consideration of (A) - (L)

The dotted lines (....) indicate findings unique to this report (ecdysteroids) and Rembold and Bownes (personal communication) (JH) at the time of adult cuticle melanisation in Drosophila.

Fig. 7.7

Manduca: Ecdysteroids

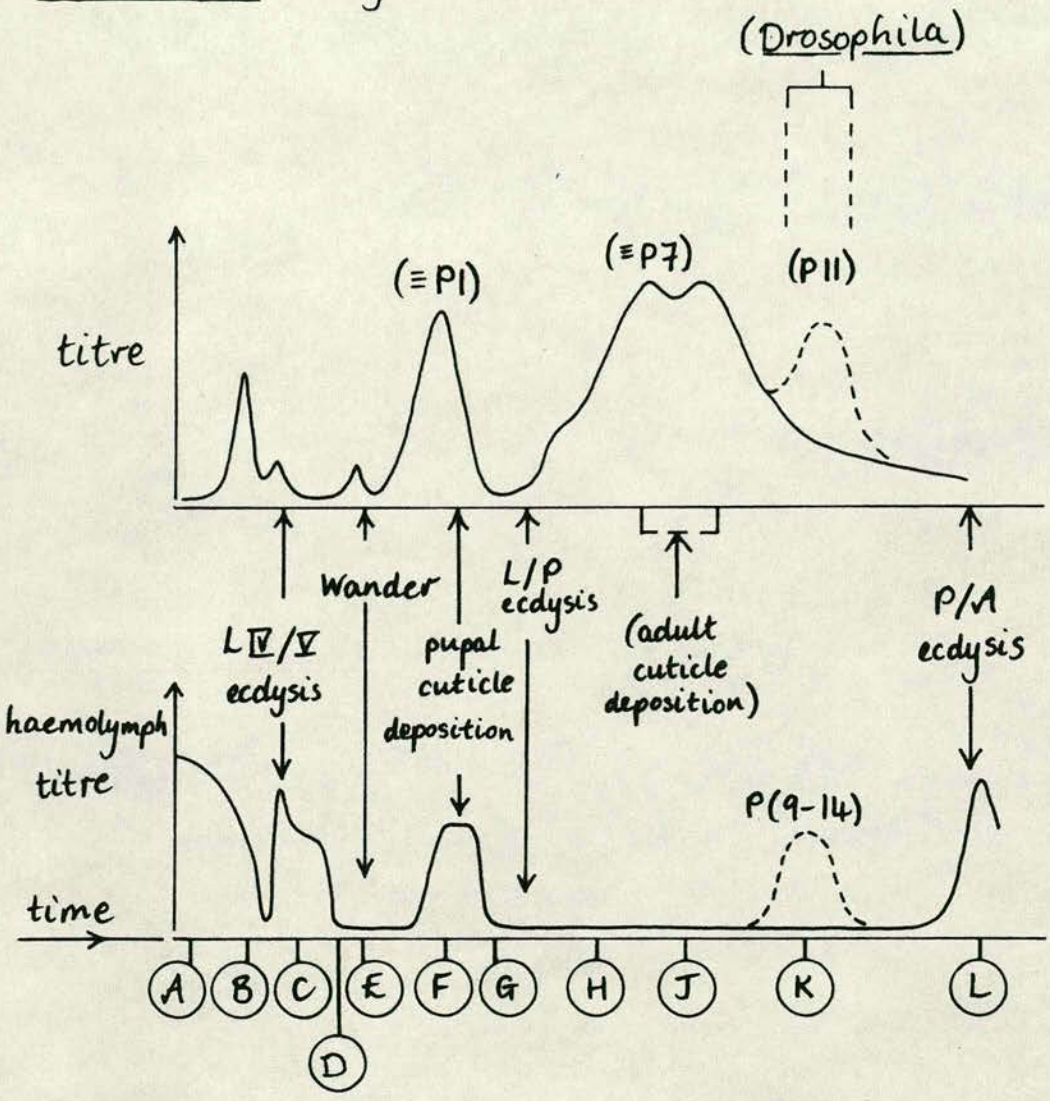

Manduca: JH

moult (B). The cells are recommitted to the production of larval cuticle so the JH titre can fall. It reappears to prevent melanisation of the new larval cuticle (C). The fall in JH titre during the final larval instar (D) allows the imaginal discs to undergo multiple mitoses and to become competent to metamorphose when next exposed to a moult-inducing (high) titre of ecdysteroids. This decline in JH titre (D) also triggers programmed cell death in specifically larval (e.g. "crochet") epidermis. A small rise in ecdysteroid titre (transient in Manduca) in the absence of JH (E) causes pupal reprogramming of the abdominal epidermis such that larval cuticle may no longer be secreted at the next ecdysteroids peak, even in the presence of JH, although larval cuticle continues to be deposited meanwhile. This reprogramming requires the synthesis of RNA and protein (Riddiford, 1981) and involves the irreversible termination of transcription of many larval-specific genes and the initiation by 20-OH-ecdysone of a cascade of synthesis of new non-cuticular proteins (Riddiford, 1982). The change in epidermal commitment, although accompanied by DNA replication, does not seem to require it: reprogramming occurs even in cells exposed to cystosine arabinoside which inhibits DNA synthesis (Riddiford, 1981). (This observation runs counter to the "quantal mitosis" model of cytodifferentiation whereby differentiation occurs first covertly at the stage of DNA synthesis and is expressed overtly in the daughter cells resulting from mitosis; (see Sridhara, 1981).)

After this unusual period with respect to relative titres of the two hormones the epidermis becomes aloof to JH, and at the next ecdysteroid peak (F) it is unaffected (non-juvenilised) by the

reappearance of JH. Now the imaginal discs undergo morphogenesis and then begin pupal cuticle secretion. (In Drosophila, disc evagination is elicited by peak ecdysteroid titre, and a declining titre allows first epicuticle, then procuticle to be secreted: Fristrom, 1984). JH at this time (F) seems to inhibit premature adult differentiation of Manduca discs (Riddiford 1980), although its presence is not required by Drosophila discs (late LIII) cultured in vitro - 20-OH-ecdysone is sufficient to stimulate pupal differentiation (Milner 1977). JH may also stimulate Manduca prothoracic glands to produce ecdysone; and the ecdysteroids peak acts on the reprogrammed abdominal epidermis to elicit pupal-specific gene expression (Riddiford 1981). Transcription of most pupal cuticle mRNAs begins at this time (Riddiford 1982). Once the epicuticle has been deposited pupal cuticle secretion continues as both titres fall (G). The withdrawal of JH allows the abdominal histoblasts to respond to an increasing ecdysteroid titre at (H) by spreading to replace the larval abdominal epidermis - this response is prevented in Sarcophaga by administration of JH at (G), although it does not affect mitosis in the histoblasts (Bhaskaran, 1972). Riddiford (1980) supposes the imaginal discs to be reprogrammed for subsequent adult cuticle production by this early rise in ecdysteroid titre (again in the absence of JH); but, although an increasing ecdysteroid titre could be involved in adult differentiation at this stage in Drosophila abdomens, it is not essential to thoracic disc differentiation in vitro (Milner, 1977). At the onset of adult cuticle secretion (J), (Drosophila P7/8 + 1 hour; Bodenstein, 1950) JH might be expected, by analogy with (F), (Riddiford 1980), to

stimulate ecdysone production; but no JH is found in Drosophila until adult cuticle melanisation begins (K) when ecdysone-production also seems to occur. JH reappears in Manduca at about the time of eclosion (L) (cf. Fig. 7.5; Drosophila).

Overall, the Manduca reprogramming model corresponds well with the information available concerning Drosophila if we allow that imaginal rudiments of the higher Diptera achieve a relatively highly determinate state in the embryo or young larva. Thus the imaginal discs are largely unaffected by JH once they begin to metamorphose - they do not produce adult cuticle prematurely without it - and cuticle-secreting cells proceed through a predetermined sequence of cuticles. In Tenebrio, by contrast, Roberts and Willis (1981) report the capacity to move from larval to adult cuticle-secretion directly, given the appropriate hormonal stimuli, and also to secrete a true second pupal cuticle (not merely an untanned adult cuticle). This may be true in Drosophila in response to JH but it probably derives from the larval abdominal epidermis, not from the imaginal histoblasts (Madhavan, 1973; Bhaskaran, 1972).

Figure 7.8 shows that no cells in Drosophila secrete more than two cuticle-types, larval and pupal or pupal and adult; and of the two cell lines which produce pupal cuticle, namely larval abdominal epidermis and imaginal discs, the disc-derived epidermis becomes aloof to the reappearance of JH once its absence has stimulated their development. The putative association of adult cuticle melanisation with a coincident rise in titres of JH and

Figure 7.8

JH and Drosophila cell lines secreting cuticle

Schematic theoretical representation of the cell lines in Drosophila which secrete one or more cuticles in response to 20-OH-ecdysone and the presence or absence beforehand of JH (cf. Fig. 7.7). Forks in the courses of development represent changes in commitment of the cells (i.e. reprogramming). L = larval cuticles; P = pupal cuticle; A - adult cuticle.

1. Cells secreting exclusively larval structures (e.g. mouth hooks) maintained in activity by JH and programmed to die after the JH titre declines in the last larval instar (LIII).

2. Abdominal epidermis secretes larval cuticle repeatedly until its commitment is changed by an ecdysteroid titre elevation in the absence of JH before stage L1. Subsequent exposure to JH during P(1-3) does not prevent secretion of the pupal cuticle. Programmed cell death or destructive displacement then follows as the imaginal histoblast cells spread over the pupal abdomen. The original larval epidermis may continue to secrete pupal cuticle unless the histoblast nests take over by spreading. This would be consistent with the observation of "second pupal' or "undifferentiated adult" cuticle on the abdomen after treatment of the pupa with JH (Bhaskaran 1972; Postlethwait 1974).

3. Thoracic imaginal disc cells become competent to react to ecdysteroids by differentiating when JH is withdrawn during LIII. They are unable to secrete adult cuticle before pupal cuticle and are unable to secrete a larval-type cuticle, so they are unaffected by the reappearance of JH during P(1-3). In response to 20-OH-ecdysone at pupariation they evaginate (morphogenesis) and, as the titre declines, they secrete pupal epicuticle followed by procuticle

(Fristrom, 1984). During a period of undectable JH-titre (P4-8) and increasing ecdysteroid titre (not essential *in vitro*; Milner 1977) they switch to the adult program of gene expression, developing the sculpted adult surface and secreting adult cuticle (P8). This is melanised during a period of elevated JH titre (P9-14) (not essential *in vitro*; Milner 1977). Imaginal disc derivatives secrete normal adult cuticle even when exposed to JH in the pupal period (Postlethwait 1974) i.e. they become aloof to JH after the onset of differentiation in the larva.

4. Adult abdominal histoblasts undergo mitosis in the prepupa/pupa and begin to replace the larval epidermis by spreading after the withdrawal of JH before P4; (Spreading is inhibited by JH at about stage P5 in *Sarcophaga*; Bhaskaran, 1972). They secrete only adult cuticle. Perhaps these cells require JH for melanisation of the adult cuticle during P9-14; but the establishment of the cuticle *pattern* can be disrupted by the application of JH before stage P5 (0-12h; Postlethwait 1974). JH is present in *Drosophila* in P(1-3). Postlethwait (1974) found that inhibition of abdominal adult cuticle differentiation was possible by topical JH treatment, or by implantation of active corpus allatum cells (LI ring glands), at stage P1; but the critical period for JH-inhibition of histoblast cell spreading could well be after P3 since the duration of the JH pulse was uncontrolled in these experiments: this tends to suggest stage P4 as the critical period, (i.e. rather than P(1-4) cf. Postlethwait 1974).

Fig. 7.8

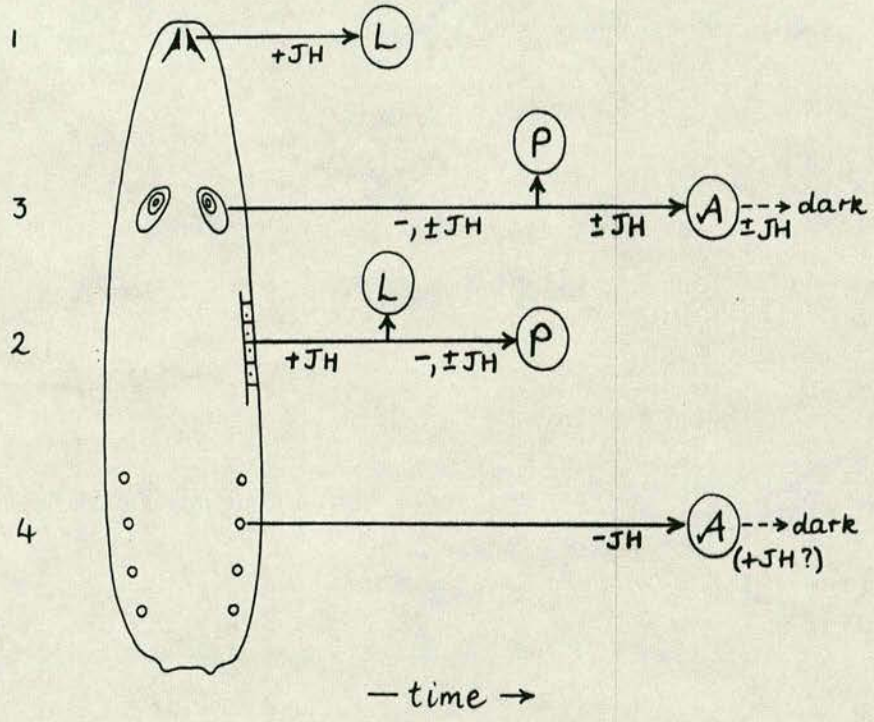

ecdysone suggested by this report is merely circumstantial, and the disc derivatives at least are independent of JH stimulation when differentiating fully *in vitro*. Perhaps the function of any JH present at this time must be sought elsewhere amongst the tissues of the pharate adult.

Appendix One

Glossary

Acrididae (f.)

Short-horned grasshoppers including locusts.

Adult:

Reproductive, typically winged stadium of insect life-cycle. After secretion of the adult cuticle in Drosophila stages P7+, the animal remains pharate until A1 and is immature (i.e. sub-imaginal) until A3. But the adult form is achieved by the morphogenetic events involving disc fusion and evagination before stage P5 in the pupa.

Apis mellifera:

Honey or hive-bee (o. Hymenoptera)

Apolysis:

Separation of epidermis from the most recently secreted cuticle.

Beer's-Lambert's Law:

The optical density of a solution depends only upon the number of absorbing molecules through which the light passes, i.e.

$$A = \log_{10} I_o/I = e.c.l$$

where A = absorbance

I_o = intensity of incident light

I = intensity of transmitted light

c = concentration

l = path length (1cm)

e = absorptivity, a measure of the likelihood that a given photon will be absorbed by a given type of molecule at λ_{max}.

$c = (A/e_m) \times l$

where e_m = molar extinction coefficient

= absorptivity of 1 molar solution of a particular solute.

In practice $c = (OD/e_m) \times 1$

i.e. $c \propto OD$.

Substances which obey Beer's-Lambert's Law show e_m independent of concentration; (solvent specified - λmax and e_m vary with solvent).

Blattaria (s.o.):

Cockroaches (o. Dictyoptera).

Blattella spp. :

Genus of cockroaches (o. Dictyoptera; s.o. Blattaria)

Bombyx mori:

Common or mulberry Silkworm moth (o. Lepidoptera).

Bombus terrestris:

Bumble bee (o. Hymenoptera).

Calliphora erythrocephala (= vicina):

The blow-fly (o. diptera; s.o. cyclorrhapha)

Carbon dioxide (solid):

Temperature = -80°C.

Coleoptera (o.):

Beetles. Metamorphosis is complete.

Correlation coefficient:

$$r = \frac{\Sigma x y - n \bar{x} \bar{y}}{n S_x^{n-1} S_y^{n-1}}$$

to selected level of confidence, where

x and y = variables

n = sample number (<30)

s = sample standard deviation.

Cryptocephalic:

Condition of the dipteran pupa before eversion of the head sac formed from fused imaginal discs. (cf. phamerocephalic). In Drosophila, until stage P4 (ii).

Cyclorrhapha (s.o.):

Sub-order of dipteran insects having a puparium within which complete metamorphosis takes place.

Diptera (o.):

Order of insects having two wings and mouthparts modified for sucking. Metamorphosis is complete.

Disintegration (d):

Radioactive decay. 1 d. per second = 1 Bq (Beqerel); 37 kBq = 1μ Ci (microCurie).

Liquid scintillation counting efficiency = c m^{-1}/d m^{-1}.

To calculate d m^{-1}: ln final dm^{-1} =

ln original dm^{-1} - (ln2 x No. elapsed half-lives).

Drosophila melanogaster:

Fruit fly (o. Diptera; s.o. Cyclorrhapha); literally "dew-lover, black stomach".

Ecdysis:

Shedding of unresorbed cuticle, i.e. moulting (cf. apolysis); precedes deposition of new cuticle.

Ecdysteroid:

Ecdysone or related compound, usually a C_{27} (e.g. 20-OH-ecdysone) or C_{28} (Makisterone A) compound.

Eclosion:

Adult ecdysis, i.e. transition from pharate to exarate condition of imago. In Drosophila the operculum of the puparium is opened by expansion of the ptilinum using haemolymph hydrostatic pressure and the imago emerges through an antero-dorsal split in the pupal cuticle. The meconium may be expelled inside the puparium.

Exarate:

Condition of a stadium after ecdysis, e.g. the adult is exarate after ecdysis (cf. pharate).

Exuvial:

Phase(s) in development of some insects after an apolysis when the epidermis remains naked i.e. before the onset of secretion of pre-ecdysial cuticle. (lit. divested of covering).

Galleria mellonella:

Greater wax moth (o. Lepidoptera).

Gametogenesis:

Process of differentiation of germ cells in the gonad. In Drosophila oogenesis begins during metamorphosis but uptake of yolk proteins from the haemolymph commences at eclosion, while spermatogenesis is advanced by the time of eclosion - males are fertile early in stage A3.

G.C.:

Gas Chromatography.

G.L.C.:

Gas-Liquid Chromatography.

Glossina morsitans:

Tsetse fly (o. Diptera); a bloodsucking genus which is the vector for trypanosomiasis (sleeping sickness).

Hemimetabola/Heterometabola/Exopterygota (sub-class):

Insects showing incomplete metamorphosis by way of nymphal instars to achieve adult status (e.g. cockroaches).

Hemiptera (= Rhychota) (o.):

Bugs; parasitic, exopterygote insects (i.e. incomplete metamorphosis through nymphal stadia rather than a pupa).

Holometabola/Endopterygota (sub-class):

Insects showing complete metamorphosis from larva to adult by way of a pupal stadium (e.g. Drosophila).

HPLC: High performance (high pressure) Liquid chromatography

Hyalophora cecropia:

Silkmoth (o. Lepidoptera).

Hymenoptera (o.):

Bees, wasps and ants. Metamorphosis is complete.

Imago:

Final, perfect state of an insect after completion of all metamorphosis. In Drosophila, sexually mature stage A3: strictly the pharate adult (q.v.) is sub-imaginal. (Latin = image, idea).

Instar:

Stage in insect larval development between two moults. (More

loosely = stadium).

Larva:

Pre-adult form which emerges from the egg; a structurally embryonic feeding stadium which in insects achieve full growth by a series of moults and adult status by metamorphosis (q.v.). A feeding embryo, it is not sexually mature; (Latin = ghost/mask).

Lepidoptera (o.):

Moths and butterflies. Metamorphosis is complete.

Locusta migratoria:

Migratory locust (o. Orthoptera; f. Acrididae).

L.S.C.:

Liquid Scintillation Counting.

Mamestra brassicae:

Cabbage army worm.

Manduca sexta:

Tobacco hornworm moth (o. Lepidoptera).

Mass Action, Law of:

The velocity of a chemical change is proportional to the molecular concentrations of the reacting substances.

Mass Fragmentography (MF):

Mass spectrometry - selected/multiple ion monitoring (MS-SIM/MS-

MIM).

Metamorphosis:

Transformation; change from larval to adult (imaginal) form. Insects show either incomplete m. (gradual through nymphal stages; the Hemimetabola, e.g. locusts) or complete m. (radical, through a pupal stadium; the Holometabola, e.g. Drosophila).

Molar Extinction coefficients, e_m:

Ratio optical density:concentration, when light path = 1cm. (See Beer's-Lambert's Law)

e.g. at λ_{max} = 243nm

$e_{ecdysone}$ = 11,600 and

$e_{20\text{-}OH\text{-}ecdysone}$ = 10,300

~~Musca domestica~~:

House fly (o. Diptera; s.o. Cyclorrhapha)

Nauphoeta spp. :

Genus of cockroaches.

Nitrogen (liquid):

Temperature = -195.8°C

Temperature of vapour above liquid = -140°C.

Nymph:

Larval stadium which bears a strong resemblance to the imago and undergoes incomplete metamorphosis through several instars to

achieve adult status, e.g. locusts, cockroaches. (Young form; from Greek = bride).

ODS:

Octadecylsilane (C_{18}) chains linked to silica by siloxane bonds.

Oncopeltus fasciatus:

Greater milkweed bug (o. Hemiptera).

Periplaneta americana:

"American" cockroach (o. Dictyoptera; s.o. Blattaria).

Phanerocephalic:

Condition of the dipteran pupa after eversion of the head sac (cf. cryptocephalic); in Drosophila, achieved at stage P4 (ii).

Pharate:

Condition of a stadium before ecdysis e.g. the adult is pharate until eclosion (cf. exarate). In the Cyclorrhapha the pupa is always pharate (i.e. still within the larval-cuticular puparium) whereas the Lepidoptera, for instance, shed the larval cuticle at "pupation" to become exarate pupae.

Polar:

The property of having electrically positive and negative centres in a molecule; including, for the purposes of liquid chromatography, hydrogen-bonding.

POPOP:

1,4-bis-2-(5-phenyloxazolyl) benzene.

Population mean, limits of:

$\mu = \bar{x} \pm (t_{0.95} \cdot s_{n-1})$ to 95% level of confidence;

where $\bar{x}$ = sample mean

t is at p = 0.05

s = sample standard deviation

(n = sample number (<30)).

Postfeeding/Wandering larva:

In the higher Diptera, a last-instar larva which has: irreversibly stopped feeding; emptied its crop; and (often) commenced wandering behaviour.

(Formerly, sometimes called "prepupa" (not = prepupa, q.v.).

PPO:

2,5-diphenyloxazole.

Prepupa:

Distinctive phase at the end of the last larval instar in cyclorrhaphous flies during which tanning of the puparium and larval-pupal apolysis occur. (The pupa then secretes the pupal cuticle). There is no discrete prepupal cuticle. Histolysis of many larval tissues occurs and, in Drosophila, disaggregation of the fat body, change in the pattern of polytene chromosome puffs, and evagination of the imaginal discs, etc.

Prepupation/pupariation:

Becoming a prepupa (q.v.); prepupation by analogy with pupation (q.v.); pupariation literally synonymous with puparium formation (q.v.), a process, but used with the sense of transition to prepupal status. Marked by establishment of the shape (but not the colour) of the puparium.

Pupa:

Stadium in complete insect metamorphosis which intervenes between the larval and imaginal stadia. There is no feeding and little or no movement. Extensive reorganisation occurs to assemble the pharate adult insect and suppress larval structures. There is a discrete pupal cuticle. (Latin = girl/doll).

P. refers very loosely to any stage enclosed within a puparium, cocoon or pupal cuticle. (i.e. chrysalis = lepidopteran "pupa").

Pupariation/prepupation:

(See prepupation).

Puparium:

(By analogy with aquarium etc.; case housing the pupa). Modified last larval cuticle inside which Cyclorrhaphous metamorphosis occurs; functionally analogous (anchorage, etc.) to the cocoon of the Lepidopteran pupa (chrysalis). In Drosophila the anterior spiracles are extended, the cuticle becomes bullet-shaped, an opercular ridge develops, and larval-pupal apolysis and hardening/darkening of the exuvium (undigested exocuticle) occurs.

This exuvium (cf. LI, LII) is not shed until eclosion (P15 ii), i.e. during the next-but-one stadium (adult). The so-called "white puparium" is really translucent, the larval tissues being white and seen as such until the puparium darkens at stage P2.

Puparium formation:

Often used synonymously with pupariation/prepupation, but better restricted to describing the transformation of the larval cuticle to form the puparium (q.v.). This occurs gradually, over stages L2-P2 in Drosophila; but formation of the "white puparium" is a shape-change visible to the naked eye at L2/P1.

Pupation:

Becoming a pupa. In insects which shed the larval cuticle earlier than the pupal, e.g. Lepidopterans (cf. the Cyclorrhapha) "pupation" usually refers to the pupal ecdysis. In Drosophila this is marked by the muscular contractions of stage P4 (ii) culminating in head evagination (P4/5) inside the puparium - there is no ecdysis. However, the pupal cuticle is complete before this stage and the term is perhaps best avoided.

P. also refers very loosely to metamorphosis involving a pupal stadium.

"Repelcote":

2% dimethyldichlorosilane in 1,1,1-trichloroethane (Hopkin and Williams, BDH) - gives a silicone surface on glass/ceramic.

Rhodnius sp.

A blood-sucking bug (o. Hemiptera).

RRT (Rt_R); RR_F:

Retention time, RT or R_F respectively relative to a given value of same.

Sarcophaga bullata:

Flesh fly (o. Diptera; s.o. Cyclorrhapha).

Schistocerca gregaria:

Desert locust (o. Orthoptera; f. Acridiidae)

Sem:

Standard error (deviation) of the mean

$$Sem = s / \sqrt{n}$$

where s = sample standard deviation

n = sample number ($n > 30$)

Population mean,

$\mu = (\bar{x} \pm 2\ sem)$ to 95% level of confidence

where $\bar{x}$ = sample mean ($n \geqslant 30$)

Spodoptera littoralis:

Cotton leafworm

Stadium/Stadia:

Distinct phase(s) of the insect life cycle, often differing ecologically; e.g. egg/embryonic, larval or nymphal, pupal, adult ss. (From medicine = stage, period of disease).

Standard deviation of sample:

$$S = \sqrt{\frac{\Sigma (x - \bar{x})^2}{n-1}}$$

where x = value of variable

$\bar{x}$ = sample mean

n = sample number (<30)

Tenebrio molitor:

Mealworm (o. Coleoptera).

TLC:

Thin-Layer Chromatography.

Tritium, T:

Radionuclide, isotope of hydrogen, ^{3}H; half-life 12.35 yrs.

Wandering larva:

(See postfeeding larva).

Appendix Two

Timecourse of metamorphosis: Sequence of changes (observed, and reported in the literature) in Drosophila melanogaster at 25°C correlated with the staging system (Chapter 3)

Selected sources: 1) Author's Observations:-

*direct timing (extremes);

X stage transition-times estimated by frequency (Section 3.3.1);

2) Bodenstein, 1950;

3) Bownes, M. (personal communication)

4) Fraenkel and Bhaskaran, 1973;

5) King, 1970;

6) Lindsley and Lifschytz, 1972;

7) Postlethwaite and Schneiderman, 1973;

8) Robertson, 1936;

9) Schubiger, G. (personal communication).

Sex(s) M = male F = female	Stage (estimated) (diagnostic change)	Time after L2/P1(h) (*,X See (1) above)	Observation Changes visible with dissecting microscope are numbered 1-51 (cf. Figs. 3.1-3.6)	Reference Sources(s) 1-9 above
F/M	LIII		Testes larger than ovaries	1,2
F	(LIII-P7)		Ovary growth	2
FM	.LIII		1) Stops feeding	

			(empties crop,	
			wanders)	1,4
FM	L111/L1	-4.3^{X}	Climbs bottle wall	1
F	(L1)	-2	Ovarioles differentiating.	
			Terminal filament cells	
			present.	3
FM	.L1		2)Stops crawling	
			reversible until body	
			shortens).	1
FM	L1/L2	-0.5^{X}	3)Everts anterior	
			spiracles	1
FM	L2		4)Withdraws 3 apparent	
			anterior segments	1
FM	L2		5) Body shortens	1
			Cuticle becomes smooth.	1
FM	L2/P1		(Glue expelled from salivary	
			glands)	
			6)Sticks to glass	1
FM	P1	0	Fails to crawl when wetted	1
F	P1	0	Some ovarioles present	2
M	P1	0+	Meiotic divisions I and II	6
FM	P1	+0.1-	7)Posterior spiracular	
		0.2*	papillae and anterior	
			margin of puparium tan	
			(orange)	1
FM	P1	0-1.0*	8)wriggling movements stop	1
FM	P1/2	0.3-1.0*	9)Puparium becomes brown to	
		(1.7^{X})	unaided eye	1

M	P2	(0)-3*	10) Testes became less distinct (still faintly distinguishable in P5)	1
FM	P2	1-5*	11) Oval armature movements stop permanently	1
FM	P2	1-6.5*	12) Median dorsal (heart) contractions stop	1
F	(P2-3)	2	Ovary is an eclipsoid, polarised cell mass with a membrane	5
FM	P2/P3	0.3-3* (4.8^{X})	13) Gas bubble becomes visible within abdomen (it has tracheal associations when dissected out, and it fails to develop in submerged prepupae).	1
FM	(P3)	4	Anterior muscle histolysis begins;	2
			Malpighian tubules and mid-intestine isolated	2
FM	P3	3-6*	14) Opercular ridge becomes distinct	1
FM	(P3)	4-6	Larval-pupal apolysis begins anteriorly	4
FM	(P3)	3	Pupal cuticle cuticulin distinguishable by E.M.	7
FM	(P3)	6	"Yellow body" forms (larval gut)	2
FM	(P3)	6+	Thoracic imaginal discs evaginated but not yet extended	2

FM	P3/4i	6.5-7*	15)Becomes positively buoyant	
		(5.8^{X})		1
FM	P4i	6.5-8*	16)Lateral trunk tracheae	
			become obscured	1
FM	(P4i)	7	Imaginal hypoderm of thorax	2
			complete	
FM	(P4i)		Larval ring gland begins to move	
			posteriorly	2
FM	P4i	9-5-13.5*	17)Median abdominal contractions	
			seen (mid-intestinal peristalsis)	1,8
FM	(P4i)	10	Larval salivary glands	
			histolysis advanced	2
FM	P4i		18)Everted leg and wing discs	
			become distinguishable	1
M	(P4i)	11	Testis elongation begins	2
FM	P4i/ii	12-13.5*	19)Bubble appears at posterior tip	
		(8.0^{X})	of puparium, displacing pupa	
			anteriorly; and bubble within	
			abdomen disappears	1
FM	P4ii	12-13.5*	20)Bubble displaced to anterior	
			of puparium and pupa displaced	
			posteriorly	1
FM	P4ii/5i	12-13.5*	21)Head eversion and expulsion of	
		(8.2^{X})	oral armature	1
M	P5	(12.2+)	Testes no longer visible	1
FM	P5i	12.5-13.6*	22)Legs and wings achieve full	
			extension along abdomen	1
FM	P5i		23)Enlarged initial segments of	

			anterior pair of Malphigian tubules (Mt) move from thorax into abdomen	1
FM	P5i		24) Transluscent patch lacking adhering fat body cells becomes apparent in eye	1
FM	P5i/ii	13-48* (9.3^{X})	25) Two white Mts become visible dorsally in abdomen (viewed in shadow)	1
FM	(P5ii)	14	Crop begins to form.	2
			Most abdominal muscles destroyed	2
FM	(P5ii)	16	Bristle-forming cells appear	2
FM	P5ii/P6	13-48*, (18.7^{X})	26) Mts become prominent and green	1
FM	P5/6	19+	Pigmentation of Malphigian tubules	2
FM	(P6)	20	Wing vein development begins	2
FM	(P6)	20	Wing muscle differentation	2
F	(P6)	20	Ovarioles recognisable in whole ovaries	2
F	(P6)	22	Outgrowth (oviduct) from genital disc begins	2
M	(P6)	24	Nearly-mature spermatozon present + all earlier stages	2
M	(P6)	30	Testes-vasa efferentia attachments form	2
FM	(P6)	30	Bristle formation begins	2
FM	(P6/7)	c.32	Yellow body appears and darkens	2

FM	P6/7	25-46* 32.4^{x})	27)"Yellow body" appears (dark-green) between anterior ends of the two anterior Mts, mid-dorsally at anterior of abdomen.	1
F	(P7)	34-36	Ovaries-oviducts attachments form.	2
			Oogonia only present.	2
FM	(P7)	34	Abdominal imaginal hypoderm complete.	2
FM	P7		28)Yellow body moves back between anterior Mts	1
FM	(P7-8)	34-50	Pupal/adult apolysis begins posteriorly	4
F	(P7-14)	34-84	Genital disc derivatives and ovaries completed	2
M	(P7)	34	Coiling of testes begins (promoted by vasa efferentia)	2
FM	P7	(42)	Tarsal claw morphogenesis	1
FM	"mid-pupal"		Tarsal claw morphogenesis	9
FM	P7/8	43-47* (44.3^{x})	29)Eye pigmentation begins-eye cup becomes yellow at perimeter	1
FM	e.P8		30)Eye becomes pale yellow	1
FM	e.P8	(44.3^{x})	Leg bristle morphogenesis and differentiatioin spreads proximally	1
FM	P8	c. 45-50	Adult cuticle secretion on thoracic appendages begins	

			(...Femur and tibia first; bristle morphology completed in P8)	1
FM	P8		31)Eye becomes bright yellow	1
FM	(P8)	48	Bristle and socket formation complete	2
FM	(P8)	48	Abdominal muscles have been destroyed	2
FM	(P8)	50	Wing muscles striated	2
FM	(P8)	50	Large polytene cells of larval wing gland degenerate (after pupal/adult "moult"). Primordia of Corpus allatum and Corpus cardiacum continue to prothoracic gland	2
FM	P8/9	49-57* (56.6^{X})	32)Eye colour changes to amber	1
FM	(P9)	60	Abdominal imaginal muscles present	2
FM	(P9)	60	Crop folded	2
M	(P9)	64	Testis pigmentation begins	2
FM	m.P9		33)Eye colur darkens to deeper amber	1
FM	(P9)	66	Abdominal imaginal muscles are striated	2
FM	P9/10	71-78* (74.5^{X})	34)Eyes become very pale pink	1
FM	P10		35)Eyes become bright red	1

FM	P10/11i	(74.6^{X})	36) Orbital and ocellar bristles and vibrissae darken	1
FM	P11i/ii	72.5-77* (75.9^{X})	37) Dorsal thoracic micro- and macrochaetes become visible	1
FM	P11ii/12i	(76.6^{X})	38) "Tips" of folded wings become grey	1
FM	P12i	73-97*	39) Bristles on abdominal tergites become visible	1
FM	P12i/ii	73-78* (77.5^{X})	40) Wings become grey	1
M	P12ii		41) Sex combs darken	1
FM	P12ii/13	75-86* (78.6^{X})	42) Wings darken to black	1
FM	P13/14	(81.9^{X})	43) Tarsal claws darken and claws become bleak	1
FM	P14		44) Legs twitch	1
FM	P14/15i	87-103* (91.5^{X})	45) Meconium (green patch) appears dorsally at posterior tip of abdomen	1
F	(P15i)		First oocytes appear	2
FM	P15i	90-103*	46) Malphigian tubules and yellow body no longer distinguishable	1
FM	P15i	90+*	Pharate adults able to walk if removed from puparium prematurely	1
FM	P15i/ii	93-105*	47) Ptilinum expanded by	

		(99.6x)	hydrostatic pressure, opening the operculum	1
M	(P15ii)	102	Testes contain mostly spermatozoa with some younger stages	2
F	(P15ii)	98	Meiosis	2
FM	P15ii/A1	c.100 48)	Eclosion completed	1
F	(A1-3)	Eclosion + 2d	Growth and maturation of oocytes	2
FM	A1/2	c.100.5*49) (102.2^{X})	Wings unfold, flatten and harden; and	1
		50)	Abdomen becomes broad.	1
FM	A2/3	(115.7^{X})51)	Abdomen tergites become brown and shiney (sexes differ in pattern)	(1)

TABLE A2.1

Time elasped between mid-points of stages (hours at 25°C)

x 2.05 for 18°C
x 0.80 for 29°C

L2/P1																	
0.15	P1																
0.85	0.7	P2															
4.4	4.2	3.6	P3														
9.5	9.3	8.6	5.1	P4													
15.4	15.2	14.6	11.0	5.9	P5												
25.6	25.4	24.7	21.2	16.1	10.2	P6											
38.3	38.1	37.4	33.9	28.8	22.9	12.7	P7										
50.4	50.2	49.6	46.0	40.9	35.0	24.8	12.1	P8									
65.6	65.4	64.7	61.2	56.1	50.2	40.0	27.3	15.2	P9								
74.6	74.4	73.7	70.2	65.1	59.2	49.0	36.3	24.2	9.0	P10							
76	76	75	72	66.5	61	50.4	38	26	10	1	P11						
78	78	77	74	68.5	63	52	40	28	12	3	2	P12					
80	80	79	76	70.5	65	54	42	30	14	5	4	2	P13				
87	87	86	83	77.5	72	61	49	37	21	12	11	9	7	P14			
96	96	95	92	86.5	81	70	58	46	30	21	20	18	16	9	P15		
100	100	99	96	90.5	85	74	62	50	34	25	24	22	20	13	4	A1	
108	108	107	104	98.5	93	82	70	58	42	33	32	30	28	21	12	8	A2

Appendix Three

Analysis of the pupal cuticle polypeptides

A3.1 Introduction

The secretion of the pupal cuticle begins shortly after pupariation and is detectable in electron micrographs at 3-6h (Poodry and Schneiderman, 1970, Wehman, 1969). The larval-pupal apolysis, or separation of the larval cuticle from the underlying epidermis, also begins at about this time (4-6h; Fraenkel and Bhaskaran, 1973), proceeding from anterior to posterior, and reaches completion before the pupal moult itself in stage P4(ii) (before 12h at 25°C). The pupal cuticle can therefore develop in the intervening space and when complete it is a thin transparent bag of pupal shape with no surface markers (Fig. A3.1). Beneath this the secretion of the patterned adult cuticle later occurs.

The origin of the pupal cuticle is complicated by the fact that, while the anterior part is secreted by the complex of fused imaginal discs destined to become the head and thorax, the abdomen at this time is still essentially larval and retains the larval hypodermis which will not be replaced by the abdominal histoblasts until after head evagination, (the pupal moult, P4 ii). Thus there are two lineages of cells involved in the secretion of the pupal cuticle which have been separated since embryionic development, (Poodry and Schneiderman, 1970).

Fraenkel and Bhaskaran (1973) observe that "the epidermis is

Figure A3.1

a) Pupal cuticle from stage P5 ii, dorsal view

The thin transparent bag of cuticle has been punctured and the haemolymph and histolysed organs, viscera etc. have been removed. The larval trachea (t) may be removed with watchmaker's forceps. Head (H), Leg (not shown) Wing (W), Thorax (T), Abdomen (A) and Genitalia (G) regions may be separated with a microknife.

b) Larval and pupal cuticles after eclosion, dorsal view. The pupal cuticle (pc) is separated from the adult cuticle and fragile by this stage (P15) and is remains within the puparium at eclosion. The larval lateral trunk tracheae (t) and oval armature (or) are still as they were left at head eversion (P4(ii)) on the anterior ventral lining of the puparium. (Dissected in 1% Agar).

Fig. A3.1

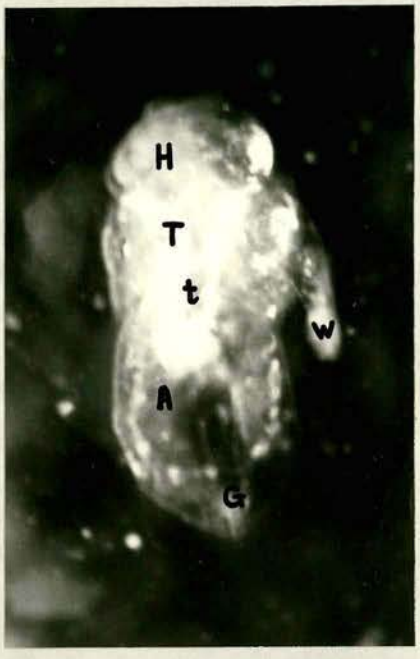

a)

b)

exceptional (during this period) in that a mixed population of imaginal and larval epidermal cells turn on the same genes at this stage in development". Such a situation is interesting with regard to the control of these genes, but the question arises - are they really the same genes? Are the anterior and posterior cuticles of the same composition ? This question was the basis for a preliminary investigation of pupal cuticle proteins.

A3.2 Materials and methods

Animals were selected in stages P4, P5, P8-10 and P14 (see 3.1) and the puparia were removed by dissection in Ringer's solution. A microknife was used to divide the cuticles into the fragments shown in Fig. A3.2. Some of the contents of the cuticle (haemolymph etc.) were removed during this procedure. The various fragments were made discrete (non-overlapping) by excluding intervening strips from the analysis and so effectively "enriching" the samples for head, thoracic or abdominal cuticle respectively (Fig. A3.2). To clean the cuticles further they were opened dorsally and gently scraped free of adhering cells and tracheae. The leg and wing pouches were squeezed, and the cuticle fragments were then vortexed vigorously in microcap tubes containing insect Ringer's solution.

Cuticle fragments were sonicated for 10 sec. in Laemmli buffer and the samples were separated into their respective polypeptides by SDS-polyacrylamide gradient gel electrophoresis (Bownes and Hodson, 1980). Molecular weight markers included: Ovalbumin (42K), Penicillinase (28K), Myoglobin (16K) and Lysozyme (14K) in a

Figure A3.2

Pupal cuticle fragments - dissection scheme

H, head; T, thorax; W, wings; L, legs; A, abdomen; C, complete cuticle. Lateral view, "neck" and "waist" regions were discarded to avoid ambiguity in sample composition. Genital disc region, G only removed from whole abdomens, i.e. (H+T+A) = (C-G).

Fig. A3.2

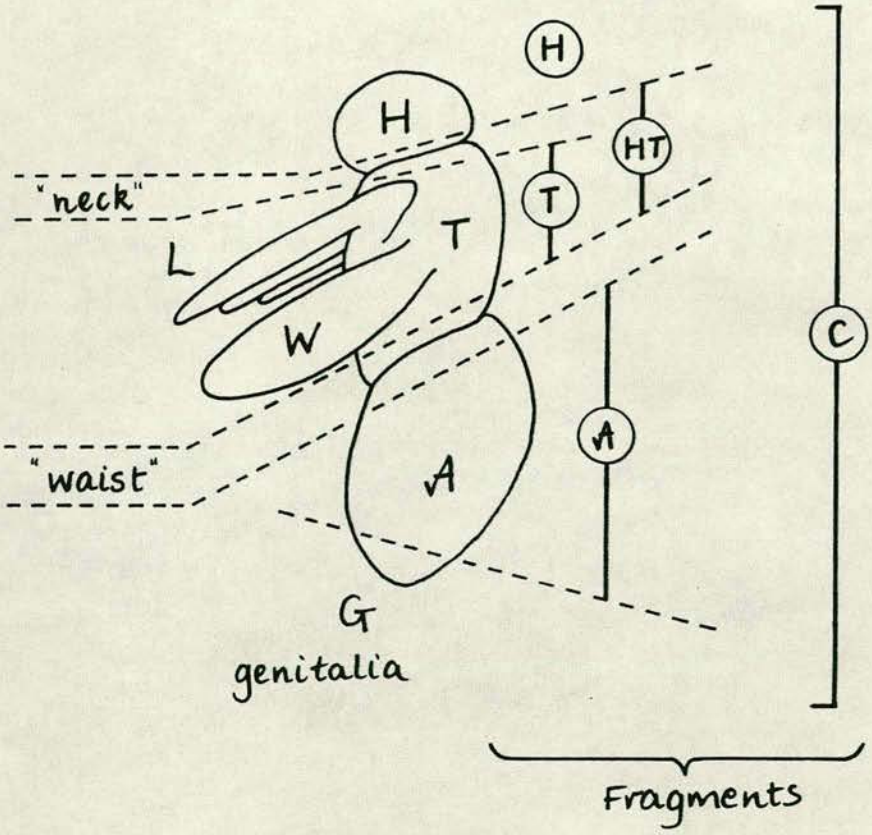

cocktail; and Drosphila Yolk polypeptides (c.45K).

A3.3 Results

The sources of the fragments of pupal cuticle, together with the sex of the animals where known and the number of individuals represented are shown at Fig. A3.3 where the polypeptide components of these samples are visualised as electrophoretic binding patterns. The molecular weights were estimated from the marker tracks (Fig. A3.4); and the differences between tracks, allowing for variations in amount of extracted sample (extraction efficiency only assumed to be uniform), are presented in Fig. A3.5 to bring out comparisons between fragments, between stages and between the sexes.

The following three features emerge from these comparisons: (A) There is, at least between stages P4 and P5, a difference in apparent composition between cuticles of the head (i.e. imaginal cell lineage) and abdomen (larval cell lineage) - bands of molecular weights 17...33K appear earlier in the abdomen, and sizes 36...115.5K, while present in the abdomen and cuticle in P4, fail to appear in that of the head in P5. Also, sizes 23K and 68K are present only in the abdominal cuticle of P14-15 (male only examined) while 12...55.5K are restricted to the head and/or thorax. (B) Considering the pupal cuticle as a whole (sexes mixed) the data suggest many changes with developmental time from before the completion of the larval-pupal apolysis until the pharate adult is mature. Some "early" polypeptides seem to disappear before P8 (17,

Figure A3.3

Pupal cuticle polypeptides separated by SDS-polyacrylamide gel electrophoresis

Tracks 1-10 are fragments of cuticle as shown. Tracks 11 and 17 are molecular weight markers. Compare especially (a) tracks 1 and 3 (anterior) with 2 and 4 (posterior); (b) track 5 (stage P8) with track 6 (P9); and (c) track 8 (female) with tracks 9 and 10 (male). Molecular weight markers: 12K, cytochrome; 14K lysozyme; 16K, myoglobin; 28K, Penicillinase; 42K Ovalbumin; c. 45K YP2 (Drosophila yolk); 68K, Bovine serum albumin; (Cocktail from Professor Neil Willetts, YPs from Dr. Bownes). (Estimates of unknowns are based on Fig. A3.4). Method: (Bownes and Hodson, 1980) 7-20% acrylamide, + TEMED, Ammonium persulphate, 15% APS; overlay buffer = SDS-TRIS; run at 0.15KV; soak in TCA (10%); stain with 0.1% Coomassie Blue 5:5:1 MeOH:H_2O: acetic acid; soak in aqueous MeOH/Acetic acid (10%); dry.

Fig. A3.3

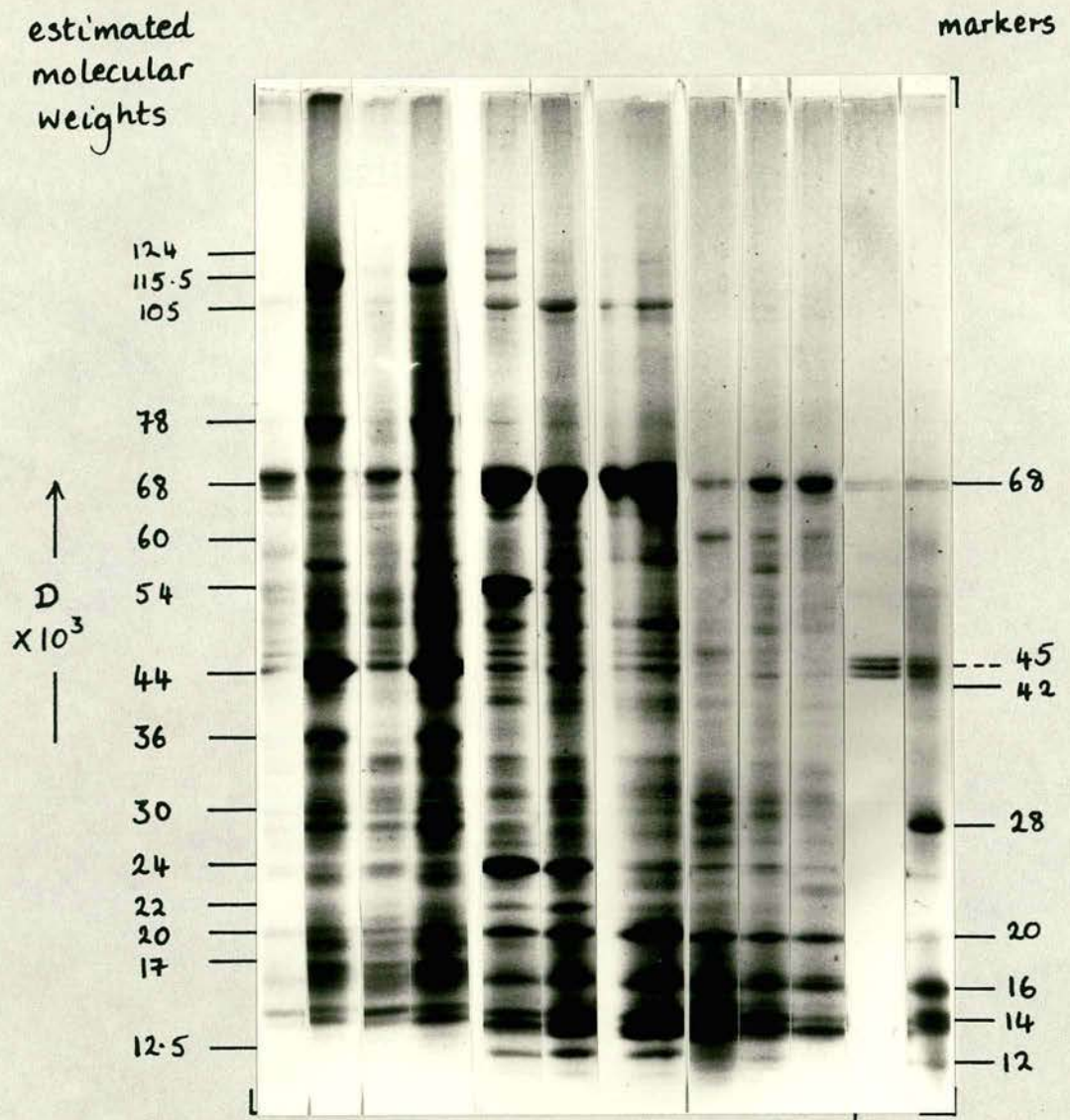

Track	1	2	3	4	5	6	7	8	9	10	11	12
Stage (P)	4	4	5	5	8	9	10	14	14	14	–	–
Fragment	H	A	H	A	W	W	W	W	HT	A	(YP)	(Cocktail)
Sex ♀	+	+	+	+	+	+	+	+				
Sex ♂	+	+	+	+	+	+	+		+	+		
No. Animals	18	29	21	21	16	32	29	40	35	35		

Figure A3.4

Molecular weight conversion curve

Log_{10} gel electrophoresis R_F vs. molecular weight (daltons x 10^3). Extrapolated to limits of gel tracks. Markers as Fig. A3.3.

Fig. A3.4

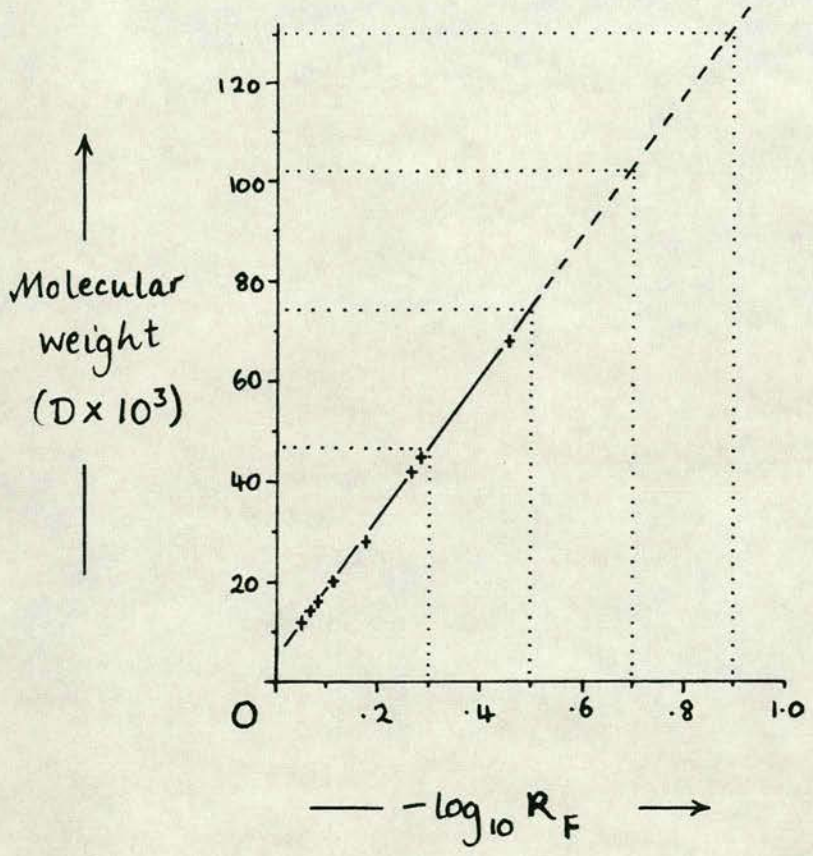

Figure A3.5 Comparison of polypeptide components of pupal cuticle by stage, sex and fragment, (semi- systematic): Account has been taken of the numbers of animals and relative sizes of fragments in comparing densities of bands in Fig. A3.3 (equal extraction efficiencies assumed). Sizes (kilodaltons) are listed where they first appear on the grid, and subsequent increases (+) or decreases (-) are noted. Major changes are underlined. Larval-pupal apolysis extends from c. P3-P4/P5; Pupal-adult apolysis occurs c. P7. Boxes for which there are no data are scored out (x). H, head; T, thorax; A, abdomen without genital region; C, complete cuticle. All material came from mixed-sex populations except P14-15.

Fig. A3.5

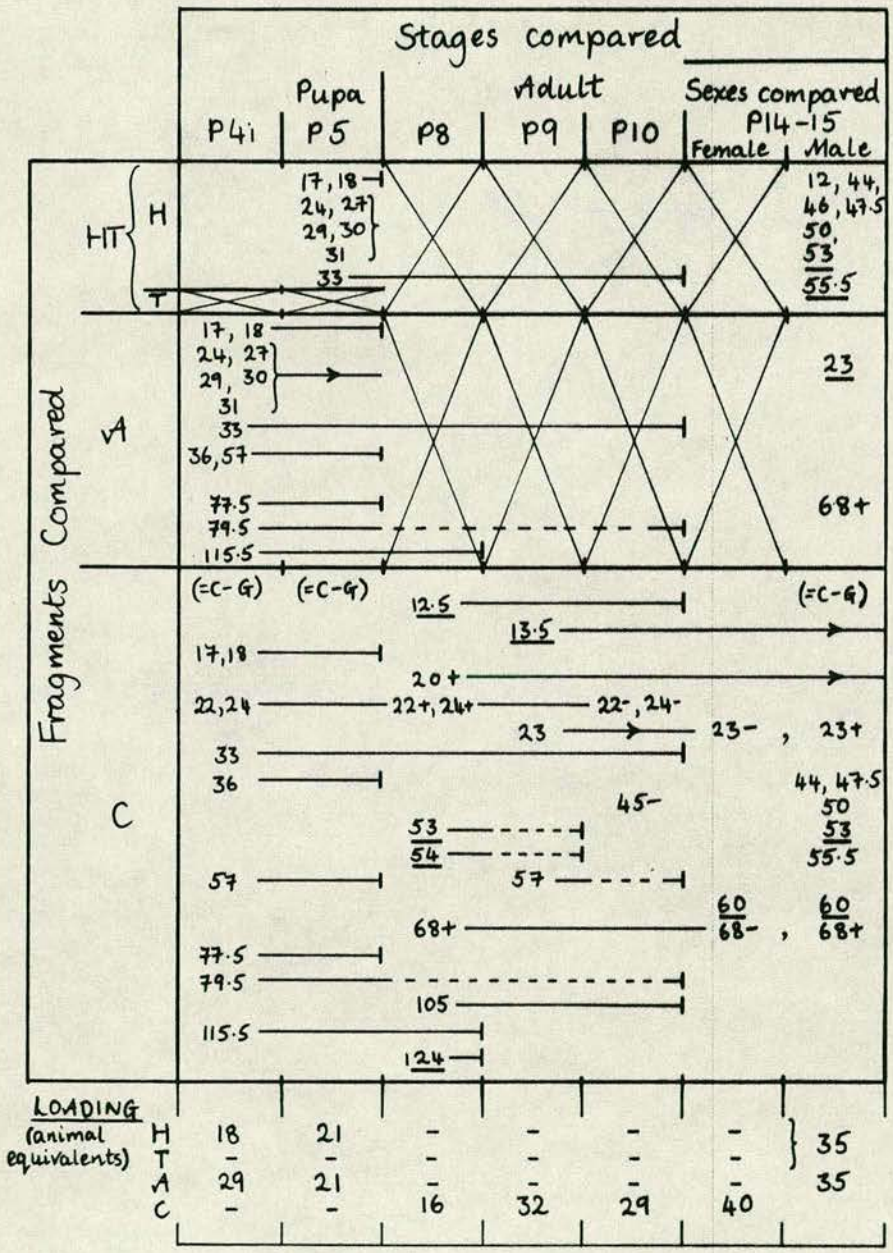
Stages compared
Pupa
Adult
Sexes compared
P4i
P5
P8
P9
P10
P14-15
Female
Male
Fragments Compared
H
T
A
C
17, 18
24, 27
29, 30
31
33
36, 57
77·5
79·5
115·5
(=C-G)
12·5
13·5
20+
22+, 24+
22-, 24-
23
23-, 23+
45-
53
54
57
60
68+
68-, 68+
105
124
12, 44, 46, 47·5
50
53
55·5
LOADING
(animal equivalents)
18
21
29
16
32
40
35

18, 36, 57, 77.5K), some appear transiently in the pharate adult (e.g. 45K, 54K) and some appear only after the underlying adult cuticle is already melanised (e.g. 60K) while several bands disappear before this stage (<P14-15; 12.5, 33, 57, 79.5, 105K). Other bands vary in density (e.g. 22, 24, 68K) or may be absent altogether for some time (53K, 57K). (C) The data suggest that, at least where the comparison has been made (late pharate adults), this cuticle differs between the sexes: bands of molecular weight 44...55.5K are restricted to the male in P14-15, and 23K and 68K decrease in the female but increase in the male.

A3.4 Discussion:

This analysis is incomplete and the comparisons are not quantitative. The details are therefore of little interest; but the overall impression is one of great complexity (cf. Roberts and Willis (1980a) for Tenebrio cuticles in larvae, pupae and adults, all of which show unique banding patterns), and the system is of interest because the material is available in relatively large quantities which offers an opportunity to analyse developmental control of the expression of some important genes. However, it cannot be assumed that the efficiency of extraction of all polypeptides, from all fragments of the cuticle, in all stages and both sexes, would be the same, even were the samples to be of equivalent mass to begin with, which they were not. The loading of tracks might be roughly equated by preliminary assays of the relative amounts of extractable protein present (e.g. Schaffner and Weissmann, 1973) before comparisons are made; and the fragments may

be contaminated by adhering epidermis, especially in the legs, before pupal adult apolysis makes the cuticle easier to dissect clean. (In a related study Chihara et al. (1982) performed repeated homogenizations of pupal cuticles in 8.5% sodium chloride or split the cuticles and scraped them clean). Also, given equivalence of loading and reasonable purity of the samples, an analysis of this type still would not reveal the level of control of gene products. Changes seen here could as well result from modifications of the polypeptides (e.g. phosphorylation, de-/glycosylation, clearage) as from synthesis and secretion de novo. But with this in mind the control of cuticle polypeptides appears nevertheless to be far from simple.

In Tenebrio abdomens (Roberts and Willis, 1980b) the patterns of cuticle protein synthesis as determined by ^{3}H-leucine incorporation are very similar in larvae, pupae and adults despite the differences in banding patterns (Roberts and Willis 1980a) - the differences in time are related to the phase of the moult cycle (pre/post-ecdysis). However, these cuticles are all produced by the same population of epidermal cells showing changes in commitment (cf. the more complex situation with respect to abdominal histoblasts in Drosophila).

The Drosphila samples examined by Chihara et al. (1982) were timed from preparation but their data are roughly comparable with these. (See 3.3.1, Table 3.IV; but note that 58-60h (=P9) is probably P8: pupal adult apolysis = 58h, pupal cuticle is readily dissected out at 60h). Examining the period 13-96h (c.P5i -

c.P15i), they find a difference in (urea-soluble) polypeptides between head-plus-thorax and abdominal cuticles between 13h and 54h (c.P5-P8): Five polypeptides are traced to the pupal cuticle of the head + thorax (pcp 1-5) one of which is missing from the abdomen (pcp 2) on SDS-polyacrylamide gel electrophoresis. This may represent a larval/imaginal cell lineage difference, but the abdominal fragments included the cuticle derived from the genital disc region, so it could result from a positional difference (anterior vs. posterior, imaginal lineage). They do report a reduction in bands near the origin at 84-96h (c. P14) compared to earlier times, but otherwise they find no differences between samples of different ages (13 cf. 54h; approx. P5 cf. P8). They do not compare the sexes. So Chihara et al. (1982) find some differences when comparing lineages (or positions) and some in a comparison of ages (i.e. stages). More importantly, it may be that they examined only a small subset of the polypeptides separated here which themselves constitute a limited subclass of the full complement of cuticle proteins; (Chihara et al. extracted in 7M Urea-TRIS, pH 8.6; cf. Laemmli-buffer).

The pupal cuticle suggests itself as a promising subject for an investigation of the control of enkaryotic gene expression; but it would be necessary before drawing further conclusions to identify those polypeptides (if any) which when they seem to appear for the first time do so as a result of new gene expression; (e.g. ^{35}S-methionine pulse labelling and antoradiography; Seybold and Sullivan (1978) found temporal and positional (disc-specific) differences between Drosphila imaginal discs during metamorphosis in vitro

using this technique, and their tissues included both pupal and adult cuticles, so some of these differences may be traceable to the pupal cuticle; but Greenburg and Adler (1982) were unable to confirm such differences in a similar study). It would be of interest to develop this investigation, i.e. to isolate and raise antisera against selected gene products; to perform cell-free translation of extractable mRNA (e.g. Mitchell and Petersen, (1981) who used Drosophila wing discs) and screening of products with antiserum; to produce a cDNA library from epidermal mRNA; and to hybridise cDNA in situ to polytene chromosomes in order to map the genes being expressed and compare their puffing response patterns to ecdysteroids. The interaction of 20-OH-ecdysone with epidermal genes during metamorphosis could therefore be characterised. (It was understood when such a program of experiments was considered that Professor Fristrom (Berkeley) was well advanced with the same investigation (published later as Chihara et al., 1982); so instead, a broad analysis of the hormones themselves was attempted - the subject of this report).

Appendix Four

Ecdysteroid Recovery Efficiencies

The use of C_{18} cartridges for short column reverse-phase liquid chromatography and Silica-gel plates for thin layer chromatography (TLC) were investigated before being employed in the preparation of samples for HPLC (Section 2.14). This section demonstrates that recoveries from TLC are sufficiently variable to make the use of (and hence contamination by) an internal concentration standard essential if quantification of endogenous steroids, as well as their identification, is to be attempted for Drosophila extracts. It also shows that such quantification cannot be performed by HPLC-coupled-UV spectrophotometry alone (cf. Section 5.3) but must involve subjecting the compounds separated by HPLC to quantification by, for example, GLC-MS (6.1) or RIA (5.6) with reference to an internal concentration standard which behaves as much as possible like the subjects of the analysis.

Two techniques were employed to assess these steps in the protocol - Liquid Scintillation counting (LSC) and HPLC-UV-spectrophotometry. In experiment 1 the recovery from C_{18} cartridges is found to be effectively 100%, and this value is assumed in experiments 2 (a)-(f), (six measurements of recovery from TLC). A comparison of measured recovery efficiencies will be presented in Table A4.III (q.v.) and the conclusions from these experiments characterising TLC are presented in Section A4.3. They were considered when the protocol adopted for Chapter 5 was

developed (Section 2.14).

A4.1 Materials and methods

Manufacturers as for Chapter 2 unless otherwise stated.

All glassware was silonised (Repelcote).

Solvents: Methanol, HPLC-grade

Ethanol, (AR)

Chloroform (HPLC)

Hexane (AR)

Water: double-distilled, than "Norganic".

Ecdysteroids: Ecdysone 8.5 x 10^{-5}M stock solution;

20-OH-ecdysone 5.1 x 10^{-5}M stock solution;

Makisterone A (gift from Dr. Wilson, Dr. Morgan, Keele) 7 x 10^{-5}M stock solution;

3H-ecdysone (MEM; 80 Ci.mMol).

Procedures:

A) Extractions: (Expts. 1, 2b, f)

Stages P10-13 0.5g (Experiments 1 and 2b),

stage P1 1.035g (Experiment 2f);

Homogenized in 70% aqueous methanol until supernatant came away clear (c. 10ml total); pooled; Sonicated c. 20 secs; Spun 10 min 10K;

B) Partitions (Expts. 1, 2b, e,f)

v.s. Hexane and chloroform; with back extractions;

Reduced to c. 1ml water (rotary evaporation);

C) C_{18} Liquid Chromatography (Expts. 1, 2d, e, f)

Sep-PAK prepared (3ml MeOH; 5ml H_2O);

Aqueous sample loaded from siliconised syringe;

Cartridge washed with 5ml water;

Eluted with methanol;

Reduced to dryness (rotary evaporation);

D) Thin Layer Chromatography (TLC): (Expts. 2a-f)

Silica-gel plates pre-run x 2 in 3:17 95% ethanol/$ChCl_3$;

Samples and R_F-standards loaded in ethanol with 5µl or 25µl capillaries or with an adjustable pipette (Gilson pipetman, P200, tips siliconised);

Develop 60-70 min. in 3:17 95% ethanol/$CHCl_3$

in TLC tank (vapour saturated);

Chromatograms viewed under UV-light;

Silica-gel zones scraped and eluted in 3+

aliquots of cold ethanol;

Eluates centrifuged 10 min. (10K or 12,000 r.p.m.);

Reduced to dryness (Nitrogen, c. 30°C);

Samples subjected to (E) or (F):-

E) Liquid Scintillation Counting (L.S.C):

(Expts. 1, 2 a-c)

Samples taken up in 100µl water and vortexed;

1 ml scintillant ("Aquasol", MEM) added, vortexed;

Vials kept in the dark 1h;

Counted 10 min x 2 with water/asquasol background-subtraction;

F. High Performance/Pressure Liquid Chromatography - Ultra-violet spectrophotometry (HPLC-UV spec.):

(Expts. 2d-f)

Samples taken up in water and filtered (Millipore HA).45µm);

Brought to 200µl 50% aqueous methanol;

HPLC: see Appendix A5 for details of apparatus. Column = C_{18}, 8mm i.d. (Rad-PAK, Waters Ass.), room temperature; mobile phase 50% aqueous methanol, 1ml min^{-1}; quantification by reference to external concentration standards, by pre-programmed "cailbration averaging" method (recalibration after five unknowns); repeated injections; samples alternated with injector purges (methanol); isocratic runs, 20 min, with 10 min equilibration delay including column-flush with methanol.

A4.2 Experiments

Experiment (1) Use of C_{18} Sep-PAK cartridges for sample purification before TLC

An extract of stages P10-13 (0.5g) was partitioned against hexane to remove lipids and then "spiked" with c. 400K counts of 3H-ecdysone (= 100%). The sample was loaded onto a prepared C_{18} cartridge and the water retained, after which the cartridge was washed, the water being retained again. Serial methanol elutions were performed (3 x 1ml) and the eluates were taken to water. Aliquots of all samples were counted (L.S.C.) to determine proportional recovery of 3H-ecdysone.

Results: Counts transmitted at aqueous loading = 0.15%

" eluted at wash = 0.08%

(volume transmitted = 8ml)

Counts eluted in 1st ml methanol = 95.58%

" " " 2nd" " = 3.54%

" " " 3rd" " = 0.11%

Activity accounted for = 99.46%

(95.58% + 3.54% = 99.12%; 99.12% + 0.11% = 99.23%)

Conclusion: recovery in 2ml methanol > 99% efficient (in the presence of a Drosphila extract).

Experiments (2) a - f Characterisation of TLC as a preparative step for HPLC samples

Experiments a - c are measurements of recovery of radio-labelled ecdysone by LSC, whole experiments d - f are based on HPLC-UV spec. for which unlabelled ecdysteroids were used.

Experiment 2 (a) Distribution of recoverable ^{3}H-ecdysone on a silica-gel thin-layer chromatogram

About 450K counts ^{3}H-ecdysone were subjected to TLC and their recoveries from the various zones were determined by elution in 3 x 1ml ethanol (pooled) and L.S.C.

Results: (See Fig. A4.1) Recovery from R_f-ecdysone $\pm$ 2 spot-diameters = 42.5%. 37% was recovered within two spot-diameters of the ecdysone standard (ecdysone + trailing ecdysone). 12% was retained at origin. (Zones 8/9 and 9/10 were unlikely to yield high percentages and were not examined.) Total recovered = 62% (approx.).

Conclusions: 42.5% activity was recovered between R_Fs .23 - .45 (RR_F- -α .68-1.36). More than 10% was retained at the origin (and was recoverable). About 40% was irreversibly bound in Silica-gel under these conditions (1ml elution x 3; no native extract present).

Experiment 2(b) Effects on recovery of ^{3}H-ecdysone through TLC of:-

i) the presence of a Drosophila extract;

Figure A4.1

Experiment 2 (a), Recovery of ^{3}H- ecdysone from TLC by ethanol elution. Percentage recovery from R_F zones (100% = 451109 cpm), showing recoveries in the vicinity of an ecdysone marker, (α; plate viewed under U.V. illumination). Length of loading zone = 2cm. RR_F-α is relative R_F with respect to ecdysone.

Fig. A4.1

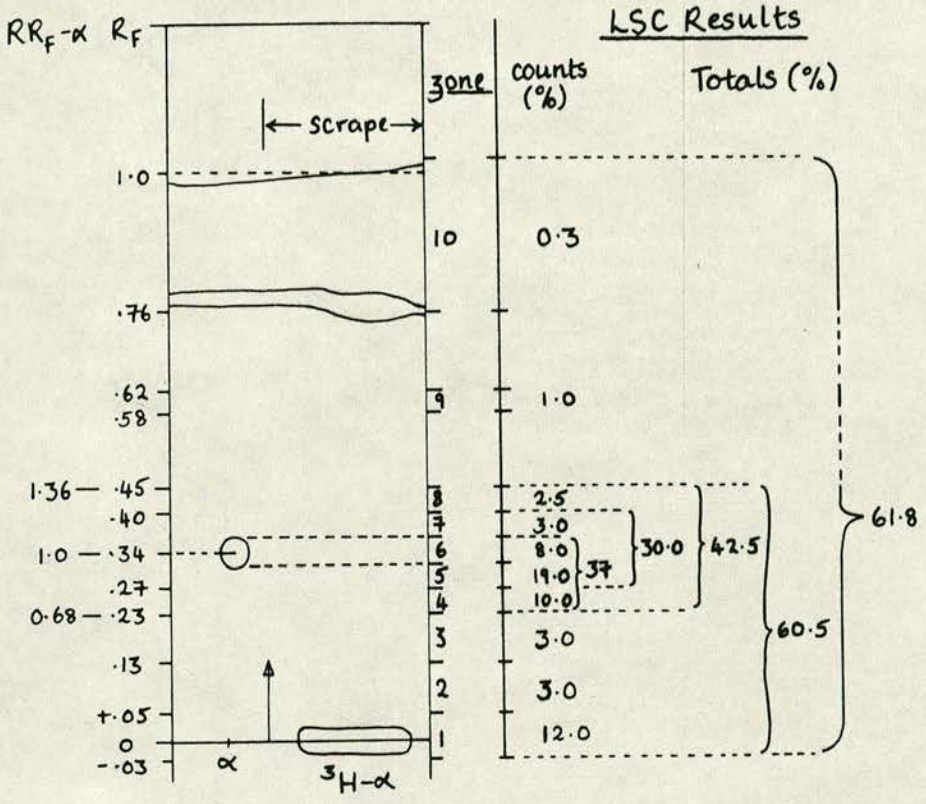
RR_F-α
R_F
scrape
1·0
·76
·62
·58
1·36 — ·45
·40
1·0 — ·34
·27
0·68 — ·23
·13
+·05
0
-·03
α
³H-α
zone
10
9
8
7
6
5
4
3
2
1
LSC Results
counts (%)
Totals (%)
0·3
1·0
2·5
3·0
8·0
19·0
10·0
3·0
3·0
12·0
37
30·0
42·5
60·5
61·8

ii) elution volume/number of elutions; and

iii) plate area

An extract from stages P10-13 (0.5g) was partially purified by being hexane-partitional and passed through a C_{18} cartridge and then "spiked" with about 300K counts ^{3}H-ecdysone (=100%). The sample was subjected to TLC and the zones visible under UV-illumination were serially-eluted in 300µl ethanol x 3 or x 6 (not pooled). Recovery was determined by L.S.C.

Results: Total recoveries (3 or 6 elutions) per zone are shown at Fig. A4.2. Most of the recoverable activity was located between R_F .33 - .66, while about 75% available counts were recovered altogether by 6 serial ethanol elutions (1.8ml). Less than 1% of loaded counts recovered from the (ecdysone + trailing ecdysone) region (zones 9-11) represent 91% of recoverable counts. About 9% loaded counts of ecdysone comigrated with 20-OH-ecdysone (zone 9).

Fig. A4.3a shows the proportions of recovered activity present in successive eluates 1-6 for the region spanning ecdysone and yielding more than 1% loaded counts (zones 9-12). Values are expressed as mean percentages of total activity recovered from each of these four zones. The curve is very similar to that for zones 1-12 (not shown); but zone 14 considered alone shows a different pattern (Fig. A4.3b). This is too far from the R_F-markers to be of interest when eluting ecdysteroids.

It seems, then, that a fourth 300µl-elution of activity from the ecdysteroid region can only improve on approximately 95% of that recoverable by 6 elutions. But there could be a load effect whereby

Figure A4.2 Experiment 2 (b): Distribution of counts ^{3}H-ecdysone (α) recovered from TLC by pooling 3 or 6 ethanol eluates. Zones showing very low activity (zones 2-8) were only eluted three times. The position of 20-OH-ecdysone (β) is predicted from that of ecdysone. The length of the loading zone for stage P10-13 spiked with radiolabelled ecdysone = 3.5cm. 100% loaded activity = 293,280 cpm.

Fig. A4.2

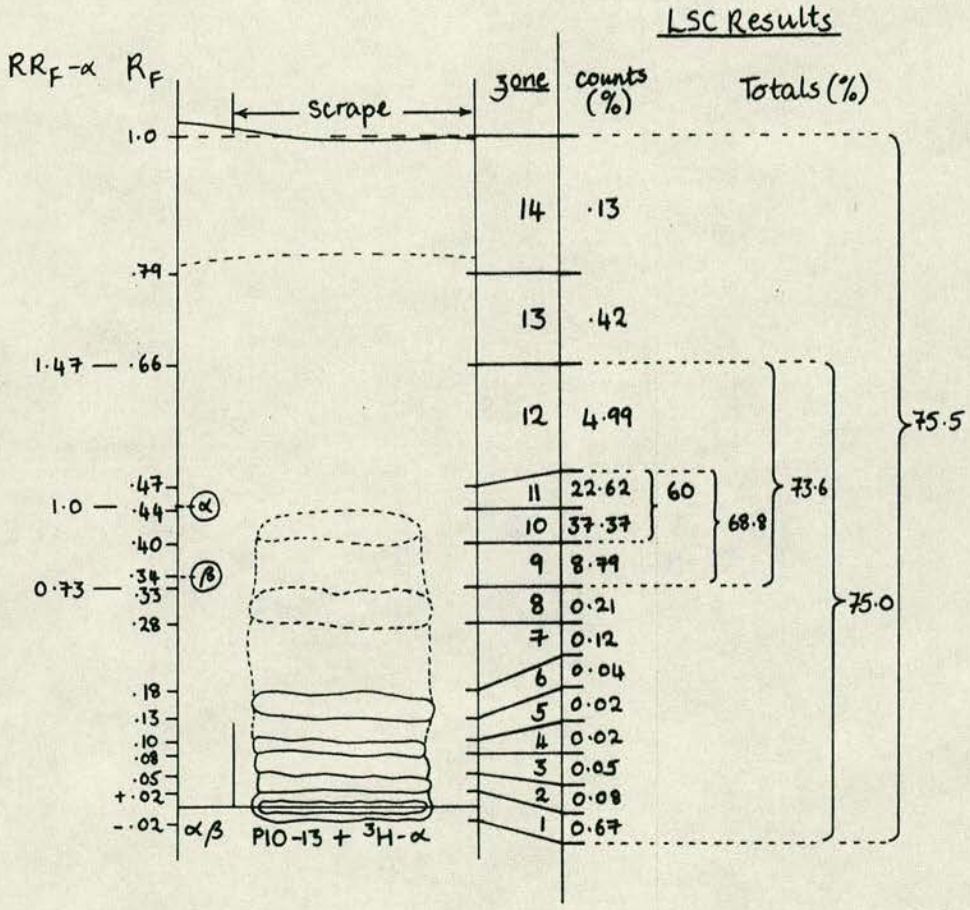
LSC Results
RR_F-α
R_F
scrape
zone
counts (%)
Totals (%)
1·0
·79
1·47
·66
1·0
·47
·44
·40
·34
·33
·28
0·73
·18
·13
·10
·08
·05
+·02
-·02
α
β
αβ
P10-13 + ^{3}H-α
14 ·13
13 ·42
12 4·99
11 22·62
10 37·37
9 8·79
8 0·21
7 0·12
6 0·04
5 0·02
4 0·02
3 0·05
2 0·08
1 0·67
60
68·8
73·6
75·0
75·5

Figure A4.3

Experiment 2 (b): Recovery from TLC- zones by successive 300µl ethanol elutions

a) Mean recoveries from zones 9-12 (ecdysone region, R_F 0.33-0.66) expressed as cumulative percentages of the total counts recovered by six elutions ($p = 0.05$). The means of zones 1-14 give an almost identical curve. Eluates 4-6 only contributed 2.8% to the total. Zones 2-8 yielded little activity and were only eluted three times. Error-bars show 95% confidence limits.

b) as (a) for zone 14 alone (R_F 0.79-1.0; atypical): eluates 4-6 contributed 30% to the total from six elutions.

Fig. A4.3

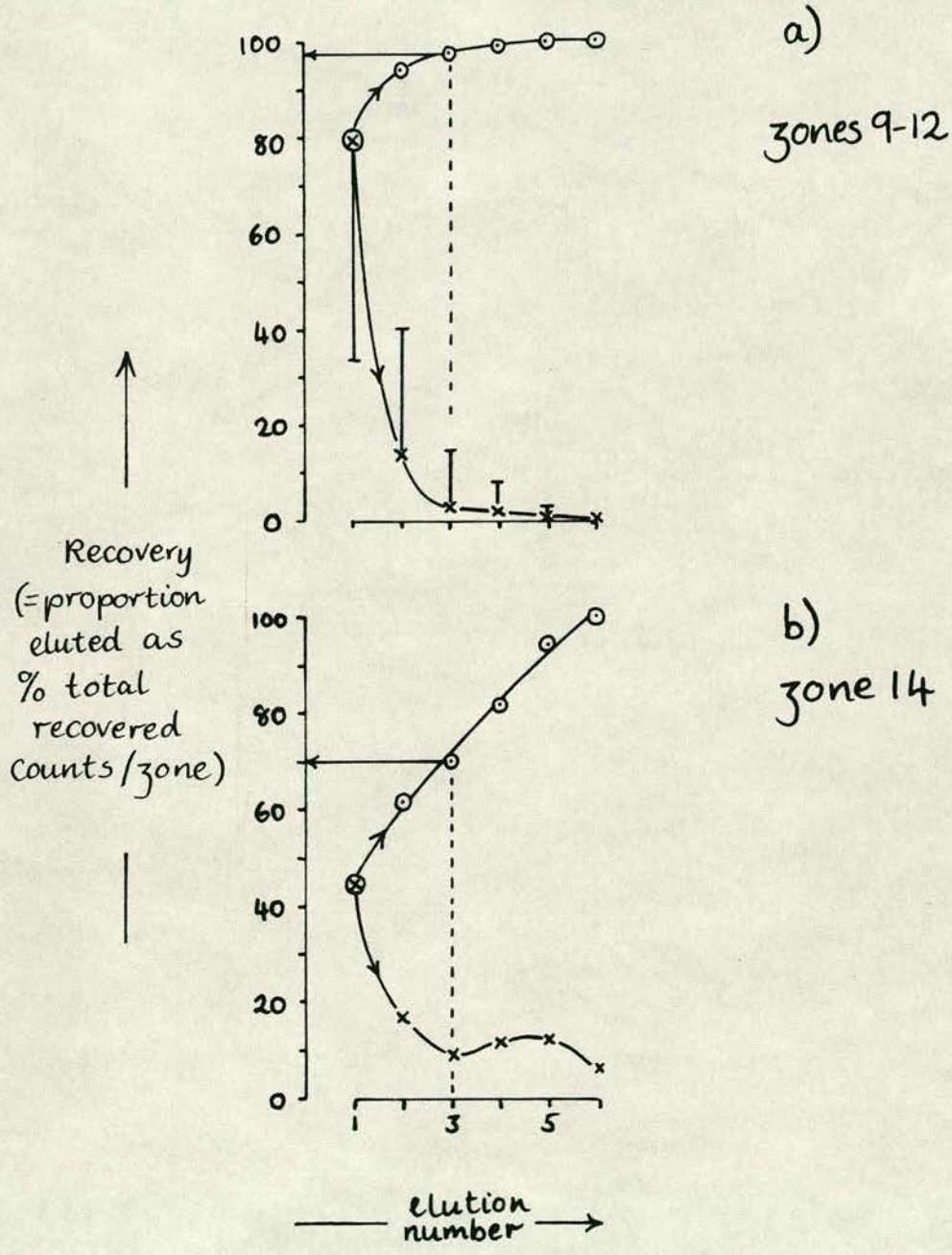
a)
zones 9-12
b)
zone 14
Recovery
(= proportion
eluted as
% total
recovered
counts/zone)
100
80
60
40
20
0
1
3
5
elution
number

binding to the plate coating increases or decreases with the load at a given R_f zone (R_F>0, i.e. this is not the "loading density" at the origin; cf. experiments c and f). This is examined at Fig. A4.4 by plotting load against recovery for the first three elutions; and it is apparent there that initial recovery of activity is directly related to load, but also that recovery by a second elution is inversely related to load; i.e. the binding effect is reversible so that a heavily-loaded zone being eluted for a second time behaves like a new sample carrying less steroid. This is not to say that recovery can be complete - a quarter of the activity loaded at the origin was never recovered - but there is little to suggest a differential effect of load on recovery from the ecdysone region after three elutions.

The areas of zones 1-14 are not equal. The activity recovered by the nth member of a series of elutions tends to be proportionally higher in comparison to that by a subsequent elution when the quantity of Silica-gel is relatively small, irrespective of the steroid load for each zone (Fig. A4.5). This indicates that large areas of silica-gel will yield up ecdysteroid(s) more gradually than small areas during serial elution, which would make little difference when excess ethanol is used; but when comparing samples they should be eluted from equal plate areas.

Conclusions: 73.6% of loaded activity was recovered between R_F .33-.66 (RR_F-α .73 - 1.475). Less than 1% was recoverable from the chromatogram origin in the presence of a Drosophila extract. About 95% recoverable counts from the ecdysone region (c.20cm^2) was obtained by 3 serial elutions of 300µl (1.8ml)

Figure A4.4

Experiment 2 (b): Independence of recovery by 0.9ml Oution volume and Load a) Recovery of ^{3}H-ecdysone is considered to have been exhaustive, and loads are taken to be total counts recovered per zone as percentages of the total available counts (= 293,280 cpm). Zone loads are plotted against the proportions represented by single 0.3ml elutions. Only the first three elutions are shown, together with their sum (i.e. 1-3 pooled). Areas of the TLC plate represented by load are similar for zones 9-11 ($3.0cm^2$; s.d. 0.93). Zone 12 represents $10.8cm^2$. Curve 1 shows that binding to silica-gel is enhanced when load is relatively small; curve 2 that a second elution compensates for this.

b) Hypothetical situation where high load density enhances recovery but binding to silica- gel at low load density is irreversible.

c) Interpretation of (a) for zones 9-12 (ecdysone region).

Fig. A4.4

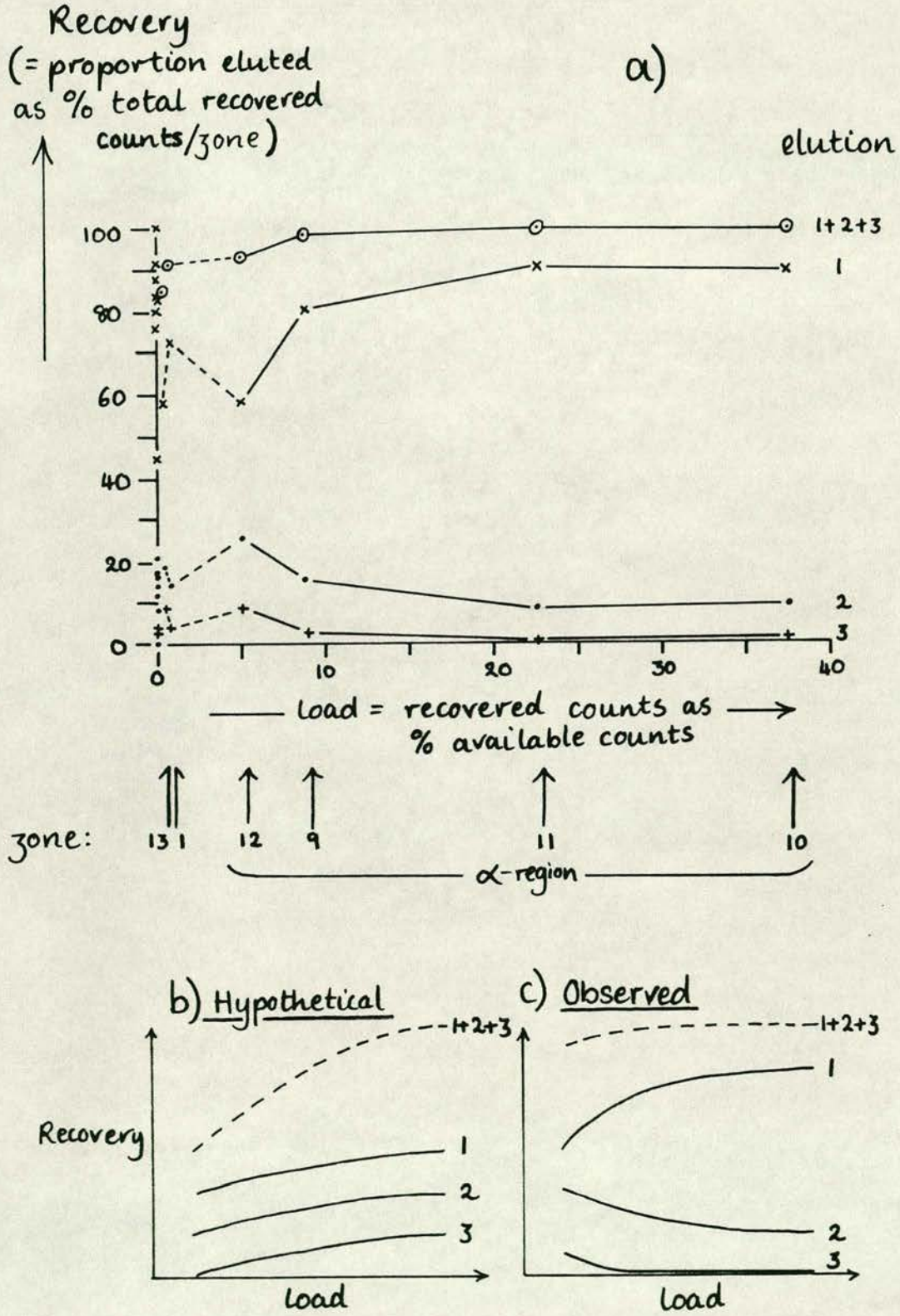
Recovery
(= proportion eluted as % total recovered counts/zone)
a)
elution
100
80
60
40
20
0
0
10
20
30
40
1+2+3
1
2
3
Load = recovered counts as % available counts
zone:
13 1
12
9
11
10
α-region
b) Hypothetical
c) Observed
Recovery
1+2+3
1
2
3
Load
1+2+3
1
2
3
Load

Figure A4.5 Effect of silica-gel plate-area on proportional recovery of ^{3}H-ecdysone in serial elutions

Zone areas (cm^2) vs. $\log_{10}$ ratio of counts recovered by 300µl ethanol elutions, numbers 1 and 2 (a) and 2 and 3 (b). (fitted by eye; 0 = mean centre). Ratios = infinity when the second elution of a pair gives zero yield of activity, and in no such case did a subsequent elution yield any activity. Correlation coefficients, r for these and later pairs of elutions are as follows:-

Elutions Ratio	r (area vs. ratio)	>r when P =	r (load vs. ratio)	>r when P =	n
1:2	-.74	0.01	+.47	>0.1	13
2:3	-.72	0.02	+.66	0.05	9
3:4	-.04	0.1	-.16	0.1	7
4:5	-.73	0.05	+.72	0.05	7
5:6	-.14	0.01	+.68	0.1	7
3.6	-.58	0.01	+.72	0.05	7

This Table also shows r for the same ratios plotted against load (the activity recovered from each zone, i.e. replacing this abscissa with that of Fig. A4.4). At least in the case of the first elution, there is no dependence of the ratio on the load of ^{3}H-ecdysone - serial recovery is probably unaffected by load. The relationship between the third and fourth elutions is anomalous. There is no correlation in this experiment between area and load (plot not shown; r = -0.20).

Fig. A4.5

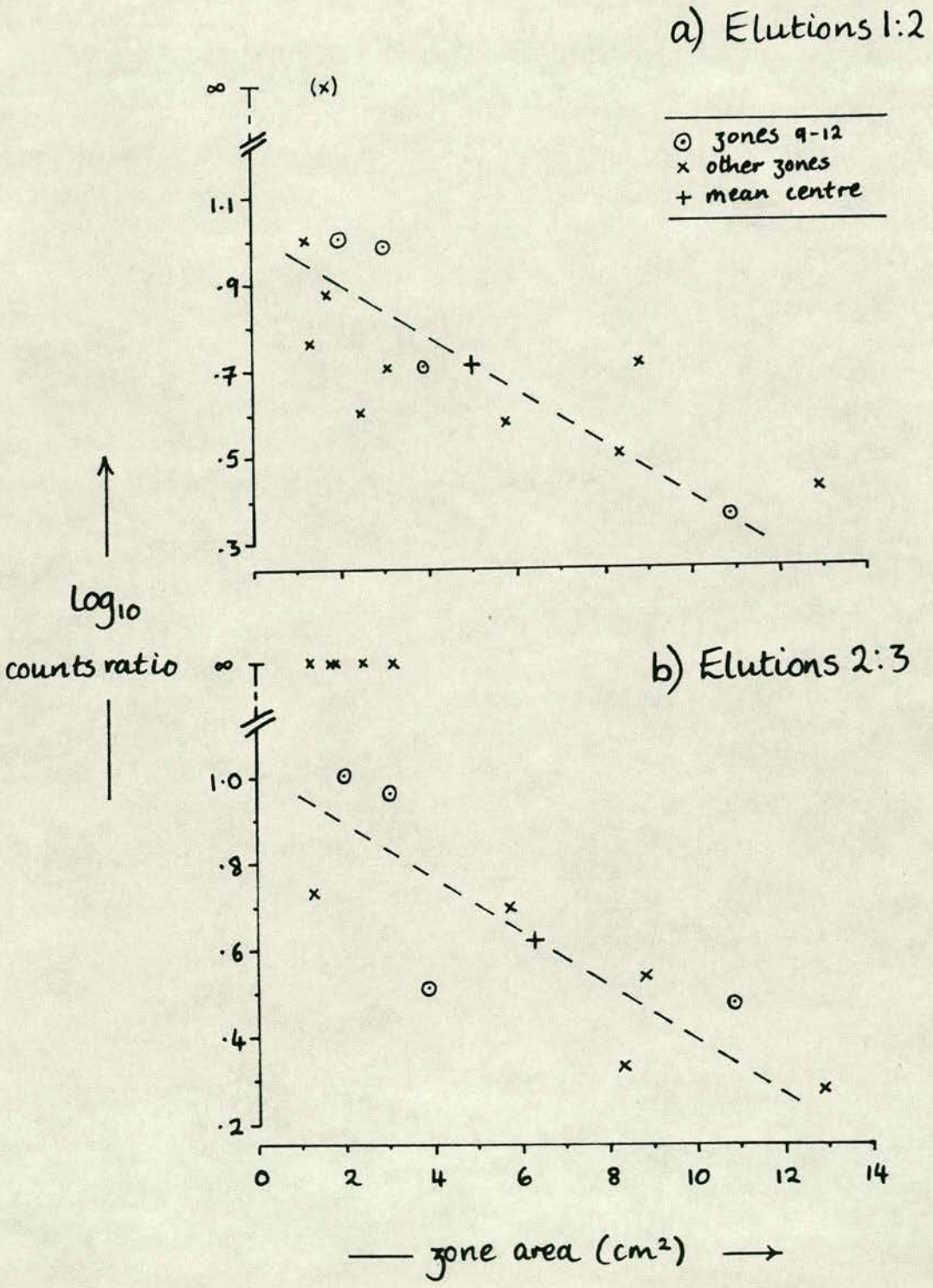
a) Elutions 1:2
⊙ zones 9-12
× other zones
+ mean centre
∞
(×)
1.1
·9
·7
·5
·3
log10 counts ratio
b) Elutions 2:3
1·0
·8
·6
·4
·2
0
2
4
6
8
10
12
14
zone area (cm²)

ethanol. Any differential effect of load on recovery tends to be corrected by 3 serial elutions in the ecdysone region. Comparisons between chromatograms should be based on similar areas of TLC plate.

Experiment 2(c) Effect on recovery of ^{3}H-ecdysone through TLC of loading - density at the origin (determined by L.S.C.)

A stock solution of 3^{3}H-ecdysone was made to contain c. 1700 counts per unit volume, and 1, 3, 5, 7 or 9 unit volumes of activity were applied to 1, 3 5, 7 or 9 units of TLC plate area, as shown in Fig. A4.6. The developed chromatogram was analysed for activity comigrating with ecdysone and 20-OH-ecdysone by ethanol elution (600µl x 3, pooled) and L.S.C.

Results: Table A4.I gives values for the recovery of ^{3}H-ecdysone from the ecdysone/20-OH-ecdysone region as shown in Fig. A4.6. There was no significant difference between recoveries of counts over a nine-fold increase in loading density using radio-labelled ecdysone. The volumes of label used here corresponded to the range 0.02-0.25pg ecdysone (0.04-0.54pMoles) per mean loading area of 1.25cm^{2} (i.e. approx. 0.5-0.65pM cm^{-2}; 0.025-0.30pg cm^{-2}.

Recovery of trailing-ecdysone in the 20-OH-ecdysone zone (B) was less than 5% both of loaded counts and of counts recovered from this ecdysteroid region (A + B; Relative R_F (ecdysone = 1.0) 0.53-1.06).

Conclusions: Recovery = 53.8 $\pm$ 25.3% (n = 20, p = 0.05) from RR_F (ecdysone) 0.53-1.06 at a loading density of 0.025-0.30pg ^{3}H-ecdysone per cm^{2}. Recovery does not vary with loading density over this range. More than 95% of recoverable

Figure A4.6

Experiment 2 (c): Effect of loading-density

Schematic TLC-plate showing experimental design for the detection of any effect of density of loading at the origin on recovery of ^{3}H-ecdysone in the ecdysone (α) and 20-OH-ecdysone (β) regions. RR_F-S = Relative R_F with respect to standard ecdysone or 20-OH-ecdysone. d = spot diameter at the origin.

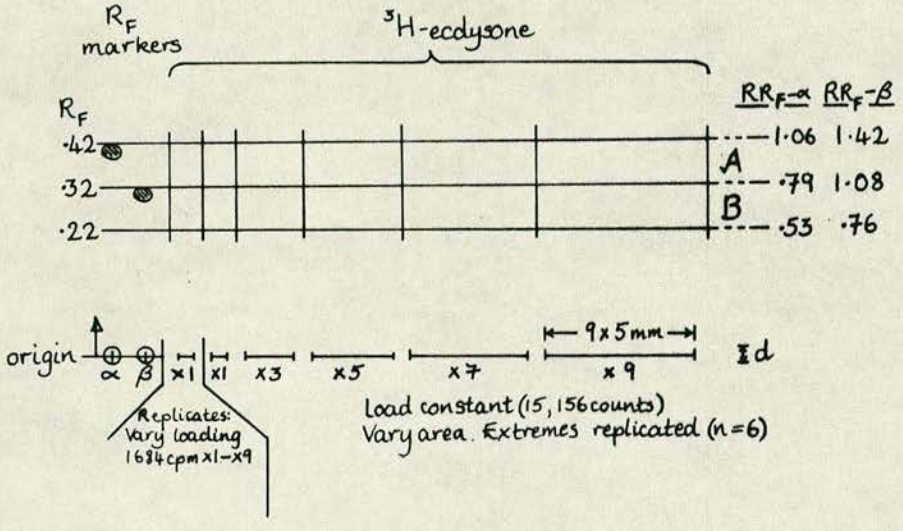
R_F markers
^{3}H-ecdysone
R_F
·42
·32
·22
RR_F-α
RR_F-β
1·06 1·42
A
·79 1·08
B
·53 ·76
origin
α
β
×1
×1
×3
×5
×7
9×5mm
×9
Σd
Replicates:
Vary loading
1684cpm ×1-×9
Load constant (15,156 counts)
Vary area. Extremes replicated (n=6)

Fig. A4.6

TABLE A4.I

Experiment 2(c) Recovery from (A + B) (% total loaded).

	% Recovery	mean % (p = 0.05)		
Vary load on 1 unit area:	53.0			
	42.0			
	42.0	32.13-57.87		
	43.0			
	45.0			
Load constant on 1 unit area:	55.0		32.5-58.96	
	49.1			
	40.8			
	39.1	28.6-64.04		
	53.9			53.8%
	40.1			(28.5-79.1)
" " " 3 " "	73.9			(n = 20)
" " " 5 " "	68.4			
" " " 7 " "	75.5			
" " " 9 " "	77.0			
	49.6			
	53.6	35.6-82.7		
	60.0			
	54.5			
	60.4			

Recovery from B:

Recovery from B as percentage of total loaded: mean 2.23± 2.53%
(-.31-+4.76; p = 0.05)% i.e. < 5%

Recovery from B as percentage recovery from A=
(223/53.8 =) 4.1% < 5%.

ecdysone in this region migrates ahead of 20-OH-ecdysone, (i.e. R_F markers are reliable, although their loading densities may be relatively large compared with unknowns - they must show up under U.V.-illumination).

Experiment 2(d) Recovery of three ecdysteroids through C_{18} L.C. cartridges and TLC (determined by HPLC-U.V. spectrophotometry

A stock solution containing ecdsyone, 20-OH-ecdysone (each x 10^{-5}M) and makisterone A (10^{-6}M) was prepared. Twelve 200µl aliquots were passed through C_{18} cartridges (elution by 3ml methanol) and subjected to TLC, ethanol elution (3 x 1ml, pooled) and HPLC-UV spec. (3 x 50µl injection volume) with the original steroid mixture as a concentration standard.

Results: Table A4.II shows percentage recoveries of ecdysone, 20-OH-ecdysone and makisterone A after TLC-HPLC as measured by optical density (UV) comparison with standard solutions. There was no significant difference here between the more polar and less polar ecdysteroids (20-OH-ecdysone cf. ecdysone); and the mean recovery-value for these data considered as a whole places the population mean within broad limits (95% confidence: 3.7-79.1%). HPLC of the TLC-eluates showed some false positives especially for 20-OH-ecdysone, (i.e. quantities ostensibly of 20-OH-ecdysone, measured in terms of O.D. peak area, when that compound was not included in the loaded sample,) which suggests that HPLC-UV spectrophotometry alone is an unreliable means of identifying and quantifying ecdysteroid components from biological extracts.

Conclusions: Recovery of those ecdysteroids from $RR_{F-\mu}$ 0.48-1.53 = 41.42 $\pm$ 37.7% (u = 12, p = 0.05). Therefore an internal

Table A4.II

Experiment 2(d) Steroid recovery through TLC determined by HPLC-UV spec.

Steroid	load ($\mu g\ cm^2$)	Recovery (%)	mean% ± t.s.		
20-OH -ecdysone (β) (from RR_F-β= 0.57-1.8)	8.89	a 75.1 b 50.8 c 35.0 d 24.1 e 40.9	45.18 ± 53.63	40.49 ± 36.87	41.42 ± 37.7% (3.7-79.1) n = 12
Ecdysone (α) (from RR_F-α = 0.40-1.31)	9.74	a 22.8 b 36.2 c 27.3 d 56.7* e 36.0*	35.80 ± 36.15		
Mak. A (μ) (from RR_F-μ= 0.48-1.53)	0.91	a 65.8* b 26.3	46.05		

*20-OH-ecdysone false positives reported
+Ecdysone " " "
Value of mean % ± t.s. to 95% confidence level.

concentration standard is required. (Loading density range = 0.91-8.89µg cm^{-2}).

HPLC-UV spectroscopy is not sufficiently accurate for quantification since it yields false positive results in identifying peaks under these conditions. Therefore HPLC-coupled RIA or its equivalent is required.

Experiment 2(e) Recovery of Makisterone A through C_{18} LC cartridges and TLC

200µl of Makisterone A, 10^{-5}M was subjected to partitioning, elution from a Sep-PAK C_{18} cartridge using 4ml methanol, TLC (double-developed, 70 min. x 2; elution in 6 x 1ml Ethanol) and HPLC-UV spectrophotometry (injection volume 10µl) with 10^{-5}M Makisterone A as the reference concentration to determine recovery efficiency.

Results; Recoveries with reference to standard Makisterone A concentration were as follows:

	R R_F (Mak. A = 1.0)		
	<.38	.38-1.85	>1.85
%	0	51.88	0
	0	54.49	0
	0	40.07	0
	0	58.165	0
mean %	0	51.15 ± 24.7	0
(Limits (p = 0.05):		26.25-76.05)	

Conclusions: Recovery of Makisterone A = 51.15 (±24.7%, n = 4, p = 0.05) from RR_F (Mak. A) 0.38-1.85 (Loading density = 3.45µg cm^{-2}.)

Experiment 2 (f) Effect of Loading density on ecdysteroid recovery through the several procedures employed in sample preparation for HPLC (Section 2.14); and analysis of the contributions from these procedures to HPLC-UV-spectrophotometry chromatograms

An extract from stage P1 (1.035g) and aliquots of an ecdysteroid "cocktail" containing ecdysone, 20-OH-ecdysone and Makisterone A (10^{-5}M; 100, 200, 300µl) were subjected to: partitioning; passage through a C_{18} L.C. cartridge; transfer from methanolic (4ml) to ethanolic solution through siliconised glassware; TLC (double-developed) ethanol elution from 25.2cm^2 silica-gel (6 x 1ml ethanol, pooled) and HPLC-UV spectrophotometry (injections = 50µl). Three controls were prepared omitting parts of the preparative procedure. Quantification of recovery through this protocol was performed with reference to the original ecdysteroid mixture; and all samples were compared for peak areas to within an order of magnitude. Samples 1 and 2 were HPLC controls.

Samples:

1. 50% methanol/water (i.e. HPLC mobile phase);
2. Untreated standard solution (3 ecdysteroids, 10^{-5}M);
3. A pre-run TLC plate (unloaded), scraped R_F .24-.78 (1.5cm^2) and eluted;
4. Ethanol transferred to a siliconised round-bottomed flask and vortexed with silonised glass beads; TLC as (3);
5. Methanol passed through prepared Sep-PAK C_{18} cartridge; reduced to dryness in a siliconised round-bottomed flask; as (4) (This constitutes a full control for sample 9);
6. 100µl standard ecdysteroids solution (10^{-5}M) applied to a

TLC plate and recovered by ethanol elution;

7. as (6), 200µl ecdysteroids solution;
8. as (6), 300µl " "
9. Stage P1 (604 animals) extract prepared as for Chapter 5 (sections 2.14 and 5.1).

Results: Recoveries of ecdysone, 20-OH-ecdysone and makisterone A are shown in Fig. A4.7 as a function of loading density. In this experiment recovery decreased with increasing loading density but it appears to have stabilised at about 52.5% when loading at the origin was about 10µg ecdysteroid/cm^2 silica-gel. The semi-log graph shows that the three ecdysteroids behaved similarly but it also suggests two inflexions in the relation of recovery to loading density.

Fig. A4.8 shows the patterns of U.V. absorbing compounds contributed by the several steps in the protocol in terms of HPLC retention time. It can be seen that false-positive identifications of ecdysone and, especially, of 20-OH-ecdysone should be expected from HPLC-UV spectrophotometry alone.

Sources of peaks (nos. 1-22) based on Fig. A4.8 are as follows:-

1. 50% aqueous methanol; (therefore ubiquitous, from extraction);
2. Standard aqueous alcohol ecdysteroids solutions; TLC;
3. 50% aqueous methanol (unless preparation includes TLC);
4. Standard ecdysteroids solutions (" " " ");
5. Ethanol/siliconised glassware;
6. TLC;

7 + 8 Standard ecdysteroid solutions;

9 + 10 TLC;

11 Standard ecdysteroids solutions; TLC (unless P1-extract present);

12 Standard ecdysteroids solutions; TLC; P1-extract;

Figure A4.7

Experiment 2 (f): Effect of loading density on recovery of ecdysteroids through the HPLC preparation protcol

Loading density at the TLC origin (µg ecdysteroid per cm^2) vs. log_{10} recovery efficiency as measured by UV-spectrophotometry with reference to a standard mixture containing ecdysone (α), 20-OH-ecdysone (β) and Makisterone- A (µ). r, correlation coefficient for curve (b) = -0.80 > r(p = 0.1). Inflections occur at approx. 3.05µg cm^{-2} (65.6%) and 5.3µg cm^{-2}) (54%); Slopes (%/load) are (a) 0.57, (b) 0.32, (c) 0.14.

Fig. A4.7

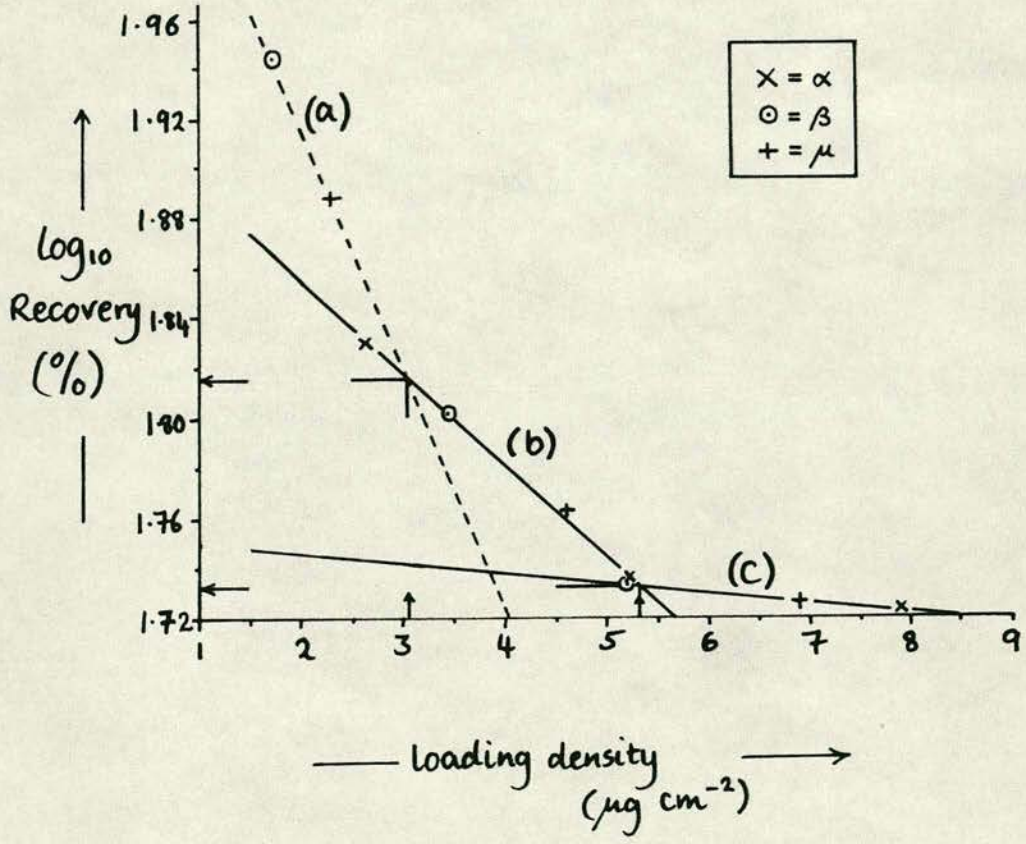
1·96
1·92
1·88
1·84
1·80
1·76
1·72
log10 Recovery (%)
(a)
(b)
(c)
× = α
⊙ = β
+ = μ
1
2
3
4
5
6
7
8
9
loading density (μg cm⁻²)

Figure A4.8

Experiment 2 (f): Analysis of sources of HPLC - UV spectrophotometry peaks in the protocol adopted for Drosophila sample preparation (λ = 254nm)

Samples 1-9 are shown as stylised chromatograms in terms of the order of magnitude (x) of the UV-peaks areas (units, 0-10) of their liquid chromatograms. Retention times are shown $\pm$ 5%. 22 peaks were recorded altogether. Sample 1-9 as in text. Standards: ecdysone (α), 20-OH-ecdysone (β) and Makisterone A (μ). Values are based on n chromatograms.

Fig. A4.8

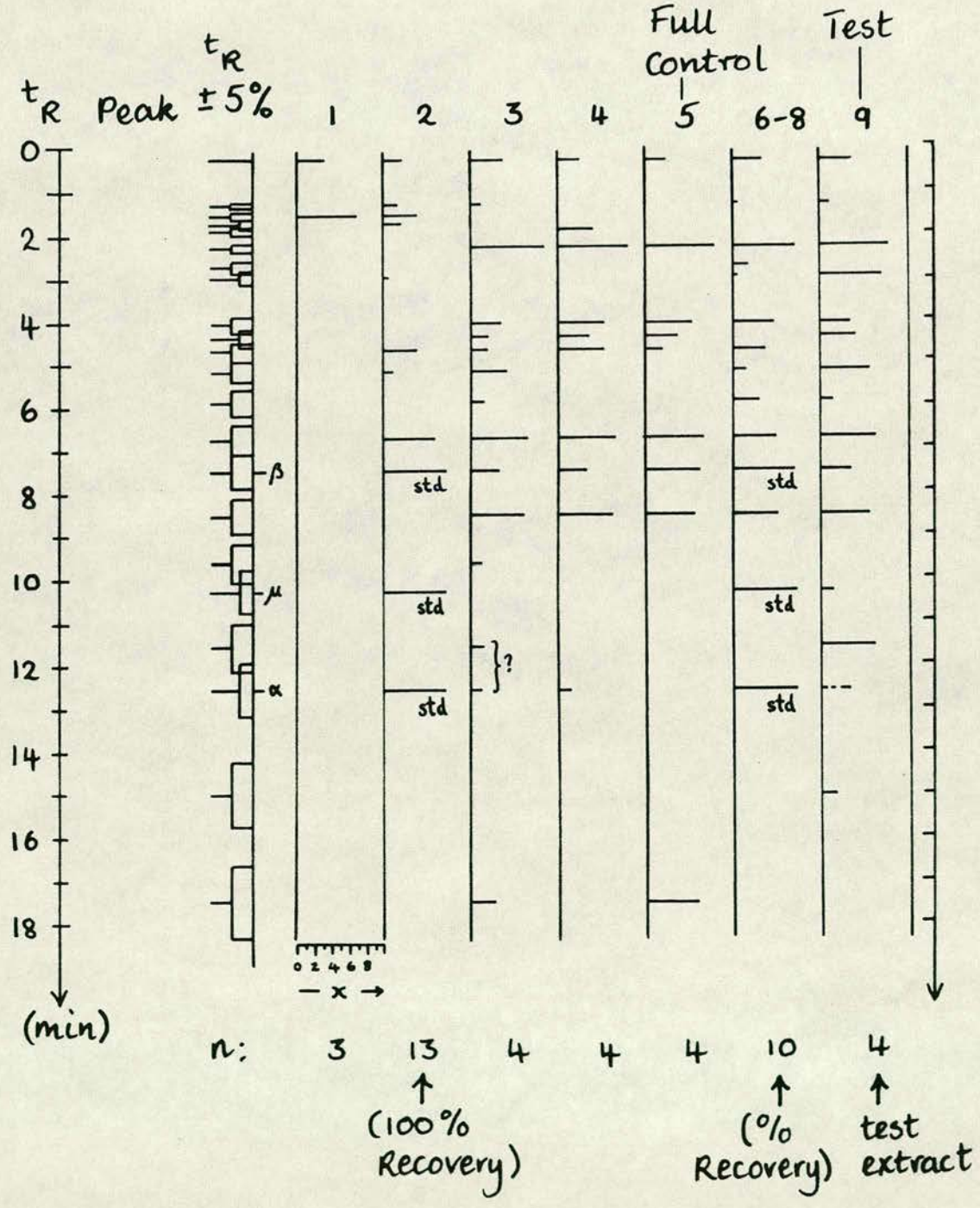
t_R Peak
t_R ± 5%
1
2
3
4
Full Control
5
6-8
Test
9
0
2
4
6
8
10
12
14
16
18
(min)
β
μ
α
std
std
std
?
std
std
0 2 4 6 8
— x →
n: 3 13 4 4 4 10 4
(100% Recovery)
(% Recovery)
test extract

13 TLC;

14 Standard ecdysteroids solutions; TLC;

15 20-OH-ecdysone; TLC;

16 + 17 TLC;

18 Makisterone A; P1 extract;

19 TLC; P1 extract;

20 Ecdysone;

21 P1 extract;

22 TLC;

In general; C_{18} cartridges (Sep-PAKs) and siliconised glassware do not contribute important U.V.-absorbing contaminants to the samples; and TLC contributes many contaminants but retains some contributed by earlier steps in the protocol (peaks 3 and 4).

Conclusions: Recovery of ecdysteroids from TLC = approx. 52.5% at high loading density (c. 10µg cm^{-2}). Recovery at lower densities of loading varies unpredictably with density, so an internal standard is required to measure concentrations of native ecdysteroids. Many UV-absorbing compounds are contributed to samples by steps in the purification procedure, especially TLC; so HPLC-UV spectrophotometry must be followed by quantification using another method (e.g. RIA).

A4.3 TLC: general conclusions

Table A4.III summarises the recovery efficiencies determined in Section A4.2 and presents a mean percentage recovery based on the six TLC determinations; but the variability is very high and, especially in view of experiment 2 (f) which shows a dependence of

Table A4.III

Summary: Ecdysteroid recovery estimates

Exp.	% Recov. (p=0.05)	n	Estimated load	*RR_F	No. Elutions	**Ratio plate area: total vol.
1	99.23	1	8.27pg (+P10-13)	-	-	-
2 a	42.5	1	8.37pg/cm^2	α:0.68-1.36	3	0.3
b	73.6	1	3.11pg/cm^2 +P10-13	α:0.73-1.47	6	2.75
	71.8	"	"	"	3	5.5
c	53.8 ± 25.3	20	0.025-0.3pg/cm^2	α:0.53-1.06	3	0.7-28.0
d	41.4 ± 37.7	12	0.91-8.89µg/cm^2	α:0.40-1.31 µ:0.48-1.53 β:0.57-1.80	3	2.2
e	51.15 ± 24.7	4	3.45µgcm^{-2}	µ:0.38-1.85	6	7.4
f	variable 52.5	9 -	1.73-7.89µg/cm^2 c. 10µgcm^{-2}	α:0.41-1.30 µ:0.46-1.46 β:0.52-1.64	6	4.2
2 a-f	52.5 + 29.8 (highly variable)	(6)	(max. range 0.025 -10,000 pg/cm^2	(max. 0.38-1.85)	(max. = 6)	(min. =0.3)

(* standard ecdysteroid R_F = 1.0)

(** cm^2 Silica gel/ml ethanol)

recovery on loading density, it is apparent that an internal concentration standard must be employed to monitor recovery through any protocol involving TLC that may be adopted for quantification of endogenous steroids in Drosphila. Furthermore, such quantification is unlikely to be effective by HPLC-UV spectrophotometry alone since false positive identifications of ecdysteroids were made by this method (experiments 2d and f), and, at least as far as 20-OH-ecdysone is concerned, this may be traced to a contaminant eluted from the TLC matrix which co-elutes with 20-OH-ecdysone in HPLC and is measurable at 254nm (experiment 2f). (In contrast to this finding in the microgram range of loading densities per cm^2 (experiment f), experiment 2 (c) in the picogram range suggests that loading density is unrelated to recovery efficiency).

Sometimes, then, low loading density enhances recovery. Once the thin layer chromatogram has been developed, recovery from the ecdysteroids zone is enhanced by high load (i.e. ecdysteroid burden cm^{-2}; experiment 2b) but this effect is reversible with serial elution. However, for a given load at $R_F > 0$ and a given elution volume, larger areas of silica-gel yield up their burden of ecdysteroid(s) more slowly than smaller areas (experiment 2b); so the ratio of silica-gel to eluent (ethanol) and the number of serial elutions should be considered in devising a protocol: In experiment 2(b) they were 2.75-5.5 and 3-6 respectively. Therefore the values adopted in experiment 2 (f) are acceptable, being 4.2 and 6 respectively; and note that in experiment 2 (b) 95% recoverable counts were obtained by only three serial elutions). The presence of a Drosophila extract appears to enhance ecdysteroid recovery

from the ecdysteroids zone (experiments 2(a) cf. 2 (b)), presumably by competitive irreversible binding of material to the silica-gel at the origin.

Makisterone A behaves very like ecdysone and 20-OH-ecdysone in its elution characteristics over a range of loading densities (experiment 2f; Fig. A4.7); so from this point of view it is a good candidate for the role of internal standard to facilitate sample preparation by HPLC and subsequent quantification by RIA.

Overlap of ecdysone with 20-OH-ecdysone in TLC is less than 10% (c. 9%, experiment 2(b); < 5%, experiment 2(c)).

Appendix Five

HPLC: Theoretical and technical information

A5.1 Aspects of lquid chromatography theory

For a given component:-

Retention (elution) time, t_R = injection-to-elution interval.

Retention (elution) volume V_R = volume of eluent equivalent to t_R.

Volumetric flow rate, $f_V = \frac{V_R}{t_R}$

Volume of column = Void volume, V_o (tube length to/from column negligible (= narrow gauge)).

Unretained conponents elute at the void volume, i.e.

$V_o = t_o$ = retention time for unretained solute.

Degree of retention of a solute is indicated by the Phase Capacity Ratio (capacity factor), K'

$$K' = \frac{t_R - t_o}{t_o} = \frac{V_R - V_o}{V_o}$$

i.e. retention time is measurable in units of void volume.

(Retention time, t_R has been referred to directly throughout this study).

If rate of movement of eluent (1ml min^{-1}), Linear flow velocity = u, then:

$u = L/t_o$ and

$u = f_v/a$

....where L = column length (10cm)

a = mean cross-sectional area of eluent in column

(pi x 0.42 cm^2)

Let linear velocity of a given solute be U_s;

then $U_s/u = t_o/t_R = {}^1/(1+K')$

i.e. $U_s \alpha 1/t_R$

Band width W for a given solute increases as the square of
the distance migrated within the column, d_R;
the elution volume V_R; and
the retention time, t_R.

Band dispersion, or "Height equivalent to a theoretical plate",

$$H = \frac{(\text{Band width, W in terms of distance})^2}{\text{Column length, L}} \times 0.0625$$

$$= \frac{(\text{Band width, W in terms of time})^2}{t_R} \times 0.0625.L$$

N = number of plates equivalent to the column (Theoretical Plate Number)

= L/H = 16(L/W in terms of distance)^2

= 16(t_R/W in terms of time)^2

= 16(V_R/W in terms of elution volume)2

In practice

$$N = 16(V/\text{Peak width})^2 \quad (= 1{,}000\text{-}20{,}000)$$

For two components A and B:-

Resolution, R = Peak separation/mean peak width

$$= \frac{t_R((B)) - t_R((A))}{0.5(W_{(B)} + W_{(A)})}$$

where W is peak width in terms of distance;

$$= \frac{V_R(B) - V_R(A)}{0.5(W_{(B)} + W_{(A)})}$$

where W is peak width in terms of volume (R is dimensionless)

References: Knox, J. H. (1978)

Waters Associates Inc. (1982).

A5.2 HPLC-system operation (Waters/LKB)

Apparatus: Waters Associates Tri-module automated HPLC system:-

Waters Intelligent Sample Processor, WI-SP 710B;

System Controller 720;

Data Module M730;

in conjunction with "SuperRac" 221 Fraction Collector (LKB, Broma) (all programmable); and Red-pak C_{18} column (8mm i.d.) mounted in RCM-100 radial compression module, (Rad-PAKs protected by Guard-PAK pre-column inserts);

Fixed wavelength UV-absorption detector 441 (filter = 254nm);

Two constant-delivery pumps, A and B (6000A Waters' Solvent

delivery system pumps);

4ml sample vials ± limited-volume inserts

± self-sealing septa;

Pre-column filter interposed between Wisp and RCM-100.

A5.2.2 HPLC Program

Program for 20 min. isocratic operation with (1) collection of eluate fractions from unknowns and (2) standards directed to waste, (as Chapter 5)

A)Data module:

Parameter number	Function	Value/Status
2	Chart speed	0.3 (cm min^{-1})
3	Plot mode	0 (OFF)
4	Pen 2	0 (OFF)
5	Pen 1 zero-position	10 (% Full-scale)
6	Pen 2 zero-position	0
7	Auto-zero	1 (ON)
8	GPC/LC	1 (LC)
9	Calibration	(0) (ON/OFF automatic)
20	Auto-parameters	0 (OFF)
21	Peak width	(optimised)
22	Noise rejection	(optimised)
62	Percent window (i.e. t_R recognition)	5 (%)
11-14	Calibration Table - see below	
36-39	Calibration Averaging Routine-see below.	

Calibration Table:

Parameter:	11	12	13	14
Code:	id	RT	Co	R_F
Function:	(standard peak No)	(t_R, min)	(Concentration) x 10^{-5}M	(Response Factor)
Example:	1 (=β)	7.8	5.1	
	2 (=μ)	10.75	7.0	
	3 (=α)	13.2	8.5	

(Response Factors are computed automatically and revised).

Calibration Averaging Routine - coordinated with System Controller Operation and Methods tables (q.v.)

Parameter	Function	Value
36	Injections per vial	3
37	No. standard injections	(1 x 3 =) 3
38	Samples between standards	4
39	Number of cycles (for averaging of response factors)	0

System operated from System Controller (RUN/STOP).

B) System Controller:- Pump Set 1 (for standards):

Pressure: high limit = 2000 psi (with Rad-PAK)

Pump	Solvent
A	1:1 MeOH/water
B	Methanol

Initial Conditions/Gradient Table:

Time(m)	Flow(ml min^{-1})	%A	%B	Curve
0	1	100	0	-
20	1	100	0	6
21	1	0	100	6
25	9	0	100	6
26	9	0	100	6
27	3	100	0	6
29	3	100	0	6
30	1	100	0	6
45	0	100	0	11

Pump Set 2 (for samples):

As Pump Set 1 with the addition of "external events" to control the fraction collector:-

External Events

Time	No	Status	(Function =)
0.01	1	ON	Start (i.e. first tube)
20.00	3	ON	Hold (i.e. Waste)
29.90	3	OFF	"
30.00	2	ON	Return (i.e. recommence cycle)

Operation Table:

Op. No.	Time	Vials From	Vials Thru	Method
1	-	1	1	1
2	-	2	5	2
3	-	1	1	1
4	-	6	9	2

Method Table

Method No.	Name	Pump Set	Column	Detector
1	-	1	-	-
2	-	2	-	-

C) WI-SP:-

Injection volume 100(µl)

Number of injections (e.g.) 3

Run Time 20 (min)

Equilibration Delay 10 (min)

Standards routine:

Number of standards in set = 1 (82XX = 8201)

Rerun standards every 4 vials (72XX = 7204)

These system messages are not used unless the run is to be operated from the WISP (using only one pump set): "Zero-case" programming).

(Injector-system purges may be programmed only when the run is operated from the WISP:

89XX (Purge duration 0.1 min) = 8910

90XX (Compression check for bubbles in sample) = 9001).

D) LKB SuperRac

Collected in the Time mode:

Rac: B

Mode: time

Fraction size: 30 (sec)

Fraction number: 40

Delay Size 35 (sec)

A5.2.3 Technical details

Mobile-phase preparation (1:1 methanol/water): Water was filtered/degassed first using HAWP 04700 (0.45μm); followed with an equal volume of methanol using IFHUP 04700 (0.50μm) (Millipore). Components were mixed in situ and degassing continued for c. 2 minutes.

Priming of the pumps: Both pumps were operated on methanol and were therefore maintained indefinitely without priming from scratch. After degassing solvents in the reservoirs, the delivery lines to pumps A and B were cleared of residual solvent from the last operation to avoid bubble-formation in the detector cell.

Sample vials were not filled to capacity, and PTFE septa, when used (not self-sealing), were pierced with a pin to allow rapid pressure- equilibration during injection.

Pumping rate: Zero flow-rate was approached through 1ml/min to avoid instantaneous depressurisation of the column. This would otherwise produce "fines" which migrate within the column and affect the chromatography.

Pre-column filter: This fine mesh filter was cleaned frequently

by sonization in "Decon" (1:40 water) followed by rinses in water and methanol.

Pump inlet manifold filters were cleaned periodically by passage of DMSO through solvent select valve 3, (approached and left via methanol).

Cleaning the fluid-line: (The Rad-PAK column was replaced by a dummy cartridge).

a) Injector to fraction-collator: Injected aliquots of DMSO (50µl).

b) Solvent reservoirs to fraction-collector: reservoirs filled with DMSO; Gradient Table Initial conditions = 50% pump A + 50% pump B; Program WISP to purge 5 mins. (7950); Flushes controlled manually, increasing flow rate to high pressure (less than 2000 p.s.i.); Returned to aqueous methanol, methanol.

Other solvents employed: Decon (1:40 aqueous); n-heptan; dichloroethane.

c) Column: Column reversed in RCM-100, (Guard-PAK replaced), and subjected to protracted methanol flush.

Use of the "WISP": Although it was useful to be able to perform automatic quantification from many samples, and despite the fact that it was desirable to inject small aliquots of dilute sample so as not to overload the column, nevertheless the WISP was prone to mechanical failure and, because the program-capability of this systemn did not allow purges to be performed whilst at the same time collecting sample fractions and rejecting standards, it injected progressively smaller amounts of sample during exhaustive preparative-HPLC of 1ml extracts. This gave more opportunity for chromatographic conditions, and hence retention times, to change during the accumulation of eluate fractions, necessitating the

collection of more than one set of fractions from a given sample for RIA. In retrospect it can be seen that the samples should have been injected as single aliquots (followed by a few washes); and a Waters model U6K manual injector was obtained for this purpose (currently in use).

Appendix Six

Can Drosophila imaginal discs serve in an ecdysteroid bioassay?

The classical "ecdysone" bioassays involved injection of moulting hormone into ligatured dipteran abdomens (e.g. Calliphora; Shaaya and Karlson, 1965). They share one disadvantage of RIA in being unable to indicate which ecdysteroid is causing a given response; and they offer an additional hazzard - abdomens can metabolise the prohormone ecdysone to its 20-hydroxylated active derivative. (see review by Richards, 1981b). Imaginal discs will evaginate in vitro in the presence of 20-OH-ecdysone (Guillermet and Mandaron, 1980; and Chihara et al. (1972) have reported the inhibition of evagination by JH - Richards, 1981b). Richards, (1981b) comments that it is important to obtain effective titres of ecdysteroids both within individual tissues and within the haemolymph, and that despite the value of RIA we still need new bioassays for function, preferably with tissues shown to have little or no metabolic capacity for ecdysteroids and also responding rapidly enough to exclude indirect stimulation. So could imaginal discs serve in this capacity ? Their response (evagination), being morphological initially, could be monitored more conveniently than the responses of other tissues (e.g. salivary gland polytene chromosome puffing; fat body polypeptide secretion; cuticle-secretion from epidermal cells, Richards, 1981b); they show a differential response to ecdysone and 20-OH-ecdysone in respect of the concentration required to effect morphogenesis (Granger and Bollenbacher, 1981); but they do not

effect conversion from ecdysone to 20-OH-ecdysone (Gilbert, 1974): Unlike ligatured abdomens, discs are relatively discrete tissue-types, which is important when the hormones subject to analysis are known to be interconverted *in vivo*; (cf. juvenile hormones (Richards 1981b); Postlethwait (1974) uses whole abdomens in a bioassay for JH activity in disrupting adult cuticle development). RIA must be matched by a procedure which can distinguish between moulting hormone analogues. Perhaps for routine analyses where HPLC or GLC-MF are impracticable a disc bioassay could have a role.

Experimental

In a preliminary investigation leg and wing imaginal discs were removed from late third instar larvae (LIII) and cultured overnight in 50µl Sheilds and Sang's medium NS + Serum V (a gift from Dr. Martin Milner) in Falcon tissue culture wells (3040F Microtest II) with or without male larval fat body from which the testes had been removed. At time zero the cultures were charged with the additives shown at Table A6.I including ecdysone, 20-OH- ecdysone, and these steroids as recovered from silica-gel TLC plates (with fluorescent indicator; Eastman) together with control preparations lacking steroid. After one day at room temperature the cultures were scored for evagination.

Like bioassays employing whole abdomens the results shown at Table A6.I are based on the predominant response of a group of tissues/animals, so not all of the false positive or negative results are shown. A model has been tested: It is assumed that

Table A6.I Ecdysteroid Bioassay trial

Additives	Culture	+/- Male Larval Fat body (- testes)	3 Experiments: Predominant Response (d.1) (+/- evagination)	Prediction (+/- evagination)	Contra-dictions
None	1	-	-	-	
	2	+	-	-	
α	3	-	+	-	*
	4	+	+	+	
β	5	-	+	+	
	6	+	+	+	
TLC: (ethanol eluate)	7	-	-	-	
	8	+	-	-	
Methanol/TLC	9	-	-	-	
	10	+	-	-	
α/TLC	11	-	-	-	
	12	+	+/-	+	(*)
β/TLC	13	-	-	+	*
	14	+	+	+	

Culture conditions:
Imaginal discs = approx. 8 (prothoracic legs and wings mixed);
Medium = Shields and Sang's tissue culture medium + Bovine Serum V (Milner);
Ecdysteroid solutions 10^{-5}M, ecdysone (α) or 20-OH-ecdysone (β)

discs will respond to 20-OH-ecdysone 10^{-5}-10^{-6}M by evaginating (Guillermet and Mandaron, 1980) but that ecdysone will be relatively ineffective in inducing evagination unless accompanied by metabolically-active fat body able to convert the prohormone into its 20-hydroxylated derivative. Results which do not confirm the predictions of this model are indicated (*). The system is not worth calibrating since the number of discs involved would make RIA a more useful assay for quantity; but in general there is a trend towards qualitative discrimination between the two steroids. However, there are false results, both positive and negative, (not involving the controls - the system is capable of recognising the presence of ecdysteroid without being confounded by contaminants from TLC plates). The contradictions may well result from the small number of discs employed (= never more than 15; about 5 when *). The cultures were not prepared in a sterile flow hood. It remains to be seen whether precursors of ecdysone or other metabolites apart from 20-OH-ecdysone are recognised in this system.

This pattern of results is in marked contrast to that reported by Mandaron (1973) who found (in contrast to most other studies - see his introduction) that discs evaginated (and indeed, differentiate) <u>in vitro</u> with ecdysone, not 20-OH-ecdysone to which they were unable to respond physiologically. 20-OH-ecdysone instead inhibited development of the discs, regardless of the presence of larval fat body. These results may have been an artifact of the culture medium, (medium M, Mandaron, (1973)).

Conclusion

Late third instar imaginal discs respond *in vitro* to ecdysteroids by evaginating, a response which is not elicited by blank controls or contaminants likely to be eluted from silica gel in the course of recovery of steroids after methanolic extraction. With some refinement the system may be able to distinguish between ecdysone and 20-OH-ecdysone; or, by comparing the disc responses with and without fat body quantitatively, it may be useful in recognising mixtures of these ecdysteroids without resorting to chromatography.

Appendix Seven

J. Embryol. exp. Morph. Vol. 66, pp. 57–80, 1981
Printed in Great Britain © Company of Biologists Limited 1981

Staging the metamorphosis of *Drosophila melanogaster*

By S. PAUL BAINBRIDGE AND MARY BOWNES[1]
From the Department of Molecular Biology, University of Edinburgh

SUMMARY

A sequence of 51 visible changes is described during the course of metamorphosis in *Drosophila melanogaster*, and a series of 24 convenient stages is defined for use in the experimental analysis and exploitation of this part of the insect life cycle. The duration of each stage is estimated and times are suggested for batch collections of symphasic animals.

INTRODUCTION

The imaginal discs of *Drosophila* have been widely used in the study of animal development because they exhibit a wide difference between the time of cell determination and that of the expression of the determined state which results in the formation of the adult cuticle. The embryo is the site of the formation of the discs; the larval instars are the sites of cellular proliferation and the source of the discs for experimentation; and the adult bears the results of such experiments in the form of cuticle markers, either on its surface or on metamorphosed implants in the abdomen; so these phases of development are well known. But the events of metamorphosis have generally received less attention, possibly because of the technical difficulties involved. In the cyclorrhaphous Diptera, including *Drosophila*, the last larval cuticle is tanned and retained throughout metamorphosis as a hard case inside which the developing imaginal hypoderm is at first extremely delicate. In addition, much of the larval structure disintegrates as the various organ systems are histolysed and reconstituted. Nevertheless, 'pupation' has recently attracted attention because during this period the realization of the determined state is achieved.

Methods for staging a continuous process have been developed for other systems, e.g. Bownes (1975), for *Drosophila* embryos; Nieuwkoop & Faber (1967), for *Xenopus* tadpoles. No method exists for *Drosophila* pupae, however, although *timed* animals were employed by Robertson (1936) and Bodenstein (1950) to construct a timecourse of the anatomical changes seen in sectioned material. This takes no account of differences in rate of development between

[1] *Authors' address:* Department of Molecular Biology, University of Edinburgh, Kings Buildings, Mayfield Road, Edinburgh EH9 3JR, Scotland.

individuals and between the sexes. Rate studies on timed animals were reviewed by Ashburner & Thompson (1978). Bliss (1926) noted four staging criteria but found their timing to be erratic. Several authors recorded the effect of a diurnal rhythm upon eclosion and the greater time required by males to reach eclosion (e.g. Powsner, 1935; Kalmus, 1940; Bakker & Nelissen, 1963).

This paper presents a practical system for the staging of living prepupae and pupae and a method for collecting some batches of animals all in the same stage from timed plates without laborious hand sorting. However, it must be emphasized that staging is useful precisely because it eliminates variation due to stock and culture condition differences, and therefore any timings adopted from our data must be checked first and, if necessary, modified accordingly. Where possible our teminology follows that recommended by Fraenkel & Bhaskaran (1973) for cyclorrhaphous dipterans in general.

It is hoped that this staging method will facilitate a precise approach to the study of metamorphosis together with its underlying molecular mechanisms regulating gene expression.

MATERIALS AND METHODS

All observations were made using an Ore-R stock of *D. melanogaster* maintained on yeasted Lewis's medium at $25 \pm 0{\cdot}1$ °C and exposed to a 12:12 h day/night cycle until collected for use in this study unless otherwise stated in the text. The colour of the 'yellow body', identified according to Bodenstein (1950), was checked on Instant Drosophila Food (Carolina Biological Supply Co.). The Malpighian tubules are identified according to Wessing & Eichelberg (1978).

(*a*) *Establishing the sequence of events and some extreme timings*

White prepupae were picked from the sides of culture bottles at random times throughout the day/night cycle and placed in pupation plates consisting of sealed Petri dishes lined with moist filter paper. Collections continued for about 20 min, after which time some individuals had become pale brown and were discarded. Any larvae still able to crawl were also discarded. The plates were stored in the dark and withdrawn for observation at various times throughout metamorphosis. Time zero was therefore puparium formation (P.F) + 20 min. max. Records of observations were made at 30 min. intervals and the data were pooled. The flies remained fairly synchronous during puparation, becoming less so as pupation proceeded. 256 observations were made of 44 plates, each of which contained about 25 flies. In a separate experiment we determined the viability under these conditions to be 97 % (total 946).

The typical sequence of events (i.e. visible changes) was assembled, together with a range of times at which each event had been seen to occur. The animals were examined on a white background using a Wild dissecting microscope with lateral illumination close to the stage, interposing the tip of a pair of watchmaker's forceps between the lamp and the puparium to cast a shadow over any feature which may be obscured by surface reflexion but which would show up with light scattered inside the animal – this was particularly true of the Malpighian tubules and the meconium. The puparia were wetted for observation.

(*b*) *Durations of stages by frequency in a population of continuous age distribution*

Five mature males and five mature females were placed in each of four fresh culture bottles and kept in constant darkness to encourage continuous egg laying. On days 11–14 mixed populations of prepupae and pupae could be seen on the sides of the bottles. Adult flies were etherized, sexed, staged and counted.

Prepupae and pupae were then removed, washed, staged and counted. Staging was performed on a random sample from a bottle's total population and lasted no more than 1 h, because development continued during this time. Living animals were employed since freezing and fixation altered their coloration and other staging characteristics.

(*c*) *The photography*

Animals were collected, washed and staged as above (*b*). The characteristics employed here as staging criteria may be observed through the puparium, but to facilitate the taking of photographs this cuticle is best removed from pupae. The dissections and subsequent photography were performed on animals submerged in 1 % agar in a tissue culture dish. A Wild dissecting microscope was used with a × 50 objective and fitted with a Photoautomat MPS 55 and camera attachment. Illumination was from above using Volpi Intralux Fibre Optics 150H against a dark field.

OBSERVATIONS AND RESULTS

(*a*) *The sequence of visible events during metamorphosis*

The following list of 52 numbered events is presented in the order most typical of animals observed under the conditions defined above. Each stage is given both a numerical and a verbal designation, and each is preceded by the change(s) diagnostic of its beginning. Extreme times at which events have been observed to occur in individual animals are given where available (Ext.). Note that these are not extreme stage *durations* from the pooled observations, (c.f. Table 3). Numbered changes 1–47 are indicated on Figs. 1–6 for which the following list constitutes a running legend. A developmental series of photographs of whole animals is shown (Figs. 7–12) and photographic details of staging criteria are given (Figs. 22–31).

Third-instar larva

(1) Stops feeding, climbs bottle wall:

Stage L1 (*Post-feeding*) (Fig. 1)

(2) Stops crawling (reversible until 5);
(3) Everts anterior spiracles:

Stage L2 (*Spiracles everted*) (Fig. 1)

(4) Withdraws three apparent anterior segments;
(5) Body shortens;
(6) Sticks to wall of culture bottle:

Prepupa

Stage P1 (*White puparium*) (Figs. 1, 7)

(7) Posterior spiracles and ridge between anterior spiracles tan orange (Ext. 0–½ h);
(8) Stops wriggling completely (Ext. 1 h);
(9) Puparium becomes brown to the unaided eye (Ext. 20 min–1 h):

Stage P2 (*Brown puparium*) (Fig. 1)

(10) Male gonads become less distinct; (may still be faintly distinguished in stage P3) (Ext. 0–3 h);
(11) Oral armature stops moving permanently (Ext. 1–5 h);
(12) Dorsal medial abdominal contractions stop, (i.e. heart stops pumping) (Ext. 1–6½ h);
(13) Gas bubble becomes visible within the abdomen (Ext. 3 h). (It is not known how this bubble forms; but it appears to have tracheal associations when dissected out, and it fails to develop in submerged prepupae):

Figs. 1–6. Diagrammatic representation of the visible events observed during metamorphosis. Segments of individual figures are presented in reading order: *a*, *b*, *c*, *d*. Not all changes are employed as criteria for staging. Numbers in parentheses correspond to the list of visible changes presented in the text. Staging criteria are further illustrated by photographs (Figs. 7–31). Figs. 1–5 are dorsal views, Fig. 6 ventral.

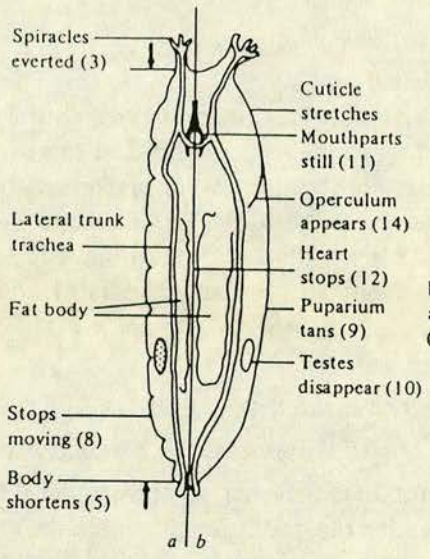

Fig. 1

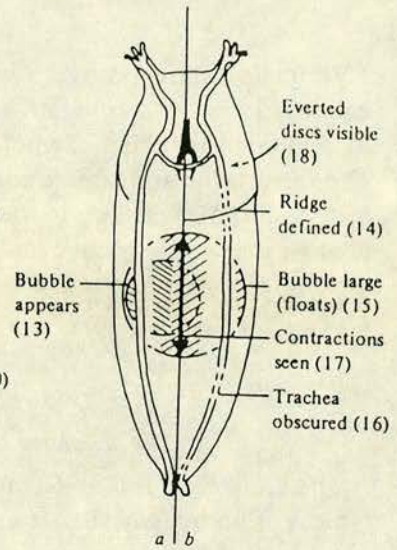

Fig. 2

Fig. 1. Stages L1 (Post-feeding) to P2 (Brown puparium). The left side shows half of the un-contracted late third instar larva, drawn the same length as its other half a few hours later, which is shown on the right. Thus the boundary divides the drawing unequally, and the two halves are not to scale.

Fig. 2. Stages P3 (Bubble prepupa) to P4 (Buoyant). The bubble which appears within the abdomen is shown firstly small and often to one side of the animal, and secondly large and visible dorsally. Contracting muscles are seen stretched across the surface of the bubble.

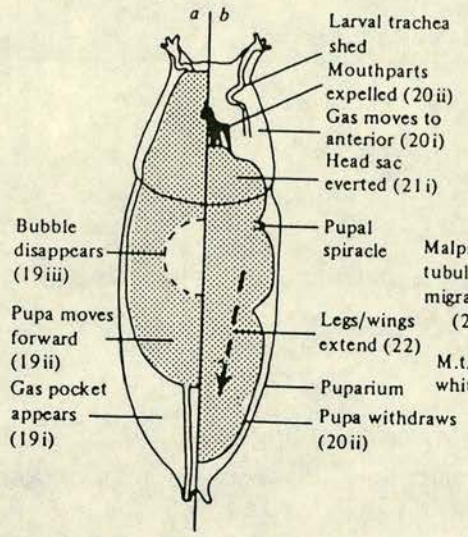

Fig. 3

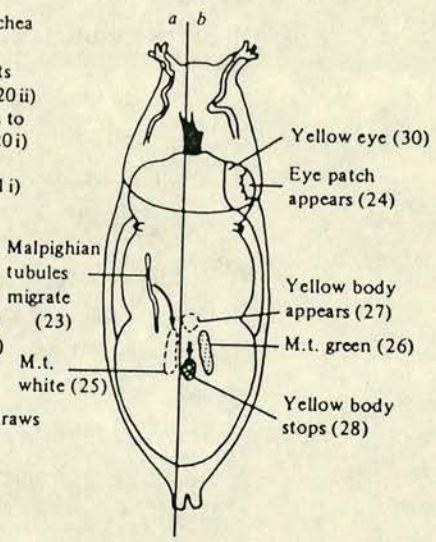

Fig. 4

Fig. 3. Stages P4 (Moving bubble) to P5 (Malpighian tubules migrating). The pupa is shown in two positions within the puparium, firstly at the anterior end during shedding of the posterior tracheal linings and secondly in its final position after displacement of gas to the anterior end (see also Figs. 24–26) and head eversion. All tracheal connexions with the outside of the puparium are broken. The arrow represents the ventral extension of the appendages by hydrostatic pressure. The pupal spiracle marks the insertion of the lateral trunk trachea in the larva/pupa.

Fig. 4. Stages P5 (Malpighian tubules migrating) to P7 ('Yellow body'). The white enlarged initial segments of the anterior Malpighian tubules (M.t.) are first visible in the thorax but move through the constriction into the abdomen where they may at first be completely obscured. Later, they become faintly visible again and eventually turn green. The 'yellow body' appears at the thorax–abdomen junction as a dark shadow and is most prominent after moving to lie between the M.t.'s.

Stage P3 (*Bubble prepupa*) (Figs. 2, 22)

(14) Ridge of operculum becomes distinct (Ext. 3–6 h):
Fraenkel & Bhaskaran (1973) place the larval-pupal apolysis at this point (4–6 h); i.e. the puparium becomes separated from the underlying epidermis, starting anteriorly. The resulting stage is termed the *Cryptocephalic pupa*. (However, see Figs. 24, 25. The movements of gas associated with pupal morphogenesis seem to be involved in the final shedding by the prepupa of the larval endocuticle, and so the larval/pupal apolysis is not *strictly* completed until a few seconds before head evertion (P4 (ii)). The cryptocephalic pupa is then to be regarded as only a transient stage if *physical separation* of successive cuticles is taken into account, i.e. stage P4 (ii) represents pupation.)

(15) Becomes positively buoyant (Ext. 6½–7 h):

Stage P4(i) (*Buoyant*) (Figs. 2, 23)

(16) Lateral trunk tracheae become obscured (Ext. 6½–8 h);

(17) Dorsal medial abdominal contractions observed, (also ventral; mid-intestinal peristalsis (Robertson, 1936)) (Ext. 9½–13½ h);

(18) Everted leg and wing discs become visible (translucent);

(19) Bubble appears in posterior portion of puparium, displacing the pupa anteriorly, and the bubble within the abdomen disappears (Ext. 12–13½ h):

Stage P4(ii) (*Moving bubble*) (Figs. 3, 24–26)

(20) Bubble is gradually displaced to the anterior portion of the puparium and the pupa withdraws to the posterior end (Ext. 12–13½ h);

(21) Imaginal head sac is everted and the oral armature of the larva is expelled (Ext. 12–13½ h):

Phanerocephalic pupa

Stage P5(i) (*Malpighian tubules migrating*) (Fig. 4)

(22) Legs and wings achieve their full extension along the abdomen (Ext. 12½–13½ h);

(23) Enlarged initial segments of anterior pair of Malpighian tubules move from thorax into abdomen;

(24) Translucent patch lacking adhering fat body cells becomes discernible in the middle of the eye region;

(25) Pair of white Malpighian tubules becomes visible dorsally in the abdomen when viewed in the shadow of forceps (Ext. 15–48 h):

Stage P5(ii) (*White Malpigian tubules*) (Figs. 5–7; Figs. 4, 8–10)

(26) Malpigian tubules become prominent and green (Ext. 13–48 h):

Stage P6 (*Green Malpigian tubules*) (Fig. 4)

(27) Dark green 'yellow body' appears between the anterior ends of the two Malpighian tubule segments, mid-dorsally at the anterior of the abdomen (Ext. 25–46 h):

Stage P7 (*'Yellow body'*) (Fig. 4)

(28) The 'yellow body' moves back between the Malpighian tubules:
Fraenkel & Bhaskaran (1973) place the pupal-adult apolysis at this point (34–50 h), i.e. the transparent pupal cuticle separates from the underlying epidermis, starting posteriorly. The resulting stage is termed the *Pharate adult;*

(29) Eye cup becomes yellow at its perimeter (Ext. 43–47 h):

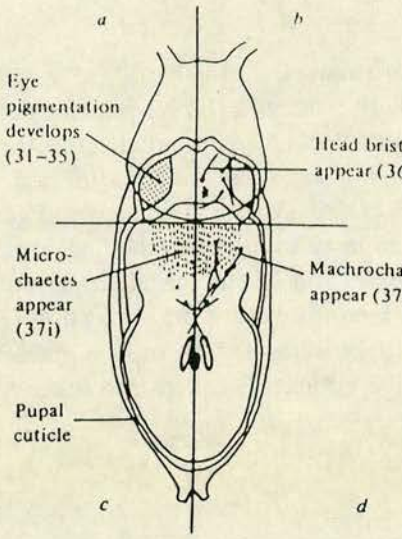

Fig. 5

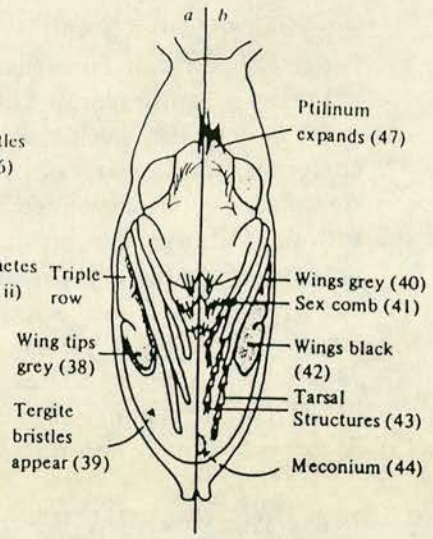

Fig. 6

Fig. 5. Stages P8 (Yellow-eyed) to P11 (Thoracic bristles). Pigmentation of the eye begins with yellowing of the perimeter. The rest of the eye colours (P8) and later darkens to amber (P9). The perimeter followed by the whole eye becomes pink at the beginning of P10 and this colour darkens to the mature bright red of adults (P10).

Fig. 6. Stages P11 to P15 (Meconium). The 'distal' part of the folded wing blade becomes grey (P12(i)), then the whole blade darkens (P12(ii)). The wings then undergo further darkening to appear black when folded, usually beginning with the 'distal' part again (P13). Tanning of the sex comb in P12(ii) allows one to separate the sexes from now on instead of sexing prepupae. Tarsal claws do not darken until P14 when the legs may also begin to twitch. The meconium appears dorsally as a green patch (P15(i)) which persists until eclosion (P15(ii)). Then, the ptilinum, an extensible sac between the eyes, is expanded by hydrostatic pressure from the contracting abdomen. The operculum breaks open anteriorly, the fly emerges and the ptilinum contracts while the abdomen shortens and widens (A1). The wings are unfurled (A2) and the banding of the abdomen becomes distinct (A3).

Stage P8 (*Yellow-eyed*) (Figs. 5, 11, 27)

(30) Pale yellow pigmentation spreads inwards across the eye;
(31) Eye becomes bright yellow;
(32) Eye colour changes to amber (Ext. 49–57 h):

Stage P9 (*Amber*) (Fig. 5, 12)

(33) Eye colour darkens to deep amber;
(34) Eyes become very pale pink (Ext. 71–78 h):

Stage P10 (*Red-eye Bald*) (Fig. 5)

(35) Eyes become bright red;
(36) Orbital and ocellar bristles and vibrissae darken:

Stage P11(i) (*Head bristles*) (Fig. 5)

(37) Dorsal thoracic micro- and macrochaetes become visible (Ext. 72½–77 h):

Stage P11(i) (*Thoracic bristles*) (Figs. 6, 28, 29)

(38) 'Tips' of folded wings become grey:

Stage P12(i) (*Wing tips grey*) (Figs. 6, 13–15)

(39) Bristles on abdominal tergites become visible, (Ext. 73–97 h):
(40) Wings become grey (Ext. 73–78 h):

Stage P12(ii) (*Wings grey*) (Fig. 6)

(41) Sex comb darkens;
(42) Wings darken to black (Ext. 75–86 h):

Stage P13 (*Wings black*) (Figs. 6, 16–18, 30, 31)

(43) Tarsal bristles darken and claws become black:

Stage P14 (*Mature bristles*) (Figs. 6, 19, 20)

(44) Green patch (the meconium) appears dorsally at the posterior tip of the abdomen (Ext. 87–103 h):

Stage P15(i) (*Meconium*) (Figs. 6, 21)

(45) Malpighian tubules and 'yellow body' become obscured by tanning of the tergites (Ext. 90–103 h);
(46) Legs are seen to twitch: flies able to walk if the puparium is removed prematurely (Ext. 90 h);
(47) Ptilinum expands by hydrostatic pressure, opening the operculum (Ext. 93–c. 105 h):

Stage P15(ii) (*Eclosion*)

(48) Eclosion is completed:

Exarate adult

Stage A1 (*Newly eclosed*) (Fig. 30)

(49) Wings unfold, flatten and harden;
(50) Abdomen becomes broader:

Stage A2 (*Wings extended*)

(51) Abdominal tergites tan to shiny brown:

Stage A3 (*Tergites tanned*)

Two other species of Drosophila were checked for the presence of the stages listed above. *D. simulans* (sibling species) is very similar to *D. melanogaster* except for the site of metamorphosis (on the food) which makes it impossible to collect L1 (post-feeding) as wandering larvae. *D. pseudo-obscura* (obscura group) also shows this character to a lesser extent, but some individuals do move away from the food. However, the diagnostic feature of Stage P7 is lacking in this species since the 'yellow body' is not observed until P8 and even at P9 has still to move into position between the M.t.'s. In both spp. the larval male gonads and the sex comb(s) (two in *D. pseudo-obscura*) are available as criteria for sexing individuals. In general then, the stages of metamorphosis in related species are similar to *D. melanogaster* though their proportional durations may differ.

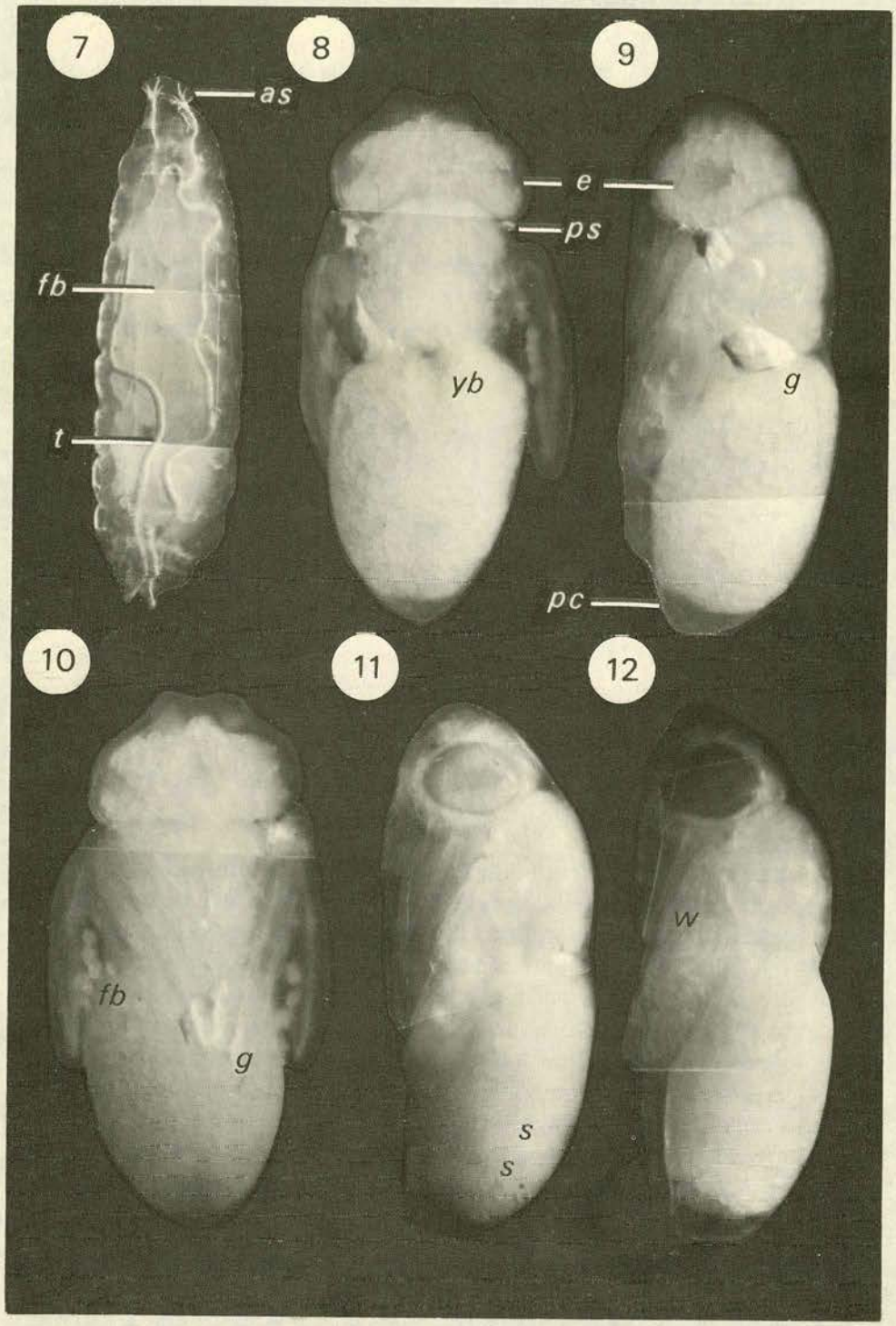

Fig. 7. Female of stage P1 (white puparium), dorsal view. Everted anterior spiracle (*as*); fat body (fb); lateral trunk trachea (*t*). Scale smaller then subsequent figures – contraction of the cuticle is incomplete.

Figs. 8–10. Stage P5(ii) (White Malpighian tubules), dorsal, lateral and ventral aspects respectively, after removal of the puparium. Pupal morphogenesis is complete. Fat body cells (*fb*) have entered the wing pouches by hydrostatic pressure and line the hypoderm except in the middle of the eye (*e*). Malpighian tubules must be viewed in shadow at this stage. The first signs of the 'yellow body' (*yb*) are visible here but it will move posteriorly by stage P7. The pupal spiracles (*ps*) were severed from the anterior larval spiracles at head eversion (P4/P5). Pupal cuticle (*pc*); gas pockets (*g*) adhering to *pc*.

Fig. 11. Stage P8 (Yellow-eyed), lateral view. Yellow pigment defines the extent of the compound eye. Abdominal segment margins (*s*) would not be distinct through the puparium.

Fig. 12. Stage P9 (Amber), lateral view. Eye colour has darkened. The wing is visibly folded within its sleeve of pupal cuticle (*w*).

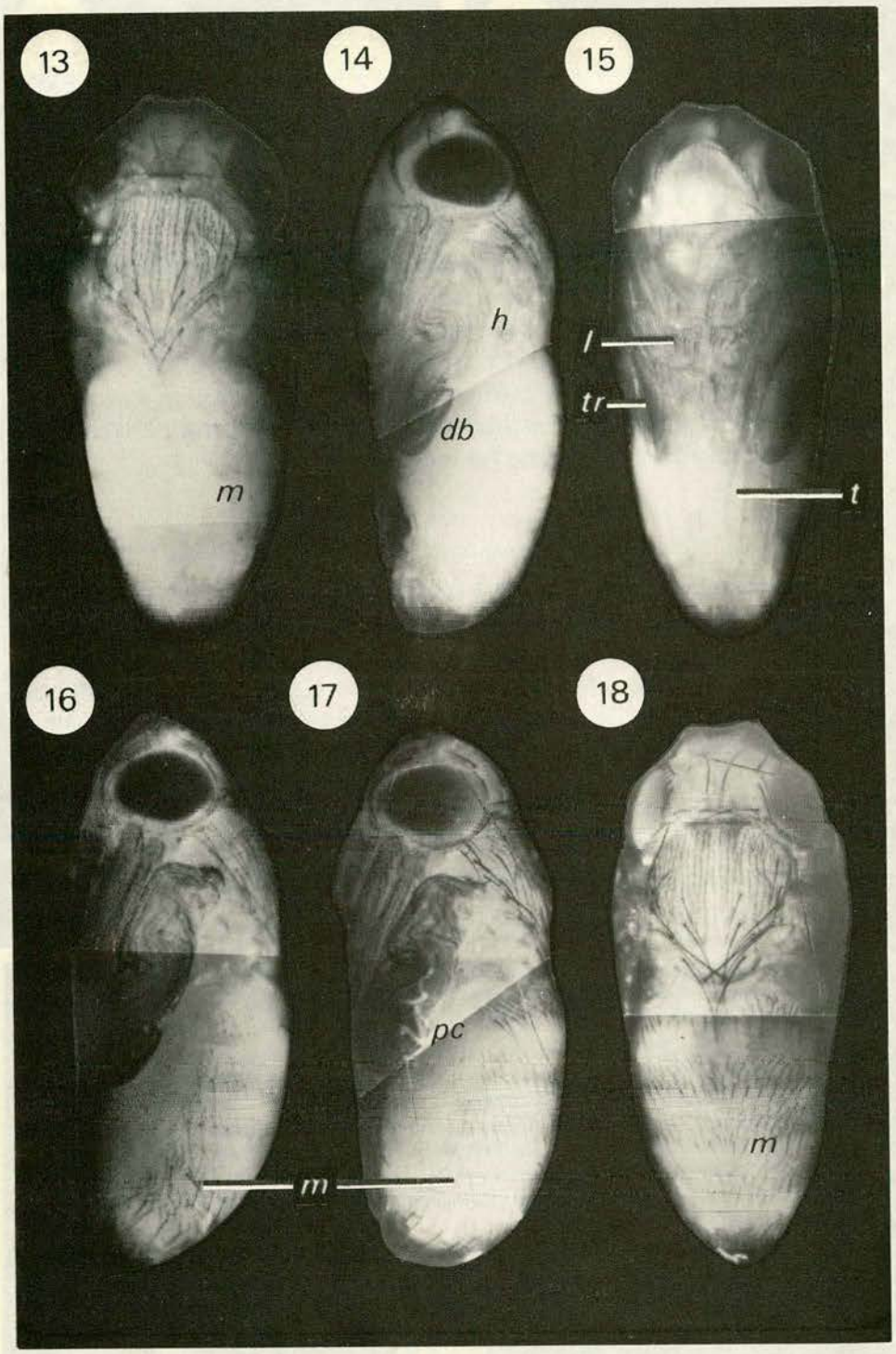

Figs. 13–15. Stage P12(i) (Wing tips grey), dorsal, lateral and ventral views respectively. Macrochaetes along the posterior margins of the abdominal tergites are beginning to darken (*m*). The wing hinge region (*h*) is untanned while the distal blade has darkened (*db*). Triple row (*tr*); dark proximal leg bristles (*l*); untanned tarsi (t).

Fig. 16. Early stage P13 (Wings black), lateral view. The wing has darkened further. Macrochaetes of tergites 2 to 6 (*m*).

Figs. 17 and 18. Late stage P13 (Wings black), lateral and dorsal views respectively. The whole wing is deeply tanned. After the pupal-adult apolysis, the degradation of the pupal cuticle (*pc*) continues. Here it has torn during removal of the puparium. At eclosion it is left inside the puparium. The Malpighian tubules and yellow body are no longer prominent. Tergite macrochaetes are very dark (*m*).

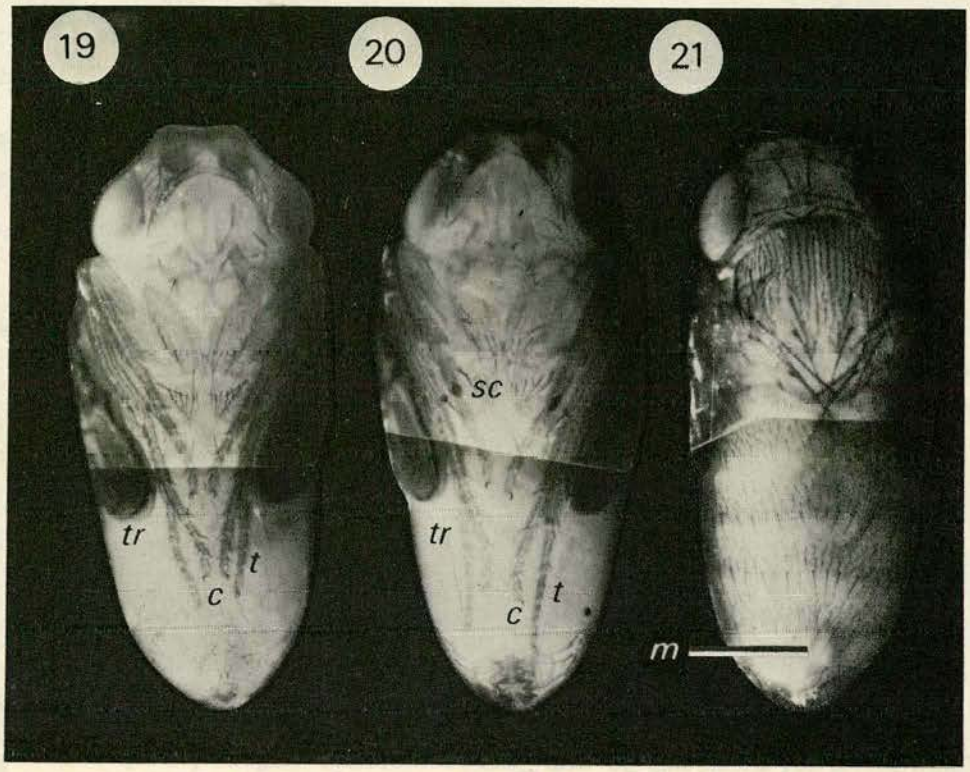

Figs. 19 and 20. Stage P14 (Mature bristles), female and male ventral aspects respectively. Tarsal bristles (*t*), claws (*c*), sex comb (*sc*) and triple row (*tr*) are black. The genital disc derivatives are obscured by the posterior spiracular papillae until the puparium is removed.

Fig. 21. Stage P15(i) (Meconium), dorsal view. The meconium (*m*) is a pale green patch. It will be expelled soon after eclosion (A1) or sometimes inside the puparium during eclosion (P15(ii)). It is composed of fluid derived from the 'yellow body' (Robertson, 1936).

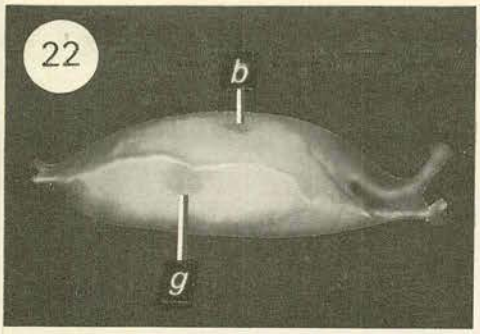

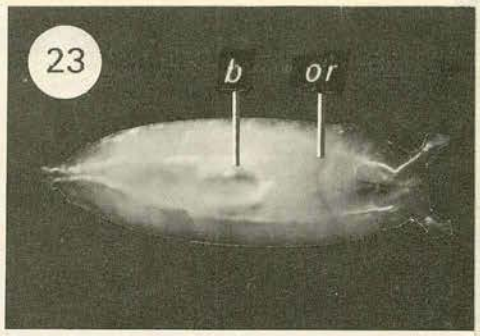

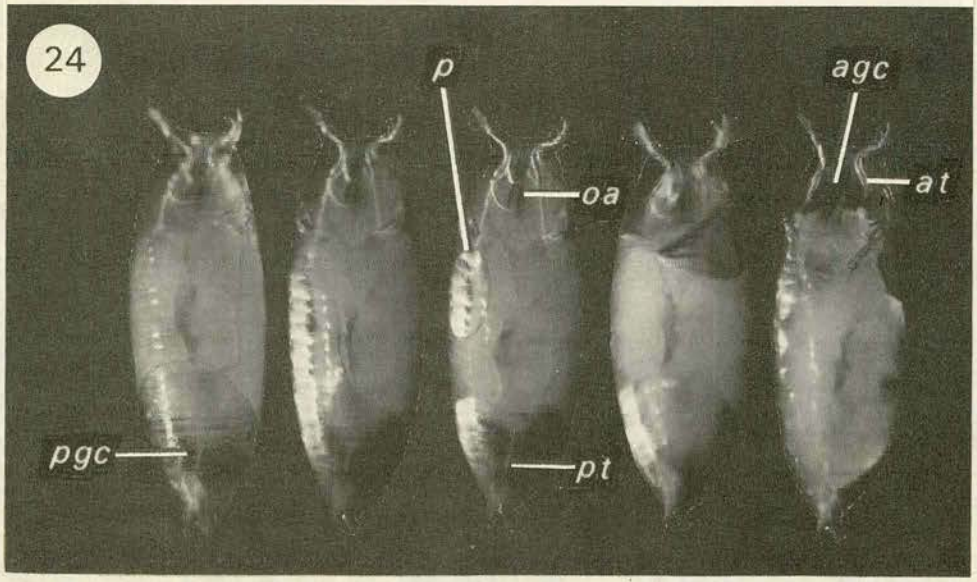

Fig. 22. The appearance of the translucent male gonads (*g*) of the larva/prepupa, seen here still visible in Stage P3 (Bubble prepupa) and distinct from the gas bubble (*b*). The female gonads are indistinguishable from fat body. Lateral view.

Fig. 23. The gas bubble (b) in an animal from Stage P4(i) (Buoyant), lying between and beneath the lobes of the fat body. The lateral trunk tracheae are still intact and, since head eversion has yet to occur, the pupa is cryptocephalic. Opercular ridge (*or*). Dorsal view.

Figs. 24–26 show pupal morphogenesis of the head and thorax in Stage P4(ii) (Moving bubble).

Fig. 24. Unequal time-lapse series of gas bubble movements within the puparium, and head eversion. Dorsal view. The first three photographs represent 1 min, and the whole process takes from 2–10 mins. Note the absence of a gas bubble. Posterior gas chamber (*pgc*); posterior tracheal lining (*pt*); gas pocket (*p*); larval oval armature (*oa*); anterior tracheal lining (*at*); anterior gas chamber (*agc*).

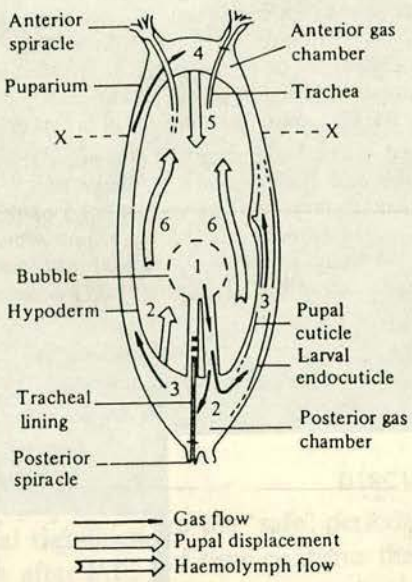

Fig. 25. Diagrammatic interpretation of the morphogenetic events shown at Fig. 24. Numbered arrows represent the sequence of events. (1) The bubble within the animal disappears as (2) the posterior gas chamber develops inside the puparium and the animal moves accordingly toward the anterior spiracles. As a result, the posterior linings of the lateral trunk tracheae are stretched across the chamber and so are shed (Robertson, 1936; Whitten, 1957*a*, *b*). Tracheal connexions are schematic, and gas may also exit through more anterior abdominal ecdysial openings (Whitten, 1957*a*). (3) The gas is shunted forward by slow wriggling using the larval abdominal muscles. Small pockets of gas pass between the pupal cuticle and the larval endocuticle or lining of the puparium (formerly called the 'prepupal cuticle') (Robertson, 1936; Poodry & Schneiderman, 1970), thus effecting the final physical step in the larval/pupal apolysis. The pupal cuticle is already continuous and rather tough. (4) The increase in size of the anterior gas chamber is accompanied by the backward-displacement of the pupa (5) and the withdrawal of the anterior tracheal linings. These and subsequent changes are independent of all the spiracles (Robertson, 1936) and the pupa now has no tracheal connexions with the puparium. Pupal spiracles mark the sites of connexions to the larval anterior spiracular papillae, (see Fig. 8). (6) By sudden muscular contractions, haemolymph and dissociated larval fat body is pumped into the folded head sac which then everts into the anterior gas chamber. The larval oral armature is expelled and lies ventrally inside the puparium. X–X marks the level of the antennal hypoderm within the puparium. The leg and wing discs, which are already evaginated, evert more slowly and extend along the abdomen during stage P5(i) to reach their pupal positions (see Fig. 10).

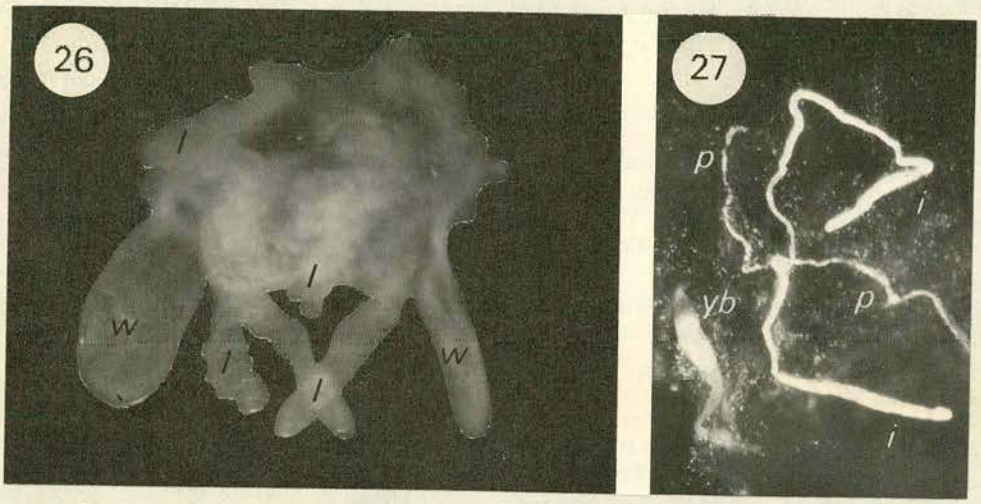

Fig. 26. The state of the thoracic imaginal discs towards the end of pupal morphogenesis, Stage P4(ii). The complex of fused discs with its continuous layer of pupal cuticle has been dissected out of the puparium. Evertion of legs (*l*) and wings (*w*) by hydrostatic pressure is incomplete. In the intact pupa, the anterior region is translucent while the abdominal hypoderm, of larval origin, is opaque.

Fig. 27. Displayed visceral dissection of the pupa shown at Fig. 11 to show the Malpighian tubules and 'yellow body' in Stage P8 (Yellow-eyed). Dissection performed in 1 % agar. Enlarged initial segments (*i*) of the anterior pair (*p*) of Malpighian tubules join the more slender posterior pair which are invisible in the intact animal. The 'yellow body' (*yb*) is the imaginal mid-intestine containing the larval mid-intestine, gastric caecae and proventriculus (Bodenstein, 1950).

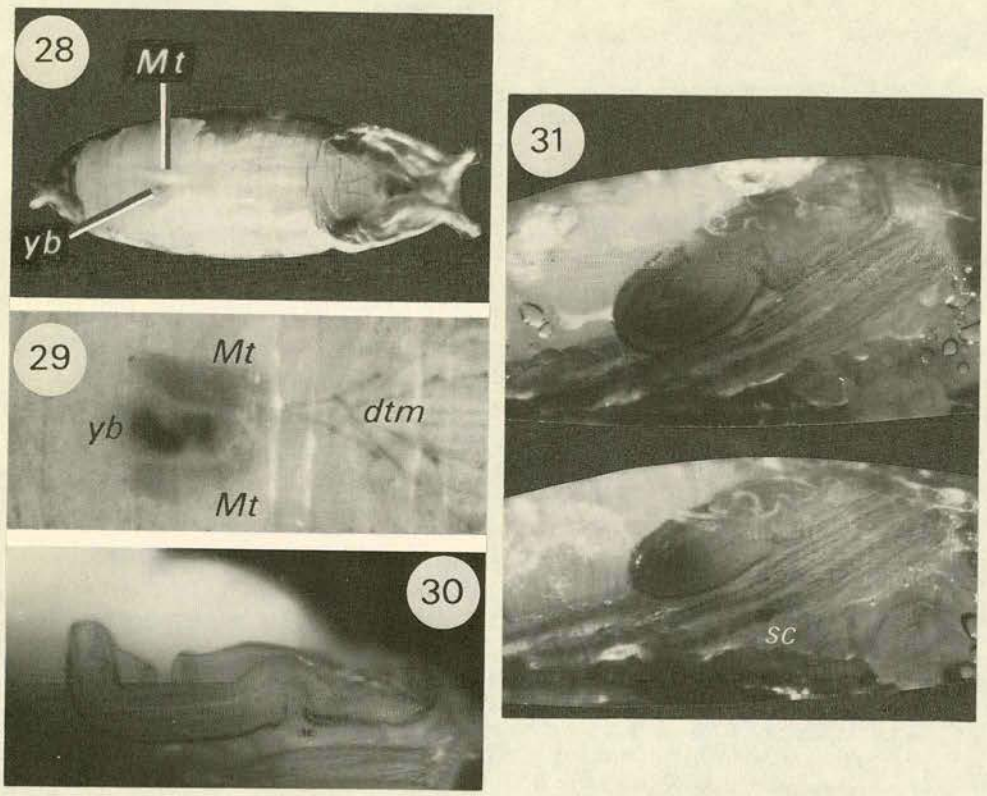

Fig. 28. The relationship between the Malpighian tubules (*Mt*) and the 'yellow body' (*yb*) *in situ*. Dorsal view, stage P11(ii) (Thoracic bristles). These structures are by now distinctly green. Note also the orbital and ocellar bristles, and the dark (i.e. red) eyes. Reflexions are due to gas trapped beneath the puparium.

Fig. 29. The mature relationship between the green Malpighian tubules (*mt*) and the almost black 'yellow body' (*yb*) in their most prominent condition in a stage P11(ii) animal before they begin to be obscured. Dorsal thoracic macrochaetes (*dtm*).

Fig. 30. The folding of the imaginal wing before eclosion. The puparium and pupal cuticle of the pharate adult shown at Fig. 16 (Stage P13 (Wings black)) have been removed, allowing the wing blade to unfurl prematurely. Compare Fig. 31.

Fig. 31. Comparison of the sexes after the darkening of the male-specific sex comb (*sc*) in stage P12(ii). Ventrolateral views, early stage P13 (Wings black). The wings are blackening distoproximally. Droplets of water line the puparium.

(*b*) *Estimation of durations of stages L1–A2 by frequency*

Flies were scored from cultures of four ages, namely 11, 12, 13 and 14 days. When the culture contained both F1 adults in stage A3 and post-feeding larvae (stage L1) it was deemed acceptable. Since laying commenced on day 0 and eclosion on day 10, this composite population approximated to a continuous age distribution, and mean percentage frequencies were then obtained for each stage within it. Table 1 shows the sampling procedure and the proportions L:P:A involved.

Table 1. *Sampling procedure*

Days after oviposition begins:			11	12	13	14	Mean
L1–A3 (total = 2286)			367	688	373	858	571·5
Sample size (= 100 %)			159	140	196	119	
Classes	L %		3·1	5·7	2·5	1·7	3·25 %
within	P %		93·1	88·6	71·5	44·5	74·4 %
sample	(Total*)		(148)	(124)	(140)	(53)	
	A %	♀	3·2	2·9	18·4	30·3	13·7 %
		♂	0·6	2·8	7·6	23·5	8·6 %
		Total	3·8	5·7	26·0	53·8	22·3 %

* These values become 100 % in Table 2, q.v.

Table 2 shows the observed frequencies of each stage in the various cultures and their calculated means. However, in order to relate the frequencies to a known time-span (P.F. to eclosion), the scores for all stages (L1–A2) are expressed as percentages of the total P1–P15 taken from Table 1 (*). The time taken from P.F. to eclosion was estimated from the observation of pupation plates. The mid-point of the range of eclosion times was about 100 h, that for females being 98 ± 5 h, and that for males 102 ± 4 h, giving a difference of 4 h which is in agreement with that reported by Powsner (1935), i.e. 3·7 h at 25 °C.

Table 2. *Frequencies of stages L1–A2, expressed as percentages of total P (i.e. P1–P15; see Table* 1*)

Day after oviposition begins:		11	12	13	14	Mean %
Total P		148	124	140	53	
Stage:						
L1	(Post-feeding)	2·0	5·6	3·6	3·8	3·8
L2	(Spiracles everted)	1·4	0·8	0	0	0·5
P1	(White puparium)	0	0·8	2·1	3·8	1·7
P2	(Brown puparium)	1·4	3·2	2·1	5·7	3·1
P3	(Bubble prepupa)	0·7	2·4	0·7	0	1·0
P4(i)	(Buoyant)	3·4	1·6	4·3	0	2·2
P4(ii)	(Moving bubble)	0	0	0·7	0	0·2
P4		3·4	1·6	5·0	0	2·4
P5(i)	(M.T. migrating)	0·7	0	0	3·8	1·1
P5(ii)	(White M.T.)	8·8	7·3	12·1	9·4	9·4
P5		9·5	7·3	12·1	13·2	10·5
P6	(Green M.T.)	14·9	27·4	10·7	1·9	13·7
P7	('Yellow body')	23·6	16·1	2·1	5·7	11·9
P8	(Yellow-eyed)	20·3	19·4	5·7	3·8	12·3
P9	(Amber)	17·6	12·9	14·3	11·3	14·0
P10	(Red eye bald)	0·7	0·8	1·4	13·2	4·0
P11(i)	(Head bristles)	0	0·8	0·7	3·8	1·3
P11(ii)	(Thoracic bristles)	0	0	0·7	1·9	0·7
P11		0	0·8	1·4	5·7	2·0
P12(i)	(Wing tips grey)	0	0·8	0·7	1·9	0·9
P12(ii)	(Wings grey)	0·7	1·6	2·1	0	1·1
P12		0·7	2·4	2·8	1·9	2·0
P13	(Wings black)	2·7	0	2·8	7·6	3·3
P14	(Mature bristles)	4·1	2·4	15·0	16·9	9·6
P15(i)	(Meconium)	0·7	1·6	20·7	9·4	8·1
P15(ii)	(Eclosion)	0	0·8	0·7	0	0·4
P15		0·7	2·4	21·4	9·4	8·5
A1	(Newly eclosed)	0	0	4·2	3·8	2·0
A2	(Wings extended)	0	0·8	8·6	45·3	13·7
						Total P = 100 %

So for a mixed-sex population the approximate duration of the period P1–P15 may be taken to be 100 ± 7 h. If we now assume that the size of any given stage in a random sample is directly related to the time spent in that stage, then a 1 % stage size indicates a duration for that stage of 1 h. This principle is employed in Table 3 to describe a timecourse for metamorphosis.

Table 3. *Timecourse of metamorphosis estimated by stage frequencies*

P1–P15 =	100 h: % ≡ h	100 h: Cumulative percentages ≡ timecourse	100 h: (Timed extremes (h) for comparison)	98 h (♀) Cumulative percentages Stage ends (h)	102 h (♂) Cumulative percentages Stage ends (h)	∴ ♀/♂ overlap (h)
Stage:						
(L.III)		−4.3		−4·2	−4·4	
L1	3·8	−0·5		−0·5	−0·5	
L2	0·5	0		0	0	
P1	1·7	+1·7		+1·6	+1·7	0–1·6
P2	3·1	4·8	½–3	4·6	4·9	1·7–4·6
P3	1·0	5·8	3–7	5·6	5·9	4·9–5·6
P4(i)	2·2	8·0		7·8	8·2	5·9–7·8
P4(ii)	0·2	8·2*	12–13½*	8·0	8·4	—
P4	2·4	8·2	6½–13½	8·0	8·4	5·9–8·0
P5(i)	1·1	9·3		9·1	9·5	8·4–9·1
P5(ii)	9·4	18·7		18·3	19·1	9·5–18·3
P5	10·5	18·7	12½–48	18·3	19·1	8·4–18·3
P6	13·7	32·4	13–46	31·7	33·1	19·1–31·7
P7	11·9	44·3	25–47	43·4	45·2	33·1–43·4
P8	12·3	56·6	43–57	55·5	57·7	45·2–55·5
P9	14·0	70·6	49–78	69·2	72·0	57·7–69·2
P10	4·0	74·6	71–77	73·1	76·1	72·0–73·1
P11(i)	1·3	75·9		74·4	77·4	—
P11(ii)	0·7	76·6	72½–	75·1	78·1	—
P11	2·0	76·6		75·1	78·1	—
P12(i)	0·9	77·5		76·0	79·0	—
P12(ii)	1·1	78·6	73–	77·1	80·1	—
P12	2·0	78·6		77·1	80·1	—
P13	3·3	81·9		80·3	83·5	(80·1–80·3)
P14	9·6	91·5		89·7	93·3	83·5–89·7
P15(i)	8·1	99·6	87–(100+)	97·6	101·6	93·3–97·6
P15(ii)	0·4	100·0	93–106	98·0	102·0	—
P15	8·5	100·0		98·0	102·0	93·3–98·0
A1	2·0	102·0		100·0	104·0	—
A2	13·7	115·7		113·4	118·0	104–113·4

* See Discussion.

(*c*) *Times for harvesting batches of symphasic animals*

The timecourse obtained from stage frequencies may be compared with timed extremes of stage durations which have been derived from pupation plate data and are shown in Table 3. For the most part these extremes will lie on either side of the frequency-ranges. Timecourses may also be calculated for males and females separately and these, when compared, reveal periods during which we can expect animals of both sexes to be in the same stage. This comparison is made in Table 3. A dash indicates that no such overlap occurs. We now consider the general timecourse and limit the durations of its component stages using both the extreme timings and the predicted male/female overlaps. In this way we define periods of development during which a high proportion of the animals collected together at P.F. may be expected to be in the same stage, i.e. symphasic. Such 'safe' collection periods are indicated at Fig. 32.

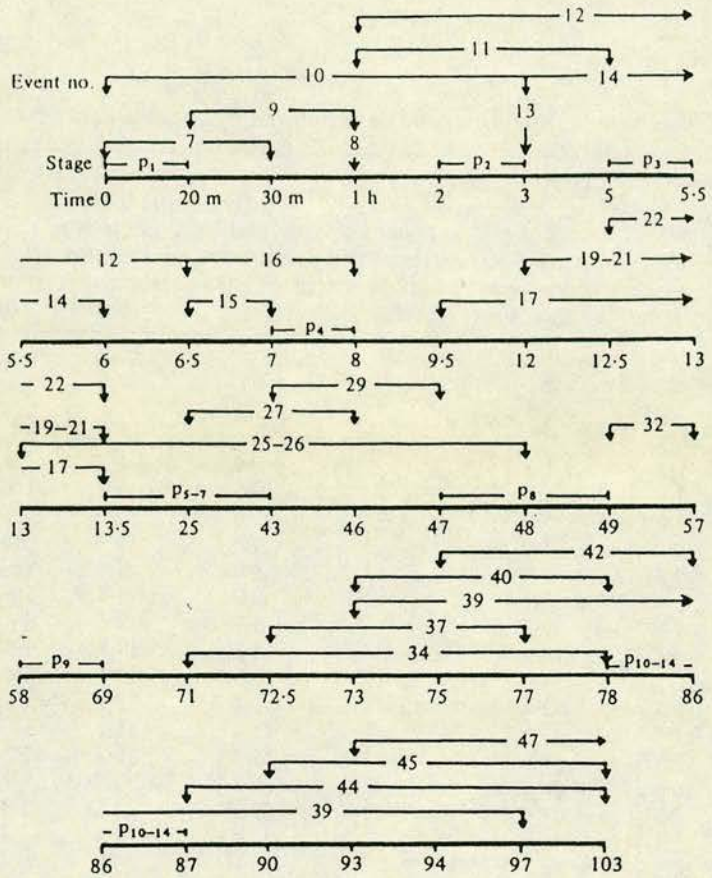

Fig. 32. Suggested periods for symphasic batch collections. Extreme times for numbered visible changes during metamorphosis are displayed against a non-linear time scale. The numbers refer to the order in the text, and arrows indicate the ranges over which these events were seen to occur in the pooled observations of pupation plates (mixed males and females). Where there is no overlap between staging criteria, 'safe' periods are predicted for the collection of homogeneous batches of animals, and these are restricted further where appropriate by the estimated male and female timecourses calculated from stage frequencies (Tables 2 and 3), to give bands of time when asynchronous males and females might be expected to be largely of the same appearance, i.e. symphasic. Due to the clustering of stages beyond P10 and the increasing asynchronization of the animals, this is impossible for a given stage beyond P9. Thus a visual check is always required, (see text) and stages P5–7, 10–15 must be hand-sorted from non-uniform batches. Some events are not respected, e.g. eye colour (no. 29) supersedes the appearance of the Malpighian tubules (nos. 25/26) in predicting entry into stage P8. Note that strictly this chart may not be used to age untimed pupae, which may very well lie beyond the safe periods chronologically.

Note that some stages cannot be obtained homogeneously by timing alone, (e.g. P6); and that in any case no sub-stages (i or ii) may be reliably obtained without there first being a visual check performed. So large symphasic batches of animals may be collected by plating prepupae at the beginning of P1, maintaining them at 25 °C in continuous darkness, and harvesting stages P2–P14 at the times shown. It must be emphasized, however, that these absolute times may vary between stocks, so, at least initially, batches must be checked and times modified if necessary. It is often convenient to segregate males and females as larvae or prepupae and time them separately, but still hand-sorting is required for the short stages P11(i)–P13. Note also that after P2 no sexing of flies may be done until P12(ii), though the females are generally larger than the males, so we recommend prior sexing of prepupae in stage P1 for experimental analysis of these stages. This is best done with wet animals on black filter paper. Some difficulty may be encountered at first in drawing the line between two stages, e.g. P8 (Yellow-eyed) and P9 (Amber). To avoid ambiguity in the resulting batches it is best to sort the plate into three sub-groups and discard the animals of intermediate colour. Subdivision of stages may also be performed given a large enough number of flies by employing an internal standard within a given

plate: e.g. 'early P9' may be collected when most of the members of the plate are still in P8, and similarly 'late P8' when most are already in P9. With practice, colour sorting may become sufficiently reproducible, though subjective, to allow of the collection of 'mid-stage x' in addition to 'early' and 'late' by sub-sorting of a plate. It is not convenient, however, to *sub-time* within a given stage, due to the large number of P1s required to yield a small group of synchronous animals later on.

DISCUSSION

The narrowness of the 'safe' periods (Fig. 32) where all flies are in the same stage for a period of time confirms that staging rather than timing is essential to studies of *Drosophila* metamorphosis since the members of a timed batch are unlikely to fall unequivocally into one developmental stage. It is possible that the extreme timings are partly due to the effect of the diurnal rhythm, as the prepupae were withdrawn from a day/night cycle and had therefore pupariated under these conditions. It seems likely, however, that the diurnal rhythm induces a block in the latter part of pupation: thus some flies eclose before the meconium becomes visible, while others retain this character but do not eclose for some time. But certainly the difference between males and females is established early, to the extent that, if pupae are segregated on the basis of early or late accession to P5 (i.e. time of head eversion), then they are also segregated sexually with an accuracy of about 70 %. The effects of the day/night cycle are decreased in the estimation of stage durations by frequency, as both oviposition and P.F. took place in the dark to avoid gating.

It is interesting to note that, whilst the timing and frequency data generally correspond, there is one short stage, that of bubble displacement and head eversion (P4(ii)) which is exceptional (see *Table 3). On the basis of frequency the duration of this stage is found to be 0·2 h, i.e. 12 min, which agrees with several observations of the process in action. It is predicted to begin at 8 h post-P.F., and repeated timings have shown P4(ii) to begin no earlier than 12 h at 25 °C. However, this is of no practical significance since P4(ii) can be most conveniently collected at 18 °C, 24–25 h after P.F. Here we assume that morphogenetic and other events employed in staging are not unrelated to the underlying biochemistry and so will not be uncoupled from the metabolism of the organism when metamorphosis occurs at other temperatures. Should the assumption prove to be justified, we may exploit other temperatures to obtain all stages at convenient times of day. Table 4 shows factors by which durations P1–15 at 18, 22 and 29 °C are shown in the literature to differ from that at 25 °C, (Ludwig & Cable, 1933; Powsner, 1935; Davidson, 1944). If we further assume that the proportions of time devoted to the various stages will remain constant, then these factors may be used, together with Table 3, to predict collection times for stages at other temperatures if these are more convenient; but now hand sorting becomes more than ever essential.

Table 4. *Durations of period from P1–P15 inclusive at four temperatures, estimated from the literature on timing of metamorphosis*

Temperature (°C)	Factor	Estimated durations (h)	
		Female	Male
		(our conditions)	(our conditions)
25	× 1 (reported)	98 (calculated)	102 (calculated)
18	× 2·07	203*	211*
22	× 1·31	128	133
29	× 0·79	77*	80*

* These eclosion times are in rough agreement with our observations of eclosion at these temperatures.

The abdominal bristles are found to tan unreliably in stage P12(i), and they have been observed to appear asynchronously across the abdomen, e.g. they appeared (tanned) first across the second tergite, then along the flanks of the abdomen, then dorsally. This may be related to Trepte's observations (1980) on *Sarcophaga barbata*, where the chromosome puffing pattern of bristle cells and the associated process of bristle differentiation were found to be autonomous in different regions of the body surface. In *Drosophila* the tanning of these bristles cannot be employed as a strict diagnostic feature for staging. The tanning of the tarsi is less variable but not unique to stage P13, although the tanning in the leg does appear to follow a sequence in which the tarsi are tanned last. This is in contrast to the order of acquisition of differentiative competence in the leg disc, (distoproximal to medial; Schubiger, 1974) and the sequence of bristle differentiation in the pupal leg, (distal to proximal; authors' observations).

The staging system presented in this paper constitutes a more precise approach to the problems of insect metamorphosis than has previously been available to *Drosophila* workers, who have used timed batches of animals, often of mixed sexes. The visible changes described here presumably do reflect the underlying metabolic state of the animal, so symphasic individuals may be assumed to be reasonably synchronous in metabolic terms, though they may well be of widely differing chronological ages. The hormonal basis of morphogenesis and differentiation could now be readily investigated by assaying hormone titres of the various stages to produce a profile for each sex (in preparation). Protein synthesis may be examined, e.g. in the tanning of cuticle and in those tissues – brain, fat body and Malpighian tubules – which survive metamorphosis. Finally, the involvement of hormones and other factors in the control of gene expression may be studied in relation to the secretion of both pupal and adult cuticles, the latter having well-characterized surface markers whose sequential appearance may be followed in successive stages. The clustering of stages at P10–P12 is fortunate since by this time asynchrony is most significant.

We should like to thank Jo Rennie for her excellent assistance with the photography. The work was supported by the Science Research Council.

REFERENCES

ASHBURNER, M. & THOMPSON, J. N. (1978). The laboratory culture of *Drosophila*. In *The Genetics and Biology of* Drosophila (ed. M. Ashburner & T. R. F. Wright), Vol. 2a. Academic Press.

BAKKER, K. & NELISSEN, F. X. (1963). On the relations between the duration of the larval and pupal period, weight and diurnal rhythm in emergence in *Drosophila melanogaster*. *Entomologia Experimentalis et Applicata* **6**, 37–52.

BLISS, C. I. (1926). Temperature characteristics for prepupal development in *Drosophila melanogaster*. *J. gen. Physiol.* **9**, 467–495.

BODENSTEIN, D. (1950). The postembryonic development of *Drosophila*. In *The Biology of* Drosophila (ed. M. Demerec). Hafner.

BOWNES, M. (1975). A photographic study of development in the living embryo of *Drosophila melanogaster*. *J. Embryol. exp. Morph.* **33**, 789–801.

DAVIDSON, J. (1944). On the relationship between temperature and rate of development of insects at constant temperatures. *J. Anim. Ecol.* **13**, 26–38.

FRAENKEL, G. & BHASKARAN, G. (1973). Pupariation and pupation in cyclorrhaphous flies (Diptera): terminology and interpretation. *Ann. ent. Soc. Amer.* **66**, 418–422.

KALMUS, H. (1940). Diurnal rhythms in the axolotl larva and in *Drosophila*. *Nature* **145**, 72–73.

LUDWIG, J. & CABLE, R. M. (1933). The effect of alternating temperatures on the pupal development of *Drosophila melanogaster*. *Physiol. Zool.* **6**, 493–508.

NIEUWKOOP, P. & FABER, J. (1967). *Normal Table of* Xenopus laevis (*Daudin*), 2nd ed. Amsterdam: North-Holland.

POODRY, C. A. & SCHNEIDERMAN, H. A. (1970). The ultrastructure of the developing leg in *Drosophila melanogaster*. *Wilhelm Roux' Archiv. devl Biol.* **166**, 1–44.

POWSNER, L. (1935). The effects of temperature on the durations of the developmental stages of *Drosophila melanogaster*. *Physiol. Zool.* **8**, 474–520.

ROBERTSON, C. W. (1936). The metamorphosis of *Drosophila melanogaster*, including an accurately timed account of the principal morphological changes. *J. Morph.* **59**, 351–399.

SCHUBIGER, G. (1974). Acquisition of differentiative competence in the imaginal leg discs of *Drosophila*. *Wilhelm Roux' Archiv. devl Biol.* **174**, 303–311.

TREPTE, H.-H. (1980). Autonomous puffing patterns in thoracic and abdominal polyten bristle cell chromosomes of the flesh fly *Sarcophaga barbata*. *Devl Biol.* **75**, 471–480.

WESSING, A. & EICHELBERG, D. (1978). Malpighian tubules, rectal papillae and excretion. In *The Genetics and Biology of* Drosophila (ed. M. Ashburner & T. R. F. Wright), Vol. 2c. Academic Press.

WHITTEN, J. (1957*a*). The post-embryonic development of the tracheal system in *Drosophila melanogaster*. *Ql J. Microsc. Sci.* **98**, 123–150.

WHITTEN, J. (1957*b*). The supposed prepupa in cyclorrhaphous Diptera. *Ql J. Microsc. Sci.* **98**, 241–250.

(*Received 16 June 1981*)

BIBLIOGRAPHY

ALDRICH, J. R., KELLY, T. J. and WOODS, C. W. (1982) Larval moulting hormone of trichophoran hemiptera-heteroptera: makisterone A, not 20-hydroxyecdysone. J. INSECT PHYSIOL. 28, 857-861

ASHBURNER, M. and THOMPSON, J. N. (1978) The Laboratory Culture of Drosophila In: The genetics and biology of Drosophila; Vol. 2a. Eds. ASHBURNER, M. and WRIGHT, T. R. F. Academic Press.

BAINBRIDGE, S. P. and BOWNES, M. (1981) Staging the metamorphosis of Drosophila melanogaster. J. EMB. EXP. MORPHOL. 66, 57-80.

BAKKER, K. and NELISSEN, F. X. (1963) On the relations between the duration of the larval and pupal period, weight and diurnal rhythm in emergence in Drosophila melanogaster. ENT. EXP. et. APPL. 6, 37-52.

BALLS, M. and BOWNES, M. (In Press). Metamorphosis. O.U.P.

BENTLEY, D., KESHISHIAN, H., SHANKLAND, M. and TOROIAN-RAYMOND, A. (1979) Quantitative staging of embryonic development of the grasshopper, Schistocerca nitens. J. EMB. EXP. MORPH. 54, 47-74.

BERGOT, B. J., JAMIESON, G. C., RATCLIFF, M. A. and SCHOOLEY, D. A. (1981) Identification of a new insect juvenile hormone and a method for JH titre determination using gas chromatography - mass spectroscopy. In: KLOZA (1981).

BERREUR, P., PORCHERON, P., BERREUR-BONNENFANT, J. and SIMPSON, P. (1979) Ecdysteroid levels and pupariation in Drosophila melanogaster. J. EXP. ZOOL. 210, 347-352 (ZIPGRAM).

BHASKARAN, G. (1972) Inhibition of imaginal differentiation in Sarcophaga bullata by juvenile hormone. J. EXP. ZOOL. 182, 127-142.

BLISS, C. I. (1926) Temperature characteristics for prepupal development in Drosophila melanogaster. J. GEN. PHYSIOL. 9, 467-495.

BODENSTEIN, D. (1947) Investigations on the reproductive system of Drosophila. J. EXP., ZOOL. 104, 101-152.

BODENSTEIN, D. (1950) The Postembryonic development of Drosophila. In: The Biology of Drosophila. Ed. DEMEREC, M. Hafner. (pp. 275-367).

BORDES, N., HANDLER, A., GHARIB, B. and DE REGGI, M. (1983) Changes in ecdysteroid and juvenile hormone titres in Drosophila, related to the initiation of vitellogenesis. Personal communication (preprint of a conference poster).

BORST, D. W., BOLLENBACHER, W. E., O'CONNOR, J. D., KING, D. S. and FRISTROM, J. W. (1974) Ecdysone levels during metamorphosis of Drosophila melanogaster. DEVELOP. BIOL. 39, 308-316.

BORST, D. W. and O'CONNOR, J. D. (1974) Trace analysis of ecdysones by gas-liquid chromatography, radioimmunoassay and bioassay. STEROIDS. 24, 637-655.

BOWNES, M. (1975) A photographic study of development in the living embryo of Drosophila melanogaster. J. EMB. EXP. MORPHOL. 33, 789-801.

BOWNES, M. (1980a) Ovarian synthesis of yolk proteins in Drosophila melanogaster. GENETIKA. 12, (1) 13-20.

BOWNES, M. (1980b) The use of yolk protein variations in Drosophila species to analyse the control of vitellogenesis. DIFFERENTIATION, 16, 109-116.

BOWNES, M. (1983) Interactions between germ cells and somatic cells during insect oogenesis. In: McLAREN and WYLIE (Eds.) Current Problems in Germ Cell Differentiation. C.U.P.

BOWNES, M., BLAIR, M., KOZMA, R. and DEMPSTER, M. (1983) 20-hydroxyecdysone stimulates tissue-specific yolk-protein gene transcription in both male and female Drosophila. J. EMBRYOL. EXP. MORPHOL. 78, 249-268.

BOWNES, M., DEMPSTER, M. and BLAIR, M. (1983b). Expression of the yolk protein genes in the mutant doublesex dominant (dsx^D) of Drosophila melanogaster. J. EMB. EXP. MORPHOL. 75, 241-257.

BOWNES, M., DUBENDORFER, A., and SMITH, T. (1984a) Ecdysteroids in adult males and females of Drosophila melanogaster. J. INSECT. PHYSIOL. (In Press).

BOWNES, M., BLAIR, M. and JOHNSON, P. (1984b) Transcription of the genes coding for the yolk-proteins in adult Drosophila females. (IN PRESS).

BOWNES, M., BLAIR, M. and SMITH, T. (1984c) Personal communication: The regulation of expression of the genes coding for the yolk-proteins in Drosophila. Paper for Hamburg International Entomology Congress (August 1984) (IN PRESS).

BOWNES, M. and HODSON, B. A. (1980) Mutant fs(1) 1163 of Drosophila melanogaster alters yolk protein secretion from the fat body. MOL. GEN. GENET. 180, 411-418.

BOWNES, M. and NÖTHIGER, R. (1981) Sex determining genes and vitellogenin synthesis in Drosophila melanogaster. MOL. GEN. GENET. 182, 222-228.

BOWNES, M. and REDFERN, C. P. F. (1984) Insect metamorphosis and its hormonal control. In: BALLS and BOWNES (IN PRESS).

BRIERS, T. and de LOOF, A. (1980) The molting hormone activity in Sarcophaga bullata in relation to metamorphosis and reproduction. INT. J. INVERT. REPROD. 2, 363-372.

CHIHARA, C. J., PETRI, W. H., FRISTROM, J. W. and KING, D. S. (1972) The assay of ecdysones and juvenile hormones on Drosophila imaginal dics in vitro. J. INSECT PHYSIOL. 18, 1115-1123.

CHIHARA, C. J., SILVERT, D. J., and FRISTROM, J. W. (1982). The cuticle proteins of Drosophila melanogaster: stage specificity. DEV. BIOL. 89, 379-388.

CHOMYN, A., MOLLER, G. and MITCHELL, H. K. (1979) Patterns of protein synthesis following heat shock in pupae of Drosophila melanogaster DEV. GENETICS. 1, 77-95.

DAVID, J. and CLAVEL, M. F. (1966) Essai de définition d'une température optimale pour le développment de la Drosophile. C. R. ACAD. SCI. PARIS. 262D, 2159-2162.

DAVID, J. and CLAVEL, M. F. (1967) Influence de la température d'élevage sur la mortalité larvo-nymphale et la durée de développment de la Drosophile. NATURALISTE CANAD. 94, 209-219.

DEAN, R. L., BOLLENBACKER, W. E., LOCKE, M., SMITH, S. L. and GILBERT, L. I. (1980) Haemolymph ecdysteroid levels and cellular events in the intermolt/molt sequence of Calpodes ethlius. J. INSECT PHYS. 26, 267-280.

DELACHAMBRE, J., BESSON, M. T., CONNAT, J. L. and DELBECQUE, J. P. (1980) Ecdysteroid titres and integumental events during the

metamorphosis of Tenebrio molitor. In: HOFFMAN (1980)

DELBECQUE, J. P. (1981) Production of ecdysteroids outside prothoracic glands in Tenebrio. In: LANZREIN, B. (1981) Abstracts of Vth ecdysone symposium, Gurten-Berne, Switzerland; May (1981).

DELBECQUE, J. P., HIRN, M., DELACHAMBRE, J. and de REGGI, M. (1978) Cuticular cycle and molting hormone levels during the metamorphosis of Tenebrio molitor (Insecta, Coleoptera). DEV. BIOL. 64, 11-30.

EL-IBRASHY, M. T. (1981) Bimodal effect of the corpus allatum on morphogenesis and reproduction of Spodoptera littoralis. In: KLOZA (1981).

FRAENKEL, G. and BHASKARAN, G. (1973) "Pupariation and pupation in cyclorrhaphous flies (Diptera): terminology and interpretation". ANN. ENT. SOC. AMER. 66, 418-422.

FRISTROM, J. W., NATZLE, J., DOCTOR, J. and FRISTROM, D. (1984) The regulation of a developmental sequence during imaginal disc metamorphosis. In: BALLS and BOWNES (IN PRESS).

GAREN, A., KAUVAR, L. and LEPESANT, J. A. (1977) Roles of ecdysone in Drosophila development. PROC. NAT. ACAD. SCI. 74, (11) 5099-5103.

GAVIN, J. A. and WILLIAMSON, J. H. (1976) Synthesis and deposition of yolk protein in adult Drosophila melanogaster. J. INSECT. PHYS. 22, 1457-1464.

GAVIN, J. A. and WILLIAMSON, J. H. (1978) J. INSECT. PHYSIOL. 24, 413-416.

GEE, J. D., WHITEHEAD, D. L. and KOOLMAN, J. (1977) Steroids stimulate secretion by insect Malphigian tubules. NATURE, 269, 238-239.

GIETZ, R. D., SAGE, B. A., O'CONNOR, J. D. and HODGETTS, R. B. (1983) A characterisation of the ecdysteroids and their relation to the appearance of Dopa Decarboxylase in Drosophila embryos. Personal communication.

GILBERT, L. I. (1974) REC. PROG. in HORMONE RES. 30, 347-390.

GILBERT, L. I. and FRIEDEN, E. (EDS) SECOND EDITION. Metamorphosis. A problem in developmental biology. PLENUM PRESS, NEW YORK (1981).

GILBERT, L. I. and GOODMAN, W. (1981) Chemistry, metabolism and transport of hormones controlling insect metamorphosis. In: GILBERT and FRIEDEN, (1981).

GRANGER, M. A. and BOLLENBACHER, W. E. (1981) Hormonal control of insect metamorphosis. In: GILBERT AND FRIEDEN, (1981).

GREENBERG, R. M. and ADLER, P. M. (1982) Protein synthesis and accumulation in Drosophila melanogaster imaginal discs: Identification of a protein with a non-random spacial distribution. DEV. BIOL. 89, 273-286.

GUILLERMET, C. and MANDARON, P. (1980) In vitro imaginal disc development and moulting hormone. J. EMB. EXP. MORPH. 57, 107-118.

HANAOKA, K. and HAGEDORN, H. H. (1980) Brain hormone control of ecdysone secretion by the ovary in a mosquito. In: HOFFMAN, (1980).

HANAOKA, Z. and OHNISHI, E. (1974) Changes in ecdysone titre during pupal-adult development in the silkworm, Bombyx mori. J. INSECT PHYS. 20, 2375-2384.

HANDLER, A. M. (1982) Ecdysteroid titres during pupal and adult development in Drosophila melanogaster. DEVELOP. BIOL. 93, 73--82.

HARKER, J. E. (1965) The effect of a biological clock on the developmental rate of Drosophila pupae. J. EXP. BIOL. 42, 323-337.

HARKER, J. E. (1965) The effect of photoperiod on the developmental rate of Drosophila pupae. J. EXP. BIOL. 43, 411-423.

HIRN, M. H. and DELAAGE, M. A. (1980) Radioimmunological approaches to the quantification of ecdysteroids. In: HOFFMANN (1980).

HODGETTS, R. B., SAGE, B. and O'CONNOR, J. D. (1977) Ecdysone titres during postembryonic development of Drosophila melanogaster. DEV. BIOL. 60, 310-317.

HOFFMANN, J. A. (ED) (1980). Progress in ecdysone research. ELSVERIER/NORTH HOLLAND BIOMEDICAL PRESS.

HORN, D. H. S., WILKIE, J. S., SAGE, B. A. and O'CONNOR, J. D. (1976) A high affinity antiserum specific for the ecdysone nucleus. J. INSECT PHYS. 22, 901-905.

JOESTEN, M. E., ROYSTON, M. E., JIMENEZ, M., WADEWITZ, A., MELIAN, D. and LOCKSHIN, R. A. (1982) Gain and loss of fluid in metamorphosing larvae of Manduca sexta. J. INSECT PHYSIOL. 28, 589-599.

JOWETT, T. AND POSTLETHWAITE, J. H. (1980). The regulation of yolk polypeptide synthesis in Drosophila ovaries and fat body by 20-OH-ecdysone and a juvenile hormone analogue. DEVELOP BIOL. 80, 225-234.

JUNGREIS, A. M. (1979) Physiology of moulting in insects. In: TREHERNE, BERRIDGE and WIGGLESWORTH; Advances in insect physiology. 14, 109-183. ACADEMIC PRESS.

KALMUS, H. (1940) Diurnal rhythms in the axolotl larva and in Drosophila. NATURE, 145, 72-73.

KAPLANIS, J. N., THOMPSON, N. J., DUTKY, S. R. and ROBBINS, W. E. (1979) The ecdysteroids from the tobacco hornworm during pupal-adult development five days after peak titres of moulting hormone activity. STEROIDS 34, (3) 333-345.

KAPLANIS, J. N., WEIRICH, G. F., SVOBODA, J. A., THOMPSON, M. J. and ROBBINS, W. E. (1980) Moulting hormones of the tobacco hornworm and milkweed bugs. Their chemistry and biochemistry. In: HOFFMANN (1980).

KARLSON, P. and SHAAYA, E. (1964) Der ecdysontiter während der insektentwicklung - I. Eine methode zur bestimmung des ecdysongehalts. J. INSECT PHYS. 10, 797-804.

KING, R. C. (1970) Ovarian development in Drosophila melanogaster. ACADEMIC PRESS, (N.Y.).

KISS, I., SZABAD, J. and MAJOR, J. (1978) Genetic and developmental analysis of puparium formation in Drosophila. MOLEC. GEN. GENET. 164, 77-83.

KLAGES, G., EMMERICH, H. and REMBOLD, H. (1981) Identification and titre of juvenile hormones in the fruit fly, Drosophila hydei. In: KLOZA (1981).

KLOSE, W., GATEFF, E., EMMERICH, H. and BEIKIRCH, H. (1980) Developmental studies of two ecdysone deficient mutants of Drosophila melanogaster. WILHELM ROUX ARCH. 189, 57-67.

KLOZA, A. M. (1981) Regulation of insect development and behaviour (Part 1). (International Conference in Karpacz, Poland, June 1980) Technical University of Wroclaw (1981)

KOOLMAN, J., SCHELLER, K. and BODENSTEIN, D. (1979). Ecdysteroids in the adult male blowfly Calliphora vicina. EXPERIENTIA 35, 134-135.

KOOLMAN, J. (1982) Ecdysone metabolism. INSECT BIOCHEM. 12, 225-250.

KRAMINSKY, G. P., CLARK, W. C., ESTELLE, M. A., GIETZ, R. D., SAGE, B. A., O'CONNOR, J. D. and HODGETTS, R. B. (1980) Induction of translatable mRNA for dopa decarboxylase in Drosophila: an early response to ecdysterone. PROC. NAT. ACAD. SCI. USA. 77, (7) 4175-4179.

KUMARAN, A. K. (1981) Reprogramming in insect epidermal cells: role of hormones. In: KLOZA (1981).

LAFONT, R., BEYDON, P., MAUCHAMP, B., SOMME-MARTIN, G., ANDRIANJAFINTRIMO, M. and KRIEN, P. (1981) Recent progress in ecdysteroid analytical methods. In: KLOZA (1981).

LAFONT, R., SOMME- MARTIN, G., MAUCHAMP, B., MAUME, B. F. and DELBECQUE, J. P. (1980) Analysis of ecdysteroids by high-performance liquid chromatography and coupled gas-liquid chromatography - mass spectrometry. In: HOFFMANN (1980).

LAGUEUX, M., HIRN, M. and HOFFMANN, J. A. (1977) Ecdysone during ovarian development in Locusta migratoria. J. INSECT. PHYSIOL. 23, 109-119.

LANGLEY, P. A. and ELY, R. (1978) X-ray investigation of gas bubble formation, and water loss in tsetse fly pupae. PHYSIOL. ENTOMOL. 3, 303-307.

LANZREEN, B., HASHIMOTO, M., PARMAKOVICH, V. and NAKANISHI, K. (1975) Identification and quantification of juvenile hormones from different developmental stages of the cockroach Nauphoeta cinere. LIFE SCIENCES, 16, 1271-1284.

LINDSLEY, D. L. and LIFSCHYTZ, E. (1972) The genetic control of spermatogenesis in Drosophila. In: The genetics of the spermatozoan. BEATTY, R. A. and GLUECKSOHN-WAELSH, S. (Eds); Edinburgh University, Department of Genetics.

LUDWIG, D. and CABLE, R. M. (1933) The effect of alternating temperatures on the pupal development of Drosophila melanogaster. PHYSIOL. ZOOL. 6, 493-508.

MADHAVAN, K. (1973) Morphogenetic effects of juvenile hormone and

JH mimics on adult development of Drosophila. J. INSECT PHYS. 19, 441-453.

MAETERLINCK, M. (1901) The life of the bee; translated by A. Sutro. George Allen, London.

MALTÉTE, F. (1962) Contribution a l'étude chronologique de l'embryogēnèse chez Locusta migratoria migratorioides R et F; développement des corps allates et des glandes ventrales de la tête. These de 3° cycle. Bordeaux.

MANDARON, P. (1973) Effects of α-ecdysone, β-ecdysone and inokosterone on the in vitro evagination of Drosophila leg discs and the subsequent differentiation of imaginal integumentary structures. DEVELOP. BIOL. 31, 101-113.

MARÓY, P. and TARNOY, K. (1978) Moulting hormone level during the last instar of Galleria mellonella larva. J. INSECT PHYS. 24, 325-327.

MAUCHAMP, B., LAFONT, R., PENNETIER, J-L and DOUMAS, J. (1981) Detection and quantification of the juvenile hormone 1 during the postembryonic development of Pieris brassicae L. In: KLOZA (1981).

MAVOR, J. D. (1927) A comparison of the susceptibility to X-rays of Drosophila melanogaster at various stages of its life cycle. J. EXP. ZOOL. 47, 63.

MILNER, M. (1977) The time during which β-ecdysone is required for the differentiation *in vitro* and *in situ* of wing imaginal discs of *Drosophila melanogaster*. DEVEL. BIOL. *56*, 206-212.

MILNER, N. P., CLARKE, G. S. and REES, H. H. (1982) Ecdysteroid metabolism in the Cotton Leafworm, *Spodoptera littoralis*. Abstract of presentation to the workshop: Hormones and Insect Development, held at the Royal Entomological Society, (March 1982).

MITCHELL, H. K. and MITCHELL, M. (1964) Mass culture and age selection in *Drosophila*. DROS. INFO. SERVICE *39*, 135-137.

MITCHELL, H. K. and PETERSEN, N. S. (1981) Rapid changes in gene expression in differentiating tissues of *Drosophila*. DEV. BIOL. *85*, 233-242.

MITCHELL, H. K., WEBER-TRACY, U. M. and SCHAAR, G. (1971) Aspects of cuticle formation in *Drosophila melanogaster*. J. EXP. ZOOL. *176*, 429-444.

MORGAN, E. D. and WILSON, I. D. (1980) Progress in the analysis of ecdysteroids. In: HOFFMANN (1980).

NEVILLE, C. (1978) The biology of arthropod cuticle. CAROLINA BIOL. SUPPLY CO.

NIEUWKOOP, P. and FABER, J. (1967) Normal table of *Xenopus laevis*

(Daudin). 2nd Edition, North-Holland, Amsterdam.

OHTAKI, T. and TAKAHASHI, M. (1972). Induction and termination of pupal diapause in relation to the change of ecdysone titre in the fleshfly, Sarcophaga peregrina. JAPAN. J. MED. SCI. BIOL. 25, 369-376.

PITTENDRIGH, C. S. and SKOPIK, S. D. (1970) Circadian systems V. The driving oscillation and the temporal sequence of development. PROC. NAT. ACAD. SCI. USA. 65, 500-507.

POODRY, C. A. and SCHNEIDERMAN, H. A. (1970) The ultrastructure of the developing leg in Drosophila melanogaster. WILHELM ROUX ARCHIV. 166, 1-44.

PORCHERON, P., FOUCRIER, J., GROS, C., PRADELLES, P., CARRIER, P. and DRAY, F. (1976) Radioimmunoassay of arthropods moulting hormone: β-ecdysone antibodies production and 125I-iodinated tracer preparation. FEBS LETTERS, 61, 159-162.

POSTLETHWAITE, J. H. (1974) Juvenile hormone and the adult development of Drosophila. BIOL. BULL. 147, 119-135.

POSTLETHWAIT, J. H. and SCHNEIDERMAN, H. A. (1970) A clonal analysis of development in Drosophila melanogaster: morphogenesis, determination, and growth in the wild-type antenna. DEV. BIOL. 24, 477-519.

POWSNER, L. (1935) The effects of temperature on the durations of the developmental stages of Drosophila melanogaster. PHYSIOL. ZOOL. 8, 474-520.

PRYDE, A. and GILBERT, M. T. (1979) Applications of high performance liquid chromatography. CHAPMAN AND HALL, LONDON.

REDFERN, C. P. F. (1981) Ecdysterone and ovarian development in Anopheles stephensi Liston (Diptera: Cuticidae). J. INSECT. PHYS. IN PRESS.

REDFERN, C. P. F. (1983) Ecdysteroid synthesis by the ring gland of Drosophila melanogaster during late-larval, prepupal and pupal development. J. INSECT. PHYSIOL. 29, 65-71.

REDFERN, C. P. F. (1984) Makisterone-A: A possible additional moulting hormone in Drosophila melanogaster grown on cornmeal-yeast media. PROC. NAT. ACAD. SCI. (IN PRESS).

REDFERN, C. P. F. and BOWNES, M. (IN PRESS) Prothoracic glands and the production of steroid hormones during the metamorphosis of holometabolous insects. In: BALLS AND BOWNES (IN PRESS).

REES, H. H. (1977) Insect biochemistry. CHAPMAN AND HALL, LONDON.

de REGGI, M., HIRN, M. H. and DELAAGE, M. A. (1975) Radioimmunoassay of ecdysone - an application to Drosophila larvae and pupae. BIOCHEM. BIOPHYS. RES. COMM. 66, (4) 1307-1315.

REMBOLD, H. (1981) Modulation of JH 111-titre during the gonotrophic cycle of Locusta migratoria, measured by gas chromatography - selected ion monitoring mass spectrometry. In: PRATT, G. E. and BROOKS, G. T. (EDS.) (1981) JUVENILE HORMONE BIOCHEMISTRY ELSEVIER/NORTH-HOLLAND.

REMBOLD, H. and HAGENGUTH, H. (1981) Modulation of hormone pools during postembryonic development of the female honey bee castes. In: KLOZA (1981).

REMBOLD, H., KREMER, J. P. and ULRICH, G. M. (1980) APIDOLOGIE 11.

RICHARDS, G. (1976) The control of prepupal puffing patterns in vitro; implications for prepupal ecdysone titres in Drosophila melanogaster. DEV. BIOL. 48 191-195.

RICHARDS, G. (1980) Ecdysteroids and puffing in Drosophila melanogaster. In: HOFFMANN (1980).

RICHARDS, G. (1981a) The radioimmune assay of ecdysteroid titres in Drosophila melanogaster. MOL. CELL. ENDOCRINOL. 21, 181-197.

RICHARDS, G. (1981b) Insect hormones in development. BIOL. REV. 56, 501-549.

RIDDIFORD, L. M. (1980) Interaction of ecdysteroids and juvenile

hormone in the regulation of larval growth and metamorphosis of the tobacco hornworm. In: HOFFMANN (1980).

RIDDIFORD, L. M. (1982) Changes in translatable mRNAs during the larval-pupal transformation of the epidermis of the tobacco hornworm. DEVELOP. BIOL. 92, 330-342.

RIDDIFORD, L. M. and KIELY, M. L. (1981) The hormonal control of commitment in insect epidermis - cellular and molecular aspects. In: KLOZA (1981).

ROBERTS, B., BAKER, M., KOTZMAN, M. and WENTWORTH, S. L. (1982) A possible role of ecdysteroids in pre-ecdysial tanning in larvae of Sarcophaga bullata (Diptera: Sarcophagidae). J. INSECT PHYSIOL. 28, 123-127.

ROBERTS, J. D. and CASERIO, M. C. (1964) Basic principles of organic chemistry. BENJAMIN, INC. NEW YORK.

ROBERTS, P. E. and WILLIS, J. H. (1980) The cuticular proteins of Tenebrio molitor I. Electrophoretic banding patterns during postembryonic development. DEVELOP BIOL. 75, 59-69.

ROBERTS, P. E. and WILLIS, J. H. (1980) The cuticular proteins of Tenebrio molitor II. Patterns of synthesis during postembryonic development. DEVELOP. BIOL. 75, 70-75.

ROBERTS, P. E. and WILLIS, J. H. (1981) Effects of juvenile

hormone, ecdysterone, actinomycin D, and mitomycin C on the cuticle proteins of Tenebrio molitor. J. EMB. EXP. MORPH. 56, 107-123.

ROBERTSON, C. W. (1936) The metamorphosis of Drosophila melanogaster including an accurately timed account of the principal morphological changes. J. MORPHOL. 59, 351-399.

RUHLAND, U. and ROMER, F. (1977) Nachweis von häutungsaktiven Stoffen in isolierten prothorakaldrüsen und Oenocyten bei Bombyx mori während des 5. Larvenstadiums. WILHELM ROUX'S ARCH. 181, 123-134.

RUSSELL, G. B. and PRICE, G. M. (1977) Metabolism of β-ecdysone during the larval and white puparial stage of the blowfly. Calliphora erythrocephala. INSECT BIOCHEM. 7, 197-202.

SCATCHARD, G. (1949) The attractions of proteins for small molecules and ions. ANAL. N.Y. ACAD. SCI. 51, 660-672.

SCHAFFNER, W. and WEISSMANN, C. (1973) ANALYTICAL BIOCHEM. 56, 502.

SCHUBIGER, G. (1974) Aquisition of differentiative competance in the imaginal leg discs of Drosophila. WILHELM ROUX' ARCHIV. 174, 303-311.

SEYBOLD, W. D. and SULLIVAN, D. T. (1978) Proteinsynthetic patterns

during differentiation of imaginal discs in vitro. DEVELOP. BIOL. 65, 69-81.

SHAAYA, E. and KARLSON, P. (1965) Der ecdysontiter während der Insektentwicklung. IV Die entwicklung der Lepidopteren Bombyx mori (L) und Ceruta vinula L. DEV. BIOL. 11, 424-432.

SHAAYA, E. and LEVENBOOK, L. (1982) The effects of starvation and 20-hydroxy-ecdysone on feeding and pupariation of early 3rd-Instar Calliphora vicina larvae. J. INSECT PHYSIOL. 28, 683-688.

SHAAYA, E. and SEKERIS, C. E. (1965) Ecdysone during insect development III. Activities of some enzymes of tyrosine metabolism in comparison with ecdysone titre during the development of the blowfly, Calliphora erythrocephala. GEN. COMP. ENDOCRINOL. 5, 35-39.

SHACKLETON, C. H. L. and WHITNEY, J. O. (1980) Use of "Sep-pak" cartridges for urinary steroid extraction. Evaluation of the method for use prior to gas chromatographic analysis. CLINICA CHIMICA ACTA. 107, 231-243.

SMITH, S. L., BOLLENBACHER, W. E. and GILBERT, L. I. (1980) Studies of the biosynthesis of ecdysone and 20-hydroxy-ecdysone in the tobacco hornworm, Manduca sexta. In: HOFFMANN (1980).

SRDIC, Z., REINHARDT, C., BECK, H. and GLOOR, H. (1979) Autonomous yolk protein synthesis in ovaries of Drosophila cultured in

vivo. WILHELM ROUX ARCHIV. *187*, 255-266.

SRIDHARA, S. (1981) Macromolecular changes during insect metamorphosis. In: GILBERT AND FRIEDEN (1981)

STEEL, C. G. H., BOLLENBACHER, W. E., SMITH, S. L. and GILBERT, L. I. (1982) Haemolymph ecdysteroid titres during larval-adult development in *Rhodnius prolixus*: correlations with moulting hormone action and brain neurosecretory cell activity. J. INSECT PHYSIOL. *28* (B), 519-525.

STELLWAAG-KITTLER, F. (1954) (BIOL. ZENTRALBL. *73*, 12-49) Cited by Delachambre et al in Hoffmann, J. A. (1980).

TREPTE, H-H (1980) Delayed vitellogenesis due to larval food deficiency in the housefly. J. INSECT PHYS. *26*, 801-806.

TRUMAN, J. W., LEVINE, R. B., and WEEKS, J. C. (1984) Reorganisation of the nervous system during metamorphosis of the moth, *Manduca sexta*. In: BALLS and BOWNES (IN PRESS).

WEHMAN, H. J. (1969) Fine structure of *Drosophila* wing imaginal discs during early stages of metamorphosis. WILHELM ROUX ARCHIV. *163*, 375-390.

WEIS-FOGH, T. (1970) Structure and formation of insect cuticle. SYMP. R. ENTOMOL. SOC. LOND. *5*, 165-185.

WENTWORTH, S. L., ROBERTS, B. and O'CONNOR, J. D. (1981) Ecdysteroid titres during postembryonic development of Sarcophaga bullata. J. INS. PHYS. 27, (7) 435-440.

WHITTEN, J. M. (1957a) The post-embryonic development of the tracheal system in Drosophila melanogaster. QUART. J. MICROSCOP. SCI. 98, 123-150.

WHITTEN, J. (1957b) The supposed pre-pupa in cyclorrhaphous Diptera. QUART. J. MICROSCOP. SCI.

WILSON, I. D., BIELBY, C. R. and MORGAN, E. D. (1982) Evaluation of some phytoecdysteroids as internal standards for the chromatographic analysis of ecdysone and 20-hydroxyecdysone from arthropods. J. CHROMATOG. 236, 224-229.

WILSON, T. G. (1980) Studies on the female-sterile phenotype of l(1) su (f)^{ts76a}, a temperature-sensitive allele of the suppressor of forked mutation in Drosophila melanogaster J. EMBRYOL. EXP. MORPHOL. 55, 247-256.

WOLSKY, A. (1938) The effect of carbon monoxide on the oxygen consumption of Drosophila melanogaster. J. EXP. BIOL. 15, 225-234.

YOUNG, N. L. (1976) The metabolism of ^{3}H-molting hormone in Calliphora erythrocephala at the mature larval and white puparial stages. INSECT BIOCHEM. 6, 1-12.

ZDAREK, J. (1981) The role of hormones in the control of premetamorphic behaviour in insects. In: KLOZA (1981).